1. CONTROL NUMBER		BATCH NUMBER
U 208105		231. 24

3. COL. CD.: 4

2 SOURCE CODE: N A S A

4. ACCESSION NUMBER: N73-74270

2A. RECOGNITION NUMBER: NASA-CR-55894

10 TRANSACTION N NEW D DUPLICATE P PRIOR S SUPERSEDES: N

10A.

6. MGT. CD. (C D A R K V): Q X F F V F

7. PROCESS ACCTG. CD.: Ø1

8 PROD. MGR.

9 RECEIPT TYPE: 1
- 0 N/A   3 ERRATA
- 1 RETAIN 4 LOAN
- 2 LAST

9A. LOAN DUE OUT (Y Y D D D)

11. PRICE: 1
- 1. STD.
- 2. EXC.

12. RETURNS: Ø
- 0 N/A   5 REST
- 1 PAGES 6 MISC.
- 3 REPRO
- 4 BDS

12A RETURN DATE (Y Y M M D D)

13 PROCESS: 1
- 0 STANDARD 3 UNEDIT
- 1 INVENTORY 4 REANNOUNCE
- 2 HIGHLIGHT 5 SPECIAL BIB

14. PAT. POTENTIAL: Ø
- 0 NO   3 GOOD
- 1 POOR 4 EXCEL
- 2 FAIR

16. BILL: 1 Ø Ø

17. FORM/PRICE: 1 2 0 0 1

18. ANNOUNCE (GRA WGA D/B): Ø Ø 0 Ø

19. PUBLICATION-1: U 7 8 2 Ø

20. PUBLICATION-2:

20A PUBLICATION-3:

21 LIMITATION: Ø
- 0 N/A
- 1 DISCLAIMER
- 2 COLOR
- 3 COMBO

	BIN	STOCK	PAGES/SHEETS	DOMESTIC PRICE	FOREIGN PRICE	ACTION CD.
23. PAPER COPY	Ø Ø Ø		Ø 8 / 3	2 4 Ø Ø	4 8 Ø Ø	B X
30. MICROFICHE						X M

37. REL CD.: J

38. MF PRINT: D

39. ADD. INFO: N

40. PRINT PC: N

43

41 PC DUE: N

42. SOURCE ORDER: N

COPYRIGHT: YES ☐ NO ☒ **INITL:** F

44. BATCH NO

02C) COM. CAT

03S) ADDITIONAL SOURCE CLIENTS

03L) LANGUAGE

03C) COMP. ENTRY CODE

34) SERIAL

35) CORP. AUTHOR CD.

MGT. CD. (CAT REV KEY VER)

PCA 99

1) ACC.#

6) TITLE

11) DATE

14) REPT. #(I-C)

45. REMARKS (DO NOT KEY)
RD_____

RECEIVE
NO.3

ANGLE
MEAS

TRACKING
NETWORK

TRAFFIC
CONTROL

WEATHER
BUREAU

SYNCHRONI
NO.3

BUFFER

BUFFER

BUFFER

BUFFE

3602
COMMUNICATIONS
MODULE

3604
COMPUTE
MODULE

16
BIDIRECTIONAL
DATA CHANNELS

3602
COMMUNICATIONS
MODULE

3602
COMMUNICATIONS
MODULE

3604
COMPUTE
MODULE

16
BIDIRECTIONAL
DATA CHANNELS

3602
COMMUNICATIONS
MODULE

6-379/6-380

RECEIVER NO.2

RECEIVER NO.1

RANGE MEAS.

ANGLE MEAS

RANGE MEAS.

ANGLE MEAS.

RANGE MEAS.

TRANSMITTER NO. 3

TRANSMITTER NO. 2

TR

SYNCHRONIZER NO.2

SYNCHRONIZER NO.1

GMT TIME

TRANSMITTER SELECTOR FOR FREQUENCY CONTROL

BUFFER

BUFFER

BUFFER

BUFFER

OMPUTER INTERFACE

3603 STORAGE MODULE

PRIVATE STORE

COMMON STORE

3603 STORAGE MODULE

3603 STORAGE MODULE

3603 STORAGE MODULE

3603 STORAGE MODULE

3603 STORAGE MODULE

PRIVATE STORE

2

6-379/6-380

```
                    ANTENNA· TRACKING ·EQUIPMENT              NORMAL INPUT — OUTPUT EQUIPMENT

  ┌──────────┐   ┌────────────┐  ┌────────────┐  ┌────────────┐
  │ANSMITTER │   │ANTENNA NO.3│  │ANTENNA NO.2│  │ANTENNA NO.1│
  │          │   │  TRACKING  │  │  TRACKING  │  │  TRACKING  │
  │  NO. 1   │   │  DISPLAY   │  │  DISPLAY   │  │  DISPLAY   │
  └──────────┘   └────────────┘  └────────────┘  └────────────┘

  ┌──────────┐   ┌────────────┐  ┌────────┐   ┌────────┐   ┌────────┐
  │MODULATOR │   │  ANTENNA   │  │  TAPE  │   │        │   │ CONSOLE│
  │          │   │  TRACKING  │  │        │   │PRINTER │   │   AND  │
  │(MESSAGES)│   │SYSTEM SELECTOR│ UNITS  │   │        │   │ DISPLAY│
  │          │   │    FOR     │  └────────┘   └────────┘   └────────┘
  │          │   │INITIAL POINTING│
  └──────────┘   └────────────┘

  ┌──────────┐   ┌────────────┐  ┌────────┐   ┌────────┐   ┌────────┐
  │  BUFFER  │   │   BUFFER   │  │ BUFFER │   │ BUFFER │   │ BUFFER │
  └──────────┘   └────────────┘  └────────┘   └────────┘   └────────┘
```

Figure 6. 3-7.   Computer Complex and Peripheral Equipment,
. Functional Block Diagram

3

The Antenna Tracking and Control Equipment receives only initial pointing commands through its buffer thus performing another output function for the central data processor. It is tentatively planned to incorporate three antennas, each with its own tracking and control equipment. Each of these equipments would receive pointing and activation commands separately.

Other buffered peripheral equipments which communicate with the central data processor are those normally required input-output equipments such as central control operating consoles, minimum operational console visual display, a printer, and tape recorders.

Also, a very accurate clock communicates with the buffer associated with the input telemetry equipment, and through its own buffer to the central data processor. The input telemetry buffer adds the time of message receipt to all incoming messages, and the clock buffer communicates the time to the central data processor.

System Time Standard

The Navigation Satellite System time throughout the world should be based on a common standard. Such a standard is available to the various parts of the system (in particular the vehicles and ground stations) in the WWV signals transmitted throughout the world by the Bureau of Standards. The accuracy of time of fix reported to the user vehicles is to the nearest second. Accordingly, for this purpose a timer synchronized to the WWV signals should suffice for both the ground stations and the user vehicles.

6: 3. 7. 1. 2 Characteristics Desired in the Computer of the Ground Control Station.

Word Length

A computer with 36-bit word length is more than enough to satisfy the Navigation Satellite System requirements, but when one can get a computer with a 48-bit word length with even greater computational ability for a lesser price, the choice is obvious.

Operation Time

The add time of a computer is a real measure of its potential speed. However, unless the latest techniques for multiplication and division are utilized, the add time may be a misleading guide to the computer's comparative speed capability. That is, since the ratio of the time for operations other than add to the add time is not the same for all computers, it does not necessarily follow that the computer with the best add time is the best computer for a given problem. Only a detailed analysis of the programming required for a given problem can positively determine which computer is fastest for solving the problem. This is so because certain operations most frequently used in solving a given problem can cause the preferred computer to be other than the one with the fastest add time. An add time of less than four microseconds was considered desirable in the computer to be used in the Navigational Satellite System.

Memory Requirements

Partial programming on an IBM 7094 of some of the tasks to be performed by the computer of the ground control station has given an indication that a thirty-two thousand word memory

would probably suffice initially, but the inevitable growth of the system should be considered along with the estimate of the initial memory requirements. Therefore, one of the prime requirements of the computer recommended for the ground station complex was that it should have an expandable memory, preferably expandable to greater than one hundred thousand words. An additional requirement was that this expandable memory be implemented by magnetic cores rather than magnetic discs or drums so that its access and cycle times would be short, preferably less than two microseconds.

Input-Output Buffering Requirements

The required computer, or computer complex as it should be called, must have a significant input-output capability. It has input and/or output interfaces with the Tracking Network, the Traffic Control Center, the Weather Bureau, three Receiving Synchronizers associated with the Data Receiving Equipment, a Transmitter Selection Unit and a Transmitter Frequency Control Unit associated with the Data Transmitting Equipment, an Antenna Tracking System Selector for initial pointing commands, several magnetic tape units, a printer, and a console. Each of these units should be capable of operation concurrently with the operation of the main computer; however, it is possible to allow the computer to momentarily interrupt its operations to initiate the input or output operation. After initiating the input or output operation, the computer should be enabled to continue its computation.

Redundancy Requirements in Ground Computer Complex

To provide uninterrupted operation of the ground control station, an adequate use of redundancy is required. It is necessary that the buffering equipment be duplicated and the output signals sent to each of two computers, one used as a standby for the other. There should be a common memory used by both of the computers, and this common memory should also be redundant to provide for possible failure of one of the common memories. Such redundancy is essential to provide a reasonable assurance of continuous operation of the ground station.

6.3.7.2 Computer Configuration

6.3.7.2.1 Choice of the Recommended Computer. - The computer requirements of the ground control station must be approached from a reasonable point of view. The prime goal of the study has been to ascertain the feasibility of the system. With the present state of development of the computer field there was even initially little doubt that a computing system could be developed for the ground complex which could satisfy the needs of the navigation satellite program. However, the detailed design of such a complex ground computing system was never implied in this feasibility study, nor could it have been implemented with the funding provided if an adequate effort was to be directed to the less feasible portions of the system.

As the study progressed and the system began to take a more final form, the major systems equations to be solved were derived and partial programming of some was implemented on an

IBM 7094 Computer. Analysis of the partial programming along with rough estimating of the additional computational load, led to conclusions about the desirable and practical characteristics of the ground station computing system. Comparing the necessary characteristics of presently available computers and then reviewing the computers satisfying these requirements for further desirable characteristics implied by the nature of the navigation satellite program, led to narrowing the choices to a very few computers that seemed capable of handling the navigation satellite program in a satisfactory way.

A necessary computer attribute which was used to eliminate many computers that could otherwise have been possible contenders was the availability of a high-speed random access memory of greater than one hundred thousand words. Such a memory capacity was found available on only about eight computers of which two (namely LARC and STRETCH) were discontinued computers. Another three utilized 186,000-word drum memories (namely the IBM models 7090, 7094 Model I, and 7094 Model II) to realize the greater than 100,000-word capacity and were accordingly eliminated because of the slower drum access time. The remaining three computers were the CDC 6600, the IBM 7080, and the CDC 3600.

The IBM 7080 was eliminated because of its much slower operational speed. The CDC 6600 is one of the most capable computers thus far available, but its capability is considered much in excess of the requirements of the Navigation Satellite System, and its price is in keeping with its excess capability. The remaining system to be considered is the CDC 3600 computer, a less capable computer built by the same company, Control Data Corporation.

Of the several computers having adequate computational rates and memory capacity the CDC 3600 seems to have the most desirable overall characteristics. Its computational speed is greater than that of the IBM 7094, its price is less, it has a greater memory capacity as well as a greater word length, and its planned modularity makes it more amenable to the navigation satellite task.

From the analysis of the partial programming of the computational load, it appears that one operable CDC 3600 could handle the job, but for improved performance and the requirement that the ground station be continuously operable, it is necessary to have at least two such computers at the ground station. One could be in operation while necessary maintenance was undertaken on the other machine. Should the performance of just one machine prove inadequate, a third machine could later be added to the computer complex to take on the additional computational load. The system then would consist of two operating computers and one in a standby mode.

The CDC 3600 is designed for just such a multiple computer system.

6.3.7.2.2 Description of the Recommended Computer. - Basically each CDC 3600 system consists of three modules:

1) The High-Speed 3602 Communication Module with up to eight bi-directional 3606 Data Channels.

2) The High-Speed 3603 Storage Module with 32,768 48-bit words, each with an additional 3 parity bits.

3) The High-Speed Compute Module.

Included in the basic computer is a 3601 console, which contains an electric typewriter, which when used as an input device has direct access to the accumulator. Used as an output device its data is buffered through the Communication Module. Also included in the basic 3600 Computer is a 250 card per minute reader which has direct access to the accumulator.

The 3604 Compute Module

This module is the heart of the 3600 Computer and performs all computing and logical operations, and provides the control for initiating input-output operations. This module operates in the parallel binary mode and has direct access to the 3603 core storage module.

The 3603 Storage Modules

This module provides a high-speed, random access magnetic core storage of 32,768 48-bit words divided into two independent storage banks of 16,384 words. Within each such bank, storage addresses are consecutive, permitting the 3603 to be treated as two independent storage units. The storage cycle time of each 16,384 word submodule is 1.5 microseconds and is totally independent of other submodules.

The 3602 Communication Module

The 3602 Communication Module contains a storage access control section, an arithmetic and control section, and up to 8 bi-directional data channels. Its input or output operations are initiated by the Compute Module, but the arithmetic and control portion of the 3602 Communication Module supervises all of the remaining input or output activity.

The basic 3600 Computer can be smoothly expanded to include up to eight 3603 Storage Modules (each with 32,768 words) for a total capacity of up to 262,144 48-bit words, each with 3 additional parity bits. Furthermore, the basic 3600 Computer can be expanded to include up to four 3602 Communication Modules, each with a capacity of eight bi-directional data channels, for a total of 32 possible data channels, each with a capacity for up to 8 control and/or peripheral devices attached to each bi-directional data channel.

6.3.7.2.3 Description of the Recommended Computer Complex. - A multiple computer complex such as envisioned for the navigation satellite ground control station can readily be formed from the 3600 modules. Figure 6.3-7 shows the modular layout of such a multi-computer complex.

Each of the two basic 3600 Computers requires two Communication Modules, one Compute Module, and one (or more) Memory Modules. In addition a memory consisting of two (or more) Memory Modules will serve as a memory that is capable of being used by both computers.

The number of Memory Modules used exclusively by one computer plus the number used by the same computer in the common memory cannot exceed eight modules. Upon failure of computer A, computer B could immediately utilize the contents of the common memory.

The common memory should be formed of two simultaneously addressed memories. In case of failure, of one of the two common memories, the currently used computer would use the available common memory until the other was repaired. The private memories would consist of only one storage module for each computer to be used when trouble shooting either computer.

Only by the incorporation of such redundancy can continuous operation of a ground station be assured.

Characteristics of the 3600 which make it appropriate for the navigation satellite application are:

1) a satisfactory input-output capability

2) modular expandability in input-output, number of storage modules in private or common storage, number of computers in complex

3) more than adequate word length

4) adequate operational speed

5) adequate interrupt facilities

6) simultaneous computation and input-output operations.

6.3.7.3. Event Sequencing at the Ground Computer.

6.3.7.3.1 <u>Initial Antenna Pointing, Satellite Position and Attitude Determination</u>. The ground computer operations associated with initial antenna pointing, satellite position and attitude determination, and satellite transfer from one control station to another control station are listed in this section.

After the several necessary computer programs have been loaded into the computer, the satellite ephemeris data is acquired from a tracking network to enable the ground station to initially point its two antennas to the satellites required by the given station for coverage of the vehicles in its assigned area. The computer then decides to which satellites its antennas should be pointed for coverage of the area assigned to the given ground station. It then formats and outputs an appropriate pointing command to each of the Antenna Tracking Control Units.

When the antennas have acquired their assigned satellites, the computer formats and outputs a command to each of the satellites, commanding each (in time sequence) to supply satellite status data. Upon receipt of the satellite status data, the computer makes a comparison of the satellite status data with stored data limits and prints out any out-of-limits data and determines whether the satellite is capable of being used.

The computer then determines, by position relative to the satellite's position, four appropriately positioned reference stations for use in determining the given satellite's exact position and attitude. It then formats and outputs to the Data Transmitting Equipment a fix command to each of the reference stations, four for each of the two satellites.

Upon receipt of each message from the satellite, the ground Data Receiving Equipment affixes the time of receipt to the message and generates, by decoding the function code, a specific interrupt signal for each type of message received. The computer then inputs the data to the appropriate part of its memory in keeping with the specific interrupt program which is activated by receipt of the interrupt signal.

After receipt of the range and angle data by the computer it proceeds to compute the position and attitude of the satellite at the time each reference station fix was made. By appropriate computation the satellite's position and attitude can then be predicted for fixes on vehicles made during the next second, at which time the satellite position and attitude is determined again to provide more accurate satellite position and attitude data for the following vehicle fixes.

Depending upon transfer rules yet to be established, the computer determines when a given satellite is to be transferred to the control of another ground station. When the satellite position relative to the ground station is greater than the maximum allowed by the transfer rules, the computer formats a transfer message and outputs it to the Interstation Communicating Equipment, through which it is transmitted to the appropriate ground station, thus effecting a transfer of the satellite control to the adjacent ground control station. The former ground station

then discontinues use of the given satellite until it receives another satellite transfer message from another ground control station.

Ground Processing to Implement Initial Antenna Pointing and Satellite Transfers from One Control Station to Another Control Station:

1. Input satellite ephemeris data from satellite tracking network (only necessary with new satellite)

2. Compute initial antenna pointing parameters for #1 antenna

3. Format antenna pointing command for #1 antenna

4. Output antenna pointing command for #1 antenna to Antenna Tracking Control

5. Format satellite #1 status data command

6. Output satellite #1 status data command to Data Transmitting Equipment

7. Compute antenna pointing parameters for #2 antenna

8. Format antenna pointing command for #2 antenna

9. Output antenna pointing command for #2 antenna to the Antenna Tracking Control

10. Format satellite #2 status data command

11. Output satellite #2 status data command to Data Transmitting Equipment.

12. Choose by position relative to satellite's position (as determined from satellite ephemeris data), 4 appropriate reference stations for satellite #1 position and attitude determination, compute doppler shift correction and output to transmitter to be used to track satellite #1 (update as required).

13. Format fix command for first reference station (reference station #1) used for satellite #1 position and attitude determination.

14. Output fix command (for reference station #1, to Data Transmitting Equipment)

15. Format fix command for second reference station (reference station #2) used for satellite #1 position and attitude determination.

16. Output fix command for reference station #2 to Data Transmitting Equipment

17. Format fix command to third reference station (reference station #3) for satellite #1 position and attitude determination.

18. Output fix command for reference station #3 to Data Transmitting Equipment.

19. Format fix command to fourth reference station (reference station #4) for satellite #1 position and attitude determination.

20. Output fix command for reference station #4 to Data Transmitting Equipment

21. Receive satellite #1 status data interrupt signal from Data Receiving Equipment

22. Input satellite #1 status data from Data Receiving Equipment

23. Compare to stored status data limits

24. Print out out-of-limits data (if any)

25. Determine whether satellite is capable of being used by analysis of limit comparison. If satellite is in satisfactory condition, continue position and attitude determination. If not, stop further use of the satellite and print out the results of the limit analysis.

26. Receive satellite #2 status data interrupt signal

27. Repeat 22 for satellite #2 ⎫
28. Repeat 23 for satellite #2 ⎪ Input satellite status data compared to limits,
29. Repeat 24 for satellite #2 ⎬ print out out-of-limits data, determine usability
30. Repeat 25 for satellite #2 ⎭ of satellite #2.

31. Repeat 12 for satellite #2 ⎫
32. Repeat 13 for satellite #2 ⎪
33. Repeat 14 for satellite #2 ⎪ Choose 4 reference stations for position and
34. Repeat 15 for satellite #2 ⎪ attitude determination of satellite #2 format
35. Repeat 16 for satellite #2 ⎬ and output the appropriate fix commands
36. Repeat 17 for satellite #2 ⎪ (ref. sta. 5 thru 8)
37. Repeat 18 for satellite #2 ⎪
38. Repeat 19 for satellite #2 ⎪
39. Repeat 20 for satellite #2 ⎭

40. Receive data interrupt signal from Data Receiving Equipment

41. Input fix data on reference station #1 from Data Receiving Equipment

42. Receive fix data interrupt signal from Data Receiving Equipment

43. Input fix data on reference station #2 from Data Receiving Equipment

44. Receive fix data interrupt signal from Data Receiving Equipment

45. Input fix data on reference station #3 from Data Receiving Equipment

46. Receive fix data interrupt signal from Data Receiving Equipment

47. Input fix data on reference station #4 from Data Receiving Equipment

48. Check consecutive receipt of fix data on the four reference stations.

49. - 57. Repeat 40 through 48 on fix data received on reference stations 1 through 8 used for determination of satellite #2 position and attitude.

58. Compute satellite #1 position using the range data on reference stations 1 through 4.

59. Compute satellite #1 attitude using the angle data on reference stations 1 through 4.

60. Compute satellite #2 position using the range data on reference stations 5 through 8. (Repeat operations 12 through 20, and 31 through 61 at one second intervals until a satellite leaves the control station area.)

61. Compare satellite range from control station (i. e., range from reference station located at station control with maximum allowable range from control station to satellite. (When greater than <u>allowable</u> range, transfer position data on last two or three satellite positions to next control station through appropriate link, thus effecting a transfer of satellite control to the adjacent control station; then discontinue use of given satellite and cease tracking it.)

62. Format satellite transfer message.

63. Output satellite transfer message to Inter Station Communication link(teletype).

6. 3. 7. 3. 2 <u>Vehicle Transfer Between Control Stations</u>. The necessity of transferring a vehicle from one ground control station to an adjacent one is brought about by the movement of the vehicle from the area controlled exclusively by a given ground station into the peripheral area controlled by the given station and an adjacent station. Based on the vehicle's present position, velocity, and heading, the ground computer determines whether or not a satellite will be available to enable the given ground station to obtain the next scheduled position fix on the vehicle. If it turns out that no satellite will then be available, the given station must effect a transfer of the given vehicle to the appropriate adjacent ground station.

Rules for transfer rather than physical limits will control the transfer of a vehicle from one station to another. Rules of usage of the satellites by the several ground stations will also be required so that when a given satellite is required by a given station for its prime coverage it will not be in use by an adjacent station. These rules for transfer and usage are dependent upon the satellite orbit configuration and the number of satellites as well as the number of ground stations and their configuration.

When it is found necessary to transfer the responsibility for fixing a given vehicle from one ground station to another, the station tentatively controlling the fixes on the vehicle formats a vehicle transfer message containing the following information for the adjacent station to which the vehicle is to be transferred.

1) Time to effect transfer

2) Vehicle identification

3) Last known position and time of fix for vehicle

4) Time next fix is due

There are two basic approaches to obtaining the communications link required for this hand-off; one is to use the Navigation Satellite itself as a relay satellite, and the other is to use existing or projected worldwide communications circuits.

The first approach appears attractive since it would keep the entire operational procedure within the Navigation Satellite System. However, the hand-off data rate should be very low and would require at most one conventional teletype channel. The instantaneous reliability required for the fix procedures is not present for this data link since a delay for several minutes to several hours (depending on the type of vehicles) would not impair the performance of

the system. In addition, the initial and operational costs of adding the communications link
to the navigation satellite and installing the additional relay equipment in the reference
stations for use when a common satellite is not available between the ground stations, would
more than offset the cost of leasing external communication facilities.

Thus, it is suggested that the hand-off problem be solved by leasing a conventional two-
way teletype channel from the Com-Sat system. If operational circuits are not available dur-
ing the initial phases of the Navigation Satellite program, a similar channel on submarine
cable, H. F. radio or any other common carrier facility will suffice.

6.3.7.3.3 <u>Satellite Transfer Between Control Stations.</u> The satellite array is a system of two
orthogonal orbits of 6000 n.m. altitude, each with four uniformly spaced satellites, all with
identical inclination angles of from $45°$ to $90°$.

The ground station array consists of six ground stations, arranged to provide worldwide·
coverage.

With two orthogonal orbits, each with four satellites, the coverage will be 100%. Each
orbit of four satellites will cover all of the earth except for a small section on opposite
sides of the earth on the axis perpendicular to the orbit. These two areas are covered in-
stead by the other orthogonal orbit of four satellites. The two areas where the two orbits
intersect is provided double coverage by the two orbits. Also a significant area of overlap
exists between the two orbits.

Transfer of a satellite from one ground station to another is effected by transfer commands
between ground stations. A satellite under the present system cannot be shared simultan-
eously be two adjacent ground stations. The given ground control station must first finish
using the satellite and must then notify the appropriate adjacent ground station when it has
done so before the adjacent station can make use of the satellite.

Each time a vehicle is serviced, a new computation is made to determine which satellite
and ground station will be used for the vehicle's next fix. If it is determined that another
adjacent ground station should provide the next fix, the vehicle will immediately be transferred
It will be treated as a new vehicle entering the new ground control area and will be given an
immediate fix and a listing in the sequence lists of the new ground station. Satellites must be
acquired by the tracking antennas of a station prior to actual use by the station. The ground
station initiates tracking of a satellite even while it is being used by an adjacent station.
However, the given ground station cannot begin to use it until the adjacent station relinquishes
use of it.

To ascertain which satellite will be available to obtain the next fix on a given vehicle it
must first be determined which satellites will be located within the specified geocentric
angle from the ground station at the time of the next desired fix. Theoretically (on a single
station basis), all such satellites could be used by the given ground station, but realistically
some of them will be in use by adjacent stations. For use with a given vehicle, the usable

satellites must be within a specified geocentric angle from the given vehicle. Next it must be ascertained which satellites are available, that is, which of those satisfying the previous tests are not still being used by an adjacent station. Also, with a limited number of dish antennas located at a given ground station it must be further ascertained whether or not one of the local antennas is directed to the desired satellite.

With the rotation of the satellites in their orbits, assuming orthogonal polar orbits, and the rotation of the earth being in a ratio of about 6 to 1, the patterns shift primarily in the north to south direction or vice versa. Since the overlap patterns are constantly changing, the checks relating to usage of a given satellite must be based on the geocentric angles relating the satellites to the ground station and on the geocentric angles relating the satellites to the vehicle. Such a scheme can adequately determine which satellite can be used for obtaining a given vehicle fix.

Obviously, the availability of a given satellite in terms of not being used by an adjacent ground station is data that must be stored by the computer in addition to the established rules of usage by the ground stations (which rules of necessity are different for different satellite and ground station configurations).

6.3.7.3.4 Vehicle Entry Request. The ground computer operations associated with processing vehicle entry requests are listed in items a through p of this section.

A vehicle entry request is a vehicle-originated action which arrives at the ground station out of sequence with the planned operations. The Data Receiving Equipment generates a specific interrupt signal which alerts the computer to the receipt of a vehicle entry request and causes the computer to momentarily interrupt its normal sequence of operations to take care of the entry request. From the vehicle address, the computer determines the type of vehicle and its fix rate and stores it in the appropriate vehicle list for proper fix rate and position message format.

The computer then formats and outputs a fix command to the requesting vehicle and checks to insure that fix data is received within a maximum allowed time. If the fix data is not received, the computer repeats the fix command up to three times. If it has still not been received, the computer formats a message to both the vehicle and Traffic Control indicating failure to receive the fix data.

Assuming receipt of the fix data, the computer proceeds to compute the actual time of fix on the vehicle. The computer then computes the position and attitude of the satellite at the actual time of the vehicle fix. Using the position data and satellite position and attitude, the computer then computes the position in latitude and longitude of the vehicle at the time of fix, formats the vehicle position report and includes it with the next vehicle fix command and report message sent to the Data Transmitting Equipment. Receipt of subsequent vehicle entry requests produces lists of vehicles to be serviced with different message formats and different fix rates. After servicing the vehicle entry request, the computer resumes its normal sequence of operations.

If a vehicle desiring entry into the system should happen to be in an area between two adjacent ground stations covered simultaneously by two satellites, one satellite in use by one ground station and the other in use by the adjacent station, the vehicle would stimulate a repetition of its entry request by both satellites, which would in turn heterodyne repeat the message to their respective ground stations. To avoid the problem of both ground stations simultaneously transmitting the vehicle's fix, each station would first determine the position of the given vehicle. Then, according to the rules pertaining to area coverage by the ground stations, one station would determine that it should not service the given vehicle and the other station would determine that it should service the vehicle. The rules should definitely avoid ambiguity as to which station should service the vehicle.

    a. Receive vehicle N_1 entry request interrupt signal from Data Receiving Equipment (This will determine through which satellite the request was repeated).

    b. Input vehicle N_1 entry request from Data Receiving Equipment.

    c. Determine vehicle fix rate and store in appropriate vehicle list.

    d. Format vehicle N_1 fix command.

    e. Output vehicle N_1 fix command to Data Transmitting Equipment.

    f. Receive fix data interrupt signal from Data Receiving Equipment.

    g. Input fix data on vehicle N_1 from Data Receiving Equipment.

    h. Check that fix data on given vehicle is received within specified maximum time allowance. If it has not been received, repeat fix command up to three times. If it has still not been received, format and output a message to both the vehicle and Traffic Control indicating failure to receive fix data.

    i. Compute actual time of fix on vehicle N_1.

    j. Compute satellite position at actual time of fix of vehicle N_1.

    k. Compute satellite attitude of actual time of fix of vehicle N_1.

    l. Compute position in latitude and longitude of vehicle N_1 at actual time of fix.

    m. Format vehicle N_1 position report.

    n. Output vehicle N_1 position report to Data Transmitting Equipment.

    o. Receipt of subsequent vehicle entry requests produces lists of vehicles to be serviced with different message formats and different fix rates.

    p. Resume interrupted sequence of operations.

6.3.7.3.5 <u>Vehicle Exit Request.</u> - The ground computer operations associated with processing vehicle exit requests are listed in items a through g, this section.

A vehicle exit request is another vehicle-originated action which arrives at the ground station out of sequence with the planned operations. The Data Receiving Equipment generates a specific interrupt signal which alerts the computer to the receipt of a vehicle exit request and causes the computer to interrupt its planned operations momentarily to service the exit request. After receipt of the message the computer removes the vehicle from the fix sequence

listing, and formats and outputs a message to Traffic Control indicating that the vehicle is no longer actively being serviced. The computer then returns to its normal sequence of operations.

    a. Receive vehicle exit request interrupt signal from Data Receiving Equipment.

    b. Immediately interrupt present operation such as to allow a later return to complete it.

    c. Input vehicle exit request message from Data Receiving Equipment.

    d. Remove vehicle from fix sequence listing.

    e. Format vehicle exit message for Traffic Control.

    f. Output vehicle exit message to Traffic Control.

    g. Continue interrupted sequence of operations.

6.3.7.3.6 Vehicle Emergency Request The ground computer operations associated with processing a vehicle emergency request are listed in items a through r, this section.

A vehicle emergency request is another vehicle-originated action whose receipt at the ground station causes the Data Receiving Equipment to generate a specific interrupt signal which in turn causes the computer momentarily to interrupt its current operation, input the message, and initiate the emergency procedure. The computer then immediately formats and outputs a fix command to the vehicle and temporarily increases its fix rate to more accurately track it. The increased fix rate continues until the Traffic Control discontinues the emergency status of the vehicle.

After receipt of the fix data on the given vehicle the same necessary fix computations as described in the vehicle entry description are performed by the computer (as listed) ending with a position report to both the vehicle and the Traffic Control. The computer then continues its normal sequence of operations.

    a. Receive emergency request interrupt signal from Data Receiving Equipment.

    b. Immediately interrupt present operation such as to allow a later return to complete it

    c. Input vehicle E emergency request message from Data Receiving Equipment.

    d. Format a vehicle E fix command.

    e. Output Vehicle E fix command to the Data Transmitting Equipment.

    f. Temporarily increase the vehicle E fix rate.

    g. Check that fix data on given vehicle E is received within specified maximum time allowance. If it has still not been received, repeat fix command up to three times. If it has still not yet been received format and output a message to both the vehicle and Traffic Control indicating failure to receive fix data.

    h. If successful, receive emergency fix data interrupt signal from Data Receiving Equipment.

    i. Input emergency fix data on vehicle E from Data Receiving Equipment.

    j. Compute actual time of fix on vehicle E.

k. Compute satellite position at actual time of fix on vehicle E.

l. Compute satellite attitude at actual time of fix on vehicle E.

m. Compute position in latitude and longitude of vehicle E at actual time of fix (and put into vehicle position storage).

n. Choose next vehicle N_n (i. e. repeat the one that was interrupted).

o. Format vehicle N_n fix command and vehicle E position report.

p. Output position report on vehicle E to Traffic Control.

q. Output vehicle N_n fix command and vehicle E position report to Data Transmitting Equipment.

r. Restore normal fix rate for vehicle E only when advised to do so by Traffic Control.

6.3.7.3.7 Satellite Operational Commands and Operability Check. The ground computer operations associated with implementing satellite operational commands are listed in items a through k, this section.

Assuming that antenna A is pointing to satellite S, the computer simply formats the desired specific satellite command and outputs it to the Data Transmitting Equipment. To check on the results of the given command, the computer then formats and outputs a status data command to the given satellite. Upon receipt of the status data, the computer compares the several parameters with the stored limits and in particular verifies that the commanded change (if measured by the normal status data) has taken place in the satellite.

a. Assume an antenna A is pointing to a satellite S.

b. Format the desired specific satellite command.

c. Output the satellite command to the specific antenna pointing to satellite S.

d. After allowing sufficient time for the satellite S to implement the command, format a satellite S status data command.

e. Output the satellite S status data command to the specific Data Transmitting Equipment.

f. Receive satellite status data interrupt signal from Data Receiving Equipment.

g. Input satellite S status data from Data Receiving Equipment.

h. Compare to stored status data limits.

i. Store status data on magnetic tape for further off-line processing.

j. Print out out-of-limits status data. In particular the parameter/s modified by the satellite command should be printed out.

k. The normal sequence of obtaining fixes is resumed pending initiation of corrective action, if required.

6.3.7.3.8 Sequencing the User Vehicles. Sequencing the user vehicles is necessary to properly service the user vehicles according to the required service rate and the type of vehicle. Slow moving vehicles are serviced infrequently because their positions change slowly with

time, and fast moving vehicles are serviced frequently (with the exception of special survey ships, etc.)

The sequential listing can best be described as a commutator where the total commutation cycle is a cycle of length in time equal to the period of time between servicing the least frequently serviced vehicles. Such vehicles are serviced only once per commutation cycle. Other vehicles are serviced an integral number of times per commutation cycle.

. The number of vehicles in a class varies approximately inversely as a function of the class, the greatest number of vehicles being located in the least frequently serviced class and the least number of vehicles in the most frequently serviced class. Accordingly, the lesser number of vehicles in the more frequently serviced classes must be interspersed among the much greater number of vehicles in the less frequently serviced classes at appropriate intervals to satisfy all of the servicing rates. Although the number of vehicles that could be serviced in a given interval of time in the initial implementation is much less than the number forecast for the year 2,000, the procedure for sequencing the user vehicles will be essentially the same. The type of vehicle and its desired fix rate is an inherent property of its specific address code. Initially, with the reduced number of vehicles in the system, a count field (or a portion) of the total count can be allocated to specific user categories, where each category is a specific type of vehicle requiring a specific report format and a specific fix rate. Upon receipt of an entry message with such a vehicle address appropriate checks are made to ascertain which field the vehicle address is a part of and accordingly what kind of message format is required and what fix rate is also required. At a later date when the number of vehicles of all types has greatly increased, it might cause considerable confusion if the several categories start overflowing their initial field (or count) allocations. It therefore seems much more straightforward to incorporate additional data (in addition to the address code) specifically informing the ground station what kind of vehicle it is and what its fix rate is. The computer could then straightforwardly assign the vehicle to the appropriate list without further checks and without the possible later confusion resulting from inadequate initial count allocations.

After ascertaining the type of vehicle and its fix rate the computer lists the vehicle in the list determined by these two factors. It then increases the tally of vehicles in that particular list by one and recalculates the number of vehicles that should be taken from that list in a given 5-minute time period.

When a vehicle exits from the system, it must be removed from the list, and the computer must again change the tally of the given list and recompute the number of vehicles to be serviced from the given list in a 5-minute interval of time. The updated tally N of vehicles in the given list is divided by the number of groupings G associated with the particular class (or list) to satisfy the given fix rate. The integer quotient Q is the number of vehicles that should be serviced in a 5-minute interval with the present tally of the given class. The

remainder of the quotient R defines the number to be serviced more precisely by saying in effect that the first R groupings of the class (if R is the remainder, modulo G) should be augmented by one to most evenly distribute the list over the entire commutation cycle.

The computer services the vehicles at a fix rate commensurate with the tentative system load. This simple computation involves the determination of the total number of fixes required for a given interval of time which is simply the sum of the vehicles in a given class, N, divided by the number of groupings in the class, G, for the given interval of time (assumed to be 5 minutes at this time) divided by the number of seconds in the 5-minute interval (300).

$$\frac{1}{300}\left(\frac{N_1}{G_1} + \frac{N_2}{G_2} + \frac{N_3}{G_3} + \frac{N_4}{G_4} + \dots \frac{N_N}{G_N}\right) = \text{No. of vehicle fixes per second}(F/sec.)$$

According to available estimates for the year 2000, in the North Atlantic (theoretically the busiest ocean area on the earth), 1600 active minimum user marine vehicles will require fixes about once every 6 hours, whereas about 5100 typical marine users will require fixes every hour. No estimates are available on the number of special marine users so a figure of 100 (probably too large) was chosen. The marine special users would require fixes at five-minute intervals. Likewise, the total of 100 was used as the largest number of jet transports or sequence transports active over the Atlantic, each requiring a fix every five minutes. For commercial propeller aircraft requiring fixes every 10 minutes, a total of 800 was estimated. The general aviation category requiring fixes every 15 minutes numbered 3800 active vehicles. Distributing the appropriate portion of each category over the 6-hour interval as shown in the following equation,

$$\frac{1600}{72} + \frac{5100}{12} + \frac{100}{1} + \frac{100}{1} + \frac{800}{2} + \frac{3800}{3} = \begin{array}{l} 2315 \text{ fixes in a 5-minute period over} \\ \text{North Atlantic by year 2000} \end{array}$$

A figure of 2315 fixes in a given 5-minute interval was computed (adequately less than the maximum allowable of 3000 at the 10 per second fix rate), or,

$$F/sec. = 2315 \times \frac{1}{300} = 7.7 \text{ fixes per second at year 2000.}$$

To properly service the entire listing of vehicles, the number of vehicles serviced in a second would be set to eight per second, with a short resultant slack period of 11 seconds available before the next 5-minute group is serviced. If messages other than the required fix and report messages are desired, the fix rate can be increased to allow more time at the end of the five-minute intervals as desired.

6.3.7.3.9 Operational Timing Sequence of Navigation Satellite System. - Two very important system parameters are the vehicle fix rate and the message bit rate. A change in either of these parameters affects the satellite power requirements as well as the system interference. This section is intended to clarify the timing associated with the system with regard to message content and fix rate.

The planned system requires attitude calibration of the satellite interferometer antennas once each second by means of consecutive angle measurements to four reference stations. Table 6.3-1 shows the message formats for links 1, 2, and 5. The transmission time has been computed for a 25,000 bits/sec rate and for a 2,500 bits/sec rate over link 2. The total transmission time required for 10 fixes has been computed for each case. Referring to Table 6.3-1, the sequence of events is as follows:

Items 1 through 4.	Obtain angle measurement on reference station no. 1.
Items 5 through 16.	Obtain angle measurements on reference stations 2, 3, and 4.
Items 17 through 28.	Obtain fix on vehicle N.
Items 29 through 32.	Send position report to vehicle N-10.
Items 33 through 49.	Obtain a fix on vehicle N + 1 and send a position report to vehicle N-9.
Items 50 through 167.	Obtain fixes on vehicles N + 2 through N + 9 with interspersed position reports to vehicles N-9 through N-2.

The time, t, required for transmission propagation between the satellite and a reference station or a vehicle is given by:

$$t = \frac{r}{c}$$

where

r = range

c = velocity of light = 161,000 nmi/sec

then for maximum and minimum ranges we have:

Range	Propagation Time
8500 nmi	52.8 m sec
6000 nmi	37.3 m sec

It should be noted in table 6.3-1 that some dead time has been placed before each position fix (items 4, 28 and 49). Adequate dead time is necessary to insure that no interference occurs between the range and angle pulses from two consecutive position fixes due to differences in lengths of transmission paths.

Table 6.3-2 shows the message format over links 3a, 3b, and 4, where the bit rate is 10,000 bits/sec.

TABLE 6.3-1

MESSAGE FORMATS, LINKS 1, 2, AND 5

Item	Description	Link	No. Bits	25000 bits/sec		2500 bits/sec	
				Bit Length (μsec)	Time (μsec)	Bit Length (μsec)	Time (μsec)
1	Sync	1, 2	6	40	240	400	2400
2	Function Command (Ref. Sta. Angle Fix)	1, 2	4	40	160	400	1600
3	Ref. Sta. #1 Address	1, 2	8	40	320	400	3200
4	Space (Propagation Time)				41,280		34,800
--	Subtotal (Items 1 through 4)				42,000		42,000
5 thru 8	Repeat 1 thru 4 for Ref. Sta. #2						
9 thru 12	Repeat 1 thru 4 for Ref. Sta. #3						
13 thru 16	Repeat 1 thru 4 for Ref. Sta. #4						
--	Subtotal (Items 1 thru 16)				168,000		168,000
17	Sync	1, 2	6	40	240	400	2400
18.	Function Command (Vehicle Fix)	1, 2	4	40	160	400	1600
19	Vehicle (N) address	1, 2	24	40	960	400	9600
20	Space, (to allow switching from link 2 to link 5)				80		300
21	Radar Sync	1, 5	6	100	600	100	600
22	Range Pulse I	1, 5		320	320	320	320
23	Space				15		15
24	Range Pulse II	1, 5		320	320	320	320
25	Space				25		25
26	Range Pulse III	1, 5		320	320	320	320
27	Space (to allow switching from link 5 back to link 2)				80		800
--	Subtotal (Items 17 thru 27)				3,120		16,800

TABLE 6.3-1 (Continued)

Item	Description	Link	No. Bits	25000 bits/sec Bit Length (μsec)	25000 bits/sec Time (μsec)	2500 bits/sec Bit Length (μsec)	2500 bits/sec Time (μsec)
28	Space (Propagation Time)				38,800*		25,200**
29	Sync	1, 2	6	40	240	400	2400
30	Function Command (Report)	1, 2	4	40	160	400	1600
31	Vehicle (N-10) Address	1, 2	24	40	960	400	9600
32	Report Format	1, 2	153	40	6120	400	61,200
--	Subtotal (Items 28 thru 32)				7480		74,800
--	Subtotal (Items 17 thru 32)				10,600		91,600
33 thru 48	Repeat 17 thru 32 For Fix on Vehicle N+1 and report to vehicle N-9				10,600		91,600
49	Space (Propagation time)				31,400*		0**
50 thru 167	Repeat 17 thru 32 8 more times for remaining 8 vehicle fixes and 8 vehicle reports				84,800		732,800
--	Total time to fix 4 reference stations 10 vehicles and report to 10 vehicles				588,000		1,084,000

*The total time between fixes must be at least 38,880 μsec. Part or all of the time may be used for transmission of one or more reports. The dead time at the end of a report (or series of reports) must be such that it, plus the report transmission time, will be at least 38,880 μsec. (For purposes of calculating average power requirements it is assumed that one report follows each vehicle fix.)

**A space of at least 25,200 μsec must follow a vehicle fix before another vehicle fix can be made. Part or all of the 25,200 μsec may be used for a vehicle report.

The first part of table 6.3-2 shows the format for links 3a (vehicle to satellite) and 4 (satellite to ground) when the ground station has requested a vehicle or reference station fix. The second part of table 6.3-2 shows the format over links 3b (vehicle to satellite) and 4 (satellite to ground) when the message is one of the several evergency requests or an entry or exit request.

TABLE 6.3-2

MESSAGE FORMATS, LINKS 3A AND 4

Item	Description	No. Bits	Bit Length (μ sec)	Time (μ sec)
1	Radar sync	6	100	600
2	Range pulse #1			320
3	Space			15
4	Range pulse #2			320
5	Space			25
6	Range pulse #3			320
7	Partial Address	10	100	1000
8	Angle Pulse			7000
	Total 1 through 8			9600

PULSE FORMAT, LINKS 3B AND 4

1	Sync	6	100	600
2	Function Command	4	100	400
3	Address	24	100	2400
	Total 1 through 3			3400

Figures 6.3-8 and 6.3-9 show the time sequence of links 2 and 3a. The ordinate is propagation time in milliseconds and the abscissa is elapsed time in milliseconds. Figure 6.3-8 is based on a 25,000 bit/sec rate on link 2. Referring to Figure 6.3-8, the sequence of events is as follows:

Point 0, 0   transmission of a fix command to vehicle N begins at the satellite.

Point 3.12, 0   end of transmission of fix command to vehicle N, beginning of report to vehicle N-10
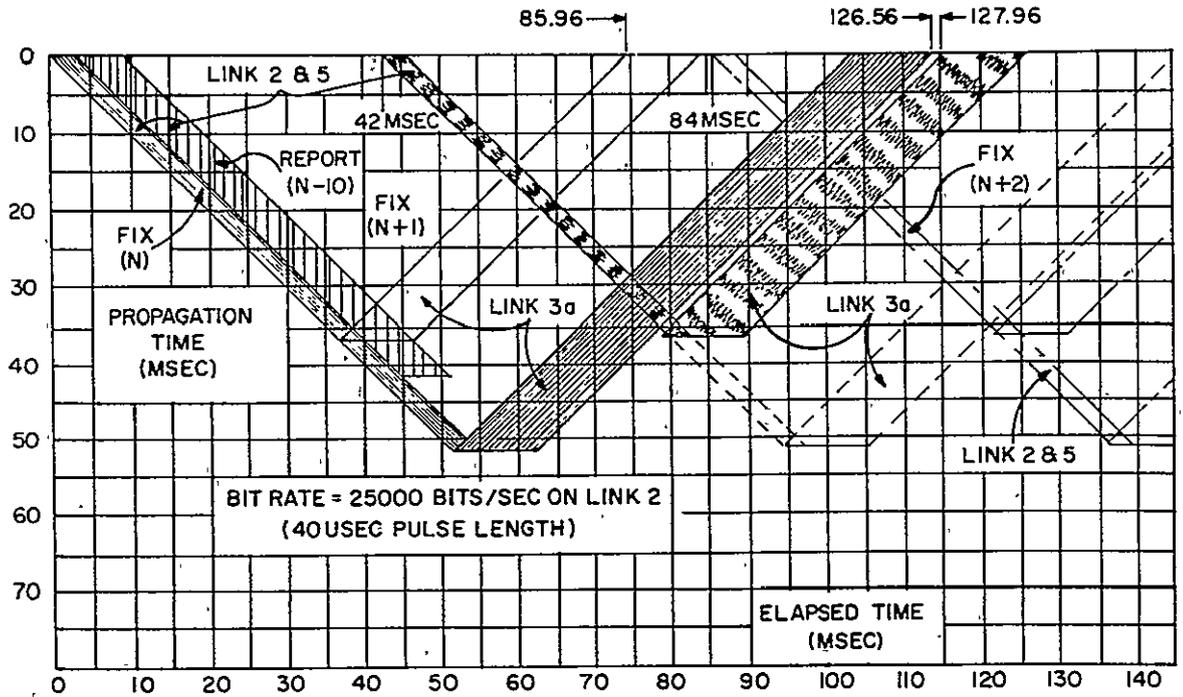
Figure 6.3-8. Propagation Sequence for 25,000 Bits Per Second
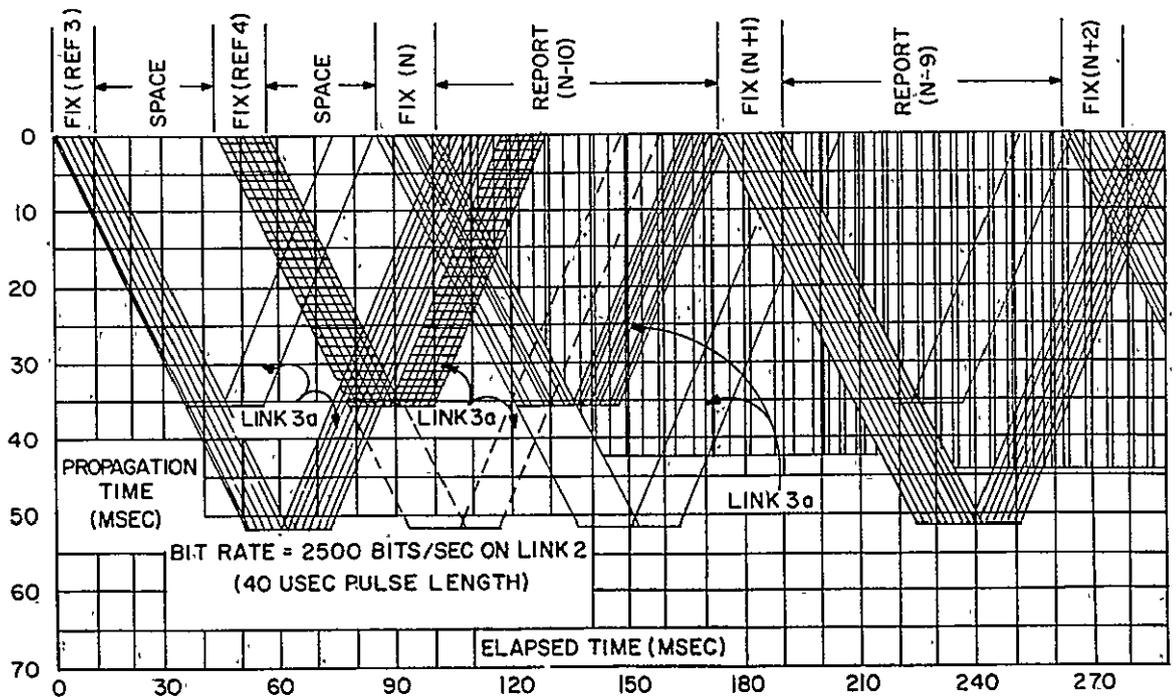
Figure 6.3-9. Propagation Sequence for 2,500 Bits Per Second

Point 37.3, 37.3	the first bit of the fix command to vehicle N travels the shortest possible distance (6000 nmi) to a vehicle. If vehicle N were at this point it would set up to heterodyne repeat the range pulse
Point 52.8, 52.8	the first bit of the fix Command has reached vehicle N (arbitrarily placed at a maximum range from the satellite)
Point 73.36, 52.8	the last bit is sent from vehicle N to the satellite
Point 126.16, 0	the last bit from vehicle N is received by the satellite.

The space between fixes is so arranged that the first bit from vehicle N + 1 will always arrive at the satellite after the last bit from vehicle N. Part or all of the space between fixes can be used for transmitting position reports to the vehicle without causing interference.

Figure 6.3-9 is based on a bit rate of 2500 bits/sec on link 2 and therefore, the transmission time is greater than that shown in figure 6.3-8 where the bit rate is 25000 bits/sec. Referring to figure 6.3-9, the sequence of events is as follows:

Point 0, 0	satellite starts transmitting fix command message to Reference Station 3
Point 42, 0	satellite starts transmitting fix command message to Reference Station 4
Point 84, 0	satellite starts transmitting fix command message to Vehicle N
Point 100.8, 0	satellite starts transmitting position report to vehicle N-10 (end fix to vehicle N).

It should be noted that the space between reference station fixes is determined by the propagation time just as in figure 6.3-8. The space between vehicle fixes however, is determined by the length of the report, since the report transmission time is greater than the propagation time. Examination of figure 6.3-9 will show that interference can never occur at the satellite, in the reception of consecutive range and angle transmission from vehicles or reference stations that are under control of a common ground station.

Table 6.3-3 shows the variation of Per Cent Duty Cycle of links 1, 2, 4 and 5 as a function of the Vehicle Fix Rate for a 2500 bit per second data rate on links 1 and 2. Table 6.3-4 shows the same data when the data rate on links 1 and 2 is 25,000 bits per second.

Link 3 (vehicle to satellite) is not shown since the duty cycle on this link is not a function of the system fix rate but only of the individual vehicle fix rate which is in the order of once every several minutes to several hours and therefore is not critical. Link 1 is also not

TABLE 6.3-3

TRANSMITTER DUTY CYCLE AT 2500 BITS PER SECOND
DATA RATE ON LINKS 1 AND 2

Vehicle Fix Rate (Vehicle/sec)	% Duty Cycle			
	Link 1	Link 2	Link 4	Link 5
0 (Ref. sta. only)	2.9	2.9	3.4	0
1	11.9	11.7	4.4	.16
2	20.9	20.6	5.4	.32
3	29.9	29.4	6.3	.48
4	38.9	38.2	7.3	.64
5	47.9	47.1	8.2	.80
6	56.9	55.9	9.2	.96
7	65.9	64.8	10.1	1.12
8	74.9	73.6	11.2	1.28
9	83.8	22.4	12.1	1.44
10*	92.9	91.3	13.0	1.60

*A 2500 bits/sec system is limited to nine vehicle fixes per sec because the total time required for 10 complete fixes could exceed the one second time allowed.

TABLE 6.3-4

TRANSMITTER DUTY CYCLE AT 2500 BITS PER SECOND
DATA RATE ON LINKS 1 AND 2

Vehicle Fix Rate (Vehicle/Sec)	% Duty Cycle			
	Link 1	Link 2	Link 4	Link 5
0	.29	0.29	3.4	0
1	1.3	1.17	4.4	.16
2	2.4	2.05	5.4	.32
3	3.4	2.94	6.3	.48
4	4.5	3.82	7.3	.64
5	5.5	4.71	8.2	.80
6	6.6	5.59	9.2	.96
7	7.6	6.48	10.1	1.12
8	8.6	7.36	11.2	1.28
9	9.7	8.24	12.1	1.44
10	10.7	9.13	13.0	1.60

critical so far as interference is concerned since it employs a directional antenna which discriminates against undesired satellites. It is also not cricital of power requirements since it is located at a fixed ground location where more or less unlimited power is available.

Interference in the system is a function of the data rate and vehicle fix rate used. It is clear in tables 6.3-3 and 6.3-4 that the satellite is kept busy a much greater part of the available system time when the slower bit rate of 2500 bits per second is used. A vehicle desiring to enter the system, to exit from the system, or to notify the ground station of an emergency condition is not dependent upon the available free time of the system because a special offset frequency channel is set aside for this purpose, but the concurrency of such messages with resultant interference is less probable if the data rate is increased.

The slower bit rate of 2500 bits per second would apply only until the faster bit rate of 25,000 bits per second becomes necessary.

The satellite average power requirements are also a function of the data rate and vehicle fix rate used. The transmitters for links 2, 4, and 5 are aboard the satellite and as shown, eleswhere in this report they require peak powers of 20W, 2W and 5KW respectively. The average power for any desired vehicle fix rate is this peak power times the duty cycles shown in tables 6.3-3 and 6.3-4. It can be seen that with a data bit rate of 2500 and a vehicle fix rate of one per second, the following average powers are required:

> Link 2 - 2.34 watts
>
> Link 4 - 88 milliwatts
>
> Link 5 - 8.0 watts

6.3.8 Data Processor Calculations. This section of the report describes the mathematical computations performed by the ground computer. These include the navigation problem solution as well as the determination of satellite position and attitude. Computations related to satellite position and attitude will be treated first, followed by the fix equations.

6.3.8.1 Satellite Position Calculation From Keplerian Orbital Elements.

a. Inertial reference frame. A necessary prelude to the discussion of satellite calculations is a description of the fundamental coordinate system. The system adopted is a geocentric, equatorial, inertial, cartesian coordinate reference frame, designated the E-frame. The X-axis of this non-rotating coordinate system is aligned in the direction of the vernal equinox, the Z-axis coincides with the earth's polar axis, positive in the direction of north, and the Y-axis completes an orthogonal "right hand" system. Satellite positions and velocities will be first computed in the E-frame coordinates then transformed to geographic polar coordinates.

b. Orbital elements. It is assumed that a set of satellite parameters will be available from an external tracking net. The set of 6 parameters assumed, together with 2 additional precessional rates, are as follows:

Semi-major axis, a, in earth radii

Eccentricity, e, dimensionless

Inclination, i, in degrees

Time of perigee, t_p, in seconds UT

Argument of perigee, ω_p, in degrees

Right ascension of ascending node, Ω_n, in degrees

Precession of perigee, $\dot{\omega}_p$, in degrees/day

Precession of node, $\dot{\Omega}_n$, in degrees/day

c. The equations used in computing satellite position in E-frame coordinates (X_s, Y_s, Z_s) are outlined in table 6.3-5. Kepler's equation (3), will be solved by Newton-Raphson iteration with mean anomaly being taken as a first estimate of eccentric anomaly. This procedure is based on the assumption of a low eccentricity orbit.

d. The sequence of calculations given in table 6.3-5 will be followed for 2 satellite position calculations near the beginning of a pass as the satellite enters the coverage area of a ground station. Subsequent positions will be obtained by a different method described below.

6.3.8.2 Satellite Position Refinement.

As a satellite enters the control area of the ground station two successive positions will be determined. Satellite inertial coordinates will be calculated from Keplerian elements and will then be differentially corrected with the aid of three simultaneous range readings to different reference stations. Thereafter, satellite position, whenever required, will be calculated from the two most recently corrected position fixes by a variation of Gibb's method. At intervals of one minute, the satellite position will be differentially corrected using range data obtained from scheduled interrogation of three reference stations. See figure 6.3-10.

Three simultaneous radar range measurements R_1, R_2, R_3 will be made from the satellite to reference stations located at positions $(X_i, Y_i, Z_i: i = 1, 2, 3)$. These same three ranges will also be calculated using a satellite position (X_s, Y_s, Z_s) obtained from orbital elements of Gibb's method. Calculated range from satellite to i the reference station will be

$$R_{ic} = \left[(X_s - X_i)^2 + (Y_s - Y_i)^2 + (Z_s - Z_i)^2 \right]^{1/2} \quad i = 1, 2, 3$$

Let A denote the matrix whose elements are the partial derivatives of the calculated ranges with respect to the satellite coordinates, i.e.

$$A = \begin{pmatrix} \partial R_{1c}/\partial X_s & \partial R_{1c}/\partial Y_s & \partial R_{1c}/\partial Z_s \\ \partial R_{2c}/\partial X_s & \partial R_{2c}/\partial Y_s & \partial R_{2c}/\partial Z_s \\ \partial R_{3c}/\partial X_s & \partial R_{3c}/\partial Y_s & \partial R_{3c}/\partial Z_s \end{pmatrix}$$
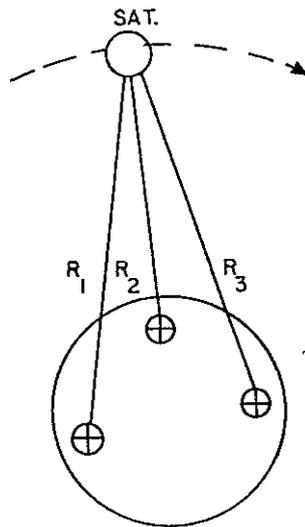
Figure 6.3-10. Position Refinement Measurements

Then the differential correction method yields corrections to satellite position $(\Delta X_s, \Delta Y_s, \Delta Z_s)$ as the solution to the linear system:

$$(A) \begin{pmatrix} \Delta X_s \\ \Delta Y_s \\ \Delta Z_s \end{pmatrix} = \begin{pmatrix} R_1 - R_{1c} \\ R_2 - R_{2c} \\ R_3 - R_{3c} \end{pmatrix}$$

It can be readily seen that the rows of the A matrix are comprised of the three sets of direction cosines associated with the reference station to satellite range vectors. The entire process may be iterated until the incremental corrections to satellite position fall below some preassigned threshold value.

6.3.8.3 Satellite Position Extrapolation By Gibb's Method.

Following the method outlined by Cole and Deutsch[1], from known satellite positions R_{s1} and R_{s2} at times t_1 and t_2, a position vector is calculated for t_3.

---

[1] ARS Journal, September 1962

Let

$$\tau_{21} = t_2 - t_1$$

$$\tau_{31} = t_3 - t_1$$

$$\tau_{32} = t_3 - t_2$$

Coefficients M_1 and M_2 are calculated as follows:

$$M_1 = \frac{\tau_{32}}{\tau_{21}} \left[1 + \frac{\mu(\tau_{21}^2 - \tau_{32}^2)}{6\,R_{s1}^3} \right]$$

$$M_2 = -\frac{\tau_{31}}{\tau_{21}} \left[1 + \frac{\mu(\tau_{21}^2 - \tau_{31}^2)}{6\,R_{s2}^3} \right]$$

Then the satellite position vector at t_3 is given by:

$$R_{s3} = -M_1 R_{s1} - M_2 R_{s2}$$

μ appearing in the expressions above is the earth's gravitational constant. It is expected that the satellite position will be differentially corrected once every minute so that the time intervals involved are of that magnitude or less.

A variation of the method will yield the satellite velocity vector. With two known positions $\overline{R}_{s1}$, $\overline{R}_{s2}$ at times t_1 and t_2, the velocity vector at time t_2 is obtained:

$$\overline{V}_2 = \overline{R}_{s2} = \frac{\overline{R}_{s2} - \overline{R}_{s1}}{t_2 - t_1} - \frac{\mu(t_2 - t_1)}{3} \left[\frac{\overline{R}_{s2}}{R_{s2}^3} + \frac{\overline{R}_{s1}}{2R_{s1}^3} \right]$$

This is an adaptation of equation 10 in the reference paper. Velocity is used in the determination of the time of fix as outlined in section 5.

6.3.8.4 Attitude Determination.

By attitude determination, is meant the finding of the E-frame inertial direction cosines (or components) of a unit vector presumed to be collinear with the arm of each interferometer in addition to a determination of the interferometer scale factor and delay. The orientation of the unit vector in inertial space is time varying due to 1) satellite orbital motion,

2) satellite rotation and possibly 3) warping of the interferometer arm. Additionally the scale factor and delay must be assumed to vary with time. Thus, an attitude fix on the satellite is essentially associated with a single point of time. For navigation purposes, there is a requirement to know satellite attitude at any given instant of time. Two possible approaches toward meeting this requirement are 1) infrequent attitude fixes, accompanied by tracking and prediction with the ground data processor 2) attitude determination made so frequently that the variations between fixes may be neglected. The second approach is adopted here, satellite attitude being determined nearly simultaneously with every navigation fix on a user vehicle.

See figure 6.3-11. A set of four independent angle readings on separate ground reference stations is necessary and sufficient to calculate the orientation, scale factor, and delay of a single interferometer. Ideally, the four measurements should be taken simultaneously. Since this is not possible the interval over which they are taken should be kept as short as the measuring process will allow. It will be assumed here that over the duration of the measurement interval, the satellite attitude remains constant.

The location of each reference station in a rotating geocentric coordinate system will be known. With the X-axis of this coordinate system lying in the plane of the Greenwich meridian, the transformation of reference station coordinates to the E-frame involves a rotation of the X, Y components through the Greenwich hour angle.

θ_{ij} = ANGLE BETWEEN AXIS OF INTERFEROMETER i AND LINE OF SIGHT TO REFERENCE STATION j.
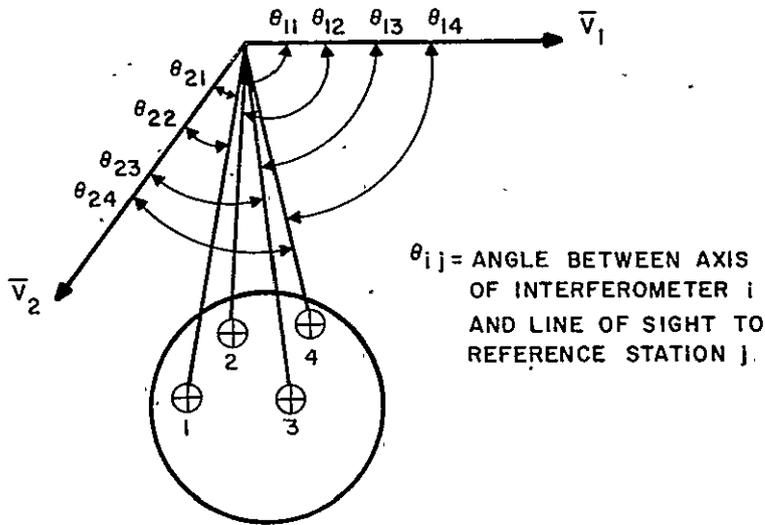
Figure 6.3-11. Attitude Determination Measurements

$$X_{ni} = X'_{ni} \cos \theta - Y'_{ni} \sin \theta$$

$$Y_{ni} = X'_{ni} \sin \theta - Y'_{ni} \cos \theta$$

$$Z_{ni} = Z'_{ni}$$

(X_{ni}, Y_{ni}, Z_{ni}) is the location of the i th reference station in inertial coordinates. The corresponding primed quantities are the known components in the rotating coordinate system. θ is the GHA effective at the time of measurement.

$$\theta = GHA_O + \omega_e t_m$$

Here GHA_O is the hour angle of Greenwich at the beginning of the day, t_m the time of measurement and ω_e the rotation rate of the earth.

The components of the satellite-to-reference-station range vector are obtained from:

$$R_x = X_{ni} - X_s$$

$$R_y = Y_{ni} - Y_s$$

$$R_z = Z_{ni} - Z_s$$

where (X_s, Y_s, Z_s) is the satellite position vector at t_m, calculated by the method of paragraph 6.3.8.3. Next a unit vector $\bar{r}$ is calculated in the direction satellite-to-ground-station.

$$r_x = R_x/D, \qquad r_y = R_y/D, \qquad r_z = R_z/D,$$

$$D = \sqrt{R_x^2 + R_y^2 + R_z^2}$$

Unit vectors are calculated in this manner for the four separate ground reference stations. They are designated $\bar{r}_1, \bar{r}_2, \bar{r}_3$ and $\bar{r}_4$ corresponding to reference stations number 1 through 4. Denoting by $\bar{V}_1$ a unit vector collinear with the base line of interferometer number 1 and by $\cos \theta_n$ the cosine of the angle this vector makes with the vector $\bar{r}_n$, the following relations hold:

$$\bar{V}_1 \cdot \bar{r}_1 = \cos \theta_1$$

$$\bar{V}_1 \cdot \bar{r}_2 = \cos \theta_2$$

$$\bar{V}_1 \cdot \bar{r}_3 = \cos \theta_3$$

$$V_1 \cdot r_4 = \cos \theta_4.$$

The effects of interferometer scale factor A, and delay, D, are assumed to be such that the actual measurement C is of the form

$$C = A (\cos \theta - D)$$

Subtracting the unknown delay from each side of the four equations above, then multiplying them by the unknown scale factor A:

$$A\overline{V}_1 \cdot \overline{r}_1 - AD = C_{11}$$

$$A\overline{V}_1 \cdot \overline{r}_2 - AD = C_{12}$$

$$A\overline{V}_1 \cdot \overline{r}_3 - AD = C_{13}$$

$$A\overline{V}_1 \cdot \overline{r}_4 - AD = C_{14}$$

Here C_{ij} denotes the angle measurement made by interferometer number 1 on the j the reference station. This system of linear equations is solved for the quantities AV_{1x}, AV_{1y}, AV_{1z} and AD. From the first three of these, A is obtained,

$$A = \left[(AV_{ix})^2 + (AV_{iy})^2 + (AV_{iz})^2 \right]^{1/2}$$

The individual components of the unit vector $\overline{V}_1$ follow from

$$V_{1x} = \frac{(AV_{1x})}{A} , \qquad V_{1y} = \frac{(AV_{1y})}{A} , \qquad V_{1z} = \frac{(AV_{1z})}{A}$$

D follows from $D = \frac{(AD)}{A}$

This sequence of calculations is repeated using measurements C_{21}, C_{22}, C_{23}, C_{24} made on interferometer number 2. Direction cosines, scale factors and delays for each interfero-meter are then stored in computer memory for use in the vehicle fix calculations.

6.3.8.5 Calculation of Time of Fix.

The precise time assigned to the navigation fix will be defined as the time of reception of the target vehicle angle CW transmission at the satellite interferometers. Since all precision time measurements will be made at the ground station this fix time must be calculated from such data as the time of receipt of the angle signals at the ground station, the fixed delays in various items of equipment and the transmission time from satellite to ground station.

Let T_m be the time at which the interferometer measurements are received at the ground station. Denote by ΣD_f the sum of all hardware time delays in the satellite and ground station plus any delay within the data message between time mark and actual angle data. The trans-mission time from satellite to ground station, tw, is an unknown since the exact position of the satellite at the time of fix, T_f, is not known.

Subtracting the fixed delays and transmission time from the time of signal reception at the ground station,

$$T_f = T_m - \sum D_f - t_w$$

The satellite position (X_s, Y_s, Z_s) and velocity $(\dot{X}_s, \dot{Y}_s, \dot{Z}_s)$ in inertial coordinates at time $t = T_m - \sum D_f$ are calculated from two known previous positions using Gibb's method; the ground station position (X_g, Y_g, Z_g) is also calculated for this same time.

An expression in terms of these variables represents the range from satellite to ground station at time T_f,

$$(X_s - t_w\dot{X}_s - X_g)^2 + (Y_s - t_w\dot{Y}_s - Y_g)^2 + (Z_s - t_w\dot{Z}_s - Z_g)^2 = (Ct_w)^2$$

Here C is the speed of light. The motion of the ground station due to earth rotation during the time between t and T_f is neglected because it is too small to be of significance.

Expanding and regrouping,

$$(X_s - X_g)^2 + (Y_s - Y_g)^2 + (Z_s - Z_g)^2 - 2 t_w \left[(X_s - X_g) \dot{X}_s + (Y_s - Y_g) \dot{Y}_s + (Z_s - Z_g) \dot{Z}_s \right]$$
$$+ t_w^2 (\dot{X}_s^2 + \dot{Y}_s^2 + \dot{Z}_s^2) = C^2 t_w$$

Rewritten in vector rotation with the satellite position vector being denoted by R_s and the ground station-to-satellite range vector by $\overline{R}$ this equation becomes,

$$\overline{R}^2 - 2 t_w (R \cdot R_s) + t_w^2 R_s^2 = C^2 t_w^2$$

or, when transposed

$$(C^2 - \dot{R}_s^2) t_w^2 + 2t_w \overline{R} \cdot \dot{\overline{R}}_s - \overline{R}^2 = 0$$

The coefficients of this quadratic equation involve quantities which are known or can be calculated; its solution, t_w, is then entered into the equation $T_f = T_m - \sum D_f - t_w$ to yield the effective time of fix T_f.

6.3.8.6 Navigation Fix Calculation.

It is assumed that for each of the two interferometers mounted on the satellite, the inertial direction cosines specifying the orientation of the axis collinear with the base line as well as scale factor and delay are available in computer storage. See figure 6.3-12.

The measurements received from the two interferometers and assumed to be of the form

$$C_1 = A_1 (\cos \theta_1 - D_1)$$

$$C_2 = A_2 (\cos \theta_2 - D_2)$$
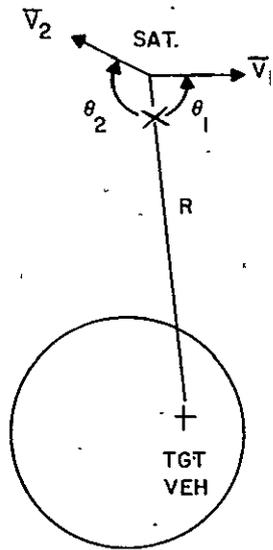
Figure 6.3-12. Navigation Vehicle Fix Measurements

The A's are interferometer scale factors, the D's are time delays and the θ's represent the angles between interferometer baselines and the satellite to vehicle line of sight. The problem is to determine the direction cosines (r_x, r_y, r_z) of the range vector, given the directional orientation of the interferometer axes in inertial space. From the measured and known data, the following equations are set up:

$$V_{1x} r_x + V_{1y} r_y + V_{1z} r_z = \cos\theta_1 = {}^{C_1}/A_1 + D_1$$

$$V_{2x} r_x + V_{2y} r_y + V_{2z} r_z = \cos\theta_2 = {}^{C_2}/A_2 + D_2$$

where (V_{nx}, V_{ny}, V_{nz}) is the set of direction cosines describing the orientation of the effective axis of interferometer n (= 1, 2) at the time of fix. Eliminating r_x from these equations and obtaining r_y in terms of r_z,

$$r_y = K_1 - k_1 r_z$$

Substituting this value of r_y in the first equation, r_x is obtained in terms of r_z.

$$r_x = K_2 - k_2 r_z$$

These values of r_x and r_y are then inserted into the relation

$$r_x^2 + r_y^2 + r_z^2 = 1$$

$$(K_z - k_2 r_z)^2 + (K_1 - k_1 r_z)^2 + r_z^2 = 1$$

$$A r_z^2 - 2B r_z + C = 0$$

where

$$A = 1 + k_1^2 + k_2^2$$

$$B = K_1 k_1 + K_2 k_2$$

$$C = K_1^2 + K_2^2 - 1$$

The roots of this quadratic yield two values of r_z and thus two sets of direction cosines (r_x, r_y, r_z), each of which represents the components of a unit vector. The scalar product of each of these unit vectors with the satellite position vector is calculated; the set of direction cosines yielding a negative product is taken to be the "true" set associated with the satellite to vehicle range vector.

$$r_x R_{sx} + r_y R_{sy} + r_z R_{sz} < 0$$

The measured range to the target vehicle < R is obtained from an independent radar determination. After conversion to units of earth radii, multiplication by the respective direction cosines r_x, etc, will result in the inertial range vector components.

$$R_x = R r_x; R_y = R r_y; R_z = R r_z$$

Components X_n, Y_n, Z_n of the target vehicle position vector at the time of fix are simply the sums of the corresponding satellite position and satellite to vehicle range components.

$$X_n = R_{sx} + R_x$$

$$Y_n = R_{sy} + R_y$$

$$Z_n = R_{sz} + R_z$$

Geocentric latitude of the target vehicle is given by

$$\beta = \tan^{-1}\left[\frac{Z_n}{\sqrt{X_n^2 + y_n^2}}\right]$$

From this geodetic latitude can be obtained as

$$\phi = \tan^{-1} \left[\frac{\tan \beta}{(1 - f)^2} \right]$$

where f is the flattening of the earth.

Inertial longitude (right ascension) of the vehicle is obtained from

$$\chi = \tan^{-1} (X_n, Y_n)$$

where the notation signifies four quadrant determination of the angle

This is converted to geodetic longitude

$$\lambda = \lambda^1 - GHA_o - \omega_e t_f$$

Here GHA_o is the Greenwich hour angle for 0000 hrs. UT on the day of fix; ω_e, the rotational rate of the earth; and t_f, the time of fix. Since altitude is not determined, the fix outputs will be ϕ and λ after conversion from radians to degrees and minutes. The five quantities t_f, ϕ°, ϕ^{min}, λ° and λ^{min} are the final navigation fix outputs.

6.3.8.7 Interferometer Ambiguity Resolution

The inner pair of antennas are separated by 6 wavelengths and constitute a channel for coarse measurements. The output of a counter associated with this channel will be equivalent to ϕ radians of phase difference. The total phase difference is

$$\Phi_i = \phi_i \pm 2n_\pi \qquad n = 0, 1, 2$$

yielding 5 possible values of Φ_i. The outer pair of antennas, constituting the vernier channel, will have its own count equivalent to a phase difference ϕ_v, where $0 \le \phi_v \le 2_\pi$ radians. Total phase difference for the vernier channel will be

$$\Phi_v = \phi_v \pm 2m_\pi \qquad m > n$$

Letting Lv, Li denote the spacing between outer and inner antenna pairs respectively, then

$$\Phi_v = \frac{L_v}{L_i} \Phi_i$$

Of all possible values of Φ_v, 5 will correspond to the possible values of Φ_i multiplied by the ratio L_v/L_i. The remaining problem is that of selecting the correct value of Φ_v.

One possible approach to this problem would utilize an apriori rough estimate of vehicle position, obtained from the traffic control system or by extrapolation from previous position information retained in data memory. The interferometer measurements expected to be received from such a position could be calculated and by comparison therewith, the spurious values associated with ambiguities could be eliminated.

An alternative to be explored involves the computation of position fixes corresponding to the several ambiguities using only angle data and an assumed sphericity of the earth, followed

by elimination of the spurious fixes on the principle that the calculated ranges associated with them would differ appreciably from the measured radar range.

A solution, though undesirable, is to mount a third interferometer having antennas separated by a half wavelength on the satellite. It is recommended that the above two alternatives be more thoroughly investigated before adding the additional weight to the satellite.

<div align="center">

TABLE 6.3-5

E-FRAME COORDINATE EQUATIONS

</div>

1) $P = 5069.4\, a^{3/2}$

2) $M = \dfrac{2\pi}{P}\, (t - t_p)$

3) $M = E - e \sin E$

4) $\sin V = \dfrac{\left(1 - e^2\right)^{1/2} \sin E}{1 - e \cos E}$

5) $\cos V = \dfrac{\cos E - e}{1 - e \cos E}$

6) $R_s = a\,(1 - e \cos E)$

7) $X_s = R_s \left[\cos\Omega n \cos(\omega p + V) - \cos i \sin\Omega n \sin(\omega p + V)\right]$

   $Y_s = R_s \left[\sin\Omega n \cos(\omega p + V) + \cos i \cos\Omega n \sin(\omega p + V)\right]$

   $Z_s = R_s \sin i \sin(\omega p + V)$

P = satellite period seconds

a = semi-major axis

M = mean anomaly

E = eccentric anomaly

e = eccentricity

V = true anomaly

R_s = length of satellite radius vector

X_s, Y_s, Z_s = satellite coordinates in E-frame

6.3.9 Housing and Layout

6.3.9.1 Site Planning.

The ground control station should be situated in the center of several hundred acres of level terrain, free of projecting structures which may interfere with a line of sight path to the horizon. The control building shall be surrounded by at least three tracking antennas.

6.3.9.2 Antenna Spacing

The tracking antennas shall be placed far enough apart and in such a manner as to prevent masking of the satellite signals by each other at elevation angles above 5 degrees. Trees

must be cleared to avoid interference at low angles. For the same reason any commercial power lines shall be placed underground as they approach the control building.

6.3.9.3 Control Building

The control building may be considered as being made up of three areas. One area will contain heating, power and utility equipment for the control building and the outlaying tracking antennas. Another area will contain the communications terminal equipment which will link the control station with traffic control, and other control stations. The third area will contain the ground station control consoles, antenna pointing computers, and other computing and buffering equipment necessary to formulate outgoing messages and process incoming messages.

6.3.9.4 Air Conditioning and Heating

Neither the equipment nor personnel heating, cooling, or humidity control are expected to present much of a problem. Electronic equipment operates very efficiently in a stabilized ambient of 60 degrees to 85 degrees F. and low humidity. Most people are comfortable at about 72 degrees F. and 50 percent relative humidity.

6.3.10 Ground Station Power

6.3.10.1 Requirements

The power requirements of the ground station will be divided into three classes:

a. Primary Essential Services

b. Secondary Essential Services

c. Utility Power

The primary essential services consist of items such as:

a. Computers

b. Buffers

c. Receivers

d. Transmitters

e. Tracking Antennas

f. Emergency Lighting

The secondary essential services consist of items such as:

a. Radome Blowers

b. Equipment Air Conditioners

c. Equipment Heating

Utility Power consists of items such as:

a. Regular Lighting

b. Personnel Comfort Air Conditioning or Heating

c. General Housekeeping Power.

For the primary essential service to each of the three radomes, commercial power of 480 volts, 3 phase, four wire will be used. The backup to commercial power will be a

150 KW to 300 KW No-Break Emergency Power Generating Set (described in a subsequent section) for each of the three radomes, and a 50 KW No-Break Emergency Unit for the computer building. Any interruption of this power is intolerable, therefore, the system recommended will provide for no interruption of operation regardless of failures of commercial power.

The secondary essential services are those for which an interruption of prime power is tolerable for a period of up to 10 minutes, but not desirable. For this service, manual start generators will be used as a back-up to commercial power except where time is a critical function, such as power for the radome blowers. In this case, an automatic starting unit which will respond to either or both an undervoltage or under frequency will be used. Since the probability of human error is greatest during the first few minutes of an emergency, this system is designed to perform all time-critical functions automatically.

The utility service will also be provided with a back-up of manual start generators and a primary service of commercial power.

To protect such items as the computers and data circuits from input voltage fluctuations, an induction regulator will be used to regulate AC power to the receivers, transmitters, computers and data processing equipment. The induction regulator will be designed to compress any voltage variation between ±50 percent to ±1.5 percent of nominal voltage.

For the secondary essential services and utility power, under voltage relays will cause the primary line circuit breakers to open and the emergency breakers to close. Audible and visible alarms powered from batteries will sound when a power failure occurs. When commercial power reaches 95 percent of normal, a transfer back to commercial power will be implemented automatically after a preset delay.

6.3.10.2 No-Break Emergency Power Generator Set

The generating set will consist of a diesel engine coupled through a heavy-duty induction clutch to a flywheel, induction motor and brushless generator. All rotating components will be connected by flexible couplings.

During normal operation, the electric motor receives power from the incoming commercial power source and drives the inertia flywheel and generator at a constant speed. The generator will feed the critical load of preferred power distribution panel. There will be no electrical connection between utility power and the critical load. In the event of commercial power failure, or dip in voltage, below 90 percent of normal value, controls will function to disconnect the electric motor from the commercial source; and the induction clutch is energized connecting the engine driveshaft to the inertia flywheel. The energy of the rotating flywheel shall instantly crank and start the engine, and the engine, and the engine shall then drive the generator with no interruption in the voltage supplied to the load.

Generator voltage shall be maintained within plus or minus 2 percent of normal output voltage during normal power service, during any fault condition, during any automatic transition period, and during diesel operation.

The generator shall maintain at all times a frequency of 60 cycles per second within plus or minus 1.0 cycle per second during operation from the electric motor or diesel engine. During transition from diesel engine to electric motor or vice versa, frequency dip shall not exceed 2.0 cycles per second.

6.3.10.3 Switchgear

Switchgear will be selected from standard commercial switchgear with conservative application. All lines will be protected with circuit breakers and all motor loads will be handled with standard line contactors and breakers. Sufficient indicators and voltage and frequency measuring devices coupled with audible and visible alarm and warning devices will be used to reduce the chance of human error to a minimum.

6.4 REFERENCE STATION

6.4.1 Introduction

This section of the report discusses the reference station each of which contains a transponder placed at a specific known point on the earth's surface to serve as a reference point for calibrating the interferometer attitude of the Navigation Satellite. These stations will make it possible to determine satellite orbital data when the system becomes operational. For worldwide coverage, approximately twenty four stations, strategically located, will be required. There will be no need for these stations to be manned, since adequate redundancy and automatic substitution techniques will be employed to assure maximum reliability.

6.4.2 Equipment

The equipment used in the reference stations will be a re-packaged version of the vehicle transponder. Figure 6.4-1 is a simplified block diagram of the station. The components used will be identical to those for the user vehicle, except that the "L" band antenna will be a tracking type of antenna, rather than omni-directional. The data processing and display equipment of the user vehicle will be deleted, since only identification coding and gating capabilities will be required for the transponder operation.

6.4.3 Antenna

For the simplest, least expensive installations, the reference station antenna(s) will be the same omni-directional antenna(s) employed on the vehicle (Section 6.2.2). However, to increase the accuracy of system calibration for the special users (6.2.2.3) the gain of the "L" band antenna can be improved by approximately 10 db. There are two possible approaches to improving the antenna gain, both of which tend to increase the cost of the reference station.

6.4.3.1 Conventional Tracking

The simpler approach to increased accuracy is the use of small tracking dishes (approx. 2 ft. diam.) with very coarse pointing data which is transmitted to the station by the VHF data channel and received via an omni-directional antenna. Since the beamwidth of a 2 foot antenna at "L" band frequencies is about 40 degrees, continuous tracking data will not be required. The hemisphere surrounding the station can be divided into approximately 20 sectors, wherein the gain of the antenna will equal or exceed 10 db, and the antenna drive can be made to track in increments corresponding to these sectors. The ground station, upon acquisition of a satellite, can then compute the appropriate sector for the reference stations in its coverage area and transmit this information in coded form to each station. The segment data will be updated three to five times during each satellite pass, and 26 bits of data will be used each time this function is performed.

6.4.3.2 Electronic Scanning

Recently, a new approach to eliminate the problem of mechanically tracking a directive antenna on interplanetary spacecraft has been advanced. It consists of a planar array of radiating elements which are triggered by an approaching signal in such a phase relationship
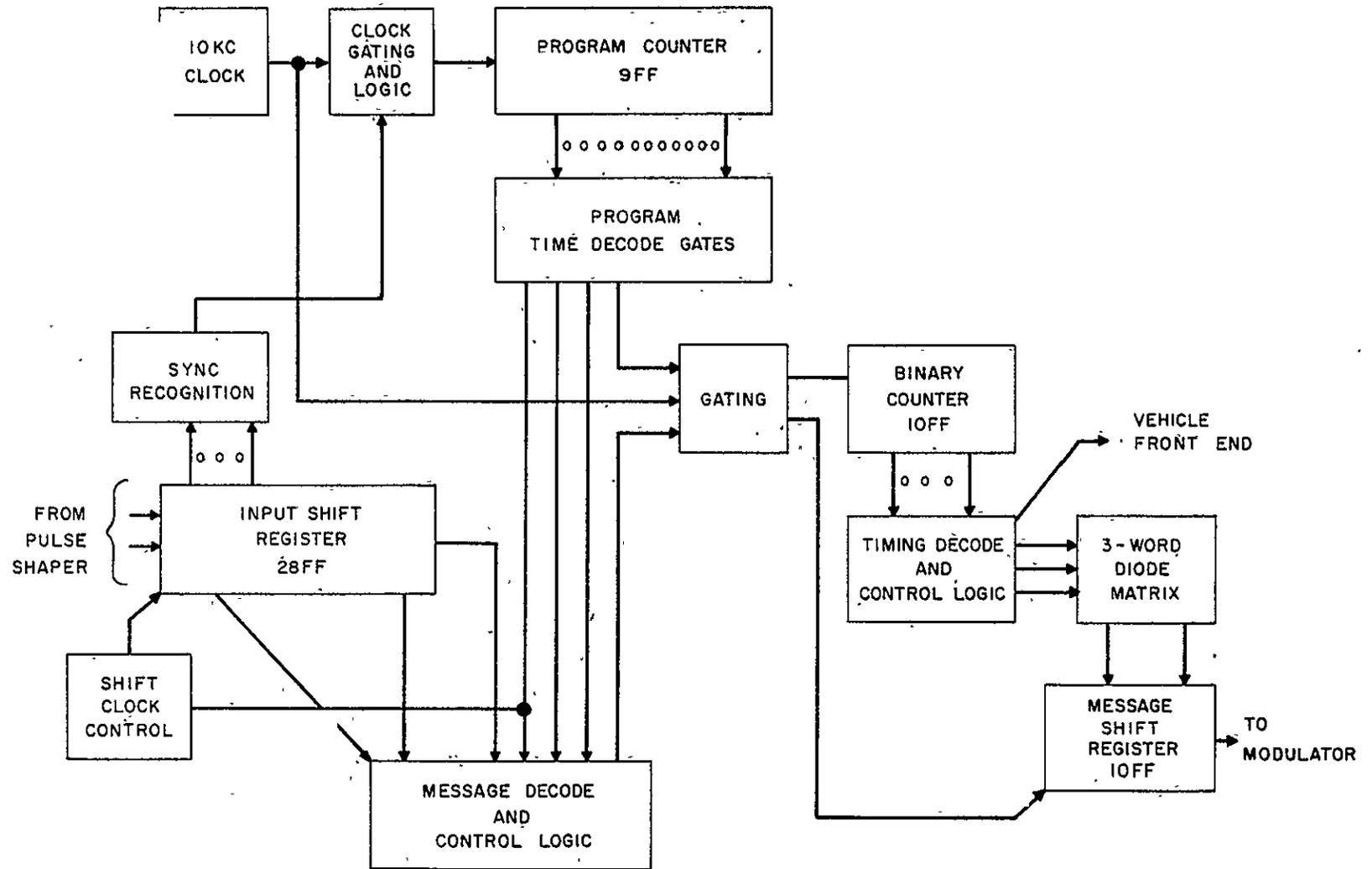
Figure 6.4-1. Station Simplified Block Diagram.

that sensitivity, oriented in the direction of the arriving signal results. This concept can be applied to the reference station; however considerable development will be required to provide hemispherical coverage. Its cost, compared to the conventional tracking system described above will be high, but it will afford the advantage of eliminating moving parts, and consequently will not require as much computer capacity, data channel capacity and data processing in equipment at the reference station as that needed for conventional tracking antennas.

6.4.4 Transponder Repeater

The transponder repeater will be identical to that of the transponder receiver described (in paragraph 6.2.3) for the user vehicle equipment. The reference station transponder repeater will operate at a higher signal to noise ratio than user vehicle equipment, due to the use of high gain reference station antennas. The packaging of the reference station equipment will be somewhat different from that of the vehicle. However, to take advantage of mass production economy, the same units that are produced for the user vehicle equipment (such as the IF strips, the mixers, and the circulators) will be used for both types of equipment.

6.4.5 Data Processor

The functions which will be performed by the Data Processor are:

a. To receive and decode incoming message at the required bit rate.

b. To format the reference station identification code.

The equipment needed to perform these functions are shown in Figure 6.4-2.
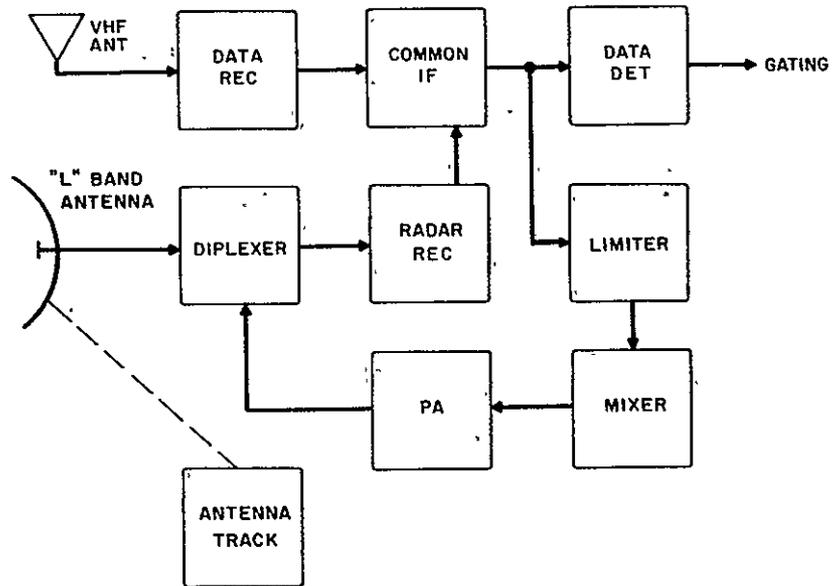
Figure 6.4-2. Reference Station Equipment.

6.4.5.1 The Reception and Decoding of Incoming Messages.

Information received from the pulse shaper is serially read into the input Shift Register. When sync recognition occurs, the clock gating and control logic permits a pulse train to

drive the program counter and to act as the shift clock for the input shift register. This shifting of the ISR is continual throughout the message. ISR decoding gates in the message decoder and control logic are time gated by outputs from the program time decode gates to provide a source of control signals for the control logic. The output of the last flip-flop in the ISR is coupled through logic channels to the area processor at selected times.

6.4.5.2 Reference Station Identification Code Message Formation

Generation of an identification code is initiated by a program time decode gate which permits a 10 KC clock to trigger a 10 flip flop Binary Counter. The time gates generated by the timing decode and control logic govern the inputs to the message shift register, and the switching controls for the RF front end of the user vehicle equipment. The different bit rates of incoming and outgoing messages prevents utilization of logic for more than one message rate. The necessity of understanding all parts of the incoming message also precludes the sharing of logic.

The output of the message shift register goes to the modulator.

6.4.6 Power Supply

The power supplies for the reference station will be the same as those for the user vehicle. Although less power is consumed by the reference station equipment than is needed for the user vehicle equipment, the power requirement differential is not sufficient to justify the expense of designing separate power supply units for the two facilities.

6.4.7 Reference Station Housing

6.4.7.1 Location

All reference station sites shall be selected in areas which are protected from present and/or anticipated sources of rf interference (paragraph 6.3.9.1).

Each ground control station will house one reference station. Wherever possible, additional reference stations will be housed by cooperating universities, research centers, and similar institutions. Such institutions will consequently have an ideal opportunity to conduct earth-space rf propagation research experiments.

When necessary, a reference station can be housed in a remote area, and will be completely automated, although it will include the necessary accommodations to logistically support a maintenance crew.

6.4.7.2 Weather Protection

In order to achieve the maximum degree of reliability, the electronic equipment in each reference station will be protected from extremes of temperature and humidity. No special construction technique will be required to accomplish this.

6.4.7.3 Size

An 8' x 10' area will provide enough floor space to accommodate the operational and service equipment required by each reference station.

7. SYSTEM DESIGN INTEGRATION

7.1 NUMBER AND DISTRIBUTION OF GROUND STATIONS

This section lists three proposed ground station groupings arranged in an optimum octahedral distribution. Absolute requirements in site location are: a. land areas (excluding the polar regions) and b. 100% world coverage. Requirements recognized as desirable but not absolute are: a. large, non-remote land areas, b. one, at minimum, in the U.S.A. and c. none in the USSR or China.

Locations were based on a radius of coverage for satellite altitudes of 6000 nmi and a minimum elevation angle of 5°. Optimum and non-optimum station groupings other than those listed below are assumed to exist.

PROPOSED LOCATIONS

Group A	Group B	Group C
Argentina	Ecuador	Japan
Aral Sea Region/USSR	Nova Scotia	Kerguelen Islands/ France
Virginia/USA	India	Tahiti
Naysaland	New Zealand	Paraguay
Hawaii	South Africa	Virginia/USA
Australia	Midway Islands	Sudan

Group A has the unique advantage of two locations on US soil but includes one USSR location. Group B excludes both the USA and USSR. Other six station groups proved similar to Group C where small remote island areas make site location questionable. The method used to indicate possible site locations was crude but time saving. Use was made of the equation (from Appendix B)

$$\frac{h + R_o}{R_o} = \frac{\cos E}{\cos (d_o + E)}$$

where
E = minimum station elevation angle
h = altitude
R_o = earth's radius
d_o = great circle radius of satellite coverage

for
$h = 6,000$ nmi
$R_o = 3,440$ nmi
$E = 5°$

$d_o = 63.7°$

Six wire circles were constructed of radius d and mounted on a world globe. The circles were loosely joined together, as shown in figure 7-1 using string, such that no manipulation would reduce any triple overlap area to zero. This guaranteed 100% world coverage. The six circles were then manipulated over the globe until land areas appeared at the centers of each circle. These land areas then became station locations.
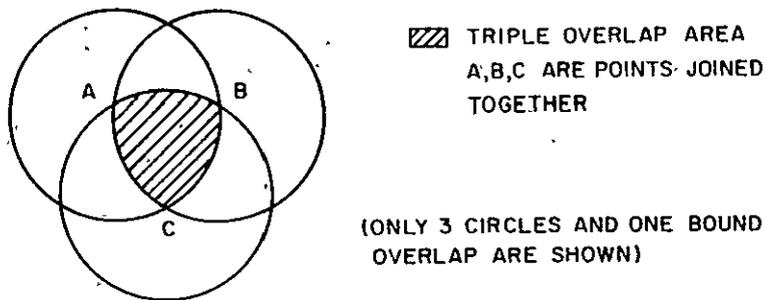
Figure 7-1. Ground Station Location

7.2 FREQUENCY ALLOCATIONS

7.2.1 General Requirements

The Navigation Satellite System described in this report requires several worldwide frequency allocations in the VHF and UHF bands to provide channels for the operational radar, data and maintenance telemetering and developmental tracking, and telecommand and telemetering. Specifically, the following links are required:

Channel	From	To	Functions
		Operational	
1	Ground Control	Satellite	(1) Radar Ranging (2) Data
2	Satellite	Vehicle	Data
3a	Vehicle	Satellite	(1) Radar Ranging & Angle (2) Data
3b	Vehicle	Satellite	Data
4	Satellite	Ground Control	(1) Radar Ranging & Angle (2) Data
5	Satellite	Vehicle	Radar Ranging
		Developmental	
6	Tracking Net	Satellite	(1) RARR* Tracking (2) Telecommand
7	Satellite	Tracking Net	(1) RARR[1] Tracking (2) Autotrack (3) Telemetry

The description of the specified channels are as follows:

a. Channel 1. This link shall utilize a high gain ground-tracking-antenna and under suitable regulations, this channel can be shared with other terrestial and perhaps, space services. Since this link carries the radar ranging pulses, it must be above about 800 to 900 MC to avoid a serious range error due to ionospheric refraction. The upper frequency limit is not critical and can be as high as 7 GC before propagation medium limitations occur. But, hardware availability and economy indicate an upper limit of about 3 GC is more desirable.

b. Channel 2. Only data is carried by this link, therefore; ionospheric refraction does not preclude lower frequency operation. In fact, since the satellite and vehicle antennas are wide beamwidth with their gain effectively constant with frequency, it is necessary to operate this channel as low as possible to minimize satellite power. However; below about 100 MC, extraterrestial galactic noise rises to a level that the satellite power requirements again begin to rise. Since this channel uses wide coverage antennas on both the satellite and vehicle, it is required that the channel be a world-wide clear channel and not shared with other services to avoid mutual interference problems.

c. Channel 3. Since this channel carries radar ranging and angle pulses, the lowest feasible frequency as described for channel 1 is in the order of 800 to 900 MC. However, it also employs wide beamwidth antennas, similar to Channel 2, which causes the transmitter power on the vehicle to increase as the square of the frequency. Thus, little latitude of choice is available and the optimum frequency is in the vicinity of 900 to 1100 MC. A secondary choice would be for the frequency to go as high as 1500 to 1600 MC realizing, that more than twice the vehicle power would be required. Again this channel, the same as channel 2, cannot be shared with other services.

d. Channel 4. The "down-link" from the satellite to the ground control station carries all the radar range and angle information as well as data relayed from the vehicle. The frequency for this link is required to be between 800 MC and 3 GC for the same reasons as described for channel 1. It also can be shared with other terrestial services under suitable regulations since a highly directive ground antenna is employed.

e. Channel 5. This channel is similar to channel 2 since it employs wide coverage antennas and thus shall use the lowest possible frequency to conserve satellite power. However, it carries radar range pulses and therefore, shall operate above 800 to 900 MC. For the same reasons as channel 3, there is little choice of frequency other than about 900-1100 MC. Operation at 1500 to 1600 MC would impose high power requirements on the satellite. Again, this frequency is required to be an exclusive world wide allocation.

f. Channel 6 and 7. Four channels are required for the Developmental (or pre-operational phase of the program. The precision tracking requirements for orbit injection require the use of the Goddard Range and Range Rate System which operates on the 136-137, 148.25, 1700-1710, and 2271 MC space research frequencies.

7.2.2 Available Allocations

The conference called by the International Telecommunications Union (ITU) in Geneva in October 1963, resulted in the allocation of frequencies for various space services including radio navigation for satellite and space research. These allocations become effective on 1 January 1965 with additional time (extending to 1 January 1970 in some cases) for various administrations to re-allocate certain other services presently operating in the specified bands. The only applicable operational allocations made by the ITU for the Radio Navigational Service are shown in Table 7-1. These frequencies can be shared by maritime, aeronautical and land mobile services. Only the 149.9 - 150.05 MC band has the possibility of technically satisfying the needs of the system under study. Even this frequency has certain disadvantages: a. it requires approximately 3 db more satellite power than the 110 MC frequency currently assumed and b. it would require sharing the band with an existing navigation satellite system.

TABLE 7-1

RADIO NAVIGATION-SATELLITE SERVICE

(Maritime, Aeronautical, Land Mobile Services)

149.9 - 150.05 MC	Cessation date for fixed and mobile
	services in these bands is 1 January
399.9 - 400.05 MC	1969 except in a number of European
14.3 - 14.4 GC	countries and Cuba.

It can be seen that there is no suitable frequency allocated for the radar system since it is required that the system operate at a frequency of about 1 GC or compromise satellite and vehicle power with ionospheric refraction errors.

Lacking suitable operational frequencies in the present allocations, the system requirements for a set of worldwide frequencies to be shared by maritime, aeronautical, and land mobile services shall be found by considering frequencies allocated to other services and looking to the next Plenary Conference in 1966 as an opportunity to define and request frequencies suitable to the navigation satellite. The presently allocated space frequencies are not considered inflexible, and future ITU conferences will undoubtedly offer opportunities to make revisions commensurate with the advances in the state of the art and needs of the moment.

Tentatively, the frequencies chosen to exemplify the system design concepts contained in this document are as acceptable as any other frequencies for the purpose. The impact of using other frequencies, as a result of official allocation problems, are discussed in this section and in other pertinent sections of this report.

7.2.3 Aeronautical Services

Table 7-2 shows the frequencies applicable to an operational Radio Navigation Satellite System used exclusively by the Aeronautical Services. The 1540-1660 MC band can be used for the radar system with two major disadvantages. First, it would require approximately twice the power in the satellite transmitter and the vehicle transponder than the approximate 1 GC frequency; and second, the transmitting tubes on the vehicle can no longer be an inexpensive tetrode.

TABLE 7-2

AERONAUTICAL RADIO NAVIGATION SERVICE

(EXCLUSIVELY AERONAUTICAL-SPACE)

1540 - 1660 MC	These bands are reserved on a worldwide basis for the development of airborne electronic aids to air naviga-
4200 - 4400 MC	tion and any directly associated ground based or satellite
5000 - 5250 MC	borne facilities. They are also allocated to the aero-
15.4 - 15.7 GC	nautical mobile (R) service for the use and development of systems using space communication techniques.

The data link can use the frequencies designated in Table 7-3 and are entirely suitable for the system.

TABLE 7-3

AERONAUTICAL MOBILE (R) SERVICE

(EXCLUSIVELY AERONAUTICAL-SPACE)

117.975 - 132 MC	This band is currently in use on a worldwide basis for aeronautical mobile (R) service.
132 - 136 MC	This band has been further authorized (1963) for the use and development for this service of systems using space communication techniques. It is initially limited to satellite relay stations of the aeronautical mobile (R) service.

In addition to tables 7-2 and 7-3 which open to space systems, the allocations in
table 7-4 are also for exclusive aeronautical use but are restricted to non-space systems.
The frequencies currently under study in the program lie within these allocations for both the
data and the radar systems. It is possible, that specific frequencies suitable to the system
can be negotiated within these bands at some future conference. The frequencies of 149.0 -
150.05 and 399.9 - 400.05 MC were allocated to the radio navigation satellite service in the
1963 Conference had originally belonged to other services when the AN/BRN-3 system was
originally proposed several years ago. Since the Aeronautical Services will be an outstanding
beneficiary of the system, it may not be difficult to open the specific frequencies required to
system operation.

TABLE 7-4
ON-SPACE AERONAUTICAL SERVICES
(EXCLUSIVELY AERONAUTICAL)

108 - 117.975 MC	Aeronautical radio navigation (worldwide)
138 - 143.6 MC	Aeronautical mobile (region 1; fixed, mobile and radio location in regions 2 and 3)
960 - 1215 MC	Aeronautical radio navigation (worldwide)
1300 - 1350 MC	These bands are restricted by the Aeronautical Radio Navigation Service to the use of ground-based radars and associated airborne transponders that transmit only in this band and only when actuated by radars in the band.

7.2.4 Space and Space Research Services

Table 7-5 shows a number of allocations designated for the space and space research
services. Particularly, the 136 - 138 MC band can be used for the data and the 900 - 960 MC
band can be used for the radar system with little change from the current system concepts and
parameters under study. In addition, the 143.6 - 143.65 MC and 1427 - 1429 MC (or 1525 -
1535 MC) can similarly be used with the disadvantage previously discussed for similar
frequencies in paragraph 7.2.3.

TABLE 7-5

SPACE SERVICE - SPACE RESEARCH SERVICE

136 - 138 MC	Space research (telemetering and tracking) band and is shared with fixed and mobile services in regions 1 and 3. The space, space research (telemetering and tracking) is to be used mainly for research concerning the establishment, technical improvement, and maintenance of operational space system. This band is shared with other services in Australia and parts of Europe, Africa, and the Far East.
143.6 - 143.65 MC	Space Research (telemetering and tracking) band and is shared with other services in all three regions of the world.
267 - 273 MC	Space (telemetering and tracking) band and is shared with fixed and mobile services in all three regions of the world.
400.05 - 401 MC	Space Research (telemetering and tracking) band and is shared with meterological aids and meterological - satellite services in all regions and with other services in parts of Europe and United Kingdom.
401 - 402 MC	Space (telemetering and tracking) band and is shared with meterological aids services in all regions and fixed and mobile services in some parts of the world.
900 - 960 MC	Specific portions of this band can be used on a secondary basis for experimental purposes and space research. The primary allocated services in each region are varied.
1427 - 1429 MC	Space (telecommand) band and is shared with fixed and mobile services in all three regions of the world.
1525 - 1535 MC	Space (telemetering and tracking) band and is shared with fixed and mobile services in various parts of the world.

APPLICATION FOR RADIO FREQUENCY AUTHORIZATION

	1. DATE OF PREPARATION
	1/7/64

2. SECURITY CLASSIFICATION OF FREQUENCY AS ASSIGNED	3. CONTRACT NO.	4. PROJECT NAME/NO.
Unclassified	NASw-785	Navigation Satellite System

5. FREQUENCY REQUIRED (Kc/s) (Mc/s) (Gc/s)	A. BANDWIDTH (Kc/s) & EMISSION
Between 900 and 1215 Mc/s	250 Kc/s (incl. guard band) P-9

B. PEAK PULSE POWER	C. AVERAGE POWER
50 watts (nominal)	Variable 5 to 50 watts

D. PULSE DURATIONS (Microseconds)	E. PULSE RECURRENCE RATE
Variable to approx. 80,000	Variable - 9 to 49 per second

F. RANGE IN NAUTICAL MILES	G. HOURS OF OPERATION
8500	Unlimited

H. CALL SIGN REQUIREMENT	I. CATEGORY OF STATION
--	Radio navigation (fixed)

6. TYPE OF ANTENNA	A. DIRECTIVITY OF ANTENNA	B. BEAMWIDTH OF AZIMUTH	C. BEAMWIDTH IN ELEVATION
Reflector	Conical Beam	Approx. 1°	Approx. 1°

7. TRANSMITTER NOMENCLATURE	A. TUNABLE FREQUENCY RANGE OF TRANSMITTER	B. METHOD OF FREQUENCY CONTROL
Developmental	To be determined	Precision Standard

8. TRANSMITTER LOCATIONS

A. FIXED	(1) NO. TO BE EMPLOYED	(2) LOCATION (Names of nearest cities and geographical coordinates-to nearest minute.)
	6 (max)	To be determined

B. MOBILE	(1) NO. TO BE EMPLOYED	(2) AREA (Enter the radius in miles with respect to a fixed geographical coordinates.)
	None	--

C. AIRBORNE AND/OR SPACE	(1) NO. TO BE EMPLOYED	(2) ALTITUDE AND AREA (Include type of operation, i.e. air to air, air to ground, space to ground, etc.)
	None	--

9. JUSTIFICATION, EXPLANATION AND REMARKS. *THIS IS THE MOST IMPORTANT SINGLE ITEM IN THIS APPLICATION.* (Explain why this particular Frequency or Band is necessary and why an existing assignment cannot be shared. Continue on additional sheet(s) of 8x10½" paper.)

This channel will utilize a high gain ground tracking antenna and under suitable regulations could be shared with other terrestial and perhaps space services. Since this channel carries the radar ranging pulses, it must be above about 900 Mc to avoid serious range error due to ionospheric refraction. The upper frequency limit is not critical and might be as high as 7 G_c before propagation medium limitations occur except that hardware availability and economy indicate an upper limit of about 3 G_c is more desirable.

10. TYPED NAME OF CONTRACTOR REPRESENTATIVE	A. ADDRESS

11 TYPED NAME OF NASA REPRESENTATIVE	A. ADDRESS

12. SIGNATURE OF AUTHORIZED NASA PROJECT MANAGER	A. OFFICE CODE	B. ADDRESS

13. DATE AND LENGTH OF TIME REQUIRED	14. IDENTITY NO.	15. SIGNATURE OF AREA FREQUENCY COORDINATOR

16. TYPED NAME OF NASA FIELD INSTALLATION FREQUENCY MANAGER RESPONSIBLE FOR ALL ENTRIES ON THIS APPLICATION	A. SIGNATURE OF RESPONSIBLE FREQUENCY MANAGER

B NASA INSTALLATION FREQUENCY MANAGERS THROUGH WHOM APPLICATION IS ROUTED.	
(1) NAME	(2) NAME

NASA FORM 566 AUG 61

Figure 7-2. Application for Frequency Authorization. Channel 1

APPLICATION FOR RADIO FREQUENCY AUTHORIZATION	1. DATE OF PREPARATION 1/7/64

2. SECURITY CLASSIFICATION OF FREQUENCY AS ASSIGNED Unclassified	3. CONTRACT NO. NASw-785	4. PROJECT NAME/NO. Navigation Satellite System

5. FREQUENCY REQUIRED *(Kc/s) (Mc/s) (Gc/s)* Between 108 and 136 Mc/s	A. BANDWIDTH *(Kc/s)* & EMISSION 15 Kc (incl. guard band) P-9 .

B. PEAK PULSE POWER 75 w (nominal)	C. AVERAGE POWER Variable 2 to 75 watts

D. PULSE DURATIONS *(Microseconds)* Variable to approx. 80,000	E. PULSE RECURRENCE RATE Variable - 6 to 22 per second

F. RANGE IN NAUTICAL MILES 8500	G. HOURS OF OPERATION Unlimited

H. CALL SIGN REQUIREMENT --	I. CATEGORY OF STATION Radio Navigation (Space)

6. TYPE OF ANTENNA Conical Spiral	A. DIRECTIVITY OF ANTENNA Conical Beam	B. BEAMWIDTH OF AZIMUTH Approx. 60°	C. BEAMWIDTH IN ELEVATION Approx. 60°

7. TRANSMITTER NOMENCLATURE Developmental	A. TUNABLE FREQUENCY RANGE OF TRANSMITTER Fixed	B. METHOD OF FREQUENCY CONTROL AFC/Precision Std.

8. TRANSMITTER LOCATIONS

	(1) NO. TO BE EMPLOYED	(2) LOCATION *(Names of nearest cities and geographical coordinates to nearest minute.)*
A. FIXED	None	

	(1) NO. TO BE EMPLOYED	(2) AREA *(Enter the radius in miles with respect to a fixed geographical coordinates)*
B. MOBILE	None	

	(1) NO. TO BE EMPLOYED	(2) ALTITUDE AND AREA *(Include type of operation, i.e. air to air, air to ground, space to ground, etc.)*
AIRBORNE c. AND/OR SPACE	8	6000 nmi altitude -- Space to Mobile

9. JUSTIFICATION, EXPLANATION AND REMARKS. *THIS IS THE MOST IMPORTANT SINGLE ITEM IN THIS APPLICATION. (Explain why this particular Frequency or Band is necessary and why an existing assignment cannot be shared. Continue on additional sheet(s) of 8x10½" paper.)*

Only data is carried by this channel, therefore ionospheric refraction does not preclude operation in the VMF band. In fact, since the satellite and vehicle antennas are wide beamwidth with gain effectively constant with frequency, it is necessary to operate this channel as low as possible to minimize satellite power. However, below about 100 M_c extraterrestial galactic noise rises at such a rate that the satellite power requirements begin to rise. Since this channel uses wide coverage antennas on both the satellite and vehicle, it must be a world-wide clear channel, not shared with other services, to avoid mutual interference problems.

10. TYPED NAME OF CONTRACTOR REPRESENTATIVE	A. ADDRESS	
11. TYPED NAME OF NASA REPRESENTATIVE	A. ADDRESS	
12. SIGNATURE OF AUTHORIZED NASA PROJECT MANAGER	A. OFFICE CODE	B. ADDRESS
13. DATE AND LENGTH OF TIME REQUIRED	14. IDENTITY NO.	15. SIGNATURE OF AREA FREQUENCY COORDINATOR
16. TYPED NAME OF NASA FIELD INSTALLATION FREQUENCY MANAGER RESPONSIBLE FOR ALL ENTRIES ON THIS APPLICATION	A. SIGNATURE OF RESPONSIBLE FREQUENCY MANAGER	

B. NASA INSTALLATION FREQUENCY MANAGERS THROUGH WHOM APPLICATION IS ROUTED.	
(1) NAME	(2) NAME

NASA FORM 566 AUG 61

Figure 7-3. Application for Frequency Authorization, Channel 2

APPLICATION FOR RADIO FREQUENCY AUTHORIZATION		1. DATE OF PREPARATION 1/7/64	
2. SECURITY CLASSIFICATION OF FREQUENCY AS ASSIGNED Unclassified		**3. CONTRACT NO.** NASw-785	**4. PROJECT NAME/NO.** Navigation Satellite System
5. FREQUENCY REQUIRED (Kc/s) (Mc/s) (Gc/s) Between 900 and 1215 Mc/s		**A. BANDWIDTH (Kc/s) & EMISSION** 250 K_0 (incl. offset & guard band) P-9	
B PEAK PULSE POWER 3.6 KW Nominal		**C. AVERAGE POWER** Variable 12 to 35 watts	
D. PULSE DURATIONS (Microseconds) 3400 or 9600		**E. PULSE RECURRENCE RATE** One per second (per transmitter)	
F. RANGE IN NAUTICAL MILES 8500		**G. HOURS OF OPERATION** Unlimited	
H. CALL SIGN REQUIREMENT --		**I. CATEGORY OF STATION** Radio Navigation (Mobile & fixed)	

6 TYPE OF ANTENNA	A. DIRECTIVITY OF ANTENNA	B. BEAMWIDTH OF AZIMUTH	C. BEAMWIDTH IN ELEVATION
To be determined	Hemispherical	360°	Approx. 180°

7. TRANSMITTER NOMENCLATURE	A. TUNABLE FREQUENCY RANGE OF TRANSMITTER	B. METHOD OF FREQUENCY CONTROL
·Developmental	To be determined	AFC/Crystal Ref.

8.		TRANSMITTER LOCATIONS	
A. FIXED	**(1) NO. TO BE EMPLOYED** Approx. 24	**(2) LOCATION** *(Names of nearest cities and geographical coordinates to nearest minute.)* To be determined (worldwide)	
B. MOBILE	**(1) NO. TO BE EMPLOYED** Unlimited	**(2) AREA** *(Enter the radius in miles with respect to a fixed geographical coordinates.)* Worldwide	
AIRBORNE C. AND/OR SPACE	**(1) NO. TO BE EMPLOYED** None	**(2) ALTITUDE AND AREA** *(Include type of operation, i.e. air to air, air to ground, space to ground, etc.)*	

9. JUSTIFICATION, EXPLANATION AND REMARKS. *THIS IS THE MOST IMPORTANT SINGLE ITEM IN THIS APPLICATION.* *(Explain why this particular Frequency or Band is necessary and why an existing assignment cannot be shared. Continue on additional sheet(s) of 8x10½" paper.)*

The channel carries radar ranging and angle pulses, in addition to a limited amount of data. Therefore, the lowest feasible frequency is in the order of 900 Mc to avoid serious range error due to ionospheric refraction. However, it employs wide beamwidth antennas on both the satellite and vehicle which causes the transmitter power on the vehicle to increase as the square of the frequency. Thus, little latitude of choice is available and the optimum frequency is in the vicinity of 900 to 1215 M_c. A secondary choice would be in the vicinity of 1500 to 1600 M_c realizing that more than twice the vehicle power would be required. This·channel cannot be shared with other services due to use of essentially non-directional antennas.

10. TYPED NAME OF CONTRACTOR REPRESENTATIVE	A. ADDRESS	
11. TYPED NAME OF NASA REPRESENTATIVE	A. ADDRESS	
12. SIGNATURE OF AUTHORIZED NASA PROJECT MANAGER	A. OFFICE CODE	B. ADDRESS

13. DATE AND LENGTH OF TIME REQUIRED	14. IDENTITY NO.	15. SIGNATURE OF AREA FREQUENCY COORDINATOR
16. TYPED NAME OF NASA FIELD INSTALLATION FREQUENCY MANAGER RESPONSIBLE FOR ALL ENTRIES ON THIS APPLICATION		A. SIGNATURE OF RESPONSIBLE FREQUENCY MANAGER

B. NASA INSTALLATION FREQUENCY MANAGERS THROUGH WHOM APPLICATION IS ROUTED.	
(1) NAME	(2) NAME

NASA FORM 566 AUG 61

Figure 7-4. Application for Frequency Authorization, Channel 3

APPLICATION FOR RADIO FREQUENCY AUTHORIZATION	1. DATE OF PREPARATION 1/7/64

2. SECURITY CLASSIFICATION OF FREQUENCY AS ASSIGNED Unclassified	3. CONTRACT NO. NASw-785	4. PROJECT NAME/NO. Navigation Satellite System.

5. FREQUENCY REQUIRED *(Kc/s) (Mc/s) (Gc/s)* Between 900 and 1215 Mc/s	A. BANDWIDTH *(Kc/s)* & EMISSION 250 Kc/s (incl. offset & guard band) P-.9

B. PEAK·PULSE POWER 2 watts	C. AVERAGE POWER Variable 50 to 200 mW

D. PULSE DURATIONS *(Microseconds)* 3400 or 9600	E. PULSE RECURRENCE RATE Variable 5 to 13 per second

F. RANGE IN NAUTICAL MILES 8500	G. HOURS OF OPERATION Unlimited

H CALL SIGN REQUIREMENT --	I. CATEGORY OF STATION Radio Navigation (Space)

6. TYPE OF ANTENNA Phased Array	A. DIRECTIVITY OF ANTENNA Conical Beam	B. BEAMWIDTH OF AZIMUTH Approx. 60.$^{\circ}$	C. BEAMWIDTH IN ELEVATION Approx. 60°

7. TRANSMITTER NOMENCLATURE Developmental	A. TUNABLE FREQUENCY RANGE OF TRANSMITTER Fixed	B. METHOD OF FREQUENCY CONTROL AFC/Precision Std.

8. TRANSMITTER LOCATIONS

	(1) NO. TO BE EMPLOYED	(2) LOCATION *(Names of nearest cities and geographical coordinates to nearest minute.)*
A. FIXED	None	
B. MOBILE	(1) NO. TO BE EMPLOYED None	(2) AREA *(Enter the radius in miles with respect to a fixed geographical coordinates.)*
C. AIRBORNE AND/OR SPACE	(1) NO. TO BE EMPLOYED 8	(2) ALTITUDE AND AREA *(Include type of operation, i.e. air to air, air to ground, space to ground, etc.)* 6000 nmi altitude--Space to Ground

9. JUSTIFICATION, EXPLANATION AND REMARKS. *THIS IS THE MOST IMPORTANT SINGLE ITEM IN THIS APPLICATION.* *(Explain why this particular Frequency or Band is necessary and why an· existing assignment cannot be shared. Continue on additional sheet(s) of 8x10½" paper.)*

This channel will utilize a high gain ground tracking antenna and·under suitable regulations could be shared with other terrestial and perhaps space services. Since this channel carries the radar ranging pulses, it must be above about 900 M_c to avoid serious range error due to ionospheric refraction. The upper frequency limit is not critical and might be as high as 7 G_c before propagation medium limitations occur except that hardware availability and economy indicate an upper limit of about 3 G_c is more desirable.

10. TYPED NAME OF CONTRACTOR REPRESENTATIVE	A. ADDRESS

11. TYPED NAME OF NASA REPRESENTATIVE	A. ADDRESS

12. SIGNATURE OF AUTHORIZED NASA PROJECT MANAGER	A. OFFICE CODE	B. ADDRESS.

13. DATE AND LENGTH OF TIME REQUIRED	14. IDENTITY NO.	15. SIGNATURE OF AREA FREQUENCY COORDINATOR

16. TYPED NAME OF NASA FIELD INSTALLATION FREQUENCY MANAGER RESPONSIBLE FOR ALL ENTRIES ON THIS APPLICATION	A. SIGNATURE OF RESPONSIBLE FREQUENCY MANAGER

B. NASA INSTALLATION FREQUENCY MANAGERS THROUGH WHOM APPLICATION IS ROUTED.	
(1) NAME	(2) NAME

NASA FORM 566 AUG 61

Figure 7-5. Application for Frequency Authorization, Channel 4

APPLICATION FOR RADIO FREQUENCY AUTHORIZATION

	1. DATE OF PREPARATION 1/7/64

2. SECURITY CLASSIFICATION OF FREQUENCY AS ASSIGNED	3. CONTRACT NO.	4. PROJECT NAME/NO.
Unclassified	NASw-785	Navigation Satellite System

5. FREQUENCY REQUIRED (Kc/s) (Mc/s) (Gc/s)	A. BANDWIDTH (Kc/s) & EMISSION
Between 900 and 1215 Mc/s	250 Kc/s (incl. guard band) P-9

B. PEAK PULSE POWER	C. AVERAGE POWER
8 KW (nominal)	Variable 60 to 170 watts

D. PULSE DURATIONS (Microseconds) .	E. PULSE RECURRENCE RATE
320	Variable 3 to 27 per second

F. RANGE IN NAUTICAL MILES	G. HOURS OF OPERATION
8500	Unlimited

H. CALL SIGN REQUIREMENT	I. CATEGORY OF STATION
--	Radio Navigation (Space)

6. TYPE OF ANTENNA	A. DIRECTIVITY OF ANTENNA	B. BEAMWIDTH OF AZIMUTH	C. BEAMWIDTH IN ELEVATION
Phased Array	Conical Beam	Approx. 60°	AFC/Precision Std.

7. TRANSMITTER NOMENCLATURE	A. TUNABLE FREQUENCY RANGE OF TRANSMITTER	B. METHOD OF FREQUENCY CONTROL

8. TRANSMITTER LOCATIONS

A. FIXED.	(1) NO. TO BE EMPLOYED None	(2) LOCATION (Names of nearest cities and geographical coordinates to nearest minute.)
B. MOBILE	(1) NO TO BE EMPLOYED None	(2) AREA (Enter the radius in miles with respect to a fixed geographical coordinates.)
C. AIRBORNE AND/OR SPACE	(1) NO. TO BE EMPLOYED 8	(2) ALTITUDE AND AREA (Include type of operation, i.e. air to air, air to ground, space to ground, etc.) 6000 nmi Altitude -- Space to Mobile

9. JUSTIFICATION, EXPLANATION AND REMARKS. *THIS IS THE MOST IMPORTANT SINGLE ITEM IN THIS APPLICATION.* *(Explain why this particular Frequency or Band is necessary and why an existing assignment cannot be shared. Continue on additional sheet(s) of 8x10½" paper.)*

Since this channel carries radar ranging and angle pulses, the lowest feasible frequency is in the order of $900 \cdot M_c$ to avoid serious range error due to ionospheric refraction. However, it employs wide beamwidth antennas on both the satellite and vehicle which causes the transmitter power on the satellite to increase as the square of the frequency. Thus, little latitude of choice is available and the optimum frequency is in the vicinity of 900 to 1215 M_c. A secondary choice would be in the vicinity of 1500 to 1600 M_c realizing that more than twice the satellite power would be required. This channel cannot be shared with other services due to use of non-directional antennas.

10. TYPED NAME OF CONTRACTOR REPRESENTATIVE	A. ADDRESS

11. TYPED NAME OF NASA REPRESENTATIVE	A. ADDRESS

12. SIGNATURE OF AUTHORIZED NASA PROJECT MANAGER	A. OFFICE CODE	B. ADDRESS

13. DATE AND LENGTH OF TIME REQUIRED	14. IDENTITY NO.	15. SIGNATURE OF AREA FREQUENCY COORDINATOR

16. TYPED NAME OF NASA FIELD INSTALLATION FREQUENCY MANAGER RESPONSIBLE FOR ALL ENTRIES ON THIS APPLICATION	A. SIGNATURE OF RESPONSIBLE FREQUENCY MANAGER

B. NASA INSTALLATION FREQUENCY MANAGERS THROUGH WHOM APPLICATION IS ROUTED.

(1) NAME	(2) NAME

NASA FORM 566 AUG 61

Figure 7-6. Application for Frequency Authorization, Channel 5

TABLE 7-5 (Continued)

1535 - 1540 MC	Space (telemetering and tracking), band and is shared with fixed services in a number of European countries and with aeronautical radio navigation in Morocco and Yugoslavia.
1700 - 1710 MC	Space Research (telemetering and tracking) band and is shared with fixed and mobile services in regions 1 and 3 and Cuba (in Region 2).
2290 - 2300 MC	Space Research (telemetering and tracking in deep space) band and is shared with fixed and mobile services in regions 1 and 3 and in Cuba.
8400 - 8500 MC	Space Research band and is shared with fixed and mobile services in regions 1 and 3 and in Cuba.

7.2.5 Application for Radio Frequency Authorization

Contained in figures 7-2 through 7-6 are the sample application forms for radio frequency authorization for the five operational channels of the Navigational Satellite System. The developmental tracking channels are not included since these channels are already allocated for space research and are currently being implemented in the NASA tracking network.

7.3 SUMMARY OF SYSTEM PARAMETERS

Tables 7-6 through 7-10 contain a summary of the system parameters used to evaluate the overall system performance and feasibility. The detailed calculations can be found in appendices A and Z.

7.4 PARAMETRIC ANALYSES

The goal of the parametric analyses is to derive the subsystem requirements subject to the constraints of the system requirements and at minimum system costs. These analyses are divided into two areas:

    a. Optimization studies
    b. Error analyses

These are discussed in the following paragraphs. Following this discussion is a summary of the subsystem requirements.

7.4.1 Optimization Studies

The subsystem requirements model is a mathematical model of the relationships between the various subsystem parameters and costs of the Navigation Satellite System. This model is used to generate the optimum subsystem parameters that are based on the criteria of

TABLE 7-6

LINK 1 - GROUND TO SATELLITE

(RADAR RANGING AND DATA)

Transmitter peak power	44 watts
Frequency	1190 MC
Ground Station Ant. Gain	44 db
Free Space Loss	177 db
Polarization Loss	3 db
Atmospheric Loss	2 db
Component Losses	1 db
Fading Margin	6 db
Safety Factor	2 db
Satellite Antenna Gain	9.7 db
Total System Effective Noise Temperature	2700°K
Receiver Noise Figure	9.3 db
Receiver Bandwidth	190 KC

TABLE 7-7

LINK 2 - SATELLITE TO VEHICLE

(DATA)

Transmitter Peak Power	20 watts
Frequency	110 MC
Satellite Antenna Gain	9.7 db
Free Space Loss	157 db
Polarization Loss	3 db
Atmospheric Loss	0.6 db
Component Losses	1.2 db
Fading Margin	6 db
Safety Factor	2 db
Vehicle Antenna Gain	2 db
Total System Effective Noise Temperature	1835°K
Receiver Noise Figure	5.5 db
Receiver Bandwidth	10 KC
Data Rate	2500 bits/sec

TABLE 7-8
LINK 3 - VEHICLE TO SATELLITE
(RADAR RANGING, ANGLE, AND DATA)

Transmitter Peak Power	3600 watts
Frequency	1050 MC
Vehicle Antenna Gain	2 db
Free Space Loss	177 db
Polarization Loss	3 db
Atmospheric Loss	.2 db
Component Losses	1 db
Fading Margin	6 db
Safety Factor	3 db
Satellite Antenna Gain	9.7 db
Total System Effective Noise Temperature	$1160°K$
Receiver Noise Figure	6 db
Receiver Bandwidth	170 KC

TABLE 7-9
LINK 4 - SATELLITE TO GROUND
(RADAR RANGING, ANGLE, AND DATA)

Transmitter Peak Power	2 watts
Frequency	970 MC
Satellite Antenna Gain	9.7 db
Free Space Loss	176 db
Polarization Loss	3 db
Atmospheric Loss	2 db
Component Losses	1 db
Fading Margin	6 db
Safety Factor	2 db
Ground Station Antenna Gain	42.5 db
Total System Effective Noise Temperature	$50°K$
Receiver Bandwidth	159 KC

TABLE 7-10

LINK 5 - SATELLITE TO VEHICLE
(RADAR RANGING)

Transmitter Peak Power	5200 watts
Frequency	990 MC
Satellite Antenna Gain	9.7 db
Free Space Loss	176.5 db
Polarization Loss	3 db
Atmospheric Loss	2 db
Conponent Losses	1 db
Fading Margin	6 db
Safety Factor	3 db
Vehicle Antenna Gain	2 db
Total System Noise Temperature	$1270°$ K
Receiver Noise Figure	7 db
Receiver Bandwidth	219 KC

minimum total system cost. In doing this, it generates trade-off relationships between the various subsystem parameters and between these parameters and system cost.

The model functions in the following manner. The system is subject to performance constraints such as fix accuracy and traffic handing capability. Within the framework of these constraints, the subsystem parameters are manipulated until a minimum system cost is obtained. By performing these manipulations, the trade-off relations are generated. The end result is an optimum set of subsystem parameters.

As described in the discussions of the system concept, the navigation satellite system has four major subsystems:

    a. the ground control stations

    b. the network of satellites

    c. the user vehicle equipments

    d. the network of reference stations

Therefore, any complete model should analyze each of these subsystems. In the study reported here, the study constraints preclude this complete analysis. The system design shall first minimize the cost of the user vehicle equipments. Therefore, the parameters of these equipments are not available for manipulation in a general optimization study. Rather, they become constraints on the optimization of the remainder of the system. It is, however, instructive to show the effects of the user vehicle equipment parameters on the system cost.

It is also assumed, in deriving the subsystem requirements model, that the costs of the reference stations are negligible compared to the costs of the ground control stations and the satellites. This assumption is justifiable since the reference stations are no more than simplified user vehicle equipments. The user vehicle equipment must have a low cost to be commercially valuable. Therefore, the model discussed here only considers the ground control stations and the network of satellites.

The following paragraphs first describe the subsystem requirements model in general and then present more detailed discussions of each element of the model.

7.4.1.1 General Model Description

Figure 7-7 is a block diagram of the elements and flow of information of the subsystem requirements model. Given a set of inputs or system constraints; the satellite weight, number of satellites, number of ground stations, and the payload weight capability of the launch vehicles can be determined. From these values; the satellite cost, ground station cost, and minimum booster cost are calculated. These costs are then combined to obtain satellite subsystem cost and the total system cost. By varying the input values, a range of total system costs are generated. This allows trade-off curves, between the input values and costs, to be plotted.

Table 7-11 contains a list of those input parameters and performance requirements which are used in this model. The inputs which are varied in addition to the performance requirements and the inputs which have been fixed due to design considerations are shown. The fixed inputs are classified according to their use in figure 7-7.

Each of the sections of the model shown in figure 7-7 shall now be discussed in detail.

7.4.1.2 Satellite Weight

Figure 7-8 is a detailed breakdown of the satellite weight block shown in figure 7-7. With the inputs previously mentioned, the maximum range from the satellite to the vehicle and the ground station and the signal to noise ratios on the range and data channels can be determined. This defines the satellite antenna beamwidth, which with the two signal to noise ratios, allows the various satellite peak powers to be calculated. With the peak powers known, the average output and input powers for the various channels can be determined.
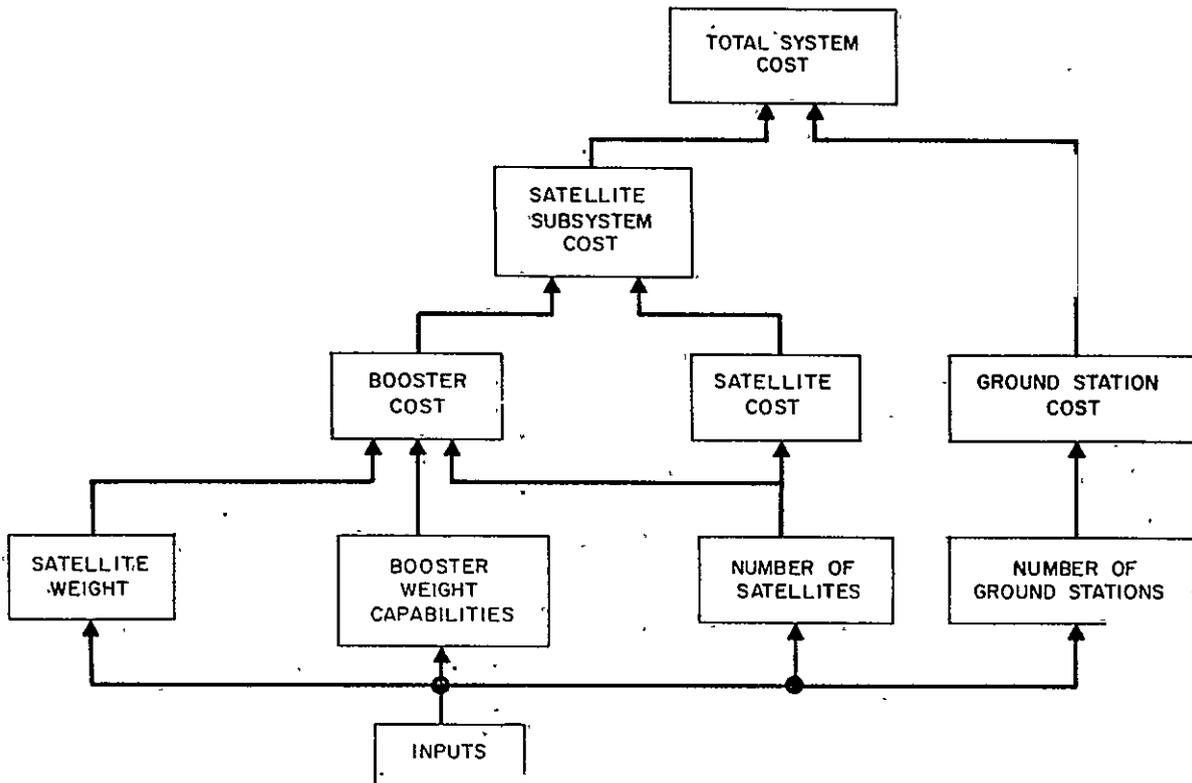
Figure 7-7. Subsystem Requirements Model

TABLE 7-11

INPUTS TO MODEL

Variable Inputs

    1. Altitude

    2. Radar Channel Frequency

    3. Ground Station Antenna Gain

    4. Transponder Peak Power

    5. Data Channel Bandwidth

Performance Requirements

    1. Vehicle Fix Rate

    2. Range Error due to Noise

    3. Angle Error due to Noise

Fixed Inputs

A. Satellite Weight

    1. Antenna Elevation Angles

    2. Satellite Attitude Drift

    3. Vehicle Antenna Gain

    4. Losses due to Polarization, Fading and Atmosphere

    5. Data Channel Frequencies

    6. Range Channel Bandwidth

    7. Angle Channel Bandwidth

    8. Receiver Noise Temperatures

    9. Pulse Compression Ratio

    10. Data Channel Bit Error Rates

    11. Fix Data Channel Bandwidth

    12. Range Channel Pulses/Fix

    13. Reference Station Fix Rate

B. Number of Satellites

    1. Number of Orbital Planes

    2. Vehicle Elevation Angle

    3. Satellite Ground Path Width

C. Number of Ground Stations

    1. Ground Station Elevation Angle

D. Booster Weight Capability

    1. Latitude of Launching Station

    2. Orbital Plane Inclination Angle

TABLE 7-11 (Continued)

Fixed Inputs (Continued)

3. Specific Impulses of Boosters' Last Stages

4. Radius of Perigee

5. Velocity at Perigee

6. Boosters' Weight Capability at 100 Nautical Miles

E. Booster Costs

1. Boosters' Reliabilities

2. Boosters' Costs

The summation of these input powers allow total input power and secondary power supply weight to be calculated.

Range and antenna beamwidth permit the angle channel signal noise ratio to be determined for a given angular accuracy requirement. This ratio defines the interferometer antenna separation. The antenna and arm weight and the radar electronics weight are then determined.

With the average output power on the radar channel known, radar transmitter weight is calculated and combined with the antenna and electronics weights to find the weight of the satellite's radar portion. The communications transmitter and electronics weight are similarly determined from the average output powers of the data channel.

The weight of the initial and final stabilization equipment is then determined and combined with other major weights to give the total satellite equipment weight. This weight is then added to the necessary structure weight to determine the total satellite weight which is to be injected into orbit.

It can be seen that as the inputs are varied; certain powers, weights, etc. shall also vary. This allows the total satellite weight variation to have its effect on choice of boosters, booster costs, and system cost.

7.4.1.3 Number of Satellites

The decision has been made that the Navigation Satellite System, at the time of its full deployment, shall have launch and tracking facilities available that are capable of providing highly accurate orbital injections. This decision implies that injection velocity can be controlled so that a network of satellites can be established that can maintain precise relative positions from three to five years. This decision results in a minimum number of satellites to achieve complete worldwide coverage.

With these stipulations, the following relations are used to calculate the number of satellites as a function of altitude.
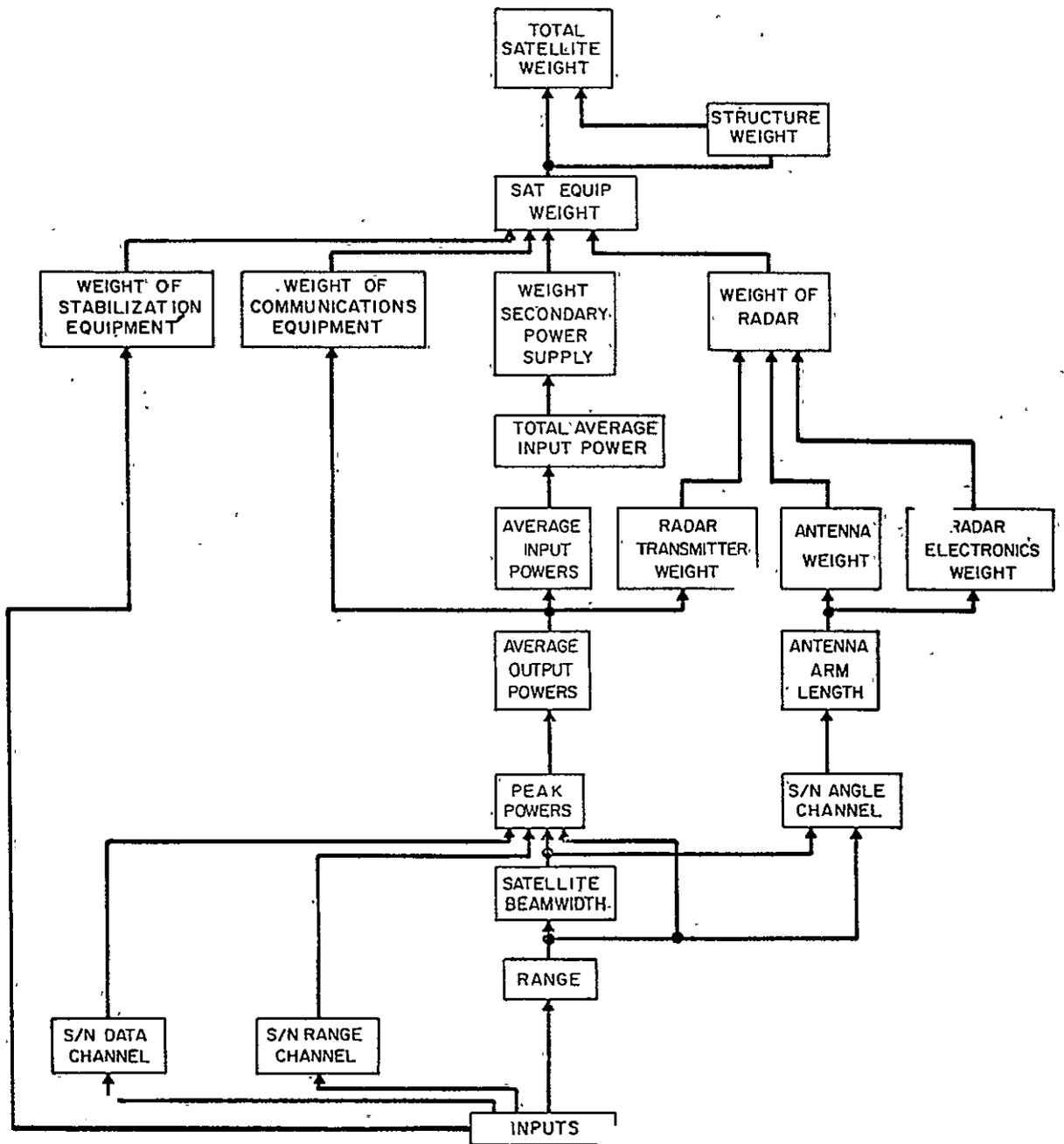
Figure 7-8. Satellite Weight Relations

$$\phi = \cos^{-1}\left(\frac{R_e}{R_e + H} \cos g\right) - g$$

$$NS/p = \frac{\pi}{\cos^{-1}\dfrac{\cos\phi}{\cos D}}$$

where

ϕ = satellite great circle radius of coverage

R_e = earth radius

H = altitude

g = vehicle elevation angle

NS/p = number of satellites required per orbital plane

D = satellite ground path width

The minimum number of orbital planes and consequently the minimum number of satellites that will allow 100 percent coverage of the earth is two.

Therefore: NS = 2 (NS/P)

where   NS = total number of satellites required

7.4.1.4 Number of Ground Stations

A ground station network is to be established so that the coverage of the satellite orbital sphere shall be complete. That is, a satellite will always be in sight of at least one ground station.

With this constraint, the required number of ground stations can be calculated knowing the satellite altitude and the minimum elevation angle of the ground station antenna. The following relations are used

$$H = \frac{6880 \sin(1/2\ \phi + g) \sin(\phi/2)}{\cos(\ + g)}$$

$$\cos\ = \frac{1}{\sqrt{3}}\ \tan\left(\frac{NGS-3}{NGS-2}\ \cdot\ 60°\right)$$

where:

H = satellite altitude

ϕ = satellite great circle radius of coverage

g = ground station elevation angle

NGS = number of ground stations required

The actual number of ground stations considered in this requirements model varies from four to fifteen. The cost of each station is highly dependent on how many are used. For example, if only four are used, the per station cost would be significantly more than it would if fifteen were used. Also, because of the uneven distribution of traffic throughout the world, some ground stations, such as one controlling the South Atlantic, would have much less traffic to handle and would cost less in proportion to one controlling the North Atlantic.

7.4.1.5 Booster Weight Capability

To launch into the selected circular orbit, the booster shall initially launch the payload in a low circular orbit; approximately 100-400 nautical miles. At this time, the last stage shall inject the payload into an elliptical transfer or parking orbit whose perigee corresponds to the initial low orbit and whose apogee is at the altitude of the circular orbit desired. At elliptical transfer or parking orbit apogee, a final stage shall transfer the payload to the desired circular orbit.

The desired weight capability is the payload weight that the booster can place into the final circular orbit. The known weight capability is the payload weight that various boosters can orbit at 100 nautical miles altitude and at an inclination angle equal to the latitude of the launching station. The total weight capability that will be lost between 100 nautical miles and the desired altitude is a summation of the following three weight losses

      a. the weight loss in orbiting the payload at an inclination angle other than above, ΔW_i.

      b. the weight loss due to the injection of the payload at perigee into the elliptical transfer orbit, ΔW_p, and

      c. the weight loss due to the injection of the payload at apogee into the desired circular orbit, ΔW_a.

Therefore

$$\Delta W_t = \Delta W_i + \Delta W_p + \Delta W_a$$

where

ΔW_t = Total weight loss for a given booster and altitude.

and

$$W_H = W_{100} - \Delta W_t$$

where

    W_H = weight a given booster can orbit at altitude H

    W_{100} = weight a given booster can orbit at 100 nautical miles.

The relations used to calculate these weight factors are derived in Appendix Y.

7.4.1.6 Booster Costs

The cost of each booster is considered as the combination of both production and launch costs. A more accurate cost to the system, however, shall include the backup booster cost that is defined by the reliability of the booster. With the assumption that total booster cost will vary in proportion to reliability, the total booster cost is

$$CBR = \frac{CB}{RELB}$$

where

    CBR = total booster cost including reliability

    CB = launch plus booster cost

    RELB = reliability of booster

7.4.1.7 Satellite Subsystem Cost

Before discussing the method of determining satellite system cost, it is mentioned that there are two methods of launch which shall be investigated. The first is the single launch method where one satellite is launched per booster. The second is the multiple or piggyback launch method where more than one satellite per booster can be launched.

Regardless of which method is used, the objective of determining satellite system cost is to choose the combination of boosters that is capable of launching the satellite at minimum cost. This combination is initially defined by the number of satellites desired, the weight of each satellite, and the orbital altitude and inclination angle.

7.4.1.7.1 <u>Single Launch</u>. - The costs for this method can be determined simply by multiplying the sum of booster and satellite costs by the number of satellites desired.

Of course, only those boosters capable of launching the required satellite weight into the desired orbit can be used. The cost shall then be calculated, and the minimum cost and booster chosen accordingly.

Similar to booster cost, the cost of the satellite on a particular booster will vary proportionally to that boosters' reliability.

$$CSR = CS/RELB$$

where

   CSR = cost of each satellite including reliability

   CS = initial cost of each satellite

   $RELB$ = booster reliability

therefore

   $$TC = NS (CBR + CSR)$$

where:

   TC = total satellite system cost

   NS = number of satellites

7.4.1.7.2 <u>Multiple Launch</u> The minimum satellite system cost for this case is difficult to determine. A search through the various combinations of boosters to find optimum points for each value of the satellite number, weight, and orbital altitude and inclination is required. Each booster's weight capability is divided by the satellite weight to obtain the number of satellites, NS_i, that the ith booster is able to launch. This value can vary from 0 to the maximum number of necessary satellites in one orbital plane. The satellite system cost for all the various combinations of boosters is then calculated, and the minimum cost is chosen. Again, the reliability of each booster shall be included.

A possible minimum cost combination can then be NS_1 satellites on NB_1 of one booster, and NS_2 satellites on NB_2 of another booster. The total satellite system cost in this case would be

$$TC = NB_1 \left(\frac{NS_1 \times CS + CB_1}{RELB_1}\right) + NB_2 \left(\frac{NS_2 \times CS + CB_2}{RELB_2}\right)$$

where:

TC = total satellite subsystem cost

NB_1 = number of first type of booster used

NB_2 = number of second type of booster used

NS_1 = number of satellites per first booster

NS_2 = number of satellites per second booster

$NS_1 = NS_2 = NS$ = total number of satellites required

CS = cost of one satellite

CB_1 = cost of the first type of booster

CB_2 = cost of the second type of booster

$RELB_1$ = reliability of the first type of booster

$RELB_2$ = reliability of the second type of booster

There are various combinations which can be chosen for minimum cost. However, the general format will be similar to the example shown above.

7.4.1.8 Total System Cost

The total system cost is the sum of the satellite subsystem cost and the ground station costs.

System Cost = TC + CGS.

7.4.1.9 Results

The objective of this evaluation is to present the values of the inputs which are used in the subsystem requirements model and a discussion of the results obtained.

7.4.1.9.1 Input Values. The values of the inputs previously discussed in table 7-1 that have been fixed due to subsystem design consideration are presented in the succeeding paragraphs. The inputs are classified according to their use in the model.

7.4.1.9.1.1 Satellite Weight

Ground station antenna elevation angle	5°
Vehicle antenna elevation angle	5°
Satellite attitude drift	$\pm 5^{\circ}$
Vehicle antenna gain	2 db
Losses due to polarization, fading and atmosphere	14 db
Fix data channel frequency	110 MC
Range channel bandwidth	159 KC
Angle channel bandwidth	150 CPS
Effective noise Temperature on link 1	2700 K
Effective noise Temperature on link 2	2750 K
Effective noise Temperature on link 3	1160 K
Effective noise Temperature on link 4	50 K
Effective noise Temperature on link 5	1270 K

Pulse compression ratio	50. 6
Fix data channel bandwidth	10. KC
Range channel pulses/fix	3 pulses/fix
Reference Station fix rate	1 fix/sec.

7.4.1.9.1.2 Number of Satellites

Number of orbital planes	2
Vehicle elevation angle	$5.^\circ$
Satellite ground path width	45°

7.4.1.9.1.3 Number of Ground Stations

Ground station elevation angle	5°

7.4.1.9.1.4 Booster Weight Capability. Five boosters were considered in the model. Subscripts on the input values listed in this paragraph and in 7.4.1.9.1.5 indicate the following boosters:

a. Thor Delta

b. Thrust Augmented Delta

c. Super Delta

d. Atlas Agena

e. Atlas Centaur.

Latitude of launching station	28.4°
Orbital plane inclination angle	45°
Specific Impulse$_{a, b, c, d}$	260 sec.
Specific Impulse$_e$	350 sec.
Radius of perigee	3538 nmi
Velocity at perigee	4.2064 nmi/sec.
Weight capability at 100 nmi$_a$	810 lb.
Weight capability at 100 nmi$_b$	920 lb.
Weight capability at 100 nmi$_c$	1500 lb.
Weight capability at 100 nmi$_d$	5000 lb.
Weight capability at 100 nmi$_e$	8500 lb.

7.4.1.9.1.5 Booster Cost

Booster reliability$_a$	0.95
Booster reliability$_b$	0.75
Booster reliability$_c$	0.75
Booster reliability$_d$	0.60
Booster reliability$_e$	0.50
Booster cost$_a$	$2.1 (10^6)
Booster cost$_b$	$2.6 (10^6)

Booster Cost$_c$ $3.5 (10^6)$

Booster Cost$_d$ $6.3 (10^6)$

Booster Cost$_e$ $7.8 (10^6)$

7.4.1.9.2 <u>Discussion of Results</u>. — A discussion of the effects on total system cost of varying the input parameters and performance requirements is presented in the succeeding paragraphs.

7.4.1.9.2.1 Orbital Altitude Input Parameter Variations. — Shown in figures 7-9 and 7-10 is the effect on total relative system cost caused by varying altitude. The cost shown is relative to the minimum system cost obtained. Figure 7-9 represents the relative cost variation for the single launch case and figure 7-10 represents the relative cost variation for the multiple launch case. As can be seen, the only range of altitudes that shall be considered is between 3,000 and 13,000 nautical miles. The extreme variation below 3000 nautical miles is caused by two factors. The first is great number of satellites required for 100 percent coverage and second is the larger number of ground stations necessary for 100 percent coverage. As the number of satellites increases, the number of boosters required for the single launch case, or the size of the booster(s) required for the multiple launch case increases. Both conditions cause an increase in cost. The rise in cost above approximately 13,000 nautical miles is caused by the large satellite weight required. This weight increase necessitates a larger and more costly booster. The increase in weight at this high altitude is necessary because of the large power requirements and long antenna arms necessary to satisfy the performance requirements.

The optimum altitude is between 3600 and 4400 nautical miles for a single launch and between 5000 and 5400 or 10,400 and 12,800 nautical miles for a multiple launch. However, 6000 nautical miles is considered the minimum altitude for this satellite system due to radiation belt effects. Also, the range of altitudes between 10,400 and 12,800 nautical miles must be discounted because of the extreme values of peak power, antenna arm length, etc. that are required.

The next best region for minimum system cost is the single launch case at an altitude between 5000 and 7200 nautical miles. As previously mentioned, however, 6000 nautical miles is the minimum altitude to be considered. Any increase above that value does not affect system cost but will increase satellite requirements such as weight, power, etc. Based on the above considerations and total system cost, the decision was made that the optimum altitude is approximately 6000 nautical miles. Using this selected altitude requires an eight percent increase in system cost over the optimum value.

With an altitude selected, the rest of the input variables and performance requirements are varied at that particular altitude to generate the trade off relationships.

7.4.1.9.2.2 Radar Channel Frequency Input Parameter Variations. — The variation of cost versus transponder peak power for different radar channel frequencies is shown in figure 7-11. As the radar frequency increases, the path attenuation increases and this requires that transponder and satellite powers rise to satisfy the various accuracy requirements.
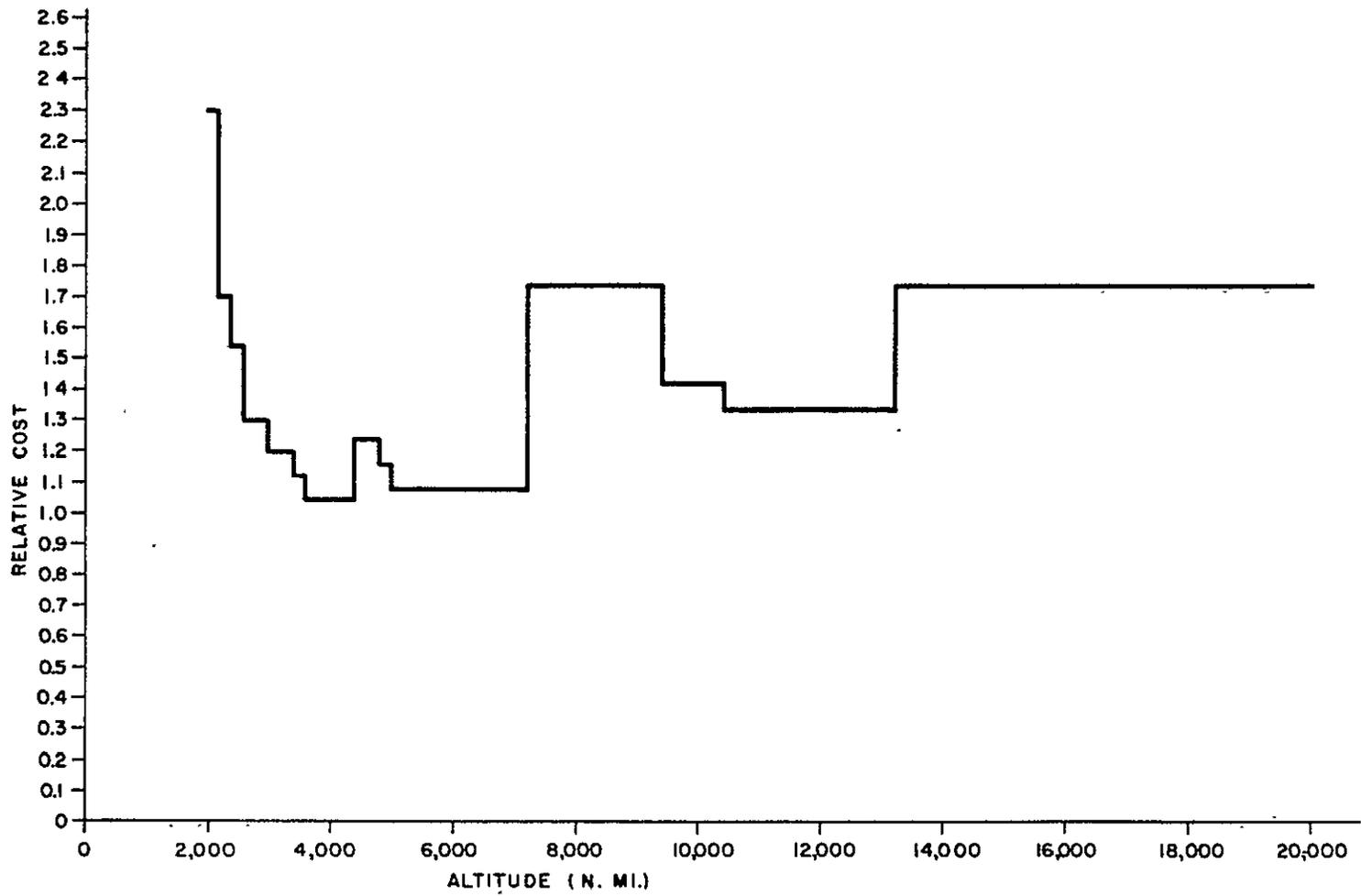
Figure 7-9. Total System Cost vs Altitude (Single Launch Case)
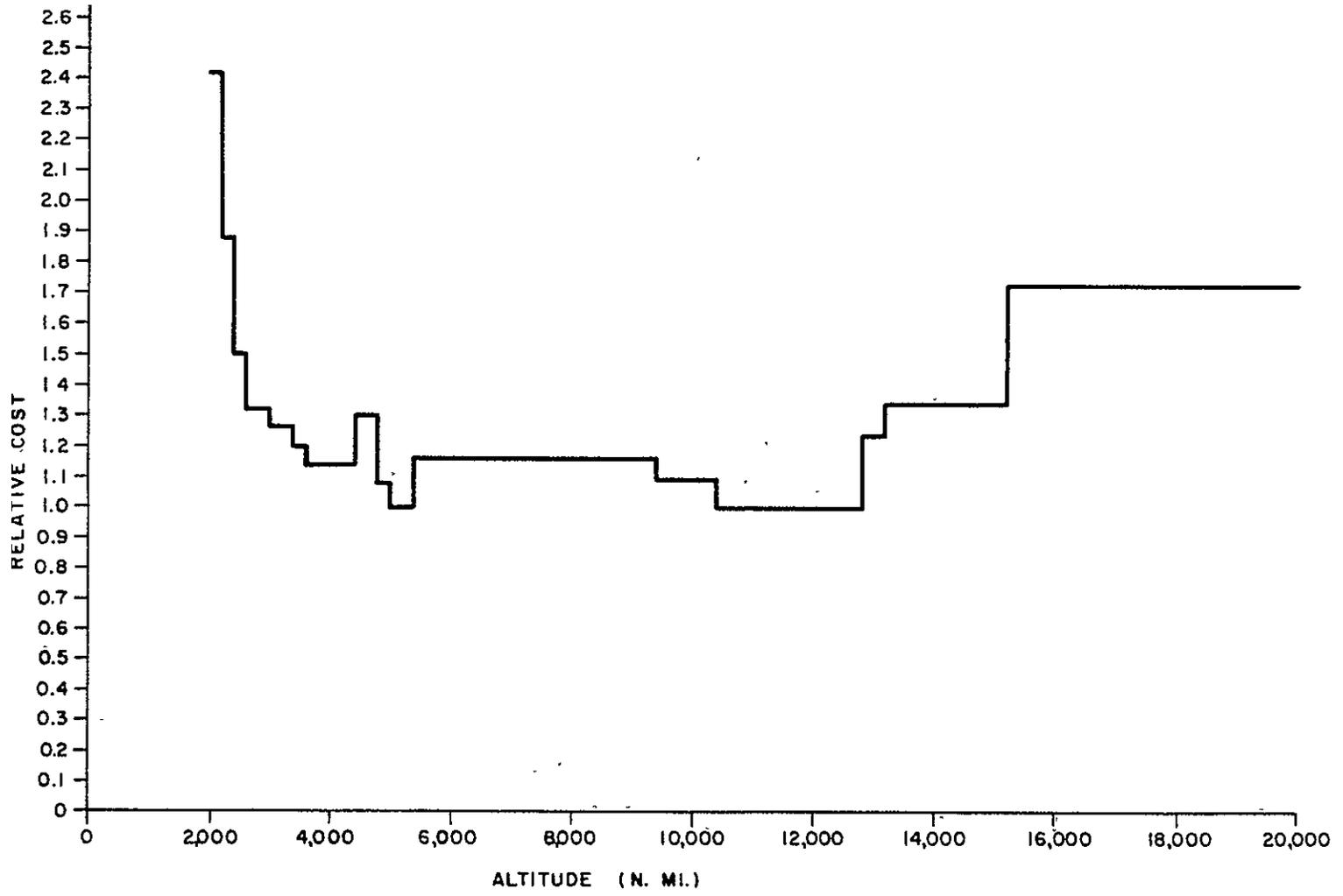
Figure 7-10. Total System Cost vs Altitude (Multiple Launch Case)
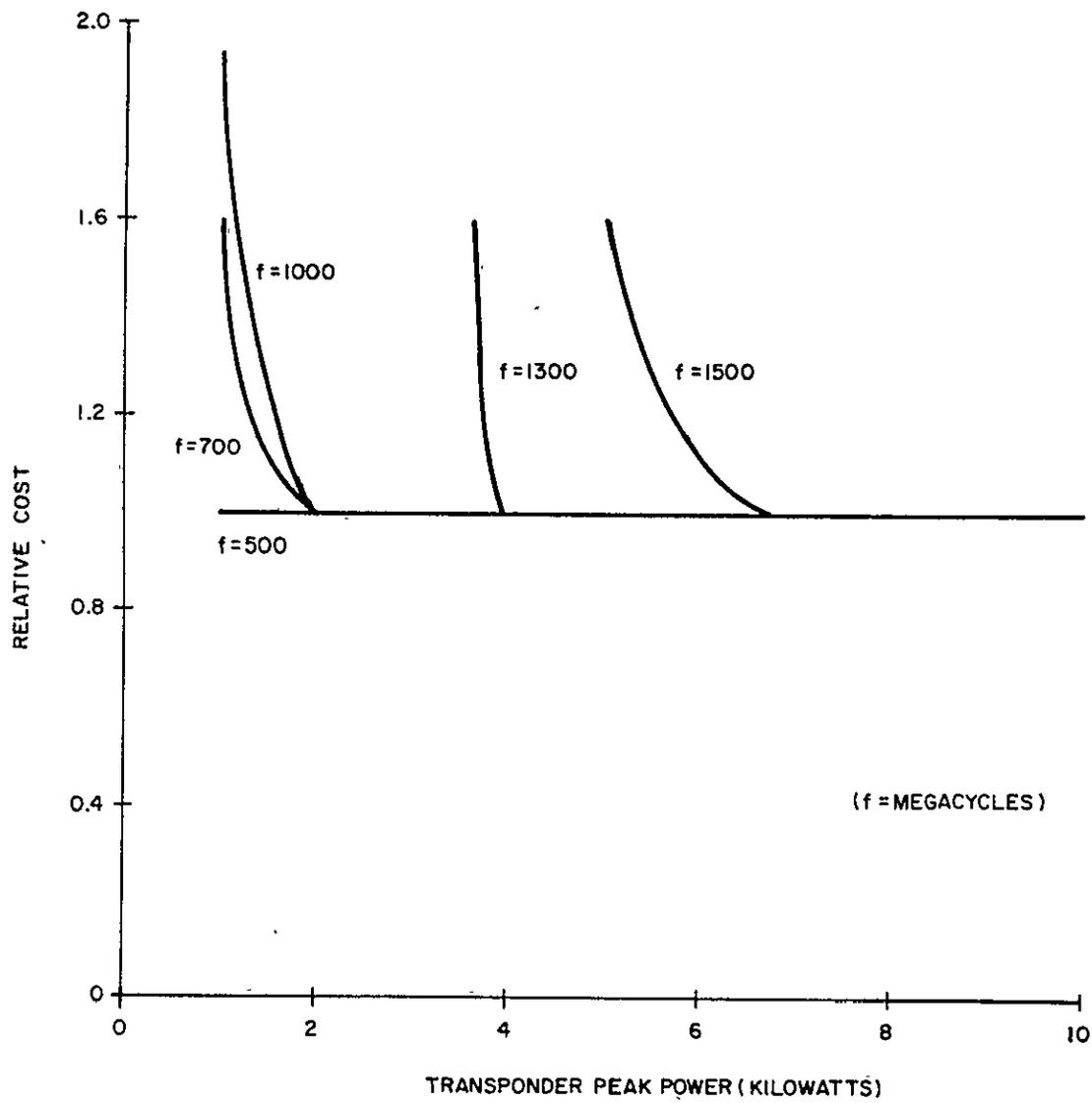
Figure 7-11.   Transponder Peak Power vs Relative Cost
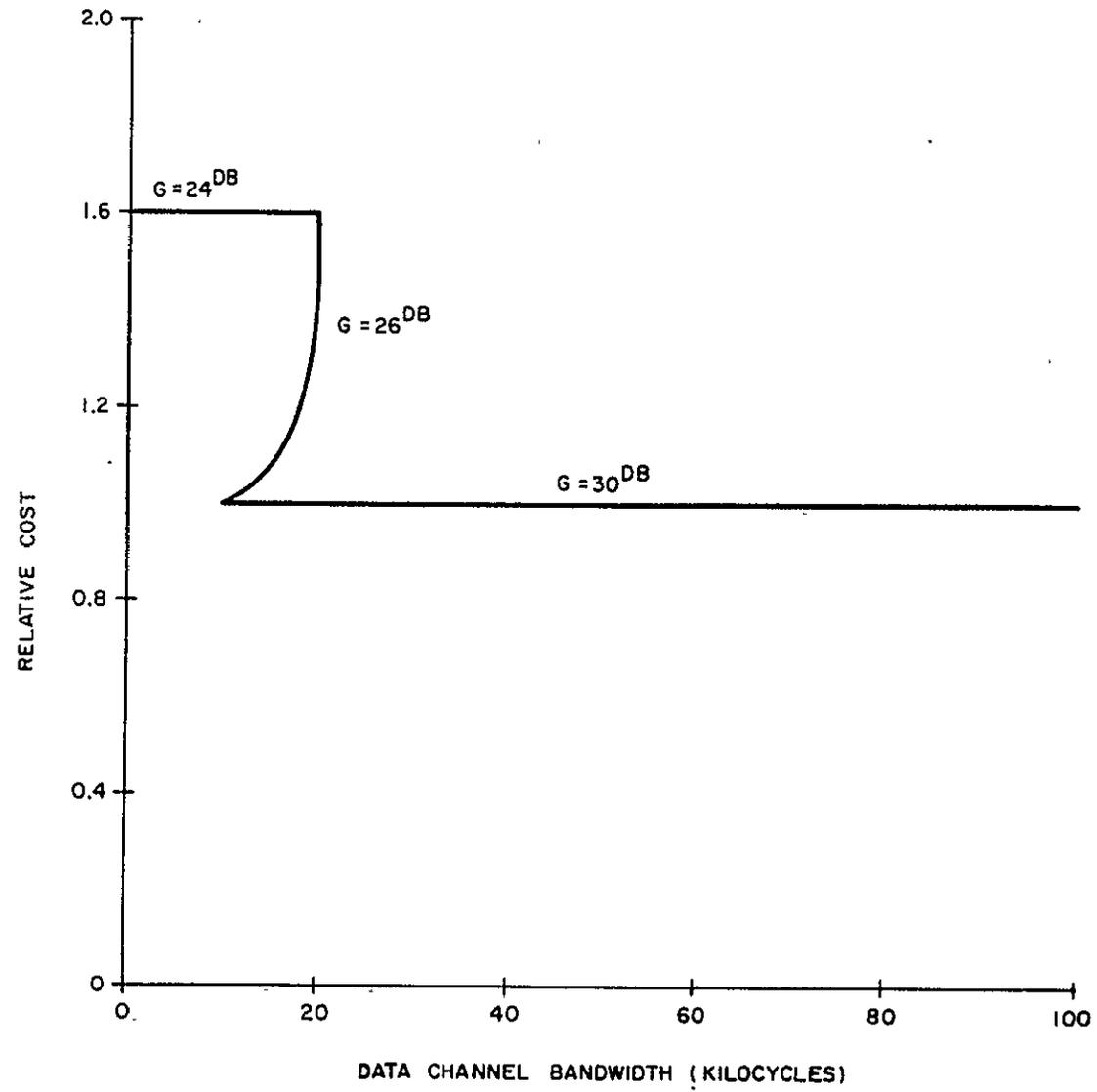
Figure 7-12.   Data Channel Bandwidth vs Relative Cost
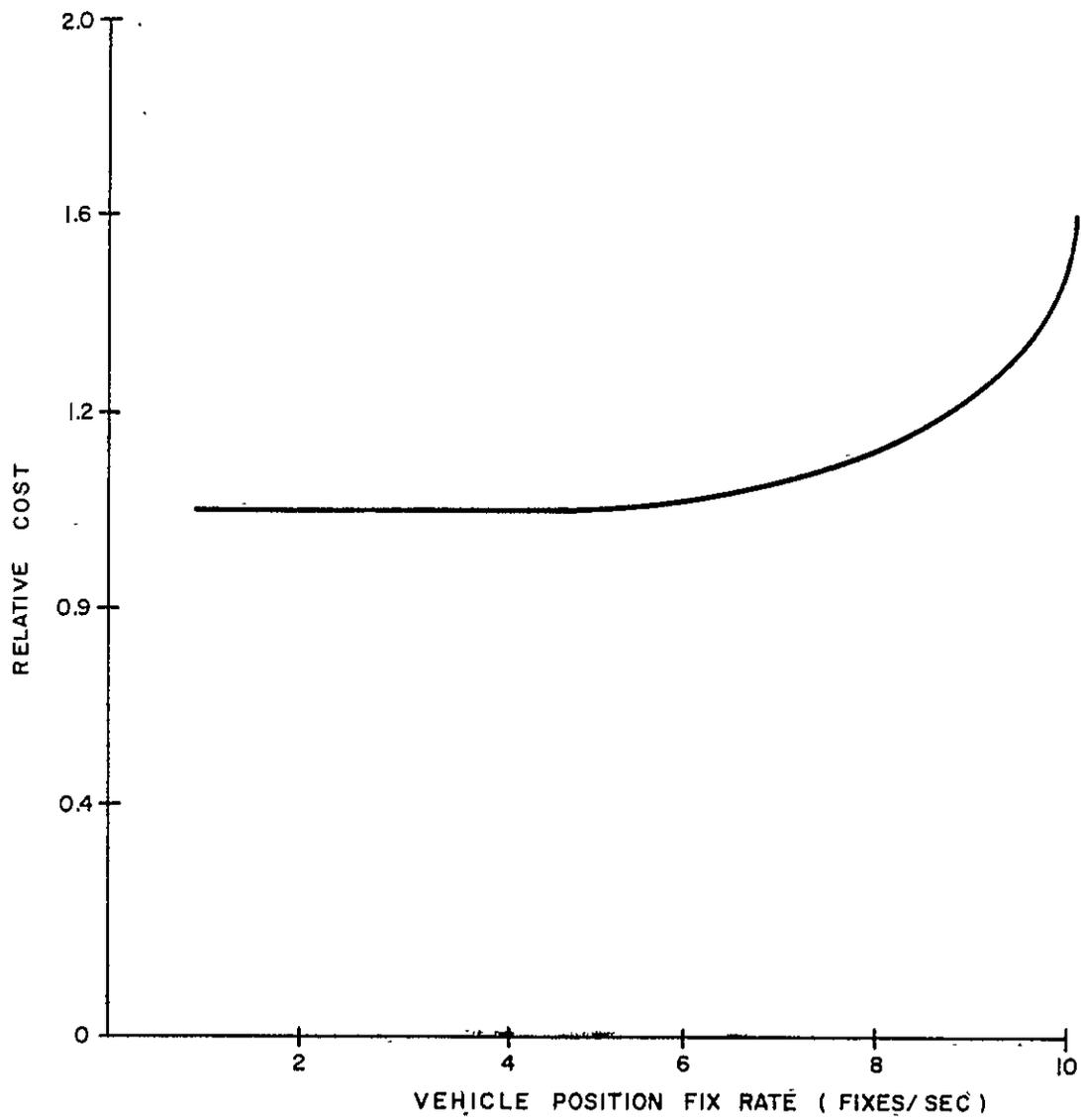
Figure 7-13.   Vehicle Position Fix Rate vs Relative Cost

Providing the transponder peak power is at least 2 kilowatts, any radar frequency of 1000 megacycles or less shall not increase the system cost from its optimum value. However, when the frequency decreases, atmospheric measurement errors become larger. Therefore, a radar frequency should be chosen with a value of approximately 1000 megacycles and a minimum useable frequency of 800MC.

7.4.1.9.2.3 Transponder Peak Power Input Parameter Variations. - Referring to figure 7-11, the effect of transponder power on system cost will be considered. For a given radar frequency, as the transponder power is decreased, the antenna arm length, satellite power, etc. increases, the results is an increase in the system cost. For any radar frequency value of 1000 megacycles or less, a transponder peak power of 2 kilowatts or more is adequate and causes no increase in system cost. There are no other significant reasons why the system frequency should be raised above 1000 megacycles. Therefore, a peak power of 2 kilowatts or more shall be chosen.

7.4.1.9.2.4 Data Channel Bandwidth and Ground Station Antenna Gain Input Parameter Variations. - Figure 7-12 describes the variation in system cost with the bandwidth of a data gathering channel for various values of ground station antenna gain. For low antenna gain values, small increases in the bandwidth of this data channel causes large increases in the power required to be radiated from the satellite. This power increase results in larger satellite weight and system cost. As the antenna gain is raised, the increase in satellite power required for increased bandwidth begins to have a negligible effect on satellite weight, necessary booster, and system cost.

As can be seen from figure 7-12, a 26 db antenna gain allows a bandwidth up to 10 kilocycles with no increase in cost. A 30 db antenna will reduce the required power increase with increasing bandwidth, so that bandwidth values up to 100 kilocycles can be utilized with no increase in cost. Therefore, a ground station antenna gain of 30 db or more, with a data bandwidth of 100 KC or less, is optimum for the system.

7.4.1.9.2.6 Vehicle Fix Rate Performance Requirements. - In the model, the effect of increasing the vehicle fix rate is to increase the values to the average radar link powers on the satellite. This shall cause the satellite weight to increase and consequently, the launch costs.

In figure 7-13 the increase in weight caused by increasing the fix rate does not affect the system cost (i. e., no larger booster is necessary) until the fix rate is increased above five vehicles per second. Therefore, the system can handle up to approximately 18,000 fixes per hour with no increase in cost. For a fix rate above five per second, the weight increase begins to become a factor in the boosters necessary for launch and consequently, in the cost.

7.4.2 Error Analysis

A rigorous analysis of the position fix equations is very complex. However, the problem can be greatly simplified by geometrically handling the error propagation. Other simplifications are made by taking note of the system involved.

Satellite position is measured by measuring the ranges to reference stations. Measurement of the user vehicle position, relative to the satellite, is equivalent to measuring the position of the user vehicle relative to the reference stations. Therefore, bias errors introduced by errors in the reference station location can be added directly to the bias error computed in the user vehicle position. These errors are not required to be carried through the error propagation equations.

Relative positions of stations on the surface of the earth can now be computed from satellite observations to within approximately 25 feet. This is accomplished using an earth model that is only valid to the third harmonic. Programs are currently under way in NASA to carry this model out to the ninth harmonic. Therefore, when this navigation system is implemented, it can reasonably be expected that the positions of the reference stations shall be known with greater accuracy compared to the one mile approximation of this system. Because of this reason, errors in reference station position are ignored in this analysis.

Similarly, if the measurements of satellite position and user vehicle position are taken nearly simultaneously, small errors in satellite position can be considered as bias errors. If these errors are sufficiently small, they will cancel and can be neglected in the analysis. Tracking systems are currently being studied to determine the positions of spacecraft with better than 50 feet accuracies. With expected improvements in use by the time this navigation system is operational, it is reasonable to neglect errors in satellite position.

The time that measurements of reference stations and user vehicles are made can be very accurately determined by the ground control stations . Therefore, timing errors shall also be neglected in this analysis.

The major sources of system error are the radar measurements and the atmosphere. This analysis considers the manner in which these errors, when measuring four reference stations and the user vehicle, propagate and contribute to the final error in user vehicle position.

For the purposes of this analysis, the system can be considered as if photographed and stopped at one instant of time. For convenience in numerical evaluation, the situation shown in figure 7-14 is chosen. The central coordinate system is the inertial set of axes. The satellite is located on the X-axis. The two interferometer arms are taken parallel to the Y and Z axes, respectively. The user vehicle is located on the earth's surface in the X-Y plane and its line of sight to the satellite is at an elevation angle of $5°$. These assumptions made merely for convenience in calculation and in no way invalidate the results of the error analysis.
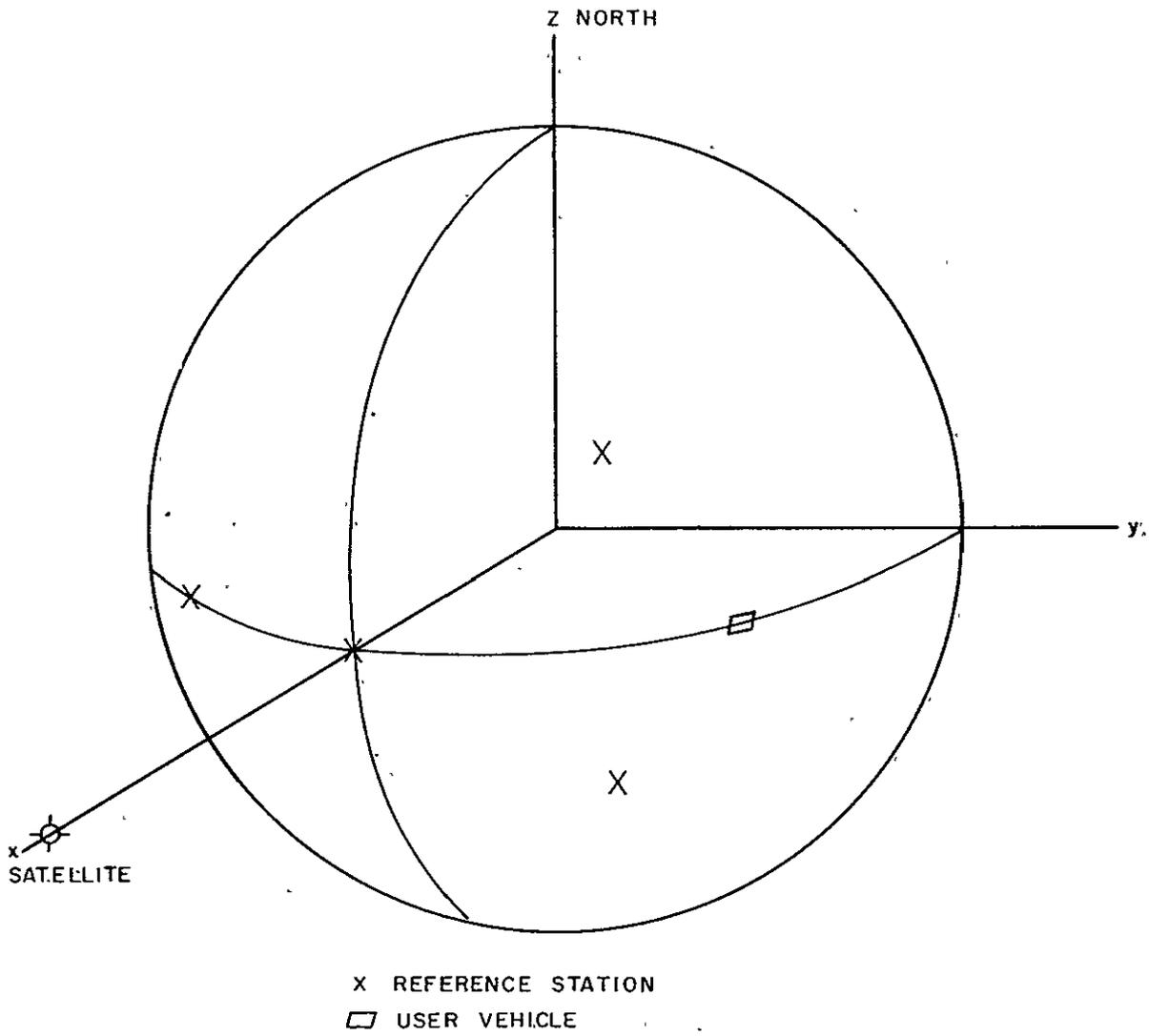
Figure 7-14. System Geometry

7.4.2.1 Error Equations

The equations describing vehicle position error as a function of the reference station measurement errors and the vehicle measurement errors are derived in this paragraph.

Consider a satellite-centered sphere, as shown in figure 7-15, with the numbered points on the surface of the sphere representing directions of the following quantities.

0, 1, 2, 3 - reference stations

        4 - vehicle

        5 - interferometer

        6 - intermediate step in locating 7

        7 - the error

        8 - north

        9 - center of earth

also

ϕ_1, ϕ_5 - the spherical distance between 0 and 1 and between 0 and 5, respectively

ϕ_{15} - the distance between 1 and 5

λ_{15} - the angle between ϕ_1 and ϕ_5

Similarly; ϕ_i, ϕ_j, ϕ_{ij} and λ_{ij} are used for any of the other points with 0 used as the origin. Knowing the quantities ϕ_i, ϕ_j and λ_{ij}, determines ϕ_{ij}.

$$\cos \phi_{ij} = \cos \phi_i \cos \phi_j + \sin \phi_i \sin \phi_j \cos \lambda_{ij} \tag{7-1}$$

and an $_i$ such that may be defined

$$\cos \alpha_i = \frac{\cos 2\, \theta_i + \cos 2\, \theta_j \cos 2\, \theta_k}{\sin 2\, \theta_j \sin 2\, \theta_k} \tag{7-2}$$

where

$$2\, \theta_i = 180° - \phi_{jk}$$

Then

$$\sin \beta_i = \sin \theta_j \sin \alpha_j \tag{7-3}$$

where

$$\sin \alpha_j = \frac{\sin \theta_i \sin \alpha_k}{\sin \theta_k}$$
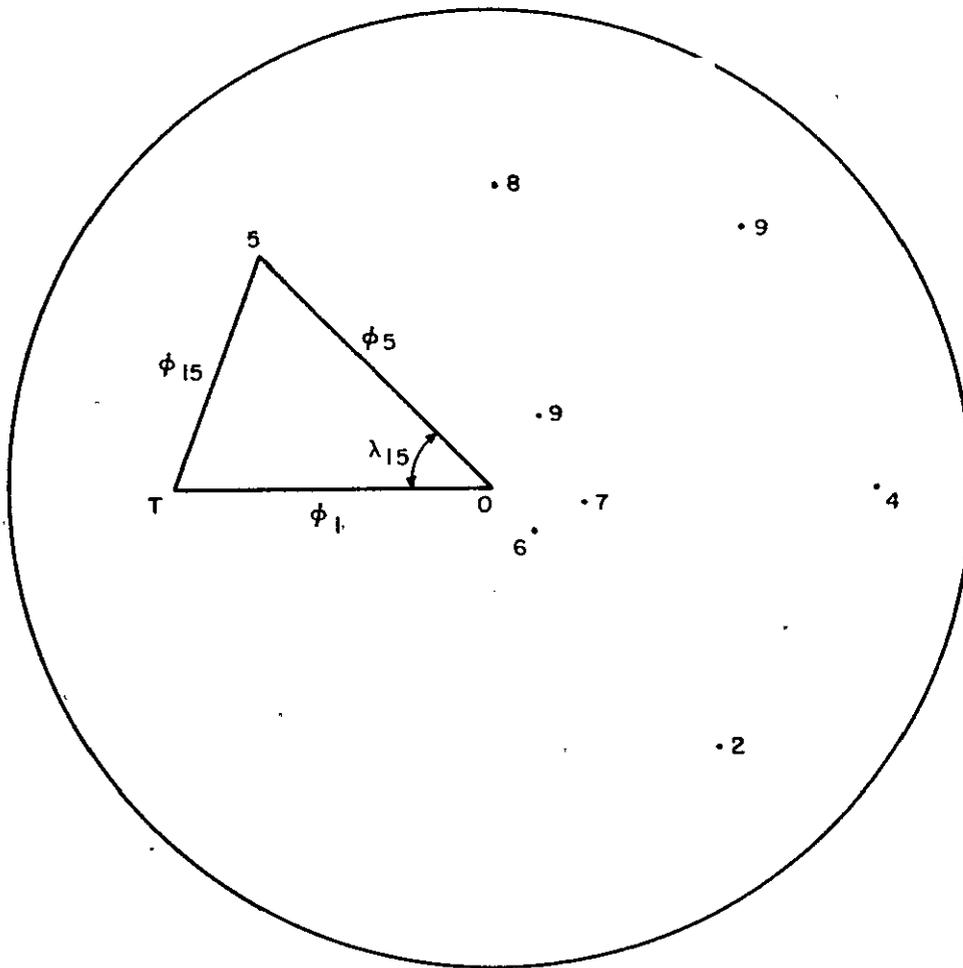
Figure 7-15. Satellite-Centered Sphere

and

$$\cos \phi_k = -\cos_i \cos_j + \sin_i \sin_j \cos_k$$

The quantity ϕ_{16} is derived as

$$\cos \phi_{16} = \frac{\sin \beta - \cos \phi_6 \cos \phi_1}{\sin \phi_6 \sin \phi_1} \tag{7-4}$$

with $\sin \beta = \cos \phi_6 \cos \phi_1 + \sin \phi_6 \sin \phi_1 \cos \phi_{16}$

and $\cos \phi_6 = \cos \phi_3 \sin \beta + \sin \phi_3 \cos \beta \cos \beta_3''$

but $\beta_i'' = \beta_i''' - \beta_i'$

and $\cos \beta_i''' = \dfrac{\sin \beta - \sin \beta \cos \phi_{ij}}{\cos \beta \sin \phi_{ij}}$

$\cos \beta_i' = \dfrac{\cos \phi_j - \cos \phi_i \cos \phi_{ij}}{\sin \phi_i \sin \phi_{ij}}$

For an error in the reference station located directly below the satellite, d_0, τ_0, ϕ_7° are defined as

$$d_0 = \frac{a_0}{\cos \phi_6 - \sin \beta} \tag{7-5}$$

$$\tau_0 = d_0 \sin \beta \tag{7-6}$$

$$\phi_7^\circ = \phi_6 \tag{7-7}$$

where a_0 is the input error and ϕ_6 and β have been previously determined.

For an error in one of the outer stations define a ρ_i and a g_i'' as

$$\rho_i = \frac{a_i}{\sin 2 \theta_j \sin \alpha_k} \tag{7-8}$$

where a_i is the input error

$$g_i'' = g_i + g_i' \tag{7-9}$$

where

$$\cos g_i' = \frac{\cos \phi_i - \cos \phi_{ik} \cos \phi_k}{\sin \phi_{ik} \sin \phi_k}$$

and

$$\cos g_i = \frac{\sin 2\theta_j \sin\alpha_k}{\sin\phi_{ik}}$$

also ψ'_i and g_i''' are determined as

$$\cos \psi'_i = \sin\phi'_k \cos g_i'' \tag{7-10}$$

$$\cos g_i''' = \frac{\cos\phi_i - \cos\psi'_i \cos\delta_i}{\sin\psi'_i \sin\delta_i} \tag{7-11}$$

·so that

$$\psi_i = \psi''_i - \delta_i \tag{7-12}$$

$$\tan\psi''_i = -\frac{1}{\tan\psi'_i \cos g_i'''}$$

Define d_i' and ω_i as

$$d_i' = \frac{b_i \cos\gamma}{\cos\gamma - \sin\beta} \quad, \quad \gamma = \phi_6 \tag{7-13}$$

·where

$$b_i = \rho_i \cos\delta_i + C_i \cot\psi'_i$$

and

$$C_i = \rho_i \sin\delta_i$$

$$\omega_i = 90° + \delta_i - \omega'_i \tag{7-14}$$

$$\tan\omega'_i = \frac{d_i' - \rho_i \cos\delta_i}{C_i}$$

Then for an error in one of the outer stations d_i, τ_i and ϕ_7^i are given as

$$d_i = \frac{C_i}{\cos\omega_i'} \qquad i = 1, 2, 3 \tag{7-15}$$

$$\tau_i = d_i' \sin\beta$$

$$\cos\phi_7^i = \cos\psi'_i \cos\omega_i + \sin\psi'_i \sin\omega_i \cos g_i''' \tag{7-17}$$

Then the resultant error (h_i') in the interferometer measurements is given by the equation

$$h_i' = d_i \cos \phi \, _{74}^i - \tau_i \tag{7-18}$$

where $\phi \, _{74}^i$ is defined in equation (7-1)

The angular error which will result from the error (h_s) will equal

$$\Delta \epsilon_i = \frac{h_i}{L \sin \phi_{54}} \tag{7-19}$$

in which L is the interferometer baseline then

$$\Delta \epsilon_i = \frac{\sin \, ^V 5_j 49}{\sin \, ^V 5_k 45_j} \tag{7-20}$$

$$\Delta a_i = \frac{\cos \, ^V 5_j 49}{\sin \, ^V 5_k 45} \tag{7-21}$$

where the $_j$ and $_k$ refer to the respective interferometer and

$$\cos V_{ijk} = \frac{\cos \phi_{ik} - \cos \phi_{ij} \cos \phi_{jk}}{\sin \phi_{ij} \sin \phi_{jk}}$$

A ΔS_a and ΔS_e is defined in terms of Δa and Δe

$$\Delta S_e = R \cos g \, \Delta e \tag{7-22}$$

$$\Delta S_a = R \, \Delta a \tag{7-23}$$

R is the slant range

and

$$g = \phi_{94} + \sin^{-1} \left\{ \frac{R_4 \sin \phi_{94}}{R_e} \right\}$$

R_e is the earth radius. And finally, the vehicle error in latitude and longitude are given by

$$\Delta \text{Lat.} = \frac{\Delta S_e \cos \beta_e + \Delta S_a \sin \beta_e}{R_e} \tag{7-24}$$

$$\Delta \text{Long.} = \frac{\Delta S_e \sin \beta_e - \Delta S_a \cos \beta_e}{R_e \sin Z} \tag{7-25}$$

where $\cos Z = \cos f_4 \cos f_8 - \sin f_4 \sin f_8 \cos V_{498}$

$$\sin \beta_e = \sin f_8 \frac{\sin V_{498}}{\sin Z}$$

$$\sin f_i = \frac{R_i \sin \phi_{9i}}{R_e}$$

Equations (7-18) through (7-25) express the latitude and longitude error in terms of a_i; a distance error in interferometer orientation. However, a_i is given simply in terms of angular measurement error as

$$a_{ij} = \Delta \theta_{ij} \, L \sin \theta_{ij} \tag{7-26}$$

where θ is the angle measured from the interferometer axis to the line of sight with i representing the interferometer number and j the reference station.

In order to apportion input angular errors in θ_{ij} into both equipment and atmospheric errors, $\Delta \theta_{ij}$ is further resolved into component errors in the azimuth and elevation directions.

$$\Delta \theta_1 = \frac{\Delta \epsilon_1}{\sin V_{5_1 45_2}} \tag{7-27}$$

$$\Delta \theta_2 = \frac{\Delta \epsilon_2}{\sin V_{5_1 45_2}} \tag{7-28}$$

Equations 7-18 through 7-28 give the sensitivity factors for errors in measuring reference stations. The sensitivity factors for the vehicle position measurements are obtained from equations 7-20 through 7-25 with errors in latitude and longitude as functions of Δe_i and Δa_i. The radar range sensitivity factor is obtained from equations 7-24 and 7-25 and the following relationship

$$\Delta S_{e_R} = \Delta R \sin g, \quad R - \text{radar range} \tag{7-29}$$

The errors in latitude and longitude position can now be written as

$$\bar{\epsilon}_\rho \text{ lat.} = S_{2 \text{ lat.}} \, \bar{\epsilon}_R + \sum_{K=3}^{6} S_{K \text{ lat.}} \, \bar{\epsilon}_{\phi 1(K-2) a} +$$

$$+ S_{7 \text{ lat.}} \, \bar{\epsilon}_{\theta 1a} + S_{8 \text{ lat.}} \, \bar{\epsilon}_{\theta 2a} + \sum_{K=9}^{12} S_{K \text{ lat.}} \, \bar{\epsilon}_{\theta 2 (K-8) a} \tag{7-30}$$

where the $\bar{\epsilon}_i$ s are the bias errors in i and S_i s are the corresponding sensitivity factors. The subscript, a, denotes errors that are due to the atmosphere. The bias errors that are due to the equipment are assumed to be zero.

Then the longitude error, $\bar{\epsilon}_{p\,\text{long.}}$ is of exactly the same form as equation (7-30) except for the appropriate notation changes.

The random errors in latitude and longitude are given by

$$
\sigma^2_{p\,\text{lat.}} = S^2_{2\,\text{lat.}}\left(\sigma^2_{R_m} + \sigma^2_{Ra}\right) + \sum_{K=3}^{6}\left[S^2_{K\,\text{lat.}}\left(\frac{\sigma\theta_m}{3}\right)^2 + \right.
$$

$$
\left. + \left(S_{K\,\text{lat.}}\;\sigma\theta_{1(K-2)a} + S_{(K+6)\,\text{lat.}}\;\sigma\theta_{2(K-2)a}\right)^2\right] +
$$

$$
+ \sum_{K=9}^{12} S^2_{K\,\text{lat.}}\left(\frac{\sigma\theta_m}{3}\right)^2 + \left(S_{7\,\text{lat.}}\;\sigma\theta_{1a} + S_{8\,\text{lat.}}\;\sigma\theta_{2a}\right)^2 +
$$

$$
+ \left(S^2_{7\,\text{lat}} + S^2_{8\,\text{lat.}}\right)\sigma\theta_m^2 \tag{7-31}
$$

and similarly for longitude, $\sigma_{p\,\text{long.}}$. In these expressions, the atmospheric errors on measurements by the two interferometers on the same point on the earth's surface are assumed to be correlated. It is also assumed, that the error in measuring the vehicle is greater than that in measuring a reference station by a factor of three.

7.4.2.2 Sensitivity Factors

In this situation, one reference station is placed directly below the satellite and the other three stations are placed in a circle about the first station and are symetrically distributed. The interferometer arms are orthogonal. One arm is directed towards one of the outer reference stations. The vehicle is placed directly opposite this particular reference station at a distance such that the line of sight elevation angle is $5°$. The reference station circle is at approximately 90% of the distance between the user vehicle and the satellite. With this geometry, the sensitivity factors previously defined have the values shown in table 7-11.

TABLE 7-11

SENSITIVITY FACTORS

Factor	Error Source	Value	Units
S_2 lat.	R	0	nmi/nmi
S_3 lat.	θ_{11}	-879.03	nmi/rad
S_4 lat.	θ_{12}	3449.7	nmi/rad
S_5 lat.	θ_{13}	-6212.4	nmi/rad
S_6 lat.	θ_{14}	-6212.4	nmi/rad
S_7 lat.	θ_1	8489.6	nmi/rad
S_8 lat.	θ_2	0	nmi/rad
S_9 lat.	θ_{21}	0	nmi/rad
S_{10} lat.	θ_{22}	0	nmi/rad
S_{11} lat.	θ_{27}	0	nmi/rad
S_{12} lat.	θ_{24}	0	nmi/rad
S_2 long.	θ_R	.99619	nmi/nmi
S_3 long.	θ_{11}	0	nmi/rad
S_4 long.	θ_{12}	0	nmi/rad
S_5 long.	θ_{13}	0.	nmi/rad
S_6 long.	θ_{14}	0	nmi/rad
S_7 long.	θ_1	0	nmi/rad
S_8 long.	θ_2	739.97	nmi/rad
S_9 long.	θ_{21}	-71.04	nmi/rad
S_{10} long.	θ_{22}	228.94	nmi/rad
S_{11} long.	θ_{23}	-519.57	nmi/rad
S_{12} long.	θ_{24}	-519.57	nmi/rad

7.4.2.3 Atmospheric Errors

The atmospheric errors in the measured angles are calculated in terms of azimuth and elevation angles as shown in figure 7-16.

.Figure 7-16. Error Geometry

then

$$\cos \theta_1 = \cos E \cos A \qquad (7\text{-}32)$$

$$\cos \theta_2 = \cos E \sin A \qquad (7\text{-}33)$$

Solving for A and E

$$\sin A = \frac{\cos \theta_2}{\left[\cos^2 \theta_1 + \cos^2 \theta_2 \right]^{1/2}} \qquad (7\text{-}34)$$

$$\cos A = \frac{\cos \theta_1}{\left[\cos^2 \theta_1 + \cos^2 \theta_2 \right]^{1/2}} \qquad (7\text{-}35)$$

$$\cos E = \left[\cos^2 \theta_1 + \cos^2 \theta_2 \right]^{1/2} \qquad (7\text{-}36)$$

$$\sin E = \left[1 - (\cos^2 \theta_1 + \cos^2 \theta_2) \right]^{1/2} \qquad (7\text{-}37)$$

and the errors in θ_1 and θ_2 are

$$\epsilon_{\theta_1} = \frac{\partial \theta_1}{\partial E} \, \epsilon_E + \frac{\partial \theta_1}{\partial A} \, \epsilon_A \tag{7-38}$$

$$\epsilon_{\theta_2} = \frac{\partial \theta_2}{\partial E} \, \epsilon_E + \frac{\partial 2}{\partial A} \, \epsilon_A \tag{7-39}$$

and

$$\epsilon_{\theta_1} = \frac{\sin E \cos A}{\sin \theta_1} \, \epsilon_E + \frac{\cos E \sin A}{\sin \theta_1} \, \epsilon_A \tag{7-40}$$

$$\epsilon_{\theta_2} = \frac{\sin E \sin A}{\sin \theta_2} \, \epsilon_E - \frac{\cos E \cos A}{\sin \theta_2} \, \epsilon_A \tag{7-41}$$

Combining these relations

$$\epsilon_{\theta_1} = \operatorname{ctn} \theta_1 \left\{ \frac{1}{\left[\cos^2 \theta_1 + \cos^2 \theta_2 \right]^{1/2}} - 1 \right\}^{1/2} \epsilon_E - \frac{\cos \theta_2}{\sin \theta_1} \, \epsilon_A \tag{7-42}$$

$$\epsilon_{\theta_2} = \operatorname{ctn} \theta_2 \left\{ \frac{1}{\left[\cos^2 \theta_1 + \cos^2 \theta_2 \right]^{1/2}} - 1 \right\}^{1/2} \epsilon_E - \frac{\cos \theta_1}{\sin \theta_2} \, \epsilon_A \tag{7-43}$$

The bias error in elevation angle is shown in figure 7-17. The bias error in azimuth is assumed to be zero.

The random error in angular measurement due to the atmosphere is found as a function of the bias error for any given elevation angle, from the curve in figure 7-18. The random azimuth error is approximately equal to the elevation error, therefore,

$$\sigma^2_{\theta_{ij}} = \left\{ \operatorname{ctn}^2 \theta_{1j} \left[\frac{1}{(\cos^2 \theta_{1j} + \cos^2 \theta_{2j})^{1/2}} - 1 \right] - \frac{\cos^2 \theta_{2j}}{\sin^2 \theta_{1j}} \right\} \sigma^2_E \tag{7-44}$$

$$\sigma^2_{\theta_{2j}} = \left\{ \operatorname{ctn}^2 \theta_{2j} \left[\frac{1}{(\cos^2 \theta_{1j} + \cos^2 \theta_{2j})^{1/2}} - 1 \right] - \frac{\cos^2 \theta_{1j}}{\sin^2 \theta_{2j}} \right\} \sigma^2_E \tag{7-45}$$

The bias error in random range measurement due to refraction is obtained from the curve in figure 7-19. This figure shows range bias as a function of elevation angle. The elevation angle is derived from:

$$E_\pm = \cos^{-1} \left\{ \frac{(R_e + h) (\cos^2 \theta_{1j} + \cos^2 \theta_{2j})^{1/2}}{R_e} \right\} \tag{7-46}$$

The random error in range is small enough to be assumed negligible.
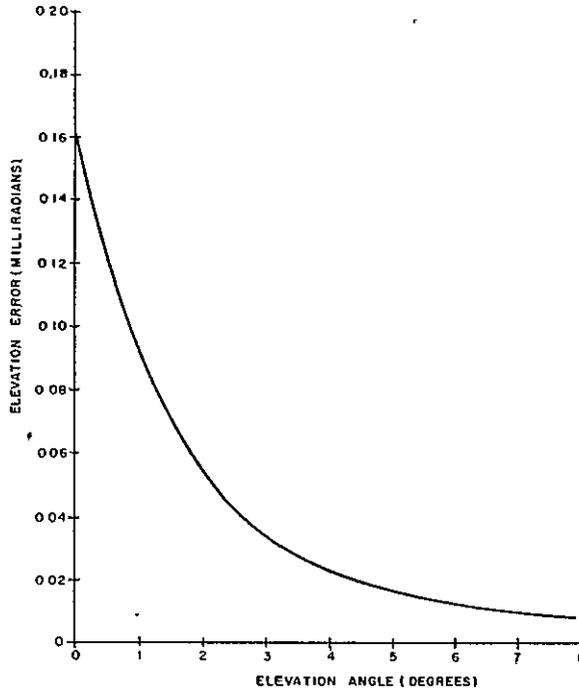
Figure 7-17. Elevation Bias Error vs Elevation Angle

7.4.2.4 Results

If there are no equipment errors in the system, the atmospheric error contributions are shown in table 7-12.

TABLE 7-12

ATMOSPHERIC ERROR CONTRIBUTIONS

Bias

Latitude	0.00464 nmi
Longitude	0.01854 nmi

Random

Latitude	0.069106 nmi
Longitude	0.010923 nmi
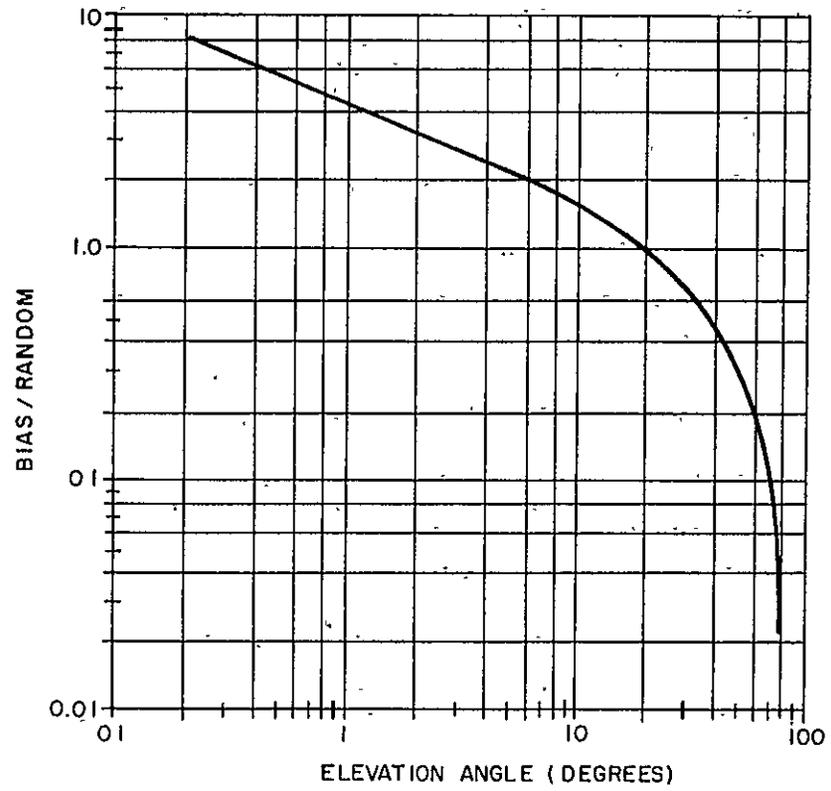
Figure 7-18. Conversion for Random Elevation Errors
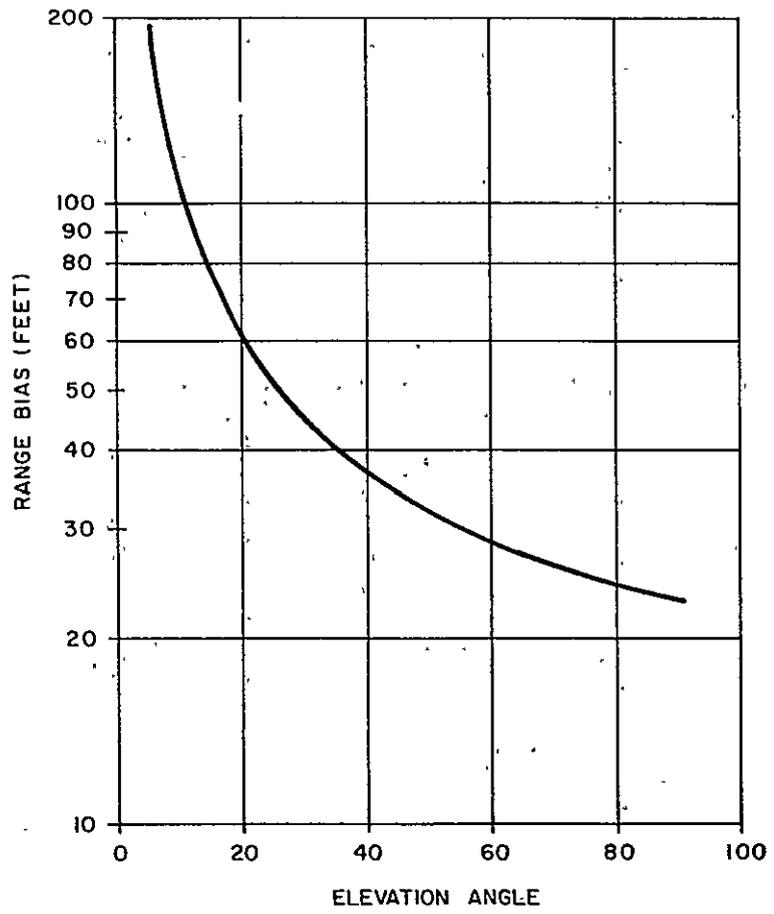
Figure 7-19. Atmospheric Range Bias

If the system is required to position the vehicle with an error no greater than one nautical mile with a 90 percent probability of confidence, then

$$\overline{\epsilon}_{\rho \text{ lat.}} + \sqrt{\left(1.6 \sigma_{\rho \text{lat. A}}\right)^2 + \left(1.6 \sigma_{\rho \text{lat. M}}\right)^2} = 1 \qquad (7\text{-}47)$$

$\sigma_{\rho \text{lat. M}}$ is the random error due to equipment inaccuracy with $\overline{\epsilon}_{\rho \text{long.}}$ and $\sigma_{\rho \text{ long.}}$ assumed to be negligible. For this case, $\sigma^2_{\rho \text{lat. M}}$ is found to be equal to 0.38223 nautical miles. Then from equation 7-31,

$$\sigma^2_{\rho \text{ lat. M}} = \sigma^2_{\theta m} \left[\frac{1}{9} \sum_3 S^2_{K \text{ lat.}} + S^2_{7 \text{ lat.}}\right] \qquad (7\text{-}48)$$

and assuming a 0.1 nmi accuracy in range, the angular accuracy required is 68..25 microradians for the vehicle measurement and 22.75 microradians for the reference station measurements.

7.5 EMERGENCY SITUATIONS

This section describes the method of alerting traffic control and the user to an emergency situation and of monitoring the remedial action.

7.5.1 Recognition of Emergency Situation

Traffic control shall be notified if any of the following symptoms exits:

a. Failure of a vehicle to respond to a "position fix" command after three attempts have been made within a five second time interval.

b. Receipt of an emergency condition code transmitted from a vehicle.

c. Failure of the system to operate normally in any respect.

Traffic control shall be supplied with all the available "fix" and weather information for each vehicle. From this information, traffic control shall determine which vehicles shall be notified of the possibility of collision, grounding, or other hazards.

7.5.2 Responsibility for Initiation and Direction of Emergency Action

Based on the information described in paragraph 7.5.1 traffic control shall determine when an emergency condition exists. Traffic control will originate all emergency messages and decide which vehicles are to be informed of the emergency condition. Traffic control determines the emergency services that the system provides to the distressed vehicle and to other vehicles in the area.

7.5.3 Emergency Message Format and Vehicle Display

The message format shown in table 7-13 shall be used to notify any vehicle of an emergency condition or to send emergency instructions to a vehicle.

TABLE 7-13

EMERGENCY MESSAGE FORMAT (SATELLITE TO VEHICLE)

Item	Description	No. of Bits
1.	sync	6
2.	Function command (vehicle report)	4
3.	Vehicle address	24
4.	Position code (binary)	20
5.	Alarm (on-off)	4
6.	Information code (100 possibilities)**	8

    1. collision is imminent, change course as follows

    2. fix information

    3. unchartered danger at following location

    4. change course as follows to aid distressed vehicle at following location

    5. change course as follows to avoid iceberg at following location

    ---

    00

Item	Description	No. of Bits
7.	latitude (as per item 6)	20
8.	longitude (as per item 6)	24
9.	time of fix**	24
10.	$\overline{V}$ or range* (as per item 6)	8
11.	$\overline{H}$ or bearing* (as per item 6)	12
12.	weather report (as per item 6)	28
13.	error detection code (not displayed)	8

*Not displayed on visual display

**The information code will be displayed in the "seconds" position of the time of fix display.

7.5.4 Acknowledgement of Emergency Message

The user vehicle shall be equipped to respond, via the offset transmitter, to any emergency instruction. The response format is given in table 7-14. The response will acknowledge receipt of the emergency message and shall indicate compliance with the message content.

TABLE 7-14
MESSAGE FORMAT OVER OFFSET CHANNEL (VEHICLE TO SATELLITE)

Item	Description	No. of Bits
1.	sync	6
2.	Function command (10 possibilities)	4
	1. emergency (class I)	
	2. emergency (class II)	
	3. enter system	
	4. exit system	
	5. acknowledge, yes	
	6. acknowledge, no	
	7. increase fix rate	
	8. return to normal operation	
	9. repeat report (internally generated by error detection circuit)	
	0. (available for use)	
3.	vehicle address	24

The system shall be capable of changing the position fix rate of any vehicle as directed by traffic control. By increasing the fix rate of vehicles in the emergency area, the vehicles may be "tracked" by traffic control.

7.6 SYSTEM CONSIDERATIONS FOR PROVIDING HIGH ACCURACY POSITION INFORMATION FOR SPECIAL CLASSES OF USERS

The objective of this contract has been to obtain position information for the general user to an accuracy of one nautical mile. In achieving this objective, considerable emphasis has been placed on minimum cost of the equipment on the user vehicle and minimum cost and weight of the satellite. There are some users, such as the Coast and Geodetic Survey ships, who would prefer to have a considerably greater accuracy. However, these requirements are basically outside the scope of this contract. Greater accuracy implies more cost. Since a vast majority of the users are not interested in this accuracy, it is unnecessary to burden them, or the overall system, with any significant increase in cost which can be associated with a generally more accurate system. However, there is one approach for achieving greater accuracy which would be acceptable and which has been given some consideration.

For the high accuracy user, the requirement for the equipment to be of very low cost can be considerably relaxed. It is acceptable to ask the user who is getting extra service to buy the more expensive equipment. The problem of achieving greater accuracy for special users, then reduces to the problem of determining means for increasing accuracy by introducing major changes into the equipment on the user vehicle but, only minor changes into the remaining system.

Within this acceptable framework for achieving greater accuracy the problem reduces to two parts. For an accuracy of the order of 0.1 nautical miles, one set of techniques is appropriate. For an accuracy of the order of 100 feet, another set of techniques shall be employed. These techniques are essentially independent of each other. Any particular user has the option of selecting those techniques which are most appropriate.

7.6.1 Accuracy Increase to 0.1 Nautical Miles

In order to achieve an accuracy of 0.1 nautical miles for all users that are willing to carry the extra equipment, two techniques shall be used. These techniques employ increased radiated energy from the user vehicle plus a multiplicity of position measurements.

7.6.1.1 Increased Vehicle Power or Antenna Gain

In order to determine means for achieving greater accuracy, one approach is to examine those factors which limit the accuracy of the unmodified equipment. The major contribution of error to this system comes from the thermal noise in the angle measuring interferometer. If the effective power radiated from the ground is increased, this error can be reduced. It can be shown, that the reduction in angle error will be equal to the increase in the ratio of signal voltage to noise voltage at the output of the interferometer receivers. The increased power from the ground can be obtained by either increasing the power generated or increasing the antenna gain; or both. The cost of increasing the power is basically the cost of the larger transmitter. The cost of increasing the antenna gain is essentially the cost of the larger antenna plus the cost of steering so that it will point its beam toward the satellite. Both of these costs are, of course, completely associated with the user vehicle equipment and therefore represent acceptable costs for achieving the desired objective.

Unfortunately, thermal noise in the interferometer is not the only contributor to error in the navigation system. Increasing power will achieve an improvement only to the point where the original second order errors now become primary errors. The point that this occurs is a function of the remaining system. Now, the design work on any portion of the original system was considered completed when the error from that portion of the system was reduced to a minor role in comparison to the interferometer noise error. Thus, it is found that the limit of accuracy for the special user is determined by the errors which were unexplored for the general user. The question then remaining is, how much improvement can be achieved without any real cost to the system by a more careful examination of these errors? There does not appear to be anything fundamental about any of the equipment errors. In the critical satellite location the reduction in these errors is basically dependent on increasing the precision of the hardware. Because of the nature of hardware, many of the tolerances required for the general user will be easily exceeded; leaving only a few critical items the improvement of which must be weighed according to their cost. The fundamentally limiting error of the high accuracy system will be the atmospheric propagation errors. These errors can be considerably reduced by making calibration corrections based on surface

refractometer data taken at the reference stations. It has been considered outside the scope of this contract to make the hardware and propagation investigations needed for a determination of the high accuracy system. Thus, it is not possible to specify how much increase in power or antenna gain should be inserted at the user vehicle nor the effectiveness of this increase. It would however appear, that an increase in power or antenna gain of about 15 db would almost certainly make possible an increase in the accuracy of the system by a factor of four.

7.6.1.2 Increased Data Rate to Vehicle

The basic accuracy of the system is the accuracy achieved with one single measurement. If multiple measurements are taken and an average position is determined from the sum of all of the measurements, then the resulting accuracy will be greater than that of any one measurement. If the individual measurements are statistically independent, that is, if there are no bias errors that persist throughout a multiplicity of measurements, then the error of the average position will be smaller than the individual errors by a factor equal to the square root of the number of measurements. If, for example, there are nine measurements, then the error of the average will be one third the error of the individual measurements. In achieving this type of improvement, it is important that the measurements be independent. In the system described in this report, bias errors are removed by calibration from signals coming from fixed reference stations at known locations. This calibration is repeated once a second. Thus, it would be expected that if any bias errors were to accumulate over an interval of a second, they would be eliminated at the next calibration interval of a second. Therefore, if the measurements are taken once a second they should be nearly independent. Of course, there are some errors which do not fit into this category. The most important of these are the propagation errors. However, these errors are amenable to compensation from data taken at the reference stations. The ranging system is somewhat different because it is not re-calibrated every second. This, however, becomes unimportant since the range error on a single sample is only 0.1 nautical miles and the bulk of this error can be attributed to the thermal noise that is statistically independent from measurement to measurement. Thus, it would be expected that nine measurements, spaced with intervals of a second, should produce the nine essentially independent measurements that are needed to achieve a factor of three improvement in accuracy.

It should be noted, that these nine measurements do cost the overall system a reduced traffic capacity. However, since the high accuracy special type of users are expected to be very small in number, increasing their data rate by a factor of nine would have only a negligible effect on the overall traffic capacity and this would be considered acceptable.

From the preceding considerations, it would not appear desirable to attempt to push either the increased power technique or the averaging technique to the point where a 0.1 mile error would be realized. However, a combination of the two techniques would appear to make the desired accuracy achievable.

7.6.2 Accuracy Increase to 100 Feet

The accuracy increase described in the preceding section would be available to any type of vehicle at any time provided only that the user be willing to carry the extra equipment. When an accuracy of 100 feet is required, it is found that such general service will not be available. For example, it will not be possible to provide such an accuracy to aircraft. Fortunately, it does not appear that there is any need for this accuracy by this type of vehicle. The approach taken will not provide general service to all users but will study the requirement of the specific users in order to meet their particular requirements.

7.6.2.1 Stationary User

All very high accuracy users, who are at non-moving positions on earth, can be lumped into a single class. An example of this is the U.S. Geological Survey. They are interested in a convenient means to measure the location of points to an absolute accuracy of 100 feet. With this type of user, range data alone can be utilized to determine positions. The principal error, normally associated with range only systems, comes from uncertain motion of the user. For the stationary user, this error is eliminated. This essentially reduces the error to that of the ranging equipment.

For the general user, range accuracy for the designed equipment is 0.1. To achieve a greater range accuracy, a modification to the system shall be introduced. Unfortunately this modification will have to be made to the user equipment and to the satellite and ground equipment. The extra cost of the user vehicle equipment will not be a problem and the ground equipment cost should be negligible. Thus, the modification to the satellite becomes the most critical item. In the equipment designed for the general user, a pulse packet of energy, having a complicated wave shape, is generated and then relayed via hetrodyne repeaters from the ground, to the satellite, to the user vehicle, back to the satellite, and then to the ground. The final pulse received is processed by the ground equipment to yield range information with an accuracy of 0.1 nautical miles. An improvement by a factor of ten can be achieved in the system accuracy. First, the original pulse of energy generated at the ground can be divided into two pulses of energy. Each pulse has a bandwidth equal to that of the original pulse. Next, the second pulse is shifted in frequency by 500 kilocycles and the entire signal radiated from the ground. The satellite and user equipment must now be modified to relay both pulses. The procedure, which can be used at both locations, is to employ hetrodyne receivers that shift their local oscillators by 500 kilocycles between the reception of the first and second pulses. On transmission, these repeaters will shift the signal back by the same 500 kilocycles so the radiated signals will maintain the desired frequency separation.

By the utilization of this technique, the only change in the equipment at the satellite will be the replacement of a fixed hetrodyne oscillator with an oscillator capable of shifting the frequency by 500 kilocycles. The associated circuitry to tell the oscillator when to shift shall also be included. With this modified equipment, it will be possible to make range measurements accurate to 60 feet. Therefore, navigation fix accuracies of approximately 100 feet would be realized. For user equipment at known altitudes, postion data can be obtained from one pass of a satellite provided its path does not pass near the zenith. For unknown altitudes, two passes of a satellite should be employed to achieve the greatest accuracy.

The degree of equipment modification required at the satellite appears to be minor and therefore a stationary user can be accommodated within the framework of this system.

7.6.2.2 100 Foot Accuracy For Moving Ships

Having provided very high accuracy for the stationary user, there now remains only one type of user requiring this service. This is the moving ship. Unfortunately, the motion of the ship destroys the possiblity of using range from a single satellite to determine position. For this purpose, even a ship adrift at sea will be moved enough by winds and current to completely destroy the accuracy of the system. However, there is one factor which may be employed to avoid this difficulty. There does not appear to be any moving vehicle which continuously requires 100 foot accuracy data. For example, the Coast and Geodetic Survey ship can normally operate with an accuracy of 0.1 miles. For the few occasions that an accuracy of 100 feet is required, they are quite willing to wait until the circumstances to achieve this accuracy are satisfactory. This gives the system the right amount of flexibility. If range data from a multiplicity of satellites are obtained simultaneously, then the errors resulting from vehicle motion do not appear. Since the vehicle is a ship located at the known altitude of the ocean surface, two satellites viewed simultaneously are adequate to determine position. Thus, if the satellites are modified to obtain the high accuracy range information described in the preceding section, ships may obtain precision navigation information by the process of waiting until two satellites are in suitable positions for simultaneous measurements.

The basic system, described in the report, measures range and angle to the navigating user vehicles. As a result, only one satellite need be in view to obtain navigation information. The number of satellites launched will therefore be those necessary to provide single coverage over the earth. However, regardless of the method of obtaining single coverage, multiple coverage over some portions of the globe will be unavoidable. For example, if the satellites are launched in two orthogonal planes, double coverage will occur near the axis of the two intersecting planes. If this axis is inclined at 45 , there will be a double coverage zone in northern latitudes and a double coverage zone in southern latitudes. As the earth

rotates, any vehicle on the earth will pass one or the other of these double coverage zones at least once a day. During this period, the very high accuracy data for the moving ship can then be obtained.

Unfortunately, the ability to see two satellites simultaneously is not entirely sufficient for navigation purposes. There are, in fact, four conditions which must concurrently fulfilled before a navigation fix can be obtained. First, the user shall be able to see two satellites. Second, neither of these satellites can be near the zenith. Ranging information becomes valueless when the satellite is directly overhead. Third, the two satellites cannot be near the same azimuthal plane. For example, if they are both in the same aximuthal plane, their ranging lines will be tangent to each other at the location of the user vehicle. The position data in one direction therefore will be valueless. This would not occur if the azimuth angles of the two satellites were nearly separated by $90°$. The fourth requirement is that both satellites be within view of one ground station. The ground stations shall be arranged so that all satellites will be seen by at least one ground station. Unfortunately, the two satellites seen by the user vehicle may be visible only to two different ground stations. In this circumstance, navigation fix information can be obtained only by processing the raw data between ground stations. While it is possible to do this, it is felt that this degree of complexity should be avoided.

Although there appears to be a number of things that must happen simultaneously in order for very high accurancy information to be available, there will still be reasonably large time periods available for this information. The ground stations can be programmed to track the satellites and to inform any special user, on request, the time for the next high accuracy interval. This mode of operation appears to be satisfactory to all the users requiring this information.

7.6.3 Summary

Accuracy of approximately 0.1 nautical miles can be obtained for any user who is willing to carry more expensive equipment. This can be done without any alteration to the satellite equipment. It would involve more careful design for accuracy than might otherwise be necessary.

Accuracy of approximately 100 feet can be supplied to all users who required this type of information. To do this, the ground equipment, the satellite equipment, and the user vehicle equipment all must be modified. It appears that the modification in the critical location of the satellite would be sufficiently minor to make such an alteration acceptable.

8. SYSTEM EVALUATION

The evaluation of a system is made on the basis of its effectiveness and cost. This section contains discussions of the effectiveness of the Navigation Satellite System. Costs are discussed in the following section.

Effectiveness of a system concept is measured in terms of the benefits gained from performing its mission, its capabilities to perform its mission, the feasibility of implementing the concept, and any bonus features which might accrue in implementing the system. Each of these factors is discussed below for the Westinghouse Navigation Satellite System.

8.1 USER BENEFITS

Ships and air craft, especially at sea, now have no way of accurately determining their positions at all locations and under all conditions. The navigation system proposed here will provide frequent and accurate position information to traffic control centers, and to participating ships and aircraft, on a worldwide, all-weather basis. Receipt of this information will mean two things to the user:

1. Increased safety
2. More effective utilization of equipment.

Since the positions of all participating ships and aircraft will be continuously monitored by the responsible traffic control agency, the air/sea rescue problem is greatly reduced. At present, when a ship or aircraft crashes or sinks at sea, large areas must be searched for survivors. But this system determines the position of each vehicle within every 100 miles of travel. Therefore, the maximum search area can be confined to a 100 mile circle about the last reported position, if a vehicle fails to report at its next fix interrogation time. Since the mean velocity and heading of the vehicle are also available at the ground control station, the search area can be still further reduced and accurately pinpointed.

Because the system also provides a relay function between the user vehicles and the traffic control agencies, the user vehicles can receive warnings of uncharted dangers, bad weather, heavy traffic areas, and other vital information. In addition, the traffic control agency can advise the vehicle of the safest and fastest route which will avoid these dangers. This warning capability will mean fewer accidents.

This data relay is a two way channel. Therefore, the user vehicles can alert the cognizan traffic control agency of an emergency, real or impending. The system can then increase the fix rates and track the vehicle right to splash. This track capability reduces the search area to a one mile circle.

The combination of the position monitoring by the traffic control agencies and the data relay capability provide an additional benefit. When an emergency situation arises, vehicles in the area of the vehicle in trouble can be requested to lend aid. In fact, airplanes going down over the open sea could be vectored to the vicinity of the nearest ship.

In addition, the user vehicle, by adding to his basic equipment, can receive and display the positions of all vehicles in his immediate area. This capability, provided at only a small increase in cost to the user, has obvious advantages in heavy traffic areas or bad weather.

Therefore, the implementation of this navigation system will mean fewer accidents resulting in a saving of both lives and equipment. In case of an accident, this system will enable search and rescue forces to be alerted immediately, to know accurately the position of the vehicle at the time of the emergency, and to know what vehicles are in the area to participate in rescue operations. Also, the Air/Sea Rescue Service can direct the rescue operations remotely. Thus, many lives that are normally lost in a crash or sinking will be saved.

Besides increased safety, implementation of a navigation system of the type discussed in this report will mean lower operating costs and more effective utilization of equipment. First, by obtaining frequent and accurate position fix information, the master of a ship or pilot of an aircraft can approximate more closely a pre-planned optimum course. Thus, more rapid transit times can be made. This means more distance, and hence, more ton-miles or passenger-miles in a given time. Warnings of storms and hazards provide the user with the capability to choose the optimum course for avoiding these dangers. This will result in faster passages through bad weather and decreased costs from weather damage.

The amount of data that a merchant ship must return to its home office during a voyage is extremely small. However, the law now requires these vehicles to have radio equipment for emergency functions. The system described here performs the emergency function. It can also handle the small amount of data exchange between the vessel and its home office with little increase in cost and complexity, eliminating the necessity for the vessel to carry an additional expensive piece of radio equipment. Also, since the equipment that this navigation system will place on the vessel is inexpensive, reliable, and requires no operator in attendance, the need for a radio officer on board will be eliminated. These two factors will result in a continuous saving in costs per voyage. The costs per ton-mile or passenger-mile are correspondingly lowered.

Thus, implementation of this navigation system will result in more ton-miles or passenger miles for a participating user vehicle in a given time. It will also result in a lower cost per ton-mile or passenger-mile.

8..2 PERFORMANCE

The Navigation Satellite System considered here will gather position data on participating ships and aircraft, and provide an accuracy of one nautical mile, 90 percent of the time. This means that the bias plus one sigma errors in user vehicle position will not exceed 0.6 nautical miles, with the method of calibrating interferometer constants and claculating the position fix, previously described.

This navigation system is required to provide fixes at rates between about 13,000 and 36,000 per hour, depending upon the time period. The system described above will provide fixes at the rate of 3600 per hour. It is, then, an interim system, and because of the natural reluctance of users to accept a new idea, its fix rate will be entirely adequate for the first few years of operation. As the system effectiveness is demonstrated to ship and aircraft users in terms of increased safety and profits, the required fix rate will begin to approach the required values stated, as justified by the number of users. The present system fix rate can be increased to 18,000 per hour with no increase in system cost. This rate will be adequate beyond 1980. When the fix rate exceeds 18,000 per hour, larger boosters will be required, resulting in increased system cost.

In addition to its primary function of gathering position information, the Navigation Satellite System is required to provide a data link between traffic control centers and user vehicles. It is shown above that the system can relay all the data required by the user vehicles. This relay function will be accomplished with high reliability, at high speed, and at a negligible contribution to system cost.

The speed factor is very important with respect to the reporting of position fix information to the user vehicles. The system will make the position fix and report it to the traffic control center and the user vehicle in less than one second. This means that for the fastest vehicle, the supersonic transport, the reporting of the position fix will coincide with determination of position fix for a travel distance of less than 0.5 nautical miles. This distance is within the accuracy of the fix, and hence, is entirely adequate.

The final function to be performed by the system is the gathering of general data from remote locations. This data can include weather and oceanographic information. It is shown in the previous discussions that data bandwidths up to 100 kilocycles can be handled with this system at low error rates with no increase in system cost. These data bandwidths are more than adequate for the remote data gathering and data dispersal functions which the system will be required to perform at any future date.

8.3 FEASIBILITY

The system described in this report is technically feasible under the projected state-of-the-art. The user vehicle and reference station subsystems are feasible under the current state-of-the-art. The most critical component in these subsystems is the

transmitter power tube. An existing tube has been found which meets the requirements for performance and reliability.

The ground control station is also feasible under the present state-of-the-art. Existing general purpose computers have sufficient speed and storage capacity to perform the data handling and processing required in this system.

Extensions in the state-of-the-art are required in the satellite subsystem, both in the satellite itself and in the launching system. Power and reliability are a problem in the spacecraft. Currently available transmitter power tubes that meet the power requirements are not sufficiently reliable to be economically feasible. In addition, tubes are inefficient due to the large filament powers required. However, high power, high frequency semi-conductor amplifiers, which are both efficient and reliable, are not yet available. Therefore, an extension in the state-of-the-art is required in this area.

Work is currently being performed on long life tubes for space applications, and on high power, high frequency semiconductor amplifiers. Since this system will not become operational prior to 1970, it is reasonable to expect that by then, one or both of these devices will be available. The tubes currently available can provide the power outputs required for short life, experimental spacecraft.

To achieve zero outage time for periods of three to five years requires low drift rates of the satellites relative to each other. This, in turn, requires precise injection into orbit. Velocity accuracy is most critical, but currently available guidance systems will not give sufficient accuracy. Advanced tracking and guidance systems are now being studied by various missile test range contractors which will provide the required accuracy. These systems are expected to be available by the time this navigation system becomes operational.

High injection accuracies are not required for an experimental system since multiple satellites for worldwide, continuous coverage will not be required at this stage. Hence, relative satellite spacing is not critical for the experimental system.

Therefore, the equipment and techniques necessary to implement the experimental system are currently available. Development programs are currently being pursued for the critical equipment and techniques necessary to implement the operational system. It is reasonable to expect that these critical equipments and techniques will be available prior to the operational date of this navigation system.

8.4 BONUS FEATURES

The navigation system discussed here is required to provide position accuracies of one mile. However, for a special class of user, the Geological Survey and the Coast and Geodetic Survey, much higher accuracies are necessary to effectively perform their mission. Techniques are described elsewhere in this report, which are easily incorporated into the system, and which will satisfy the requirements of this special class of user.

The system is ideally suited to the performance of a multi-purpose mission. This is evidenced by the large data bandwidths which the system can handle in a data gathering mode with no increase in system cost. This increase indicates that booster capabilities are not being effectively utilized. Therefore, additional functions which this satellite system can perform within the framework of a minimum cost as determined in this study, should be investigated. Adding additional functions to the satellite until the system cost begins to markedly increase, will insure maximum effectiveness for a given cost.

9. SYSTEM COSTS

The estimated costs for development and achievement of initial operational capability are summarized in table 9-1. Funds are shown by the fiscal year in which they would be obligated, rather than expended.

The basic operational system would consist of one ground control station, eight reference stations, and 8 medium altitude satellites; 4 each in two orthogonal orbits at 55 degrees inclination. This system will provide complete coverage for all ships and aircraft in the North Atlantic Ocean, Caribbean Sea, and eastern Pacific Ocean areas.

Extension of the system to give complete world-wide coverage would not require more satellites but would call for additional ground control stations and reference stations as discussed in Section 6. 1. Cost for implementing additional ground stations are not given here, because they will depend on the specific locations involved. In any event, the cost for each additional control station will be lower than for the first ground complex. The design concept for the ground control station is one of modular increments, since the capacity (and therefore the amount of equipment required) will be a function of the user activity in the control station's sector. Additional ground stations will have much less traffic to handle than the basic, or initial, system control station. Thus both investment and operating costs of each additional station will be only a portion of the corresponding estimates for the initial ground control station.

Table 9-1 includes all system operating costs through fiscal year 1972, as a part of the development flight program. Post-1972 operating costs are estimated at $24 million per year, including an allowance for launching an average of 4 satellites per year.

Development of the user equipment for both ships and aircraft is included, together with procurement and maintenance of approximately 100 equipments for experimental use aboard host ships and aircraft during the development program. However, operational user equipment is not included in the costs, since it is assumed that these will be purchased or leased by the user. The production unit price of 1 set of user equipment is estimated at $5,000.00. In the event leasing is adopted, the monthly rental to the user will be about $125.00. Equipment for some of the special, or bonus, system services discussed in the report will be more expensive. User equipment price reductions below the $5,000.00 level will be encouraged by designing the equipment so that a number of manufacturers will be qualified to market the sets.

Table 9-2 shows the recommended launch schedule on which the cost estimates are based.

Tables 9-3, 9-4, and 9-5 are breakdowns of table 9-1. The following assumptions apply to the development flight program estimates:

1. The main development of Super Delta or a booster with equivalent weight lifting capability will not be charged to this program.

2. The gravity gradient stabilization technology program now contemplated by NASA and DOD will be carried out.

3. The development integration of Super Delta with the spacecraft will be carried out on this program.

TABLE 9-1

NAVIGATION SATELLITE BASIC OPERATIONAL SYSTEM SUMMARY
OF ESTIMATED PROGRAM FUNDING REQUIREMENTS
(Exclusive Of NASA In-House Support)
Millions Of Dollars

- Fiscal Years -

	1964	1965	1966	1967	1968	1969	1970	1971	1972	Total R&D	Prod.
Development Flight Program	$ 0.5	$ 4.3	$11.3	$16.2	$22.1	$21.0	$16.7	$ 2.6	$ 2.6	$98.3	
Supporting Research & Technology	1.0	3.9	6.5	4.8	6.5	6.5	*	*	*	29.2	
Additional (Production) Investment						12.0	39.0	27.0			78.0
Construction (1 Ground Control Station)					1.0					1.0	
										128.5	78.0
	$1.5	$ 8.2	$17.8	$22.0	$28.6	$39.5	$55.7	$29.6	$ 2.6	$206.5	

* Supporting R & T funds not envisioned for FY1970-72 period. May be required depending on future developments.

TABLE 9 - 2

RECOMMENDED LAUNCH SCHEDULE

Mission	Launch Vehicle	Launch Calendar Yr.	Launch Location
Interferometer Experiment (Piggyback on Tech. Satellite)		1966	
Development Satellites			
1 flight	TAD	1967	AMR
2 flights	TAD	1968	AMR
2 flights	TAD	1969	AMR
3 flights	Super Delta	1970	AMR
Operational Satellites			
8 flights	Super Delta	1971	AMR.
4 flights	Super Delta	1972	AMR

TABLE 9 - 3

DEVELOPMENT FLIGHT PROGRAM FUNDING REQUIREMENTS
Millions Of Dollars

Fiscal Years –

	1964	1965	1966	1967	1968	1969	1970	1971	1972	Total
Spacecraft & Subsystems	$ 0.5	$ 2.5	$ 4.6	$ 8.4	$10.0	$11.2	$ 7.1			$44.3
Launch Vehicles			2.7	2.7	5.4	6.2	7.0			24.0
Ground Control Station Equipment		0.5	3.3	2.6	3.1	1.2				10.7
Ground Control Station Operations				0.8	1.5	1.8	2.0	2.0	2.0	10.1
Equipment for Reference Stations & Experimental Users		1.3	0.5	1.2	1.5					4.5
Data Reduction & Analysis			0.2	0.5	0.6	0.6	0.6	0.6	0.6	3.7
Total Direct R & D	$ .5	$ 4.3	$11.3	$16.2	$22.1	$21.0	$16.7	$ .2.6	$ 2.6	$97.3
Construction: Ground Station				$ 1.0						1.0

Total Including Construction $98.3

TABLE 9 - 4

SUPPORTING RESEARCH & TECHNOLOGY FUNDING REQUIREMENTS
Millions of Dollars

- Fiscal Years -

	1964	1965	1966	1967	1968	1969	Total
Navigation System Research	$ 0.4	$ 0.7	$ 1.5	$ 1.5	$ 2.5	$ 2.5	$ 9.1
Angle Measurement Techniques	0.6	1.3	0.9	0.8	0.8	0.8	5.2
Synchronous Navigation Satellite Studies		1.0	2.5				3.5
Component Development		0.7	1.0	1.0	1.0	1.0	4.7
Advanced Component Development		0.2	0.6	1.5	2.2	2.2	6.7
Total Direct R & D	$ 1.0	$ 3.9	$ 6.5	$ 4.8	$ 6.5	$ 6.5	$29.2

TABLE 9 - 5

ADDITIONAL INVESTMENT FUNDING FOR BASIC OPERATIONAL SYSTEM
Millions Of Dollars

- Fiscal Years -

	1969	1970	1971	Total
Spacecraft	$ 4.0	$12.0	$ 8.0	$24.0
Launch Vehicles	7.0	21.0	14.0	42.0
Ground Control Station Equipment*		5.0	5.0	10.0
Equipment for Reference Stations*	1.0	1.0		2.0
Total Procurement	$12.0	$39.0	$27.0	$78.0

* Modular additions to development ground station complex to implement full operational capability with one ground
control station

APPENDIX A
RADAR RANGING ANALYSIS AND PARAMETER CALCULATIONS

A. 1 INTRODUCTION

A relatively simple analytical technique can be used to calculate performance and parameters of simple radar and communication systems. The straightforward radar range equation, or a modification thereof, is applicable to the cases of point-to-point transmission and reflecting-target detection. The subject Navigation Satellite System, however, requires a more involved analysis. The features of the Navigation Satellite System responsible for this are: (1) each of the three heterodyne repeaters in the signal path contributes some thermal noise to the composite signal, which is subsequently amplified and transmitted; also, (2) the presence of four transmitters in the path causes a four-way trade-off of transmitted power in order to obtain the signal-to-noise ratio required for range measurement, (3) an additional complication in the use of linear-FM pulse compression to obtain the necessary equivalent peak power.

In this Appendix, a mathematical model is presented and analyzed; parametric constraints are examined; and values substituted. The resultant trade-offs are then examined to determine the best combination of transmitted powers. The resultant transmitter powers are as follows:

Transmitter	Peak Power
Ground Station	44 watts
Satellite (to Vehicle)	5,000 watts
Satellite (to Ground)	2 watts
Vehicle	3,600 watts

A. 2 MATHEMATICAL MODEL OF ON-GROUND RADAR RANGING

This section derives the expressions for signal-to-noise ratio in the satellite, vehicle, and of most importance, the ground station when: (a) radar range measurement is done at the ground station and (b) the satellite and vehicle portions of the radar act as heterodyne repeaters.

A. 2. 1 Signal and Noise Diagram

Figure A-1 illustrates the location of the signal and noise power sources of the radar system. Also shown are the flow paths of the composite signals within and between units of the system.
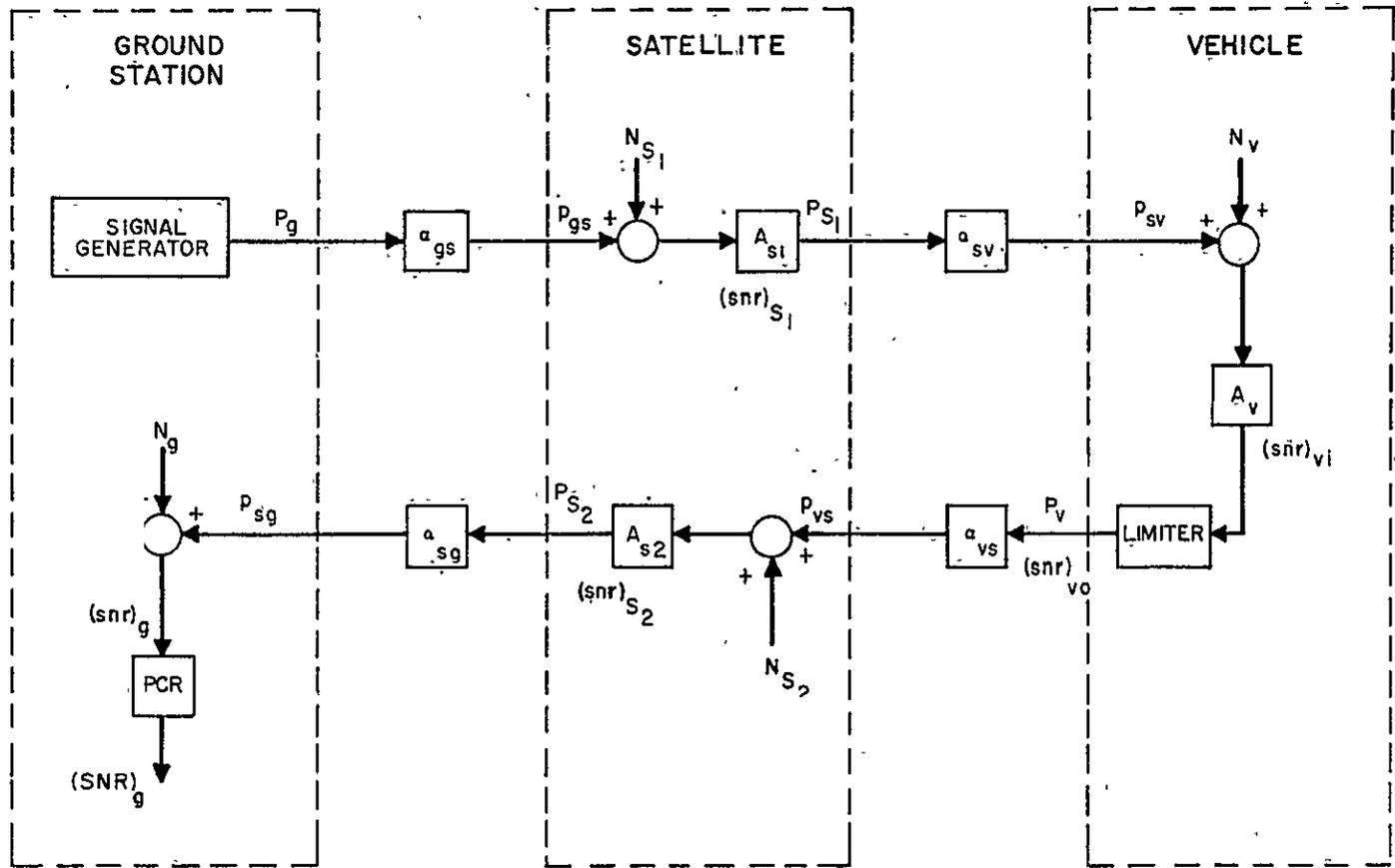
Figure A-1. Signal and Noise Diagram

A. 2. 2 Parameters

Tabulated below are the symbols and subscripts describing the various parameters needed in the derivation.

A. 2. 2. 1 Symbols

A	= power gain of repeater
B	= bandwidth
b	= normalized bandwidth
F	= noise figure
f	$\doteq$ RF carrier frequency
f( )	= a function of ( )
G	= antenna gain
K	= Boltzmann's constant
k_n	= noise adjustment factor due to limiting
k_p	= power reduction factor due to narrowbanding
k_s	= signal adjustment factor due to limiting
k_T	= snr transformation factor
L	= power losses
N	= receiver noise power
n	= noise component at the amplitude limiter
P	= transmitter peak power
p	= received power
PCR	= pulse compression ratio
R	= range
S	= signal component at the amplitude limiter
SNR	= signal-to-noise power ratio, compressed pulse
snr	= signal-to-noise power ratio, stretched pulse
T_a	= antenna noise temperature
T_s	= average sky temperature
T_e	= effective receiver noise temperature
w	= normalized power transmitted by ground station
x	= normalized power transmitted by satellite in outward link
y	= normalized power transmitted by vehicle
z	= normalized power transmitted by satellite in return link
α	= transfer constant from transmitter to receiver
λ	= RF wavelength

A. 2. 2. 2 Subscripts

g	= ground station
i	= limiter input

o = limiter output

r = receive (antenna)

s_1 = satellite in outward link

s_2 = satellite in return link

t = transmit (antenna)

v = vehicle

v_i = in vehicle before limiting

v_o = in vehicle after limiting

gs = transmission from ground station to satellite

sv = transmission from satellite to vehicle

vs = transmission from vehicle to satellite

sg = transmission from satellite to ground station

The superscript (') refers to the value after bandwidth narrowing.

A.2.3 Derivation

A.2.3.1 Ground-to-Satellite Path

The transmitter at the ground station generates a stretched linear FM pulse of peak power P_g. In travelling to and entering the satellite receiver, the pulse suffers a net attenuation of

$$\alpha_{gs} = \frac{G_g G_{s_1} (\lambda_{gs})^2}{(4\pi)^2 (R_{gs})^2 L_{gs}} \tag{A-1}$$

so that the power reaching the satellite receiver is the

$$\text{Useful Signal Power} = p_{gs} = \alpha_{gs} P_g \tag{A-2}$$

The satellite noise power, with which p_{gs} shall compete, is the

$$\text{Effective Noise Power} = N_{s_1} = K (T_e)_{s_1} B_{s_1} \tag{A-3}$$

and the first of four normalized power parameters can be defined as

$$W = \frac{\alpha_{gs} P_g}{N_{s_1}} \tag{A-4}$$

which is useful later in the derivation.

The effective signal-to-noise ratio, i.e., the ratio of (A-2) to (A-3), is:

$$(\text{snr})_{s_1} = \frac{\alpha_{gs} P_g}{N_{s_1}} = W \tag{A-5}$$

In this case the snr is identical to the normalized power parameter. This will not be true at subsequent repeaters, however, where additional noise causes snr degradation.

A.2.3.2 Satellite-to-Vehicle Path

The gain of the satellite repeater is defined as the transmitted output divided by the front-end power; that is:

$$A_{s_1} = \frac{P_{s_1}}{\alpha_{gs} P_g + N_{s_1}} = \frac{P_{s_1}}{N_{s_1}(w+1)} \tag{A-6}$$

This output power,

$$P_{s_1} = A_{s_1}(\alpha_{gs} P_g + N_{s_1}) \tag{A-7}$$

in travelling to and entering the vehicle receiver, suffers a net attenuation of:

$$\alpha_{sv} = \frac{G_{s_1} G_v (\lambda_{sv})^2}{(4\pi)^2 (R_{sv})^2 L_{sv}} \tag{A-8}$$

The composite (signal plus noise) received power is:

$$p_{sv} = \alpha_{sv} P_{s_1} = \alpha_{sv} A_{s_1}(\alpha_{gs} P_g + N_{s_1}) \tag{A-9}$$

to which is added the internal vehicle receiver noise,

$$N_v = K (T_e)_v B_v, \tag{A-10}$$

yielding a total front-end power of:

$$p_{sv} + N_v = \alpha_{sv} A_{s_1}(\alpha_{gs} P_g + N_{s_1}) + N_v \tag{A-11}$$

of which the

$$\text{Useful Signal Power} = \alpha_{sv} A_{s_1} \alpha_{gs} P_g \tag{A-12}$$

and the

$$\text{Effective Noise Power} = \alpha_{sv} A_{s_1} N_{s_1} + N_v. \tag{A-13}$$

In the radar mechanization as conceived, in order to allow for doppler shifts, the vehicle receiver passband is made wider than that of the first satellite receiver. Thus, there is no narrow banding, or reduction of the satellite noise spectrum, and the respective noise powers simply add as indicated.

The effective signal-to-noise ratio at this point, before amplitude limiting, is (A-12) divided by (A-13), or

$$(\text{snr})_{vi} = \frac{\alpha_{sv} A_{s_1} \alpha_{gs} P_g}{\alpha_{sv} A_{s_1} N_{s_1} + N_v} \tag{A-14}$$

Substituting (A-6)

$$(snr)_{vi} = \frac{\alpha_{sv} \left[\dfrac{P_{s_1}}{N_{s_1}(w+1)} \right]^{\alpha_{gs} P_g}}{\alpha_{sv} \left[\dfrac{P_{s_1}}{N_{s_1}(w+1)} \right] N_{s_1} + N_v} \qquad \text{(A-15)}$$

which, after substituting (A-5) and multiplying numerator and denominator by (w + 1), becomes

$$(snr)_{vi} = \frac{\alpha_{sv} P_{s_1} w}{\alpha_{sv} P_{s_1} + N_v (w+1)} \qquad \text{(A-16)}$$

Finally, after dividing top and bottom by N_v, the second normalized power parameter is defined and substituted,

$$x = \frac{\alpha_{sv} P_{s_1}}{N_v} \qquad \text{(A-17)}$$

yielding:

$$(snr)_{vi} = \frac{w}{w + x + 1} \qquad \text{(A-18)}$$

A. 2. 3. 3 Limiting in the Vehicle Repeater

The inclusion of an amplitude limiter in the vehicle repeater has a significant effect on signal-to-noise ratio, and this effect shall be taken into account. Following a discussion of the phenomenon itself, the effect on the system snr is shown.

A. 2. 3. 3. 1 Amplitude Limiting and Signal-to-Noise Ratio - A linear bandpass amplifier

faithfully reproduces all fluctuations of the signal plus noise within the limits of the passband. An amplitude limiter restricts the amplitude of its output by attenuating the composite signal as a function of amplitude. An ideal limiter clips the composite signal peaks at a prescribed level, thereby fixing a maximum amplitude and maximum required dynamic range of the associated amplifiers.

The effect of limiting on signal-to-noise ratio is analyzed in the literature.[1] A pertinent result of the analysis is reproduced in figure A-2, which shows the output snr of an ideal symmetrical limiter as a function of the input snr. The assumed conditions are a CW signal and Gaussian noise in a rectangular passband centered at the carrier and passing all carrier sidebands while rejecting all harmonic frequencies.

---

[1] W. B. Davenport, "Signal-to-Noise Ratios in Band-Pass Limiters", Journal of Applied Physics; Vol. 24, No. 6; June, 1953.

The most notable characteristic of the limiting phenomenon is the transition from degradation to enhancement of the signal-to-noise ratio as the input value increases. - Obviously, operation at the higher values of $(snr)_i$ pays dividends. The minimum and maximum improvement factors are:

$$\frac{(snr)_o}{(snr)_i} \approx \frac{\pi}{4}, \qquad (snr)_i \rightarrow 0 \qquad\qquad (A\text{-}19)$$

and

$$\frac{(snr)_o}{(snr)_i} \approx 2, \qquad (snr)_i \rightarrow \infty \qquad\qquad (A\text{-}20)$$

The amplitude limiter, being a nonlinear device of constant power output, is more difficult to analyze as part of a system than are simple amplifiers and attenuators. One method of accounting for its effect in the navigation satellite vehicle is to consider it as a sort of nonlinear signal-to-noise transformer at the output of the repeater. In this case, a numerical calculation of $(snr)_i$ without limiting is required in order to read from figure A-2 the value of $(snr)_o$ with limiting.

The output power, P, is constant and is composed of signal output s_o and noise output n_o. Therefore, as $(snr)_i$ increases, not only does s_o increase, but n_o actually decreases. When
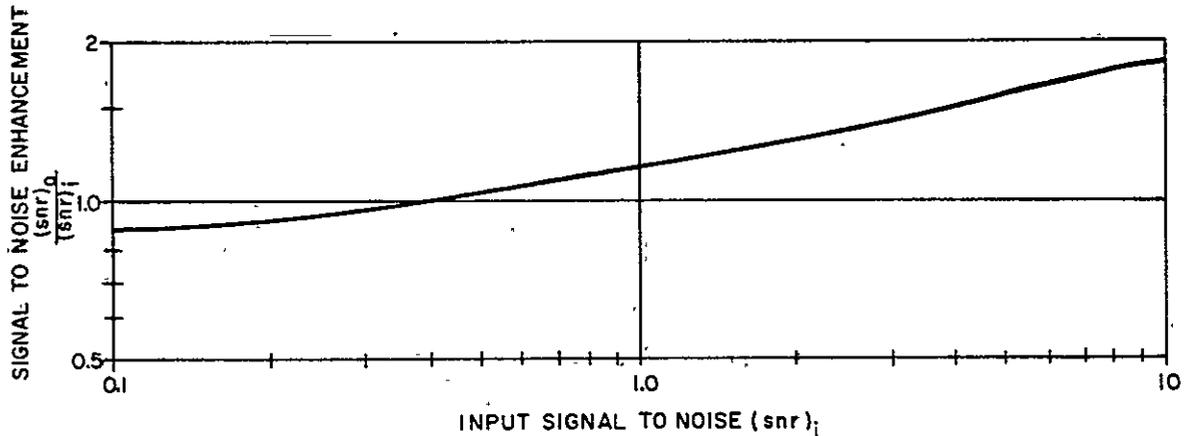
Figure A-2. Limiter Signal-to-Noise Transformation

the values in figure A-2 are translated into terms of the factors by which s_o and n_o change, the signal and noise power terms without limiting can be converted easily into those existing with limiting.

Without limiting, the output power is

$$s_i + n_i = P \tag{A-21}$$

and the signal-to-noise ratio is

$$\frac{s_i}{n_i} = (snr)_i \tag{A-22}$$

so that

$$s_i = n_i \, (snr)_i \tag{A-23}$$

combining (A-21) and (A-23),

$$n_i \, (snr)_i + n_i = P$$

$$n_i \left[(snr)_i + 1 \right] = P$$

$$n_i = P \, \frac{1}{(snr)_i + 1} \tag{A-24}$$

in which case,

$$s_i = P - n_i = P \left[1 - \frac{1}{(snr)_i + 1} \right] = P \, \frac{(snr)_i}{(snr)_i + 1} \tag{A-25}$$

By the same token, with limiting,

$$s_o + n_o = P \tag{A-26}$$

$$s_o/n_o = (snr)_o \tag{A-27}$$

so that

$$n_o = P \, \frac{1}{(snr)_o + 1} \tag{A-28}$$

and

$$s_o = P \, \frac{(snr)_o}{(snr)_o + 1} \tag{A-29}$$

The factor by which the noise component changes with limiting is therefore (A-28) divided by (A-24). The noise adjustment is

$$k_n = \frac{n_o}{n_i} = \frac{P \, \dfrac{1}{(snr)_o + 1}}{P \, \dfrac{1}{(snr)_i + 1}} = \frac{(snr)_i + 1}{(snr)_o + 1} = \frac{(snr)_i + 1}{k_T (snr)_i + 1} \tag{A-30}$$

where k_T, the limiter transformation factor, is defined as

$$k_T = \frac{(snr)_o}{(snr)_i} \tag{A-31}$$

A-8

The signal component changes by (A-29) divided by (A-25). The signal adjustment factor is therefore;

$$k_s = \frac{s_o}{s_i} = \frac{P \dfrac{(snr)_o}{(snr)_o + 1}}{P \dfrac{(snr)_i}{(snr)_i + 1}} = \frac{(snr)_o}{(snr)_i} \cdot \frac{(snr)_i + 1}{(snr)_o + 1} = k_T \cdot k_n \tag{A-32}$$

The three functions are plotted in figure A-3.

A. 2. 3. 3. 2 Effect of Limiting on System Signal to Noise Ratio.- By definition, the overall gain of the vehicle repeater is the output divided by the front-end composite power,

$$A_v = \frac{P_v}{\alpha_{s_v} P_{s_1} + N_v} = \frac{P_v}{N_v (x+1)} \tag{A-33}$$

This will hold true with or without amplitude limiting. The model of the limiter shall be considered as a device which merely juggles the relative values of output signal and noise powers while keeping the total power constant and equal to P_v. Thus, A_v includes the loss due to the limiting process.

In the vehicle receiver, both signal (A-12) and noise (A-13) are amplified by A_v, maintaining the same snr (A-14) into the limiter. From this, the limiter output is determined.

By evaluating $(snr)_{vi}$ for a particular set of parameters, the corresponding values of k_T, k_s and k_n can be determined from figure A-3. The important parameters are k_s and k_n. If desired, it is possible to calculate the quantities

$$(snr)_{vo} = k_T (snr)_{vi} = \frac{k_T wx}{w + x + 1} \tag{A-34}$$

$$S_{vo} = (\text{Signal Output})_v = k_s A_v \alpha_{sv} A_{s_1} \alpha_{gs} P_g, \tag{A-35}$$

and

$$
\begin{aligned}
n_{vo} = (\text{Noise Output})_v &= k_n \left[A_v \alpha_{sv} A_{s_1} N_{s_1} + N_v \right] \\
&= k_n A_v \alpha_{sv} A_{s_1} N_{s_1} + k_n A_v N_v
\end{aligned}
\tag{A-36}
$$

noting that:

$$P_v = s_{vo} + n_{vo} \tag{A-37}$$

A. 2. 3. 4 Vehicle-to-Satellite Path

In traveling from the vehicle back to the satellite, P_v undergoes a net attenuation of

$$\alpha_{vs} = \frac{G_v G_{s_2} (\lambda_{vs})^2}{(4\pi)^2 (R_{vs})^2 L_{vs}} \tag{A-38}$$
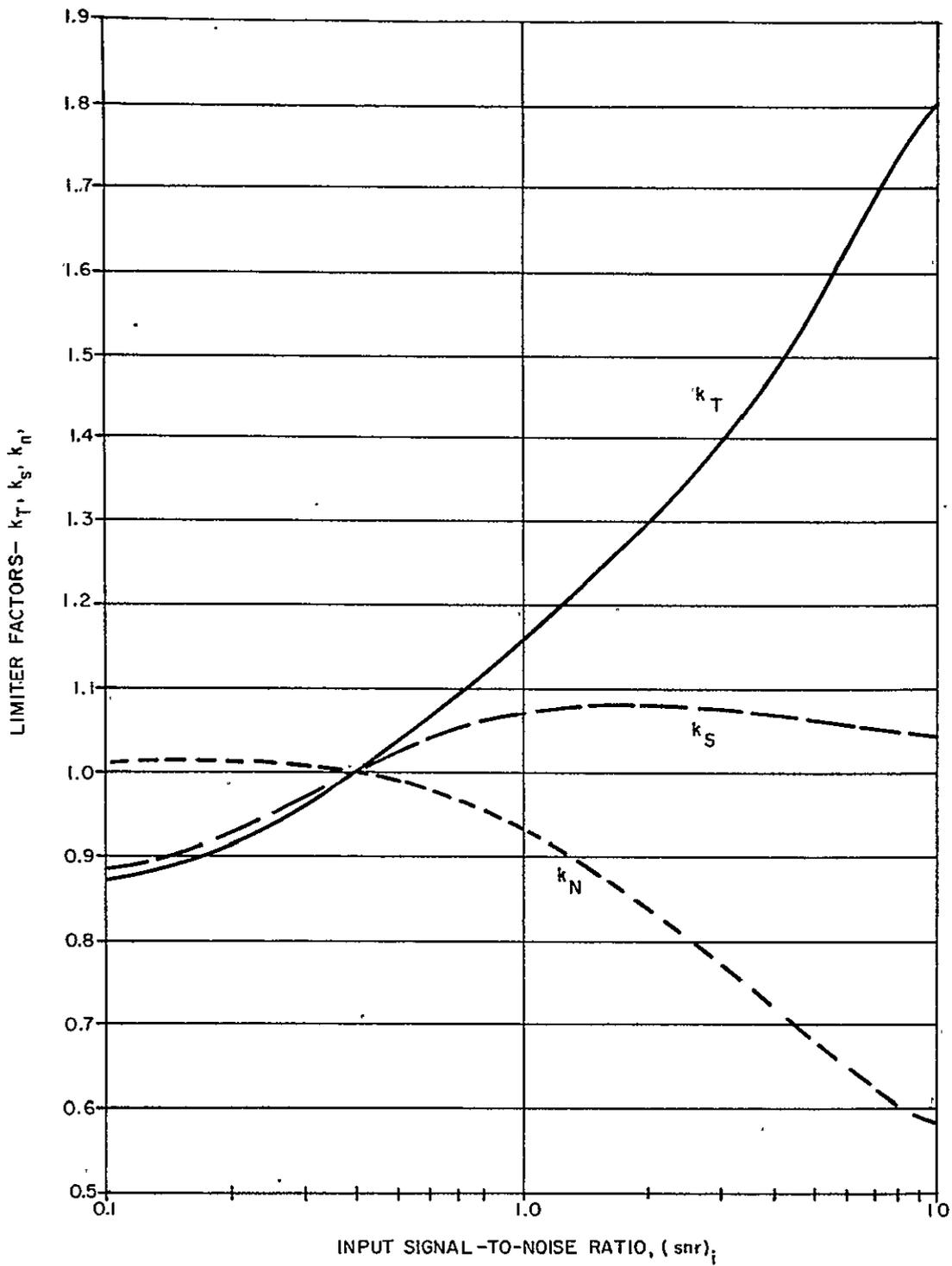
Figure A-3. Limiter Signal-To-Noise Characteristics

and appears at the receiver input as:

$$p_{vs} = \alpha_{vs} P_v = \left\{ \begin{array}{l} \alpha_{vs} k_s A_v \alpha_{sv} A_{s_1} \alpha_{gs} P_g \\ + \alpha_{vs} k_n A_v \alpha_{sv} A_{s_1} N_{s_1} + \alpha_{vs} k_n A_v N_v \end{array} \right\} \qquad (A-39)$$

At this point in the path of the composite signal, the effect of a narrowed passband is introduced. The mechanization, as conceived, embodies receiver passbands of widths such that:

$$B_g < B_{s_2} < B_{s_1} < B_v, \qquad (A-40)$$

where B_g is essentially the spectral width of the pulse stretched signal. Given such a relationship, on the return trip of the signal, the satellite receiver will reject part of the noise introduced in the vehicle and the first satellite receiver. Moreover, the bandwidth will have been narrowed even further at the ground station, yielding additional noise rejection.

With the normalized bandwidths defined as:

$$b_{s_1} = B_{s_1}/B_g \qquad (A-41)$$

$$b_v = B_v/B_g \qquad (A-42)$$

$$b_{s_2} = B_{s_2}/B_g \qquad (A-43)$$

the satellite receiver input, (A-39), entering the narrower-bandwidth circuit, becomes:

$$p_{vs} = \left\{ \begin{array}{l} \alpha_{vs} k_s A_v \alpha_{sv} A_{s_1} \alpha_{gs} P_g \\ \\ + \alpha_{vs} k_n A_v \alpha_{sv} A_{s_1} N_{s_1} \left(\dfrac{b_{s_2}}{b_{s_1}} \right) \\ \\ + \alpha_{vs} k_n A_v N_v \left(\dfrac{b_{s_2}}{b_v} \right) \end{array} \right\} \qquad (A-44)$$

To A-44 is added the interval noise power,

$$N_{s_2} = K (T_e)_{s_2} B_{s_2}, \qquad (A-45)$$

and the total power entering the receiver is:

$$p'_{vs} + N_{s_2} = \left\{ \begin{array}{l} \alpha_{vs}\, k_s\, A_v\, \alpha_{sv}\, A_{s_1}\, \alpha_{gs}\, P_g \\[2mm] + \alpha_{vs}\, k_n\, A_v\, \alpha_{sv}\, A_{s_1}\, N_{s_1} \left(\dfrac{b_{s_2}}{b_{s_1}} \right) \\[4mm] + \alpha_{vs}\, k_n\, A_v\, N_v \left(\dfrac{b_{s_2}}{b_v} \right) + N_{s_2} \end{array} \right\} \tag{A-46}$$

of which, the

$$\text{Useful Signal} = \alpha_{vs}\, k_s\, A_v\, \alpha_{sv}\, A_{s_1}\, \alpha_{gs}\, P_g \tag{A-47}$$

and the

$$\text{Effective Noise Power} = \left\{ \begin{array}{l} \alpha_{vs}\, k_n\, A_v\, \alpha_{sv}\, A_{s_1}\, N_{s_1} \left(\dfrac{b_{s_2}}{b_{s_1}} \right) \\[4mm] + \alpha_{vs}\, k_n\, A_v\, N_v \left(\dfrac{b_{s_2}}{b_v} \right) + N_{s_2} \end{array} \right\} \tag{A-48}$$

The effective signal-to-noise ratio at the second satellite receiver is:

$$(\text{snr})_{s_2} = \frac{\alpha_{vs}\, k_s\, A_v\, \alpha_{sv}\, A_{s_1}\, \alpha_{gs}\, P_g}{\alpha_{vs}\, k_n\, A_v\, \alpha_{sv}\, A_{s_1}\, N_{s_1} \dfrac{b_{s_2}}{b_{s_1}} + \alpha_{vs}\, k_n\, A_v\, N_v \dfrac{b_{s_2}}{b_v} + N_{s_2}} \tag{A-49}$$

By manipulating and substituting the same terms as in equations (A-14) through (A-18), the following result is obtained:

$$(\text{snr})_{s_2} = \frac{\alpha_{vs}\, k_s\, A_v\, w\, x}{\alpha_{vs}\, k_n\, A_v \dfrac{b_{s_2}}{b_{s_1}}\, x + \alpha_{vs}\, k_n\, A_v \dfrac{b_{s_2}}{b_v}\, (w+1) + \dfrac{N_{s_2}}{n_v}(w+1)} \tag{A-50}$$

Substituting (A-33) and multiplying numerator and denominator by $(x+1)$, equation (A-50) becomes:

$$(\text{snr})_{s_2} = \frac{k_s\, \alpha_{vs}\, P_v\, w\, x}{k_n \dfrac{b_{s_2}}{b_{s_1}}\, \alpha_{vs}\, P_v\, x + k_n \dfrac{b_{s_2}}{b_v}\, \alpha_{vs}\, P_v\, (w+1) + N_{s_2}\, (w+1)(x+1)} \tag{A-51}$$

A-12

Dividing top and bottom of A-51 by N_{s_2} and substituting the third normalized power parameter,

$$y = \frac{\alpha_{vs} P_v}{N_{s_2}} \tag{A-52}$$

yields:

$$(snr)_{s_2} = \frac{k_s \, w \, x \, y}{k_n \frac{b_{s_2}}{b_{s_1}} x \, y + k_n \frac{b_{s_2}}{b_v} (w+1) y + (w+1)(x+1)} \tag{A-53}$$

A.2.3.5 Satellite-to-Ground Path

The signal and effective noise power in the satellite front end (A-42), is amplified A_{s_2} times and transmitted as output power (P_{s_2}). The gain term is defined to be the output divided by front-end power,

$$A_{s_2} = \frac{p_{s_2}}{p'_{vs} + N_{s_2}} \tag{A-54}$$

For convenience of derivation, the first term of the denominator should be a function of p_{vs}. Therefore, introduce a factor, k_p, such that

$$p'_{vs} = k_p \cdot p_{vs} \tag{A-55}$$

in which case from (A-39) and (A-44)

$$k_p = \frac{p'_{vs}}{p_{vs}} = \frac{\alpha_{vs} k_s A_v \, \alpha_{sv} A_{s_1} \, \alpha_{gs} P_g + \alpha_{vs} k_n A_v \, \alpha_{sv} A_{s_1} N_{s_1} \frac{b_{s_2}}{b_{s_1}} + \alpha_{vs} k_n A_v N_v \frac{b_{s_2}}{b_v}}{\alpha_{vs} k_s A_v \, \alpha_{sv} A_{s_1} \alpha_{gs} P_g + \alpha_{vs} k_n A_v \, \alpha_{sv} A_{s_1} N_{s_1} + \alpha_{vs} k_n A_v N_v}$$

$$= \frac{\alpha_{sv} A_{s_1} \, \alpha_{gs} P_g + \alpha_{sv} A_{s_1} N_{s_1} \left(\frac{b_{s_2}}{b_{s_1}}\right) + N_v \left(\frac{b_{s_2}}{b_v}\right)}{\alpha_{sv} A_{s_1} \, \alpha_{gs} P_g + \alpha_{sv} A_{s_1} N_{s_1} + N_v} \tag{A-56}$$

By substituting (A-6), (A-5), and (A-7) into (A-56) and dividing top and bottom by N_v, as in steps (A-14) through (A-18), the equation reduces to

$$k_p = \frac{wx + x \left(\frac{b_{s_2}}{b_{s_1}}\right) + (w+1)\left(\frac{b_{s_2}}{b_v}\right)}{wx + x + (w+1)} \tag{A-57}$$

Because equation (A-57) is unwieldy, the factor, k_p, will be carried along in the subsequent equations. However, the above definition should be kept in mind.

Considering equation (A-54) and (A-55), the gain of the satellite second repeater is:

$$A_{s_2} = \frac{P_{s_2}}{k_p P_{vs} + N_{s_2}} = \frac{P_{s_2}}{k_p y N_{s_2} + N_{s_2}} = \frac{P_{s_2}}{N_{s_2} (k_p y + 1)} \tag{A-58}$$

In traveling to the ground-station receiver, the composite signal suffers a net attenuation of

$$\alpha_{sg} = \frac{G_{s_2} G_g (\lambda_{sg})^2}{(4\pi)^2 (R_{sg})^2 L_{sg}} \tag{A-59}$$

and appears at the receiver input as

$$p_{sg} = \alpha_{sg} P_{s_2} = \left\{ \begin{array}{l} \alpha_{sg} A_{s_2} \alpha_{vs} k_s A_v \alpha_{sv} A_{s_1} \alpha_{gs} P_g \\[2mm] + \alpha_{sg} A_{s_2} \alpha_{vs} k_n A_v \alpha_{sv} A_{s_1} N_{s_1} \left(\dfrac{b_{s_2}}{b_{s_1}} \right) \\[4mm] + \alpha_{sg} A_{s_2} \alpha_{vs} k_n A_v N_v \left(\dfrac{b_{s_2}}{b_v} \right) + \alpha_{sg} A_{s_2} N_{s_2} \end{array} \right\} \tag{A-60}$$

In entering into the narrower passband of the ground-station receiver, the front-end composite power becomes

$$p'_{sg} + N_g = \left\{ \begin{array}{l} \alpha_{sg} A_{s_2} \alpha_{vs} k_s A_v \alpha_{sv} A_{s_1} \alpha_{gs} P_g + \alpha_{sg} A_{s_2} \alpha_{vs} k_n A_v \alpha_{sv} A_{s_1} N_{s_1} \dfrac{b_{s_2}}{b_{s_1}} \left(\dfrac{1}{b_{s_2}} \right) \\[4mm] + \alpha_{sg} A_{s_2} \alpha_{vs} k_n A_v N_v \dfrac{b_{s_2}}{b_v} \left(\dfrac{1}{b_{s_2}} \right) + \alpha_{sg} A_{s_2} N_{s_2} \left(\dfrac{1}{b_{s_2}} \right) + N_g \end{array} \right\} \tag{A-61}$$

where

$$N_g = K (T_e)_g B_g \tag{A-62}$$

Of the composite power in the receiver, the

$$\text{Useful Signal Power} = k_s \alpha_{sg} A_{s_2} \alpha_{vs} A_v \alpha_{sv} A_{s_1} \alpha_{gs} P_g \tag{A-63}$$

and the

$$\text{Effective Noise Power} = \left\{ \begin{array}{l} \dfrac{k_n}{b_{s_1}}\, \alpha_{sg}\, A_{s_2}\, \alpha_{vs}\, A_v\, \alpha_{sv}\, A_{s_1}\, N_{s_1} \\[2ex] +\dfrac{k_n}{b_v}\, \alpha_{sg}\, A_{s_2}\, \alpha_{vs}\, A_v\, N_v \\[2ex] +\dfrac{1}{b_{s_2}}\, \alpha_{sg}\, A_{s_2}\, N_{s_2} + N_g \end{array} \right\} \qquad \text{(A-64)}$$

so that the effective signal-to-noise ratio is

$$(\text{snr})_g = \cfrac{k_s\, \alpha_{sg}\, A_{s_2}\, \alpha_{sv}\, A_v\, \alpha_{sv}\, A_{s_1}\, \alpha_{gs}\, P_g}{\left[\begin{array}{l} \dfrac{k_n\, \alpha_{sg}\, A_{s_2}\, \alpha_{vs}\, A_v\, \alpha_{sv}\, A_{s_1}\, N_{s_1}}{b_{s_1}} \\[2ex] +\dfrac{k_n}{b_v}\, \alpha_{sg}\, A_{s_2}\, \alpha_{vs}\, A_v\, N_v + \dfrac{1}{b_{s_2}}\, \alpha_{sg}\, A_{s_2}\, N_{s_2} + N_g \end{array} \right]} \qquad \text{(A-65)}$$

Making the same substitutions as suggested by equations (A-14) through (A-18) and (A-49) through (A-53), the following expression is obtained

$$(\text{snr})_g = \cfrac{k_s\, \alpha_{sg}\, A_{s_2}\, w\, x\, y}{\left[\begin{array}{l} \dfrac{k_n}{b_{s_1}}\, \alpha_{sg}\, A_{s_2}\, x\, y + \dfrac{k_n}{b_v}\, \alpha_{sg}\, A_{s_2}\, (w+1)\, y \\[2ex] +\dfrac{1}{b_{s_2}}\, \alpha_{sg}\, A_{s_2}\, (w+1)(x+1) + \dfrac{N_g}{N_{s_2}}\, (w+1)(x+1) \end{array} \right]} \qquad \text{(A-66)}$$

Substituting equation (A-58) for A_{s_2}, and multiplying numerator and denominator by $(k_p y + 1)$, equation (A-66) becomes

$$(\text{snr})_g = \cfrac{k_s\, \alpha_{sg}\, P_{s_2}\, w\, x\, y}{\left[\begin{array}{l} \dfrac{k_n}{b_{s_1}}\, \alpha_{sg}\, P_{s_2}\, xy + \dfrac{k_n}{b_v}\, \alpha_{sg}\, P_{s_2}\, (w+1)\, y \\[2ex] +\dfrac{1}{b_{s_2}}\, \alpha_{sg}\, P_{s_2}\, (w+1)(x+1) + N_g\, (w+1)(x+1)(k_p y+1) \end{array} \right]} \qquad \text{(A-67)}$$

Dividing numerator and denominator of (A-67) by N_g and substituting the last normalized power parameter,

$$z = \frac{\alpha_{sg}\, P_{s_2}}{N_g} \qquad \text{(A-68)}$$

yields the final signal-to-noise expression, i.e., that at the ground station;

$$(snr)_g = \frac{k_s \, w \, x \, y \, z}{\dfrac{k_n}{b_{s_1}} x \, y \, z + \dfrac{k_n}{b_v}(w+1)\, y \, z + \dfrac{1}{b_{s_2}}(w+1)(x+1)z + (w+1)(x+1)(k_p y + 1)} \qquad (A\text{-}69)$$

which, after pulse compression, is

$$(SNR)_g = (PCR)(snr)_g \qquad (A\text{-}70)$$

The interrelationships of the several parameters will be demonstrated after an examination of the constraints upon, and the calculation of, the signal-to-noise ratio.

A.3 PARAMETRIC CONSTRAINTS

This section examines the relationships which determine the required SNR at the range-pulse detector. This will influence the specification of satellite, vehicle, and ground-station transmitted power.

A.3.1 Additional Parameters

In addition to the parameters defined in paragraph A.2.2.1, the following parameters will be used in the discussion of constraints.

c = speed or light

e_g = energy in the signal received by the ground-station

$f(\;)$ = a function of $(\;)$

$(N_o)_g$ = noise power density of ground-station receiver

PCR = pulse compression ratio

P_D = probability of detection

δR = rms error in range measurement

T_R = round-trip delay time of radar pulse

δT_R = rms error in round-trip delay time.

dt/df = slope of dispersive delay line characteristic

τ_n = compressed (narrow) pulse width

τ_w = stretched (wide) pulse width

A.3.2 Range Accuracy

In the absence of noise, a transmitted pulse will echo from a target (or will be retransmitted by a repeater) and will return to a radar receiver delayed by the two-way transit time. A threshold level in the receiver will be exceeded at time

$$T_R = \frac{2}{c} R \qquad (A\text{-}71)$$

Superimposing noise upon the above pulse waveform, however, causes an uncertainty or error in the range information. The randomness of the noise will cause threshold tripping sometimes before, or sometimes after, the nominal delay time. In this case, the rms time-delay error will cause an rms ranging error of

$$\delta R = \frac{c}{2} \cdot \delta T_R$$

(A-72)

Assuming independent measurements in the satellite on both the leading and lagging edges of the compressed pulse, the ranging error of a pulse stretch radar is given[1] by

$$\delta T_R = \frac{\sqrt{3}}{\pi B_g \sqrt{2 e_g/(N_o)_g}}$$

(A-73)

For a single measurement per pulse, as would be done in the assumed system, the error would be $\sqrt{2}$ times greater. Multiplying (A-73) by $\sqrt{2}$ gives

$$\delta T_R = \frac{\sqrt{3}}{\pi B_g \sqrt{e_g/(N_o)_g}}$$

(A-74)

This may be put in terms of signal-to-noise ratio by substituting

$$e_g \approx \tau_w \text{ (useful signal power)}$$

(A-75)

and

$$(N_o)_g \approx \text{(total effective noise power)}/B_g$$

(A-76)

in (A-74) so that

$$\delta T_R = \frac{\sqrt{3}}{\pi B_g \sqrt{(\tau_w B_g)\left(\frac{\text{useful signal power}}{\text{total effective noise power}}\right)}} = \frac{\sqrt{3}}{\pi B_g \sqrt{(\tau_w B_g)(\text{snr})_g}}$$

(A-77)

The time-bandwidth product in the denominator is very nearly equal to the pulse compression ratio,[2, 3, 4]

$$\tau_w B_g \approx \tau_w \left(\frac{1}{\tau_N}\right) \equiv PCR$$

(A-78)

The range error is then

$$\delta T_R = \frac{\sqrt{3}}{\pi B_g \sqrt{(PCR)(snr)_g}}$$

(A-79)

Solving for the required swept bandwidth,

$$B_g = \frac{\sqrt{3}}{\pi (\delta T_R) \sqrt{(PCR)(snr)_g}}$$

(A-80)

Because pulse compression correlates the coherent signal and not the incoherent noise, the peak signal-to-noise after compression is multiplied by the PCR, and

[1] M. I. Skolnik, "Theoretical Accuracy of Radar Measurements," IRE Transactions on Aeronautical and Navigational Electronics, December 1960.

[2] J. R. Klander, et al, "The Theory and Design of Chirp Radars," Bell Telephone Monograph 3660; also published in the Bell System Technical Journal, Vol. 39, July 1960.

[3] G. P. Ohman, "Getting High Range Resolution with Pulse Compression Radar," Electronics, October 7, 1963.

[4] M. Bernfield & C. Cook, "Matched Filtering and Pulse Compression," Sperry Engineering Review, Spring 1963.

$$B_g = \frac{\sqrt{3}}{\pi (\delta T_R) \sqrt{(SNR)_g}} \qquad \text{(A-81)}$$

A.3.3 Delay Line Considerations

Mechanization of the pulse stretch network imposes a practical limitation on the time-bandwidth relationship. The most practical device appears to be the ultrasonic frequency-dispersive delay line. This delay line consists of an aluminum wire or strip with barium titanate transducers on each end. The input transducer converts electrical energy to acoustic energy. The energy propagates down the delay line at a velocity dependent on frequency and is reconverted to electrical energy at the delay line output.

The constraint imposed by dispersive delay lines[5],[6],[7] can be expressed in terms of the delay-frequency slope. That is,

$$\tau_w \Big/ B = dt \Big/ df \qquad \text{(A-82)}$$

where dt/df represents the possible dispersion of realizable delay lines.

A.3.4 Probability of Detection

The final constraint upon the power-related parameters is imposed by the signal-to-noise ratio of the collapsed pulse. It must be high enough to ensure an adequate probability of detecting the signal and a small probability of detecting noise. The curves of Marcum[8] indicate this relationship for a given radar configuration, once the allowable false alarm (noise-triggered detection) rate is chosen. At this point with all else being equal, it is sufficient to indicate that,

$$(SNR)_g = f (P_D) \qquad \text{(A-83)}$$

The next section will give numerical meaning to the foregoing expressions.

A.4 CALCULATION OF REQUIRED SIGNAL-TO-NOISE RATIO

This section further examines the previous parametric constraints, assigning numbers where required.

A.4.1 Allowable Range Error

Assuming that the ultimate range accuracy allows

Total Range Error = 0.1 nmi $\qquad$ (A-84)

it seems reasonable to allot one-half of this error to signal-to-noise effects.

---

[5] A. H. Meitzler, "Ultrasonic Delay Lines Using Shear Modes in Strips," IRE Transactions on Ultrasonic Engineering, June 1960, p. 35.

[6] J. E. May, "Wire-Type Dispersive Ultrasonic Delay Lines," op. cit., p. 44.

[7] T. R. Meeker, "Dispersive Ultrasonic Delay Lines Using the First Longitudinal Mode in a Strip," op. cit., p. 53.

[8] J. I. Marcum, "A Statistical Theory of Target Detection by Pulsed Radar," IRE Transactions on Information Theory, April 1960.

Therefore, within the context of paragraph A. 3. 2, assume

$$\delta R = 0.1/2 = 0.05 \text{ nmi} \tag{A-85}$$

In terms of allowable echo-time uncertainty, this then represents

$$\delta T_R = \frac{2}{c} \delta R = (12.36 \mu \sec/\text{nmi}) (0.05 \text{ nmi}) = 0.618 \mu \sec \tag{A-86}$$

A. 4. 2 Realistic Frequency Dispersion

The assumed amount of frequency dispersion is based on realizable ultrasonic delay lines. Because devices have already been mechanized[9,10,11] with time-frequency slopes of 2000 $\mu \sec/\text{mc}$, a reasonable value for dispersion is

$$\frac{dt}{df} = 2 \times 10^{-9} \sec/\text{cps} \tag{A-87}$$

so that, from (A-82),

$$\tau_w = 2 \times 10^{-9} B \tag{A-88}$$

A. 4. 3 Required Signal-to-Noise Ratio

Paragraph A. 3. a refers to the dependence of (SNR) on the probability of the threshold being tripped by the signal or by noise. The actual relationship is demonstrated here.

A. 4. 3. 1 Selection of Probability Curve

Marcum's[12] family of curves illustrates the probability of detection versus signal-to-noise for a variety of conditions. By defining those conditions applicable to the satellite-vehicle radar, a relevant curve is determined.

Each curve is valid for a unique combination of values for each of three parameters:

γ = the number of pulses received during the time allotted to signal detection

N = the number of pulses integrated

n = the number of opportunities for noise to exceed the threshold

Assuming one pulse transmitted per round-trip transit time, i. e., assuming no range ambiguities,

$$\gamma = 1 \tag{A-89}$$

so that,

$$N = 1 \tag{A-90}$$

The remaining parameter, n, known as the false alarm number, is defined as

$$n = \tau_{fa} f_r \eta \tag{A-91}$$

where

τ_{fa} = required false alarm time

f_r = pulse repetition (sweep) frequency

η = number of pulse intervals per sweep

---

[9] A. H. Meitzler, op. cit.

[10] J. E. May, op. cit.

[11] T. R. Meeker, op. cit.

[12] J. I. Marcum, op. cit.

The PRF period, $1/f_r$, shall be slightly longer than the two-way transit time of the signal, which is

$$T = \frac{2}{c} R = (12.36\,\mu\text{sec/nmi})\,(8496\ \text{nmi}) = 0.105\ \text{sec} \qquad \text{(A-92)}$$

Therefore, assume

$$1/f_r \approx 0.11\ \text{sec} \qquad \text{(A-93)}$$

or

$$f_r \approx 9.1\ \text{cps} \qquad \text{(A-94)}$$

The number of pulse intervals per sweep equals the radar listening time divided by the compressed or narrow pulse width. In this case, the satellite receiver must listen for an echo return for at least

$$T_L \approx \frac{2}{c} (R-h) = (12.36\,\mu\text{sec/nmi})\,(8496-6000) \qquad \text{(A-95)}$$

$$= 0.0308\ \text{sec}$$

The compressed pulse width is undetermined at this point, but it is probably on the order of 7 microseconds. Therefore,

$$\eta = T_L/T_N = 0.0308/7\text{x}10^{-6} = 4400\ \text{pulse intervals} \qquad \text{(A-96)}$$

The third factor, false alarm time, is somewhat arbitrary. Choose

$$\tau_{fa} = 1\ \text{hour} = 3600\ \text{seconds} \qquad \text{(A-97)}$$

Substituting equations (A-94), (A-96) and (A-97) into equation (A-91), results in

$$n = (3600)\,(9.1)\,(4400) = 1.44\text{ x }10^8 \approx 10^8 \qquad \text{(A-98)}$$

In review, then, the pertinent conditions are

$$\gamma = N = 1 \qquad \text{(A-99)}$$

$$n = 10^8 \qquad \text{(A-100)}$$

which, for a square law detector, stipulate that the Marcum curve be shown in figure A-4. (In the cited reference, it is Marcum's figure 21.)

A.4.3.2 Application of Probability Curve

For high probabilities of detection, figure A-4 illustrates the marked influence of signal-to-noise ratio. Note that the following dependency exists:

$(\text{SNR})_g$	P_D
17 db	99.99%
16 db	99.6 %
15 db	95 %
14 db	75 %
13 db	50 %

For a reasonable probability, a minimum

$$(\text{SNR})_g = 15\ \text{db} \qquad \text{(A-101)}$$

will be the assumed value for these calculations.
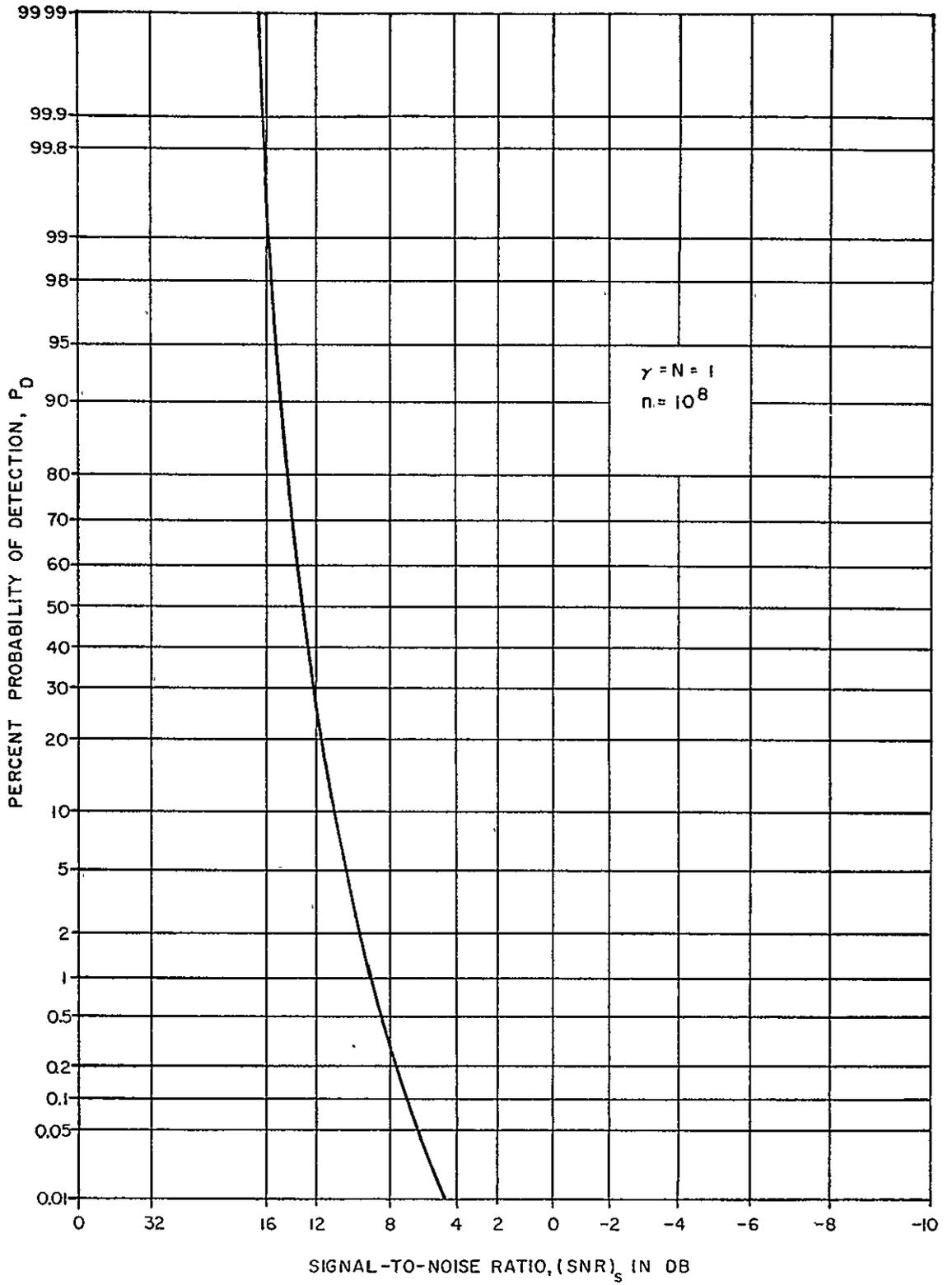
Figure A-4. Single Pulse Probability of Detection
vs. Signal-To-Noise Ratio in the Satellite

Should two pulses be transmitted, the probability that at least one of the two pulses is detected is a so-called cumulative probability. In this case, it corresponds to the probability of not having two undetected pulses:

$$P_c = 1 - (1 - P_D)^2 = 1 - (1 - 0.95)^2 = 0.9975 \sim 99.75\% \tag{A-102}$$

If three pulses are permitted, the probability of detecting at least one of them is improved even more:

$$P_c = 1 - (1 - 0.95)^3 = 0.999875 \sim 99.99\% \tag{A-103}$$

Also, the probability of detecting at least two of the three pulses is equal to the summation of the probabilities of the several possible combinations:

$$P_c = (P_D)^3 + 3\left[(P_D)^2(1 - P_D)\right]$$

$$= (0.95)^3 + 3(0.95)^2(0.05) = 0.992750 \sim 99.28\%. \tag{A-104}$$

A.4.4 Final Parameter Calculations

The constraints on the radar parameters may now be combined in order to calculate bandwidth, pulse width, pulse compression ratio, and stretched signal-to-noise ratio.

Substituting equations (A-86) and (A-101) into equation (A-81) yields

$$B_g = \frac{\sqrt{3}}{\pi(\delta T_R)\sqrt{(SNR)_g}} = \frac{\sqrt{3}/\pi}{(0.618 \times 10^{-6})\sqrt{31.6}}$$

$$\equiv \frac{0.552}{(0.618 \times 10^{-6})(5.62)} = 0.159 \times 10^6 = 159 \text{ KC} \tag{A-105}$$

This is the required frequency dispersion and the nominal bandwidth for these preliminary calculations.

The effective width of the compressed pulse, from (A-78) is essentially the reciprocal of the swept bandwidth,

$$\tau_n \approx \frac{1}{B_g} = \frac{1}{0.159 \times 10^6} = 6.29\,\mu\text{sec} \tag{A-106}$$

and, from (A-88),

$$\tau_w = 2 \times 10^{-9} B_g = (2 \times 10^{-9})(159 \times 10^3) = 318\,\mu\text{sec} \tag{A-107}$$

The pulse compression ratio, from (A-78), is established as

$$PCR = \tau_w/\tau_n = 318/6.29 = 50.6 \sim 17.04 \text{ db} \tag{A-108}$$

and, from (A-78), (A-101), and (A-108),

$$(snr)_s = 15 - 17.04 = -2.04 \text{ db} \sim 0.626 \text{ power ratio} \tag{A-109}$$

A.5 ILLUSTRATION OF NORMALIZED POWER TRADE-OFFS

This section examines the result of section A.2, the expression for signal-to-noise ratio at the ground station as a function of the four normalized power parameters, in the light of

the snr calculated in section A. 4. The resultant expression of section A. 2 was

$$(snr)_g = \cfrac{k_s \, wxy \, z}{\cfrac{k_n}{b_{s_1}} x \, yz \; + \cfrac{k_n}{b_v}(w+1) \, y \, z \; + \cfrac{1}{b_{s_2}}(w+1)(x+1) \, z \; + (w+1)(x+1)(k_p y + 1)} \tag{A-110}$$

The number of independent parameters in equation (A-110) makes it extremely difficult to illustrate the interrelationships. In order to convey an idea as to how they vary, assume that the constants are equal to unity. That is,

$$k_s = k_n = b_{s_1} = b_v = b_{s_2} = k_p = 1.0 \tag{A-111}$$

This equality implies: (a) the amplitude limiter in the vehicle is operating at a unique signal-to-noise ratio, and (b) all accumulated noise power reaches the ground station receiver. The first condition assumes a special case and the latter ignores the narrow banding effect. Obviously, neither assumption is realistic; but they do allow a simplified view of the relationships involved.

Assuming that (A-111) holds, equation (A-110) reduces to

$$(snr)_g = \cfrac{w \, x \, y \, z}{x \, yz + (w+1) \, yx + (w+1)(x+1) \, z + (w+1)(x+1)(y \quad 1)} \tag{A-112}$$

$$= \cfrac{wx \, y \, z}{1 + (w+x+y+z) + (wx+wy+wz+xy+xz+yx) + (wxy+wxz+wyz+xyz)} \tag{A-113}$$

From section A. 4 a stretched-pulse snr of -2. 04 db was required at the input to the pulse-compression delay line in order to meet the system requirements. Choosing this value for $(snr)_g$, i.e.,

$$(snr)_g = 0.626 \sim -2.04 \text{ db} \tag{A-114}$$

a curve of w versus z for each specific combination of x and y can be computed. Put another way, for each value of y, a family of curves in w, z, and x can be computed.

Figures A-5, A-6, and A-7 illustrate these relationships. The curves precisely illustrate the power trade-off that is intuitively suspected. For a given pair of normalized transmitted powers between satellite (x) and vehicle (y), the required signal-to-noise ratio can be maintained by trading-off the normalized satellite power (z) for normalized ground-station power (w). Also, the requirements on the latter two (w and/or z) can be eased by raising either of the former (x or y).

The calculation of the absolute power level depends on a numerical evaluation of each receiver noise, N, and the inter-unit transfer constant, α . This evaluation is accomplished in the succeeding section.

A. 6 NUMERICAL EVALUATION OF PARAMETERS

The inter-unit transfer constant has been defined as

$$\alpha = \frac{G_t \, G_r \lambda^2}{(4\pi)^2 \, R^2 \, L} \tag{A-115}$$
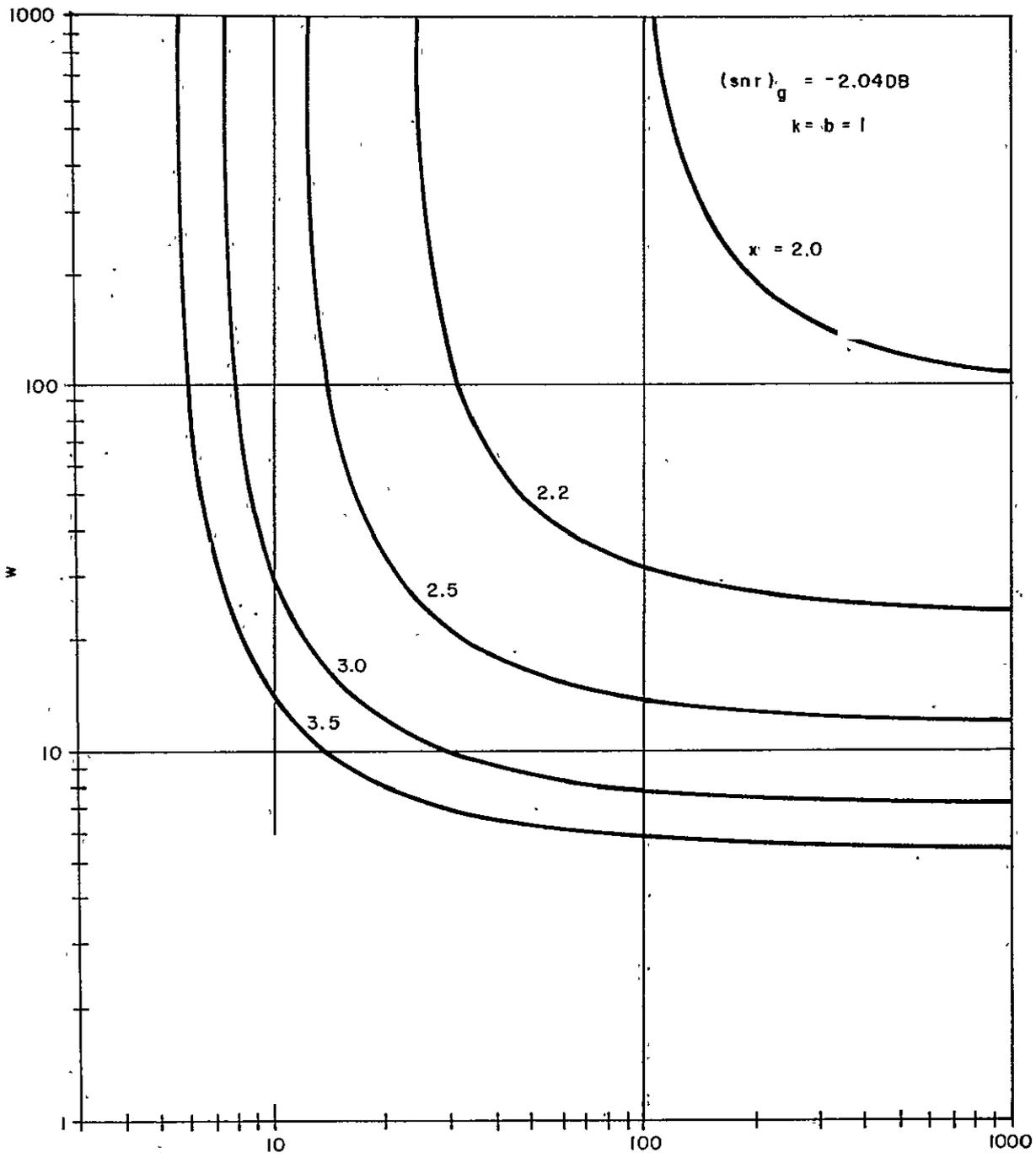
Figure A-5. Illustrative Family of Normalized Power Curves, y = 1.4
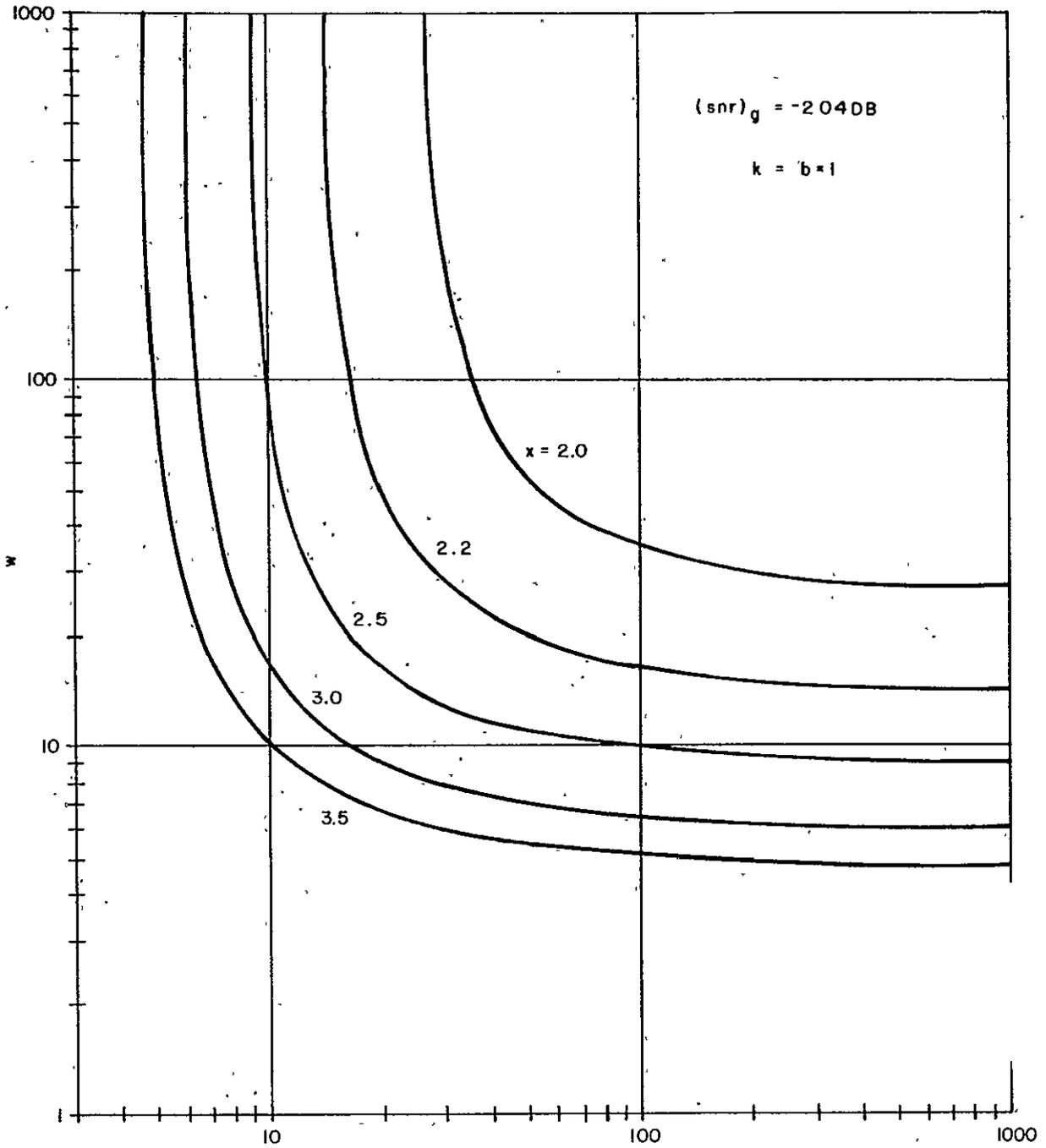
Figure A-6. Illustrative Family of Normalized Power Curves, y = 1.5
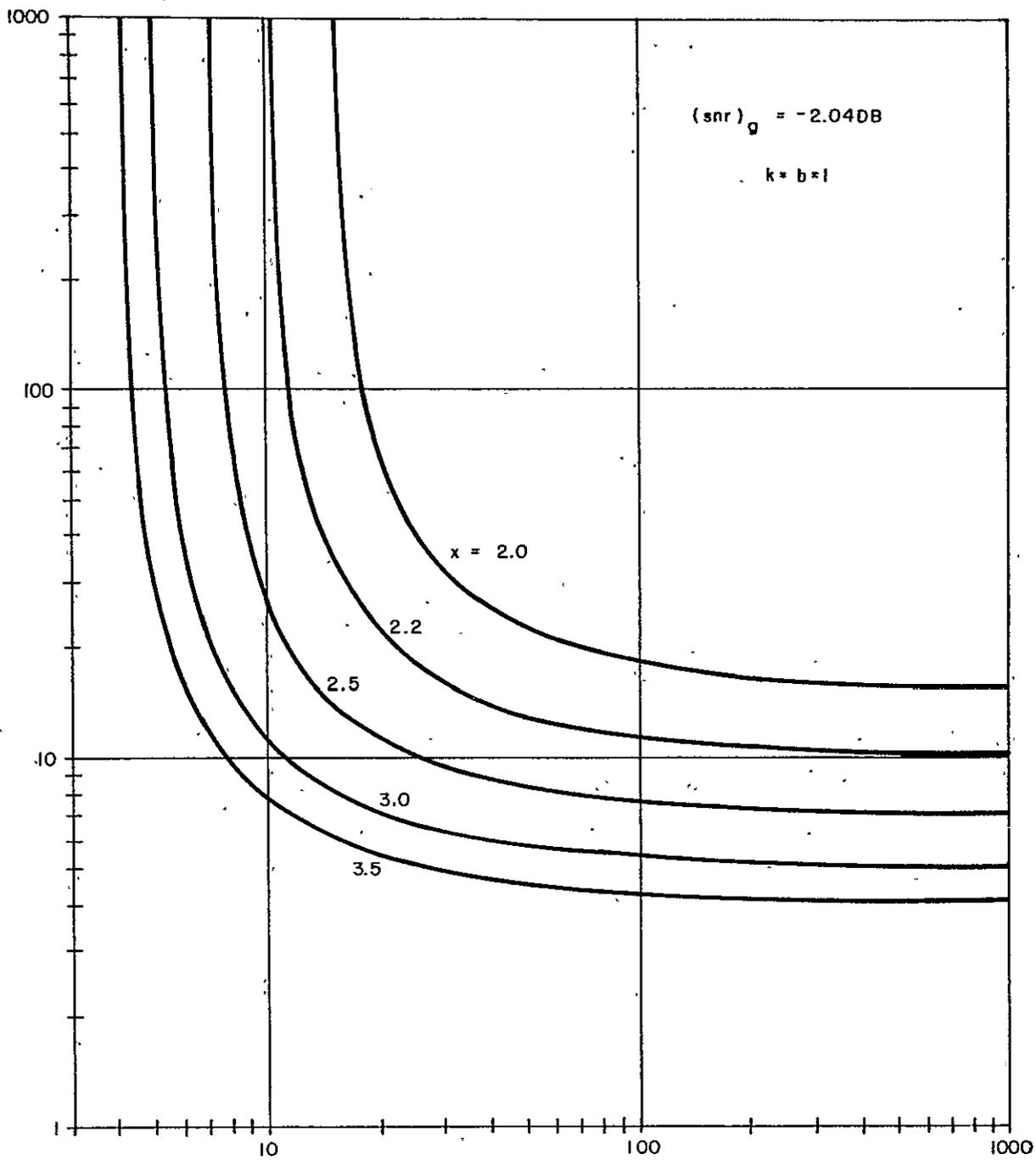
Figure A-7. Illustrative Family of Normalized Power Curves, y = 1. 6

and the receiver noise power as

$$N = K T_e B \tag{A-116}$$

The effective noise temperature in this equation is calculated by the equation

$$T_e = 290 \left[(F-1) + \frac{T_a}{290} \right] \tag{A-117}$$

The normalized power parameters relate these quantities to transmitted power,

$$w = \frac{\alpha_{gs} P_g}{N_{s_1}} \tag{A-118}$$

$$x = \frac{\alpha_{sv} P_{s_1}}{N_v} \tag{A-119}$$

$$y = \frac{\alpha_{vs} P_v}{N_{s_2}} \tag{A-120}$$

$$z = \frac{\alpha_{sg} P_{s_2}}{N_g} \tag{A-121}$$

Given the normalized parameters, the transmitted power, P, can be calculated if the respective values of N and α are known. This section evaluates these numbers.

A. 6. 1 Parametric Values

The following radar parameter values are based on a model which assumes a satellite altitude of 6000 nmi and a minimum elevation angle of 5 degrees at the ground and vehicle.

A. 6. 1. 1 Radar Range

The maximum straight-line distance between satellite and ground or satellite and vehicle is

$$R_{gs} = R_{sv} = R_{vs} = R_{sg} = 8496 \text{ nmi} \sim 39.29 \text{ db nmi} \tag{A-122}$$

A. 6. 1. 2 Losses

The losses in the ground-satellite links are

$$L_{gs} = L_{sg} = \underset{\substack{\text{(Polarization)}\\\text{loss}}}{3 \text{ db}} + \underset{\substack{\text{(Atmospheric)}\\\text{loss}}}{2 \text{ db}} + \underset{\substack{\text{(RF Transmit)}\\\text{loss}}}{1 \text{ db}}$$

$$+ \underset{\substack{\text{(Fading}\\\text{Margin)}}}{6 \text{ db}} + \underset{\substack{\text{(Safety}\\\text{Factor)}}}{2 \text{ db}} = 14 \text{ db} \tag{A-123}$$

while the losses in the satellite-vehicle links are

$$L_{sv} = L_{vs} = 3 \text{ db} + 2 \text{ db} + 1 \text{ db} + 6 \text{ db} + \underset{\substack{\text{(Safety}\\\text{Factor)}}}{3 \text{ db}} = 15 \text{ db} \tag{A-124}$$

A. 6. 1. 3 Frequencies and Wavelengths

The carrier frequencies for the four radar links are

$$f_{gs} = 1190 \text{ mc} \tag{A-125}$$

$$f_{sv} = 990 \text{ mc} \tag{A-126}$$

$$f_{vs} = 1050 \text{ mc} \tag{A-127}$$

$$f_{sg} = 970 \text{ mc} \tag{A-128}$$

so that the pertinent wavelengths are

$$\lambda_{gs} = \frac{c}{f_{gs}} = \frac{162 \times 10^3 \text{ nmi/sec}}{1190 \times 10^6 \text{ cps}} = 0.1361 \times 10^{-3} \text{ nmi} \sim -38.66 \text{ db nmi} \tag{A-129}$$

$$\lambda_{sv} = 0.1638 \times 10^{-3} \text{ nmi} \sim -37.86 \text{ db nmi} \tag{A-130}$$

$$\lambda_{vs} = 0.1543 \times 10^{-3} \text{ nmi} \sim -38.12 \text{ db nmi} \tag{A-131}$$

$$\lambda_{sg} = 0.1670 \times 10^{-3} \text{ nmi} \sim -37.78 \text{ db nmi} \tag{A-132}$$

A. 6. 1. 4 Antenna Gains

The remaining parameter calculations are the satellite, vehicle, and ground-station antenna gains. The satellite antenna gain, which is determined by the required coverage, is

$$G_{s_1} = G_{s_2} = 9.7 \text{ db} \tag{A-133}$$

The vehicle antenna gain, at the 5 degree elevation angle, is

$$G_v = 2 \text{ db} \tag{A-134}$$

and the gain of a 60-foot parabolic antenna is used for the ground station antenna gain. The gain of a parabolic antenna is

$$G = \frac{4\pi A e}{\lambda^2} = \frac{4\pi(kA)}{\lambda^2} = \frac{4\pi\left(k\frac{\pi}{4}D^2\right)}{\lambda^2} = \frac{\pi^2 k D^2}{\lambda^2} \tag{A-135}$$

where

A_e = effective aperture area

A = actual aperture area

k = antenna efficiency ≈ 0.52

D = dish diameter

For the outward link, the wavelength in feet is

$$\lambda_{gs} = \frac{c}{f_{gs}} = \frac{9.84 \times 10^6 \text{ ft/sec}}{1190 \times 10^6 \text{ cps}} = 0.827 \text{ ft.} \tag{A-136}$$

so that the ground-station antenna gain in the outward link is

$$G_g = \frac{\pi^2 (0.52)(60)^2}{(0.827)^2} = 27,000 \sim 44.32 \text{ db} \tag{A-137}$$

For the return link

$$\lambda_{sg} = 984/970 = 1.014 \text{ ft.} \tag{A-138}$$

so that the return-link gain is

$$G_g = 27,000 \left(\frac{0.827}{1.014}\right)^2 = 17,920 \sim 42.54 \text{ db} \tag{A-139}$$

A. 6. 1. 5 Receiver Bandwidths

Calculating receiver noise from equation (A-116) requires that the bandwidth and the effective noise temperature be given. The assumed bandwidths and their normalized equivalents are:

$$B_{s_1} = 190 \text{ KC} \qquad (b_{s_1} = 190/159 = 1.194) \tag{A-140}$$

$$B_b = 219 \text{ KC} \qquad (b_v = 219/159 = 1.378) \tag{A-141}$$

$$B_{s_2} = 170 \text{ KC} \qquad (b_{s_2} = 170/159 = 1.070) \tag{A-142}$$

$$B_g = 159 \text{ KC} \tag{A-143}$$

A. 6. 1. 6 Effective Noise Temperatures

A. 6. 1. 6. 1 General. The thermal noise temperature, with which a radar signal must compete, consists of two components. The first component is the internally generated noise of the receiver, symbolized by the system noise figure, and the second is that component introduced by the receiving antenna. Both components are substituted in equation (A-117) to obtain the total effective noise temperature.

The temperature of each receiver-ground, satellite, and vehicle-are examined here. A value, based on data from another space project, is assumed for the temperature of the ground station. The temperature of the satellite is based on an assumed noise figure and an inference as to antenna noise temperature. The vehicle temperature is based on an assumed noise figure and a calculated antenna temperature.

A. 6. 1. 6. 2 Ground Station. Data[1] from the Telstar program indicates that a reasonable total effective noise temperature for a low-noise front end and high-gain antenna looking toward the sky is

$$(T_e)_g = 50° \text{ K} \tag{A-144}$$

A. 6. 1. 6. 3 Satellite. The tunnel diode amplifiers of the vehicle to satellite receivers ie system noise figures of

$$F_{s_1} = F_{s_2} = 4 \qquad 6 \text{ db} \tag{A-145}$$

---

[1]Telstar I, NASA SP-32, Vol. 3; June 1963.

The noise temperature of an antenna is an average of that seen by all portions of its gain pattern. The satellite antenna is attempting to exclusively look at the earth. Neglecting the additional beamwidth allowed for attitude deviations, assume the most pessimistic case of

$$(Ta)_{s_1} = (Ta)_{s_2} = 290° \text{ K} \tag{A-146}$$

The satellite tunnel-diode receivers are assumed to yield system noise figures of

$$F_{s_1} = F_{s_2} = 4 \sim 6 \text{ db} \tag{A-147}$$

so that the total effective noise temperature, from (A-117) is

$$(Te)_{s_2} = 290 \left[(4-1) + \frac{290}{290} \right] = 290 \left[4 \right] = 1160° \text{ K} \tag{A-148}$$

The ground station to satellite noise temperature is 2700°K.

A. 6. 1. 6. 4 Vehicle

A. 6. 1. 6. 4. 1 Component Temperatures. The vehicle antenna has a nearly uniform antenna pattern. The side and back lobes, constituting approximately 0.3 of the entire pattern, senses the earth's temperature of 290°K. The nearly hemispheric main beam virtually senses the entire sky. By calculating an average sky temperature, T_{sky}, the vehicle antenna temperature can be found by

$$(Ta)_v = 0.3 (290) + 0.7 (T_{sky}) \tag{A-149}$$

The sky temperature contains three separate components. The galactic noise temperature[1] component, at 1000 mc, is about 20° K and is independent of elevation angle or antenna beamwidth because of its uniformity. The tropospheric component[2] is due to oxygen and water vapor, and because its density varies with altitude this component is a function of elevation angle. The sky temperature component due to the sun[3] is a function of the width of the antenna beam.

A. 6. 1. 6. 4. 2 Model. Figure A-8 depicts the hemispheric model for calculating the average tropospheric sky temperature. At zenith angle ϕ, the temperature in figure A-8b is seen to vary with frequency[4]. The values at 1000 mc are replotted versus angle in figure A-8c.

The method of averaging the sky temperature involves summing, over the entire hemisphere, incremental products of temperature and solid angle, and then dividing by the solid angle of a hemisphere.

---

[1]D. C. Hogg & W. W. Mumford, "The Effective Noise Temperature of the Sky", Figure 3, The Microwave Journal, March 1960.

[2]Ibid, figure 8.

[3]Ibid, figure 2.

[4]Ibid, figure 8.

(a) GEOMETRY

(b) FREQUENCY CHARACTERISTICS

(c) LOOK-ANGLE CHARACTERISTIC

f = 1000 MC
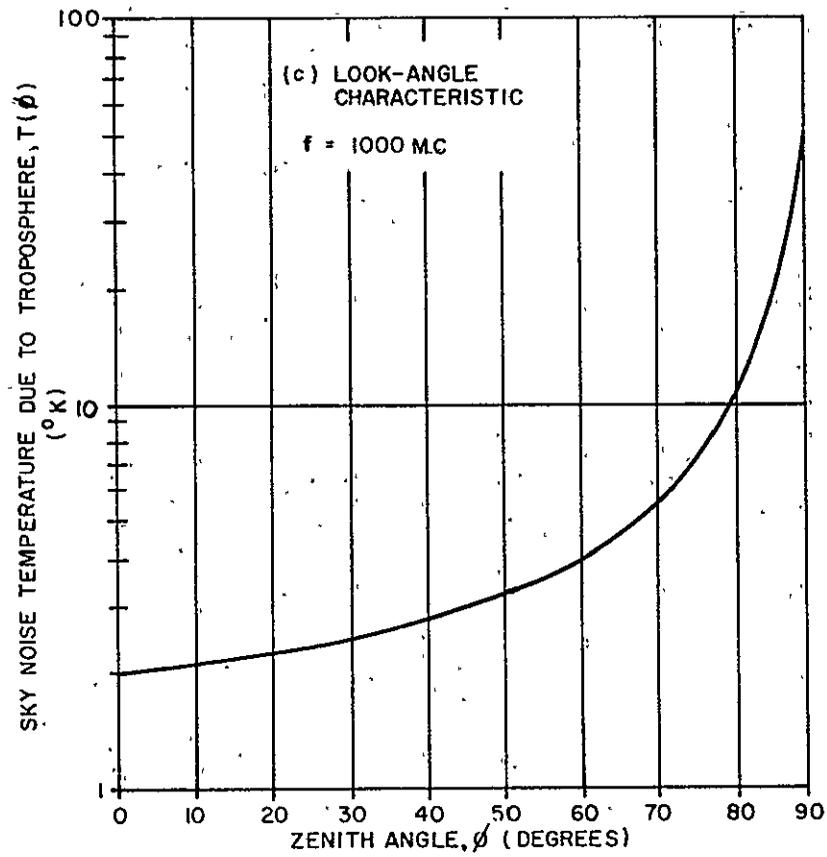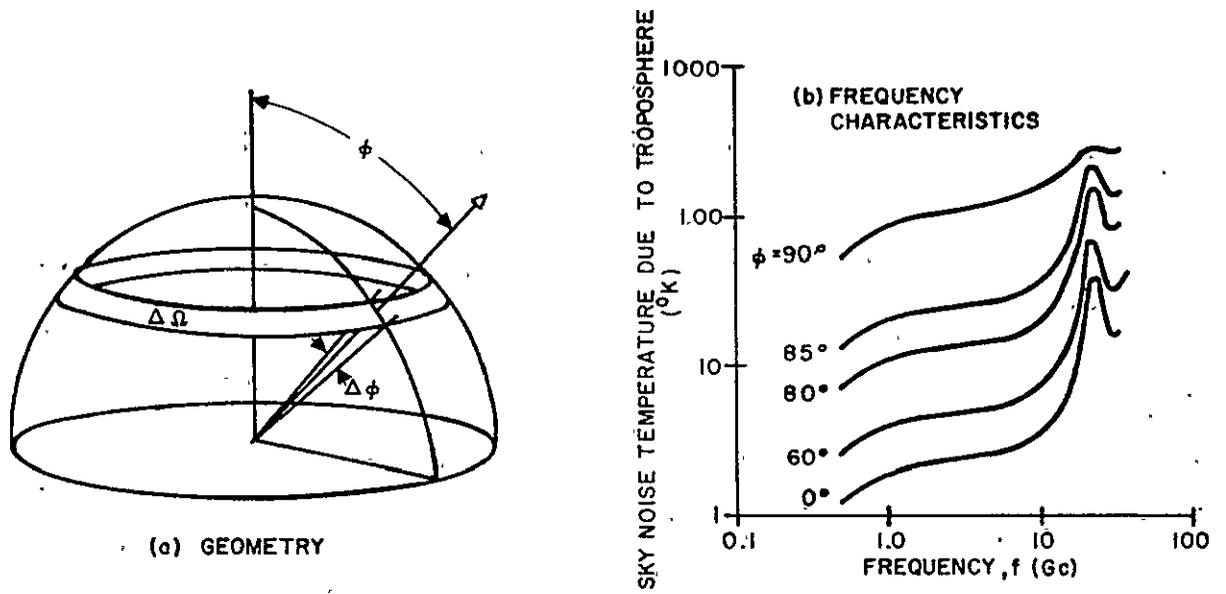
Figure A-8. Tropospheric Sky Noise

Let the temperature at a given zenith angle, ϕ, be designated $T(\phi)$. For an approximate calculation, it can be assumed that this temperature is constant over a small angular increment, $\Delta\phi$. Due to symmetry, then, the temperature is constant over the entire solid angle, $\Delta\Omega$, where the solid angle is defined as

$$\Delta\Omega = 2\pi \sin\phi \, \Delta\phi \tag{A-150}$$

Note that this is equal to the area of the concentric surface strip illustrated in figure A-8a when the hemispherical radius is of unity amplitude:

$$\text{Radius} \quad = R \tag{A-151}$$

$$\text{Strip Area} \quad = \left[2\pi (R \sin\phi)\right] (R \Delta\phi) = 2\pi R^2 \sin\phi \, \Delta\phi \tag{A-152}$$

$$\left[\text{Strip Area}\right]_{R=1} = 2\pi \sin\phi \, \Delta\phi \tag{A-153}$$

Assuming the hemisphere to be divided into m strips of equal $\Delta\phi$, where

$$m = \frac{\pi/2}{\Delta\phi} \tag{A-154}$$

and recognizing the solid angle of a hemisphere to be $1/2 \, (4\pi)$ steradians, the average temperature due to the troposphere may be calculated as

$$T_{trop} = \frac{T(\phi_1)\left[2\pi\sin\phi_1 \Delta\phi\right] + T(\phi_2)\left[2\pi\sin\phi_2 \Delta\phi\right] + \cdots T(\phi_k)\left[2\pi\sin\phi_k\Delta\phi\right] \cdots + T(\phi_m)\left[2\pi\sin\phi_m\Delta\phi\right]}{\frac{1}{2}(4\pi)} \tag{A-155}$$

$$T_{trop} = \sum_{k=1}^{m} T(\phi_k) \sin\phi_k \, \Delta\phi = \sum_{k=1}^{m} T(k \Delta\phi) \cdot \sin(k \Delta\phi) \cdot \Delta\phi \tag{A-156}$$

A. 6. 1. 6. 4. 3 Calculation of Average Tropospheric Temperature. Equation (A-156) was used to calculate average temperature using the $T(\phi)$ of figure A-8c. The angular increment chosen was

$$\Delta\phi = 1 \text{ degree} = \frac{1}{57.3} \text{ radian} \tag{A-157}$$

so that (A-156) becomes

$$T_{trop} = \sum_{k=1}^{90} T(\phi_k) \sin\phi_k \frac{1}{57.3} = \frac{1}{57.3} \sum_{k=1}^{90} T\left(\frac{k}{57.3}\right) \sin\left(\frac{k}{57.3}\right) \tag{A-158}$$

The result of the calculation is

$$T_{trop} = \frac{1}{57.3} \left[524\right] = 9.15° \text{ K} \tag{A-159}$$

A. 6. 1. 6. 4. 4 Calculation of Temperature Due to Sun. The noise temperature of the sun at 1000 mc is approximately 3×10^5 degrees Kelvin[1]. The plane angle subtended by the sun is only about 1/2 degree. Therefore, the effective sun temperature sensed by an antenna with hemispherical coverage is reduced by the ratio of the respective solid angles.

---

[1] Ibid., figure 2.

Specifically, the solid angle of a hemisphere is $1/2 \, (4\pi) = 2\pi$ steradians, and the solid angle subtended by a 1/2 degree beam is approximately

$$\Omega \approx \frac{\pi}{4} \left(\frac{1/2}{57.3}\right)^2 = 6 \times 10^{-5} \text{ steradian} \tag{A-160}$$

Note that this is equal to the area that the beam would project on the surface of a hemisphere of unit radius.

The effective sun temperature is therefore

$$T_s = T_{sun} \frac{\Omega}{\frac{1}{2}(4\pi)} = 3 \times 10^5 \frac{6 \times 10^{-5}}{2\pi} = 2.87^\circ \text{ K} \tag{A-161}$$

A. 6. 1. 6. 4. 5 Total Effective Noise Temperature. The total sky noise temperature is the sum of the three components,

$$T_{sky} = T_{gal} + T_{trop} + T_s$$
$$= 20 + 9 + 3 = 32^\circ \text{ K} \tag{A-162}$$

so that the vehicle antenna temperature is

$$(T_A) = 0.3 \, (390) + 0.7 \, (32)$$
$$= 87 + 22 = 109^\circ \text{ K} \tag{A-163}$$

The system noise figure is equivalent to the noise figure for a commercial, television-type front end,

$$F_r = 5 \sim 7 \text{ db} \tag{A-164}$$

so that the total effective noise temperature is

$$(Te)_v = 290 \left[(5-1) + \frac{109}{290}\right] = 290 \left[4.376\right] = 1270^\circ \text{ K.} \tag{A-165}$$

A. 6. 2 Calculation of α and N

The foregoing parametric values will be combined here to calculate the values of α and N, equations (A-115) and (A-116), for each of the four signal paths. This will permit relating the transmitted power requirements to the normalized power parameters via equations (A-118) through (A-121).

A. 6. 2. 1 Ground-to-Satellite Link

$$\alpha_{gs} = \left[44.32 + 9.7 + 2 \, (-38.66)\right] - \left[22.0 + 2 \, (39.29) + 14\right]$$
$$= -137.88 \text{ db} \sim 0.163 \times 10^{-13} \tag{A-166}$$

and

$$N_{s_1} = (1.38 \times 10^{-23}) \, (2.7 \times 10^3) \, (1.90 \times 10^5) = 7.1 \times 10^{-15} \text{ watts} \tag{A-167}$$

so that

$$P_g = \frac{7.1 \times 10^{-15}}{0.163 \times 10^{-13}} \text{ w} = 0.44 \text{ w} \tag{A-168}$$

A. 6. 2. 2 Satellite-to-Vehicle Link

$$\alpha_{sv} = \left[9.7 + 2.0 + 2\,(-37.86)\right] - \left[22.0 + 2\,(39.29) + 15\right]$$

$$= -179.60 \text{ db} \sim 0.1097 \times 10^{-17} \tag{A-169}$$

and

$$N_v = (1.38 \times 10^{-23})\,(1.270 \times 10^3)\,(2.19 \times 10^5) = 3.84 \times 10^{-15} \text{ watts} \tag{A-170}$$

so that

$$P_{s_1} = \frac{3.84 \times 10^{-15}}{0.1097 \times 10^{-17}}\; x = 3500\, x \tag{A-171}$$

A. 6. 2. 3 Vehicle-to-Satellite Link

$$\alpha_{vs} = \left[2.0 + 9.7 + 2\,(-38.12)\right] - \left[22.0 + 2\,(39.29) + 15\right]$$

$$= -180.12 \text{ db} \sim 0.973 \times 10^{-18} \tag{A-172}$$

and

$$N_{s_2} = (1.38 \times 10^{-23})\,(1.16 \times 10^3)\,(1.70 \times 10^5) = 2.72 \times 10^{-15} \text{ watts} \tag{A-173}$$

so that

$$P_v = \frac{2.72 \times 10^{-15}}{0.973 \times 10^{-18}}\; y = 2800\, y \tag{A-174}$$

A. 6. 2. 4 Satellite-to-Ground Link

$$\alpha_{sg} = \left[9.7 + 42.54 + 2\,(-37.78)\right] - \left[22.0 + 2\,(39.29) + 14\right] \tag{A-175}$$

$$= -137.90 \text{ db} \sim 0.1622 \times 10^{-13}$$

and

$$N_v = (1.38 \times 10^{-23})\,(50)\,(1.59 \times 10^5) = 1.098 \times 10^{-16} \text{ watts} \tag{A-176}$$

so that

$$P_{s_2} = \frac{1.098 \times 10^{-16}}{0.1622 \times 10^{-13}}\; z = 0.00676\, z \tag{A-177}$$

A. 7 POWER EQUATIONS

This section uses the equations and parametric values of the preceding sections to calculate the required transmitted power at the satellite, vehicle, and ground station.

A. 7. 1 Signal-to-Noise Ratio

The required signal-to-noise at the input of the pulse compression device at the ground station is, from equation (A-109),

$$(snr)_g = 0.626 \sim -2.04 \text{ db} \tag{A-178}$$

This result will be substituted into equation (A-69), once the other required numbers are determined.

A. 7. 2 Satellite-Vehicle Power Trade-Off (Approximate)

If the normalized power parameters of the ground-satellite links are assumed to be very large, the $(\text{snr})_g$ equation will be considerably simplified. This assumption will permit an approximate evaluation of the trade-off between satellite and vehicle transmit powers. Actually, this is not an unreasonable assumption because, due to the high-gain ground antenna, w and z may be allowed to become quite large before the actual powers, (A-168) and (A-177), become appreciable.

The fundamental equation is

$$(\text{snr})_g = \frac{k_s \, w \, x \, y \, z}{\dfrac{k_n}{b_{s_1}} x \, y \, z + \dfrac{k_n}{b_v}(w+1) \, y \, z + \dfrac{1}{b_{s_2}}(w+1)(x+1) \, z + (w+1)(x+1)(k_p \, y + 1)} \quad (A\text{-}179)$$

Dividing numerator and denominator by wz yields

$$(\text{snr})_g = \frac{k_s \, x \, y}{\dfrac{(k_n/b_{s_1}) \, x \, y}{w} + \dfrac{k_n}{b_v}\left(\dfrac{w+1}{w}\right) y + \dfrac{1}{b_{s_2}}\left(\dfrac{w+1}{w}\right)(x+1) + \dfrac{\left(\dfrac{w+1}{w}\right)(x+1)(k_p \, y + 1)}{z}} \quad (A\text{-}180)$$

Letting w and z become very large,

$$\left[(\text{snr})_g\right]_{\substack{w \to \infty \\ z \to \infty}} \approx \frac{k_s \, x \, y}{\dfrac{k_n}{b_v} y + \dfrac{x+1}{b_{s_2}}} \quad (A\text{-}181)$$

Even in this approximate form, some point-by-point evaluation is required in order to plot z versus y. Where b_y and b_{s_2} are constants, k_s and k_n depend on the actual signal-to-noise at the vehicle limiter, $(\text{snr})_{vi}$. For evaluation, the curves of figure A-3 must be used. The assumption of large w simplifies the calculation of limiter signal-to-noise ratio. From (A-18),

$$\left[(\text{snr})_{vi}\right]_{w \to \infty} = \left[\frac{x}{1 + \dfrac{x+1}{w}}\right]_{w \to \infty} \quad (A\text{-}182)$$

Substituting (A-178) and the values of normalized bandwidth, (A-141) and (A-142), into equation (A-181),

$$0.626 = \frac{k_s \, x \, y}{\dfrac{k_n}{1.378} y + \dfrac{x+1}{1.070}} \quad (A\text{-}183)$$

Then, taking into account (A-182) and figure A-3 for each value of x, the curves of figure A-8 are calculated from (A-183). These curves approximate the actual trade-off between satellite and vehicle transmitted power, provided w and z are made large.
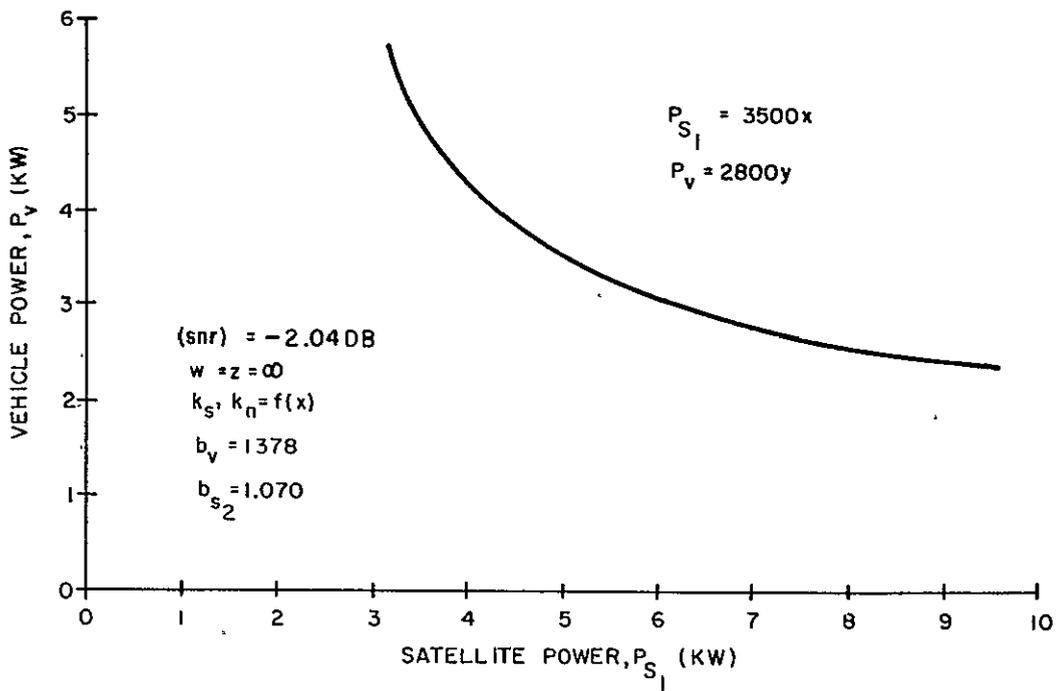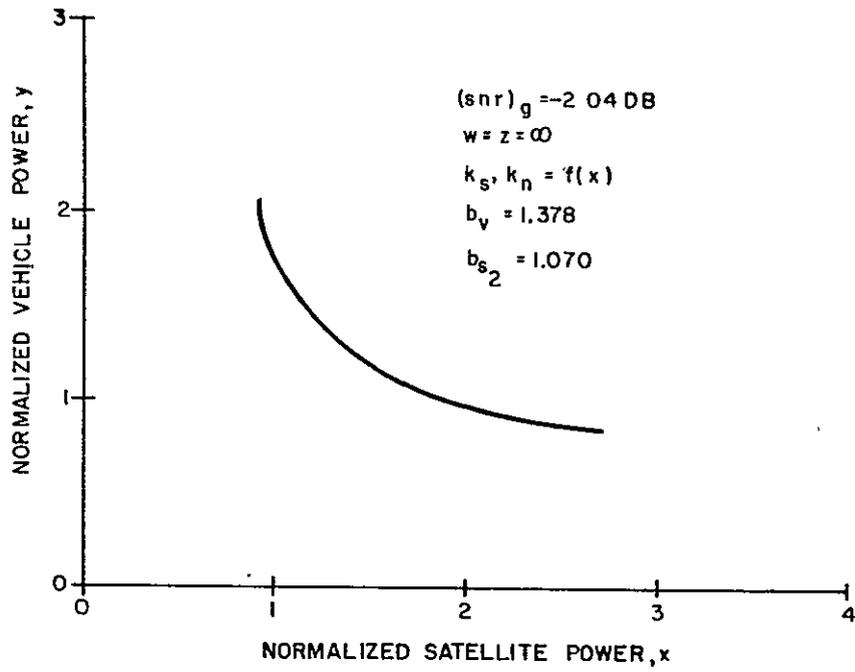
Figure A-9 Approximate Power Trade-Off Curves

A. 7. 3 Transmitted Power Calculations (Actual)

Using the exact form of the signal-to-noise equation, the power transmitted by the ground station, satellite, and vehicle will now be calculated.

A. 7.3.1 Ground-Station Transmitted Power

A suitable large value for the normalized ground-station power would be

$$w = 100 \qquad \text{(A-184)}$$

in which case, from (A-168),

$$P_g = 0.44 \times 100 = 44 \text{ watts} \qquad \text{(A-185)}$$

a small value for a ground-based radar. In fact, considerably higher values for P_g are conceivable, but little is gained from a further increase in w.

In this case, the signal-to-noise ratio at the limiter is, from (A-18) and (A-182),

$$(snr)_{vi} = \frac{x}{1 + \dfrac{x+1}{100}} \qquad \text{(A-186)}$$

A. 7. 3. 2 Satellite-to-Ground Transmitted Power

The power output of the second satellite transmitter is required to be within the capability of the proposed solid state device. Choose, as a reasonable value

$$P_{s_2} = 2 \text{ watts} \qquad \text{(A-187)}$$

In this case, from (A-177),

$$z = \frac{2.0}{0.00676} = 296 \qquad \text{(A-188)}$$

which is large enough to cause little snr degradation.

A. 7. 3. 3 Satellite-to-Vehicle Transmitted Power

The value of figure A-9 lies in its visual presentation of the satellite-vehicle power trade-off. A suitable approximate operating point can be chosen by keeping in mind the two opposing system requirements: (a) low vehicle tube power for the purpose of low cost, versus (b) low satellite tube power for the purpose of high reliability.

A reasonable value of satellite transmit power is

$$P_{s_1} = 5000 \text{ watts} \qquad \text{(A-189)}$$

in which case, from (A-171),

$$x = \frac{5000}{3500} = 1.43 \qquad \text{(A-190)}$$

A. 7. 3. 4 Equation Factors

At this point, the three factors in the $(snr)_g$ equation – k_s, k_n, and k_p – can be evaluated.

The limiter input signal-to-noise ratio is required in order to determine the limiter signal and noise adjustment factors. Substituting (A-188) and (A-190) in equation (A-186),

$$(snr)_{vi} = \frac{1.43}{1 + \frac{1.43 + 1}{100}} = \frac{1.43}{1.0243} = 1.396 \qquad (A-191)$$

From figure A-3, then,

$$k_s \doteq 1.080 \qquad (A-192)$$

and

$$k_n = 0.890 \qquad (A-193)$$

The power reduction factor is calculated by substituting (A-184) and (A-190) in equation (A-57), along with (A-140), (A-141), and (A-142).

$$k_p = \frac{(100)(1.43) + (1.43) \cdot \frac{1.070}{1.194} + (101) \frac{1.070}{1.378}}{(100)(1.43) + 1.43 + 101} = \frac{222.78}{245.43} = 0.909 \qquad (A-194)$$

A.7.3.5 Vehicle Transmitted Power

The final calculation, that of vehicle transmitted power, can now be calculated. Substituting the previously calculated numbers into equation (A-69) yields

$$0.626 = \frac{(1.080)(100)(1.43) \, y \, (296)}{\frac{0.890}{1.194}(1.43) \, y \, (296) + \frac{0.890}{1.378}(101) \, y \, (296) + \frac{1}{1.070}(101)(2.43)(296) + (101)(2.43)(0.909 \, y + 1)}$$

$$= \frac{45700 \, y}{19838 \, y + 68146}$$

$$y = \frac{42650}{33280} = 1.282 \qquad (A-195)$$

so that the vehicle transmitted power is, from (A-174),

$$P_v = 1.282 \times 2800 = 3590 \text{ watts} \qquad (A-196)$$

A.8 REPEATER GAINS

Three other quantities of interest are calculable from the equations and parametric values previously developed. They are the required net gains of the repeaters in the satellite and vehicle.

Substituting (A-189), (A-167) and (A-184) into equation (A-6) yields

$$A_{s_1} = \frac{5000}{(3.04 \times 10^{-5})(100 + 1)} = 1.63 \times 10^{16} \sim 162.1 \text{ db} \qquad (A-197)$$

which is the gain of the satellite outward repeater.

Substituting (A-196), (A-170), and (A-190) in equation (A-33) yields

$$A_v = \frac{3590}{(3.84 \times 10^{-15})(1.43 + 1)} = 3.85 \times 10^{17} \sim 175.9 \text{ db} \qquad (A-198)$$

which is the gain of the vehicle repeater.

Finally, substituting (A-187), (A-173), (A-194), and (A-195) in equation (A-58) yields

$$A_{s_2} = \frac{2}{(2.72 \times 10^{-15}) \left[(0.909)(1.282) + 1 \right]} = 3.40 \times 10^{14} \quad 145.3 \text{ db} \tag{A-199}$$

which is the gain of the satellite return repeater.

A.9 SATELLITE AND VEHICLE SIGNAL-TO-NOISE RATIOS

While the signal-to-noise ratio at the ground-station is the important quantity, it is of interest to know those ratios at the other three stations in the signal path. They may be found using the equations previously derived. For this purpose, it will be recalled that the normalized power parameters were chosen to be

$$w = 100 \tag{A-200}$$

$$x = 1.43 \tag{A-201}$$

$$y = 1.282 \tag{A-202}$$

$$z = 296 \tag{A-203}$$

and the factors were

$$k_s = 1.080 \tag{A-204}$$

$$k_n = 0.890 \tag{A-205}$$

$$b_{s_1} = 1.194 \tag{A-206}$$

$$b_v = 1.378 \tag{A-207}$$

$$b_{s_2} = 1.070 \tag{A-208}$$

A.9.1 Satellite (Ground-to-Vehicle Relay)

The signal-to-noise ratio at the satellite in the outward path is, from equation (A-5),

$$(snr)_{si} = w = 100 \sim + 20 \text{ db} \tag{A-209}$$

A.9.2 Vehicle

At the vehicle, before limiting, the signal-to-noise ratio is from equation (A-18),

$$(snr)_{vi} = \frac{wx}{w + x + 1} = \frac{(100)(1.43)}{100 + 1.43 + 1} = 1.396 \approx + 1.45 \text{ db} \tag{A-210}$$

This snr yields a transformation factor, from figure A-3 of

$$k_T = 1.224 \tag{A-211}$$

so that the snr at the limiter output is, from equation (A-34)

$$(snr)_{vo} = k_T (snr)_{vi} = (1.224)(1.396) = 1.708 \approx + 2.33 \text{ db} \tag{A-212}$$

A.9.3 Satellite (Vehicle-to-Ground Relay)

On the return trip through the satellite, the signal-to-noise ratio is, from (A-53)

$$(\text{snr})s_2 = \frac{k_s\, w\, x\, y}{k_n \dfrac{b_{s_2}}{b_{s_1}} xy + k_n \dfrac{b_{s_2}}{b_v}(w+1)y + (w+1)(x+1)}$$

$$= \frac{(1.080)(100)(1.43)(1.282)}{(0.890)\left(\dfrac{1.070}{1.194}\right)(1.43)(1.282) + (0.890)\left(\dfrac{1.070}{1.378}\right)(101)(1.282) + (101)(2.43)}$$

$$= \frac{198.2}{1.460 + 89.5 + 245.6} = \frac{198.2}{336.6} = 0.589 \approx -2.30\ \text{db} \qquad (A\text{-}213)$$

Comparing this value with the -2.04 db on the ground demonstrates the improvement in snr due to the noise reduction resulting from close AFC and bandwidth reduction at the ground station.

APPENDIX B
NUMBER OF GROUND STATIONS VS. ALTITUDE (GEOMETRIC CONSIDERATIONS)

- This Appendix examines the geometrical basis for ground station spacing to effect world-wide coverage. It is assumed that 100% minimum coverage is necessary but that minimum overlap coverage is desirable. Ground station minimum elevation angle visibility is taken into account.

B. 1 POSSIBLE DISTRIBUTIONS OF GROUND STATIONS

Assume first that uniform world-wide coverage is desired such that any satellite in any location is always in contact with at least one and preferably not more than one or two ground stations. If this is the case, then all satellites have maximum usefulness with regard to vehicle location. If ground beacons are then added to the ground complex, a given satellite will see at least one ground station whenever it sees a beacon. Then, at the worst, a complete satellite angular attitude fix may be obtained every time the satellite passes over a beacon, by a pair of (approximately) simultaneous interferometer measurements to both beacon and ground station, followed by a second pair of measurements after the direction of the beacon has changed by about 30 degrees with respect to the satellite. (However, a complete attitude and attitude rate determination may be made more quickly by taking pairs of measurements for every few degrees of directional change of beacon direction by an iterative procedure involving least squares or minimum variance data processing, which will cause the initially rough attitude-determination to converge to the correct value.)

For a first examination of the problem, we examine what perfectly uniform distributions of ground stations on a spherical earth are possible and then examine these in detail. Having done this, we then generalize to approximately regular distributions for any number of ground stations.

B. 2 PERFECTLY UNIFORM WORLD-WIDE DISTRIBUTION OF GROUND STATIONS

Given a uniform distribution of points on a sphere, a plane may be passed through every point, tangent to the sphere, and in this way a regular polyhedron is obtained. Since only five regular polyhedra exist, it follows that there are only five perfectly regular distributions of ground stations possible. The ground stations may be visualized as located at either the vertices or the face centroid of a spherical projection of the tetrahedron, cube, octahedron, dodecahedron, or icosahedron. A rundown on these is as follows, (in table B-1), where F = number of faces, V = number of vertices, and E = number of edges:

POLYHEDRONS FOR PLACEMENT OF GROUND STATIONS

Eulers Rule:		F	V	E	Edges per Vertex, e	Edges per Face, n	Face
$F + V = E + 2$	Tetrahedron	4	4	6	3	3	Triangle
	Cube	6	8	12	3	4	Square
Also $V = (\frac{Edges/face}{Edges/vertex})\, F$	Octahedron	8	6	12	4	3	Triangle
	Dodecahedron	12	20	30	3	5	Pentagon
$n\, F = (\frac{Edges}{Face})\, F = 2E$	Icosahedron	20	12	30	5	3	Triangle

The area of a spherical polygon (one face) $= \dfrac{4\pi r_o^2}{F} = (\theta - (n-2)\pi)\, r_o^2$ where n = edges/face, θ = sum of internal angles in radians. So, for a regular spherical polygon, one internal angle in degrees is:

$$A^\circ = (1/n)\theta^\circ = \frac{720}{nF} + (\frac{n-2}{n})\,180^\circ = \frac{V}{E}\,180^\circ = \frac{(n-2)V}{n(V-2)}\,180^\circ$$

If a is the great circle length in degrees of one edge, then:

For a spherical triangle: $\cos a/2 = \cos (180/n)\, \csc A/2 = \cos 60^\circ \csc (30^\circ + \frac{120^\circ}{F})$

For a spherical square: $\cos a/2 = \cos (180/n)\, \csc A/2 = \cos 45^\circ \csc (45^\circ + \frac{90^\circ}{F})$

For a spherical pentagon: $\cos a/2 = \cos (180/n)\, \csc A/2 = \cos 36 \; \csc (54^\circ + \frac{72^\circ}{F})$

If the ground station locations are regarded as at the vertices, then V is the number of stations and a is the angular great circle distance between them. If r_o = 3440 nmi, is the earth's radius, then $r_o a$ is the nmi distance between stations and we may make up table B-2.

TABLE B-2

SPACING OF GROUND STATIONS FOR VARIOUS POLYHEDRONS

	No. of Stations, V	Angular Spacing, a	Distance nmi, $r_o a$
Tetra.	4	109.4°	6560
Octa.	6	90°	5400
Cube	8	70.4°	4220
Icosa.	12	63.7°	3820
Dodeca.	20	41.8°	2510

Stations at the face-centroids of a tetrahedron can be regarded as located at the vertices of a similar tetrahedron, and stations located at the face-centroids of a cube may be considered as located at the vertices of an octahedron, so that no-additional station distributions are gained this way.

To determine satellite altitude, h, consistent with the above distributions, assume that ground station visibility (figure B-1) is limited to a minimum elevation angle, ϵ°, above the horizon.

From the law of sines:

$$\frac{h + r_0}{r_0} = \frac{\sin(90^\circ + \epsilon)}{\sin(90^\circ - \phi_0 - \epsilon)} = \frac{\cos \epsilon}{\cos(\phi_0 + \epsilon)}$$

giving: $h = 2r_0 \sin\left(\frac{\phi_0}{2} + \epsilon\right) \sin \phi_0/2 \cos(\phi_0 + \epsilon)$

Thus the region of the earth from which a satellite at altitude, h, is visible to a ground station is a circular area on the earth of great circle radius, ϕ_0 degrees. If the satellite is to be in contact with a least one ground station at all times, then at least one ground station must be within or on the edge of the circular area determined by ϕ_0 at all times. If stations are distributed to form the vertices of triangular areas as in the case of the tetrahedral, octahedral and icosahedral distrbutions, then figure B-2 may be used to find ϕ_0 minimum:
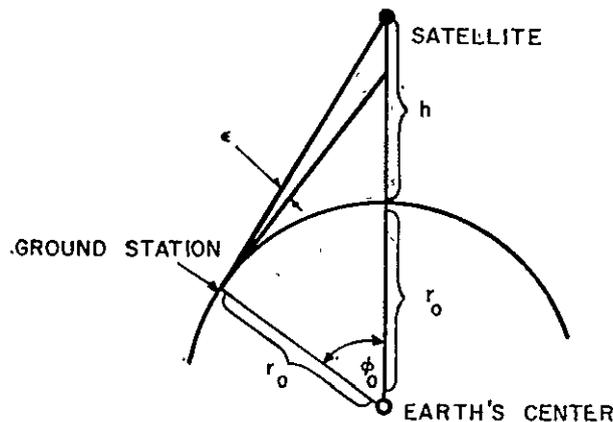
Figure B-1. Ground Station Visibility
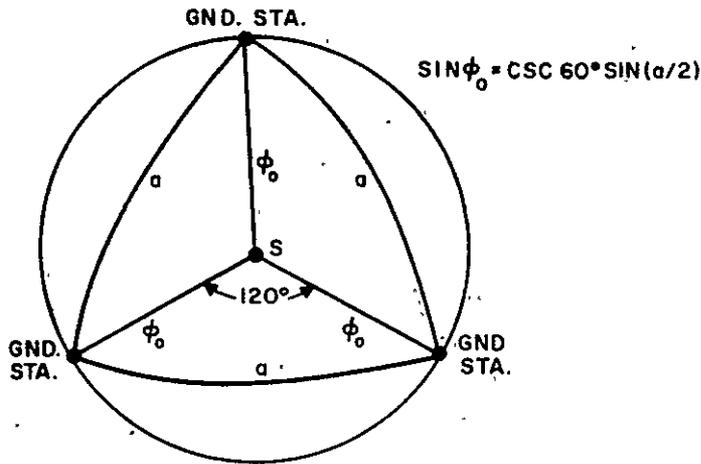
Figure B-2. ϕ_0 Minimum

For the sub-satellite point, S, as shown, if ϕ_0 were any smaller than shown, the satellite would be out of contact with any ground station. It can be seen that for $\sin \phi_0 = \csc 60 \sin(a/2)$ the satellite is always in contact with either one or two ground stations for a negligible movement of S in any direction from that shown above.

The same procedure for a cubic distribution gives:

$\sin \phi_0 = \csc 45° \sin (a/2)$

and the satellite is always in contact with one or two ground stations. Similarly for the dodecahedral (pentagonal) distribution.

Substituting for $a/2$, it will be found in general, that

$\cos \phi_0 = \text{Cot} (180°/n) \cot ((V/E)90°) = \cot (180°/n) \text{Tan} (\frac{(V-n)}{n(V-2)} 180°)$

For 4 stations: $\cos \phi_0 = \cot 60° \cot 60°$ giving $\phi_0 = 70.5°$

    6 stations: "   = $\cot 60° \cot 45°$ " $\phi_0 = 54.7°$

    8 stations: = $\cot 45° \cot 60°$ " $\phi_0 = 54.7°$

  12 stations: = $\cot 60° \cot 36°$ " $\phi_0 = 37.4°$

  20 stations: = $\cot 36° \cot 60°$ " $\phi_0 = 37.4°$

So for 4 stations: h = 3970 sin (35. 25°+ε°)/cos (70. 5°+ε°) = 6860 nmi for ε= 0°

6 or 8 " h = 3160 sin (27. 35°+ ε°)/cos (54. 7°+ ε°) = 2510 nmi for ε= 0°

12 or 20 " h " 2200 sin (18. 7° + ε°)/cos (37. 4°+ ε°) = 890 nmi for ε= 0°

For a minimum ground station elevation angle of ε° = 5°:

For 4 stations: h = 3970 sin 40. 25°/cos 75. 5° = 10, 250 nmi for ε= 5°

6 or 8 " h = 3160 sin 32. 35°/cos 59. 7° = 3,.350 nmi

12 or 20 " h = 2200 sin 23. 7°/cos 42. 4° = 1,.385 nmi

For a minimum ground station elevation angle of ε° = 10°:

For 4 stations: h = 3970 sin 45. 25°/cos 80. 5° = 16, 300 nmi for ε= 10°

6 or 8 " h = 3160 sin 37. 35°/cos 64. 7° = 4, 480 nmi

12 or 20 " h = 2200 sin 28. 7°/cos 47. 4° = 1, 560 nmi

B. 3 APPROXIMATELY UNIFORM WORLD DISTRIBUTION OF GROUND STATIONS

Eulers rule, $F + V = E + 2$ is true for any spherical polyhedron.

nF = (edges/face) $F = 2E$ is true if every spherical polygon has the same edges per face, and

$$A° \approx \frac{(n-2)V}{n(V-2)} \times 180°$$

is approximately true if the interior angles are all approximately equal. With these assumptions, approximately:

$$\cos \phi_0 = \tan (90 \frac{n-2}{n}) \tan (180 \frac{(V-n)}{n(V-2)})$$

Examination shows that ϕ_0 is smallest for n smallest, which gives minimum altitude satellite for minimum number of stations, so assume n = 3.

The $\cos \phi_0 = (1/\sqrt{3}) \tan (60° \frac{V-3}{V-2})$ where V = no. of stations

and altitude, $h = 6880$ nmi $\sin (\frac{\phi_0}{2} + \epsilon) \sin (\phi/2) / \cos (\phi_0 + \epsilon)$

Where ε° = minimum station elevation visibility angle. The above is plotted up as h versus V for values of ε° in figure B-4.

B. 4 GROUND STATION OVERLAP COVERAGE (INTERFERENCE)

For a network of ground stations, each having circular coverage, and placed on the earth in such a fashion that 100 percent coverage is obtained, there will in general be overlapping coverage. For ground station distribution as in the tetrahedral, octahedral and icosahedral distributions (that is, uniform distribution of 4, 6 and 12 stations) examined previously, a description of the overlap situation is obtained as follows. The great circle arcs between stations form triangular areas as shown in figure B-3.

(GREAT CIRCLE ARCS SHOWN AS STRAIGHT LINES)
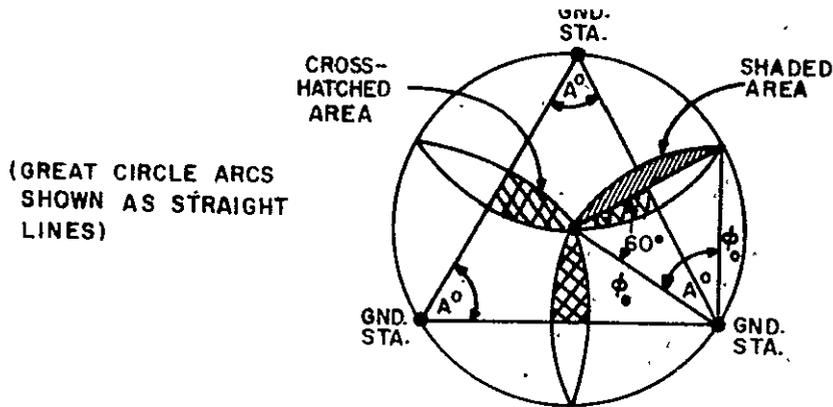
Figure B-3. Ground Station Overlap

The station overlap included in one triangular area is shown in cross hatched lines. It can be seen that the area of the shaded area is:

$$A (1-\cos \phi_0) \, r_0^2 - (A + \frac{\pi}{3} + \frac{\pi}{3} - \pi) r_0^2 = (\frac{\pi}{3} - A \cos \phi_0) \, r_0^2$$

The area of the ground station triangle is:

$$(A + A + A - \pi) \, r_0^2 = (3A - \pi) \, r_0^2$$

So the percentage overlap area within the triangle is:

$$100 \, x \, \frac{\pi - 3A \cos \phi_0}{3A - \pi} \quad , \text{ where } \cos \phi_0 = \cot 60° \cot (A/2)$$

A similar routine, run through for the 8 station (cubic) case, with stations distributed as at the corners of a square will show a percentage overlap of

$$100 \, x \, \frac{\pi - 2A \cos \phi_0}{2A - \pi} \, , \text{ where } \cos \phi_0 = \cot 45° \cot (A/2)$$

In general, for n sides, the percentage of overlap area is:

$$100 \, x \, \frac{(n-2) - nA \cos \phi_0}{nA - (n-2) \pi} \text{ where } \cos \phi_0 = \cot (180°/n) \cot (A/2)$$

$$= 100 \, x \, (V \sin^2 (\phi_0/2) - 1), \text{ where } V = \text{number of stations.}$$

Examination will show that in the case of the 4 station, 6 station, 8 station and 12 station uniform distributions previously cited, 100 percent coverage is obtained by at least one ground station and there is some overlap between pairs of stations (figure B-4), but there is no area covered or overlapped by as many as three stations. For the 20 station dodecahedral case, on the other hand, it will be found that a certain percentage of the area is covered by three stations. The percentage of three station overlap is:

$$100 \times \frac{2\pi - 20\, B \cos \phi_0}{5A - 3\pi}, \text{ where } \cot B = \tan 72° \cos \phi_0$$

$$\text{and } \cos \phi_0 = 36° \cot (A/2)$$

On the basis of the above formulas, if $A_1 \%$ is the percentage of earth's surface covered by at least one ground station, $A_2 \%$ the percentage area covered by at least two ground stations, and $A_3 \%$ the percentage of three or more station coverage (figure B-5), and if the ground station minimum elevation angle $\epsilon°$ is assumed to be 5°, then table B-3 may be drawn.

TABLE B-3

GROUND STATION COVERAGE

No. of Stations	$\epsilon = 5°$ Satellite Alt., h nmi	$A_1 \%$	$A_2 \%$	$A_3 \%$	No. of Stations Overlapping a Given Station
Tetra. 4	10,250	100	33.3	0	3
Octa. 6	3,350	100	26.7	0	4
Cube 8	3,350	100	69.0	0	3
Icosa. 12	1,385	100	23.0	0	5
Dodeca. 20	1,385	100	93.9	11.1	9
Approx. Uniform Triangular Distrib. 30	800	100	22		approx. 6
50	500	100	21		approx. 6

To obtain the figures in the last column, thought shows that for the tetrahedral distribution, any one station overlaps the other three; for the octahedral any one station is overlapped by the neighboring four equidistant stations, etc. For the dodecahedron, any one station overlaps all stations on the three joining pentagonal surfaces. For large numbers of ground stations, the maximum number of equilateral triangles that can be joined to form a vertex if there are enough stations so that the triangles are approximately planar (with internal angles approximately 60°) is six.
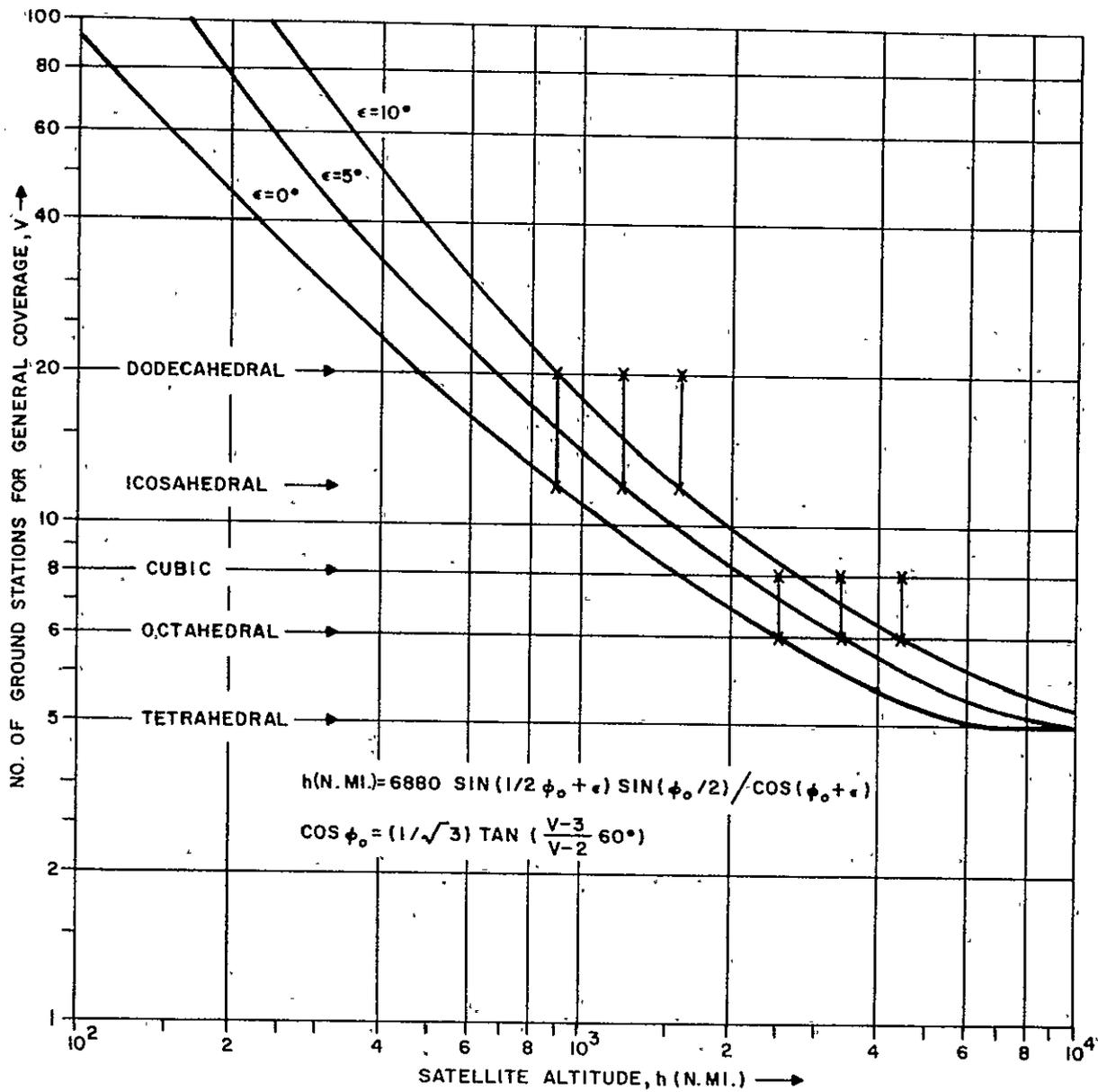
Figure B-4. Number of Ground Stations vs Satellite Altitude

A,B,C ARE TIE POINTS FOR THE THREE NEIGHBORING CIRCLES SHOWN.

TRIPLE OVERLAP AREA
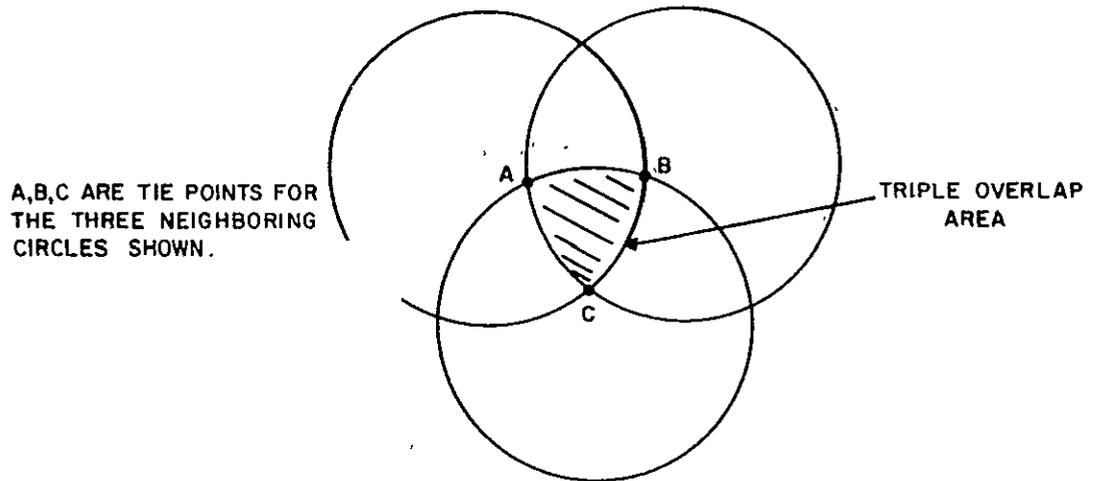
Figure B-5. Construction of Circles to Obtain Ground Station Placement

B.5 GROUND STATION LOCATION FOR 6000 NMI SATELLITE ALTITUDE

As pointed out previously in this Appendix a uniform distribution of six ground stations will insure contact at all times with satellites having a subsatellite great circle radius of coverage of ϕ_O = 54.7 degrees, or more. At an altitude of 6000 nmi we have:

For

$$\epsilon = \ \ 0°, \ \phi_O \ = 68.6°$$
$$\epsilon = \ \ 5°, \ \phi_O \ = 63.7°$$
$$\epsilon = 10°, \ \phi_O \ = 59.0°$$
$$\epsilon = 15°, \ \phi_O \ = 54.4°$$

Choosing an elevation angle of 5 degrees as an example, each station, for this altitude has a radius of coverage of 63.7 instead of 54.7 degrees. It is thus evident that for this altitude, any one or more, up to all six ground stations could be displaced by as much as 63.7 - 54.7 = 9 degrees from its nominal position without destroying 100 percent coverage The situation is actually more flexible than this, however, since a given ground station location can be moved more than the minimum 9 degrees by an amount depending upon the displacements of its neighboring ground stations. For the final solution to the ground

station placement problem for an altitude of 6000 nmi, we turn to a practical if not analytical approach. A globe of the earth is selected. Six wire circles are constructed, such that each, when placed on the globe has a great circle diameter of 2 x 63.7 = 127.4 degrees. The six circles are then mounted on the globe such that their circumferences are loosely joined together at their junction points (as shown below) using string so that no manipulation will reduce any triple overlap area to zero. This insures that 100% coverage is maintained. The six circles are then manipulated over the globe until land areas appear at the center of each circle. These are the possible ground station locations that will insure 100 percent coverage.

Possible ground station locations obtained in this way are listed in paragraph 7.2 of this document.

B.6 CONCLUSIONS

An absolutely uniform distribution of ground stations results in maximum utilization of each station for 100% coverage. Six station octahedral distribution results in 100% coverage for a satellite altitude of 2500 to 4500 nmi, depending on minimum ground station visibility elevation angle.

Numerous combinations of site locations are possible for the geometric configurations of six ground stations that will serve the system and provide world-wide coverage, with satellites at an altitude of 6000 nmi.

APPENDIX C

RADIOISOTOPE POWER SUPPLY CONSIDERATIONS

The effects of space environment on photovoltaic energy converters and the necessity of providing energy storage for night time electrical loads has resulted in a study of direct energy conversion devices for the navigation satellite. While there are many different direct energy conversion systems now in use or development, relatively few can be considered for extensive operation by 1970. Besides the photovoltaic-electrochemical (solar cell-battery) systems, the thermoelectric systems appear to have the greatest potential for applications in the power range under consideration in the 1970 period.

Since the thermoelectric couple depends on a difference in temperature to generate an electric current, some source of heat must be provided. Two sources of heat available are the sun and radioisotopes. To utilize the abundant thermal energy provided by the sun, about 130 watts per square foot in the vicinity of earth; some means of concentrating and/or collecting this energy must be provided. Orientation of this solar collector toward the sun within 2 to 5 degrees imposes a complexity and weight on the satellite which can not be justified. For this reason, a solar-thermoelectric system will not be considered.

Perhaps, the most attractive heat sources for use in space application in the electric power range being considered, are radioisotopes. A radioisotope-thermoelectric generator (RTG) would be uneffected by space radiation, has the potentiality of high reliability, can have long life, is uneffected by day-night orbits and can compare favorably with an oriented solar cell-battery system on the basis of the ratio of power output to weight. Norwithstanding these advantages, there are disadvantages which place serious doubt on possible use of an RTG as the primary source of electric power in the navigation satellite. These are the relative unavailability of suitable isotopes, their high cost and the need for heavy shielding, of some of the isotopes which may be available.

C.1 EVALUATION OF CANDIDATE ISOTOPES

With over a thousand known radioisotopes, the problem of selecting the most likely heat source candidates may seem quite formidable. However, there are criteria which can be applied to reduce this to a relatively few outstanding candidate isotopes. The main criteria influencing the selection are:

    a. Characteristics which assure the utility an isotope as a heat source:

        (1) The isotopes must have a half-life in the range of 1 to 100 years.

(2) The isotope must exist in high concentration as a stable, inert solid at the operating temperatures.

(3) The pure isotope must have a heat output greater than 0.1 watt/gram.

b. Characteristics which assure the future, practical and economical production of large quantities (thousands of grams) of the isotope:

(1) Isotopic separation processes are not required for either the target or the product.

(2) The target material must not be rare, too costly or practically unobtainable.

(3) Sufficient information must be at hand to define a realistic production process.

(4) If the isotope is a fission product, the fission yield must be greater than 0.1%. Fission yield is the number of atoms of isotope produced per hundred atoms of U-235 fissioned.

Since it establishes the time during which a device using the radioisotope may function, half-life is perhaps the most important factor in the evaluation of radioisotopes as heat sources. By applying the 1 to 100 year half-life criteria, the number of candidate isotopes is reduced to about 50. By applying the other criteria, this number can be reduced to eight candidate isotopes. Table C.1 lists these isotopes and several of their more important characteristics.

As was pointed out above, the list of eight candidate isotopes resulted from consideration of realistically usable half-lives and the practicality of the production processes. Three of the candidate isotopes are fission products, Strontium-90, Cesium-137 and Promethium-147, the remaining five are produced by neutron irradiation of special target materials.

C.1.1 Thermal Factors

In general, fission products have low specific power and irradiated products have high specific power. The heat producing properties become much more significant when the density of the compound form in which the isotope is used is taken into consideration. These differences are shown in Table C.1 in the values of power density (watts per cubic centimeter) and the volume of compound needed for a given heat output. In this table, the volume of the compound required to provide two kilowatts of heat is shown. Two kilowatts were chosen because at a realizable conversion efficiency of 5 percent (thermal to electrical energy) 100 watts of electrical energy could be produced. Figures C.1 and C.2 show the thermal watts output per initial gram versus time for various isotopes. This decay in heat output must be considered when designing an RTG because provision must be made to dissipate the excess thermal energy during the early life of the device.

C.1.2 Biological Factors

Although all radioisotopes must be regarded as very hazardous materials, the effects of isotopes on biological systems can influence the choice of isotope. Elements such as strontium and plutonium are readily deposited in human tissues (bone) and are difficult to expel. Cesium and promethium are not as readily retained in living tissue as strontium

C-2
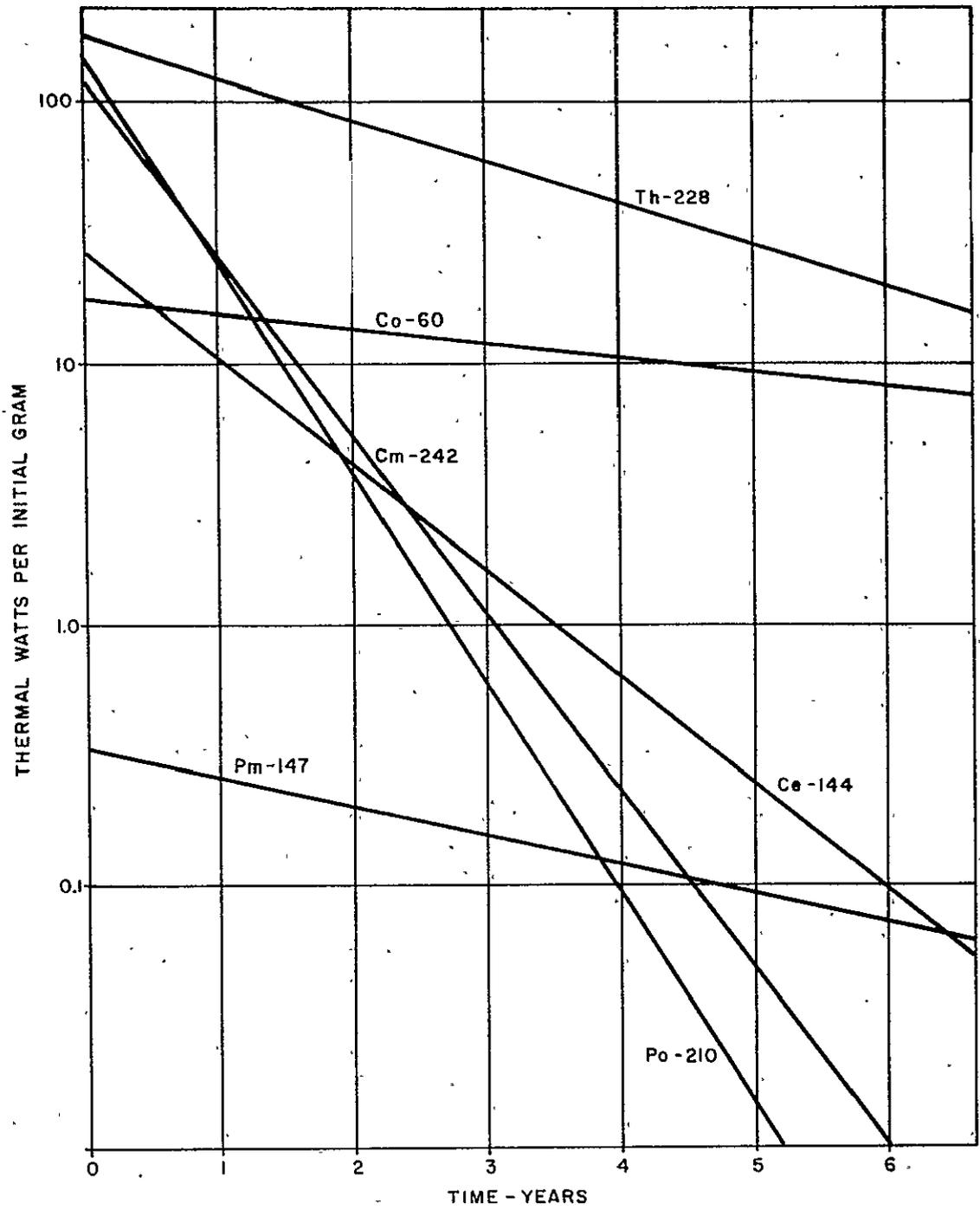
Figure C.1.   Thermal Watts Output Vs Time for Short-Lived
Radioisotopic Heat Sources
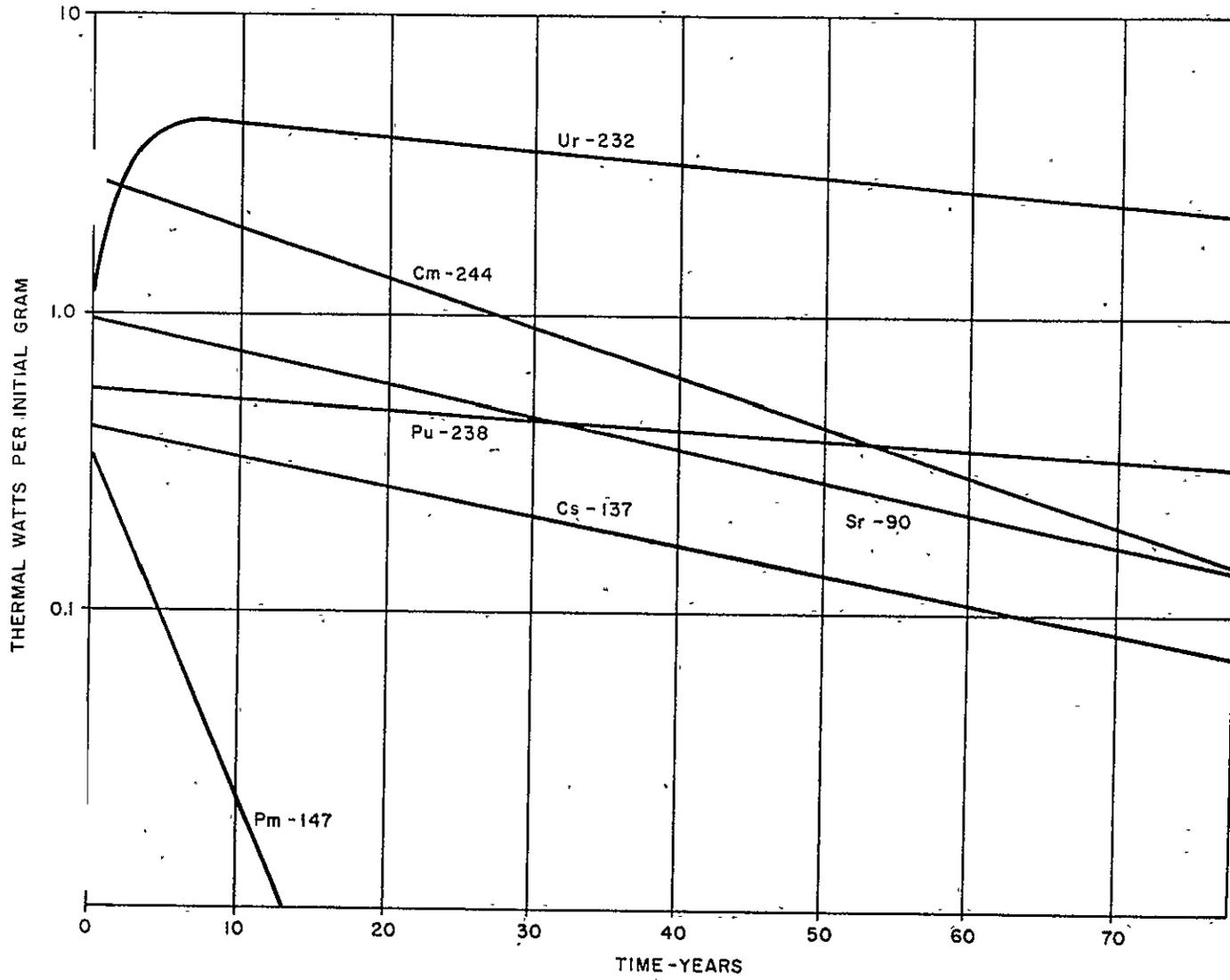
Figure C-2. Thermal Watts Output Vs Time for Long-Lived
Radioisotopic Heat Sources

and plutonium. Extensive precautions can be taken to insure the integrity of the isotope container so that it would not be ruptured during a launch abort or reentry. The least soluable compound forms can be selected and the satellite orbits can be selected such that many isotope half-lives pass before orbit decay would permit reentry into the earth's atmosphere. Regardless of these precautions, the political impact of launching certain of the biologically hazardous isotopes (strontium-90) must be considered.

C.1.3 Radiation Factors

Because energy is to be recovered by absorption of emitted radiation in matter, the easily absorbed alpha and beta radiations are of paramount interest. Alpha emitters of practical interest are available only by neutron irradiation of target materials. Beta emitters of practical interest are available as fission products and are produced as nuclear reactor by-products.

For beta emitters, there is a secondary effect which must be considered. Absorption of beta particles by any medium proceeds in part by collison energy transfer and partially by field interaction effects which result in continuous deceleration of the moving electron. Electromagnetic radiation, called bremsstrahlung, is released when the electron undergoes deceleration.

Ideally, the selected heat source would emit either no gamma radiation or would emit low energy radiation that would be absorbed by the container or encapsulating material. This condition exists in only two of the eight candidate isotopes (Promethium-147 and Plutonium -238).

The remaining six isotopes will, when fabricated into heat sources of practical size, emit electromagnetic radiation in the gamma or X-ray region. In applications where the existence of a substantial radiation field external to the source is intolerable, this field shall be attenuated with shielding materials. The amount of shielding varies with the energy of the primary beta radiation. Comparison of two pure beta emitters included in Table C.1 will illustrate this effect. In the strontium-90 system, the radio-active decay process does not produce primary gamma radiation. However, the emitted beta particles, which range in energy up to 2.26 Mev, produce bremsstrahlung gamma radiation external to a 100 thermal watt source. This requires shielding equivalent to 5 inches of lead to reduce the gamma dose rate to 10 mr/hr at 3 feet from the source. In contrast to this, the pure beta emitter Promethium-147, whose maximum energy in the beta spectrum is only about 0.23 Mev, emits only weak bremsstrahlung. The shielding required to attenuate the gamma field external to a 100 thermal watt source to a dose rate of 10 mr/hr at 3 feet is equivalent to about 0.3 inches of lead.

C.1.4 Availability and Cost

The availability and cost of the candidate isotopes are closely related and are, to a great extent, based on by-product availability, availability of target materials, and/or irradiation

source, processing facilities, and isotope fuel requirements. The quantity of isotopes made available is under study and is subject to actual isotope demand.

The fission products, Strontium-90, Cesium-137 and Promethium-147, have particular appeal because they do exist in fairly large quantities in waste from nuclear reactor fuel processing. However, dilution of these isotopes with relatively enormous volumes of other elements and salts in these wastes makes for costly isolation and purification of these materials. But the cost per kilowatt-hour on an optimum mission basis still would make the fuel costs of the fission product isotopes substantially less than the neutron irradiated isotopes.

One reason used for not considering an isotope as a preferred candidate was the need for isotope separation of either or both the target and product. This criteria for rejection is probably the only factor which has much hope for improvement. Reasonably economic isotopic separation processes, while not likely in the near future, can be anticipated for a variety of elements including those highly radioactive. The most outstanding isotope in this category is Thallium-204. This element is a pure beta emitter with a half life of 3.9 years and a specific power of about 0.65 watts per gram.

C.2 COMPARISON OF SYSTEMS

A comparison was made in Table C.2 of the RTG power supplies of likely isotopes and the solar-battery system on the basis of weight and cost for a 100 electrical watt output. Three and five year life systems were considered.

The fuel weight for the isotopes was derived for a thermoelectric generator with 5% efficiency and requiring 2 KW of thermal power. The lifetime of the isotope was considered. The "other weight" included the thermoelectric generator and the radiator. Converters and regulators were not included. This weight is based on the following:

Thermoelectric generator - 0.062 pounds per electrical watt

Radiators - 0.007 pounds per thermal watt dissipated.

The shield weight in Table C.2 includes sufficient shielding to limit the gamma and neutron does rate to a sufficiently low level so that electronic equipment in the satellite will not be damaged during a five year mission.[5,6] Shield weights assume a contoured shield that would limit gamma and neutron radiation at a distance of about one foot from the source to about 3 Rad in 48 hour period. A substantial reduction could be realized in the weight of the shield for the Sr-90 and Cm-244 isotopes if shielding for launch pad safety were not provided in the satellite. This can be done by programming of the launch with a "last minute" fueling operation that would include ground based shielding, special handling techniques and safety practices which would provide proper shielding for launch personnel. An approach such as this would make the Sr-90 isotope a much more attractive fuel.

The fuel costs were projected for availability in 1970 and are based on the Hanford Isotope Production Plant being in operation. The costs are also dependent on demand for the isotopes.

C. 3 CONCLUSION

The possibility of using an RTG as the primary source of electric power in the navigation satellite is based primarily on the availability of suitable isotopes. It is felt that the thermoelectric technology has advanced to a state which makes it entirely practical for 1970 applications. However, at this time, it appears very unlikely that suitable isotopes in sufficient quantity will be available for application to the navigation satellite. For this reason, the primary power supply for the navigation satellite will be a photovoltaic battery system.

Today, Plutonium-238 is most generally favored as a heat source because of its long half-life and that it can be used with essentially little special shielding. However, its projected high cost, scarcity, and unfavorable biological hazard encourages the search for a competitive material. It is probable, that the very long half-life of plutonium-238 cannot be considered as a strong point in its favor for use in the navigation satellite.

Although it is on the short end of the half-life scale (2.7 years) Promethium-147 can be realistically considered a substitute for Plutonium-238 in some applications. Its energy, cost, low shielding requirements, and minimum biological hazard are favorable aspects of Promethium-147.

In conclusion, it would appear that Promethium-147 should be seriously considered as a heat source, particularly if the use of Plutonium-238 is not indicated because of its cost, lack of availability, or the biological hazard. The availability of Promethium-147 is contingent on the proposed Hanford Isotope Production Plant being constructed and in production by 1970.

BIBLIOGRAPHY:

1. "Radioisotopic Heat Sources" - Atomic Energy Commission Research and Development Report, HW-76323 Rev. 1.
2. "Radioisotopic Heat Sources, Supplementary Data," AEC Research and Development Report - HW 78180
3. "The Hanford Isotope Production Plant," Engineering Study - HW-77770
4. "Nucleonics," March, 1963, Page 63, "Isotopes Costs and Availability" by H. L. Davis
5. "Shielding Requirements for Promethium Sources," HW-77375
6. "Radiation Characteristics and Shielding Requirements of Isotopic Power Sources for Space Missions." - ORNL-TM-591 (Rev.).

TABLE C-1

CHARACTERISTICS OF RADIOISOTOPES

	Cobalt -60	Strontium -90	Cesium -137	Promethium -147	Thorium -228	Uranium -232	Plutonium -238	Curium -244
Specific Power, Watts/gr	17.4	0.95	0.42	0.33	170	4.4	0.56	2.8
Half Life, years	5.3	28	30	2.7	1.9	74	89	18.4
Compound Form	Metal	Sr Ti O_3	Glass	$Pm_2 O_3$	Th O_2	UO_2	Pu O_2	Cm O_2
Compound Density, g/cc	8.9	4.6	3.2	6.6	9	10	10	11.75
Power Density Watts/cc	15.5	1.05	0.215	1.8	1270	33	3.9	27
Volume for 2KW Heat: cc	129	1840	9300	1120	1.58	61	513	74
Decay Product	Gamma	Beta	Beta-Gamma	Beta	Beta	Beta	Alpha	Alpha-Neutron
Shielding Req	Heavy	Heavy	Heavy	Minor	Heavy	Heavy	Minor	Heavy
Est. Cost, $/watt(thermal)	33	19	21	91	40	350	894	357
Production Capability (thermal KW)								
1963	Available now	19	5	0.01	–	–	1.5	–
1967	"	67	48	11.0	–	–	11.0	41
1970	"	157	110	25	–	–	25.8	129
1980	"	693	458	111	–	–	73.0	134

TABLE C-2

COMPARISON OF COST AND WEIGHT FOR SATELLITE POWER SUPPLY TO PROVIDE
100 - ELECTRICAL WATTS

3 Year System					
	Pm-147	Pu-238	Cm-244	Sr-90	Solar-Battery
Fuel Wgt. (lbs)	31.8	11.4	2.3	21.6	
Other Wgt. (lbs)	32.8	23.5	22.3	21.4	
Shielding	33.0	17.0	145.0	135.0	
Total	97.6	51.9	169.6	178.0	56.0
Fuel Cost, est.	$353,000	$1,810,000	$842,000	$42,800	$285,000*

5 Year System					
	Pm-147	Pu-238	Cm-244	Sr-90	Solar-Battery
Fuel Wgt. (lbs)	44.6	11.7	2.5	22.4	
Other Wgt. (lbs)	43.6	24.0	23.3	21.9	
Shielding	47.0	17.0	158.0	140.0	
Total	135.2	52.7	183.8	184.3	56.0
Fuel Cost, est.	$497,000	$1,850,000	$920,000	$44,300	$285,000*

*Cost of Solar Cells

APPENDIX D
TRANSPONDER ENERGY REQUIREMENT FOR ANGLE MEASUREMENT

In this appendix the relationship is established between vehicle transmitted energy and the signal-to-noise ratio in the ground station angle measurement noise bandwidth. From this relationship, the antenna spacing versus energy expression is derived as a function of angle accuracy.

D.1 ANALYSIS MODEL

The angle pulse will originate at the vehicle, be received, multiplexed and retransmitted, by the satellite, to the ground station. Angle measurement will be done in a bandwidth matched to the angle pulse width, i.e. $B = \frac{1}{\tau}$. Peak power requirements are established by the ranging requirements (Appendix A). These being fixed, transponder energy will be adjusted by varying pulse width.

The analysis model is shown in figure D-1. The transponder energy, $P_v \tau$, will be attenuated by the factor α_1 in transmission to the satellite. There receiver noise N_s will be added and the sum amplified by a factor β and retransmitted. Satellite transmitted power, P_s, will undergo attenuation (α_2) before reception at the ground station, where ground station receiver noise N_G will be added.

D.2 ANALYSIS

The vehicle transponder will transmit a peak power, P_v, and power received at the satellite will be $\alpha_1 P_v$,

where

$$\alpha_1 = \frac{G_v G_s \lambda_1^2}{(4\pi)^2 R^2 L_1}$$

G_v = vehicle antenna gain = 2 db,

G_s = satellite antenna gain = 9.7 db,

λ_1 = wavelength on vehicle to satellite link = 0.937 ft,

R = maximum range = 51.6×10^6 ft, and

L_1 = RF losses (including fade margin, polarization loss, safety factor, etc.) = 15 db.

Noise added at the satellite will be

$$N_s = K T_{es} B,$$

where

K = Boltzmann's constant
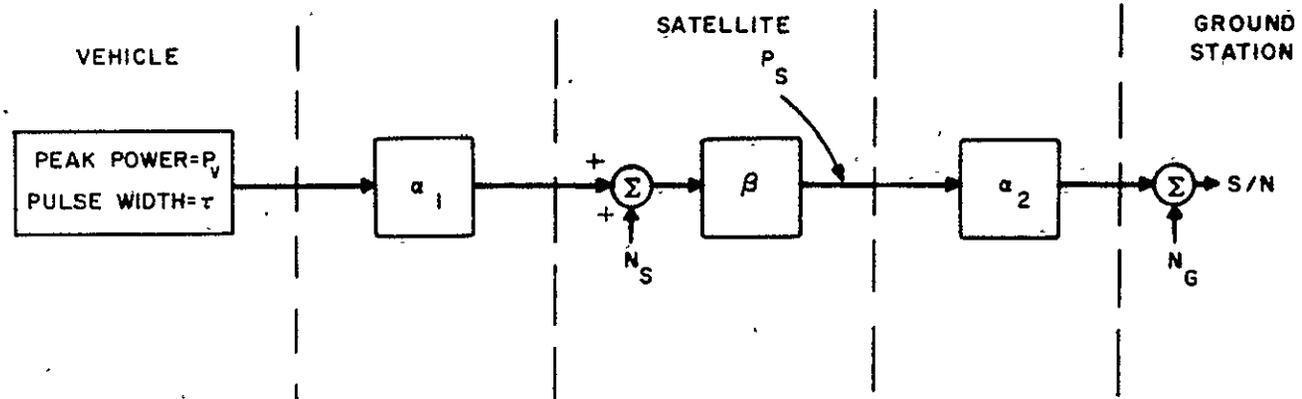
Figure D-1. Analysis Model, Angle Measurement Signal-To-Noise

T_{es} = satellite effective noise temperature

B = angle noise bandwidth

The sum of signal plus noise will be amplified by β to the level P_s.

$$P_s = (\alpha_1 P_v + N_s) \beta,$$

where

β = satellite repeater gain.

The signal plus satellite noise power received at the ground station will be

$$\alpha_2 P_s = \alpha_2 \beta (\alpha_1 P_v + N_s),$$

where

$$\alpha_2 = \frac{G_s G_g \lambda_2^2}{(4\pi)^2 R^2 L_2}$$

G_s = satellite antenna gain = 9.7 db,

G_g = ground station antenna gain = 42.5 db,

λ_2 = wavelength on satellite to ground station link = 1.014 ft,

R = maximum range = 51.6×10^6 ft,

L_2 = RF losses (including fade margin, etc.) = 14 db.

Ground station receiver noise will add to the signal power plus satellite noise power:

$$N_G = K T_{eG} B,$$

where

T_{eG} = ground station receiver effective noise temperature = 50°K.

Signal power then will be

$$\alpha_1 \alpha_2 \beta P_v$$

and total noise power will be

$$N_G + \alpha_2 \beta N_s.$$

So the signal-to-noise ratio will become

$$S/N = \frac{\alpha_1 \alpha_2 \beta P_v}{N_G + \alpha_2 \beta N_s}.$$

The satellite power, (P_s) will be 0.2 watt. (The two watt transmitter is shared by ten signals – interferometer signals and reference frequency signals. Thus the power per signal becomes 0.2 watt.)

Satellite gain will be that required to amplify signal plus noise to P_s = 0.2 watt.

$$\beta = \frac{P_s}{P_v \alpha_1 + N_s}$$

Thus, substituting into the S/N term,

$$\frac{S}{N} = \frac{\alpha_1 \alpha_2 P_s P_v}{N_G (P_v \alpha_1 + N_s) + \alpha_2 N_s P_s}$$

and substituting the value for N_G and N_s

$$\frac{S}{N} = \frac{\alpha_1 \alpha_2 P_s P_v}{KB (\alpha_1 P_v T_{eG} + \alpha_2 P_s T_{es} + KB T_{eG} T_{es})}$$

Since transponder energy $= P_v \tau = \frac{P_v}{B}$:

$$\frac{S}{N} = \frac{\alpha_1 \alpha_2 P_s}{K(\alpha_1 P_v T_{eG} + \alpha_2 P_s T_{es} + KB T_{eG} T_{es})} \text{ X transponder energy}$$

Using the values listed above, this relationship is plotted in figure 6.1-28.

S/N is related to interferometer baseline by the expression for angle error as a function of phase error:

$$\epsilon_\theta \approx \frac{\lambda}{2\pi D} \epsilon_\phi,$$

where

ϵ_θ = angle error

ϵ_ϕ = phase error

D/λ = antenna separation in wavelengths.

As shown in Section 3.5.2 (angle error analysis), the phase error (1σ) as a function of S/N is

$$\epsilon_\phi = \frac{0.463}{\sqrt{S/N}}.$$

Therefore .

$$\epsilon_\theta = \frac{\lambda}{2\pi D} \text{ X } \frac{0.463}{\sqrt{S/N}}$$

The angle error allotted to noise effects is 0.02 milliradian. Thus,

$$D/\lambda = \frac{3.69 \text{ X } 10^3}{\sqrt{S/N}}.$$

The latter is also shown in figure 6.1-28.

APPENDIX E

SOLAR CELL SURFACE CONFIGURATION EFFICIENCY

In the Navigation Satellite, the solar cells are mounted on the satellite body. The efficiency of the solar cell mounting configuration is examined in this appendix. The efficiency is examined in terms of effective solar cell area to total solar cell area.

The satellite is cylindrical with the long axis of the cylinder stabilized along the local vertical. The cylinder may be thought to be made up of two representative areas A_N and A_E as seen in Figure E-1 when A_N is the projected area of the long section of the cylinder and A_E is the end area.

The case of lowest solar cell efficiency is when the orbital plane is parallel to the sun line. It is seen in Figure E-1 that the power output from the solar cell areas A_N and A_E are rectified sine waves except for a shadow region of 2θ. The end of the cylinder away from the earth follows a half wave sine wave path and is unaffected by shadowing. The end of the cylinder facing the earth is not coated with solar cells because of the low efficiency.

The solar cell efficiency, as used in the power supply analysis, is:

$$\eta = \frac{\text{Effective Solar Cell Area During Sunlit Portion}}{\text{Total Solar Cell Area}}$$

Using Figure E-1 as a reference, the following equation is obtained:

$$\eta = \frac{\dfrac{A_N}{\pi - \theta} \displaystyle\int_0^{180° - \theta} \sin\theta \, d\theta + \dfrac{A_E}{\pi - \theta}}{\pi A_N + A_E}$$

The central angle portion of the orbit in shadow is 2θ where

$$\sin\theta = \frac{R_E}{h + R_e}$$

and for a 6000 nmi altitude

$$\theta = 21.5°$$

Solving for η and rearranging terms

$$\eta = \frac{\dfrac{A_N}{A_E} \dfrac{1}{(\pi - \theta)} \left[1 + \cos\theta\right] + 1}{\pi \dfrac{A_N}{A_E} + 1}$$

For the navigation satellite configuration, $\dfrac{A_N}{A_E} = 10$.

Substituting this value and solving the equation for η

$\eta = 24.7\%$

This value is used to determine the solar cell area required on the vehicle.
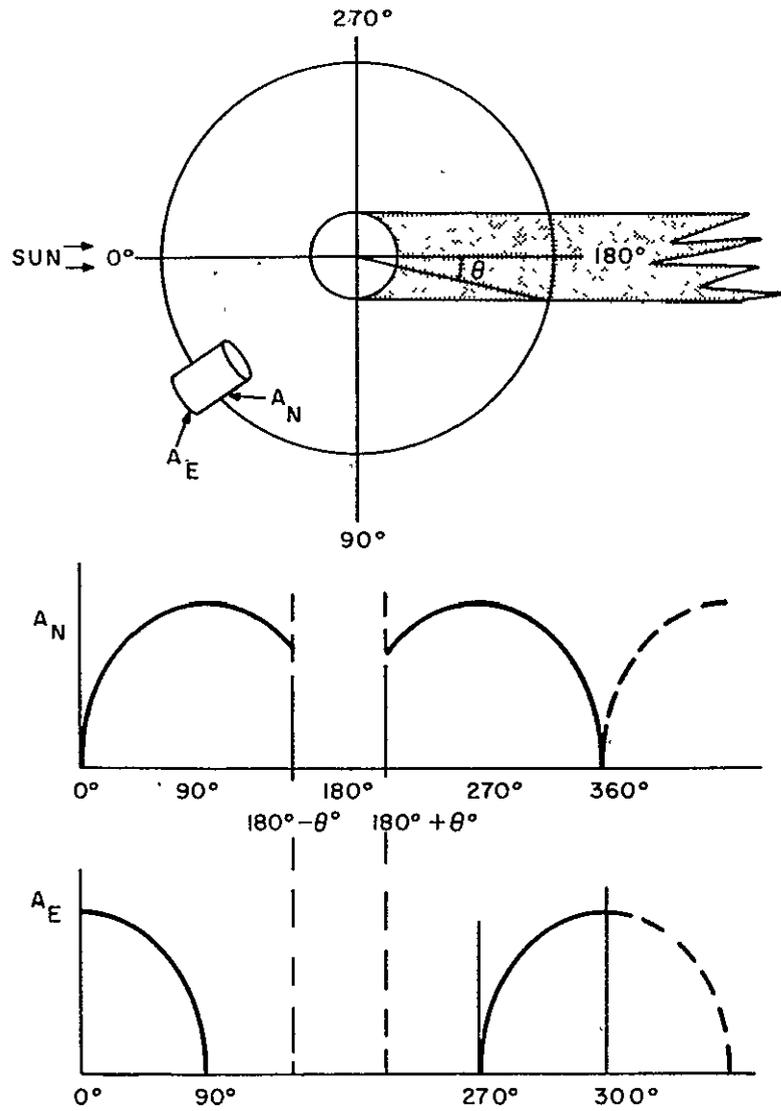
Figure E-1. Solar Cell Output in Orbit

APPENDIX F
PULSE STRETCH DEGRADATION

The accuracy of the range measurement depends on the quality of the received stretched signal. When the signal is compressed a number of time side lobes appear. No side lobe can be large enough to have a high probability of detection if a true measurement on the main return pulse is to be ensured. In addition, the compressed pulse main lobe is required to have a high detection probability to ensure reception of the pulse and a large s/n ratio to allow a precise measurement.

Because the frequency distribution of the signal is rectangular, its time transform is of a $\frac{\sin x}{x}$ form. This means that without compensation, the compressed signal will have natural side lobes at a level of -13.5 db. To reduce this effect, an amplitude weighting filter is used to reduce the natural side lobes to -20 db.

In passing through the various components in the radar links, the stretched pulse's phase and amplitude characteristics will be altered. This distortion introduces disturbance side lobes on the compressed pulse which increase the false detection probability. The effects of phase and amplitude distortion introduced in the multiple repeater system are analysed in section F.1 and the magnitude of the disturbance side lobes is calculated.

F.1 ANALYSIS

The ranging system can be considered as a linear transmission system whose steady state transfer admittance is defined as

$$Y(\omega) = A(\omega)e^{j\beta(\omega)}$$

The steady state amplitude response of the system is $A(\omega)$ and the steady state phase characteristic is $B(\omega)$. Each of these terms can be described by a Fourier series expansion about the frequency band of interest. Analysis in the literature[1] shows that this relationship is accurately given by

$$A(\omega) = a_o + a_1 \cos c\omega$$

and

$$B(\omega) = b_o \omega + b_1 \sin c\omega$$

When the stretched pulse is passed through the transmission system described by the above equations, distortion terms appear in the compressed pulse. A simplified Fourier series expansion for the first order terms of the system output pulse is

$$I(t) \approx a_o \left[E(t + b_o) + \frac{1}{2} (\frac{a_1}{a_o} + b_1) E(t + b_o + c) \right]$$

This series expansion represents the system response to amplitude and phase distortion only. The expansion does not include the natural response to the stretched pulse signal.

---

[1] J.R. Klauder, et al, "The Theory and Design of Chirp Radars", Bell System Technical Journal, Vol. 39, July 1960

It can be seen that the response consists primarily of a main pulse plus a pair of echoes produced by the amplitude and phase distortion. These echoes are, in effect, side lobes of the main response signal and can result in an erroneous range measurement if they are large enough to be detected by the range threshold. The spacing of the echoes with respect to the major response is determined by the frequency (C) of the disturbing function. When C is large enough to produce distinctive side lobes, the side lobe amplitude due to amplitude distortion is $\frac{a_1}{2a_0}$ and the amplitude due to phase distortion is $\frac{b_1}{2}$. Plots of these relationships are shown in figure F-1. The magnitude of these disturbance side lobes depends upon the total system intrapulse amplitude and phase linearity.

If the frequency, C, of the disturbing function is low, its period is less than the length of the expanded pulse, a resulting side lobe will be superimposed on the compressed pulse main lobe. The result will be a pulse distorted in amplitude and of broadened width. The amount of distortion depends on the size and frequency of the disturbance. Such a disturbance can result from an IF amplifier whose phase characteristic in the pass band is non-linear. These characteristics are associated with a single tuned band pass amplifier.

Another source of pulse distortion is quadratic phase distortion. Since the transmitted pulse has a phase characteristic which contains a square-law term, any characteristic of the system transfer function which contains a like term in the system transfer function is a potential distortion source. The effect on the pulse is to alter the expanded pulse length. When the pulse is recompressed, the resultant pulse will be broadened with a corresponding decrease in amplitude. The main source of quadratic phase distortion would be from the difference in the transfer characteristics of the delay lines used to expand and compress the pulse. This problem is essentially eliminated by mechanizing the system such that the same delay line is used for both functions. The effects of any additional incidental quadrature phase error would be reduced to an insignificant amount by the amplitude weighting filter[1].

The above effects on side lobe level by amplitude and phase distortion can be assumed to result principally from the characteristics of the IF amplifier portions of the repeaters. In addition, the microwave portions must have linear phase characteristics. Non-linearity can be caused by multiple reflections in the RF transmission lines in the repeaters[2].

If a length of lossless transmission line connects a generator and an antenna of equal mismatch, the transmitted voltage is given by

$$T = \frac{1}{\cos \theta + j \frac{1}{2} (Z + \frac{1}{Z}) \sin \theta}$$

where Z is the normalized impedance and θ is the phase shift of the lossless transformer. The maximum resulting differential phase shift is given by,

---

[1] Klauder, et al; ap. cit.

[2] J. Reed "Long Line Effect in Pulse Compression Radar", The Microwave Journal, vol. 4, pp 99-100; September, 1961.
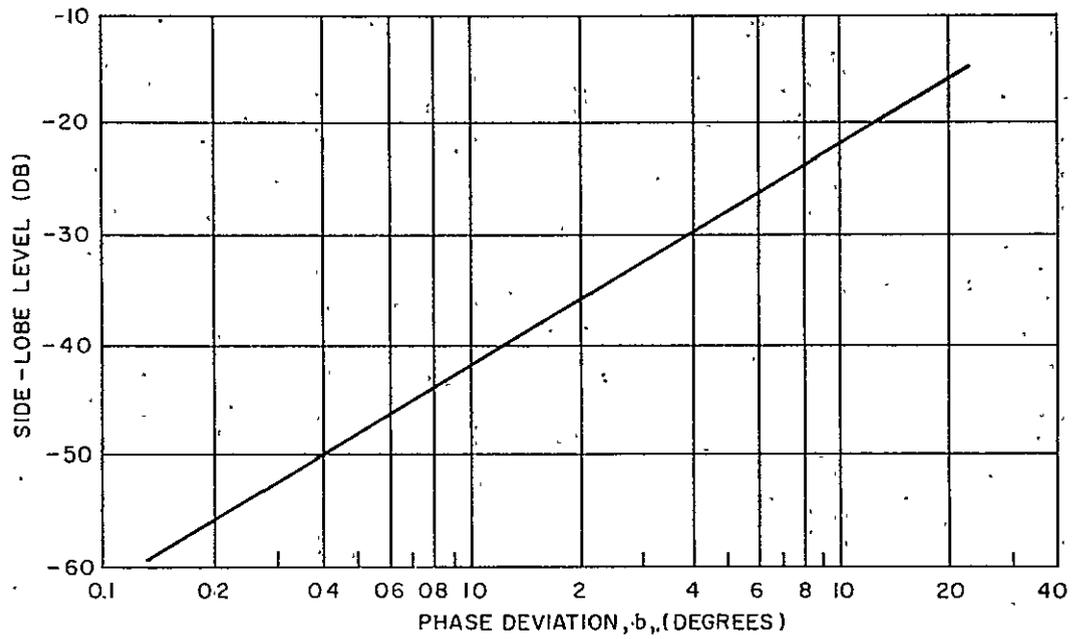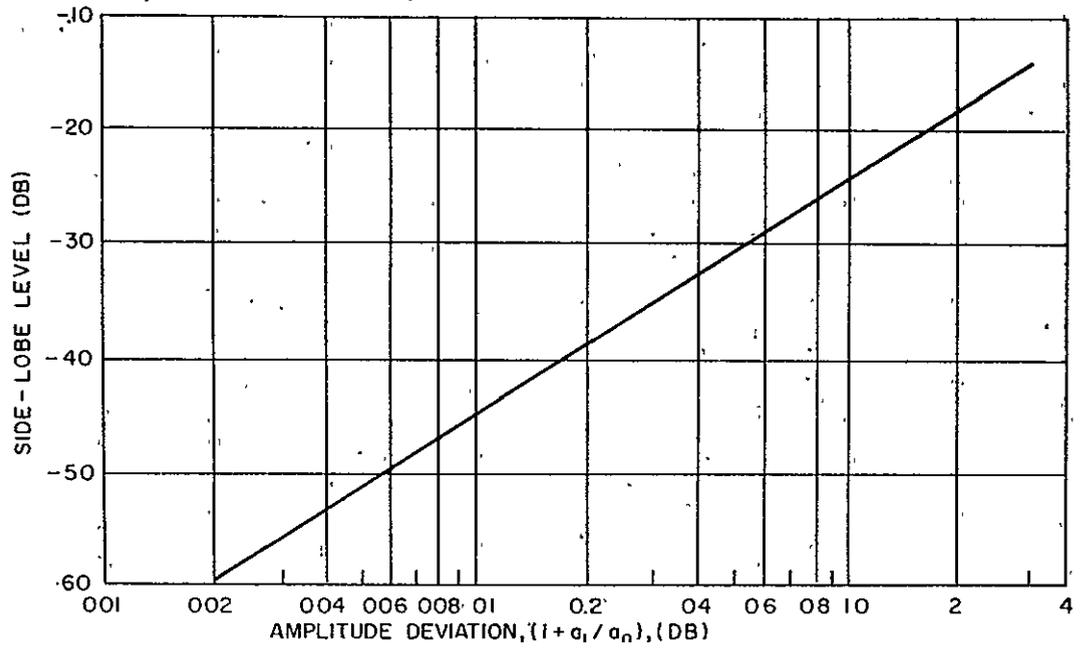
Figure F-1. Effect of Amplitude and Phase Deviations
on Side-Lobe Level

$$\alpha = \tan^{-1} \frac{(Z-1)^2}{\sqrt{8\,Z\,(Z^2+1)}}$$

Figure F-2 is a plot of this differential phase shift as a function of the mismatch VSWR. To determine whether mismatch will result in individual side lobes or in superposition of signal on the main lobe, the rate of occurance of reflections must be known. Mismatch phase distortion is essentially a sinusoidal modulation that is superimposed on a linear phase characteristic. The frequency of the modulation is given by the number of times that the pattern repeats. This is equal to the number of times that the phase shift varies by a wavelength on the frequency changer. For a coaxial cable this is given by,

$$\Delta f = \frac{f\,\lambda_0}{S}$$

where S is the length between the two mismatches. For the nominal frequency of 1 kmc of the various links of the proposed system and a frequency sweep of 159 KC, this is given by,

$$\Delta f \approx \frac{160 \times 10^3}{S}$$

The period is then

$$\Delta T \approx \frac{S}{160 \times 10^3} \ .$$

If S is equal to one wavelength, the side lobe will be spaced at the first zero crossing of the $\frac{\sin \Delta t}{\Delta t}$ output characteristic. If the length, S, is less than a wavelength the sidelobe will be superimposed on the main lobe of the compressed pulse.

F.2 DEGRADATION OF PULSE STRETCH SIGNAL IN SYSTEM COMPONENTS

F.2.1 Satellite Repeaters

The characteristic of the satellite repeaters is determined by the IF amplifiers. By allowing for a design where the amplifier is basically a wideband amplifier with a bandpass filter very good amplifier characteristics can be obtained. The two satellite repeaters are essentially the same type and the specifications for the repeaters will be considered to be similar. Amplifier amplitude ripple of 0.1 db is a reasonable design goal and will result in a side lobe of -45 db. The phase characteristic will depend on the characteristic of the filter and the stability of the local oscillator. The filter phase characteristic should be linear and contain no high frequency phase variations. Solid state multipliers, for use as local oscillators, are capable of having phase stability of 0.1 degrees. For a very conservative overall design case of 1.0 degree stability, the side lobe would be -42 db. A reasonable design goal for VSWR in the microwave portion of the circuitry is 1.2, which results in a
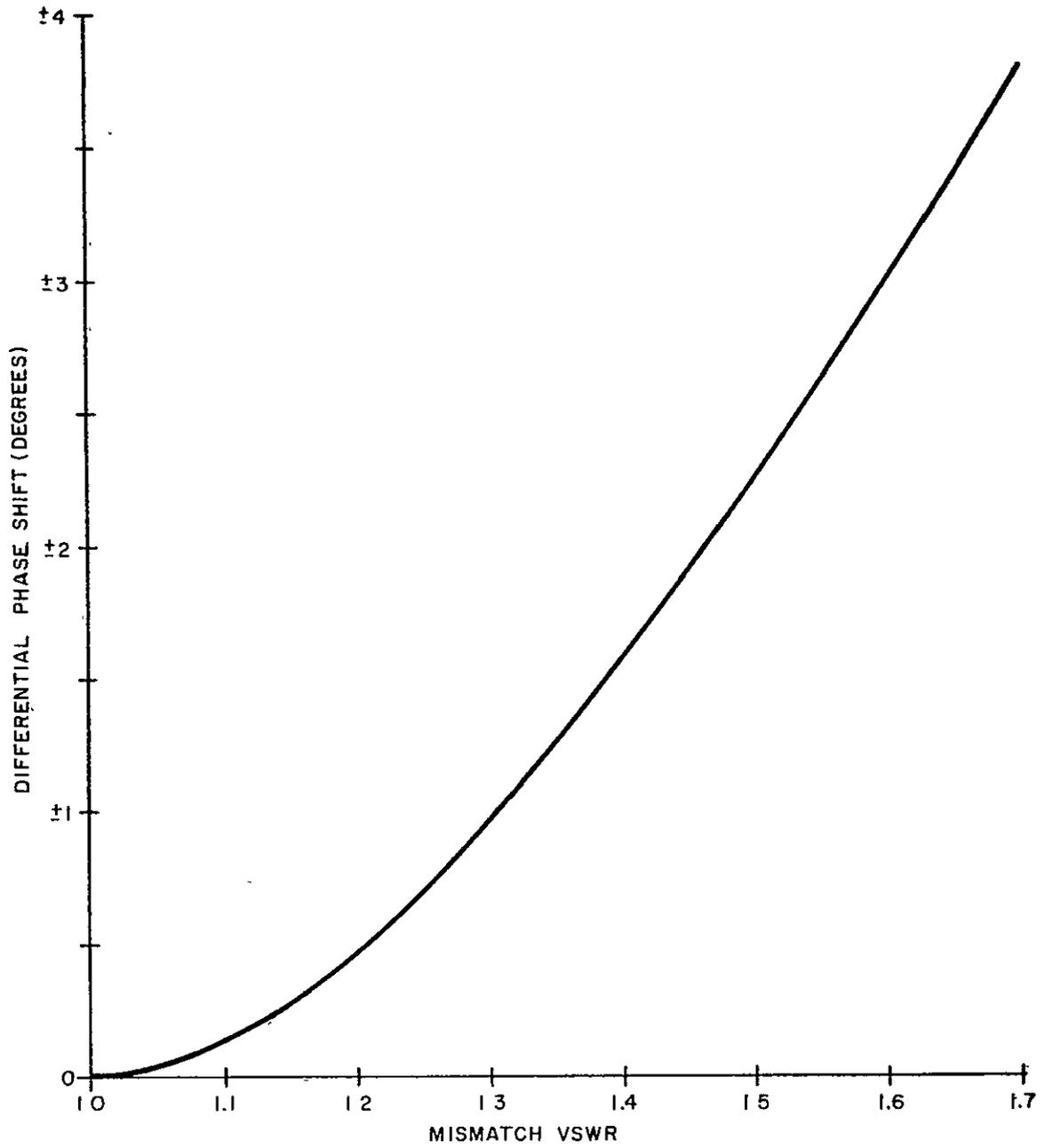
Figure F-2. Non-Linear Phase Distortion vs VSWR for
Two Equal Mismatches

maximum phase shift of 0.5 degrees. The resulting side lobe level is -47 db. There should not be an appreciable quadrature phase error due to the repeater mechanization.

F.2.2 Vehicle Repeater

The characteristic of the vehicle repeater can be considered to be that of the IF band pass filter. The specifications for this repeater will be somewhat relaxed from the specifications of the satellite repeaters. An amplitude ripple of 0.5 db results in a side lobe of -31 db. A conservative phase stability design goal of 5 degrees would result in a side lobe of -27 db. The microwave design should be as good as the design for the satellite repeaters with a corresponding side lobe of -47 db. Again there should not be significant quadrature phase error sources in the vehicle repeater.

F.2.3 Ground Station

The characteristic of the ground station receiver is that of an IF bandpass amplifier in a well controlled environment. As such, a maximum of 0.1 db amplitude ripple would be expected with a corresponding side lobe of -45 db. The phase characteristic should be sufficiently linear to insure that no high frequency phase variations are introduced. The solid state multiplier used as the local oscillator is capable of maintaining a phase stability of 0.1 degrees. Additional miscellaneous phase instabilities can be held to within 0.5 degrees. The resulting side lobe from the phase instabilities would be -47 db. Since the same delay line is used for reception and transmission, there will not be a significant quadrature phase distortion. The microwave portion of the ground station will have a VSWR of less than 1.2 and results in a maximum phase shift of 0.5 degrees with a resulting side lobe level of -47 db.

F.3 SUMMARY

To determine the possibilities of a false range measurements on a side lobe, both the natural side lobes and the disturbance side lobes must be considered. Table F-1 summarizes the effects on the pulse stretched signal resulting from the amplitude and phase response tolerances of all portions of the system hardware.

TABLE F-1

SUMMARY OF PULSE STRETCHED DEGRADATION FACTORS
DUE TO SYSTEM MECHANIZATION

Source	Amplitude Ripple $1 + \frac{a_1}{a_0}$ (db)	Phase Ripple b_1 (degrees)	$1 + \frac{a_1}{a_0}$	$\frac{1}{2}\frac{a_1}{a_0}$	$\frac{b_1}{2}$ (Radians)
Satellite Repeater #1	0.1	1.5	1.0126	0.0063	0.0131
Vehicle Repeater	0.5	5.5	1.0604	0.0302	0.0454
Satellite Repeater #2	0.1	1.5	1.0126	0.0063	0.0131
Ground Station	0.1	1.0	1.0126	0.0063	0.0087

The frequencies of the most significant disturbances would be those where the resultant side lobes occur at the same time separation as the natural side lobes. The contribution of the natural side lobes at -20 db. is 0.1000. The most significant disturbance side lobes for the satellite range measurement are:

$$S.L._S = 0.1000 + 0.0063 + 0.0131 + 0.0063 + 0.0087$$

$$= 0.1344 \sim -17.4 \text{ db}$$

The side lobe level then is so low that its detection probability is negligible. The most significant disturbance side lobes for the vehicle range measurement are:

$$S.L._V = 0.1000 + 3(0.0063) + 0.0302 + 2(0.0131) + 0.0454 + 0.0087$$

$$= 0.2294 \sim -12.8 \text{ db}$$

The most significant compressed s/n ratio is 15 db. This will result in a detection probability of 99.3% for the required detection of 2 out of 3 range pulses. The side lobes are at s/n = 2.2 db and is so low that the probability of detection is negligible.

APPENDIX G

GENERALIZED APPROACH TO SATELLITE ANGULAR ATTITUDE DETERMINATION AND ERROR ANALYSIS EQUATIONS.

In this Appendix, the necessary equations to determine satellite angular attitude and target vehicle location and the resulting equations for a system error analysis exclusive of orbit and satellite dynamics are derived. Non-simultaneous attitude measurement fixes, interferometer scale factors and time delays, and non-orthogonal interferometer axes are considered with the satellite assumed to be rotating in any known manner.

G.1 SUMMARY OF ATTITUDE MEASUREMENT CONSTRAINTS

a. Two beacon measurements (angular fixes) determine one interferometer axis if the scale factor and time delay are known.

b. Four beacon measurements determine two independent axes.

c. Three measurements determine two axes with one constraint, i.e., perpendicularity

d. One ground station (or beacon) gives one measurement per axis.

e. Two ground stations or beacons fix two independent axes (except for ambiguities) or fix one orthogonal pair of axes and give one check measurement.

f. Therefore, two ground stations or beacons give one less than the required number of measurements to fix one orthogonal pair of axes plus two interferometer constants.

g. Three beacons (6 measurements for two interferometers) determine two independent axes (4 measurements) plus two interferometer constants (2 measurements); or determine one orthogonal pair of axes and one additional check measurement.

h. To determine two axes plus 4 interferometer constants (3 [orthogonal axes] or 4 [independent axes] measurements plus 4 measurements, making a total of 7 or 8 required measurements), four beacons are required.

G.2 LIST OF SYMBOLS USED

I, J, K: The satellite angular attitude reference set of orthogonal coordinates that are centered at the satellite and are assumed known. I, J, K are unit vectors. I, J, K are fixed in space or have a known moving orientation in space and are not fixed relative to the satellite.

i, j, k: The satellite coordinate system that is approximately fixed in the satellite body and is not necessarily orthogonal. Interferometer axes are assumed fixed or aligned to i, j, and/or k where i, j, k are unit vectors.

Φ: The rotation matrix, dyadic, or tensor describing relation between i, j, k and I, J, K and not necessarily orthogonal.

$$\Phi = iI + jJ + kK \text{ and } i = \Phi \cdot I, \ j = \Phi \cdot J, \text{ etc.}$$

C_{mn} : The m_{th} measurement made by the n_{th} interferometer. This quantity is a scalar.

a_n : The n_{th} interferometer scale factor. This quantity is a scalar.

D_n : The n_{th} interferometer time delay. This quantity is a scalar.

$\overline{r_1}, \overline{r_2}, \overline{r_3}$: Unit vectors describing the known directions of the fixed ground beacons with respect to satellite and are expressed in terms of I, J, K.

$\overline{r}^1, \overline{r}^2, \overline{r}^3$: A reciprocal set of vectors (not necessarily unit vectors) to the set $\overline{r_1}, \overline{r_2}, \overline{r_3}$.

$$\overline{r_1} \cdot \overline{r}^1 = 1, \ \overline{r_2} \cdot \overline{r}^1 = \overline{r_3} \cdot \overline{r}^1 = 0, \text{ etc.}$$

$$r^1 = \frac{(\overline{r_2} \times \overline{r_3})}{(\overline{r_1} \cdot \overline{r_2} \times \overline{r_3})}, \text{ etc.}$$

Φ_1 : The satellite attitude at time t_1. This quantity is a tensor.

Φ_2 : The change in satellite attitude from time t_1 to time t_2. This quantity is a tensor.

Φ_3 : The change in satellite attitude from time t_2 to time t_3. This quantity is a tensor.

$\overline{r_1}', \overline{r_2}', \overline{r_3}'$: The beacon measurements that are taken at different times and are expressed in terms of I, J, K and W. (vectors).

W : The satellite body angular velocity vector relative to inertial space.

1 : A unit tensor, matrix or dyadic. For any vector or tensor, V, $1 \cdot V = V$.
$1 = II + JJ + KK$

H, T, J : The satellite angular momentum, external torque and inertia. These quantities are vectors and tensor.

ΔX : A small increment of X.

$|V|, \|V\|$: The magnitude of vector, V.

A, B, C : Direction cosines. These quantities are scalars.

α, β, γ : Direction cosine angles. $A = \cos \alpha$, etc. These quantities are scalars.

$\overline{R_s}$: A vector from the earth's center to the satellite's cg

$\overline{R_t}$: A vector from the earth's center to target vehicle's cg.

$\overline{R}$: A range vector from satellite to target. $\overline{R} = |R| \, \overline{r_o}$

$\overline{r_o}$: A unit vector on the satellite in the direction of the target vehicle.

R_o : The earth's radius. This is a scalar quantity and not a vector quantity.

ψ_o : The bearing of the target vehicle relative to the sub-satellite point velocity direction.

θ : The angle subtended at the earth's center by the satellite and the target vehicle $\overline{R}_s \cdot \overline{R}_t = |R_s||R_t| \cos \theta$.

h_t : The target vehicle's altitude from sea level; $|R_t| = R_o + h_t$.

A_o, B_o, C_o : The direction cosines of a unit vector from the satellite in the direction of the target vehicle.

X and . : The cross and dot vector products, respectively.

G.3 DERIVATION OF SATELLITE ANGULAR ATTITUDE

In this derivation, the method of dyadics is used. The reader is referred to pages 135 through 146 of Brand's Vector and Tensor Analysis for a complete definition of dyadics.

Let the satellite coordinate system be i, j, k where i, j, k are unit vectors, not necessarily orthogonal.

Let the satellite reference coordinate system be I, J, K where I, J, K is a known orthogonal unit vector system. Then satellite angular attitude with respect to this system is $\bar{\Phi}$ and:

$$\Phi = iI + jJ + kK \text{ so that } \bar{i} = \bar{\Phi} \cdot \bar{I}, \text{ etc.}$$

Initially assume that the interferometer measurements are made with respect to the i and j satellite axes and are of the form:

$$C_{11} = a_1 (\overline{r_1} \cdot \bar{i} - D_1)$$

$$C_{12} = a_2 (\overline{r_1} \cdot \bar{j} - D_2)$$

Where $\overline{r_1}$ is a unit vector in the direction of beacon number 1.

Initially assume that simultaneous measurements to three beacons in the directions of $\overline{r_1}$, $\overline{r_2}$ and $\overline{r_3}$ are made:

$$C_{21} = a_1 (\overline{r_2} \cdot i - D_1)$$

$$C_{31} = a_1 (\overline{r_3} \cdot i - D_1), \text{ etc.}$$

Define $C_1 = (1/a_1) C_{11} I + (1/a_2) C_{12} J + \overline{r_1} \cdot k K + D_1 I + D_2 J$

$\qquad C_2 = (1/a_1) C_{21} I + (1/a_2) C_{22} J + \overline{r_2} \cdot k K + D_1 I + D_2 J$

$\qquad C_3 = (1/a_1) C_{31} I + (1/a_2) C_{32} J + \overline{r_3} \cdot k K + D_1 I + D_2 J$

Where C_{21}, C_{22} are measurements made with respect to $\overline{r_2}$, etc.

Then $C_1 = \overline{r_1} \cdot i I + \overline{r_1} \cdot j J + \overline{r_1} \cdot k K = \overline{r_1} \cdot \Phi$, $C_2 = \overline{r_2} \cdot \Phi$, etc.

Define $\overline{r}^1 = \dfrac{\overline{r_2} \times \overline{r_3}}{\overline{r_1} \cdot \overline{r_2} \times \overline{r_3}}$, $\overline{r}^2 = \dfrac{\overline{r_3} \times \overline{r_1}}{\overline{r_1} \cdot \overline{r_2} \times \overline{r_3}}$, $\overline{r}^3 = \dfrac{\overline{r_1} \times \overline{r_2}}{\overline{r_1} \cdot \overline{r_2} \times \overline{r_3}}$

Then $\overline{r}^1, \overline{r}^2, \overline{r}^3$ is the set of reciprocal vectors to $\overline{r_1}, \overline{r_2}, \overline{r_3}$ and $\overline{r}^1 \overline{r_1} + \overline{r}^2 \overline{r_2} + \overline{r}^3 \overline{r_3}$ = unit dyadic if $\overline{r_1}, \overline{r_2}, \overline{r_3}$ are non-coplanar.

So $\overline{r}^1 C_1 + \overline{r}^2 C_2 + \overline{r}^3 C_3 = (\overline{r}^1 \overline{r}_1 + \overline{r}^2 \overline{r}_2 + \overline{r}^3 \overline{r}_3) \cdot \Phi = \Phi$

and $i = \Phi \cdot I = \overline{r}^1 C_1 \cdot I + \overline{r}^2 C_2 \cdot I + \overline{r}^3 C_3 \cdot I$

$$= (1/a_1)(C_{11} \overline{r}^1 + C_{21} \overline{r}^2 + C_{31} \overline{r}^3) + D_1 (\overline{r}^1 + \overline{r}^2 + \overline{r}^3)$$

and $\quad j = (1/a_2)(C_{12} \overline{r}^1 + C_{22} \overline{r}^2 + C_{32} \overline{r}^3) + D_2 (\overline{r}^1 + \overline{r}^2 + \overline{r}^3)$

To generalize, for an arbitrary interferometer pair along an arbitrary axis described by the unit vector, $\overline{e}_n$, with which three measurements C_{n1}, C_{n2}, C_{n3} are made to three known beacons, $\overline{r}_1$, $\overline{r}_2$, $\overline{r}_3$:

$$\overline{e}_n = (1/a_n)(C_{n1} \overline{r}^1 + C_{n2} \overline{r}^2 + C_{n3} \overline{r}^3) + D_n (\overline{r}^1 + \overline{r}^2 + \overline{r}^3)$$

Multiplying by $(\overline{r}_1 + \overline{r}_2 + \overline{r}_3)$

$$\overline{e}_n \cdot (\overline{r}_1 + \overline{r}_2 + \overline{r}_3) = (1/a_n)(C_{n1} + C_{n2} + C_{n3}) + 3D_n$$

Assume first, that D_n, the n_{th} interferometer time delay, $= 0$.

Then $a_n \overline{e}_n = C_{n1} \overline{r}^1 + C_{n2} \overline{r}^2 + C_{n3} \overline{r}^3$

$$= C_{n1} \frac{\overline{r}_2 \times \overline{r}_3}{\overline{r}_1 \cdot \overline{r}_2 \times \overline{r}_3} + C_{n2} \frac{\overline{r}_3 \times \overline{r}_1}{\overline{r}_1 \cdot \overline{r}_2 \times \overline{r}_3} + C_{n3} \frac{\overline{r}_1 \times \overline{r}_2}{\overline{r}_1 \cdot \overline{r}_2 \times \overline{r}_3}$$

Since $\overline{r}_1$, $\overline{r}_2$ and $\overline{r}_3$ are known in terms of I, J, and K, then $a_n \overline{e}_n$ is known in terms of I, J, K and the direction and magnitude of $a_n \overline{e}_n$ is known. Since the magnitude of $\overline{e}_n$ is unity, the value of a_n is known. Thus if the interferometer time delay is negligible, three measurements in three non-coplanar directions are sufficient to determine the interferometer axis and the interferometer scale-factor, a_n.

Now assume D_n, the n_{th} interferometer time delay $\neq 0$. Then measurements to a fourth beacon in direction $\overline{r}_4$ must be made.

Define $C_4 = (1/a_1) C_{41} I + (1/a_2) C_{42} J + \overline{r}_4 \cdot k K + D_1 I + D_2 J$

Define $C_1' = C_1 - C_4$, $C_2' = C_2 - C_4$, $C_3' = C_3 - C_4$

$$\overline{r}_1' = \overline{r}_1 - \overline{r}_4, \quad \overline{r}_2' = \overline{r}_2 - \overline{r}_4, \quad \overline{r}_3' = \overline{r}_3 - \overline{r}_4$$

Then, by a repetition of the previous analysis:

$$a_n \overline{e}_n = \frac{1}{\overline{r}_1 \cdot \overline{r}_2 \times \overline{r}_3 + \overline{r}_1 \overline{r}_4 (\overline{r}_2 - \overline{r}_3)} \left(\left[C_{n1} - D_{n4} \right] \left[\overline{r}_2 \times \overline{r}_3 + \overline{r}_4 \times (\overline{r}_2 - \overline{r}_3) \right] \right.$$

$$+ \left[C_{n2} - C_{n4} \right] \left[\overline{r}_3 \times \overline{r}_1 + \overline{r}_4 \times (\overline{r}_3 - \overline{r}_1) \right]$$

$$\left. + \left[C_{n3} - C_{n4} \right] \left[\overline{r}_1 \times \overline{r}_2 + \overline{r}_4 \times (\overline{r}_1 - \overline{r}_2) \right] \right)$$

giving a_n and $\overline{e}_n$.

To find D_n : $3D_n = \overline{e_n} \cdot (\overline{r_1} + \overline{r_2} + \overline{r_3}) - (1/a_n)(C_{n1} + C_{n2} + C_{n3})$

The conditions on the above are that $\overline{r_1} \cdot \overline{r_2} \times \overline{r_3} \neq 0$ and $\overline{r_1} \cdot \overline{r_2} \times \overline{r_3} \neq \overline{r_1} \cdot \overline{r_4} \times (\overline{r_2} - \overline{r_3})$

The above shows that three non-coplanar measurements are sufficient to determine both attitude and interferometer scale factor. It is also shown that four measurements, three non-coplanar and a fourth that does not lie on the circle determined by the first three, are sufficient to determine attitude, scale factors and time delays. The determinations by measurements to two beacons is shown in the latter part of thus appendix.

Now assume that measurements are not made simultaneously, but are made at successive time intervals, t_1, t_2, t_3, etc. Assume that the attitude at time t is Φ_1, at time t_2 is $\Phi_2 \cdot \Phi_1$, and at time t_3 is $\Phi_3 \cdot \Phi_2 \cdot \Phi_1$. Then Φ_2 is the change in attitude from time t_1 to time t_2 and Φ_3 is the change in attitude from time t_2 to time t_3, etc.

Proceeding as before:

$C_1 = \overline{r_1} \cdot iI + \overline{r_1} \cdot jJ + \overline{r_1} \cdot kK = \overline{r_1} \cdot \Phi_1$

$C_2 = \overline{r_2} \cdot iI + \overline{r_2} \cdot jJ + \overline{r_2} \cdot kK = \overline{r_2} \cdot \Phi_2 \cdot \Phi_1$

$C_3 = \overline{r_3} \cdot iI + \overline{r_3} \cdot jJ + \overline{r_3} \cdot kK = \overline{r_3} \cdot \Phi_3 \cdot \Phi_2 \cdot \Phi_1$

If we define $\overline{r_1}' = \overline{r_1}$, $\overline{r_2}' = \overline{r_2} \cdot \Phi_2$, $\overline{r_3}' = \overline{r_3} \cdot \Phi_3 \cdot \Phi_2$, the analysis proceeds as before, substituting $\overline{r}$ primes for $\overline{r}$'s.

To find Φ_2 :

Suppose, for the moment, that the reference frame, I, J, K is an angularly fixed inertial frame moving with the satellite and that the satellite has an angular velocity, W.

Let $\Phi_1 + \Delta\Phi_1 = \Phi_2 \cdot \Phi_1$ so that $\Phi_2 = 1 + \Delta\Phi_1 \cdot \Phi_1^{-1}$

Now Φ_1 is composed of sets of vectors with trigonometric terms for coefficients and so may be expanded in a Taylor's series expansion so that:

$\Delta\Phi_1 = \dot{\Phi}_1 (t_2 - t_1) + 1/2! \ddot{\Phi}_1 (t_2 - t_1)^2 + 1/3! \dddot{\Phi}_1 (t_2 - t_1)^3 + \text{etc.}$

giving $\Phi_2 = 1 + \dot{\Phi}_1 \cdot \Phi^{-1} (t_2 - t_1) + 1/2! \ddot{\Phi}_1 \cdot \Phi_1^{-1} (t_2 - t_1)^2 + \text{etc.}$

Since $\dot{\Phi}_1 = W \times \Phi_1$, $\ddot{\Phi}_1 = \dot{W} \times \Phi_1 + W \times (W \times \Phi_1)$, etc.

The result is:

$\Phi_2 = 1 + W \times 1 (t_2 - t_1) + 1/2! \dot{W} \times 1 (t_2 - t_1)^2 + 1/3! \ddot{W} \times 1 (t_2 - t_1)^3 + \cdots$

$+ 1/2! \, W \, W (t_2 - t_1)^2 + 1/3! (2W\dot{W} + \dot{W}W)(t_2 - t_1)^3 + \cdots$

$+ 1/2! \, W^2 \, 1 (t_2 - t_1)^2 - 3/3! (W \cdot \dot{W}) 1 (t_2 - t_1)^3 + \cdots$

$- 1/3! \, W^2 (W \times 1)(t_2 - t_1)^3 + \cdots$

If W is sufficiently slow and $t_2 - t_1$ sufficiently small then valid approximations are:

$$\Phi_2 = 1 + (W \times 1)(t_2 - t_1)$$

and $\overline{r_2}' = \overline{r_2} - (W \times \overline{r_2})(t_2 - t_1)$

The above shows that if measurements are made at successive intervals instead of · simultaneously, knowledge of satellite angular velocity relative to inertial space (or relative to a known rotating reference coordinate system) is sufficient to enable determination of satellite attitude if the time interval between measurements is known. It is also shown that the measurements may be done by the above procedure. It is evident that measurements on two beacons are equivalent to two measurements on the same beacon after either a change in vehicle attitude or a change in bearing as the satellite moves along its orbit; or a combination of both.

If J is the satellite inertia tensor, H is the momentum vector and T is the external torque (such as gravity gradient) applied to the vehicle, then

$$H = J \cdot W$$

and $T = \dot{H} = J \cdot \dot{W} + \dot{J} \cdot W = J \cdot \dot{W} + W \times J \cdot W$

These are the equations of motion of the vehicle. All of the above, by an iterative procedure, may be used to ultimately determine the satellite attitude over a period of several orbits. The differential corrections method is used if some idea of satellite attitude or angular velocity is known. The attitude may be obtained quickly if the angular velocity is sufficiently small or if W is constant. With no external torque, W is a constant and $\dot{J} \cdot W = 0$. This implies that rotation takes place only around a principal axis of inertia. This will ultimately be the case if the body is not entirely rigid. For minimum rotational energy $(W \cdot J \cdot W)$ and constant momentum, $(J \cdot W)$, rotation is about the axis of greatest inertia. How rapidly this is achieved depends on how rapidly excess rotational energy is dissipated through damping.

G.4 PRELIMINARY EQUATIONS FOR ERROR ANALYSIS

If it is assumed that the interferometer time delay is negligible, then any time delay existing is a contribution to total error. For negligible time delay assumed, equations for the attitude errors as a function of measurement errors and vehicle location errors may b obtained by taking increments on the previously derived attitude equation:

$$\overline{e_n} = (1/a_n)(C_{n1}\overline{r^1} + C_{n2}\overline{r^2} + C_{n3}\overline{r^3}) + D_n(\overline{r^1} + \overline{r^2} + \overline{r^3})$$

Where $\overline{e_n}$ is a unit vector along the N_{th} interferometer axis, a_n is the interferometer scale factor, and D_n is the time delay. Thus angular attitude error, Δe_n, is given by:

$$\Delta e_n = (1/a_n)(\Delta C_{n1}\overline{r^1} + \Delta C_{n2}\overline{r^2} + \Delta C_{n3}\overline{r^3}) + D_n(\overline{r^1} + \overline{r^2} + \overline{r^3})$$

$$+ (1/a_n)(C_{n1}\Delta\overline{r^1} + C_{n2}\Delta\overline{r^2} + C_{n3}\Delta\overline{r^3})$$

and scale factor error is given by:

$$\Delta a_n = \Delta \left\| C_{n1} \overline{r}^1 + C_{n2} \overline{r}^2 + C_{n3} \overline{r}^3 + D_n (\overline{r}^1 + \overline{r}^2 + \overline{r}^3) \right\|$$

The above equations may be reduced to useful working equations. First, the directions of $\overline{r}^1$, $\overline{r}^2$, $\overline{r}^3$ are known with respect to a reference coordinate system I, J, K, although certain direction errors do exist because of the error in beacon location with respect to the satellite, and $\overline{r}^1$, $\overline{r}^2$, and $\overline{r}^3$ may be expressed as:

$$\overline{r}^1 = A_1 \, I + B_1 \, J + C_1 \, K$$

$$\overline{r}^2 = A_2 I + B_2 \, J + C_2 \, K$$

$$\overline{r}^3 = A_3 \, I + B_3 \, J + C_3 \, K$$

If $\overline{e}_n = i$,

then $\Delta \, (i. \, I) = (1/a_1) \left(\left[\Delta C_{11} - a_1 D_1 \right] A_1 + \left[\Delta C_{12} - a_1 D_1 \right] A_2 + \left[\Delta C_{13} - a_1 D_1 \right] A_3 \right)$

$$+ (1/a_1) \, (C_{11} \, \Delta A_1 + C_{12} \, \Delta A_2 + C_{11} \, \Delta A_3)$$

$$\Delta \, (i. \, J) = 1/a_1 \left(\left[\Delta C_{11} - a_1 D_1 \right] B_1 + \left[\Delta C_{12} - a_1 D_1 \right] B_2 + \left[\Delta C_{13} - a_1 D_1 \right] B_3 \right)$$

$$+ 1/a_1 \, (C_{11} \, \Delta B_1 + C_{12} \, \Delta B_2 + C_{13} \, \Delta B_3)$$

$\Delta \, (i. \, K) = $ etc.

An error in a_1 does not enter into the attitude determination since only direction cosine ratios are necessary to determine the directions.

To find a_1:

$$a_1^2 = (a_1 \, i \, . \, I)^2 + (a_1 \, i \, . \, J)^2 + (a_1 \, i \, . \, K)^2$$

To find Δa_1:

$$a_1 . \Delta a_1 = a_1 \, i \, . \, I \, \Delta \, (a_1 \, i \, . \, I) + a_1 \, i . j \, \Delta \, (a_1 \, i . J) + a_1 \, i . K \, \Delta \, (a_1 \, i . K)$$

giving $\Delta a_1 \approx a_1 \left[i. I \, \Delta \, (i. I) + i. j \, \Delta \, (i. J) + i. k \, \Delta \, (i. K) \right]$

The other axes are determined in an identical manner.

To obtain an idea of the required minimum angles between $\overline{r}_1$, $\overline{r}_2$ and $\overline{r}_3$ to adequately determine attitude, it can be seen in figure G-1 that

$$\overline{r}^1 = \frac{\overline{r}_2 \times \overline{r}_3}{\overline{r}_1 \, . \, \overline{r}_2 \times \overline{r}_3} = \frac{1}{\sin \phi_1} \frac{\overline{r}_2 \times \overline{r}_3}{|\overline{r}_2 \times \overline{r}_3|}$$

where ϕ_1 is the angle $\overline{r}_1$ makes with the plane of $\overline{r}_2$ and r_3.
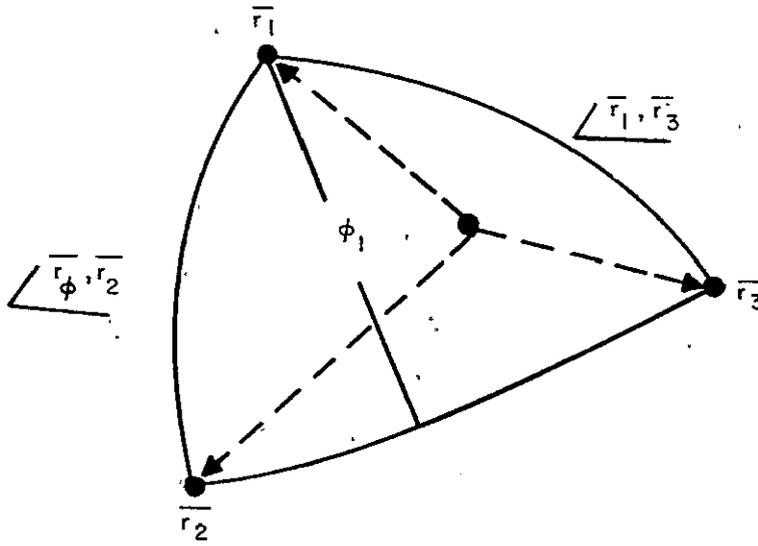
Figure G-1. Determination of Attitude Error

The attitude error due to a measurement error can be written as

$$\Delta e_n \text{ (due to } \Delta C_i) = (1/a_n)\left(\frac{\Delta C_{n1}}{\sin\phi 1}\frac{\overline{r_2} \times \overline{r_3}}{|\overline{r_2} \times \overline{r_3}|} + \frac{\Delta C_{n2}}{\sin\phi 2}\frac{\overline{r_3} \times \overline{r_1}}{|\overline{r_3} \times \overline{r_1}|} + \frac{\Delta C_{n3}}{\sin\phi 3}\frac{\overline{r_1} \times \overline{r_2}}{\overline{r_1} \times \overline{r_2}}\right)$$

In order that the attitude error caused by measurement errors be increased by not more than a factor of 2, it is required that $\sin\phi \geq 1/2$, giving $\phi \geq 30°$. If the spherical . triangle of figure G-2 is assumed equilateral:

$$\cos\theta = \cos\theta/2\cos\phi$$

giving $\cos\theta = \dfrac{\cos\phi}{4}\left(\cos\phi + \sqrt{\cos^2\phi + 8}\right)$ for $\phi = 30°$, $\cos\theta = .217$

$$(.868 + \sqrt{.752 + 8}) = .83, \quad \theta = 34°.$$

Thus, in order that the effect of measurement errors be increased by no more than a factor of 2, a minimum angular spacing of 34° between beacon fixes is required.

G.5 DIRECTIONAL MEASUREMENT ERRORS RESULTING FROM ATTITUDE ERROR

If $\overline{r}_0$ is a unit vector at the satellite in the direction of a vehicle whose position is to be measured, and if I, J, K is the satellite reference system, then
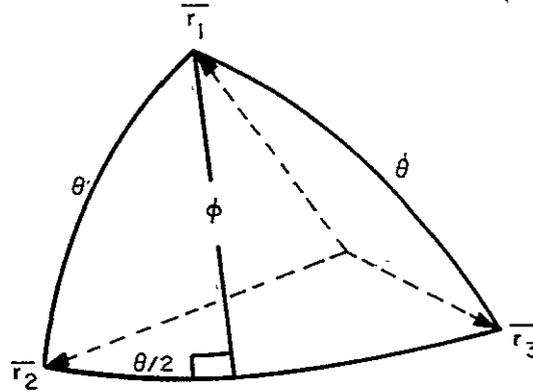
Figure G-2. Equilateral Spherical Triangle

$$\overline{r}_0 = A_0 I + B_0 J + C_0 K \text{ where } C_0^2 = 1 - A_0^2 - B_0^2$$

giving $\Delta r_0 = \Delta A_0 I + \Delta B_0 J + \Delta C_0 K$ where $C_0 \Delta C_0 = - A_0 \Delta A_0 - B_0 \Delta B_0$.

Assume a two axis interferometer system, where one axis is the i axis, the other is the j axis and the two are not necessarily perpendicular. If C_{o1} is the interferometer measurement that is made with respect to the i axis, and C_{o2} is the measurement that is made by the j axis interferometer, then

$$\overline{r}_0 \cdot i = (1/a_1) C_{o1} = A_0 I.i + B_0 J.i + C_0 K.i$$

$$\overline{r}_0 \cdot j = (1/a_2) C_{o2} = A_0 I.j + B_0 J.j + C_0 K.j$$

taking increments

$$-(1/a_1) C_{o1} (\Delta a_1/a_1) + (1/a_1) \Delta C_{o1} = \Delta A_0 I.i + \Delta B_0 J.i + \Delta C_0 K.i + A_0 \Delta (I.i)$$
$$+ B_0 \Delta (J.i) + C_0 \Delta (K.i)$$

$$- (1/a_2) \, C_{o2} \, (\Delta a_2/a_2) + (1/a_2) \, \Delta C_{o2} = \Delta A_o \, I.j + \Delta B_o \, J.j + \Delta C_o \, K.j + A_o \Delta \, (I.j)$$

$$+ B_o \Delta \, (J.j) + C_o \Delta \, (K.j)$$

and $(K.i)^2 = 1 - (J.i)^2 - (I.i)^2$ giving $K.i \quad (K.i) = - J.j \quad (J.i) - K.i \quad (I.i)$

$(K.j)^2 = 1 - (J.j)^2 - (I.i)^2 \quad K.j \quad \Delta (K.j) = - J.j \, \Delta \, (J.j) - K.j \, \Delta \, (I.j)$

Substituting for ΔC_o, $\Delta (K.i)$ and $\Delta (K.j)$, which are perturbations on quantities and are not measured;

$$(I.i - A_o/C_o) \, \Delta A_o + (J.i - B_o/C_o) \, \Delta B_o = (1/a_1) \, \Delta C_{o1} - (1/a_1) \, C_{o1} \, (\Delta a_2/a_2)$$

$$- (A_o - I.i/K.k) \Delta \, (I.i) - (B_o - J.i/K.i) \Delta \, (J.i)$$

$$(I.j - A_o/C_o) \Delta \, A_o + (J.j - B_o/C_o) \, \Delta B_o = (1/a_2) \, \Delta C_{o2} - (1/a_2) \, C_{o2} \, (\Delta a_2/a_2)$$

$$(A_o - I.j/K.j) \Delta \, (I.j) - (B_o - J.j/K.j) \, \Delta \, (J.j)$$

For any assumed attitude, the above two equations can be solved for the pointing errors, $\Delta A_o, \Delta B_o$, and ΔC_o,

$$\Delta C_o = - (A_o/C_o) \, \Delta A_o - (B_o/C_o) \, \Delta B_o,$$

to give the target vehicle location errors as a function of measurement errors $(\Delta C_{o1}, \Delta C_{o2})$ interferometer constant errors, $(\Delta a_1, \Delta a_2)$, and attitude errors $\left[\Delta (I.i), \Delta (J.j), \Delta (I.j), \Delta (J.j) \right]$.

If the satellite coordinate system is approximately orthogonal and approximately aligned with the reference system, i.e: $i \approx I$, $j \approx J$, $k \approx K$, the equations simplify and:

$$\Delta A_o = - (1/a_1) \, C_{o1} \, (\Delta a_1/a_1) + (1/a_1) \, \Delta C_{o1} - A_o \, \Delta (K.i) - B_o \, \Delta (J.i)$$

$$\Delta B_o = - (1/a_2) \, C_{o2} \, \Delta a_2/a_2 + (1/a_2) \, \Delta C_{o2} - A_o \, \Delta (K.j) - B_o \, \Delta (I.j)$$

$$\Delta C_o = - (A_o/C_o) \, \Delta A_1 - (B_o/C_o) \, \Delta B_o$$

For a non-rotating satellite that is approximately stabilized to the local vertical, a convenient choice of reference axes is to assume K pointed to the center of the earth, I along the satellite orbit in the direction of motion, and J = K X I, i.e., J is perpendicular to the orbit plane. This terminology coincides with standard aircraft axes terminology and I is the roll axis, J is the pitch axis, and K is the yaw axis.

G.6 TARGET VEHICLE COORDINATES AND ERROR EQUATIONS

Target location with respect to the satellite vehicle may be specified in terms of heading angle (ψ_0) relative to the velocity of the subsatellite point, distance $R_0 \theta$ along the earth's surface; where R_0 is the earth's radius and θ is the angle between satellite and target subtended at the earth's center, and $|R_t|$; where R_t is the radius vector from earth's center to the target.

Target altitude $h_t = |R_t| - R_0$

As shown in figure G-3, let R_s be the radius vector to the satellite; R_t the radius vector to the target; and $R = |R| \bar{r}_0$ the vector range from satellite to the target.

Then $R_t = R_s + R$ where R_s is known and R is measured.

If $\bar{r}_0 = A_0 I + B_0 J + C_0 K$

$$= \cos \alpha_0 I + \cos \beta_0 J + \cos \gamma_0 K$$

$$= \cos \psi_0 \sin \gamma_0 I + \sin \psi_0 \sin \gamma_0 J + \cos \gamma_0 K$$

then $\tan \psi_0 = \cos \beta_0 / \cos \alpha_0$

and $\sin \theta = (|R|/|R_s + R|) \sin \gamma_0$ or $\cos \theta = \dfrac{R_s| - |R|\cos \gamma_0}{|R_s + R|}$

The above assumes I, J, K are chosen so that K is toward earth's center, I and J are horizontal, and I is in direction of motion, and J = K X I.

so that $R_s = - |R_s| K.$

From the above equations

TgT . Bearing Angle, $\psi_0 = \tan^{-1} (B_0/A_0)$

TgT   Great Circle Distance, $R_0 \theta = R_0 \tan^{-1} \left(\dfrac{\sqrt{A_0^2 + B_0^2}}{\dfrac{|R_s|}{|R|} - C_0} \right)$

and since $R_t^2 = R^2 + R_s^2 - 2 R . R_s$

Target Altitude, $h_t = \sqrt{R^2 + R_s^2 - 2 |R| |R_s| C_0} - R_0$
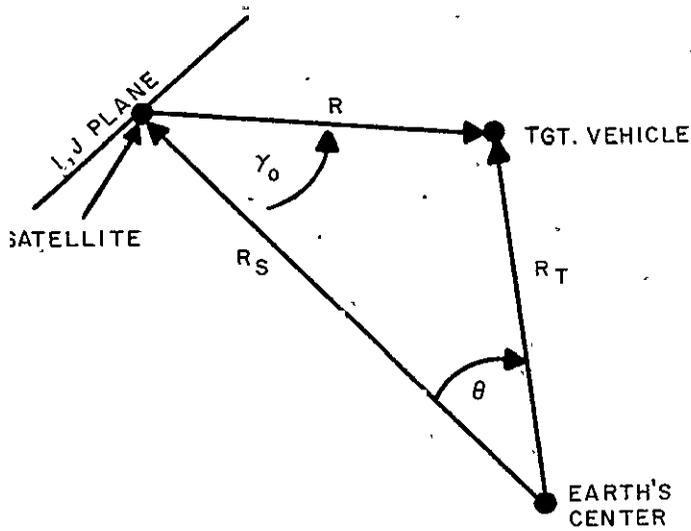
Figure G-3.   Target Location Determination

Taking increments:

$$\Delta \psi_0 = \frac{A_0 B_0}{A_0^2 + B_0^2} \left(\frac{\Delta B_0}{B_0} - \frac{\Delta A_0}{A_0} \right)$$

$$\Delta (R_0 \theta) = - \frac{R \cdot (R_s - R)}{(R_s - R)^2} \quad \frac{R_0 \, \Delta C_0}{\sqrt{1 - C_0^2}} + \frac{R \cdot R_s}{(R_s - R)^2} \quad \frac{\sqrt{1 - C_0^2}}{C_0} \quad R_0 \quad \frac{\Delta |R|}{|R|}$$

$$\Delta h_t = \left(\frac{|R|}{|R_t|} - \frac{|R_s|}{|R_t|} C_0 \right) \quad \Delta R - \frac{R \cdot R_s}{|R_t|} \quad \frac{\Delta C_0}{C_0}$$

In terms of direction cosine angles:

$$\Delta \psi_0 = (\Delta \alpha_0 \tan \alpha_0 - \Delta \beta_0 \tan \beta_0 \tan \beta_0) \frac{\cos \alpha_0 \cos \beta_0}{\sin^2 \gamma_0}$$

$$\Delta(R_o \theta) = R_o \frac{R \cdot (R_s - R)}{(R_s - R)^2} \Delta \gamma_o + R_o \frac{R \cdot R_s}{(R_s - R)^2} (\tan \gamma_o) \frac{\Delta |R|}{|R|}$$

$$\Delta h_t = (1/|R_t|) (|R| - |R_s| C_o) \Delta R + \frac{R \cdot R_s}{|R_t|} (\tan \gamma_o) \Delta \gamma_o$$

For

$$r_o \approx 0, a'_o = \pi/2 - a_o \approx 0, \beta'_o = \pi/2 - \beta_o \approx 0$$

The distance error due to heading error is $R_o \theta \Delta \psi_o$, and:

$$R_o \theta \approx \frac{R_o |R| \sin \gamma_o}{|R_s| - |R|} \approx R_o \frac{|R|}{|R_t|} \sin \gamma_o$$

$$\Delta \psi_o = \frac{\sin a'_o}{\sin^2 \gamma_o} \Delta \beta'_o - \frac{\sin \beta'_o}{\sin^2 \gamma_o} \Delta a'_o$$

and

$$R_o \theta \Delta \psi_o = R_o \frac{|R|}{|R_t|} \left(\frac{\sin a'_o}{\sin \gamma_o} \Delta \beta'_o - \frac{\sin \beta'_o}{\sin \gamma_o} \Delta a'_o \right)$$

since

$$\sin^2 \gamma_o = \sin^2 a'_o + \sin^2 \beta'_o \approx \gamma_o^2 \approx a'^2_o + \beta'^2_o$$

$$R_o \theta \Delta \psi_o \approx R_o \left(\frac{|R_s|}{|R_t|} - 1 \right) \left(\frac{a'_o}{a'^2_o + \beta'^2_o} \Delta \beta'_o - \frac{\beta'_o}{a'^2_o + \beta'^2_o} \Delta a'_o \right)$$

For a sea-level target the constraint imposed is

$$C_o = \frac{R^2 + R_s^2 - R_o^2}{2 |R| |R_s|}$$

and

$$\Delta C_o = \left[(|R| - |R_s| C_o) (C_o / R \cdot R_s) \right] \Delta R$$

since it is known that $h_t = 0$. Thus, one redundant measurement is obtained. This may be used to reduce the error volume by constraint on ΔC_o or may be used to check satellite altitude, $|R_s|$.

To find out what can be determined if sightings to only two beacons are made, let $\overline{e}_1$ of figure G-4 be a unit vector describing one interferometer pair axis and let $\overline{r}_1$, $\overline{r}_2$ of figure G-4 be unit vectors in the known directions of two beacons.
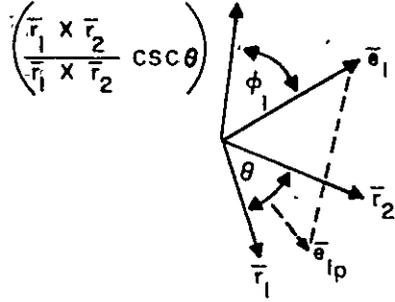
Figure G-4. Unit Vectors

Define

$$C_{11} = \overline{r}_1 \cdot \overline{e}_1, \quad C_{12} = \overline{r}_1 \cdot \overline{e}_2$$
$$C_{21} = \overline{r}_2 \cdot \overline{e}_1, \quad C_{22} = \overline{r}_2 \cdot \overline{e}_2$$

Let

$$e_1 = a \, \overline{r}_1 \times \overline{r}_2 + b\overline{r}_1 + C\overline{r}_2$$

Then

$$\overline{r}_1 \cdot \overline{e}_1 = C_{11} = 0 + b + C\overline{r}_1 \cdot \overline{r}_2 \qquad\qquad b = \frac{C_{11} - C_{12}\cos\theta}{\sin^2\theta}$$

giving

$$\overline{r}_2 \cdot \overline{e}_1 = C_{21} = 0 + b\overline{r}_1 \cdot \overline{r}_2 + C \qquad\qquad C = \frac{C_{12} - C_{11}\cos\theta}{\sin^2}$$

Also,

$$a = \frac{\overline{e}_1 \cdot \overline{r}_1 \times \overline{r}_2}{(\overline{r}_1 \times \overline{r}_2)^2} = \frac{\overline{e}_1 \cdot \overline{r}_1 \times \overline{r}_2}{\sin^2\theta} = \frac{\cos\phi_1}{\sin\theta}$$

and

$$\sin\phi_1 = \left| e \times \left(\frac{\overline{r}_1 \times \overline{r}_2}{\sin\theta}\right) \right| = (1/\sin\theta)\sqrt{C^2_{11} + C^2_{12} + 2C_{11}C_{12}\cos\theta}$$

So:

$$\overline{e}_1 = (1/\sin^2\theta)\left(\pm\sin\theta\cos\phi_1 \, (\overline{r}_1 \times \overline{r}_2) + \left\lceil C_{11} - C_{12}\cos\theta\right\rceil \overline{r}_1 \right.$$
$$\left. + \left\lceil C_{12} - C_{11}\cos\theta\right\rceil \overline{r}_2 \right)$$

Similarly, if $\overline{e_2}$ describes a second interferometer:

$$\overline{e_2} = (1/\sin^2\theta)\left(\pm\sin\theta\cos\phi_2\,(\overline{r_1}\times\overline{r_2}) + \left[C_{21} - C_{22}\cos\theta\right]\overline{r_1}\right.$$
$$\left. + \left[C_{22} - C_{21}\cos\theta\right]\overline{r_2}\right)$$

Now assume that the measurements C_{11} and C_{12} contain an unknown interferometer scale factor, a_1.

It can be seen that the direction of $\overline{e_{1p}}$ (the projection of $\overline{e_1}$ in the plane of $\overline{r_1}$, $\overline{r_2}$) is still known, since:

$$\overline{e_{1p}} = 1/a_1\left(\left[C_{11} - C_{12}\cos\theta\right]r_1 + \left[C_{12} - C_{11}\cos\theta\right]r_2\right)$$

but that the magnitude of e_{1p} is not known. While the quantity $(a_1\sin\phi_1)$ is known, the quantity $\cos\phi_1$

$$\cos\phi_1 = \sqrt{1 - \left(1/a_1^2\right)(a_1\sin\theta)^2}$$

is not known until a_1 is known. The component of $\overline{e_1}$ along $\overline{r_1}\times\overline{r_2}$ is not known and the measurements to two beacons restrict e_1 to a plane through $\overline{r_1}\times\overline{r_2}$ making a known angle (ψ_1) with respect to the $\overline{r_1}$ direction. If two interferometers are used, e_1 and e_2 are confined to known planes intersecting along $\overline{r_1}\times\overline{r_2}$. If the angle between $\overline{e_1}$ and $\overline{e_2}$ is known, this is still not sufficient to fix the attitude of the pair of axes $\overline{e_1}$ and $\overline{e_2}$ relative to $\overline{r_1}$ and $\overline{r_2}$.

G.7 CONCLUSIONS

a. Three non-coplanar beacon sightings are sufficient to determine any number of interferometer-pair axes and associated scale factors, but not the time delays. A fourth sighting, not located on the right circular cone determined by the first three, is necessary and sufficient to determine time delays also.

b. The angular spacing of the measurements with respect to the satellite axes must be at least 34 degrees if the effect of measurement errors on attitude errors is to be enhanced by no more than a factor of 2.

c. Items a. and b. also apply to a rotating satellite if the angular velocity and its derivatives with respect to inertial space is known. The velocity vector that is relative to the satellite axes does not have to be known.

d. A convenient set of coordinates to locate a target vehicle relative to the satellite are: (1) the heading (or bearing) of the target relative to the subsatellite point velocity, (2) the great circle distance from the subsatellite point to the target, and (3) the target altitude. These are all expressed in terms of two angles and range from the satellites.

APPENDIX H

SATELLITE REPLACEMENT RATE ANALYSIS

Velocity errors occurring when satellites are placed in orbit will cause the satellites to drift with respect to their nominal positions, possibly causing coverage gaps to appear. This appendix discusses the probability of such gaps, and the expected number of replacement satellites which must be used during a given period to fill these gaps. A number of satellites (n) are assumed initially equally spaced in a nominal 6000 nmi orbit. The initial satellite velocity errors are assumed to have magnitudes which are independent and normally distributed about a mean of zero, with variance σ_v^2. Each satellite covers a central angle segment of the orbit of 102 degrees, assuming that $5°$ is the minimum elevation angle for satisfactory coverage.

H.1 $T_{3\sigma_V}$ (TWO SATELLITES)

If it is assumed that two adjacent satellites have initial velocity errors of $3\sigma_V$ in opposite directions, the two satellites will tend to drift apart. For an incremental velocity of Δv, where a 6000 nmi orbit has been assumed, the drift, in degrees per year is given by $\Delta \gamma = 94.7$ (Δv in ft/sec). (S. H. Reiger, "A Study of Passive Communications Satellites", Feb. 1963, R-415-NASA, p. 94). Thus if each satellite has an error of $3\sigma_V$, in opposite directions, the equivalent value for ΔV is $6\sigma_V$, and the drift is 94.7 $(6\sigma_V)$ degrees/year. Letting θ be the central angle coverage of one satellite ($\theta = 102$ degrees) and α_0 the initial satellite spacing, the coverage gap would then be $\alpha_0 + 94.7$ $(6\sigma_V)$ $T - \theta$, where T is the elapsed time in years and negative gaps signify a coverage overlap. Where δ is the maximum permitted gap length, the elapsed time $T_{3\sigma_V}$ until this gap length is exceeded under the above conditions is

$$T_{3\sigma_V} = \frac{\theta + \delta - \alpha_0}{568\,\sigma_V} = \frac{\beta_0 - \alpha_0}{568\,\sigma_V}$$

$$\beta_0 = \theta + \delta$$

H.2 $T_{10\%}$ (FOUR OR FIVE SATELLITES)

Let $\alpha_3 = \alpha_{30} + \Delta\alpha_3$ and $\alpha_2 = \alpha_{20} + \Delta\alpha_2$ $(\alpha_{30} > \alpha_{20})$ be the relative positions of two adjacent satellites in orbit. For a small number of satellites that are initially equally spaced, the probability of a gap is approximately

$$P_G = n \times p\,(\alpha_3 > \alpha_2 + \beta_0)$$

where n is the number of satellites. This is true providing the probability of two or more gaps existing simultaneously is negligible in comparison with the probability of one gap

existing. The assumption should be reasonable for small values of P_G. However,

$$p\left(\alpha_3 > \alpha_2 + \beta_0\right) = p\left(\Delta\alpha_3 - \Delta\alpha_2 > \beta_0 - \alpha_0\right)$$

where

$\Delta\alpha_2$ and $\Delta\alpha_3$ are normally distributed about zero and have a variance $\sigma\alpha^2 = (94.7T\sigma_v)^2$.

Therefore, their difference will be normally distributed, with a zero mean and a variance of $2\sigma_\alpha^2$. This leads to the result

$$P_G = n \int_{\beta_0 - \alpha_0}^{\infty} \frac{1}{\sqrt{2}\sigma_\alpha \sqrt{2\pi}}\, e^{-\frac{y^2}{2(2\sigma_\alpha)^2}}\, dy$$

Substituting

$$z = \frac{y}{\sqrt{2}\,\sigma_\alpha},\ \sqrt{2}\,\sigma_\alpha = \sqrt{2}(94.7T)\sigma_v = 134\,T\sigma_v,$$

$$P_G = n \int_{\frac{\beta_0 - \alpha_0}{134T\sigma_v}}^{\infty} \frac{1}{\sqrt{2\pi}}\, e^{-z^2/2}\, dz$$

$$P_G = n\left(1/2 - \phi\left[\frac{\beta_0 - \alpha_0}{134\,T\sigma_v}\right]\right)$$

where

$$\phi(a) = \int_0^a \frac{1}{\sqrt{2\pi}}\, e^{-z^2/2}\, dz .$$

With $\beta_0 = 102 + 19.1 = 121.1°$; corresponding to a 20 minute gap; and $\alpha_0 = 90°$ or $72°$; corresponding to n = 4 or 5; the value of $(134\,T\sigma_v)$ may be found for which $P_G = 0.1$. From the result, T may be plotted vs $3\sigma_v$. T in this case is designated $T_{10\%}$ and is plotted in figure 6.1-20 for n = 4 and 5.

H.3 $T_{10\%}$; (EIGHT SATELLITES)

For eight satellites, the possibility that the order of the satellites may change cannot be ignored. Consider the positions of four satellites which are given by

$$\alpha_1 = \alpha_{10} + \Delta\alpha_1,\ \alpha_2 = \alpha_{20} + \Delta\alpha_2,\ \alpha_3 = \alpha_{30} + \Delta\alpha_3,\ \alpha_4 = \alpha_{40} + \Delta\alpha_4.$$

where

$\alpha_{10},\ \alpha_{20},\ \alpha_{30},\ \alpha_{40}$ are the nominal positions with $\alpha_{k0} = \alpha_{10} + (k-1)\alpha_0$ and k = 2, 3, and 4. Neglecting all other satellites than these four, a gap will appear if either

a. $\alpha_1 \le \alpha_2,\ \alpha_3 \ge \alpha_2 + \beta_0,$ and $\alpha_4 \ge \alpha_2 + \beta_0$

or

b. $\alpha_1 > \alpha_2,\ \alpha_3 \ge \alpha_1 + \beta_0,$ and $\alpha_4 \ge \alpha_1 + \beta_0$

H-2

Assuming that the probability of more than one gap appearing is negligible, the probability of a gap is approximately

$$P_G \approx n \left[p(\alpha_1 \leq \alpha_2, \; \alpha_3 \geq \alpha_2 + \beta_0, \; \alpha_4 \geq \alpha_2 + \beta_0) \right.$$
$$\left. + p\left(\alpha_1 > \alpha_2, \; \alpha_3 \geq \alpha_1 + \beta_0, \; \alpha_4 \geq \alpha_1 + \beta_0\right) \right]$$

since the probability of a gap between any two adjacent satellites is the same.

The first probability may be found by integrating the joint probability density function of α_1, α_2, α_3, α_4 over the range determined by $\alpha_1 \leq \alpha_2$, $\alpha_3 \geq \alpha_2 + \beta_0$, $\alpha_4 \geq \alpha_2 + \beta_0$. Since α_1, α_2, α_3, and α_4 are independent, this is equivalent to fixing α_2, integrating the density functions of α_1, α_3, and α_4 over the appropriate range, and then multiplying by the density function of α_2 and integrating with respect to α_2. Following this outlined procedure,

$$p\left(\alpha_1 \leq \alpha_2, \; \alpha_3 \geq \alpha_2 + \beta_0, \; \alpha_4 \geq \alpha_2 + \beta_0\right)$$

$$= \int_{-\infty}^{\infty} f_2(\alpha_2) \left\{ \int_{-\infty}^{\alpha_2} f_1(\alpha_1)\,d\alpha_1 \int_{\alpha_2+\beta_0}^{\infty} f_3(\alpha_3)\,d\alpha_3 \int_{\alpha_2+\beta_0}^{\infty} f_4(\alpha_4)\,d\alpha_4 \right\} d\alpha_2$$

Since all the α_i are normally distributed with a mean of α_{io} and a variance of $\sigma_\alpha{}^2$,

$$\int_a^b f_i(\alpha_i)\,d\alpha_i = \int_a^b \frac{1}{\sigma_\alpha \sqrt{2\pi}} e^{-\frac{(\alpha_i - \alpha_{io})^2}{2\sigma_\alpha{}^2}} \, d\alpha_i$$

$$= \int_{\frac{a - \alpha_{io}}{\sigma_\alpha}}^{\frac{b - \alpha_{io}}{\sigma_\alpha}} \frac{1}{\sqrt{2\pi}} e^{-x^2/2} \, dx$$

$$= \phi\left(\frac{b - \alpha_{io}}{\sigma_\alpha}\right) - \phi\left(\frac{a - \alpha_{io}}{\sigma_\alpha}\right)$$

Thus

$$p\left(\alpha_1 \leq \alpha_2, \; \alpha_3 \geq \alpha_2 + \beta_0, \; \alpha_4 \geq \alpha_2 + \beta_0\right)$$

$$\int_{-\infty}^{\infty} \frac{1}{\sigma_\alpha \sqrt{2\pi}} e^{-1/2\left(\frac{\alpha_2 - \alpha_{20}}{\sigma_\alpha}\right)^2} \left\{ \left[1/2 + \phi\left(\frac{\alpha_2 - \alpha_{10}}{\sigma_\alpha}\right)\right]\left[1/2 - \phi\left(\frac{\alpha_2 + \beta_0 - \alpha_{30}}{\sigma_\alpha}\right)\right] \right.$$

$$\left. \left[1/2 - \phi\left(\frac{\alpha_2 + \beta_0 - \alpha_{40}}{\sigma_\alpha}\right)\right] \right\} d\alpha_2$$

$$= \int_{-\infty}^{\infty} \frac{1}{\sqrt{2\pi}} \; e^{-z^2/2} \; \left\{ \left[1/2 + \phi \left(z + \frac{\alpha_o}{\sigma_\alpha} \right) \right] \left[1/2 - \phi \left(z + \frac{\beta_o - \alpha_o}{\sigma_\alpha} \right) \right] \left[1/2 - \phi \left(z + \frac{\beta_o - 2\alpha_o}{\sigma_\alpha} \right) \right] \right\} dz$$

$$p\left(\alpha_1 \le \alpha_2, \; \alpha_3 \ge \alpha_2 + \beta_o, \; \alpha_4 \ge \alpha_2 + \beta_o \right)$$

$$= \int_{-\infty}^{\infty} \Phi_1(z) \; \Phi_2(z) \; \Phi_3(z) \; \Phi_4(z) \, dz$$

where

$$\Phi_1(z) = \frac{1}{\sqrt{2\pi}} \; e^{-z^2/2}$$

$$\Phi_2(z) = 1/2 + \phi \left(z + \frac{\alpha_o}{\sigma_\alpha} \right)$$

$$\Phi_3(z) = 1/2 - \phi \left(z + \frac{\beta_o - \alpha_o}{\sigma_\alpha} \right)$$

$$\Phi_4(z) = 1/2 - \phi \left(z + \frac{\beta_o - 2\alpha_o}{\sigma_\alpha} \right)$$

$p\left(\alpha_1 > \alpha_2, \; \alpha_3 \ge \alpha_1 + \beta_o, \; \alpha_4 \ge \alpha_1 + \beta_o \right)$ may be found in a similar manner, so that the final probability of a gap is given by

$$P_G = n \left[\int_{-\infty}^{\infty} \Phi_1(z) \Phi_2(z) \; \Phi_3(z) \Phi_4(z) \, dz + \int_{-\infty}^{\infty} \Phi_1(z) \Phi_4(z) \Phi_5(z) \Phi_6(z) \, dz \right]$$

where

$\Phi_1, \; \Phi_2, \; \Phi_3, \; \Phi_4$ are given above and

$$\Phi_5(z) = 1/2 - \phi \left(z + \frac{\beta_o - 3\alpha_o}{\sigma_\alpha} \right)$$

$$\Phi_6(z) = 1/2 + \phi \left(z - \frac{\alpha_o}{\sigma_\alpha} \right)$$

For $n = 8$, $\alpha_o = 45°$, $\beta_o = 121.1°$ (corresponding to a 20 minute coverage gap), the value of σ_α corresponding to a gap probability of 10% was found by numerically integrating for several values of σ_α, plotting the resulting P_G vs σ_α curve, and reading off the value of σ_α corresponding to $P_G = 0.1$. This value was found to be 29.5°. Then, since $\sigma_\alpha = 94.7 T \sigma_v$, $T_{10\%}$ was found to be $T_{10\%} = \frac{29.5(3)}{94.7(3\sigma_v)} = \frac{.935}{3\sigma_v}$ years and $T_{10\%}$ was plotted vs $3\sigma_v$ in figure 6.1-20.

H.4 NUMBER OF REPLACEMENTS, $\sigma_\alpha < 25°$ (FOUR SATELLITES)

It is assumed that the probability is nearly unity that satellites remain in their original order (i.e., $\alpha_4 > \alpha_3 > \alpha_2 > \alpha_1$). If A_1, A_2, A_3, A_4 are the events that a gap appears between

α_1 and α_2, α_2 and α_3, α_3 and α_4, and α_4 and α_1, the probability of one or more gaps is given by

$$P_{1+} = p(A_1 \cup A_2 \cup A_3 \cup A_4)$$

$$= \sum_i p(A_i) - \sum_{i<j} p(A_i A_j) + \sum_{i<j<k} p(A_i A_j A_k)$$

Note that with the parameters of interest here, the probability of four gaps is zero. Similarly, the probability of two or more gaps is

$$P_{2+} = p(A_1 A_2 \cup A_1 A_3 \cup A_1 A_4 \cup A_2 A_3 \cup A_2 A_4 \cup A_3 A_4)$$

$$= p(E_1 \cup E_2 \cup E_3 \cup E_4 \cup E_5 \cup E_6)$$

$$= \sum_i p(E_i) - \sum_i \sum_j p(E_i E_j) + \sum_i \sum_j \sum_k p(E_i E_j E_k)$$

$$= \sum_{i<j} p(A_i A_j) - 3 \sum_{i<j<k} p(A_i A_j A_k) + \sum_{i<j<k} p(A_i A_j A_k)$$

$$= \sum_i \sum_j p(A_i A_j) - 2 \sum_{i<j<k} p(A_i A_j A_k)$$

The probability of three gaps is

$$P_3 = \sum_{i<j<k} p(A_i A_j A_k)$$

From these expressions, the probabilities of zero, one, and two gaps may be found as follows:

$$P_2 = P_{2+} - P_3 = \sum_{i<j} p(A_i A_j) - 3P_3$$

$$P_1 = P_{1+} - P_{2+} = \sum_i p(A_i) - 2P_2 - 3P_3$$

$$P_0 = 1 - P_1 - P_2 - P_3$$

If

$$P_3 \approx 0,$$

$$P_2 \approx \sum_{i<j} p(A_i A_j)$$

$$P_1 \approx \sum_i p(A_i) - 2P_2$$

$$P_0 \approx 1 - P_1 - P_2 - P_3$$

Four of the $A_i A_j$ terms will involve adjacent satellites and will have the same probability. The remaining two $A_i A_j$ terms involve opposite satellites, and will have equal probabilities. Also, $p(A_i)$ is the same for all A_i. Thus

$$P_2 \approx 4 p(A_1 A_2) + 2 p(A_1 A_3)$$

$$P_1 \approx 4 p(A_1) - 2P_2$$

In section 4.2, $4p(A_1)$ was found as P_G for four satellites; thus,

$$4p(A_1) = 4 \left[1/2 - \phi\left(\frac{\beta_0 - \alpha_0}{\sqrt{2}\,\sigma_\alpha}\right) \right]$$

A_1 and A_3 are approximately independent; therefore

$$p(A_1 A_3) \approx p(A_1) p(A_3) = \left[p(A_1) \right]^2 = \left[1/2 - \phi\left(\frac{\beta_0 - \alpha_0}{2\,\sigma_\alpha}\right) \right]^2$$

The probability of A_1 and A_2 may be found in a manner similar to that employed in section H.3, as follows:

$$p(A_1 A_2) = p\left(\alpha_2 > \alpha_1 + \beta_0, \ \alpha_3 > \alpha_2 + \beta_0\right)$$

$$= p\left(\alpha_1 < \alpha_2 - \beta_0, \ \alpha_3 > \alpha_2 + \beta_0\right)$$

$$= \int_{-\infty}^{\infty} f_2(\alpha_2) \left\{ \int_{-\infty}^{\alpha_2 - \beta_0} f_1(\alpha_1) \, d\alpha_1 \int_{\alpha_2 + \beta_0}^{\infty} f_3(\alpha_3) \, d\alpha_3 \right\} d\alpha_2$$

$$\int_{-\infty}^{\infty} \frac{1}{\sigma_\alpha \sqrt{2\pi}} e^{-1/2 \left(\frac{\alpha_2 - \alpha_{20}}{\sigma_\alpha}\right)^2} \left\{ \left[\phi\left(\frac{\alpha_2 - \beta_0 - \alpha_{10}}{\sigma_\alpha}\right) + 1/2 \right] \left[1/2 - \phi\left(\frac{\alpha_2 + \beta_0 - \alpha_{30}}{\sigma_\alpha}\right) \right] \right\} d\alpha_2$$

$$p(A_1 A_2) = \int_{-\infty}^{\infty} \frac{1}{\sqrt{2\pi}} e^{-z^2/2} \left[1/2 + \phi\left(z + \frac{\alpha_0 - \beta_0}{\sigma_\alpha}\right) \right] \left[1/2 - \phi\left(z + \frac{\beta_0 - \alpha_0}{\sigma_\alpha}\right) \right] dz$$

Summarizing, the formulas required to determine P_0, P_1, and P_2; with the assumption that $P_3 \approx 0$; are:

$$P_2 \approx 4 \, p(A_1 A_2) + 2 \left[p(A_1) \right]^2$$

$$P_1 \approx 4 \, p(A_1) - 2 P_2$$

$$P_0 \approx 1 - P_1 - P_2$$

where

$$p(A_1 A_2) = \int_{-\infty}^{\infty} \frac{1}{\sqrt{2\pi}} e^{-z^2/2} \left[1/2 + \phi\left(z + \frac{\alpha_0 - \beta_0}{\sigma_\alpha}\right) \right] \left[1/2 - \phi\left(z + \frac{\beta_0 - \alpha_0}{\sigma_\alpha}\right) \right] dz$$

$$p(A_1) = 1/2 - \phi\left(\frac{\beta_0 - \alpha_0}{\sqrt{2}\,\sigma_\alpha}\right)$$

The probability that the original assumption is violated, i.e. that the satellite order changes, is found in a manner similar to section H. 2.

$$P_c \approx 4p\left(\alpha_1 > \alpha_2\right) = 4p\left(\Delta\alpha_1 - \Delta\alpha_2 > \alpha_0\right)$$

$$P_c \approx 4\left[1/2 - \phi\left(\frac{\alpha_0}{\sqrt{2}\,\sigma}\right) \right]$$

If $\sigma_\alpha < 22.6°$, $P_c < 0.01$; if $\sigma_\alpha < 32.5°$, $P_c < 0.1$, since $\alpha_0 = 90°$ for four satellites. By numerical integration $p(A_1 A_2)$ was found for several values of σ_α. Since $\sigma = 94.7 T \sigma_v$, this permitted the determination of P_0, P_1 and P_2 for several values of $3\sigma_v$ and an elapsed time(T) 5 years. The limitations on σ_α imposed by P_c limited $3\sigma_v$ to less than about 0.2 feet per second. Knowing P_0, P_1, and P_2 for the 5 year period, the expected number of replacement satellites required for the five year period is given by:

$$N = P_1 + 2P_2$$

The standard deviation is given by

$$\sigma = \left[P_0 \, (N)^2 + P_1 \, (N-1)^2 + P_2 \, (N-2)^2 \right]^{1/2}$$

The probabilities that were found are plotted in figure 6.1-19 where $_0$ has been taken as 111.5°, equivalent to a 10 minute gap with a nominal orbit altitude of 6000 nmi and a minimum elevation angle for effective coverage of 5°. The expected number of replacements is plotted in figure 6.1-18, with upper and lower 1σ bounds.

H.5 NUMBER OF REPLACEMENTS, $\sigma_\alpha > 25°$ (FOUR SATELLITES)

When the possibility that the satellite order changes must be considered, the complexity of the problem is considerably increased. Techniques similar to those used in section H.4 lead to double integrations for which no analytical solutions were found. For example, the expression obtained for $p\,(A_1 A_3)$ was

$$p(A_1 A_3) \approx \int_{-\infty}^{\infty} \frac{1}{\sqrt{2\pi}} \, e^{-z_2^2/2} \int_{-\infty}^{\infty} \frac{1}{\sqrt{2\pi}} \, e^{-z_3^2/2} \quad \theta\left(z_2, z_3\right) dz_3 \, dz_2$$

where

$$\theta(z_2, z_3) =$$
$$\left[\phi\left(z_2 + \frac{\alpha_0 - \beta_0}{\sigma_\alpha}\right) - \phi\left(z_3 + \frac{\beta_0 - \alpha_0 - 90°}{\sigma_\alpha}\right) \right]\left[\phi\left(z_2 + \frac{\alpha_0 + 90° - \beta_0}{\sigma_\alpha}\right) - \phi\left(z_3 + \frac{\beta_0 - \alpha_0}{\sigma_\alpha}\right) \right]$$

for

$$z_3 > z_2 - \frac{90}{\sigma_\alpha}$$

or

$$\left[\phi\left(z_3 + \frac{90° + \alpha_0 - \beta_0}{\sigma_\alpha}\right) - \phi\left(z_3 + \frac{\beta_0 - 90° - \alpha_0}{\sigma_\alpha}\right) \right]\left[\phi\left(z_2 + \frac{90° + \alpha_0 - \beta_0}{\sigma_\alpha}\right) \right.$$
$$\left. - \phi\left(z_2 + \frac{\beta_0 - 90 - \alpha_0}{\sigma_\alpha}\right) \right] \text{for } z_3 < z_2 - \frac{90}{\sigma_\alpha}$$

In an effort to obtain an approximation to the expected number of replacements required, a short graphical analysis was performed. A list was constructed of drift rates which were independent and had an approximate normal distribution with a zero mean. Four drift rates were chosen from the list and the relative positions of the four satellites having these drift rates were plotted against time as straight lines. Whenever it was apparent that two satellites were sufficiently separated to open a gap, at that time a replacement satellite was added at the midpoint. A drift rate from the list was assigned to the replacement satellite and its relative position was plotted. This procedure was continued until t = 5 years, at which time the number of replacement satellites was counted. A second trial analysis was made using different drift rates chosen from the list. This analysis was carried out for those drift rate distributions having standard deviations of 10° per year and 20° per year. These

standard deviations correspond to $3\sigma_v$ values of 0.316 ft. per sec. and 0.633 ft. per sec. The results obtained are recorded in table H-1.

TABLE H-1

SATELLITE REPLACEMENT DUE TO DRIFT

Trial Number (i)	Number replaced (n_i)	
	$3\sigma_v = 0.316$	$3\sigma_v = 0.633$
1	3	4
2	0	2
3	1	5
4	2	3
5	1	3
6	4	4
7	4	4
8	2	2
9	4	2
10	2	2
11	2	

The average number was taken as

$$N = \frac{1}{k} \sum_{i=1}^{k} n_i$$

where the number of trials is k.

The standard deviation was $\sigma = \left[\frac{1}{k} \sum_{i=1}^{k} (N-n_i)^2 \right]^{1/2}$

The numbers obtained were

$3\sigma_v$	N	σ
0.316	2.3	1.3
0.633	3.1	1.0

These values are listed in table H-1.

APPENDIX I
LIFE LIMITATIONS FOR SEMICONDUCTORS AND INSULATION DUE TO RADIATION IN SPACE

A critical part of the space environment is the high energy charged particles encountered by an earth orbiting satellite. This space radiation plays an important part in determining the lifetime of a satellite. In this appendix, life limitations of semiconductors and insulators in circular orbits up to 10,000 nmi altitude are investigated to define the considerations involved in orbit selection and electronic system design.

This investigation requires estimation of the space radiation dose rates, with shielding, due to electron and proton fluxes and utilization of radiation damage data for semiconductors and insulation.

I. 1 SPACE RADIATION ENVIRONMENT

The artificial electron fluxes used in the calculations and shown in figures I-1 through I-3 are based upon the data of Brown and Gabbe (reference 1) with predicted variations reported by Hess (reference 2). These data include only the measurements after the Johnson Island 1.4-megaton hydrogen bomb explosion of 9 July 1962. Although additional USSR high altitude tests were subsequently conducted in the Fall of 1962, no reported data are available to correct the artificial electron fluxes. However, for semiconductor damage the artificial electron contribution is an order of magnitude smaller than the natural proton damage. Therefore, doubling or tripling the electron fluxes should not materially affect the equivalent proton dose rates.

The particle fluxes shown in figures I-1 through I-5 were then averaged for the rotation of the earth to give the effective fluxes that are shown in figures I-6 through I-10. These figures and estimated data for solar flare proton fluxes are analyzed to give the space radiation dose rates in accordance with paragraph I-2 to give the dose rates in figures I-11 through I-15. Natural belt electrons are inconsequential for electronic system damage in comparison with the artificial electron and belt protons. Particle fluxes are given above specified energy values in conformance with the data in the references.

I. 2 SPACE RADIATION DOSE RATES

Orbit plane contour maps such as shown in figures I-13 through I-15 are employed for estimating space radiation dose rates. Dose rates plotted are the effective rate of energy absorption by a thin film that is perfectly shielded on one side and shielded by 0.1-g-cm^2 aluminum on the other. Dose rates for other shielding densities and configurations are readily computed from these reference dose rates.
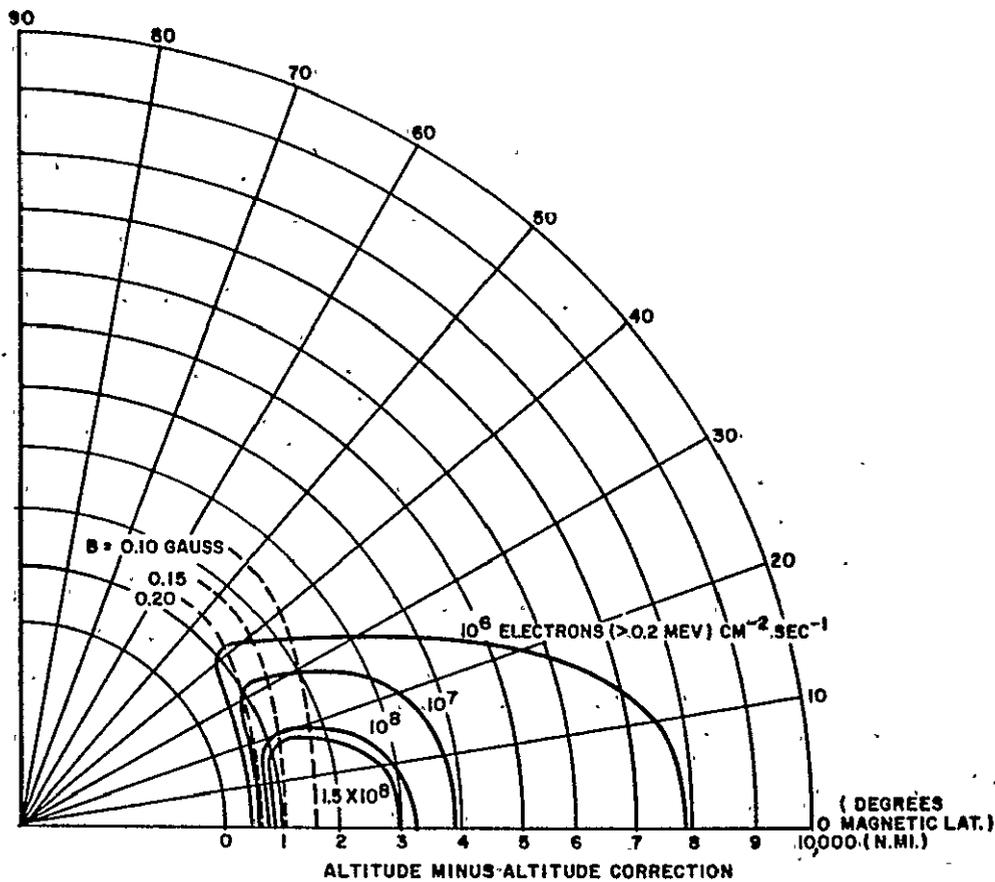
Figure I-1. Artificial Electron Flux (Mag. Coord.) 23 July 1962
(E > 0.2 mev) (Ref. 1)

Analytic representations of factors used in computing the dose rates from particle fluxes, with appropriate assumptions about the energy distributions and energy absorption characteristics, are as follows:

Linear energy absorption:

$$-\frac{dE}{dx} = a\ E^{-b}, \quad mev\ cm^2\ g^{-1}$$

Energy distribution:

$$\frac{n}{n_0} = \left(\frac{E}{E_0}\right)^{-c}$$

Minimum energy of particles passing shield density $x\ g\ cm^{-2}$:

$$E_x = x\ \frac{dE}{dx}\bigg|_{E\ =\ Ex} = x\ a\ E_x^{-b} = (a\ x)^{\frac{1}{1+b}}, \quad mev$$

I-2
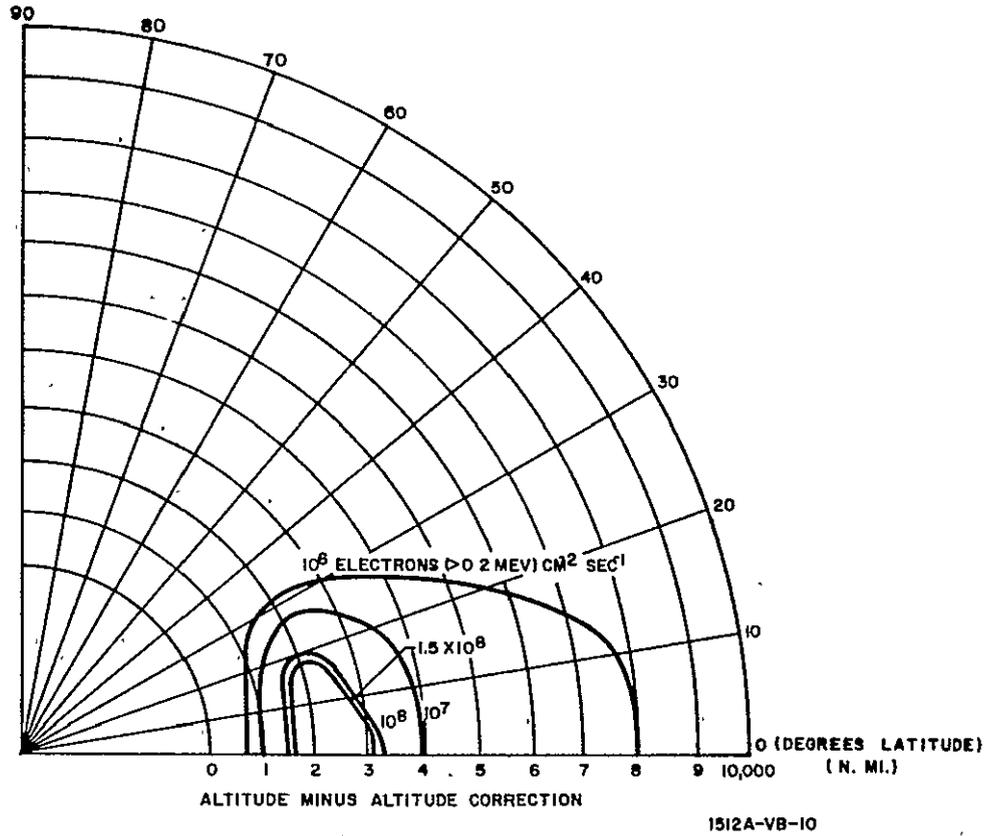
Figure I-2.   Predicted Artificial Electron Flux (Mag. Coord.) for January 1970
(E > 0. 2 mev) (Ref. 1 and 2)

Radiation dose rate:

$$D_x = \int_{E_x}^{\infty} -\frac{dE}{dx} \, dn$$

$$= \int_{E_x}^{\infty} a \, E^{-b} \, n_0 \, d\left(\frac{E}{E_0}\right)^{-c}$$

$$= \frac{a \, c \, E_0^{\,c}}{b + c} \, E_x^{\,-(b + c)} n_0$$

$$= \frac{a \, c \, E_0^{\,c}}{b + c} \, (a \, x)^{-\left(\frac{b + c}{b + 1}\right)} \quad n_0, \ \ \text{mev } g^{-1} \sec^{-1}$$

I-3
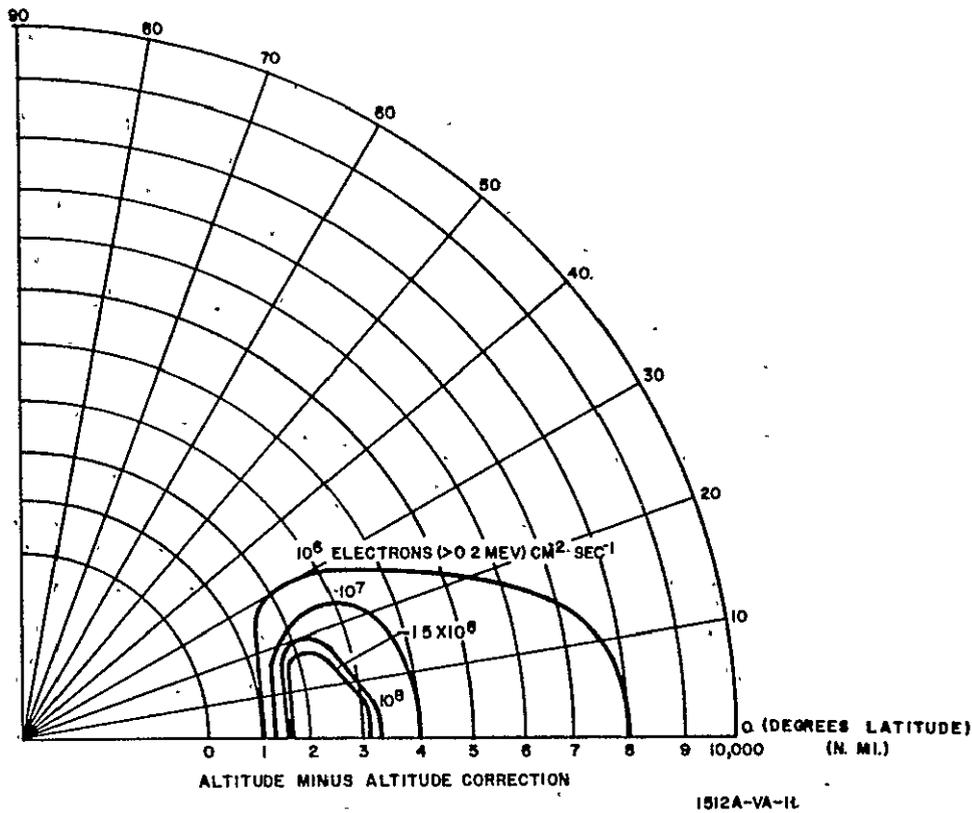
Figure I-3. Predicted Artificial Electron Flux (Mag. Coord.) for January 1980
(E > 0.2 mev) (Ref. 1 and 2)

where

a, b, and c = empirical constants

D = dose rate, mev g^{-1} sec^{-1}

D_x = shielded dose rate, mev g^{-1} sec^{-1}

E = energy, mev

E_0 = the reference particle energy, mev

E_x = the minimum energy of particles passing shield of density x, mev

n = particle flux with energy greater than E, cm^{-2} sec^{-1}

n_0 = flux of particles with energy greater than the E_0, cm^{-2} sec^{-1}

x = equivalent aluminum shielding, g cm^{-2}

The factors for artificial electron, belt proton, solar flare proton, and belt electron radiation were evaluated and given in table I-1.

Magnetic field coordinate representations of particle fluxes (figures I-1 through I-5) (references 1, 2, and 7) are averaged over one rotation of the earth to give the effective particle fluxes in geographic coordinates (figures I-6 through I-10). The average flux (reference 8) of solar flare protons (E_0 > 30 mev) is assumed to be n_0 = 34 cm^2 sec^{-1}.

I-4

TABLE I-1

RADIATION DOSE FACTORS

Radiation	$-\dfrac{dE}{dx}$ $\text{mev g}^{-1}\text{ cm}^2$ (aluminum)	$\dfrac{n}{n_0}$	E_x mev	D_x $\text{mev g}^{-1}\text{ sec}^{-1}$	$D_{0.1}$ $\text{mev g}^{-1}\text{ sec}^{-1}$
Artificial Electron	1.6	$\left(\dfrac{E}{0.2}\right)^{-1.17}$	1.6 x	$\dfrac{0.140\,n_0}{2^{1.17}}$	$2.07\,n_0$
Belt Proton	$200E^{-0.75}$	$\left(\dfrac{E}{40}\right)^{-1.66}$	$(200\text{ x})^{0.571}$	$\dfrac{42\,n_0}{x^{1.38}}$	$1010.0\,n_0$
Flare Proton	$200E^{-0.75}$	$\left(\dfrac{E}{30}\right)^{-2.13}$	$(200\text{ x})^{0.571}$	$\dfrac{33\,n_0}{x^{1.05}}$	$1470.0\,n_0$
Belt Electron	2	$\left(\dfrac{E}{0.02}\right)^{-3}$	2 x	$\dfrac{2\times10^{-6}\,n_0}{x^3}$	$0.0002\,n_0$
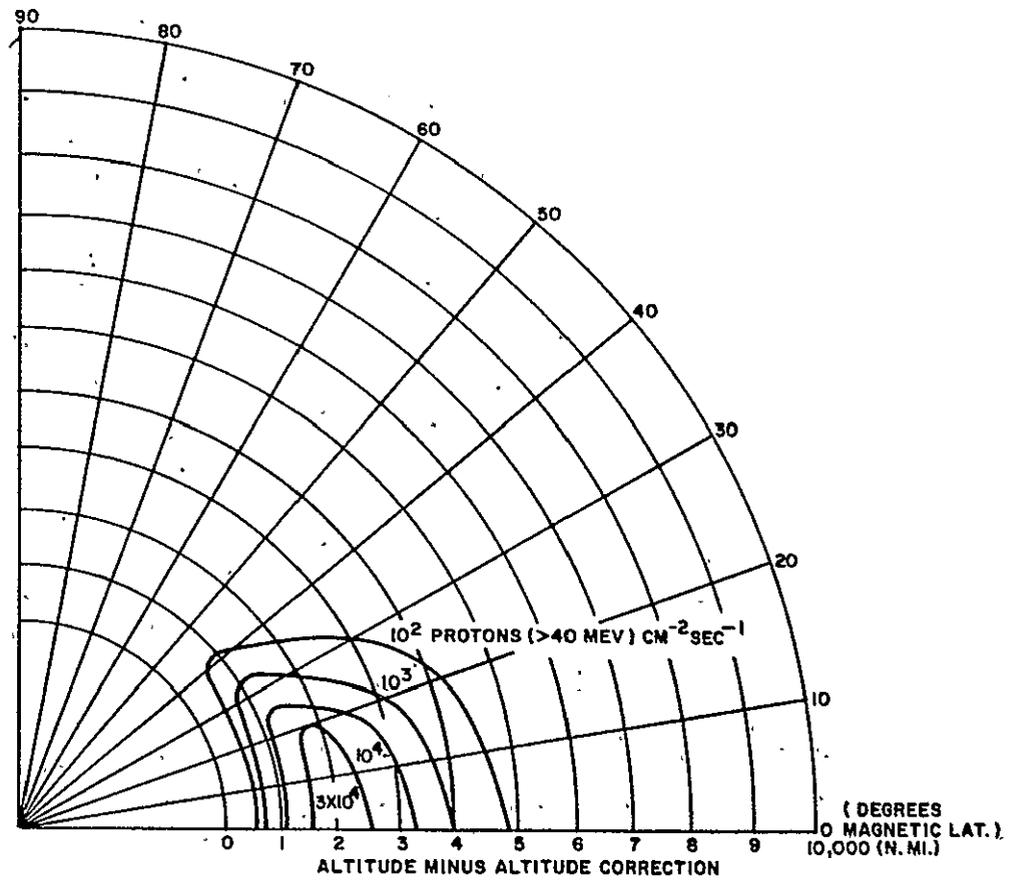
Figure I-4. Proton Flux (Mag. Coord.) E > 40 mev (Ref. 7)
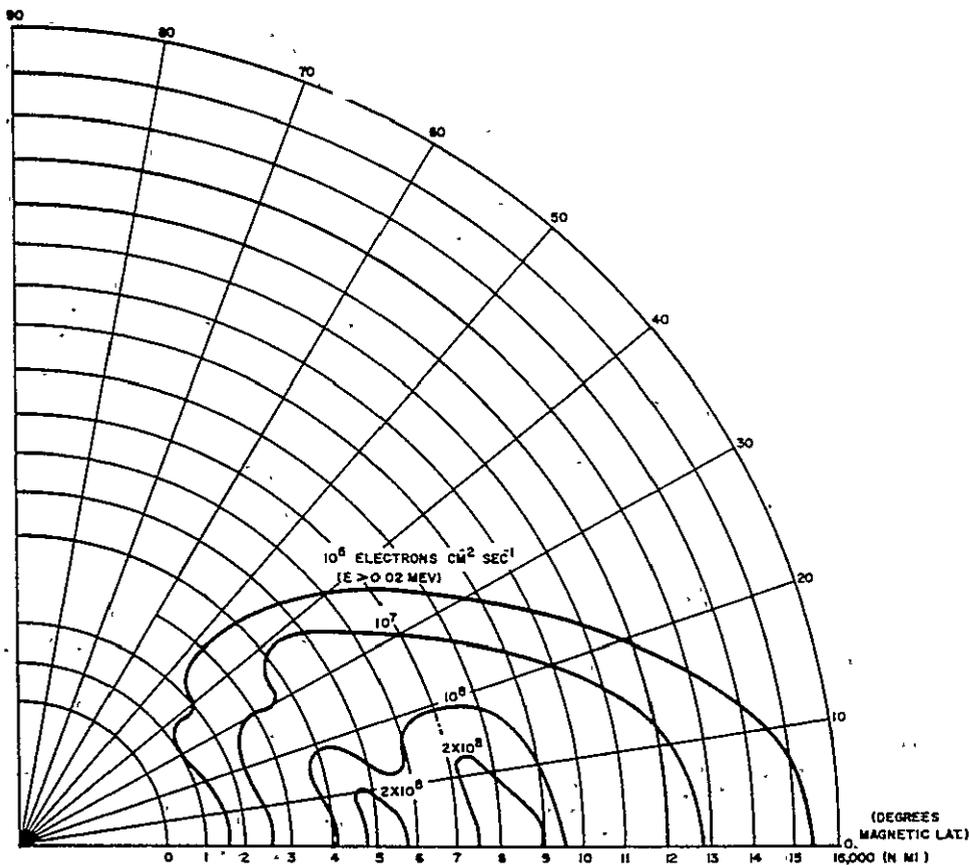
Figure I-5.   Natural Electron Flux (Mag. Coord.) E > 0. 2 mev (Ref. 7)

With 0. 1-g-cm^{-2} shielding, particles. reaching materials have sufficient energy for both ionization and atomic displacement.   Organic insulators are degraded as the extent of ionization and the total dose rate shown in figure I-10.

However, semiconductors and inorganic insulation are degraded as the atomic displacements for which the electrons are not as effective as protons for identical absorbed energy doses.   Using the ratio

$$\frac{\text{proton dose}}{\text{electron dose}} = \frac{1.3 \times 10^{15}}{.9 \times 10^{12}} \doteq 0.0069$$

for equivalent degradation (refer to section I. 4), the proton equivalent dose rates are shown in figure I-11 as a measure of the degradation of semiconductors and inorganic insulation.

Belt (natural) electrons do not contribute to dose rates of organic insulation or semiconductors with shielding adequate to give reasonable protection against the more energetic artificial electrons and belt protons.
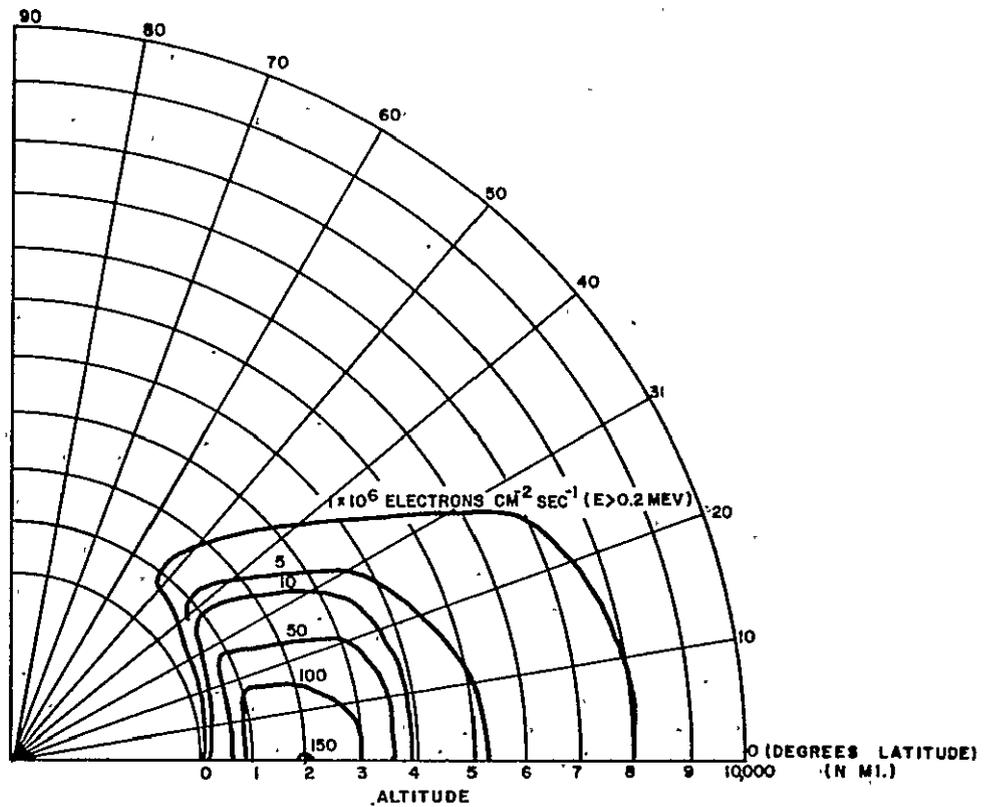
Figure I-6.   Effective Artificial Electron Flux July 1962 (E > 0. 2 mev)

Figures I-11 through I-15 include the dose rates from artificial electrons, belt protons, and solar flare protons. The estimated background average solar flare proton dose rate is $5. 0 \times 10^4$ mev g^{-1} sec^{-1}.

Artificial electrons are the major contributor to total dose rates, whereas belt protons dominate the equivalent proton dose rates.

Bremsstrahlung or secondary radiation from deceleration of artificial and natural electrons can be shown to be negligible, compared to the primary penetrating radiation, for its effects upon organic insulation or semiconductors.

The orbit plane dose rate contour drawings were prepared for special applications and are available upon request.

Total Radiation Dose Rates, 0-degree-Inclination, Sketch No. 113-S6-4234

23. 5	4235
49	4236
60	4239
65	4237
90	4238
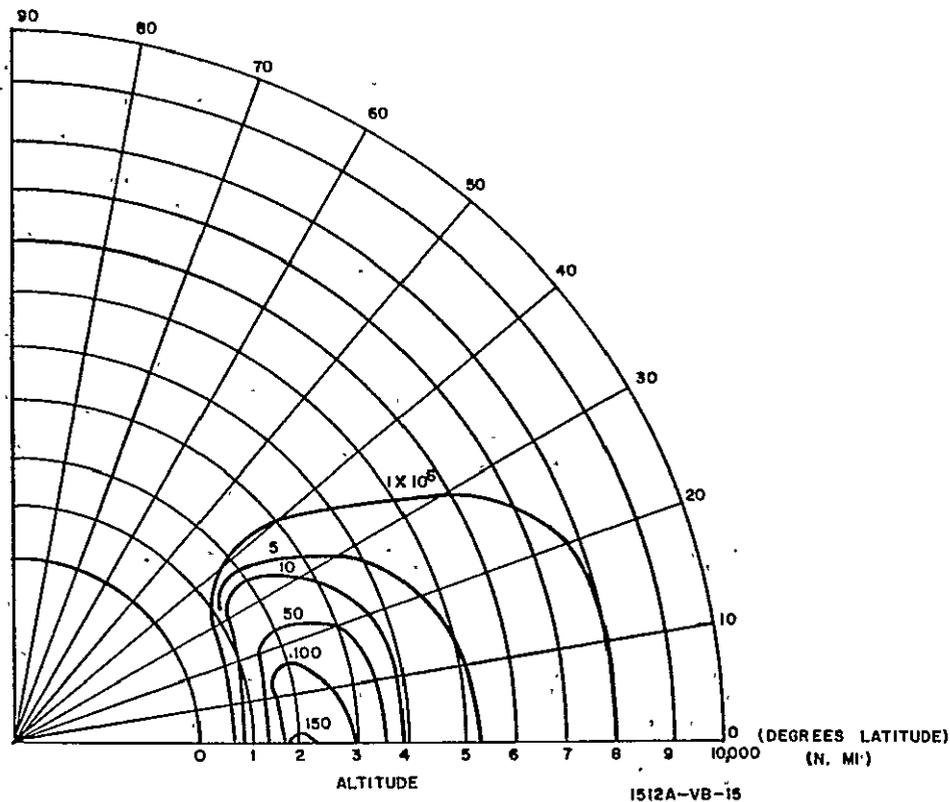
Figure I-7. Predicted Effective Artificial Electron Flux January 1970
(E > 0.2 mev)

Equivalent Proton Dose Rates, 0-degree-Inclination, Sketch No. 113-S6-4241

23.5	4243
47.5	4240
49	4244
60	4242
65	4245
90	4246

Figures I-13 through I-15 are representative of these drawings.

I.3 RADIATION TOLERANCE

Statistical reliability data for semiconductor devices subjected to doses of belt radiation after shielding is insufficient for a completely rigorous prediction of failure rates versus shielding for given orbits.

Silicon and germanium transistors may exhibit transient leakage for time ranges from seconds to minutes when subjected to a dose rate near 5×10^9 mev-g^{-1}-sec^{-1}. Unshielded exposure to belt or flare protons could give much larger dose rates, and permanent damage, rather than transient leakage, would be the primary concern. Shielding that exceeds 0.01 g cm^{-2} should eliminate any possibility of transient leakage caused by space radiation. Photovoltaic effects (transient voltage) at dose rates near 2×10^{12} mev-g^{-1}-sec^{-1} are eliminated

I-8
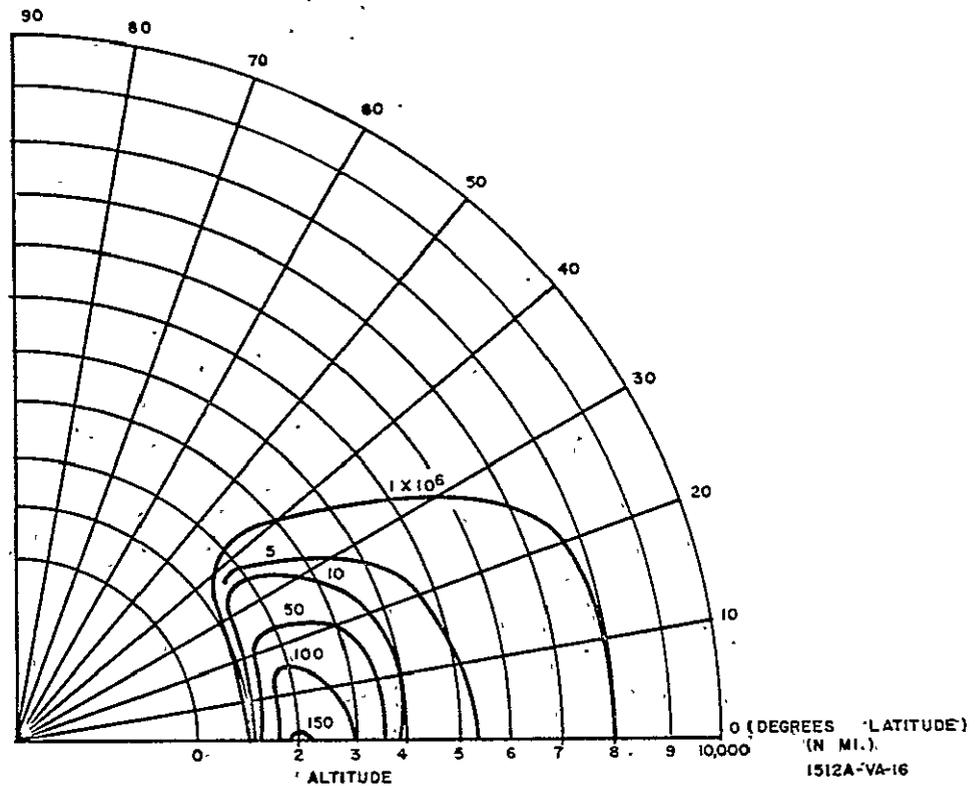
Figure I-8. Predicted Effective Artificial Electron Flux January 1980
(E > 0.2 mev)

by such shielding. Noise, similar to thermal noise, will accompany absorption of radiation particles in circuit elements and is decreased by shielding (reference 3).

Permanent damage to silicon and germanium diodes is caused by a total dose of 6×10^{12} to 2×10^{14} mev g^{-1} (reference 3). Tolerances of both diodes and transistors are about 10^{13} -nvt fast neutrons, so proton effects should be similar.

Silicon and germanium transistor small signal ac gain, h_{fe}, decreases 30 percent for a total proton dose of 10^{12} to 2×10^{13} mev g^{-1} (reference 4). Typical gain versus 40-mev proton radiation doses for transistors is shown in figure I-16. (The average rate of energy loss for 40-mev protons is 10 mev-g^{-1} cm^2.) Types 2N128(Ge), 2N743(Si), and 2N1303(Si) are examples of transistors with a superior radiation tolerance.

The thinnest base thicknesses (radii) for diodes and transistors are associated with the greatest radiation tolerance. Heavily doped N regions also increase radiation tolerance.

Deterioration of maximum power of silicon solar cells of different types and resistances is shown in figure I-17 (1-mev electron) and figure I-18 (4.6-mev protons). A decrease of 30 percent in maximum power of solar cells is caused by the electron and proton dosages in table I.2 (reference 5).

I-9
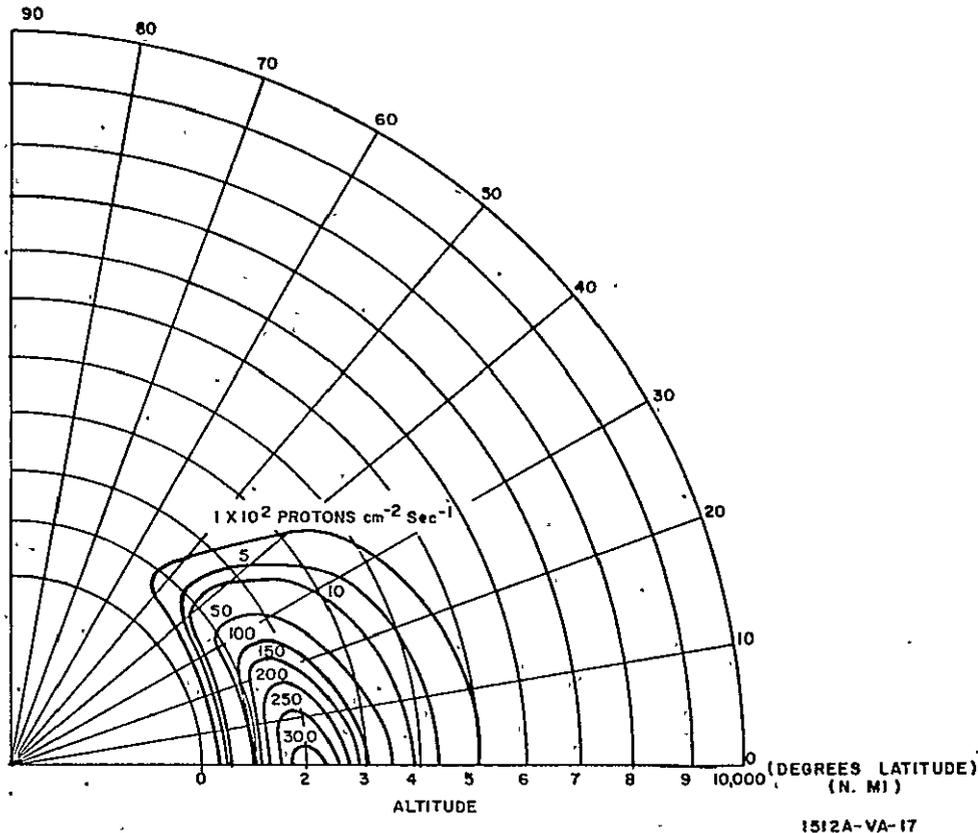
Figure I-9. Effective Proton Flux (E > 40 mev)

TABLE I-2

DOSES FOR 30-PERCENT DECREASE IN POWER OF SOLAR CELLS

Type	Electrons (1 mev)				Protons (4. 6 mev)		
	Resist-ance (ohm-cm)	Number (cm^{-2})	$-\dfrac{dE}{dX}$ (mev g^{-1} cm^2)	Dose (mev g^{-1})	Number (cm^{-2})	$-\dfrac{dE}{dX}$ (mev g^{-1} cm^2)	Dose (mev g^{-1})
np Si	25	8×10^{14}	1. 6	$1. 3 \times 10^{15}$	$1. 5 \times 10^{11}$	60	$9. 0 \times 10^{12}$
np Si	1	7×10^{14}	1. 6	$1. 1 \times 10^{15}$	$1. 1 \times 10^{11}$	60	$6. 6 \times 10^{12}$
pn Si	1	10^{13}	1. 6	$1. 6 \times 10^{13}$	10^{10}	60	$6. 0 \times 10^{11}$

The higher tolerance of the solar cells to electron doses is attributed to the low efficiency of electrons for atomic displacements associated with semiconductor degradation.

Because there are diodes and transistors with greater radiation tolerances than the np Si 25-ohm-cm solar cells and since detailed proton and electron reliability data are not

I-10
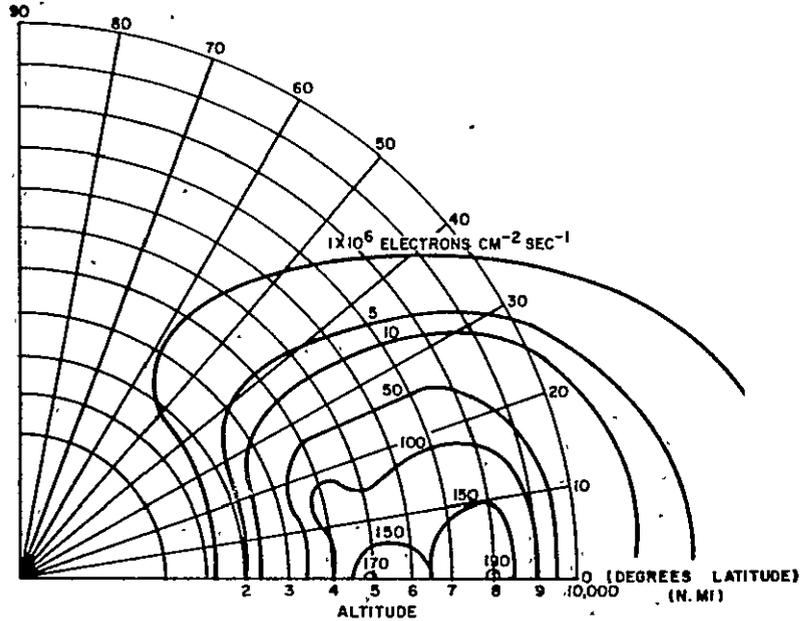
Figure I-10. Effective Natural Electron Flux (E > 0.2 mev)

available for transistors and diodes, the damage thresholds 1.3×10^{15} mev-g^{-1} for electrons and 9×10^{12} mev g^{-1} for protons are adopted as a guide for estimating the life limitations of the class of devices based upon semiconductors.

The accuracy of the dose rate charts and the tolerance of semiconductors is supported by the actual life measurement for solar cells on Relay I in section I.5.

Tolerances of organic insulating materials are based upon total dose rates since ionization is the primary damage mechanism. Semiconductor encapsulation resins, greases, and surface impurities are examples of organic insulation which are less obvious than wire insulation and potting resins.

The tolerance of organic insulation useful in space applications is assumed to be 6×10^{14} -mev-g^{-1} (10^9 erg g^{-1}) total dose. Specific materials have tolerances from 0.01 to 1000 times this reference value.

Tolerances of inorganic insulation vary widely according to composition but appear to be equal or greater than the tolerances for semiconductors. Borosilicate glass becomes severely discolored with a 10^{13} -mev-g^{-1} proton dose. Quartz slightly darkens with a 5×10^{14} mev-g^{-1} dose. Sapphire may decrease 25 percent in transmission with a 6×10^{14} mev g^{-1} dose (reference 6).

The data of figures I-16, I-17, and I-18 suggest that the radiation dose tolerance of semiconductors as a function of a parameter change, ΔY, may be approximated by equations of the form $T = A e^{B \Delta Y}$ mev g^{-1}.
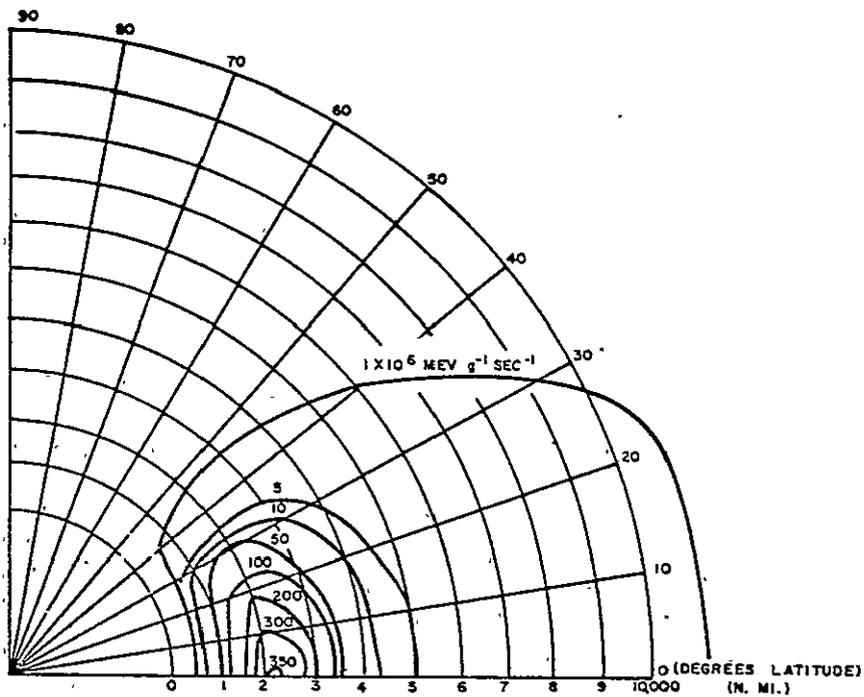
Figure I-11. Estimated Dose Rates - January 1970 (for Organic
Insulator Damage With 0. 1-g-cm^{-2} Aluminum Shield)
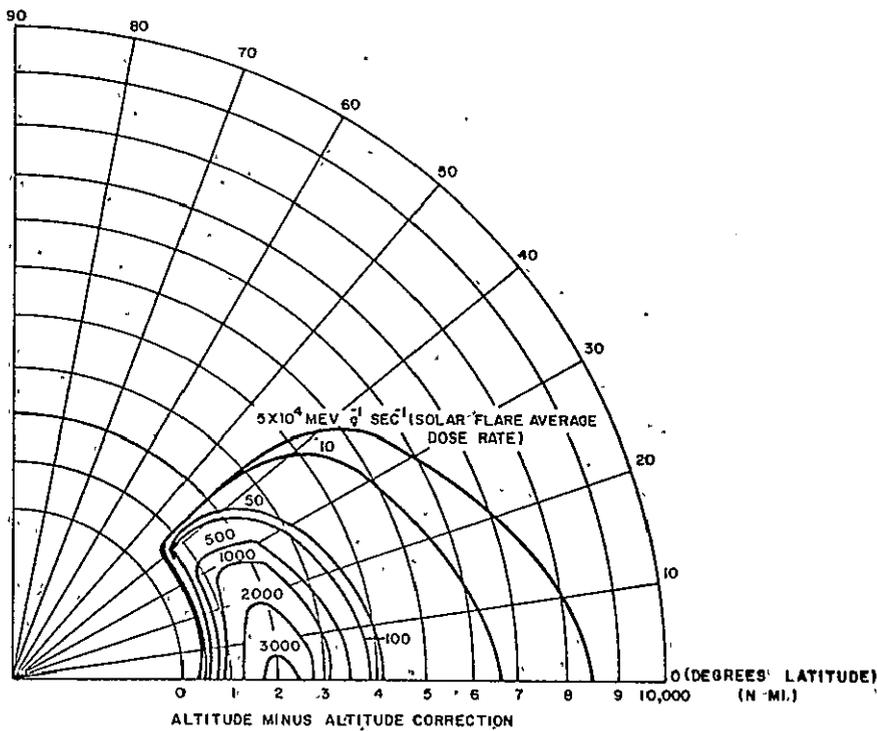
Figure I-12. Equivalent Proton Dose Rates - January 1970 (for Semiconductor
Damage With 0. 1-g-cm^{-2} Aluminum Shield)

I.4 LIFE LIMITATIONS

Damage to semiconductors by simultaneous electron and proton radiation dose rates for which the semiconductors have different tolerances requires the following relation in analogy to calculating the resistance of a parallel resistance circuit:

$$\frac{1}{\mathscr{l}} = \frac{D \text{ (protons)}}{T \text{ (protons)}} + \frac{D \text{ (electrons)}}{T \text{ (electrons)}} \sec^{-1}$$

where

$\mathscr{l}$ = the life, seconds

D = dose rate, mev g^{-1} sec^{-1} and,

T = tolerance, mev g^{-1}

Computation of semiconductor life limitations is aided by introducing the equivalent proton dose rate,

$$D_{ep} = D \text{ (protons)} + \frac{T \text{ (protons)}}{T \text{ (electrons)}} \, D \text{ (electrons) mev g}^{-1} \sec^{-1}$$

so

$$\mathscr{l} = \frac{T \text{ (protons)}}{D_{ep}}, \sec$$

using

T (electrons) = 1.3×10^{15} mev g^{-1} and

T (protons) = 9×10^{12} mev g^{-1}

$$D_{ep} = D \text{ (protons)} + 0.0069 \, D \text{ (electrons) mev g}^{-1} \sec \text{ and}$$

$$\mathscr{l} = \frac{9 \times 10^{12}}{D_{ep}} \quad \text{seconds}$$

$$= \frac{2.85 \times 10^{5}}{D_{ep}} \quad \text{years}$$

Damage to organic insulation is based upon total (ionizing) dose rate, so the life is simply

$$\mathscr{l} = \frac{T}{D}.$$

Life limitation for organic insulation with radiation tolerance not less than 6×10^{14} mev g^{-1} (polyethylene, hydrocarbons, etc) is

$$\mathscr{l} = \frac{6 \times 10^{14}}{D} \quad \text{seconds}$$
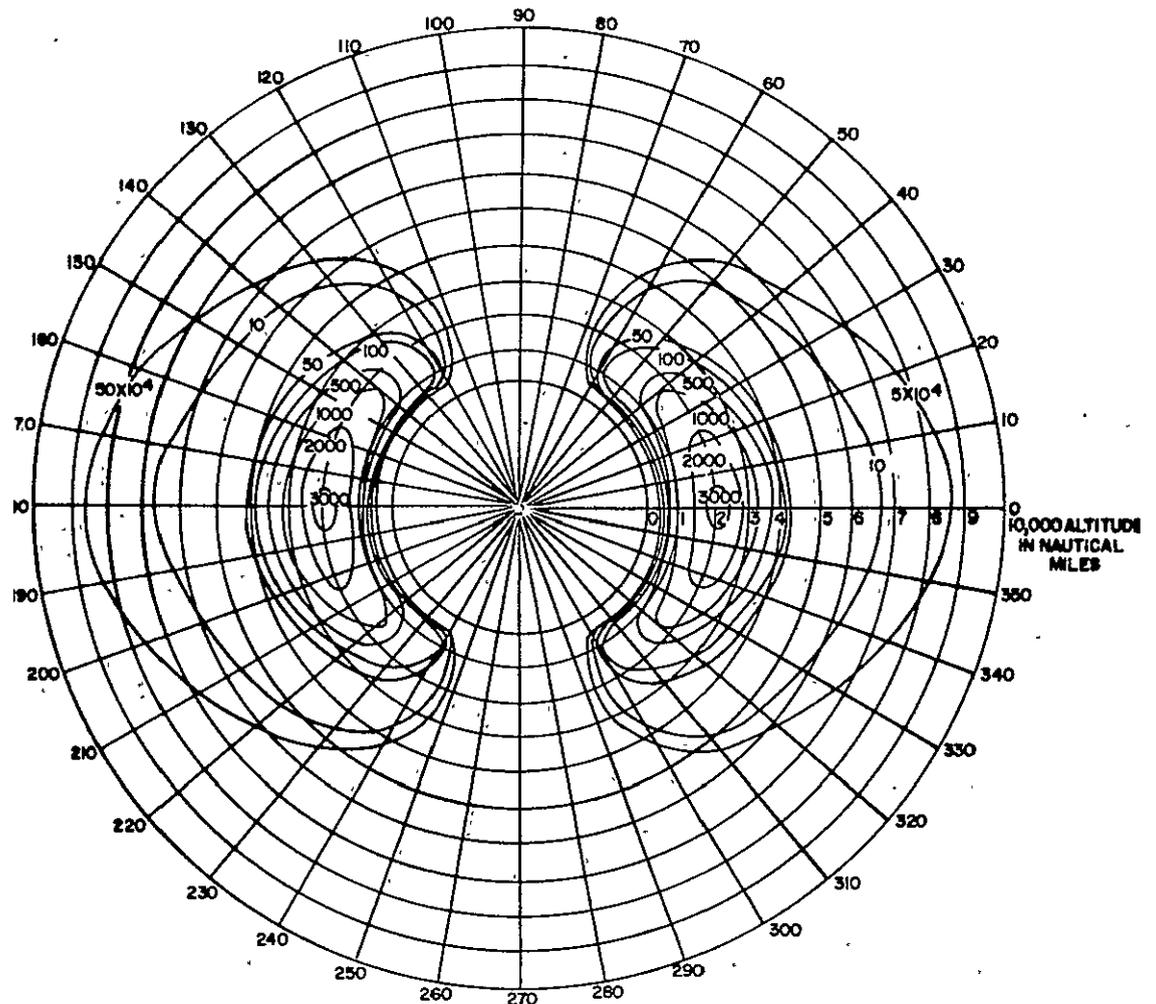
$$= \frac{1.90 \times 10^{7}}{D} \quad \text{years}$$

where D is the dose rate, mev g^{-1} sec^{-1}.

Life limits with 0.1-g-cm^{-2} shielding (aluminum) versus altitude to 10,000 nmi (in circular orbits with a 60-degree inclination) are shown in figures I-19 and I-20 for organic insulation and semiconductors respectively. Dose rates, and life limits were computed from the particle fluxes shown in figures I-6 through I-9 in accordance with section I.2. The effects
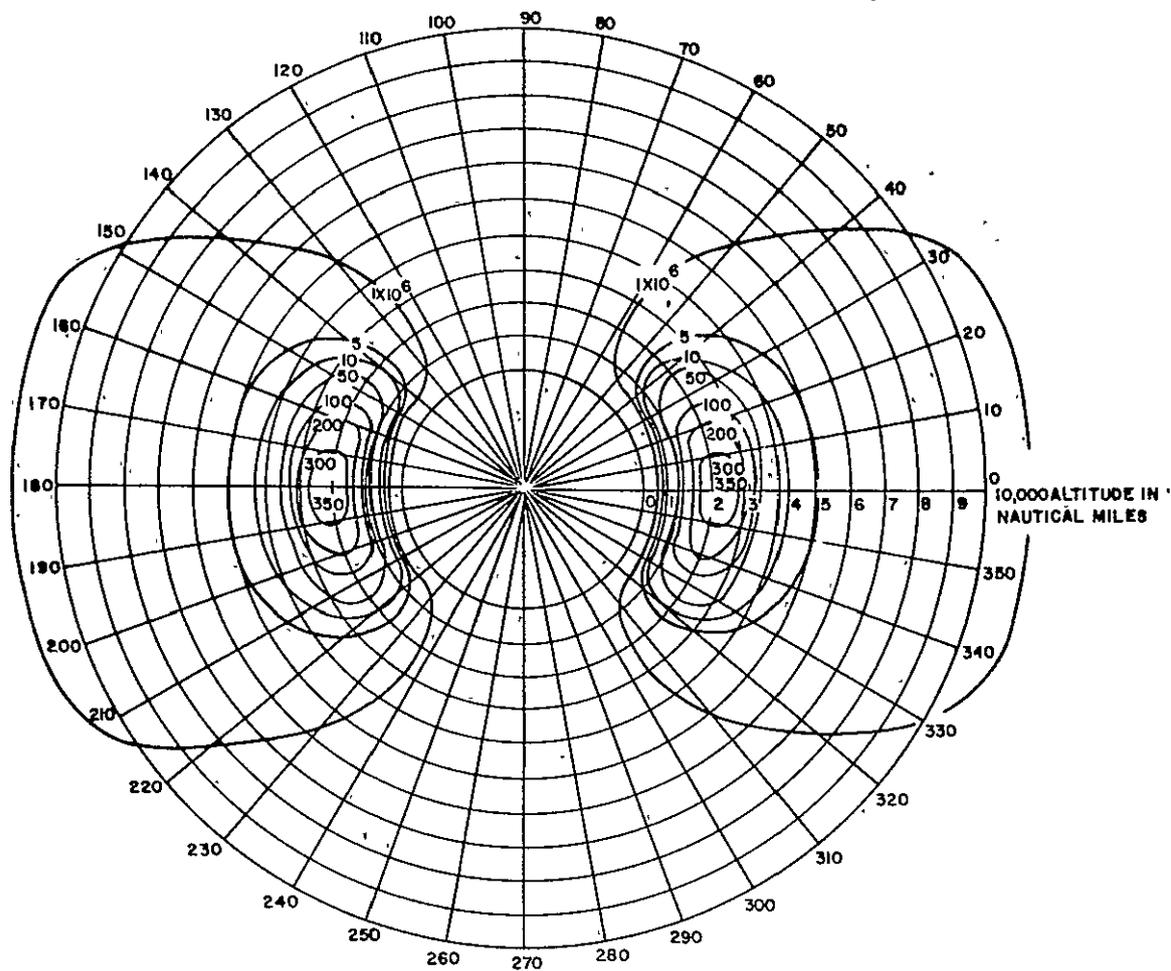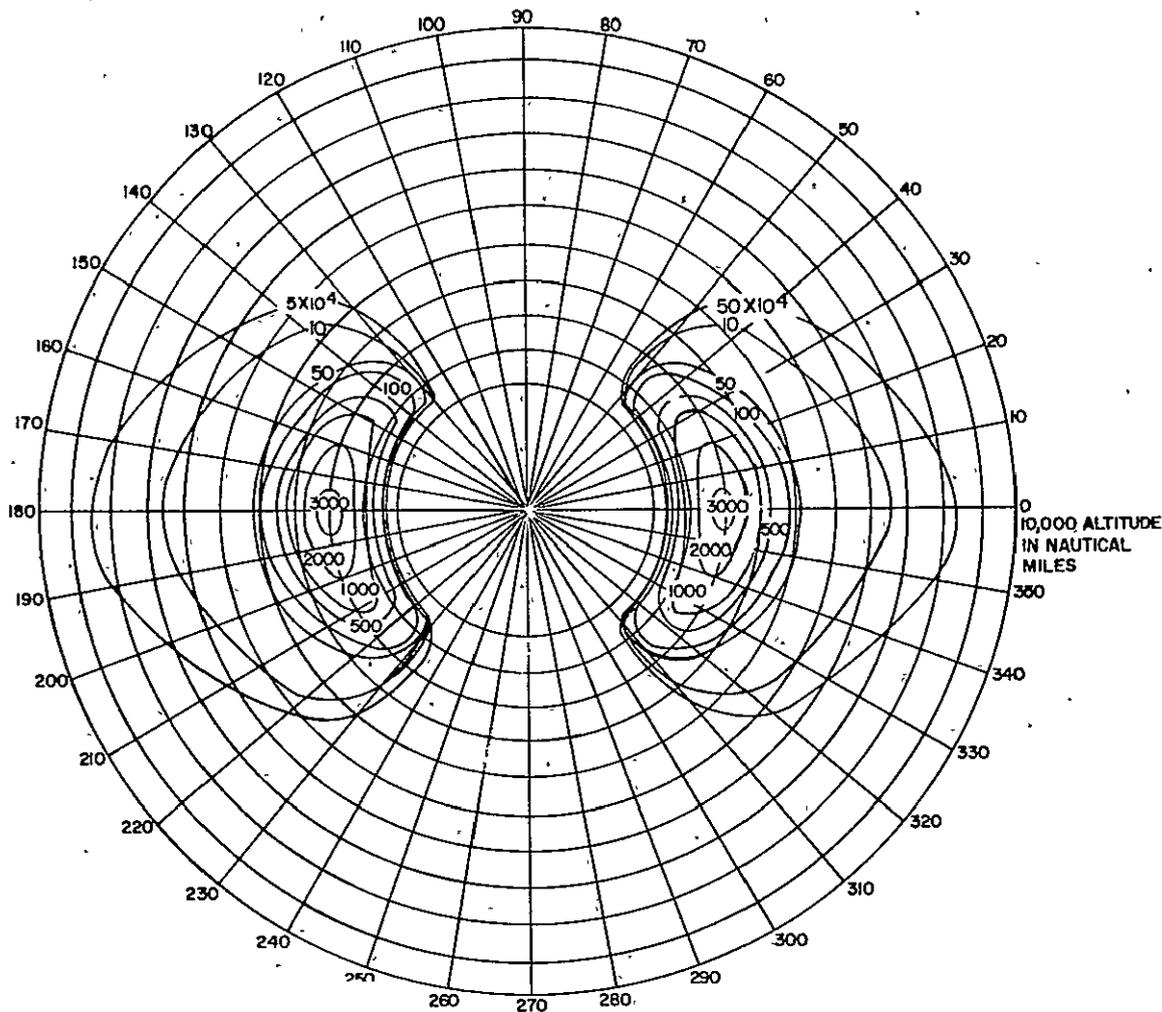
5. DOSE RATES ARE FOR ARTIFICIAL BELT ELECTRONS
(JAN 1970) NATURAL BELT PROTONS AND SOLAR
FLARE PROTONS. ARTIFICIAL BELT ELECTRONS
BELOW 2000 N. MILES GIVE HIGHER DOSE RATES
BEFORE JAN 1970. SPECIAL CHARTS SHOULD BE USED
FOR ORBITS BETWEEN 500 AND 2000 MILES AT TIMES
BEFORE JAN 1970.

4. DOSE RATES ARE FOR THIN FILMS WELL SHIELDED ON
ONE SIDE. FORMS SUCH AS WIRE INSULATION, PLATES,
POTTING AND LUBRICANTS ARE NORMALLY SUBJECT TO
TWICE THIS RADIATION DOSE RATE.

3 THE RADIUS OF THE EARTH IS ASSUMED TO BE 3440
NAUTICAL MILES.

2 THE ORIGIN OF ORBIT ANGLES IS THE LINE OF
INTERSECTION OF THE EQUATORIAL AND ORBIT PLANES

1 DOSE RATES ARE $MEV\,g^{-1}SEC$ ABSORBED IN ALUMINUM
AFTER ATTENUATION BY 0.1 g CM^{-2} ALUMINUM. THE
RADIATION IS CHARACTERIZED BY ELECTRONS FOR ITS
EFFECT UPON ORGANIC INSULATION.

Figure I-13.   Estimated Radiation Dose Rates, Orbit Plane Inclination: 60-Degree
Organic Insulation Dose Rates

5. DOSE RATES ARE FOR ARTIFICIAL BELT ELECTRONS (JAN. 1970) NATURAL BELT PROTRONS AND SOLAR FLARE PROTRONS. ARTIFICIAL BELT ELECTRONS BELOW 2000 N MILES GIVE HIGHER DOSE RATES BEFORE JAN. 1970 (LOWER AFTER JAN 1970). SPECIAL CHARTS SHOULD BE USED FOR ORBITS BETWEEN 500 AND 1000 MILES AT TIMES BEFORE JAN. 1970

4. DOSE RATES ARE FOR THIN FILMS WELL SHIELDED ON ONE SIDE. FORMS SUCH AS TRANSISTORS, DIODES, SOLAR CELLS, CERAMIC INSULATORS, GLASS COVER PLATES, AND OPTICAL ELEMENTS ARE NORMALLY SUBJECT TO TWICE THIS RADIATION DOSE RATE

3. THE RADIUS OF THE EARTH IS ASSUMED TO BE 3440 NAUTICAL MILES

2. THE ORIGIN OF ORBIT ANGLES IS THE LINE OF INTERSECTION OF THE EQUATORIAL AND ORBIT PLANES.

1. DOSE RATES ARE $MEV_g^{-1} SEC^{-1}$ ABSORBED IN ALUMINUM AFTER ATTENUATION BY 0.1g CM^{-2} ALUMINUM. THE RADIATION IS CHARACTERIZED BY PROTONS FOR ITS EFFECT UPON INORGANIC INSULATION AND SEMICONDUCTORS.

Figure I-14.   Equivalent Proton Dose Rates Orbit Plane Inclination: 60-Degree Inorganic Insulation and Semiconductor Dose Rates

Figure I-15. Equivalent Proton Dose Rates, Orbit Plane Inclination: 47-1/2-Degree
Inorganic Insulation and Semiconductor Dose Rates

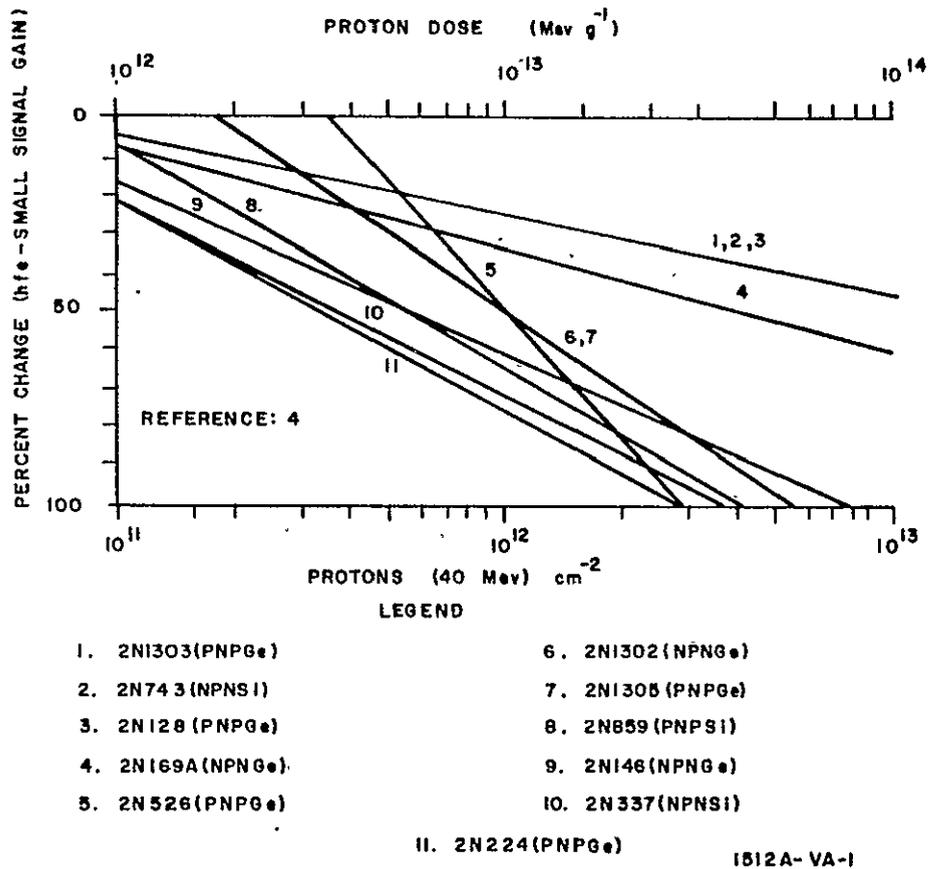Figure I-16. Gain vs Proton Radiation (Transistors)

LEGEND

1. 2N1303(PNPGe)
2. 2N743(NPNSI)
3. 2N128(PNPGe)
4. 2N169A(NPNGe)
5. 2N526(PNPGe)

6. 2N1302(NPNGe)
7. 2N1305(PNPGe)
8. 2N659(PNPSI)
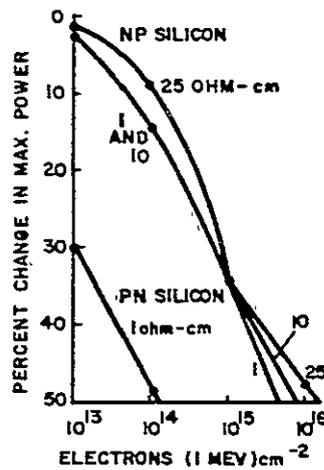9. 2N146(NPNGe)
10. 2N337(NPNSI)

11. 2N224(PNPGe)

Figure I-17. Maximum Power vs Electron Radiation (Silicon Solar Cells)
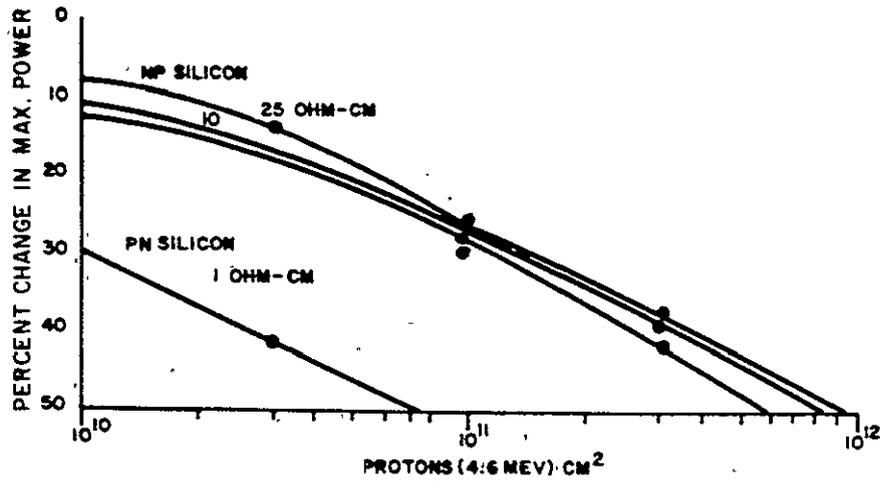
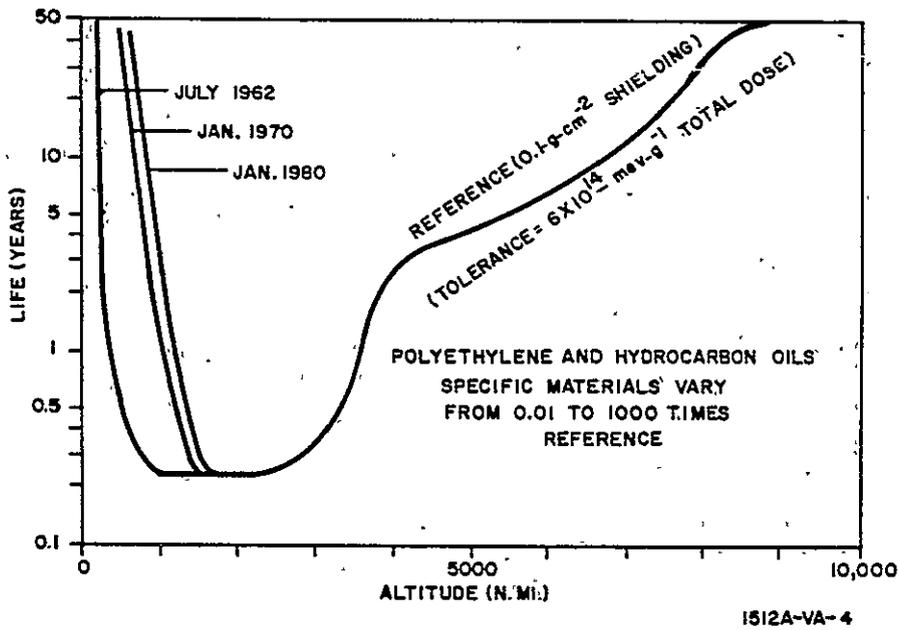Figure I-18. Maximum Power vs Proton Radiation (Silicon Solar Cells)

Figure I-19. Life Limits for Organic Insulation (60-Degree Inclination Circular Orbits)
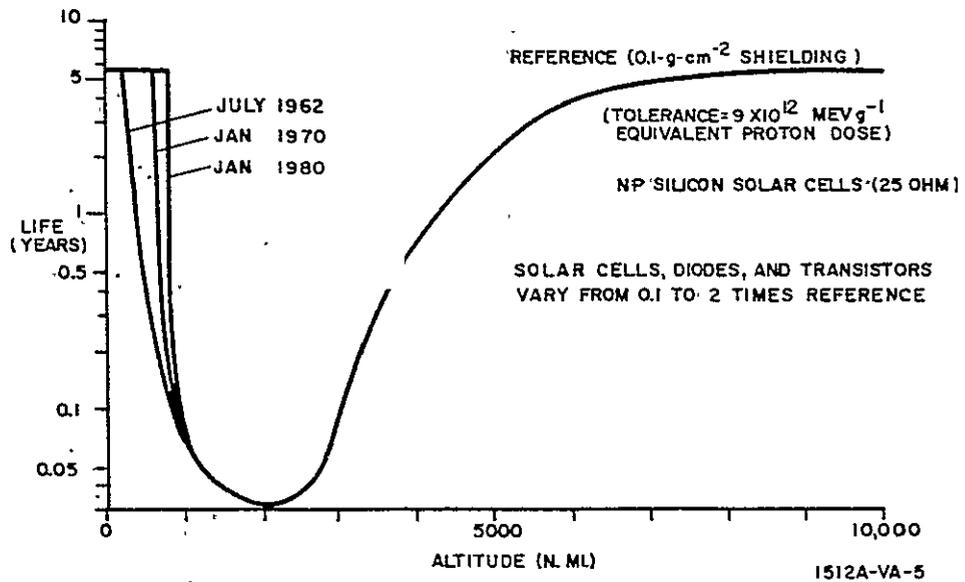
Figure I-20. Life Limits for Semiconductors (60-Degree Inclination Circular Orbits)

of variation of shielding and inclination angle are shown in figures I-21 and I-22. The life limits are conservative for materials with the radiation tolerance indicated. Section I.5 demonstrates that the dose rates used for computing the life limits in figures I-19 and I-20 are realistic.

Organic insulation and semiconductor devices should be selected discriminately for radiation tolerance with close attention to the tradeoff between redundancy and shielding. The weight increase for doubling the power of solar cells (figure I-18) effectively increases the proton radiation tolerance by a factor of 10. Redundancy or excess gain of transistors (figure I-16) also provides a disproportionate increase in effective proton radiation tolerance. This enables lower shielding weight or permitting adaptation of a subsystem to arbitrary shielding configurations.

I.5 RADIATION DAMAGE TO SOLAR CELLS ON RELAY I

The measured effects of radiation damage to np and pn silicon solar cells with different thicknesses of silicon shielding on Relay I provides a good check on the estimates of radiation dose and life limits in this document (reference 9).

Relay I was launched into orbit, 13 December 1962, with an inclination of 47.5 degrees, 7441-nmi apogee, and 4153-nmi perigee (earth center distances).

Unshielded cells degraded more than 50 percent in 3 days and shielded cells degraded more slowly.

The altitudes of Relay I are calculated at intervals in table I-3 and used to compute the average equivalent proton dose rates in tables I-4 and I-5 for the lowest dose orbit, the

TABLE I-3

COMPUTATION OF ALTITUDE AND TIME VERSUS ORBIT ANGLE - RELAY I

Orbit Angle $\pm\theta$	$\sin^2\theta$	$2.21\sin^2\theta$	$1 + 2.21\sin^2\theta\big]^{-1}$	$\left[1 + 2.21\sin^2\theta\right]^{-1}_{av}$	h	Δt	t
0	0	0	1.000	0.969+	4001	0.0966	0.00
10	0.029	0.064	0.939	0.867-	3770	0.0865	0.10
20	0.117	0.259	0.794	0.718+	3190	0.0716	0.18
30	0.250	0.553	0.643	0.583-	2530	0.0581	0.25
40	0.414	0.915	0.522	0.478+	1930	0.0476	0.31
50	0.587	1.298	0.435	0.406-	1470	0.0405	0.36
60	0.750	1.658	0.376	0.357+	1120	0.0356	0.40
70	0.883	1.951	0.339	0.329-	920	0.0328	0.44
80	0.971	2.145	0.318	0.315-	740	0.0314	0.47
90	1.000	2.21	0.311		710	0.5007	0.50

TABLE I-4

RELAY I - AVERAGE DOSE RATES VERSUS ALTITUDE MEV g^{-1} sec^{-1} (PROTON EQUIVALENT)

Orbit Angle 47.5-Degree-Inclination in Orbit	Elapsed Time Altitude	0 4000	±0.10 3770	±0.18 3190	±0.25 2530	±0.31 1930	±0.36 1470	±0.40 1120	±0.44 920	±0.47 740	±0.50 710	Fraction nmi
0		80×10^4	300×10^4	800×10^4	2400×10^4	3000×10^4	2300×10^4	1300×10^4	1000×10^4	300×10^4	200×10^4	
10		60	90	1000	2200	2700	2200	1200	900	300	300	
20		45	60	500	1600	2200	2000	1100	700	400	300	
30		40	45	200	900	1600	1400	900	600	300	200	
40		35	40	60	400	800	900	700	600	300	200	
50		25	30	40	80	300	350	350	250	200	150	
60		8	8	20	35	45	70	100	80	60	50	
70		5	5	5	5	5	5	5	5	5	5	
80		5	5	5	5	5	5	5	5	5	5	
90		5	5	5	5	5	5	5	15	5	5	
Total*		266×10^4	431×10^4	2233×10^4	6428×10^4	9158×10^4	8083×10^4	5013×10^4	3647×10^4	1723×10^4	1313×10^4	
Average**		30×10^4	48×10^4	248×10^4	715×10^4	1018×10^4	898×10^4	557×10^4	405×10^4	192×10^4	146×10^4	

Notes:

Dose rates are from figure I-14.

  * 1/2 values at 0 and 90 degrees; full values at other angles.

** 1/9 total

TABLE I-5

RELAY I - HIGHEST AND LOWEST DOSE RATES

Elapsed Time Arbitrary Units	Altitude (nmi)	Highest Dose Orbit		Lowest Dose Orbit	
		Orbit Angle (degrees)	Dose Rate (mev g^{-1} sec^{-1})	Orbit Angle (degrees)	Dose Rate (mev g^{-1} sec^{-1})
-0.50	710	230	50×10^4	270	5×10^4
0.47	740	240	40	280	5
0.44	920	250	5	290	5
0.40	1120	260	5	300	100
0.36	1470	270	5	310	350
0.31	1930	280	5	320	800
0.25	2530	290	5	330	900
0.18	3190	300	20	340	400
0.10	3770	310	30	350	100
0.00	4000	320	35	0	80
+0.10	3770	330	45	10	100
0.18	3190	340	450	20	400
0.25	2530	350	2100	30	900
0.31	1930	0	3000	40	800
0.36	1470	10	2300	50	350
0.40	1120	20	1300	60	100
0.44	920	30	700	70	5
0.47	740	40	300	80	5
0.50	710	50	200	90	5

Dose rates are from figure I-14

average dose orbit, and the highest dose orbit. Less then 25-percent variation of orbit dose rates from the average dose rate is shown in table I-6. Time variations of dose rates are shown in figure I-23.

Computation of Altitudes and Time:

Inclination $i = 47.5$ degrees

Semimajor axis, $a = 7441$ nautical miles

Semiminor axis, $b = 4153$ nautical miles.

$$\frac{x^2}{a^2} + \frac{y^2}{b^2} = 1$$

$$\frac{(h + 3440)^2}{7440^2} \left[\cos^2 \theta + \frac{7441^2}{4153^2} \sin^2 \theta \right] =$$

TABLE I-6

RELAY I - AVERAGE DOSE RATES

Elapsed Time	Lowest Dose Orbit		Average Orbit		Highest Dose Orbit	
	Dose Rate	Add	Dose Rate	Add	Dose Rate	Add
t						
-0.50	5×10^4	3×10^4	146×10^4	73×10^4	50×10^4	25×10^4
0.45	5	5	360	360	19	19
0.40	100	100	557	557	5	5
0.35	540	540	910	910	5	5
0.30	800	800	1200	1200	5	5
0.25	900	900	715	715	5	5
0.20	520	520	360	360	16	16
0.15	250	250	130	130	25	25
0.10	100	100	48	48	30	30
0.05	82	82	33	33	34	34
0.00	80	80	30	30	35	35
+0.05	82	82	33	33	37	37
0.10	100	100	48	48	45	45
0.15	250	250	130	130	150	150
0.20	520	520	360	360	720	720
0.25	900	900	715	715	2100	2100
0.30	800	800	1200	1200	3000	3000
0.35	540	540	910	910	2350	2350
0.40	100	100	557	557	1300	1300
0.45	5	5	360	360	560	560
0.50	5	2	146	73	200	100
Total*		6679×10^4		8802×10^4		10566×10^4
Average**		352×10^4		463×10^4		556×10^4
						$mev\ g^{-1}\ sec^{-1}$

* 1/2 values at t = ±0.50; full values at other times.

** 1/19 total.

$$\frac{(h + 3440)^2}{7440^2} \left[1 + \left(\frac{7441^2}{4153^2} \right) - 1 \sin^2 \theta \right] = 1$$

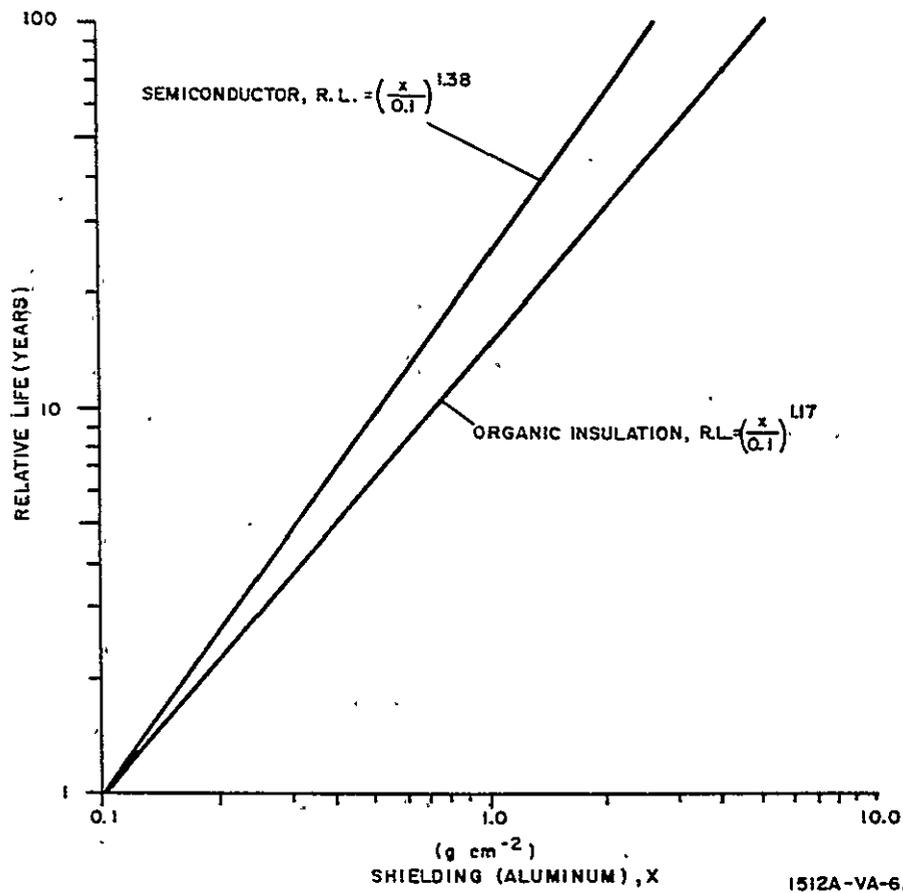$$(h + 3440)^2 = 7441^2 \left[1 + 2.21 \sin^2 \theta \right]^{-1}$$

Figure I-21. Relative Life With Increased Shielding

$$r^2 \frac{d\theta}{dt} = \frac{ab\,(360)}{p}$$

$$dt = \frac{pr^2\,d\theta}{ab\,360} \; ; \text{normalize p to 2.000}$$

$$dt = \frac{2\,(h+3441)^2\,d\theta}{7441\,(4153)\,(360)}$$

$$dt = 18.0 \times 10^{-11}\,(h+3440)^2\,d\theta$$

$$\Delta t \cong 18.0 \times 10^{-11}\,\overline{(h+3440)^2}\,\Delta\theta$$

$$\cong 18.0 \times 10^{-11}\,(7441)^2\,\overline{\left[1 + 2.21\sin^2\theta\,\right]}^{-1}\Delta\theta$$

$$\cong 0.00998\,\overline{\left[1 + 2.21\sin^2\theta\right]}^{-1}\Delta\theta$$

- Y-axis: 10, 8, 6, 4, 2, 1.0, 0.8, 0.6, 0.4, 0.2, 0.1, 0.08, 0.06, 0.04, 0.02, 0.01
- X-axis: 0, 10, 20, 30, 40, 50, 60, 70, 80, 90
- ORBIT INCLINATION ANGLE (DEGREES)

ALTITUDE   500 N. MILES OR 10,000 N. MILES

6000

5000

4000

REFERENCE SEMICONDUCTOR
WITH TOLERANCE OF 9×10^{12} MEVg^{-1}.
EQUIVALENT PROTON DOSE
SHIELDING: 0.1g CM^{-2} ALUMINUM

3000

1000

2000
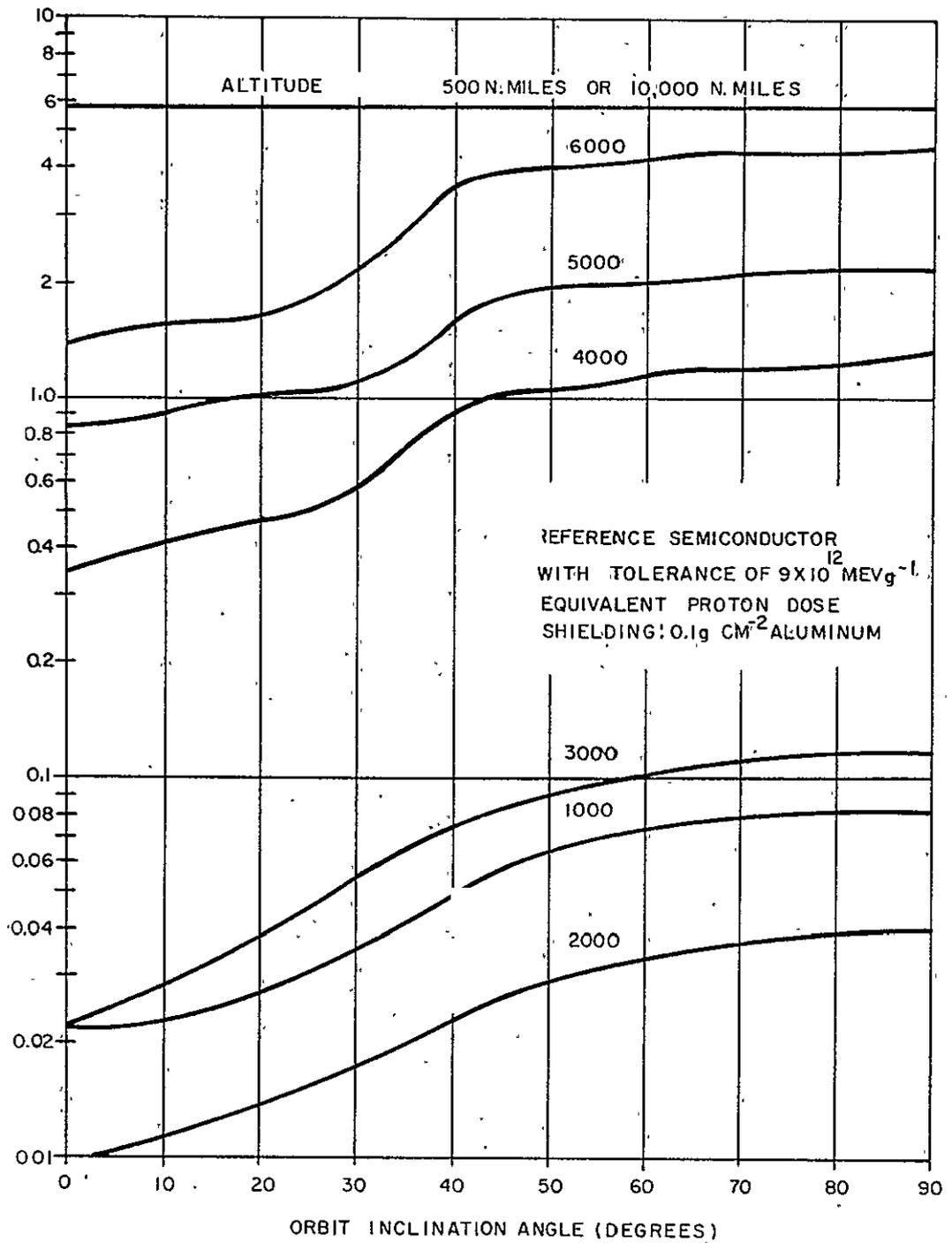
Figure I-22. Semiconductor Life vs Orbit Inclination
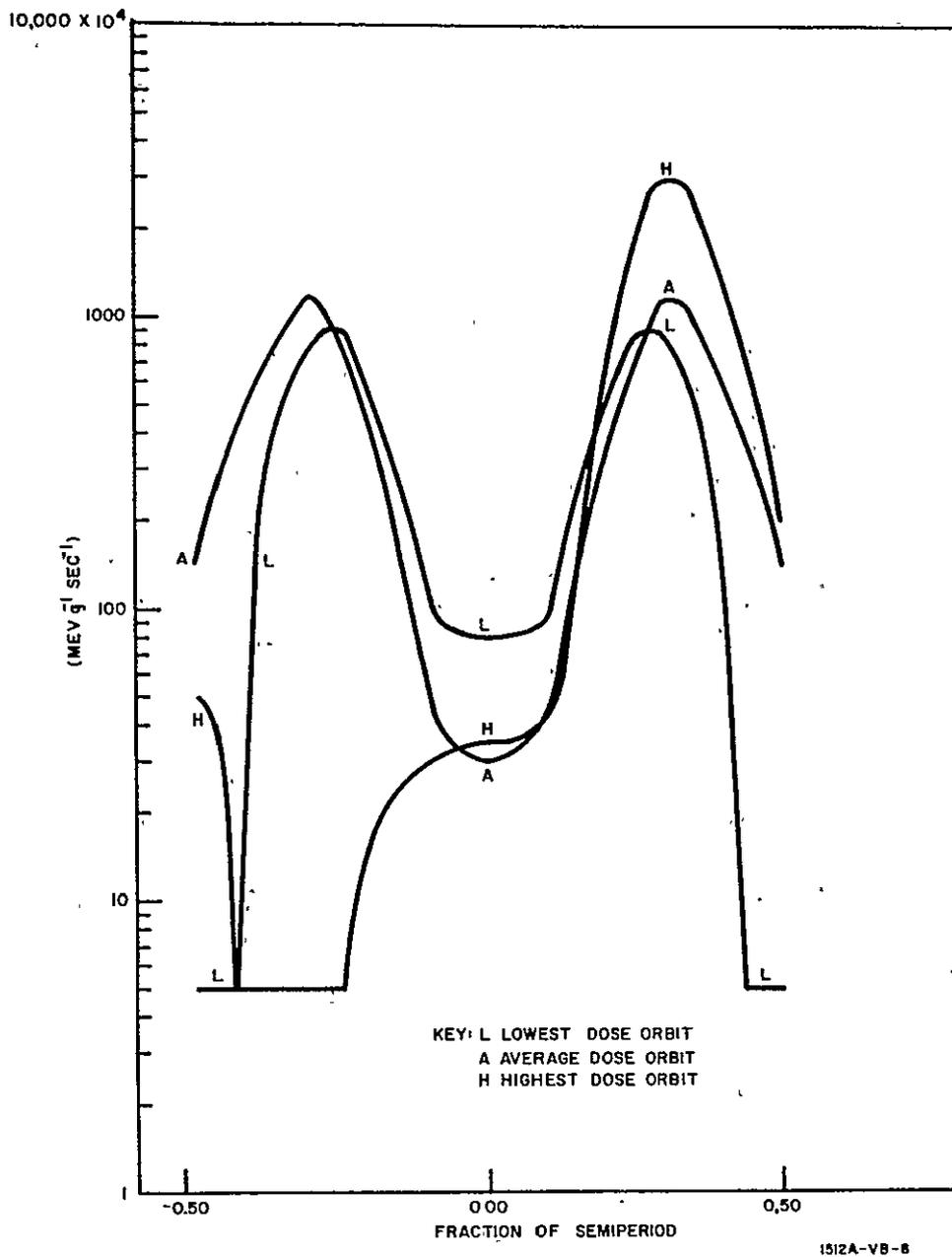
Figure I-23.   Dose Rates for Relay I Orbits

I. 5. 1   Calculation of Time for Critical Dose of Solar Cells on Relay I

The time for 30-percent decrease in short circuit current of solar cells with shielding of x g cm^{-2} subjected to radiation that would give a dose of 463×10^4 mev g^{-1} sec (proton equivalent) for 0.1-g-cm^{-2} shielding is estimated as follows: assuming the critical doses for np and pn cells to be 2.6×10^{11} and 1.9×10^{10} protons cm^{-2} (4.0 mev) (1.56 $\times 10^{13}$ and 1.14×10^{12} mev g^{-1}) respectively, (reference 5)

TABLE I-7

SOLAR CELL DEGRADATION - RELAY I

Type	Shield 7940 Silica (mils)	Shield Density x $(g\ cm^{-2})$	Time for ΔI_{sc} = -30 Percent Initial Value						% of Obs
			(sec)	Observed (reference 9) (days)	(years)	(sec)	Calculated (days)	(years)	
np Si	60	0.33	1.30×10^7	150	0.41	1.75×10^7	202	0.55	134
np Si	30	0.17	0.95	110	0.30	0.70	81	0.22	73
pn Si	60	0.33	0.39	45	0.12	0.13	15	0.041	34
pn Si	30	0.17	0.26	30	0.08	0.05	6	0.016	20

$$D_x = D_{0.1} \left(\frac{0.1}{x} \right)^{1.38}$$

$$= 463 \times 10^4 \left(\frac{0.1}{x} \right)^{1.38}.$$

$$\theta_c = \frac{T}{D_x}$$

For np cells,

$$\theta_c = \frac{1.50 \times 10^{13}}{463 \times 10^4} \left(\frac{x}{0.1} \right)^{1.38}$$

$$= 3.37 \times 10^6 \left(\frac{x}{0.1} \right)^{1.38} \text{ seconds}$$

pn cells,

$$\theta_c = \frac{1.14 \times 10^{12}}{463 \times 10^4} \left(\frac{x}{0.1} \right)^{1.38}$$

$$= 2.46 \times 10^5 \left(\frac{x}{0.1} \right)^{1.38} \text{ seconds}$$

I. 5..2 Comparison of Observed and Calculated Times for Critical Doses

The calculated times for 30-percent decrease in short circuit current of solar cells based upon the average dose rates for the Relay I satellite were 20 to 134 percent of the observed times in table I-7. The differences are attributed to the cumulative effect of errors in flux data, energy distributions, and tolerance of the particular solar cells used in this experiment.

This close agreement confirms that radiation dose rates and life limits computed in this report are realistic.

I. 6 CONCLUSIONS

Belt proton and artificial electron radiation limit the lives of reference semiconductor devices and organic insulation with standard shielding (0. 1 g cm^{-2}) to about 3 years at 600- and 5000 nmi altitude and to a few weeks at 2000 nmi altitude. Literature data show that specific types of semiconductor devices such as germanium and silicon transistors, diodes, and solar cells vary from 0. 1 to 2 times the tolerance of the reference semiconductor. Similarly, specific organic insulating materials vary from 0. 01 to 1000 times the tolerance of the reference organic insulation; some are seriously damaged before semiconductors.

Life with increased shielding is approximately proportional to the weight of shielding. Higher life is also achieved at the higher inclinations for a given altitude. Life is proportioned to time spent in the radiation belt and decreases for an increase in altitude below 2000 nmi.

Changes in parameters of specific semiconductor devices and tolerance of circuits for such changes determine the shielding requirements for the required life in specified orbits.

Since the acceptable dose as a measure of life increases exponentially with permissible parameter changes, marked advantages in reliability or decreased weight of shielding are associated with circuits designed to accommodate parameter changes (e. g. , by redundancy and adaptive functions).

BIBLIOGRAPHY

1. Brown and Gabbe, "Electron Distribution In the Earth's Radiation Belts During July 1962 As Measured by Telstar, " J. Geophys. Res. 68, 1963, pp. 607-618.

2. Hess, W. N. , "The Artificial Radiation Belt..., " J. Geophys. Res. 68, 1963, pp. 667-683.

3. Reich and Darlik, "Survey of Nuclear Radiation Effects On Semiconductor Materials and Devices, " Symposium on Radiation Effects, U. S. Army Signal Engineering Lab, Fort Monmouth, N. J. , February 1957.

4. Honaker and Bryant (NASA, Langley), "Radiation Damage to Transistors, " Space/Aeronautics, May 1963.

5. Cherry and Slifer, "Solar Cell Radiation Damage Studies, " NASA Goddard Report X-636-63-110, 1963.

6. "Radiation Effects of State of the Art 1961-1962, " REIC Report No. 24, Battelle Memorial Institute, Columbus, Ohio, June 1962.

7. Johnson, "Satellite Environment Handbook, " Stanford University Press, 1961.

8. Dugas, D. J. , "Solar Flare Radiation, " Rand Corp. , Santa Monica, Calif. , RM2825PR, November 1961.

9. Waddel, R. C. , (NASA-Goddard) "Radiation Damage Experiments on Relay, " Photovoltaic Specialists Conference, 1963, Power Information Center, Philadelphia, Penna. , Vol. 1, Section B-10.

10. Cherry, W. R. , "Solar Cells and The Application Engineer, " Astronautics and Aerospace Eng. , Vol. 1, No. 4, May 1963.

APPENDIX J
AMES GRAVITY GRADIENT CONTROL
SYSTEM AS APPLIED TO THE NAVIGATION SATELLITE

The Ames gravity gradient system, as described by Tinling and Merrick[1], is mechanized by use of a single auxiliary body that is pivoted with respect to the main satellite body through a spring and damper mechanism with one degree of angular freedom. The principle of inertial coupling is used to achieve damping for all possible modes of oscillation by use of the single body. Tinling and Merrick have extensively studied this configuration and have arrived at design criteria for optimum or near optimum performance.

These criteria can be summarized as follows:

Mass distribution: $I_1 = 1.2 I_r$

$I_d = 0.08 I_1$

$I_3 = 1.5 I_d$

$$J_3 = \left(\frac{I_2 - I_1}{I_3} \right) \cong 1.0$$

where I_j (j = 1, 2, 3) = principal moments of inertia of main satellite body excluding damper rod as shown in figure J-1

- I_r = transverse principal moment of inertia of a slim rod which has the same gravity gradient restoring torque as required in the final design.

I_d = transverse principal moment of damper rod.

Spring rate and damping: $K = 4.5 \omega_o^2 I_d$

$D = 1.5 \omega_o I_d$

where K = damper rod pivot spring.

D = damping constant for damper rod pivot.

In order to achieve the Ames mechanization, the navigation satellite must be arranged so that it has the specified mass distribution. As presently conceived, the navigation satellite has; in addition to the orientation boom; four 50 foot antenna support booms at a nominal angle of 90° between booms. At equilibrium, these booms will lie in the horizontal plane. In order to adapt this satellite to the Ames configuration, two approaches are possible. The first approach is to allow the four antenna booms to remain unpivoted (as presently conceived), add an additional damper rod pivoted with respect to the satellite body, and make other mass distribution changes as required.

---

[1] B. E. Tinling, V. K. Merrick, "The Exploitation of Inertial Coupling in Passive Gravity Gradient Stabilized Satellites." Aug 1963, AIAA Paper No. 63-342.

2

DAMPER PIVOT AXIS

PLANE OF MASS
CONCENTRATION

ORBITAL PLANE

DAMPER ROD

TIP MASS

TOP VIEW

ORIENTATION ROD

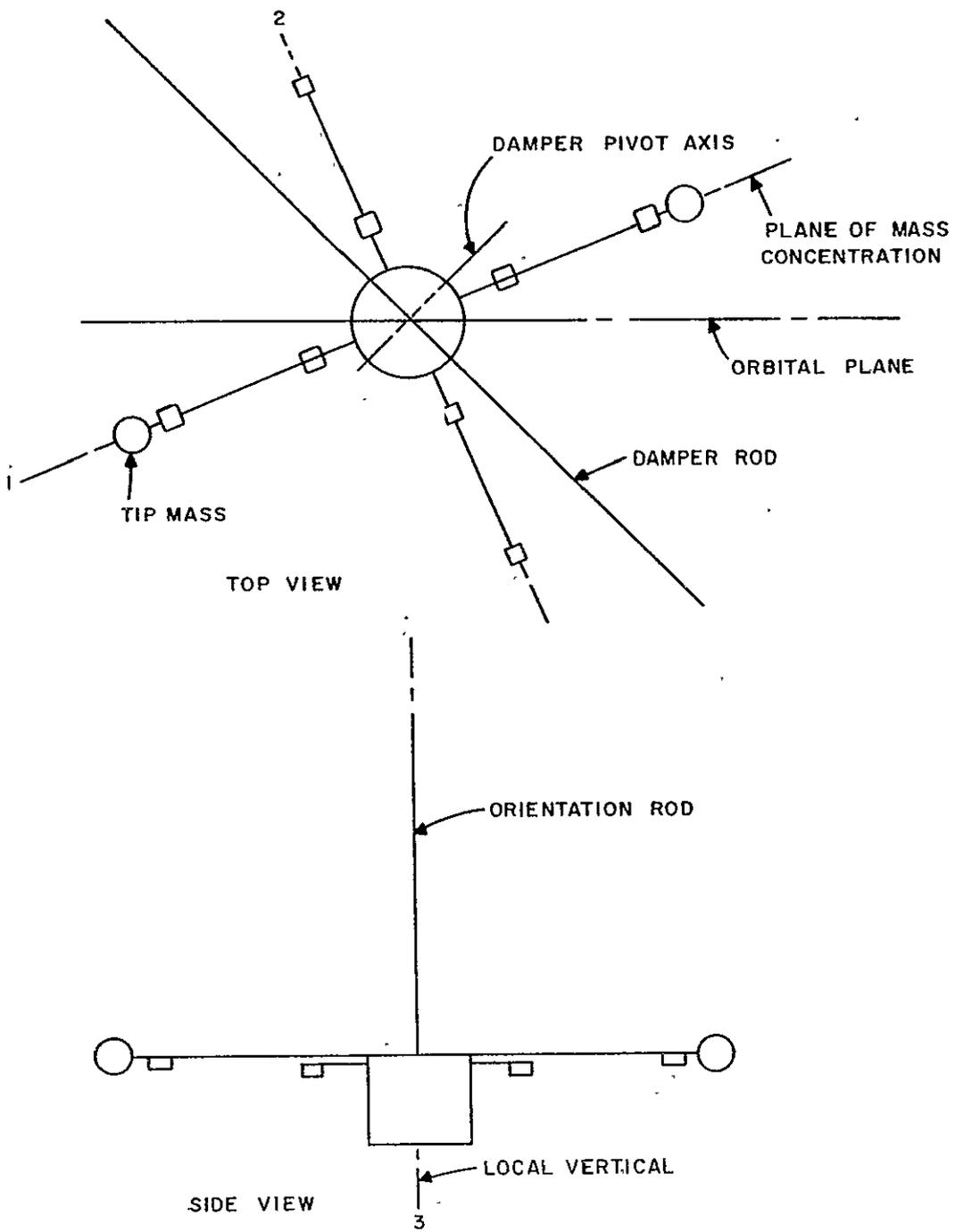LOCAL VERTICAL

SIDE VIEW

3

Figure J-1. Ames Gravity Gradient System

The second is to utilize the antenna booms to help achieve the required mass distribution.

The principal difficulty associated with the first approach is that a significant increase in system weight is necessary to obtain the required mass distribution. This can be determined by examination of the procedure necessary to obtain $J_3 \cong 1$. To have J_3 approach unity requires that the mass of the satellite body, including all fixed booms, shall approach a planar distribution. This appears physically unrealizable if four fixed orthogonal booms are used. However, J_3 can be forced to approach unity by making the moment of inertia contributed by one set of diametrically opposed booms much greater than that contributed by the second set. For example, if one set of booms has 10 times the inertia of the second set, $J \cong 0.82$, which is considered satisfactory. This alone would require the addition of considerable weight. The other listed constants on mass distribution would require the addition of a larger orientation rod inertia, I_1. In addition, the damper rod must be added, and this further increases the weight. It is true, however, that once the weight penalty is paid, performance should be near the predicted optimum by Tinling and Merrick.

In order to use the second approach, one set of diametrically opposed antenna booms would be joined together to form the damper rod and the other set would be firmly attached as before. This would, without further change, give a near planar mass distribution, $J_3 \cong 1$, and the other mass distribution constraints could be easily met. The angle between diametrically opposed pairs of antenna booms would become approximately 63° instead of 90°. This would require a slight estimated 15% increase in computing accuracy for the same overall error. The difficulty with this approach results from using one set of antenna support booms as the pivoted damper rod. This difficulty arises because each rod-mounted antenna uses one coaxial RF lead and three insulated conductors, that pass from the pivoted rod to the satellite body. These leads would mechanically interfere with the action of the damper rod pivot spring which has a very small and accurately controlled rate. A satisfactory solution to this problem is unavailable at this time. Arrangements of slip rings or conducting torsion wires either add excessive friction or make the damper unit too complex to be feasible.

It can be concluded, unless further investigation leads to a satisfactory solution of the antenna lead problem, that the application of the Ames system to the navigation satellite is feasible only by the first approach which yields near optimum performance, but carries a significant weight penalty.

APPENDIX K
INTERFEROMETER PHASE MEASUREMENT TECHNIQUE

In order to obtain the highest interferometer accuracy, the difference in phase between the signals arriving at the two interferometer antennas shall be accurately measured. The relative phases of these signals shall not be distorted in transmission to the phase comparator. In this appendix several methods of phase comparison-RF, IF, and Audio and both open and closed loop measurement techniques-are discussed. It is shown that an open loop phase measurement at audio frequencies, using a digital zero crossing phase detector, is satisisfactory.

K. 1 RF PHASE MEASUREMENT.

The need to maintain phase fidelity prior to actually making the comparison suggests that the measurement be made early in the system. This minimizes the number of phase sensitive components that are detrimental to measurement accuracy. On this premise, the possible RF phase detection techniques are examined.

Suppose the two antennas comprising an interferometer pair feed opposite ends of an RF transmission line. When a signal arrives at the interferometer, a standing wave is set up in the line. The position of the standing wave is a function of the arrival angle of the signal (See figure K-1). The signal at some point in the line, following its down conversion and amplification, can be detected. A voltage $E=A \sin \left(\frac{2\pi D}{\lambda} \sin \theta\right)$, where D/λ = antenna separation in wavelengths and θ = angle of arrival of the signal. This approach has several serious drawbacks which deny its use in this application. The principal drawbacks are:

    a. Ambiguities exist each quarter wavelength or each 90° of electrical phase shift.

    b. The measurement is sensitive to the amplitude of the incoming signal and to gain pattern mismatch of the antennas.

    c. The system noise figure cannot be optimized because of the long line lengths between the antennas and the first mixer.

A much more satisfactory performance can be obtained by changing to a closed loop system. Two additional items are necessary to implement a feedback phase demodulator. A variable phase shifter, driven by an integrator whose input is the phase detector output, is required in one of the RF channels and a dither switch is needed to polarize the error signal. Without the latter, the error signal characteristic for negative angles is the mirror image of that for positive angles. Dithering converts the error signal to one with angle sense, (shown in figure K-2), so that the servo will be capable of tracking the null in the interference pattern.
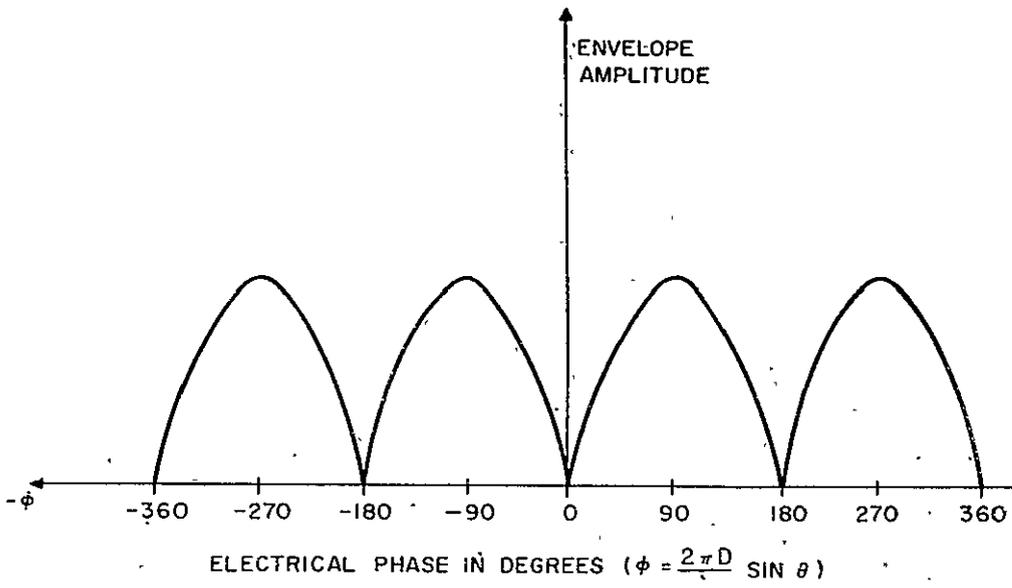
ENVELOPE
AMPLITUDE

-φ

-360   -270   -180   -90   0   90   180   270   360

ELECTRICAL PHASE IN DEGREES $(\phi = \frac{2\pi D}{\lambda} \text{ SIN } \theta)$

Figure K-1. Standing Wave Pattern

+ AMPLITUDE

WITHOUT
DITHER

-φ   -90   -45   45   90   +φ
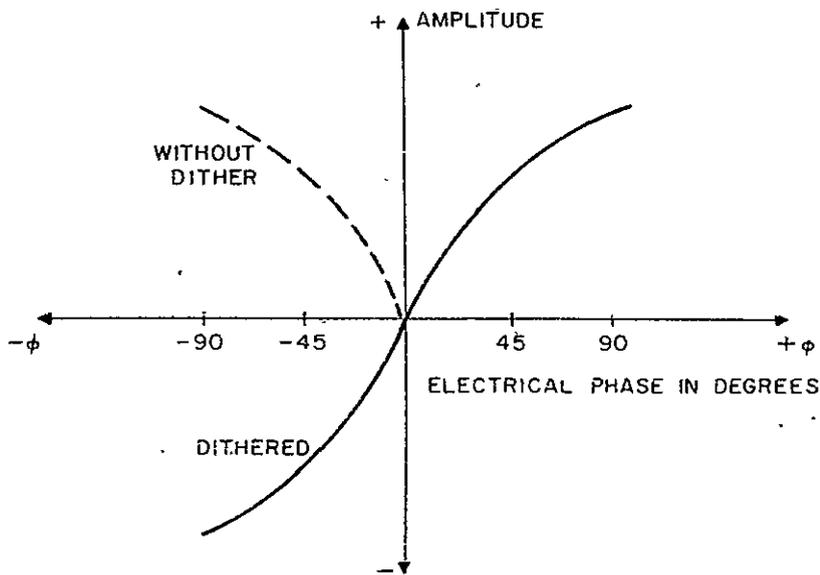
ELECTRICAL PHASE IN DEGREES

DITHERED

Figure K-2. Error Signal

The closed loop system, shown in figure K-3, has half the ambiguities of the open loop system and its accuracy is only slightly dependent upon absolute signal amplitude. These advantages are offset by other weaknesses. The first weakness is that the gain difference in the two RF channels will result in the standing wave pattern shown in figure K-4. Unlike figure K-1, which shows the infinite VSWR resulting from equal signals, figure K-4 shows a finite VSWR which has a rounded null at zero phase difference. While this introduces no boresight error in the error characteristic, it substantially reduces the slope and the loop sensitivity. This results in noisy tracking with increased angle error induced by noise.

The imperfections in the antenna patterns, which cause this reduction in performance in the presence of noise, cannot be totally eliminated. Signal-to-noise ratio must be increased to compensate for the antenna pattern imperfections.

Another objection to this system is the error introduced by imperfections in the phase shifter. The most satisfactory phase shifter is a digital delay line comprised of a number of sections of transmission lines whose lengths are integral powers of twice the basic phase quantization. These sections may be switched in and out of the signal path by digital control logic in the feedback path. The principal objection to such phase shifters is their sensitivity to environment, particularly to temperature. Unfortunately, variations due to temperature are not readily amenable to calibration. It is estimated that a phase shifter accuracy of 1/2 to 1 degree could be obtained with considerable development effort. Existing devices have twice this error over a modest temperature range. A uncertainty of $1°$ would absorb the total space angle error with 100 wavelength antenna separation.

While it appears that a closed loop system employing an RF phase shifter could be used with success, it would be demanding on other system parameters, viz, power and/or antenna separation and was eliminated from further consideration.

K. 2 IF PHASE MEASUREMENT

Next under consideration is the phase measurement techniques that can be effected at the IF level. In these systems, the signals from the two antennas are heterodyned to an IF prior to phase comparison. This approach permits optimization of the system noise figure. The long cable lengths between antenna and first mixer are eliminated. An equally important advantage of the shift to IF is that a synchronous phase detector can be used rather than the RF signal subtraction accomplished by feeding the signals into a common transmission line. (Synchronous phase detection can be accomplished at the RF level but in so doing, the system noise figure is vastly degraded.)

Two general schemes for measuring phase are again possible; open loop and closed loop. An open loop system can be implemented by comparing the two IF signals from the two antennas in a double balanced, synchronous phase detector. Such a device is sensitive only to quadrature noise. Gain imbalances in the two channels are cancelled. The principal disadvantage is the poor sensitivity of the phase detector except at small phase angles. Since the output is the sine of the phase difference, accuracy could not be expected to be adequate except over a range of about $\pm 60°$ phase.
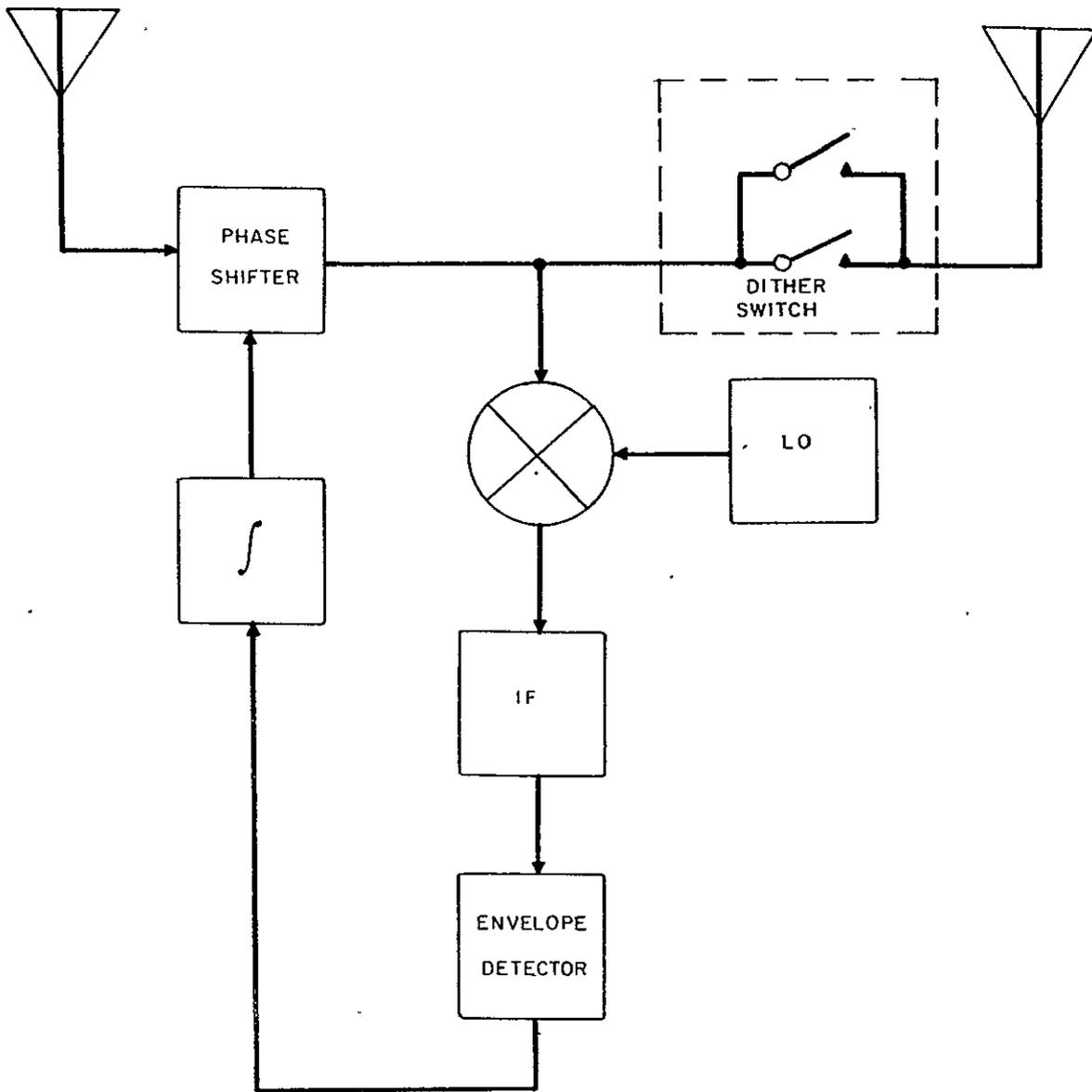
Figure K-3. Closed Loop System With RF Phase Comparison

A superior approach is to insert a digital IF phase shifter in one of the two channels and use the synchronous phase detector as an error detector in a closed loop system. Figure K-5 shows the closed loop technique. Dither is not required when operating at IF because the phase detector provides a polarized output.

But a phase shifter remains in the system. Although the temperature characteristic of an IF phase shifter is somewhat easier to compensate, temperature variations introduce some phase uncertainty which cannot easily be calibrated. This drawback accompanies any closed loop system operating in a changing environment.

K.3 LOW FREQUENCY, OPEN LOOP SYSTEMS

An open-loop system having good accuracy can be used if the interferometer signals are converted to a low frequency. Figure K-6 shows the salient features of a technique which measures phase as a function of the time between zero crossings of the two signals. Identical double conversion receivers use common local oscillators to heterodyne signals in the two channels to a relatively low frequency. Then small phase increments are represented by reasonably large time increments. The two channels must phase track with frequency and temperature variations in order to maintain accuracy.

The most critical portion of the system, with respect to phase stability, is the required narrow banding of the signals prior to the zero-crossing detectors. To indicate the nature of the problem, it is pertinent to determine the phase shifts which might be expected if the filters detune with age or temperature; or if the incoming signal frequency is not adequately controlled. The phase shift through a parallel tuned circuit at angular frequency ω is:

$$\emptyset = \tan^{-1} \left(\frac{R}{\omega L} - R \omega C \right)$$

The circuit is nominally tuned to the resonant frequency ω_m. If the filter is mistuned to frequency ω_r, then fractional mistuning is $k = \dfrac{\omega_r - \omega_m}{\omega_r}$. The resulting phase error is:

$$\emptyset = \tan^{-1} \left[\frac{R}{\omega_r L (1-k)} - R \omega_r C (1-k) \right]$$

$$= \tan^{-1} \left[\frac{Q}{(1-k)} - Q(1-k) \right].$$

$$= \tan^{-1} 2kQ$$

The angle measurement noise bandwidth shall be approximately 150 cps. The filter Q is then $Q \approx \dfrac{2\text{nd IF}}{150 \text{ cps}}$. The second IF should be reasonably high. With a low 2nd IF, the 1st IF amplifier bandpass is required to be small to avoid an appreciable degradation of S/N due to noise folding at the 2nd mixer. A narrow 1st IF bandpass would compound the phase tracking difficulties. The 2nd IF is also required to be low enough to permit adequate phase quantization by feasible digital counters. If $0.36°$ phase quantization is required, a counter with the speed of 1000 times the signal frequency is required. With a 100 mc counter, a 100 KC 2nd IF can be used. Under this condition the 1st IF must have a bandpass a little less than 400 KC.
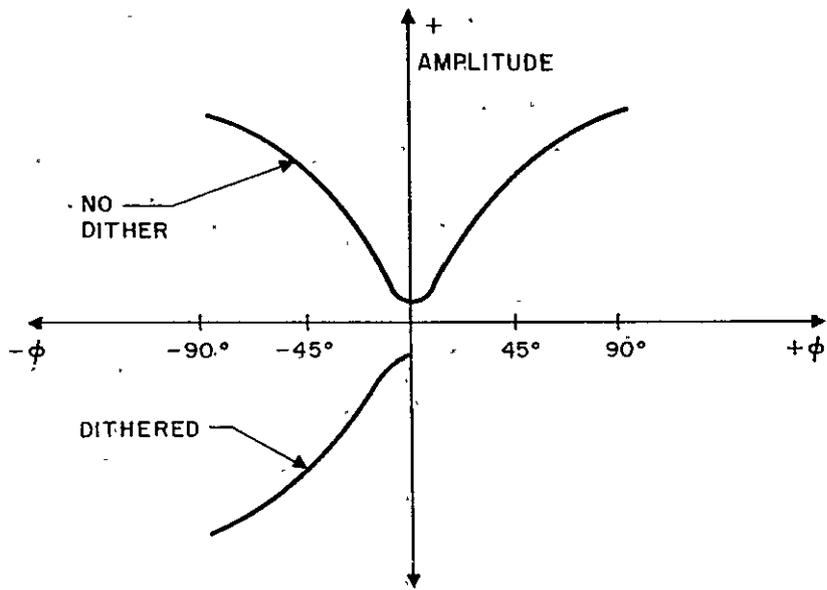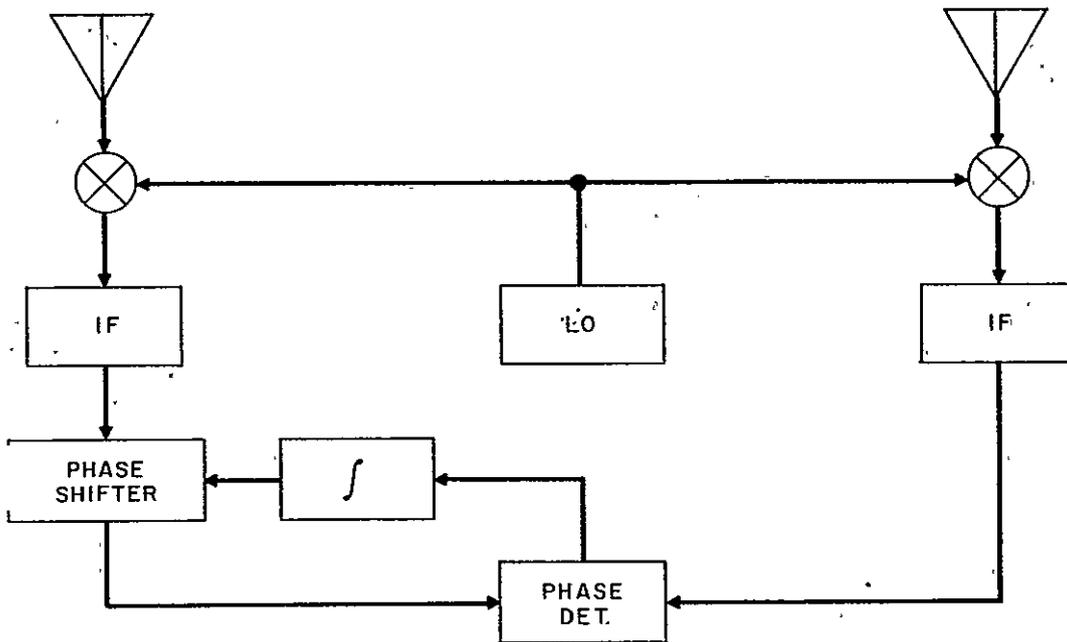
Figure K-4. Error Signal With Finite VSWR

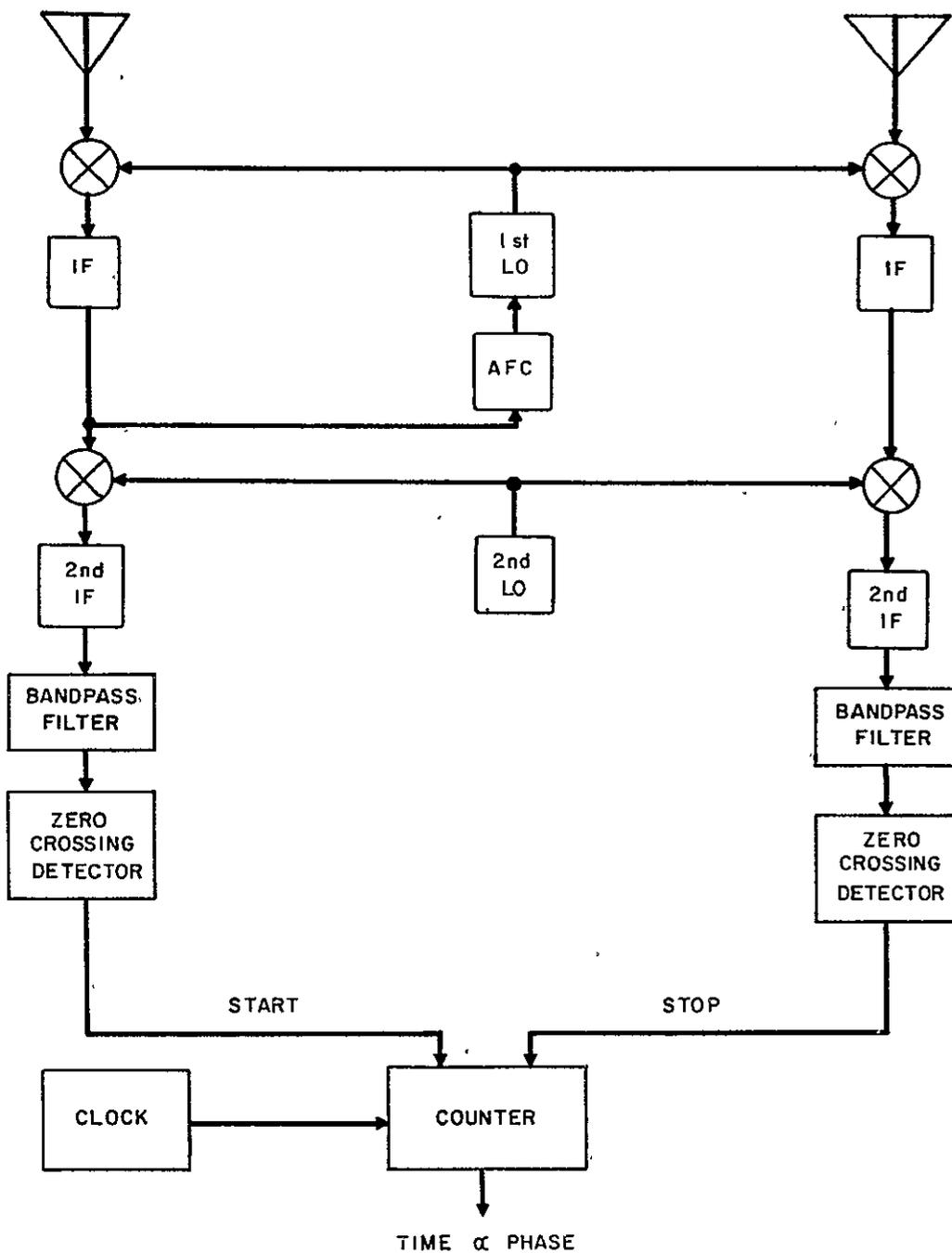Figure K-5. Closed Loop System With IF Phase Comparison

Figure K-6. Digital Phase Detection

Now with a filter $Q = \frac{100 \text{ KC}}{150 \text{ cps}} = 660$ and a permissible phase shift due to mistuning of 5 milliradians (a differential phase shift of 5 mr causes a 0.008 mr space angle error with 100 wavelength antenna separation), the allowable mistuning is

$$K = \frac{\tan 0.005}{2Q} \approx \frac{0.005}{2 \times 660} = 3.8 \times 10^{-6}$$

This is a stringent requirement, but two filters can certainly be expected to track this well between calibrations for a fixed signal frequency. The difficulty is that calibrating frequencies and vehicle frequencies will be alike only within the tolerance of the AFC and 2nd LO. The requirements on AFC and 2nd LO stability can be determined. Due to aging, the resonant frequencies of two crystal filters may drift apart several ppm. Since drifts due to aging are random (unlike temperature drifts), the filters can have differential mistuning of 3 or 4 ppm. If the input frequency changes by 3 or 4 ppm, the differential phase shift through the filters will be the same as that caused by 6 or 8 ppm mistuning of one filter alone. Thus, the 2nd LO stability must be such that it does not drift more than $4 \times 10^{-6} \times 100$ KC = 0.4 cps between calibration and vehicle fix. And the AFC must correct to within 0.4 cps. These are unreasonable requirements for light weight spaceborne equipment. If the filter environment could be controlled and their characteristics periodically measured, the requirements on AFC and 2nd LO would be relaxed. But this approach is not feasible in the satellite.

A variation of the zero crossing phase detection technique results in relaxed requirements on the oscillator and filter stability. Figure K-7 illustrates this modified technique. In this system, the signal frequencies in the two channels are offset by a reference frequency f_r, filtered, and amplified in a common 2nd IF. The two signals are mixed and the reference frequency beat between them is filtered (in a 150 cps filter) and used to trigger a zero crossing detector. At this point the desired phase is the phase between the reference oscillator signal and the beat frequency signal at the output of the mixer.

Filtering prior to 2nd IF summation is necessary for preventing doubling of the noise power in the 150 cps post detection bandwidth. Also, the signal to noise ratio at the mixer must be very high so that S/N performance approaches that of a mixer with a noise free reference.

The phase shift problem through the 150 cps filter is considerably relaxed because there is only one filter rather than two identical filters and the input frequency to the filter depends only upon the reference oscillator frequency. The problem now falls on the pre-summing noise filters. But these are at the relatively low 2nd IF (several megacycles) and their bandwidth can be nearly twice the reference oscillator frequency.

All things considered, a system, of the sort illustrated in figure K-7 has less critical phase shift specifications that than of figure K-6. The former system has been selected for use in the satellite.
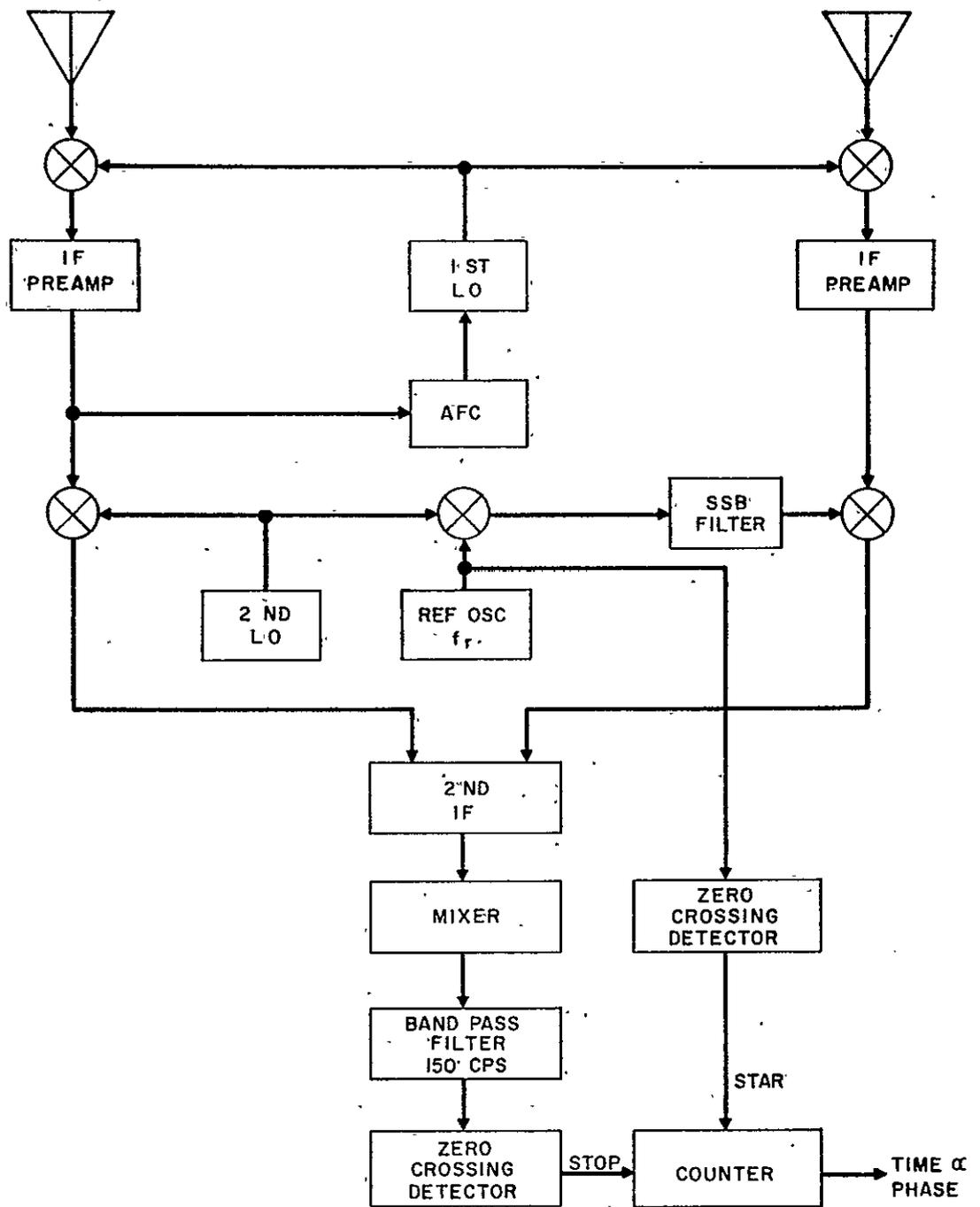
K-8

Figure K-7. Common IF Digital Phase Detection System

APPENDIX L
GRAVITY GRADIENT TORQUE DERIVATION

The principle of the gravity gradient torque expressions are well covered in the literature. But to be as general as possible, the following derivation is performed.

Figure L-1 depicts the dynamic geometry of the satellite in orbit. The figure indicates a cylindrical shape but, the analysis shall be performed to derive the torque expression for the most general shape.

From figure L-1 an expression for the force imparted to the vehicle from an incremental mass attracted by the earth's gravitation can be written. This is:

$$d\bar{F} = \frac{\mu m_e \, dm_s \bar{r}}{r^3} \tag{L-1}$$

where μ is the gravitational constant, m_e is the mass of the earth, dm_s is the incremental mass of the satellite, and r is the distance from the center of the earth to the mass center of the satellite. The vector relation

$$\bar{r} = \bar{a} - \bar{p} \tag{L-2}$$

can be obtained from the same figure. The vector $\bar{a}$ is referenced from the earth coordinates while the vector $\bar{p}$ is referenced to the satellite coordinate system. Thus, it is required to find the coordinate transformation between the two coordinate systems. To accomplish this as simply as possible, it is assumed that the order of rotation of the satellite shall be yaw, pitch, and then roll. Doing this, it is possible to write the transformation matrix, from figure L-2, as

$$\begin{vmatrix} i_1 \\ j_1 \\ k_1 \end{vmatrix} = \begin{vmatrix} \cos\psi\cos\theta & -(\sin\psi\cos\phi + \cos\psi\sin\theta\sin\phi) & (\sin\psi\cos\phi - \cos\psi\sin\theta\cos\phi) \\ \sin\psi\cos\theta & (\cos\psi\cos\phi - \sin\psi\sin\theta\sin\phi) & -(\cos\psi\sin\phi + \sin\psi\sin\theta\cos\phi) \\ \sin\theta & \cos\theta\sin\phi & \cos\theta\cos\phi \end{vmatrix} \begin{vmatrix} i \\ j \\ k \end{vmatrix} \tag{L-3}$$

From this is obtained:

$$\bar{a} = ak_1 = ai\sin\theta + aj\cos\theta\sin\phi + ak\cos\theta\cos\phi \tag{L-4}$$

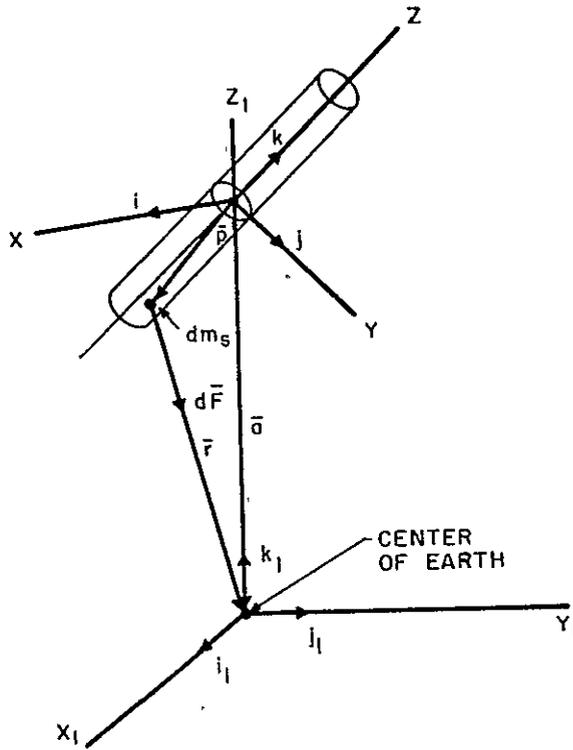$$\bar{p} = i\,x + j\,y + k\,z. \tag{L-5}$$

Figure L-1. Dynamic Geometry of the Satellite While In Orbit

Therefore:

$$\overline{r} = i\ (a\ \sin\theta - x) + j\ (a\ \cos\theta\ \sin\phi - y) + k\ (a\ \cos\theta\ \cos\phi - z). \tag{L-6}$$

The expression for the incremental torque is

$$d\ \overline{L} = \overline{p}\ X\ d\ \overline{F} \tag{L-7}$$

Inserting the expressions (L-1),(L-5), and (L-6) and taking their cross product, results in

$$d\overline{L} = \frac{\mu m_e\ dm_s}{r^3}\ \Big[\ i\ (ya\ \cos\theta\ \cos\phi - z\ a\ \cos\theta\ \sin\theta) + j\ (za\ \sin\theta - x\ a\ \cos\theta\ \cos\phi)$$
$$+ k\ (xa\ \cos\theta\ \sin\phi - ya\ \sin\theta)\ \Big] \tag{L-8}$$

The r^3 term in equation (L-8) can be derived by taking the square of equation (L-2)

$$r^2 = (\overline{a} - \overline{p})\cdot(\overline{a} - \overline{p}) = a^2 + p^2 - 2\ \overline{p}\cdot\overline{a} \tag{L-9}$$

and then taking the dot product of equations (L-4) and (L-5) as

$$\overline{p}\cdot\overline{a} = ax\ \sin\theta + ay\ \cos\theta\ \sin\phi + az\ \cos\theta\ \cos\phi, \tag{L-10}$$

and

$$r^2 = a^2 + p^2 = 2a\ (x\ \sin\theta + y\ \cos\theta\ \sin\phi + z\ \cos\theta\ \cos\phi) \tag{L-11}$$
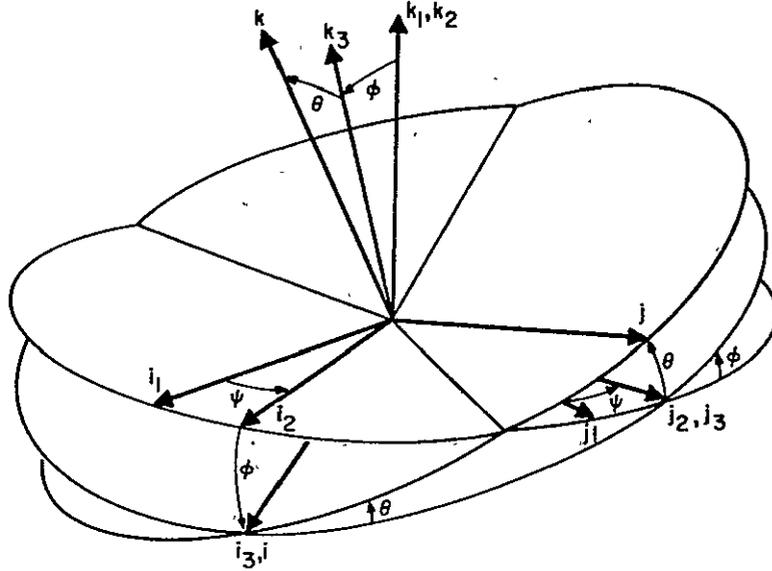
L-2

Figure L-2. Transformation Matrix Diagram

Taking the -3/2 power of equation (L-11) obtains

$$r^{-3} = \left[a^2 + p^2 - 2a \ (x \sin \theta + y \cos \theta \sin \phi + z \cos \theta \cos \phi) \right]^{-3/2} \tag{L-12}$$

$$= \frac{1}{a^3} \left[1 + \frac{p^2}{a^2} - \frac{2}{a} \ (x \sin \theta + y \cos \theta \sin \phi + z \cos \theta \cos \phi) \right]^{-3/2} \tag{L-13}$$

However, due to the very small value of p with respect to a,

$$1 \gg \frac{p^2}{a^2} \tag{L-14}$$

this term can be neglected in equation (L-13) and then using the binomial theorem to expand and accepting only the linear terms the following result is obtained

$$\frac{1}{r^3} = \frac{1}{a^3} \left[1 + \frac{3}{a} \ (x \sin \theta + y \cos \theta \sin \phi + z \cos \theta \cos \phi) \right] \tag{L-15}$$

Substituting this into equation (L-8)

$$dL = \frac{\mu m_e \, dm_s}{a^3} \cdot \left[1 + \frac{3}{a} \ (x \sin \theta + y \cos \theta \sin \phi + z \cos \theta \cos \phi) \right]$$

$$+ \left[i \ (ya \cos \theta \cos \phi - z a \cos \theta \sin \phi) + j \ (za \sin \theta - x a \cos \theta \cos \phi) \right. \tag{L-16}$$

$$\left. + k \ (xa \cos \theta \sin \phi - ya \sin \theta) \right]$$

$$= i \, dL_x + j \, dL_y + K \, dL_z$$

Solving for dL_x, dL_y and dL_z,

$$dL_x = \frac{\mu\, m_e}{a^3} \left[(ya \cos\theta \cos\phi - za \cos\theta \sin\phi) \right.$$
$$+ 3 (y \cos\theta \cos\phi - z \cos\theta \sin\phi)(x \sin\theta + y \cos\theta \sin\phi \qquad \text{(L-17)}$$
$$\left. + z \cos\theta \cos\phi \right] dm_s$$

or integrating,

$$L_x = \frac{\mu\, m_e}{a^2} \int (y \cos\theta \cos\phi - z \cos\theta \sin\phi)\, dm_s \qquad \text{(L-18)}$$

$$+ \frac{3\mu\, m_e}{a^3} \int (y \cos\theta \cos\phi - z \cos\theta \sin\phi)(x \sin\theta + y \cos\theta \sin\phi + z \cos\theta \cos\phi)\, dm_s,$$

$$dL_y = \frac{\mu\, m_e}{a^3} \left[a(z \sin\theta - x \cos\theta \cos\phi) + 3(z \sin\theta - x \cos\theta \cos\phi)(x \sin\theta \right.$$
$$\left. + y \cos\theta \sin\phi + z \cos\theta \cos\phi) \right] dm_s \qquad \text{(L-19)}$$

or

$$L_y = \frac{\mu\, m_e}{a^2} \int (z \sin\theta - x \cos\theta \cos\phi)\, dm_s \qquad \text{(L-20)}$$

$$+ \frac{3\mu\, m_e}{a^3} \int (z \sin\theta - x \cos\theta \cos\phi)(x \sin\theta + y \cos\theta \sin\phi + z \cos\theta \cos\phi)\, dm_s$$

and

$$dL_z = \frac{\mu\, m_e}{a^3} \left[a(x \cos\theta \sin\phi - y \sin\theta) + 3(x \cos\theta \sin\phi - y \sin\theta)(x \sin\theta + y \cos\theta \sin \right.$$
$$\left. + z \cos\theta \cos\phi) \right] dm_s \qquad \text{(L-21)}$$

or

$$L_z = \frac{\mu\, m_e}{a^2} \cdot \int (x \cos\theta \sin\phi - y \sin\theta)\, dm_s \qquad \text{(L-22)}$$

$$+ \frac{3\mu\, m_e}{a^3} \int x(\cos\theta \sin\phi - y \sin\theta)(x \sin\theta + y \cos\theta \sin\phi + z \cos\theta \cos\phi)\, dm_s$$

However, because x, y, and z are measured from the center of mass, the first integral terms on the left side of equations (L-18), (L-20), and (L-22) go to zero. Collecting the remaining terms

$$L_x = \frac{3\mu m_e}{a^3} \left[\int y\, x \cos\theta \cos\phi \sin\theta\, dm_s - \int z\, x \cos\theta \sin\phi \cos\phi\, dm_s \right.$$
$$+ \int y^2 \cos^2\theta \sin\phi \cos\phi\, dm_s + \int yz\, (\cos^2\phi - \sin^2\phi) \cos^2\phi\, dm_s$$
$$\left. - \int z^2 \cos^2\theta \sin\phi \cos\phi\, dm_s \right] \tag{L-23}$$

$$L_x = \frac{3\mu m_e}{a^3} \left[\frac{1}{2} \cos\phi \sin 2\theta \int xy\, dm_s - \frac{1}{2} \sin\phi \sin 2\theta \int xz\, dm_s \right.$$
$$\left. + \cos^2\phi \cos 2\theta \int yz\, dm_s + \frac{1}{2} \cos^2\theta \sin 2\phi \int (y^2 - z^2)\, dm_s \right] \tag{L-24}$$

but:

$$\int (y^2 - z^2)\, dm_s = \int (y^2 + x^2)\, dm_s - \int (z^2 + x^2)\, dm_s = I_{zz} - I_{yy}, \tag{L-25}$$

$$\int xy\, dm_s = I_{xy} \tag{L-26}$$

$$\int xz\, dm_s = I_{xz} \tag{L-27}$$

$$\int yz\, dm_s = I_{yz} \tag{L-28}$$

Therefore

$$L_x = \frac{3\mu m_e}{2a^3} \left[I_{xy} \cos\phi \sin 2\theta - I_{xz} \sin\phi \sin 2\theta \right.$$
$$\left. + 2 I_{yz} \cos^2\phi \cos 2\theta + (I_{zz} - I_{yy}) \cos^2\theta \sin 2\phi \right] \tag{L-29}$$

Similarly for L_y and L_z,

$$L_y = \frac{3\mu m_e}{2a^3} \left[2 I_{xy} (\sin^2\theta - \cos^2\theta \cos^2\phi) \right.$$
$$\left. + I_{yz} \sin\phi \sin 2\theta + (I_{xx} - I_{zz}) \cos\phi \sin 2\theta - I_{xy} \cos\theta \sin 2\phi \right] \tag{L-30}$$

$$L_z = \frac{3 \mu m_e}{2a^3} \left[2 I_{xy} (\cos^2 \theta \sin^2 \phi - \sin^2 \theta) + I_{xz} \cos^2 \theta \sin 2 \phi \right.$$

$$\left. - I_{yz} \cos \phi \sin 2 \theta + (I_{yy} - I_{xx}) \sin \phi \sin 2 \theta \right] \qquad \text{(L-31)}$$

Equations (L-29), (L-30, and (L-31) are the general expressions for the torque applied to a satellite due to the gravity gradient. The only restriction to these equations is that the center of mass remains fixed with respect to the center of the satellite coordinate system. Now if some additional assumptions are made further simplification of equations L-29, L-30, and L-31 results.

For the first assumption, fix the satellite in a circular orbit. Then applying the classical expression

$$\omega_o^2 = \frac{g'}{a} \qquad \text{(L-32)}$$

where g' is the gravitational acceleration at the altitude of the orbit, ω_o is the orbital rate, and a is the radius of the orbit from the center of the earth. The term g' can be written as

$$g' = g_o \left(\frac{R_e}{a} \right)^2 \qquad \text{(L-33)}$$

where g_o is the gravitational constant at the surface of the earth and R_e is the radius of the earth. However,

$$\mu m_e = g_o R_e^2 \qquad \text{(L-34)}$$

Therefore,

$$\omega_o^2 = \frac{\mu m_e}{a^3} \qquad \text{(L-35)}$$

Now assume that the cross products of inertia are zero and that I_{xx} is equal to I_{yy}. Then we can rewrite equations L-29, L-30 and L-31

$$L_x = \frac{3}{2} \omega_o^2 (I_{zz} - I_{yy}) \cos^2 \theta \sin 2 \phi \qquad \text{(L-36)}$$

$$L_y = \frac{3}{2} \omega_o^2 (I_{xx} - I_{zz}) \cos \phi \sin 2 \theta \qquad \text{(L-37)}$$

$$L_z = 0 \qquad \text{(L-38)}$$

These are the equations that are normally contained in the literature for the gravity gradient of a bisymmetrical satellite.

If the satellite coordinates are assigned to enable the cross products of inertia to go to zero and if the orbit is circular, the following is obtained from L-29, L-30 and L-31.

$$L_x = \frac{3}{2} \omega_o^2 (I_{zz} - I_{yy}) \cos^2 \theta \sin 2 \phi$$

$$L_y = \frac{3}{2} \omega_o^2 (I_{xx} - I_{zz}) \cos \phi \sin 2 \theta$$

$$L_z = \frac{3}{2} \omega_o^2 (I_{yy} - I_{xx}) \sin \phi \sin 2 \theta$$

Thus, if the satellite has different principle moments of inertia, it would orient itself to the direction of the orbital velocity vector and the vertical. However, the torque about the vertical axis (L_z) is dependent on the cross coupling expression $\sin \phi \sin 2 \theta$, which indicates that both angles have a value other than zero to realize any torque. This principle is employed in the NASA Ames Research Center configuration. The other configurations considered during the course of this study are the Johns Hopkins Applied Physic Laboratory and the Bell System Laboratory configurations, both of which are bisymmetrical $(I_{xx} = I_{yy})$.

APPENDIX M

PRECISION VELOCITY INJECTION ANALYSIS

This appendix presents the analysis that were performed to determine the desirable nominal parameters for the initial catch-up orbit and to evaluate the residual errors in orb parameters after a number of vernier corrections have been made. The approach was to perform the analysis by utilizing equations describing first or second order perturbations from the desired final circular orbit.

The specific factors investigated were:

    a. The effects of error sources.

    b. The choice of nominal catch-up orbit in consideration of launch opportunity duty factor, and maximum and minimum waiting times in orbit.

    c. The choice of biases for the vernier thrust corrections either to minimize the errors or to reduce the probability of requiring thrust reversal from one correction to the next.

    d. The evaluation of residual errors.

Two approaches are possible in making the precision velocity injection corrections. The first approach is to attempt the correction of the entire measured error on each trial. This approach minimizes the number of attempts for the desired accuracy. The second method is to bias each velocity impulse correction in such a way that the error in that correction will not give a total orbital velocity greater than desired. In this way, the velocity corrections are never subtractive and the total velocity impulse required is minimized. Also, it is unnecessary to provide for reverse thrust either by multiple thrusters or by thruster reorientation. Both of these approaches are analyzed in the following paragraphs.

M.1. BASIC NOMENCLATURE AND EQUATIONS

    e = orbit eccentricity

    r = orbit radius

    a = orbit semi-major axis

    v = orbit speed

    θ = velocity elevation angle

    η = angle of satellite about orbit focus

    $\omega = \dfrac{d\eta}{dt}$

    $(x)_o$ = desired value

    $(x)_i$ = initial value

    $(x)_n$ = value after nth correction

    $\Delta(x) = (x) - (x)_o$ incremental deviation

$(x)_a$ = value at apogee

For the desired orbit:

$a_o = r_o$

$v = v_o$

$e_o = 0$

$\omega = \omega_o = v_o / r_o$

For any particular orbit, the following approximation equations hold:

$$e^2 \approx \left(2\frac{\Delta v}{v_o} + \frac{\Delta r}{r_o}\right)^2 + \theta^2 \qquad = \text{constant}$$

$$\frac{\Delta a}{r_o} \approx 2\left(\frac{\Delta v}{v_o} + \frac{\Delta r}{r_o}\right) \qquad = \text{constant}$$

$$\frac{\Delta \omega}{\omega_o} \approx -\frac{3}{2}\frac{\Delta a}{r_o}$$

M.2 CATCH-UP ORBIT

If $\Delta\eta$ is the angular difference between the injection apogee and the desired orbit position, the number of orbits (n) required for catch-up is approximately

$$\frac{\Delta\omega_i}{\omega_o} \approx \frac{\Delta\eta}{2\pi n}$$

Because of the injection errors, $\Delta\omega_i$ will be a random variable. Therefore, the length of time for catch-up $(t \approx \frac{2\pi n}{\Delta\eta\omega_o}$) will vary from its predicted value. It is desirable to allow at least 2 orbits for catch-up. The first orbit for tracking and the second for position correction. It is also desirable to keep the maximum waiting time fairly low. If gaussian distributions of the injection errors are assumed, the maximum and minimum variations may be assumed to result from the respective 3σ injection deviations.

$$\overline{\frac{\Delta\omega_i}{\omega_o}} + \frac{3\sigma_{\omega_i}}{\omega_o} = \frac{\Delta\eta_{min}}{2\pi n_{min}}, \quad \sigma_i = \sigma\left(\frac{v_i}{v_o} + \frac{r_i}{r_o}\right)$$

$$\overline{\frac{\Delta\omega_i}{\omega_o}} - \frac{3\sigma_{\omega_i}}{\omega_o} = \frac{\Delta\eta_{max}}{2\pi n_{min}}$$

where

$$\overline{\frac{\Delta\omega_i}{\omega_o}} = -3\overline{\frac{\Delta v_i}{v_o}} \qquad \frac{\sigma_{\omega_i}}{\omega_o} = 3\sigma_i$$

If the preceeding equations are solved for $\overline{\Delta\omega_i}/\omega_o$, the following equation is obtained:

$$\overline{\frac{\Delta\omega_i}{\omega_o}} = \frac{\dfrac{\Delta\eta_{max} - \Delta\eta_{min}}{2\pi} + 3\left(n_{max} + n_{min}\right)\dfrac{\sigma_{\omega_i}}{\omega_o}}{n_{max} - n_{min}}$$

The quantity $\left(\dfrac{\Delta\eta\max - \Delta\eta\min}{2\pi}\right)$ is the angular interval over which the desired orbit position may be at satellite injection without requiring waiting times less than n_{min} orbital periods or greater than n_{max} periods. Therefore, this represents the duty factor or relative utility of each launch opportunity when the orbital plane is in proper phase with the launch site. For the proposed orbital altitude, the satellite position changes by nearly $90°$ in every 2 launch opportunities (24-hours). Since there will be 4 satellites in each orbit, only a very small duty factor will be required for initial placement in the orbit provided a launch can be made every opportunity (i.e., once every 12 hours for alternating orbits; or once every 24 hours for sequential orbits). This schedule is probably too rapid for convenience. Also, in the replacement problem, it will usually be undesirable to wait a long time for the selected satellite position to reach a place that is easily attained. Since this position does traverse approximately $360°$ in four $90°$ steps (each step taking 24 hours), a duty factor of 0.25 appears to provide rapid replacement without excessive catch-up rates (a maximum wait of 2 days on the ground).

Using this duty factor value, and requiring n_{min} to be 2, the bias catch up rate is given by

$$\overline{\frac{\Delta\omega_i}{\omega_o}} \approx \frac{0.25 + (n_{max} + 2)\, \frac{3\sigma\omega_i}{\omega_o}}{n_{max} - 2}$$

From this equation, the maximum velocity decrement, that shall be made up by the (biased) vernier thrust system, can be specified in terms of the maximum number of catch-up orbits and the injection errors. For the correct period,

$$\left(\frac{\Delta v_a}{v_o} + \frac{\Delta r_a}{r_o}\right)_o \longrightarrow 0$$

It will be shown that $\dfrac{\Delta r_a}{r_o} \approx \dfrac{\Delta r_i}{r_o}$ if the injection angular error is fairly small.

Therefore,

$$\Delta\left(\frac{\Delta v}{v_o}\right) = \left(\frac{\Delta v_a}{v_o}\right)_o - \frac{\Delta v_i}{v_o} \approx -\left(\frac{\Delta r_i}{r_o} + \frac{\Delta v_i}{v_o}\right)$$

$$\left|\Delta\left(\frac{\Delta v}{v_o}\right)\right|_{max} \approx \left|\overline{\frac{\Delta v_i}{v_o}}\right| + 3\sigma_i = \frac{1}{12(n_{max} - 2)} + \frac{6n_{max}}{n_{max} - 2}\,\sigma_i$$

The average velocity decrement below circular velocity at injection into the transfer orbit is

$$\overline{\frac{\Delta v_i}{v_o}} = -\overline{\frac{\Delta\omega_i}{3\omega_o}} = -\left[\frac{1}{12(n_{max} - 2)} + 3\left(\frac{n_{max} + 2}{n_{max} - 2}\right)\sigma_i\right]$$

M.3 CORRECTION OF CATCH-UP RATE

Because the catch-up rate shall be biased to ensure suitable properties for the waiting time and direction of travel, the angular steps between apogee positions are likely to

result in greater quanta than desired for the final satellite position accuracy. If it were not desired to make the period corrections at apogee in order to minimize the eccentricity, there would be no problem and the period corrections could be made whenever the desired angular position were reached. Since both corrections are desired, it is proposed that a position correction be made on the last orbit preceding catch-up.

To a good approximation, the angular increment $\Delta\eta_f$ remaining on the last catch-up orbit is likely to be equal to any value between 0 and the quantum apogee position step. That is

$$\frac{\Delta\eta_f}{2\pi} \approx a \frac{\Delta\omega_i}{\omega_o} \qquad 0 \leq a \leq 1$$

where a is uniformly distributed between 0 and 1.

Then a nominal velocity increment, should be used to bring

$$\frac{\Delta\omega_1}{\omega_o} = -3\frac{\Delta v_1}{v_o} - 3\frac{\Delta r_a}{r_o} = a\frac{\Delta\omega_i}{\omega_o} = -3a\left(\frac{\Delta v_i}{v_o} + \frac{\Delta r_i}{r_o}\right)$$

Now it can be shown, from the basic equations given in paragraph M.1, that

$$\frac{\Delta r_a}{r_o} \approx 2\left(\frac{\Delta r_i}{r_o} + \frac{\Delta v_i}{v_o}\right) + \sqrt{\left(2\frac{\Delta v_i}{v_o} + \frac{\Delta r_i}{r_o}\right)^2 + \theta_i^2}$$

Since Δv_i is biased large and negative, the θ_i^2 term under the root sign will be negligible, and

$$\frac{\Delta r_a}{r_o} \approx 2\frac{\Delta r_i}{r_o} + 2\frac{\Delta v_i}{v_o} + \left(-\frac{2\Delta v_i}{v_o} - \frac{\Delta r_i}{r_o}\right)$$

$$\frac{\Delta r_a}{r_o} \approx \frac{\Delta r_i}{r_o}$$

Then, to a good approximation,

$$\frac{\Delta v_i}{v_o} = a\frac{\Delta v_i}{v_o} + (a-1)\frac{\Delta r_i}{r_o}$$

$$\Delta\left(\frac{\Delta v_i}{v_o}\right) = \frac{\Delta v_1 - \Delta v_i}{v_o} = -(1-a)\left(\frac{\Delta v_i}{v_o} + \frac{\Delta r_i}{r_o}\right)$$

However, there will be a statistical error in this velocity increment, and it may be desired to insert a bias error. The statistical error will be assumed gaussian with zero mean and σ proportional by the factor f to the velocity increment. The desired bias, as yet undetermined, will be assumed to be in a direction to decrease the magnitude of $\Delta(\Delta v)$

$$\Delta\left(\frac{\Delta v_i}{v_o}\right) = -(1-a)(1-b_1 f)(1+f\epsilon_1)\left(\frac{\Delta v_i}{v_o} + \frac{\Delta r_i}{r_o}\right)$$

$$\frac{\Delta v_1}{v_o} = \frac{\Delta v_i}{v_o} - (1-a)(1-b_1 f)(1+f\epsilon_1)\left(\frac{\Delta v_i}{v_o} + \frac{\Delta r_i}{r_o}\right)$$

$$\overline{\epsilon_1} = 0, \quad \overline{\epsilon_1^2} = 1$$

The resulting position error at the next apogee will be

$$\frac{\Delta\eta_1}{2\pi} = -3\frac{\epsilon_{v_1}}{v_o} = -3(1-a)(b_1 f - f\epsilon_1 + b_1 f^2 \epsilon_1)\left(\frac{\Delta v_i}{v_o} + \frac{\Delta r_i}{r_o}\right)$$

In this equation, a positive $\Delta\eta_1$ indicates that the satellite has overshot the desired position.

M-4

It will be assumed that the satellite has been tracked on this new orbit and is prepared to make a period correction on the first apogee opportunity (after one orbit). It would be desir-able to know in advance if more than one orbit were required before this correction were made With this knowledge, the position correction would bring the satellite to the proper point at the time it was possible to perform the period correction. If more than one orbit were allowed to elapse, the position error would, in general be larger. But, these cases are not analyzed at this time.

The satellite apogee velocity is still given by $(\Delta v_1/v_o)$. In order to achieve the desired period, the nominal apogee velocity should be

$$\left(\frac{\Delta v_a}{v_o}\right)_o = -\frac{\Delta r_a}{r_o} \approx -\frac{\Delta r_i}{r_o}$$

Since the period accuracy must be very good to ensure low drift, at least two period corrections shall be made. On any correction, a bias can be used to minimize the possibility of reverse thrust being required on the next correction. This bias would typically be set equal to the 3 σ error for the particular correction. On the last correction, a bias is not used because the probable overshoot error is less serious than the expected bias error.

For the first period correction,

$$\frac{\Delta v_2}{v_o} = \frac{\Delta v_1}{v_o} + \left(-\frac{\Delta r_i}{r_o} - \frac{\Delta v_1}{v_o}\right)(1 + f\epsilon_2)(1 - b_2 f)$$

$$\frac{\Delta v_2}{v_o} = -\frac{\Delta r_i}{r_o} + \left(b_2 f - f\epsilon_2 + b_2 f^2 \epsilon_2\right)\left[1 - (1-\alpha)(1-b_1 f)(1 + f\epsilon_1)\right]\left(\frac{\Delta v_i}{v_o} + \frac{\Delta r_i}{r_o}\right)$$

The velocity error in this correction will cause a further position error $\Delta\eta_2$ to be added to $\Delta\eta_1$ after one orbit

$$\frac{\Delta\eta_2}{2\pi} = -\frac{3\epsilon_{v_3}}{v_o} = -3\left(b_2 f - f\epsilon_2 + b_2 f^2 \epsilon_2\right)\left[1 - (1-\alpha)\left(1 - b_1 f\right)\left(1 + f\epsilon_1\right)\right]\left(\frac{\Delta v_i}{v_o} + \frac{\Delta r_i}{r_o}\right)$$

If it is assumed that only two period corrections will be necessary, the second correction will be made without bias yielding

$$\frac{\Delta v_3}{v_o} = \frac{\Delta v_2}{v_o} + \left(-\frac{\Delta r_i}{r_o} - \frac{\Delta v_2}{v_o}\right)(1 + f\epsilon_3)$$

$$\frac{\Delta v_3}{v_o} = -\frac{\Delta r_i}{r_o} - f\epsilon_3\left(b_2 f - f\epsilon_2 + b_2 f^2 \epsilon_2\right)\left[1 - (1-\alpha)(1-b_1 f)(1 + f\epsilon_1)\right]\left(\frac{\Delta v_i}{v_o} + \frac{\Delta r_i}{r_o}\right)$$

The final velocity error is

$$\frac{\epsilon_{v_3}}{v_o} = -f^2 \epsilon_3\left(b_2 - \epsilon_2 + b_2 f \epsilon_2\right)\left[1 - (1-\alpha)(1 - b_1 f)(1 + f\epsilon_1)\right]\left(\frac{\Delta v_i}{v_o} + \frac{\Delta r_i}{r_o}\right)$$

The final rate error is

$$\frac{\Delta\omega_2}{\omega_o} = -\frac{\epsilon_{v_2}}{v_o}$$

The ellipticity is

$$e \approx \left|\frac{\Delta r_i}{r_o}\right|$$

The position error is

$$\frac{\epsilon\eta}{2\pi} = (\Delta\eta_1 + \Delta\eta_2)/2\pi$$

$$\frac{\epsilon\eta}{2\pi} = -3\left[\alpha f(b_2 - \epsilon_2 + b_2 f \epsilon_2) + (1-\alpha)f(1 + b_2 f - f\epsilon_2 + b_2 f^2 \epsilon_2)(b_1 - \epsilon_1 + b_1 f\epsilon_1)\right]$$
$$\cdot\left(\frac{\Delta v_i}{v_o} + \frac{\Delta r_i}{r_o}\right)$$

If it is assumed that three period corrections are made, the resulting errors can easily be inferred from the preceding equations to be as follows:

$$\frac{\epsilon v_4}{v_o} = -f^3 \epsilon_4 \left(b_3 - \epsilon_3 + b_3 f\epsilon_3\right)\left(b_2 - \epsilon_2 + b_2 f\epsilon_2\right)\cdot\left[1 - (1-\alpha)(1-b_1 f)(1 + f\epsilon_1)\right]$$
$$\left(\frac{\Delta v_i}{v_o} + \frac{\Delta r_i}{r_o}\right)$$

$$\frac{\epsilon\eta}{2\pi} = -3\left(\frac{\Delta v_i}{v_o} + \frac{\Delta r_i}{r_o}\right)\left\{(1-\alpha)B_1\left[1 + B_2(1 + B_3)\right] + \alpha B_2(1 + B_3)\right\}$$

where

$$B_n = b_n f - f\epsilon_n + b_n f^2 \epsilon_n$$

Notice that the velocity error is significantly reduced but the position error is only slightly increased by using the additional velocity correction.

M.4 CHOICE OF BIAS LEVELS

Notice that as far as the accuracy of the corrections is concerned, it is desirable to make all the vernier bias errors zero (including b_1). The penalty has been stated to be an increase in the fuel required and the necessity for thrust reversal. The equations for the errors in a zero-bias system are as follows

(Notice that $\overline{\alpha} = \overline{1-\alpha} = \frac{1}{2}$, $\overline{\alpha^2} = \overline{(1-\alpha)^2} = \frac{1}{3}$)

Zero Biases - n Corrections

Velocity.
$$\begin{cases} \dfrac{\epsilon v_n}{v_o} = -f^{n-1}\epsilon_n \cdots \epsilon_2 \left[\alpha - (1-\alpha)f\epsilon_1\right]\left(\dfrac{\Delta v_i}{v_o} + \dfrac{\Delta r_i}{r_o}\right). \\[2em] \dfrac{\overline{\epsilon v_n}}{v_o} = 0 \\[2em] \dfrac{\sigma^2_{v_n}}{v_o^2} = \dfrac{f^{2n-2}}{3}(1 + f^2)\left(\dfrac{\overline{\Delta v_i}^2}{v_o^2} + \sigma^2_i\right) \end{cases}$$

$$\text{Eccentricity} \quad \begin{cases} e \approx \left| \dfrac{\Delta r_i}{r_o} \right| \\[3ex] \overline{e} \approx \sqrt{\dfrac{2}{\pi}} \, {}^{\sigma}r_i/r_o \\[3ex] e_{max} \approx 3 {}^{\sigma}r_i/r_o \end{cases}$$

$$\text{position} \atop \text{n=3} \quad \begin{cases} \dfrac{\epsilon_\eta}{2\pi} = 3\left(\dfrac{\Delta v_i}{v_o} + \dfrac{\Delta r_i}{r_o} \right)\left[\alpha f \, \epsilon_2 + (1-\alpha) f \, \epsilon_1 \left(1 - f \, \epsilon_2 \right) \right] \\[3ex] \dfrac{\overline{\epsilon_\eta}}{2\pi} = 0 \\[3ex] \sigma^2_{\dfrac{\eta}{2\pi}} = 3f^2 (2 + f^2)\left[\left(\dfrac{\overline{\Delta v_i}}{v_o} \right)^2 + \sigma^2_i \right] \end{cases}$$

If thrust reversal is not desired, the bias levels should be chosen so that there is an extremely low probability that the desired nominal velocity increment is exceeded. It is assumed in this analysis that this is equivalent to biasing against $3\,\sigma$ error. Hence,

$$b_k f - f \, \epsilon_k + f^2 b_k \, \epsilon_k \geq b_k f (1 + 3f) - 3f \geq 0; \quad b_k f = \frac{3f}{1+3f} \quad , \quad 1 < k < n \; ; \quad b_n = 0$$

For b_1, it is only when $\alpha \sim 0$ that the position correction is sufficiently similar to a typical period correction that this particular bias is the best choice. Referring to the equation for the first period correction (after the position correction), it is observed that if the velocity increment is to be kept positive ($\Delta\Delta v_1 \geq 0$) and since $\left(\dfrac{\Delta v_i}{v_o} + \dfrac{\Delta r_i}{r_o} \right)$ is biased to ensure its being negative, then

$$1 - (1-\alpha)(1-b_1 f)(1+f \, \epsilon_1) \geq 1 - (1-\alpha)(1-b_1 f)(1+3f) \geq 0$$

from which

$$b_1 f \geq \frac{3f}{1+3f} - \frac{\alpha}{(1-\alpha)(1+3f)}$$

However, it is also desirable to keep the average final position error zero. For two period corrections the average position error is

$$\frac{\overline{\epsilon_\eta}}{2\pi} = -3 \left(\frac{\Delta v_i}{v_o} + \frac{\Delta r_i}{r_o} \right) \left[\alpha b_2 f + (1-\alpha)(1+b_2 f) \, b_1 f \right]$$

$$= -3 \left(\frac{\Delta v_i}{v_o} + \frac{\Delta r_i}{r_o} \right) \cdot \left[\frac{3\alpha f}{1+3f} + \frac{(1-\alpha)(1+6f) \, b_1 f}{1+3f} \right]$$

If $\overline{\epsilon_\eta}$ is set equal to zero

$$b_1 f = -\frac{3\alpha f}{(1-\alpha)(1+6f)}$$

This choice does not conflict with the previous requirement imposed on b_1 provided that

$$- \frac{3\alpha f}{(1-\alpha)(1+6f)} \geq \frac{3f}{1+3f} - \frac{\alpha}{(1-\alpha)(1+3f)}$$

or,

$$\alpha \geq \frac{3f(1+6f)}{(1+3f)^2}$$

Then for the case of 2 period corrections, the best choice for b_1 is

$$b_1 f = \left\{ \frac{3f - \left(\frac{\alpha}{1-\alpha}\right)}{1+3f} , \ 0 < \alpha \leq \frac{3f(1+6f)}{(1+3f)^2} \quad b_1 f = - \frac{3\alpha f}{(1-\alpha)(1+6f)} , \ \frac{3f(1+6f)}{(1+3f)^2} < \alpha \leq 1 \right\}$$

For more than 2 period corrections, the optimum choice for b_1 would be slightly different. The following equations for the biased thrust error assume that b_1 is chosen from the above equation. The biased thrust equations are:

$$\frac{\epsilon_{v_n}}{v_o} = - \frac{f^n \epsilon_n (3 - \epsilon_{n-1}) \cdots (3 - \epsilon_1)\left(\frac{\Delta v_i}{v_o} + \frac{\Delta r_i}{r_o} \right)}{(1 + 3f)^n} \qquad \alpha < \frac{3f(1+6f)}{(1+3f)^2}$$

$$\frac{\epsilon_{v_n}}{v_o} = - f^{n-1} \epsilon_n (3-\epsilon_{n-1}) \cdots (3 - \epsilon_2) \left\{ \alpha(1+3f) - f\epsilon_1 \left[(1-\alpha)(1+6f)+3\alpha f \right] \right\} \left(\frac{\Delta v_i}{v_o} + \frac{\Delta r_i}{r_o} \right)$$

$$\alpha > \frac{3f(1+6f)}{(1+3f)^2}$$

$$\frac{\epsilon_\eta}{2\pi} \approx - \frac{3\left(\frac{\Delta v_i}{v_o} + \frac{\Delta r_i}{r_o} \right)}{(1+3f)^2} \left[3f(1+6f) - \alpha(1+3f)^2 - 3f^2 \epsilon_2 - \epsilon_1 f(1+6f) + \epsilon_1 \epsilon_2 f^2 \right]$$

$$\alpha < \frac{3f(1+6f)}{(1+3f)^2}$$

$$\frac{\epsilon_\eta}{2\pi} \approx + \frac{3\left(\frac{\Delta v_i}{v_o} + \frac{\Delta r_i}{r_o} \right) f}{(1+6f)(1+3f)} \cdot \left\{ \left[\epsilon_1 (1+6f)\left[1+6f - \alpha(1+3f) \right] + \alpha \epsilon_2 (1+3f) \right] \right. $$

$$\left. - \epsilon_1 \epsilon_2 f \left[1+6f - \alpha(1+3f) \right] \right\}$$

$$\alpha > \frac{3f(1+6f)}{(1+3f)^2}$$

The analytical evaluations of the mean and standard deviation of these errors are given below. The evaluation of the velocity error is difficult if the statistics of α are considered. Hence, the evaluation was made when the velocity error will be greatest. ($\alpha = 1$)

$$\frac{\overline{\epsilon_{v_n}}}{v_o} = 0 \qquad \sigma^2_{v_n/v_o} \leq \frac{f^{2n-2} 10^{n-2}}{(1+3f)^{2n-2}(1+6f)^2} \left[(1+3f)^2 + 9f^4 \right] \left[\left(\frac{\overline{\Delta v_i}}{v_o} \right)^2 + \sigma^2_i \right]$$

$$(\alpha = 1)$$

M-8

The average position error is zero for $\alpha > 3f(1 + 6f) \Big/ (1 + 3f)^2$ and is finite for a smaller α. Averaged over all possible injections, the position error is

$$\frac{\overline{\epsilon_\eta}}{2\pi} \approx - \frac{27}{2} \left(\frac{\overline{\Delta v_i}}{v_o} \right) \frac{f^2 (1 + 6f)^2 (1 - 6f - 9f^2)}{(1 + 3f)^4}$$

Again, the statistics of α make the evaluation of the standard deviation of the position error difficult. However, a bound may be conveniently found by making a single evaluation for $\alpha = 0^+$. This is the condition that requires the greatest thrust impulse to correct the position, and is most subject to error.

$$\frac{\overline{\epsilon_\eta}}{2\pi} \Bigg|_{\alpha = 0} = - 9 \left(\frac{\overline{\Delta v_i}}{v_o} \right) \frac{f (1 + 6f)}{(1 + 3f)^2}$$

$$\overline{\left(\frac{\epsilon_\eta}{2\pi} \right)^2} = 9 \left[\left(\frac{\overline{\Delta v_i}}{v_o} \right)^2 + \sigma_i^2 \right] \frac{f^2 (11 + 120f + 369f^2)}{(1 + 3f)^4}$$

$$\frac{\sigma_\eta^2}{2\pi} < \left[\overline{\left(\frac{\epsilon_\eta}{2\pi} \right)^2} - \left(\frac{\overline{\epsilon_\eta}}{2\pi} \right)^2 \right]_{\alpha = 0}$$

The eccentricity error is the same as for the unbiased thrust case.

M.5 EVALUATION OF SYSTEM ERRORS

The major contributions to the errors in orbit parameters are:

a. Error in velocity at the perigee of the transfer ellipse, σ_{v_p}. A typical value for this error is

$$\frac{\sigma_{v_p}}{v_p} = 1.43 \times 10^{-3} \qquad \text{(typical)}$$

b. Error in altitude or radius at the perigee of the transfer ellipse, δr_p

$$\frac{\sigma_{r_p}}{r_p} = 1.9 \times 10^{-4} \qquad \text{(typical)}$$

c. Error in the 4th stage apogee kick $\delta (v_a - v)$

$$f_a = \frac{\sigma_{\Delta v_a}}{\Delta v_a} = 5 \times 10^{-3} \qquad \text{(typical)}$$

d. Error in the vernier thrust velocity increment

$$f = \frac{\sigma_{\Delta v_n}}{\Delta v_n} = 1.67 \times 10^{-2} \qquad \text{(typical)}$$

The effects of various thrust misalignment errors have been evaluated and found to be negligible compared to the above errors.

From the data represented by (a), (b), (c), it is necessary to determine the quantities $\sigma_{\Delta r_i}/r_o$ and σ_i and from these to determine $\overline{v_i}/v$.

From the equations for the transfer ellipse,

$$V_p r_p = v_a r_a$$

$$a = \frac{r_a + r_p}{2} = \frac{K}{\frac{2K}{r} - v^2}$$

the following errors result at the apogee of the transfer ellipse before the application of the apogee kick

$$\frac{\delta r_a}{r_a} = \frac{\delta r_i}{r_o} = \left(2 + \frac{r_o}{r_p}\right)\frac{\delta r_p}{r_p} + 2\left(1 + \frac{r_o}{r_p}\right)\frac{\delta v_p}{v_p}$$

$$\frac{\delta r_i}{r_o} + \frac{\delta v_i}{v_o} = \left[\left(2 + \frac{r_o}{r_p}\right) - \sqrt{\frac{2}{1 + \frac{r_o}{r_p}}}\left(1 + \frac{r_o}{r_p}\right)\right]\frac{\delta r_p}{r_p} + \left[2\left(1 + \frac{r_o}{r_p}\right) - \sqrt{\frac{2}{1 + \frac{r_o}{r_p}}}\left(1 + \frac{2r_o}{r_p}\right)\right]\frac{\delta v_p}{v_p}$$

The additional error added to the initial velocity v_i is given by

$$\frac{\delta v_i}{v_o} = \left(\frac{\overline{\Delta v_i}}{v_o} + 1 - \sqrt{\frac{2}{1 + \frac{r_o}{r_p}}}\right) f_a \epsilon_a \; ; \quad \overline{\epsilon}_a = 0, \; \overline{\epsilon_a^2} = 1$$

Letting $r_p = 3555$ and $r_o = 9440$, the following numerical evaluations can be made

$$\frac{\delta r_i}{r_o} = 4.66\frac{\delta r_p}{r_p} + 7.32\frac{\delta v_p}{v_p}$$

$$\frac{\sigma_{r_i}}{r_o} = 1.05 \times 10^{-2}$$

$$\frac{\delta v_i}{v_o} + \frac{\delta r_i}{r_o} = 1.96\frac{\delta r_p}{r_p} + 2.64\frac{\delta v_p}{v_p} + \left(0.26 + \frac{\overline{\Delta v_i}}{v_o}\right) f_a \epsilon_a$$

$$\sigma_i^2 = 14.35 \times 10^{-6} + \left(0.26 + \frac{\overline{\Delta v_i}}{v_o}\right)^2 .25 \times 10^{-6}$$

The quantity $\overline{\Delta v_i}/v_0$ will be small compared to 0.26, and negative, so the greatest value for

σ_i

is

$$\sigma_i < 4 \times 10^{-3}$$

Using this value, the catch-up time in orbit was evaluated as a function of the bias $(\overline{\Delta v_i})$ and the maximum vernier (Δv) as previously derived in this appendix. The results are plotted in figure M-1 and show both the maximum vernier (Δv) and the average apogee kick (Δv) as functions of the maximum number of catch-up orbits required. A time of three days, corresponding to about 11.3 orbits, was chosen. From this value, the value of $\dfrac{\overline{\Delta v_i}}{v_0}$ is determined to be

$$\frac{\overline{\Delta v_i}}{v_0} = - \frac{600 \text{ fps}}{v_0} - 3 \times 4 \times 10^{-3} \quad , \quad v_0 \sim 15,700 \text{ fps}$$

$$\frac{\overline{\Delta v_i}}{v_0} = - 2.62 \times 10^{-2}$$

Notice that since $0.026 \ll 0.26$, the original evaluation of σ_i is valid.

All the numbers required for the final error evaluation are now available, and the results are presented below (in table M-1) for the case of biased vernier thrust.

Table M-1 - Summary of Final Errors

Number of Period Corrections	2 (n = 3)	3 (n = 4)
Velocity Error Avg. 1σ 3σ	0 <0.32 fps* <0.95 fps	0 <.016 fps <.048 fps
Position Error Avg. 1σ 3σ	0.03° <0.66° <2.0°	(approximately the same as in the preceding column)
Period Error Avg. 1σ 3σ	0 <1.4 sec <4.3 sec	0 <0.07 sec <0.21 sec
Eccentricity Avg. Max.	.00835 .0315	.00835 .0315

* When the error is given as less than a number, the number was evaluated for the most unfavorable geometric relation between the initial and final orbits.
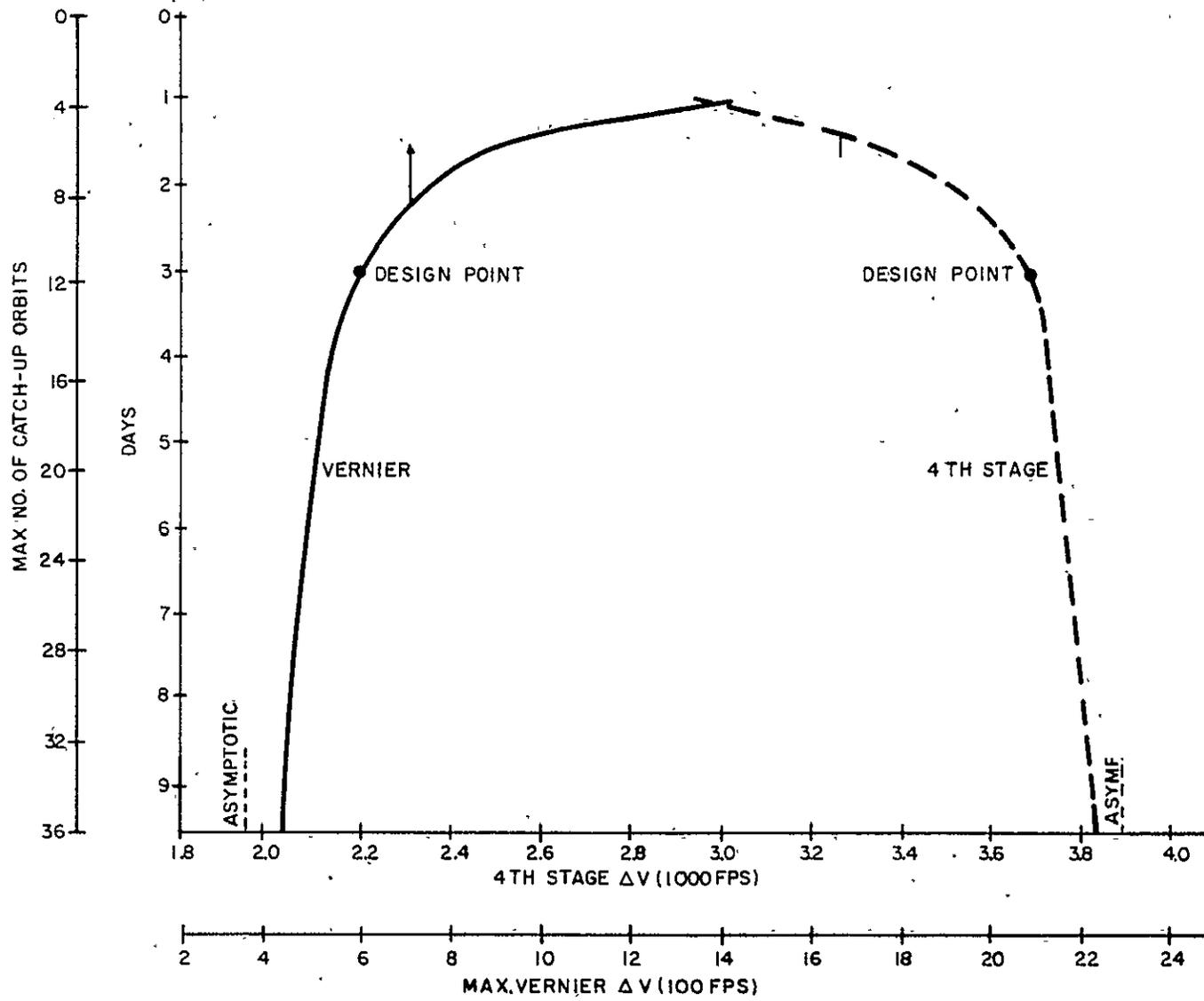
Figure M-1.   Maximum Number of Catch Up Orbits Vs Maximum Vernier Δv.

APPENDIX N
POST INJECTION DISTURBANCES

In this appendix, the perturbations of the navigational satellite orbits due to post-injection disturbances are analyzed. The effects which are considered are the following:

    a. Perturbations due to solar radiation

    b. Perturbations due to solar and lunar gravity

N.1 SOLAR RADIATION PERTURBATIONS

Analysis of the orbit perturbations due to solar radiation naturally breaks into the following two parts:

    a. Determination of the solar radiation force on the satellite.

    b. Calculation of the effects of this force on the satellite orbit.

N.1.1 Calculations of Solar Radiation Force

The force on a satellite due to direct solar radiation can be considered to originate from the direct interception of solar energy by the satellite surface and the reflection of this energy from the satellite surface. Considering the direct interuption of sunlight, a differential
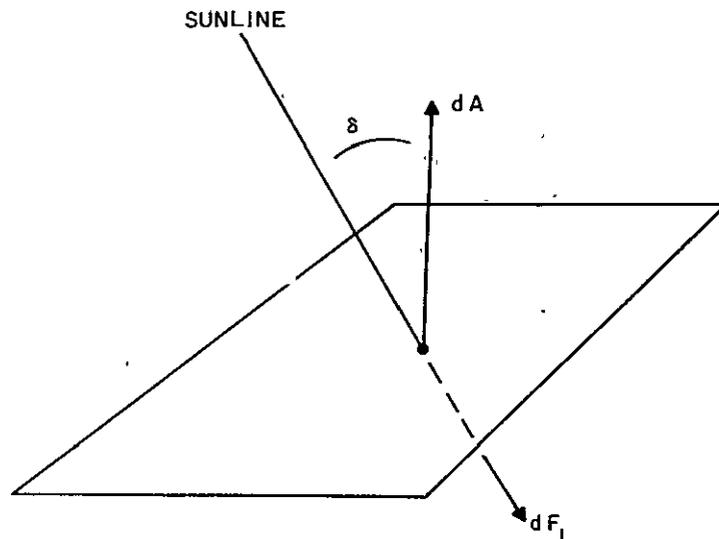

Figure N-1. Differential Surface Element of Satellite Exposed to Direct Sunlight

surface element of the satellite which is exposed to the direct sunlight and shown in figure N-1 is obtained.

From reference 1 or 2

$$dF_1 = \frac{\phi}{c} \cos \delta \, dA$$

Integrating over the surface exposed to the sunlight yields

$$F_1 = \frac{\phi}{c} \int_{A_s} \cos \delta \, dA = \frac{\phi}{c} A_n \, ,$$

where A_n is the satellite surface area projected onto a plane normal to the sunline.

From reference 2,

$$\phi = 92 \text{ lb/ft-sec.}$$

So

$$F_1 = .938 \times 10^{-7} A_n \quad \text{(directed along the sunline)}$$

The component of F due to reflected radiation (F_2) is more difficult to determine. This component is a function of the satellite's shape, orientation, and surface characteristics. In general, F_2 will not lie along the sunline. For the present analysis, F_2 was assumed to be equal to F_1 in both magnitude and direction. The approach is conservative and yields a magnitude of F which is somewhat higher than actually would be encountered. It does, however, yield some error in the direction of F.

The total force now becomes

$$F = 1.88 \times 10^{-7} A_n$$

The net projected surface area A_n will vary as a function of time. The area (A_n) is dependent upon the orbit inclination, location of the satellite in the orbit, and the satellite orientation. In the present study, a constant A_n equal to the average value during an orbit was used. A surface efficiency (average projected area/total area) of 0.33 was used for the solar cells. This is the value of the proposed configuration at the most severe orbit inclination. Using an approximate value for the projected area of the main body, the following expressions are obtained:

$$A_n = .33 \times 72 + 6.3 = 30.1 \text{ ft}^2$$

and

$$F_{av} = 0.55 \times 10^{-5} \text{ lb.}$$

Generally, the radiation force is expressed in lb per unit satellite mass. For a weight of 355 lb, the following value is obtained:

$$F' = 0.5 \times 10^{-6} \text{ ft/sec }^2$$

The main approximations, in the value of F' determined above, are the following.

    a. Components of the radiation force normal to the sunline are neglected.

    b. A constant value of the projected area of the satellite is used.

N.1.2 Investigation of Orbit Perturbations

N.1.2.1 Preliminary Calculations

In order to compute the effects of solar radiation force, approximate values of $\dot{\omega}$, $\dot{\Omega}$, and $\dot{\lambda}_s$ are needed. Symbols are defined in Section N.3.

The value of $\dot{\lambda}_s$ (apparent angular rate of the sun along the ecliptic) has been determined to be about 0.0172 radians per day.

The quantities $\dot{\Omega}$ and $\dot{\omega}$ were assumed to be caused entirely by the earth's oblateness. The necessary equations for these quantities were obtained from reference 3 and are

$$\dot{\Omega} \approx -nJ \left(\frac{r_o}{a}\right)^2 \cos i$$

$$\dot{\omega} \approx \frac{1}{2} nJ \left(\frac{r_o}{a}\right)^2 (5 \cos^2 i - 1)$$

Using the numerical values listed in table N.1 in the equations yields the following magnitudes:

$$\dot{\Omega} = -0.516 \times 10^{-2} \cos i \qquad \text{radians/day}$$
$$\dot{\omega} = 0.258 \times 10^{-2} (5 \cos^2 i - 1) \qquad \text{radians/day}$$

<div align="center">

TABLE N-1

NUMERICAL VALUES USED

(Slide Rule Accuracy)

</div>

Astronomical and Geophysical Data

c	$.984 \times 10^9$ ft/sec
ϵ	23.5 degrees
GM_e	1.408×10^{16} ft^3/sec^2
J	1.623×10^{-3} (dimensionless)
$\dfrac{M \text{ moon}}{M_e}$	1/81.45
$\dfrac{M \text{ sun}}{M_e}$	3.325×10^5
r_o	3440 nautical miles
r_{moon}	1.26×10^9 ft.
r_{sun}	$.485 \times 10^{12}$ ft.
ϕ	92 lb/ft-sec

Nominal Satellite Orbit Parameters

$a = r_c$	9440 nautical miles = .574 x 10^8 ft
n	23.9 radians per day
i	55°
$W_{satellite}$	355 lb

For i (inclination of orbit with respect to equator) of 55°, the values are

$\dot{\Omega}$ = 0.295 x 10^{-2} radians/day

$\dot{\omega}$ = 0.167 x 10^{-2} radians/day

N.1.2.2 Effect of Radiation Force on Orbit Eccentricity

Reference 4 derives the following equation for e due to solar radiation

$$\dot{e} = -\frac{3 F' n a^2 \sqrt{1-e^2}}{2 G M_e} \left\{ C^2 \frac{i}{2} S^2 \frac{\epsilon}{2} S (\omega + \Omega + \lambda_s) \right.$$

$$+ C^2 \frac{i}{2} C^2 \frac{\epsilon}{2} S (\omega + \Omega - \lambda_s)$$

$$+ S^2 \frac{i}{2} C^2 \frac{\epsilon}{2} S (\omega - \Omega + \lambda_s)$$

$$+ S^2 \frac{i}{2} S^2 \frac{\epsilon}{2} S (\omega - \Omega - \lambda_s)$$

$$- \frac{1}{2} Si \ S\epsilon \ S (\omega + \lambda_s)$$

$$+ \frac{1}{2} Si \ S\epsilon \ S (\omega - \lambda_s)$$

C = cos

S. = sin

where

   i = inclination of orbit with respect to earth's equatorial plane

   ϵ = angle between ecliptic and earth's equatorial plane

   The main approximation in this equation is that F' is constant and lies along the sunline.
The effect of the earth's shadow is not included.

To obtain an approximate integration of this equation, perform the following operations:

a. Replace $\sqrt{1-e^2}$ with 1

b. Let $a = r_c$ (constant)

c. Assume any change in i to be negligible.

d. Assume that ω, Ω, and λ_S vary linearly with time. Then, $\omega + \Omega + \lambda_S$ (for example) can be replaced by $(\dot{\omega} + \dot{\Omega} + \dot{\lambda}_S) t + \alpha_o$

e. The integration will be restricted to the case where none of the combinations of $\dot{\omega}, \dot{\Omega}$, and $\dot{\lambda}_S$ are zero.

After integration, the following expression is obtained

$$\Delta e = \frac{-3F' n r_c^2}{2GM_e} \left\{ -\frac{1}{\dot{\omega} + \dot{\Omega} + \dot{\lambda}_S} C^2\frac{i}{2} S^2\frac{\epsilon}{2} C\left[(\dot{\omega} + \dot{\Omega} + \dot{\lambda}_S) t + \alpha_1\right] \right.$$

$$-\frac{1}{\dot{\omega} + \dot{\Omega} - \dot{\lambda}_S} C^2\frac{i}{2} C^2\frac{\epsilon}{2} C\left[(\dot{\omega} + \dot{\Omega} - \dot{\lambda}_S) t + \alpha_2\right]$$

$$-\frac{1}{\dot{\omega} - \dot{\Omega} + \dot{\lambda}_S} S^2\frac{i}{2} C^2\frac{\epsilon}{2} C\left[(\dot{\omega} - \dot{\Omega} + \dot{\lambda}_S) t + \alpha_3\right]$$

$$-\frac{1}{\dot{\omega} - \dot{\Omega} - \dot{\lambda}_S} S^2\frac{i}{2} S^2\frac{\epsilon}{2} C\left[(\dot{\omega} - \dot{\Omega} - \dot{\lambda}_S) t + \alpha_4\right]$$

$$\left. +\frac{5}{\dot{\omega} + \dot{\lambda}_S} SiS\epsilon C\left[(\dot{\omega} + \dot{\lambda}_S) t + \alpha_5\right] - \frac{5}{\dot{\omega} - \dot{\lambda}_S} SiS\epsilon C\left[(\dot{\omega} - \dot{\lambda}_S) t + \alpha_6\right] \right\} + K$$

Where K is the integration constant needed to make $\Delta e = 0$ at $t = 0$. Because its large orbital radius results in small $\dot{\omega}$ and $\dot{\Omega}$ with respect to $\dot{\lambda}_S$, the navigational satellite is far removed from any of the resonance conditions. Substituting numerical values into the equation yields

$$\Delta e = 4.17 \times 10^{-6} \left\{ -2.06 C\left[0159t + \alpha_1\right] + 40.7 C\left[.0185t + \alpha_2\right] \right.$$

$$-9.37 C\left[.0219t + \alpha_3\right] + .71 C\left[.0126t + \alpha_4\right]$$

$$\left. +8.64 C\left[.0186t + \alpha_5\right] + 10.5 C\left[.0155t + \alpha_6\right] \right\} + 4.17 \times 10^{-6}$$

$$\left[2.06 C\alpha_1 - 40.7 C\alpha_2 + 9.37 C\alpha_3 - 71 C\alpha_4 - 8.64 C\alpha_5 - 10.5 C\alpha_6\right]$$

Even by using an overly conservative approach and adding all maximum values of the terms together absolutely, the following small value for Δe is obtained

$$\Delta e_{max} = 6 \times 10^{-4}$$

From this, it is concluded that solar radiation has a completely negligible effect on eccentricity since the required eccentricity is to be less than 0.03.

N.1.2.3 Effect of Solar Radiation on Orbit Orientation

Reference 4 also derives equations for $\frac{di}{dt}$ and $\dot{\Omega}$. For a near circular orbit, these expressions are as follows:

$$\frac{di}{dt} = -\frac{3}{4} \frac{F'nr_c^2 e}{GM_e} \left[S\,i\,S^2\frac{\epsilon}{2} S(\omega+\Omega+\lambda_s) - S\,i\,S^2\frac{\epsilon}{2} S(\omega-\Omega-\lambda_s) + S\,i\,C^2\frac{\epsilon}{2} S(\omega+\Omega-\lambda_s) \right.$$

$$\left. - S\,i\,C^2\frac{\epsilon}{2} S(\omega-\Omega+\lambda_s) + C\,i\,S\,\epsilon\,S(\omega+\lambda_s) - C\,i\,S\,\epsilon\,S(\omega-\lambda_s) \right]$$

$$(\sin i)\dot{\Omega} = +\frac{3}{4} \frac{F'nr_c^2 e}{GM_e} \left[S\,i\,S^2\frac{\epsilon}{2} C(\omega+\Omega+\lambda_s) - S\,i\,S^2\frac{\epsilon}{2} C(\omega-\Omega-\lambda_s) \right.$$

$$\left. + S\,i\,C^2\frac{\epsilon}{2} C(\omega+\Omega-\lambda_s) - S\,i\,C^2\frac{\epsilon}{2} C(\omega-\Omega+\lambda_s) + C\,i\,S\,\epsilon\,C(\omega+\lambda_s) \right.$$

$$\left. - C\,i\,S\,\epsilon\,C(\omega-\lambda_s) \right]$$

For the navigational satellite

$$\frac{3}{4} \frac{F'nr_c^2 e}{GM_e} = 4.17\,eF' = 2.09 \times 10^{-6} \text{ (rad/day)}.$$

The derivation in the preceding sections showed that the satellite is not near any of the possible resonances. Therefore, the terms within the brackets are periodic, and the perturbations in i and Ω due to solar radiation shall be bounded. The equations indicate that there are no perturbations when e = 0. Actually, some variations would probably be encountered, even in the circular orbiting case, due to variation in F' and the earth's shadow effect.

The technique of the preceding section can be used to obtain magnitudes of Δi and $\Delta\Omega$. To obtain rough answers however, the following approximations shall be used:

$$S^2\frac{\epsilon}{2} = 0$$

$$C^2\frac{\epsilon}{2} = 1$$

$$\dot{\omega}, \dot{\Omega} = 0$$

Using these approximations and integrating yields

$$\Delta i \approx 2.42 \times 10^{-4}\,e\left[-S\,i + S\epsilon\,C\,i \right]\left[C(\lambda_s t + \alpha_o) - C\alpha_o \right] \text{ radian} \qquad\qquad \Delta\Omega = 0$$

This expression shows that the solar radiation force should have a completely negligible effect on orbit orientation.

N.2 SOLAR-LUNAR GRAVIATIONAL PERTURBATIONS

N.2.1 In-Plane Perturbations of the Orbit

In reference 5, the following equations for the in-plane perturbations of the satellite due to extra-terrestrial gravitation are derived.

$$u = \left(\frac{M_d r_c^4}{2 M_e r_d^3} \right) (1 + 2 \cos 2\theta) \qquad \text{N-1}$$

$$v = -\frac{1}{4} \left(\frac{M_d r_c^4}{2 M_e r_d^3} \right) (8\theta + 11 \sin 2\theta) \qquad \text{N-2}$$

Figure N-2 shows the geometry which is involved. N-1 and N-2 are simplified equations which give the deviation from a circular orbit. They omit the effects of motion of the disturbing body and inclination of the satellite orbit. The quantities u and v are assumed to be small with respect to r_c. These equations are used in the present analysis in order to obtain a quick determination whether extra-terrestrial gravitation can possibly produce significant effects on navigational satellite orbit shape.
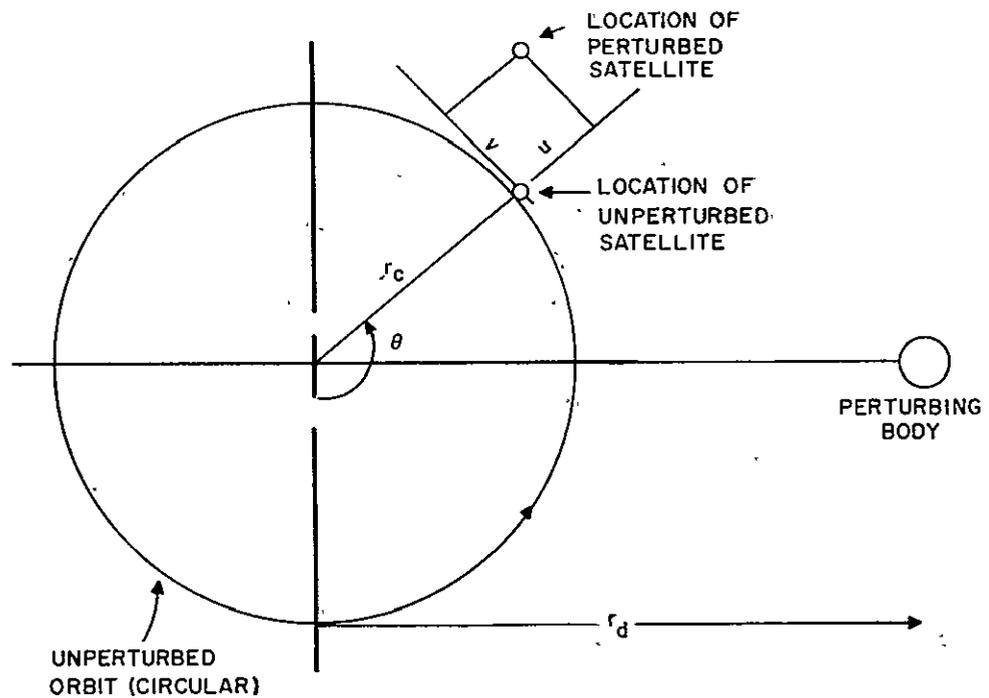

Figure N-2. In-Plane Perturbations Due to Solar Lunar Gravity (Reference 5)

Equation N-1 shows the maximum perturbation in altitude to be

$$\Delta a = \frac{M_d r_c^4}{M_e r_d^3} \qquad\qquad\qquad \text{N-3}$$

This equation is also given in reference 7

From equation N-3, the following values of Δa are obtained

sun $\Delta a = 32$ ft.

moon $\Delta a = 67$ ft.

These values are insignificant. This indicates that extra-terrestrial gravitation shall have negligible effect on the orbit shape of the navigational satellites.

Using the secular portion of equation N-2, the following drift rates are obtained:

sun $\dot{v} = 45$ nautical miles per year

moon $\dot{v} = 94$ nautical miles per year

These are drift rates of an actual, perturbed, satellite with respect to a hypothetical, non- perturbed, satellite. It is not immediately apparent that the magnitudes are small enough to have negligible effect on the performance of the Navigational Satellite System. To investigate this, the drift rates of the satellites relative to one another shall be examined. To do this, refer to equation 47 of reference 6.

$$v = -\frac{3}{8} \frac{M_d r_c^4}{M_e r_d^3} \left[\frac{4}{3} (2\cos^2 i_d - \sin^2 i_d) f - \frac{11}{6} \sin^2 i_d \sin 2\theta - \frac{2\sin^2 i_d \sin 2\gamma}{\sigma(4\sigma^2 - 1)} \right.$$

$$\left. - \frac{(4\sigma^2 + 12\sigma + 11)(1 - \cos i_d)^2 \sin 2(\gamma + \theta)}{4(\sigma + 1)^2 (2\sigma + 1)(2\sigma + 3)} + \frac{(4\sigma^2 - 12\sigma + 11)(1 + \cos i_d)^2 \sin 2(\gamma - \theta)}{4(\sigma - 1)^2 (2\sigma - 1)(2\sigma - 3)} \right]$$

where

$$\sigma \neq 0, \pm 1, \pm.5, \pm 1.5 \qquad\qquad \text{N-4}$$

For the navigational satellite

$$\frac{3}{8} \frac{M_d r_c^4}{M_e r_d^3} = 12 \text{ ft. (sun)}, \ 25 \text{ ft. (moon)}$$

For now, it will be assumed that the satellite is not at a resonant condition. The effect of resonance shall be investigated in section N.2.3. Satellites moving at different angular positions in the same orbit will have different values of θ and the same values of i_d, γ, f, and σ in the above equation. Therefore, equation N-4 indicates that such satellites shall have no secular drift rates relative to one another due to extra-terrestrial gravitation. In an actual system, some drift rates would occur due to slight differences in the

parameters. These, however, should be negligible. As an example, an error in inclination of 5 degrees in one of the satellite orbits, with a nominal inclination of 70°, would yield a relative drift of about 3 miles per year due to solar gravitation.

N.2.2 Orbit Orientation Perturbations

N.2.2.1 Nodel Regression

References 5, 6, 7 and 8 list similar, or equivalent, equations for nodal regression due to extra-terrestrial gravitation. Using equation 7 of reference 8 and neglecting the eccentricities of both the satellite and the disturbing body orbits, results in the following:

$$\Delta \Omega d/orbit = - \frac{3 \pi GM_d \sin^2 \gamma \cos i_d}{n^2 r_d^3}$$

N-5

Converting this to a time derivative yields

$$\dot{\Omega}d = -\frac{3}{2} \frac{GM_d}{r_d^3 n} \sin^2 \gamma \cos i_d = -\frac{3}{2} \frac{GM_d}{r_d^3} \sqrt{\frac{r_c^3}{GM_e}} \sin^2 \gamma \cos i_d$$

N-6

Using the average value of $\sin^2 \gamma$ over one revolution of the disturbing body, yields the following:

$$\dot{\Omega}d_{av.} = -\frac{3}{4} \frac{GM_d}{r_d^3} \sqrt{\frac{r_c^3}{GM_e}} \cos i_d$$

N-7

This equation also appears in reference 6 of the bibliography.

For the navigational satellite, equation N-7 yields the following nodal regression rates

$$sun \, \dot{\Omega}_d = -.2 \cos i_d \text{ degrees/year}$$

$$moon \, \dot{\Omega}_d = -.4 \cos i_d \text{ degrees/year}$$

N-8

The curves in reference 7 also show regression rates of roughly these magnitudes.

Euqation N-8 indicates that nodal regression due to extra-terrestrial gravity would produce no orientation displacement of the two orbit planes relative to-one another, if both planes had the same inclination with respect to the orbit of the perturbing body. Actually, however, the two planes, in general, will not have the same inclination with respect to either the sun or the moon planes. Therefore, extra-terrestrial gravitation shall produce some relative displacement of the two orbits.

The relative regression rate due to solar gravitation shall now be considered. Figure N-3 indicates the geometry involved. The development shall assume that the inclinations of the two orbit planes with respect to the earth's equatorial plane are constant and of equal magnitude. The average value of $\sin^2 \gamma$, as in equations N-7 and N-8, shall be used.
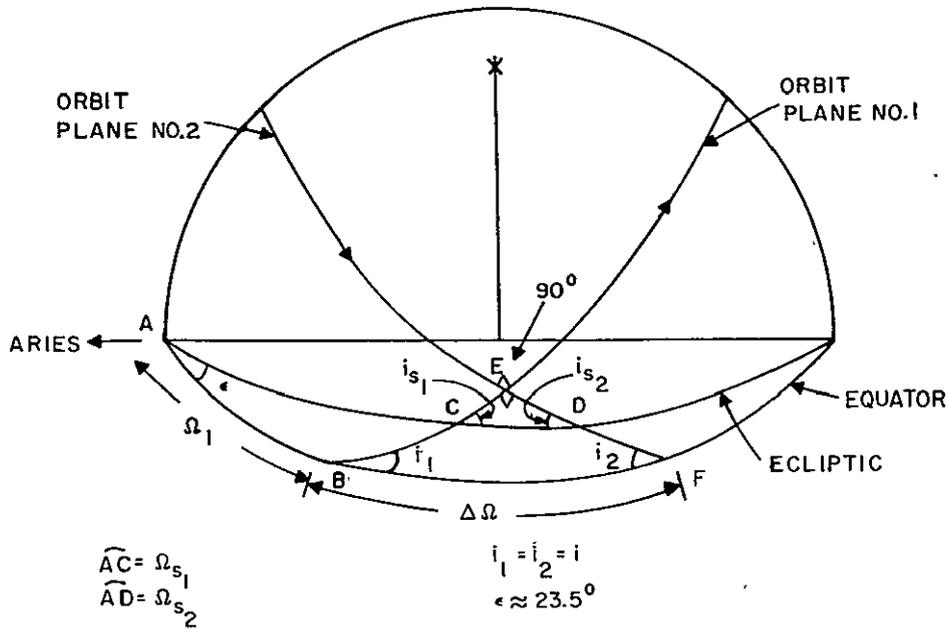
Figure N-3. Navigational Satellite Orbit Geometry

a. Using triangle BEF

$$\cos 90° = 0 = - \cos i_1 \cos i_2 + \sin i_1 \sin i_2 \cos \Delta \Omega$$

Since

$$i_1 = i_2$$

$$\cos \Delta \Omega = \left(\frac{\cos i}{\sin i} \right)^2$$

b. Using triangle ABC

$$\cos i_{s_1} = \cos \epsilon \cos i + \sin \epsilon \sin i \cos \Omega_1$$

c. From triangle ADF

$$\cos i_{s_2} = \cos \epsilon \cos i - \sin \epsilon \sin i \cos (\Omega_1 + \Delta \Omega)$$

d. Using equation N-8, the relative regression rate is

$$\dot{\Omega} r = \dot{\Omega} s_1 - \dot{\Omega} s_2 = - .2 \left[\cos i_{s_1} - \cos i_{s_2} \right] = .2 \left[\sin \epsilon \sin i \right] \left[\cos \Omega_1 - \cos (\Omega_1 + \Delta \Omega) \right]$$

But

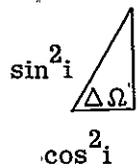$$\cos(\Omega_1 + \Delta\Omega) = \cos\Omega_1 \cos\Delta\Omega - \sin\Omega_1 \sin\Delta\Omega$$

$$\sin^2 i \sqrt{} \quad \Delta\Omega \quad \sqrt{\sin^4 i - \cos^4 i} = \sqrt{-\cos 2i}$$

$$\cos^2 i$$

$$\cos(\Omega + \Delta\Omega) = \frac{\cos\Omega_1 \cos^2 i}{\sin^2 i} - \frac{\sin\Omega_1 \sqrt{-\cos 2i}}{\sin^2 i}$$

so

$$\dot\Omega r = - \frac{.2 \sin \epsilon}{\sin i} \left[\cos\Omega_1 \sin^2 i - \cos\Omega_1 \cos^2 i + \sin\Omega \sqrt{-\cos 2i} \right]$$

$$= - \frac{.2 \sin \epsilon}{\sin i} \sqrt{-\cos 2i} \left[\sin\Omega_1 + \sqrt{-\cos 2i} \cos\Omega_1 \right] \text{ deg./year} \qquad \text{N-9}$$

The earth's oblateness causes Ω_1 to vary almost linearly. The frequency is approximately 1.1 radian per year for $i = 55°$. Equation N-9, therefore, indicates that the relative orbit displacement due to solar gravity shall be bounded. The period, however, is roughly similar to the operational life of the satellite.

Putting numerical values into equation N-9, yields

$$\dot\Omega_r = - .0575 \left[\sin(\Omega_o + 1.1t) + .59 \cos(\Omega_o + 1.1t) \right] \text{ deg/year}$$

Integrating the equation results in

$$\Omega_r = - .0522 \left[-\cos(\Omega_o + 1.1t) + .59 \sin(\Omega_o + 1.1t) + \cos\Omega_o - .59 \sin\Omega_o \right]$$

This indicates that the relative displacement of the orbits due to nodal regression resulting from solar gravity shall not exceed 0.1 degrees.

N.2.2.2 Orbit Inclination Perturbation

To evaluate the effect of solar-lunar gravitation on orbit inclination, equation 6 of reference 8 shall be used. Setting the satellite and orbiting body eccentricities equal to zero in this equation yields

$$\Delta i_{d/orbit} = - \frac{3\pi GM_d}{n^2 r_d^2} \sin i_d \sin \gamma \cos \gamma$$

Converting this to a time derivative yields

$$\frac{di}{dt} = - \frac{3 M_d \sqrt{r_c^3} GM_e}{4 M_e r_d^3} \sin i_d \sin 2\gamma \qquad \text{N-10}$$

This indicates that the variation of inclination due to extra-terrestrial gravitation is periodic, rather than divergent. Let $\gamma = \dot\gamma t + \gamma o$ in N-10 and assume that the variation in $\sin i_d$, during the period of interest, is negligible. Equation N-10 can then be integrated.

$$\tan \frac{i_d}{2} = A\epsilon^{\frac{K}{2\dot\gamma} \cos 2(\dot\gamma t + \gamma o)}$$

where

$$K = \frac{3 M_d \sqrt{r_c^3 GM_e}}{4 M_e r_d^3}$$

then

sun, $K = 0.2$ degrees per year

moon, $K = 0.4$ degrees per year

sun, $\frac{K}{2\dot\gamma} = 0.28 \times 10^{-3}$

moon, $\frac{K}{2\dot\gamma} = 0.52 \times 10^{-3}$

Clearly, these two effects will produce insignificant variation in inclination with respect to the plane of the disturbing body.

N.2.3 Resonance Effect

The work of reference 9 indicates that there are a large number of possible resonance conditions and each resonance condition would cause an initial eccentricity of the orbit to increase without bound. Since the simplified approach in section N.2.1 of this appendix did not include these effects, they are investigated here.

Reference 9 shows that satellites with perigee no smaller than that of the navigational system experience the resonance phenomena at following orbit inclinations (with respect to earth's equator):

46.4, 73.2, 56.1, 63.4, 69, 123.9, 116.6, 111, 133.6, 106.8

The purpose of the investigation in this section is to determine whether or not this phenomena might cause an initial small eccentricity to diverge to a significant magnitude during the operational lifetime of the satellite.

Using simplified notation and letting e be small, equation 55 of reference 9 can be expressed in the following form:

$$e = A e \left[\sum_{1}^{n} B_j {}' \sin \psi_j \right] \qquad\qquad \text{N-11}$$

In this equation, the B_j's are functions of i and ϵ, and both assumed constant in the present analysis. The ψ_j's are linear combinations of the angles ω, λ_d, Ω and Ω_d. Also,

$$A = -\frac{15\, M_d \sqrt{r_c^3\, GM_e}}{4\, M_e r_d^3}$$

The current development assumes a hypothetical case in which an initial eccentricity is modified only by the extra-terrestrial gravity effect.

Assuming ω, λ_d, Ω, and Ω_d to vary linearly with time, it is determined that

$$\psi_j = \dot{\psi}_j t + \psi_{j_o} .$$

Resonance occurs whenever one of the $\dot{\psi}_j$'s is zero. Consider the satellite to be at one of the resonance inclinations. Let B_n and ψ_{no} represent this condition. Equation N-11 now becomes

$$\dot{e} = Ae\left[\left\{\sum_1^{n-1} B_j \sin(\psi_j t + \psi_{jo})\right\} + B_n \sin \psi_{no}\right] \qquad \text{N-12}$$

Integrating this equation yields

$$e = D\left[\sum_1^{n-1} \epsilon^{-\frac{AB_j}{\dot{\psi}_j} \cos(\psi_j t + \psi_{jo})}\right] \epsilon^{(AB_n \sin \psi_{no})t} \qquad \text{N-13}$$

Considering the solar gravity effect we have

$A = 0.0176$ radians/year.

Let $\sin \psi_{no}$ be 1. Using equation 55 of reference 9 the maximum value of B_n for the navigational satellite is calculated to be 0.3 (for $i = 63.4$). In this case, the ϵ term has a value of approximately 1.03 at $t = 5$ years. This means that the resonance effect due to solar gravity would cause an initial eccentricity to diverge only about 3 percent or less after 5 years. The lunar effect could be expected to be roughly twice this value. Clearly, this amount is insignificant.

N.3 DEFINITION OF SYMBOLS

A_n The surface area of the satellite projected onto a plane perpendicular to the sun line

$d\overline{A}$ A vector with its magnitude equal to the area of a differential surface element and its direction perpendicular to the element

a Semi-major axis of the satellite orbit

c Velocity of light

e Orbit eccentricity

F   Force

F'   Force per unit mass

f   Angular position of satellite in orbit, measured from its position at $t = 0$

G   Universal gravitational constant

i   Inclination angle of the satellite orbit with respect to earth's equatorial plane

i_d Inclination angle of the satellite orbit with respect to orbit of disturbing body (sun or moon)

J   Coefficient of the second harmonic of the earth's oblateness

M   Mass

n   Mean angular rate of satellite

r_c Radius of circular orbit of satellite

r_d Distance from the earth to the disturbing body

r_o Earth's equatorial radius

t   Time

u, v   Defines the in-planar perturbation displacement of a satellite due to disturbing forces. The perturbation component along the line between the earth's center and the unperturbed satellite position is u. Perpendicular to u and in the plane of the unperturbed orbit is v. The unperturbed orbit is taken to be circular.

γ The angular position of the disturbing body in its orbital plane measured from the intersection of its plane and the satellite's orbit (satellite ascending node) ($\overline{\theta}$ in reference 5 and 6 notation).

δ The angle between the sunline and a perpendicular to a differential surface area of the satellite

ϵ The angle between the plane of the disturbing body and the earth's equatorial plane.

θ The angular position of the satellite in its orbital plane, measured from the intersection of its orbital plane with the plane of the disturbing body.

λ_d The angular position of the disturbing body (sun or moon) in its orbital plane measured from the intersection (ascending node) of its orbital plane and the earth's equatorial plane (λ_s refers to the sun).

σ Ratio of the angular velocity of the disturbing body to the angular velocity of the satellite (λ in reference 6 notation)

ϕ The solar radiation energy intercepted each second by a unit area in space at a mean distance of the earth and perpendicular to the radiation.

Ω The angular displacement along the earth's equatorial plane between the line of Aries and the satellite's ascending node.

$\dot{\Omega}_d$ The angular displacement along the orbit plane of the disturbing body between a reference direction and the satellite's ascending node.

ω The satellite's argument of perigee, measured from the ascending node.

N.3.1 Subscripts

d   Indicates the disturbing body (sun or moon)

e   Indicates the earth

m   Indicates the moon

r   Indicates a relative quantity

s   Indicates the sun

BIBLIOGRAPHY

1. Berman, A.I., The Physical Principles of Astronautics, John Wiley and Sons, 1961, pp. 42-46, 146-147, 258-261.

2. Ehricke, K.A., Space Flight, Vol. I, Environment and Celestial Mechanics, D. Van Nostrand Company, 1959, pp. 142-146.

3. Ehricke, K.A., Space Flight, Vol. II, Dynamics, D. Van Nostrand Company, 1962, pp. 148, 176-177, 228.

4. Musen, P., The Influence of the Solar Radiation Pressure on the Motion of an Earth Satellite, Journal of Geo Physical Research, Vol. 65, No. 5, May 1960, pp. 1391-1396.

5. Geyling, F. T., Fundamental Satellite Perturbations, American Rocket Society Journal, Nov. 1960, pp 1009-1012.

6. Geyling, F. T., Satellite Perturbations from Extra-Terrestrial Gravitation and Radiation Pressure, Journal of the Franklin Institute, May 1960, pp. 375-407.

7. Jensen, Townson, Kork, Kraft, Design Guide to Orbital Flight, McGraw-Hill Book Company, 1962.

8. Moe, M.M., Solar - Lunar Perturbations of the Orbit of an Earth Satellite, American Rocket Society Journal, May 1960, pp. 485-487.

9. Cook, G.E., Luni - Solar Perturbations of the Orbit of an Earth Satellite, Royal Aircraft Establishment, Technical Note No. G. W. 582, July 1961.

POWER PATTERN OF ANTENNAS BASED ON CARDIOID

$$P(\theta, \phi) = \frac{1 + \cos \theta}{2}$$

$$*D(\theta, \phi) = \frac{4 \, P^2(\theta, \phi)}{\int_0^{2\pi} \int_0^{\pi} P^2(\theta, \phi) \sin \theta \, d\phi \, d\theta} \quad \text{at zenith}$$

$$= \frac{8 \, P^2(\theta_o, \phi_o)}{\int_0^{\pi}(1 + 2 \cos \theta + \cos^2 \theta) \sin \theta \, d\theta}$$

$$= \frac{8 \, P^2(\theta_o, \phi_o)}{\left[-\cos \theta - \cos^2 \theta - \frac{\cos^3 \theta}{3} \right]_0^{\pi}}$$

$$= 3/4 \, (1 + \cos \theta)^2 \quad \text{from zenith}$$

Elevation angle from horizon	Gain
0°	-1.25 db
5°	-0.53 db
10°	0.14 db
15°	0.74 db
20°	1.3 db
30°	2.27 db
40°	3.06 db
50°	3.52 db
60°	4.16 db
70°	4.49 db
80°	4.70 db
90°	4.77 db

*McGraw Hill "Antennas" by Kraus, P. 542, Eq. 24a

CALCULATION OF MAXIMUM DOPPLER AND MAXIMUM DOPPLER VELOCITY

P.1 INTRODUCTION

The purpose of this appendix is to present the maximum doppler and maximum doppler velocity as a function of satellite altitude and transmitter frequency (F_s). The results are presented both in tabular form and as a series of curves.
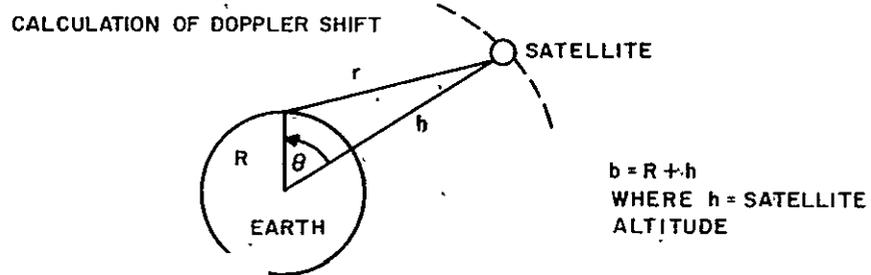
P.2 CALCULATION OF DOPPLER SHIFT

Figure P-1. Orbit Geometry

The tangental velocity, V_t, of the satellite may be calculated by equating the centripetal force and the force of gravity

$$F = \frac{mV_t^2}{b} = \text{centripetal force}$$

$$F = mg\left(\frac{R}{b}\right)^2 = \text{force of gravity}$$

where

g = force of gravity at the earth's surface

$$\frac{mV_t^2}{b} = mb\left(\frac{R}{b}\right)^2$$

$$V_t^2 = \frac{gR^2}{b}$$

the angular velocity, $\dot{\theta}$, is given as;

$$\dot{\theta} = \frac{V_f}{b}$$

<div align="right">(P-1)</div>

$$\dot{\theta} = \frac{R}{b}\left(\frac{g}{b}\right)^{1/2}$$

the range, r, is given by;

$$r = (R^2 + b^2 - 2bR\cos\theta)^{1/2}$$

$$\dot{r} = \frac{dr}{dt} = \frac{dr}{d\theta}\cdot\frac{d\theta}{dt} = \frac{dr}{d\theta}\dot{\theta}$$

therefore

$$\dot{r} = \frac{d(R^2 + b^2 - 2bR\cos\theta)^{1/2}}{d\theta}\cdot\dot{\theta}$$

$$\dot{r} = \frac{bR\sin\theta}{(R^2 + b^2 - 2bR\cos\theta)^{1/2}}\dot{\theta} = \frac{bR\sin\theta}{r}\dot{\theta}$$

for an assumed circular orbit,

$$\dot{\theta} = \text{a constant}$$
$$\ddot{\theta} = 0$$

$$\ddot{r} = \frac{d\dot{r}}{dt} = \frac{d\dot{r}}{d\theta}\cdot\frac{d\theta}{dt} = \frac{d\dot{r}}{d\theta}\ddot{\theta}$$

$$\ddot{r} = \frac{bR(\cos\theta)\dot{\theta}^2 - \dot{r}^2}{r}$$

The line-of-sight range is a maximum when the satellite is on the horizon, (r is tangential to the earth) at which time;

$$r_{max} = \sqrt{b^2 - R^2}$$

<div align="right">(P-2)</div>

The received frequency, F_r, is given as;

$$F_r = F_s\left(1 - \frac{\dot{r}}{c}\right)$$

where

F_s = source frequency

$\dot{r}$ = rate of change of range

C = velocity of light

The frequency shift due to doppler, F_d, is given as;

$$F_d = \left| F_s - F_r \right| = \left| F_s - F_s + F_s \frac{\dot{r}}{c} \right|$$

$$F_d = \left| F_s \frac{\dot{r}}{c} \right|$$

F_d is a maximum (for line of sight operation) when the satellite is on the horizon, at which time

$$\dot{r} = R\dot{\theta}$$

therefore

$$F_{dmax} = F_s \frac{R\dot{\theta}}{C} \tag{P-3}$$

The doppler velocity, $\dot{F}_d$, is given by;

$$\dot{F}_d = \frac{d}{dt} F_d = \frac{F_s}{C} \ddot{r}$$

$\dot{F}_d$ is a maximum when $\theta = 0$ (satellite is overhead) at which time $\dot{r} = 0$, $r = h$

therefore

$$\dot{F}_{d\ max} = \left(\frac{F_s}{C}\right) \left(\frac{bR\dot{\theta}^2}{h}\right) \tag{P-4}$$

Calculated values of maximum slant range, maximum angular velocity, maximum doppler and maximum doppler velocity for various satellite altitudes are presented in table P-1. Equations P-1 through P-4 were used to calculate the values listed in table P-1, using an assumed polar orbit and:

Case 1   a stationary vehicle at the earth's surface with satellite in overhead orbit

Case 2   a vehicle travelling at an altitude of 10 nmi and a speed of 2000 nmi in opposition to the satellite's orbit.

Curves of maximum doppler and maximum doppler velocity for both cases are shown in figure P-2.

TABLE P-1.

VALUES CALCULATED FROM EQUATIONS (P-1) THROUGH (P-4)

Case 1 Vehicle stationary with respect to earth's surface				
Satellite altitude n. mi.	Max. slant range n. mi.	Angular velocity (rad/sec)	Max. doppler shift (cycle/sec)	Max. doppler velocity (cycle/sec^2)
600	2107	$9.76(10)^{-4}$	$\pm 20.5(10)^{-6} F_s$	$\pm 133.5(10)^{-9} F_s$
1000	2793	$8.50(10)^{-4}$	$\pm 17.9(10)^{-6} F_s$	$\pm 78.8(10)^{-9} F_s$
3000	5426	$4.84(10)^{-4}$	$\pm 10.2(10)^{-6} F_s$	$\pm 10.50(10)^{-9} F_s$
6000	8765	$2.71(10)^{-4}$	$\pm 5.7(10)^{-6} F_s$	$\pm 2.42(10)^{-9} F_s$
10000	12960	$1.60(10)^{-4}$	$\pm 3.36(10)^{-6} F_s$	$\pm 0.72(10)^{-9} F_s$

| Case 2 Vehicle moving 2000 n. mi. per hour opposing satellite's orbit				
Satellite altitude n. mi.	Max. slant range n. mi.	Angular velocity (rad/sec)	Max. doppler shift (cycle/sec)	Max. doppler velocity (cycle/sec^2)
600	2107	$11.39(10)^{-4}$	$\pm 24.0(10)^{-6} F_s$	$\pm 181(10)^{-9} F_s$
1000	2793	$10.13(10)^{-4}$	$\pm 21.3(10)^{-6} F_s$	$\pm 95.0(10)^{-9} F_s$
3000	5426	$6.47(10)^{-4}$	$\pm 13.6(10)^{-6} F_s$	$\pm 18.8(10)^{-9} F_s$
6000	8765	$4.34(10)^{-4}$	$\pm 9.14(10)^{-6} F_s$	$\pm 6.18(10)^{-9} F_s$
10000	12960	$3.23(10)^{-4}$	$\pm 6.80(10)^{-6} F_s$	$\pm 2.94(10)^{-9} F_s$
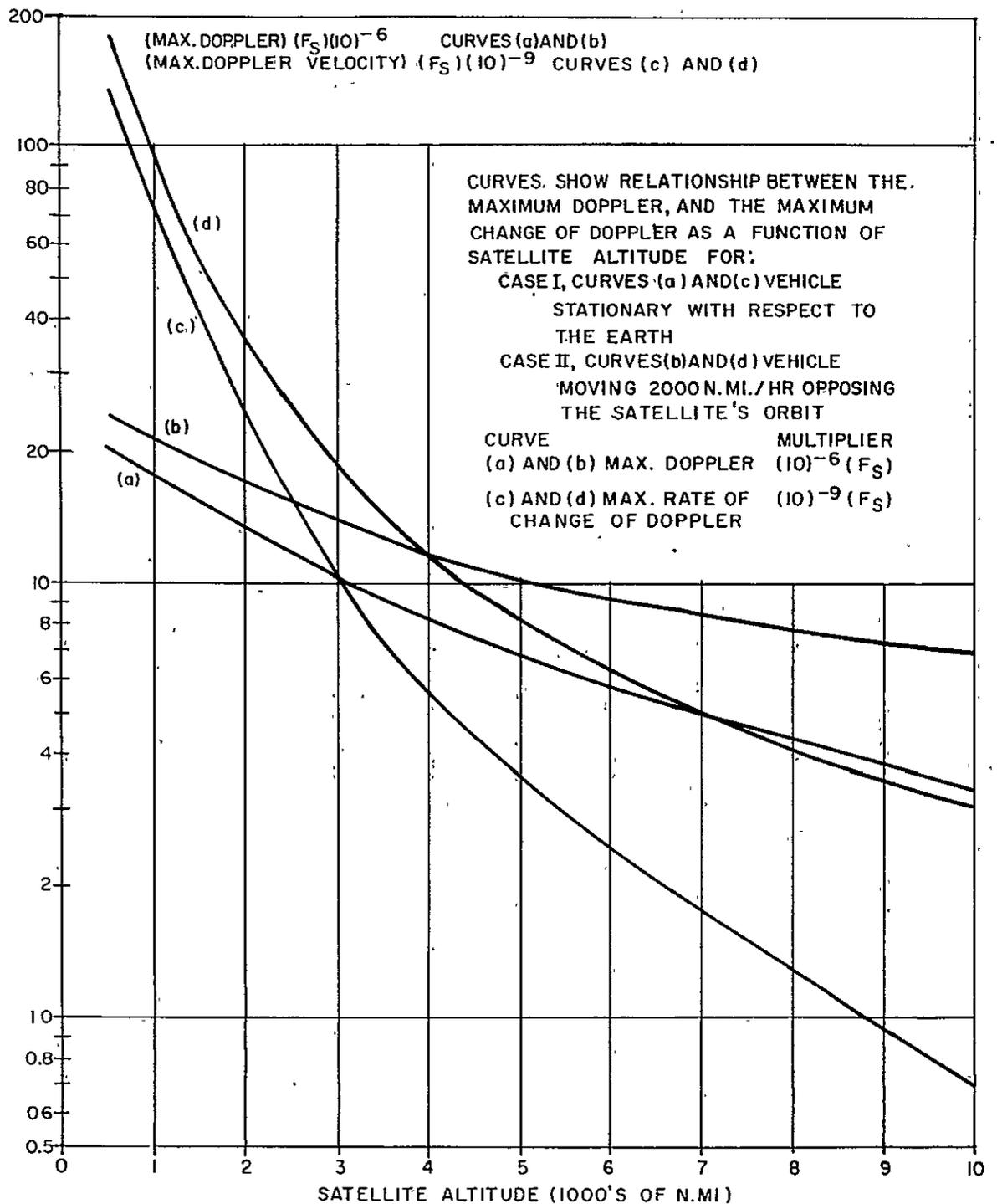
Figure P-2. Doppler Curves as a Function of Satellite Attitude

APPENDIX Q

The Bendix Corporation
Bendix Radio Division, Baltimore, Maryland

21 October 1963

Westinghouse Electric Corporation
Friendship International Airport
P. O. Box 1897, Mail Stop 811
Baltimore 3, Maryland

Attention: Mr. Keith Fellerman

Gentlemen:

Enclosed please find a copy of an interim report on SPADAT Transmitter life test data to present, October 1, 1963. This includes arc rates and emission decline of various types of 4CPX 250K's. The tubes are samples representing different phases of development of the product. Certain portions of the report have been deleted since they have no bearing on our particular common interest.

In a conversation with Mr. Washburn on October 17, 1963, the following SPADAT operating parameters for the 4CPX 250K were given:

Plate	5, 500 volts DC
Screen	1, 000 volts pulsed
Control Grid	-100 to -200 volts DC
Cathode	DC ground
Filament	6. 0 volts AC

The tube operates in a grounded grid, cathode-driven circuit where the cathode drive pulse is 250 microseconds wide at a 1 KW level and at a duty cycle of .005. The stage gain is 10 db. The tube pulsed plate current is 3 amps resulting in a plate efficiency of 60. 6% at UHF (400-500 MC). The high pulsed energy is supplied to the plate via a 2. 6 microfarad storage capacitor which is recharged during the interpulse period by the power supply. The 4CPX 250K has a 2 square centimeter cathode area and is therefore working at a pulsed current density of 1. 5 amps per square centimeter. Life testing at 3 amps per square centimeter on 4CPX 250K cathodes at .005 duty has been done with results indicating negligible reduction in tube life.

Your particular application at L-band and 2 KW output will require a pulsed plate current of approximately 1 ampere at 5000 volts. This would result in a plate efficiency of

40% which is in agreement with our experience at that frequency. The problems that need answering are:

1. Can the tube operate at 5000 volts DC reliably with no arcing?

2. Can the tube cathode operate with a 10 millisecond pulsewidth at a cathode loading of 1/2 amp. per square centimeter?

3. Will tube electrodes be able to withstand the 10 millisecond pulses without overheating?

The answer to the first question at present can only be given in terms of expected number of tube arcs in a given time interval. Circuitry can be designed to quench tube arcs without damage to the tube and then automatically turn the high voltage back on. A better solution is to get the tube manufacturer to produce an arc free tube. Because of the large quantities of 4CPX 250K's required in the SPADAT application a concerted effort by both Raytheon and EIMAC is being undertaken to accomplish this.

Tests recently run on a group of ML 7815R's planar triodes (of the 2C39 family) indicate operation at 1/2 to 1 amp per square centimeter at 10 millisecond pulse widths is possible with no cathode droop during the pulse. These tubes were operated at 3500 volts DC and have a grid to plate spacing only 1/5 to 1/6 of the 4CPX 250K screen grid to plate spacing. After operating in this manner for several hours tubes were broken open and inspected for damage. It did not appear that the electrodes were effected by the high impulse energy. Further life testing should be done before definite conclusions about 10 millisecond operation can be drawn, but the prospects of success are good.

Very truly yours,

THE BENDIX CORPORATION
Bendix Radio Division

s/S
Allen I. Sinsky
Principal Engineer
SPADAT Engineering
Department 462-4

AIS/if

Eitel-McCullough, Inc. Eimac Electron Power Tubes
301 Industrial Way, San Carlos, California
Telephone Lytell 1-1451

November 18, 1963

WESTINGHOUSE ELECTRIC CO.
Air Arm Division
Friendship Airport
Baltimore, Maryland

Attention: Keith Fellerman

Dear Mr. Fellerman,

I promised that we would comment on two requirements you have for long pulse power at 1000 mc in your study program for NASA.

Requirement I:

Power Out	3. 6 KW
Pulse Duration	9 ms
Gain	36 DB
Time between pulses	Long
Phase stability	2 1/2°

Requirement II:

Power Out	5 KW
Pulse Duration	1 to 2 ms
Frequency	1000 MC
Life Operating	25, 000 hours

Since our conversation I have also talked with Mr. J. Hrusovsky on a third requirement for the same program. Some of our comments apply to all three requirements so I promised to supply Mr. Hrusovsky with a copy of this letter.

Requirement III:

Power Out Frequency	150 to 200 watts
Frequency	110 MC
Type of signal	Data
Pulse Duration	10 ms
Time between pulses	10 to 100 sec
Required operating life	20, 000 hours

In Requirement III it is assumed that pulsed data of some form of modulation is transmitted during the 10 ms on time.

For Requirements I and II we recommend use of existing planar triodes. Power gain and efficiency of the planar triodes are high at 1000 mc compared to other devices.

Since low transit time of electrons contributes to efficiency and phase stability, electrode spacings are small and so there is a limit to the anode voltage which can be safely used. This will range from 1500 volts to possibly 4000 volts and will certainly affect reliability.

Average pulse plate current for the tube to be suggested may range from .3 a to 1.0 a for the long pulses considered here. A conservative estimate based on known information would limit this current to .3 a for the 9 ms pulse length and perhaps .5 a for the 1 ms pulse. Grid heating and power gain, as well as cathode loading must be considered here.

The Eitel-McCullough X843D planar triode is suggested as the best available tube structure for this work at 1000 mc. Power input per tube could range from 450 watts to 4 kW using the range of possible plate voltages and currents suggested above. A practical limit for moderate tube life would probably be 1500 watts input of 750 watts output per tube. Tubes would be used in clusters or diplexed to obtain the required total pulse power.

36 db of gain would be possible at the lower end of this pulse power range with three stages of the same tube type. The first stage would provide the most gain since it would have the lightest loading.

For Mr. Hrusovsky's Requirement III I suggest the high gain 4CX350A, or some modification of this off-the-shelf tetrode suitable for conduction cooling. Mr. Hrusovsky has been supplied with a data sheet on the 4CX350A and with a drawing of a similar tube type showing how the conduction cooling may be done.

The long life requirement of II and III should be the subject of a study program possibly followed or paralleled by a development program.

It is perfectly obvious that the high current density mentioned as a possible way to realize high power from an existing tube type is not likely to result in long tube life. The standard and most promising way to increase service life from vacuum tubes is to reduce cathode temperature and operate with low current density.

The suggested study program would be in two phases for the purpose of:

I   a)   Establishing the best possible cathode for use in an unusually long life device.

        b)   Establishing the highest current density for a given tube geometry to achieve extra long life.

        c)   To determine if other design modifications, such increased element spacings, would result in higher power once the current density for greatest life is established.

        d)   To consider the possibility of bunching assemblies in a common envelope which would be continuously pumped throughout life.

II   a)   To develope structures which look promising in Phase I studies.

           b)   To do limited testing on the tubes selected or developed in Phase I or Phase II a).

        Phase I would be possibly a three-month study. Phase II should be at least a year's program.

                              Very truly yours,

                              S/s
                              W. H. McAulay
                              Chief Application Engineer
                              Power Grid Tube Marketing

WHMcA/mi

RADIO CORPORATION OF AMERICA
Lancaster, Pa.

November 27, 1963

Mr. K. D. Fellerman, Sr. Engineer
Westinghouse Electric Corp.
Box 1897, Mail Stop 811
Baltimore 3, Md.

Dear Mr. Fellerman:

Subject: 3.6kw peak power output 1050 Mc rf pulsed amplifier chain.

Enclosed please find a pulse rf amplifier chain which will supply 3.6kw peak power output with three stages providing 35db gain. No plate and screen pulsing is required. All stages are grid pulse to simplify circuitry.

We have run a matrix cathode Cermolox tube type 7214 in a RCA J1853 cavity with pulses of 1 second on 59 seconds off. CW current for the 7214 would be about 1.26 amperes. In the pulsed application, we ran 3.9 amperes. This piece of evidence shows that the Cermolox tubes can be run with long pulses.

The typicals suggested in this letter will provide the type of operation you need.

Please contact George Crouchley or me if you need further information.

Very truly yours,

Paul S. Augustine
Regular Power Tube Application Eng.

ek

Enclosure (Table S-1)

cc: George Crouchley

TABLE S-1
RF PULSE AMPLIFIER CHAIN TYPICAL OPERATION IN
GRID PULSE CATHODE DRIVE AT 1050MC

	1.0W			3.6Kw
	7649	7649	7651	
Pulse Width	9000	9000	9000	usec
Pulse Rate	1	1	1	pps
DC Plate Voltage	2000	2000	5000	volts
DC Grid No. 2 Voltage	300	300	800	volts
DC Grid No. 1 Voltage	-40	-40	-120	volts
DC Plate Current during Pulse	0.025	0.28	1.5	amps
DC Plate Current	---	0.0025	.014	amps
DC Grid No. 2 Current	.0001	.0002	.001	amps
DC Grid No. 1 Current	.0001	.0002	.001	amps
Output Circuit Efficiency	80	80	80	%
Driver Power Output at Peak of Pulse (Approx.)	1	25	280	watts
Useful Power Output at Peak of Pulse (Approx.)	25	280	3600	watts

Litton Industries, Electron Tube Division
960 Industrial Rd., San Carlos, California

November 18, 1963

Mr. Fred L. Washburn, Jr., MS 129
Westinghouse Electric Corp.
Box 746
Baltimore, Maryland

Dear Mr. Washburn:

I enclose four copies each of preliminary design data on two electrostatically focused klystrons, per your conversation with Al Mixuhara. (Figures T-1 and T-2)

The phase sensitivity of these tubes to beam voltage is calculated by the relationship

$$\frac{\Delta \phi}{\Delta V} = 0.5 \, \phi \, . \, V$$

where ϕ is the tubes electrical length, about 1000°, and V is the beam voltage. For the 5 kw tube, this is about .05°/V. For the 25 kw tube, it is about .02°/V.
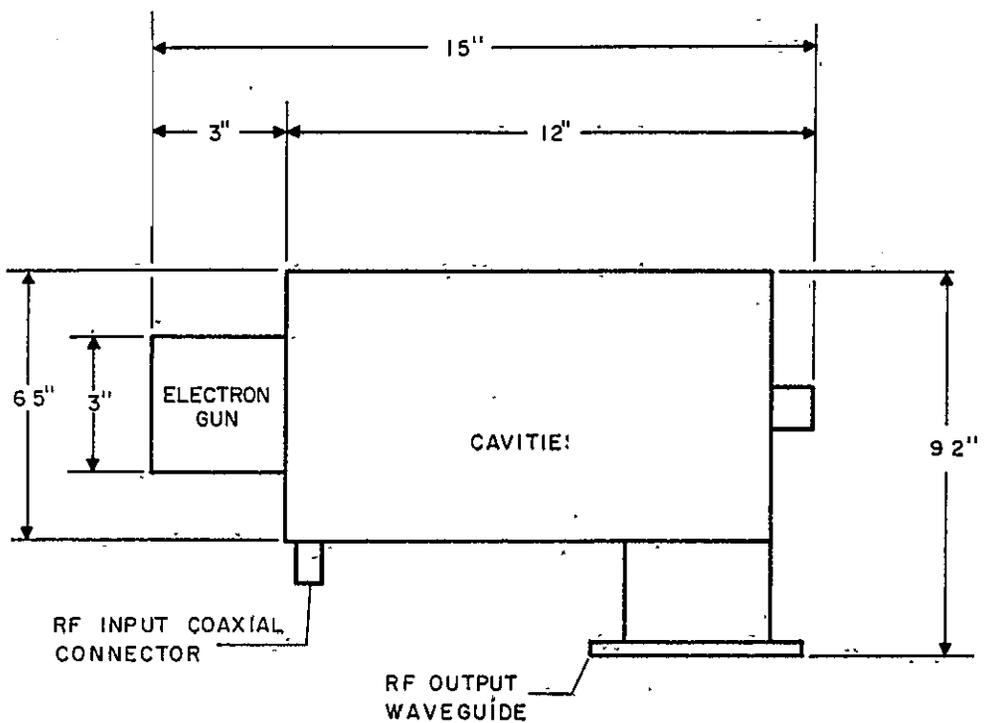
Out estimate of the selling price for the 25 kw tube is approximately $350 for 5000 tubes, after a development program amounting to about $60,000.

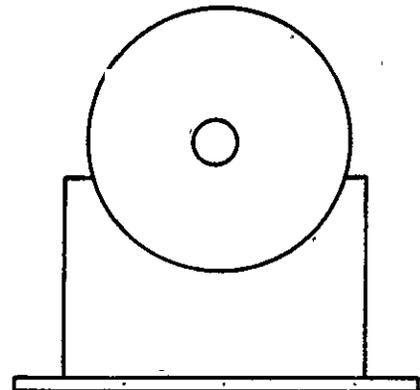We trust this information will aid you in your planning and that you will contact us if we can be of further service.

Very truly yours,

P. E. Hargrove
Sales Engineer
Research Laboratory

PEH:ka
Enclosur

NOTE: ALL DIMENSIONS ARE NOMINAL VALUES.

15"

3"   12"

6 5"   3"   ELECTRON GUN

CAVITIES

9 2"

RF INPUT COAXIAL CONNECTOR

RF OUTPUT WAVEGUIDE

TENTATIVE CHARACTERISTICS·

FREQ BAND	1000 -1100 MC/S	PULSE WIDTH	0.001 SEC
BANDWIDTH	0.5 %	ENERGY PER PULSE	25 JOULES
GAIN	36 DB	EFFICIENCY	45 %
V CATHODE	20 KV	CATHODE LOADING·	0.15 A/CM^2 PEAK
I CATHODE	2.8 A	HEATER POWER	75 WATTS
RF OUTPUT POWER, MIN	25 KW PEAK	COOLING	NATURAL CONVECTION

Figure T-1. Electrostatically Focused Klystron (Proposed) for 1050 MC

NOTE: ALL DIMENSIONS ARE
NOMINAL VALUES

12"

4"D   ELECTRON GUN   CAVITIES   65"D

TYPE N
RF OUTPUT
CONNECTOR

TYPE TNC
RF INPUT
CONNECTOR
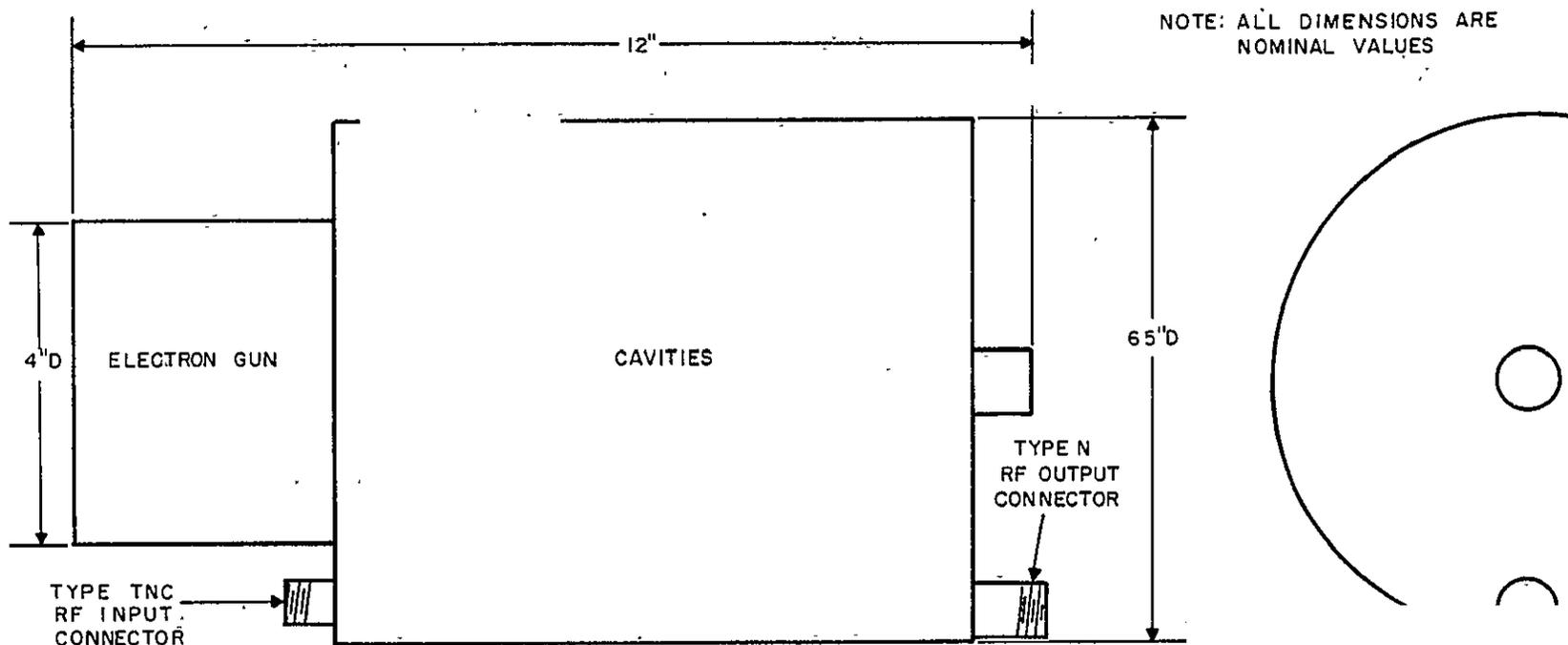
TENTATIVE CHARACTERISTICS:

FREQ BAND	1000-1100 MC/S	PULSE WIDTH	0.001 SEC
BANDWIDTH	0.5 %	DUTY	0.001
GAIN	36 DB	EFFICIENCY	45%
V CATHODE	11 KV	CATHODE LOADING	0.1 A/CM^2 PEAK
I CATHODE	1.1 A	HEATER, POWER	40 WATTS
RF OUTPUT		WEIGHT, COMPLETE	7 POUNDS
POWER, MIN	5 KW PEAK	COOLING	NATURAL CONVECTIO

Figure T-2.   Electrostatically Focused Klystron (Proposed) for Satellite Use

APPENDIX U

"L" BAND POWER AMPLIFIER OUTPUT STAGE

Technical Considerations and Calculations

As mentioned in section 6.2.3.2.4, for the driver stage a very approximate calculation was used. An i_p-e_g characteristic was drawn at 1700 volts from the published data. From this it was calculated that maximum gm = 25, 000 x 10^{-6}. It was then estimated that half of this value was a sufficiently close approximation to an effective g_m. Using this assumption effect plate loads were calculated for both the desired operation and for a published "typical operation".

Assuming that the same relation exists between the rms currents in both cases a close approximation to the peak pulse current to the plate can be calculated. The resulting value was 0.4A. Machlett confirmed that this value was well within the capabilities of the tube. Very likely the approximation of gm = 12, 500 x 10^{-6} is too high. It is however, almost certain to be within 50 percent of the correct value. The lower realized value, which will have to be obtained experimentally for other reasons, will require a larger value of plate load to get the desired gain. This will result in a smaller value of plate current and make the use of the tube even less marginal. The higher plate load is practical as the 1000 ohms calculated results in a Q of 50. In practice a value of Q of better than twice this value is easily achieved.

In both the triode driver and the tetrode final stage bias to cutoff was assumed. In neither case was pulsed electrode voltages assumed, although in practice this may be necessary. In calculating the tetrode output stage an Emiac application bulletin was used. This bulletin, in effect, gives a normalized fourier analysis for a typical tetrode. To use this it was also necessary to draw an i_p-e_g characteristic and to numerically integrate the plate current to obtain the average value. This method gives a much closer approximation to the equivalent g_m.

In both of these cases it was assumed that power gain was given by equation U-1.

$$\text{Power gain} = g_m R_p \tag{U-1}$$

This is only an approximation, but lack of information as to the true input admittance requires this approximation. The true input admittance is given by:

$$Y_{in} = \frac{1}{R_1} + \frac{R_2\,(1-g_{in}\,R_2)}{R_2^2 + \dfrac{1}{(\omega C)^2}} \tag{U-2}$$

In this equation R_1 is associated with input circuit loss and R_2 with a component of electron energy derived from the input. The capacity is the coupling capacity between these accelerated electrons and the physical grid. If it is assumed the capacitive reactance is low because of the frequency and values of R_1 and R_2 are large, then power gain as expressed in equation (U-1) results. It is extremely difficult to obtain values for R_1 and R_2 and C so that it is fortunate that the gain calculated from (U-1) is a good approximation.

An equation for the transit time was also derived. This is given in (U-3).

$$T_t = \sqrt{\frac{2}{\eta}} \left[\frac{d_g}{\sqrt{V_g}} - d_s \right] \left\{ \frac{\sqrt{V_g}}{V_s - V_g} - \sqrt{\frac{V_g}{(V_s - V_g)^2} + \frac{1}{V_s - V_g}} \right\}$$
$$-d_p \left\{ \frac{\sqrt{V_s}}{V_p - V_s} - \sqrt{\frac{V_s}{(V_p - V_s)^2} + \frac{1}{V_p - V_s}} \right\} \qquad \text{(U-3)}$$

$$\sqrt{\frac{2}{\eta}} = 3.98 \times 10^{-6}$$

d_g = cathode-grid spacing in meters

d_s = grid-screen spacing in meters

d_p = screen-plate spacing in meters

V_g = grid electrode voltage

V_s = screen electrode voltage

V_p = plate electrode voltage

To calculate the allowed supply voltage change for a small increment of total phase shift equation (U-4) may be used.

$$\Delta V = \frac{\Delta\phi T}{360 \left(\frac{\partial T_t}{\partial V} \right)} \qquad \text{(U-4)}$$

T = rf period in seconds

V = any of the electrode voltages, V_g, V_s, V_p.

In equation (U-3) above as well as equations (U-5), (U-6), and (U-7) below it should be kept in mind that the electrode voltages substituted in the equations are the instantaneous values. The incremental voltage calculated from V, is, however, the tolerance on the supply voltage for an allowed phase shift.

Equations (U-5), (U-6), and (U-7) give the incremental change in total transit time for small changes in the electrode voltages.

$\dfrac{\partial T_t}{\partial V_g}$ = change in transit time for control grid variations

$$= -\frac{1}{2}\sqrt{\frac{2}{\eta}}\left[\frac{d_g}{V_g^{3/2}} + d_s\left\{\frac{\dfrac{V_s - V_g}{\sqrt{V_g}} - 2\sqrt{V_g}}{(V_s - V_g)^2} - \frac{\dfrac{3V_s - V_g}{(V_s - V_g)^3} + \dfrac{1}{(V_s - V_g)^2}}{\left[\dfrac{V_g}{(V_s - V_g)^2} + \dfrac{1}{V_s - V_g}\right]^{1/2}}\right\}\right]$$

(U-5)

∂T_t = change in transit time for screen grid variations

$$= \sqrt{\frac{2}{\eta}}\left[d_s\left\{\frac{V_g}{(V_s - V_g)^2} - \frac{\dfrac{2V_g}{(V_s - V_g)^3} + \dfrac{1}{(V_s - V_g)^2}}{\left[\dfrac{V_g}{(V_s - V_g)^2} + \dfrac{1}{V_s - V_g}\right]^{1/2}}\right\}\right.$$

$$\left. - dp\left\{\frac{\dfrac{V_p - V_s}{2 V_s} + V_s}{(V_p - V_s)^2} - 1/2\,\frac{\dfrac{V_p + V_s}{(V_p - V_s)^3} + \dfrac{1}{(V_p - V_s)^2}}{\left[\dfrac{V_s}{(V_p - V_s)^2} + \dfrac{1}{V_p - V_s}\right]^{1/2}}\right\}\right]$$

U-6)

$\dfrac{\partial T_t}{\partial T_p}$ = change in transit time for plate voltage variations.

$$= \sqrt{\frac{2}{\eta}}\,d_p\left\{\frac{V_s}{(V_g - V_s)^2} \cdot \frac{\dfrac{2 V_s}{(V_p - V_s)^3} + \dfrac{2}{(V_p - V_s)^2}}{\left[\dfrac{V_s}{(V_p - V_s)^2} + \dfrac{1}{V_p - V_s}\right]^{1/2}}\right\}$$

U-7)

Equation (U-3) may be used to determine the transit time in a triode by setting $d_p = 0$ and substituting the real d_p' for d_s and the real V_p for V_s. The tolerances on the triode voltages can be obtained from (U-5) and U-6) by making the same substitutions.

Equations (U-3), (U-5), (U-6) and (U-7) are approximations to the transit time and the variation of the transit time with the various voltage changes. They are equations for a particular electron crossing from cathode to plate under conditions of the specific electrode voltages. To use these equations it is necessary for the user to select an electron which is considered to be typical of the phase delays or, perhaps, select an electron which is believed to give conservative results. The latter selection was chosen for the calculations. It was chosen to work with the electron which left the cathode at the time when the grid voltage was at its most positive phase and the plate voltage was at its most negative value. This selection was made because this is the phase in which the transit time will be most effected by plate voltage changes and also because this is the phase in which the current was a maximum, so that the electron represents the largest increment of current.

Second or third order approximations to the transit time effects became rapidly more complex to handle, for small increments of improvements in the results. In the ultimate, relation (U-3) defines only the transit time for the increment of current passing from cathode to plate at the equivalent electrode voltages used. The equivalent voltage would have to take into account the flight time between electrodes, the phase of arrival at a particular electrode, and the phase variation of voltage due to tuning.

These voltages would have to be estimated at the beginning of the calculation and then corrected towards the end after better numbers had been established for the phase and magnitude of the fundamental current component at the plate.

Having the transit time for the particular increment of current pulse over an rf cycle could then be constructed using this transit time and specific $i_p = e_g$ characteristic for the tube at the assumed electrode voltages. The fundamental component of the plate current could then be determined by a numerical fourier analysis. Using this component it would then, in general, be necessary to correct the transit time, etc., until a closed calculation was achieved.

An exact solution of the type outlined above can be obtained easily only if the calculations are done on a computer.

APPENDIX V

GROUND STATION LOW NOISE PREAMPLIFIER

To keep the required peak power of the satellite transmitter low, an extremely low noise preamplifier is required at the ground station. The two types of amplifier which merit consideration because of the low noise, sensitivity, stability and reliability characteristics required are the maser and the parametric amplifier. If the choice had to be made today it probably would be the maser amplifier, since the system noise figure achievable with the maser is approximately two fifths that of the system noise figure for the parametric amplifier.[1] The feasibility of a system with a noise temperature of 50°K or less is demonstrated by the Telstar system.

The maser amplifier operating at Andover, Maine, as part of the Telstar ground complex, is selected as an example of the present state of the art in respect to the use of masers. The basic components of the maser amplifier are the maser, the magnet, the pump and the liquid helium cooling system. The maser used for Telstar is a travelling wave maser with the following general characteristics.[2]

Center frequency:	4,170 mc
Effective instantaneous bandwidth:	25 mc
Effective gain:	34.5 db
Pump frequency:	30,175 mc
Pump power:	70 mw
Magnetic field:	approx. 3300 gauss
Over-all noise temperature:	3.5°K.
Bath temperature:	4.2°K.
Liquid helium consumption:	approx. 1/2 liter/hr.
Helium capacity:	10 liters
Power output at 1-db gain compression:	-38 dbm

The frequency of 4,170 MC is greater than four times the frequency (970 and 990 MC) to be used in the Navigation Satellite program. To achieve the same gain at the lower frequencies a much larger maser or a more effective slow wave structure is needed since

$$G = 27.3 \ (-x''F) \ \frac{1}{\lambda_o} \ S \ L \quad \text{where:}$$

G = electronic gain in db

x''= imaginary part of the ruby paramagnetic susceptibility

---

[1] Telstar I NASA SP-32 Vol. 3 June 1963, p. 1907.

[2] Telstar I NASA SP-32 Vol. 3 June 1963, p. 1863-1886.

F = filling factor

L = maser physical length

S = slowing = $\dfrac{\text{velocity of light}}{\text{group velocity of signal}}$

λ_o = free space signal wavelength

The magnetic field must also be stronger due to the fact that at the lower frequency the wave guide structure, and therefore the magnetic gap, is greater. Since Telstar was developed, superconductive magnets have become practical. As the maser is already being operated at 4.2°K, it is no problem to include the magnet in the bath. The supercooled magnets which can provide a powerful magnetic field are small and light in weight but they are very expensive at present. It is expected that the price will decrease as more are produced. The pump is an "X" band klystron. Since the pump frequency will be lower than that of TELSTAR, less difficulty is anticipated in acquiring satisfactory pumps and power supplies.

The bandwidth requirements for the two systems are not equivalent. The principal method of broadbanding in Telstar was accomplished by equalization following the amplifier. Thus some gain was sacrificed for broadbanded application. In the Navigation Satellite System, the principal signal from the satellite is 970 MC with 159 KC bandwidth. Since the 990 MC pulses are transmitted with sufficient power for reception at the vehicle in spite of a lossy antenna, it can be surmised that the 990 MC signal will result in operation well down on the gain curve of the maser and still be satisfactory, thus the full gain of the maser which was 42 db for Telstar may be used for the Navigation program without equalization.

One of the principal disadvantages of maser operation is that the maser must be immersed in liquid helium. The reason for the selection of the 4.2°K operating temperature is that at 4.2°K liquid helium is in equalibrium with its vapor at atmospheric pressure. If lower (and more gainful) temperatures were used the dewar would have to be maintained under a partial vacuum. This would mean periodic interruptions of service since the dewar is open to the atmosphere during each 2-hour period of liquid helium transfer. At 4.2°K Telstar was operated continuously for months since the dewar could be recharged in operation. One charge of liquid helium lasts about 20 hours. A four to five day charge of liquid helium costs about $210. The alternative of using a recycling plant will cost seventy to one hundred thousand dollars.

Telstar has demonstrated that using a travelling wave maser, a system noise figure of 50°K is achievable for navigation system since Telstar achieved a 35°K system temperature. There have been subsequent improvements in masers and the components of masers. At "L" band, a cavity maser may be used instead of a TWM, but a gain of 20 db and a noise temperature of 10°K was being achieved three years ago at various bands.

The other system that cannot be ruled out for future use is the parametric amplifier. An important point in favor of parametric amplifiers is that as the frequency decreases from "S" to "L" bands it becomes easier to design the necessary parametric amplifier, while the maser becomes more of a problem.

The parametric amplifier consists of three basic sections:

    a. A very stable pump

    b. A circulator type parametric amplifier

    c. A cryogenic system

The first advantage of the parametric amplifier in relation to a maser is that there is no highly expensive magnet in the parametric amplifier. The requirements for varactor diodes, with extremely difficult to obtain parameters, is a short coming of the parametric amplifier; however, Bell Laboratories solved this problem by using a gallium arsenide diode. It is also noted that as the frequency decreases the diode problem becomes less severe.

The gain stability of the parametric amplifier is largely dependent upon the stability of pump power level and frequency. The pump would operate at a frequency somewhat above the output frequency. For the "L" band amplifier, and "X" band pump will be necessary. Here the lower frequency of the system proposed in the navigation system compared to the Telstar system is advantageous. To get the low noise temperature required by the system the parametric amplifier must be operated at the temperature of liquid nitrogen. This created a simpler problem than the use of liquid helium in a maser. Bell Labs has developed a cyrogenic system that enables parametric amplifiers to operate for ten days without refill. About 10 liters of liquid nitrogen is used in the dewar for this purpose.

The Telstar I system utilized a two-stage parametric amplifier for test, with one amplifier refrigerated and the other at room temperature.

The following parameters were obtained:

Frequency	4.17 gc
Bandwidth	60 mc min.
System input noise temp.	less than 85° K
Gain	38 db
Gain stability	0.1 db short term
	0.3 db long term

Although the present maser makes possible lower noise temperatures and slightly better stability, a parametric amplifier can be used at lower initial costs, lower maintenance and operational costs.

APPENDIX W

DYNAMIC DEFLECTIONS OF THE GRAVITY GRADIENT MAST
AND OF THE RADAR ANTENNA BOOMS

W.1 MOTION OF THE MAST DUE TO THERMAL BENDING

Thermal bending takes place about the center of mass, and the mass distribution is such that the instantaneous angular momentum sums to zero. The c.m. is assumed to be close to the satellite by virtue of the fact $m_1 \gg m_2$. Further, the angular error encountered by assuming the end-point to end-point line is coincident with the inertial axis is small for increasing modes. The angle is conservative for the fundamental mode (30% high) and is within 7% of the actual value for higher modes. Mast bending is shown in figure W-1.

W.1.1 Equations of Motion

Therefore the equation of displacement is assumed to be sinusoidal over L, the length of the mast, and is composed of the sum of its normal modes[1]:

$$y = \sum_{i=1}^{\infty} \phi_i \, U_i \, (X)$$

where:

$$U_i \, (X) = \sin \frac{i \pi X}{L}$$

and:

$$\phi_i = i^{\text{th}} \text{ normal coordinate}$$

The kinetic energy (T) and the potential energy (V) of the moving mast are evaluated:

$$T = \frac{1}{2} \rho A \int_0^L (\dot{y})^2 \, dX = \sum_{i=1}^{\infty} \frac{\rho A}{2} (\dot{\phi}_i)^2 \int_0^L (U_i \, (X))^2 \, dX$$

$$V = \frac{EI}{2} \int_0^L (y'')^2 \, dX = \sum_{i=1}^{\infty} \frac{EI}{2} \phi_i^2 \int_0^L \left[U_i^{''} \, (X) \right]^2 \, dX$$

where the cross products $\displaystyle \int_0^L \left[U_i \, (X) \right] \left[U_j \, (X) \right] dX$

reduce to zero for i=j.

---

[1] Timoshenko & Young – Advanced Dynamics, McGraw-Hill Publishing Co., 1948

The Lagrangian is L = T - V. Operations on the Lagrangian yield the equations of motion for the mast.

$$\frac{\partial}{\partial t}\frac{\partial L}{\partial \dot{\phi}} = \rho A \sum_{i=1}^{\infty} \ddot{\phi}_i \int_0^L \left[U_i (X)\right]^2 dX$$

$$-\frac{\partial L}{\partial \phi} = EI \sum_{i=1}^{\infty} \phi_i \int \left[U_i'' (X)\right]^2 dX$$

For the ith coordinate, the equations of motion are derived from

$$\frac{\partial}{\partial t}\frac{\partial L}{\partial \dot{\phi}_i} - \frac{\partial L}{\partial \phi_i} = Q_i ,$$

whence:

$$\rho A \ddot{\phi}_i \int_0^L \left[U_i (X)\right]^2 dX + EI \phi_i \int_0^L \left[U_i'' (X)\right]^2 dX = Q_i$$

where Q_i = the generalized force.

Since

$$\int_0^L \left[U_i (X)\right]^2 dX = \int_0^L (\sin\frac{i \pi X}{L})^2 dX = \frac{L}{2}$$

and

$$\left[U_i''\right]^2 = (\frac{i \pi}{L})4, \left[U_i\right]^2$$

The Lagrangian equation of motion is therefore:

$$\frac{\rho A L}{2}\ddot{\phi}_i + \frac{EI \pi^4}{2L^3} i^4 \phi_i = Q_i$$

$$\therefore \ddot{\phi}_i + p_i^2 \phi_i = \frac{2 Q_i}{\rho A L} = Q_i'$$

$$p_i^2 = \frac{EI \pi^4}{\rho A L^4} i^4 = \left[\text{natural frequency}\right]^2 \text{ of } i^{th} \text{ mode.}$$

The solution for ϕ_i depends on the nature of Q_i.

The generalized force Q_i is determined by noting that a displacement independent moment M_t imparts energy to the boom according to:

$$M_t \, (\Delta \theta) = \Delta E = \sum M_t \left(\frac{d\theta}{dX}\right) \Delta X = \int_0^L M_t \left(\frac{d\theta}{dX}\right) dX$$

$$= M_t \int_0^L \left(\frac{d^2 y}{dX^2}\right) dX$$

$$= M_t \sum_{i=1}^{\infty} \phi_i \int_0^L (U_i'') \, dX$$

For the ith mode, the energy is:

$$\Delta E_i = M_t \, \phi_i \int_0^L \frac{d \, U_i'}{dX} \, dX$$

$$\Delta E_i = E_i = M_t \phi_i \left[U_i' \, (L) - U_i' \, (0) \right]$$

An incremental change in the normal coordinate by the generalized force causes an incremental change in the energy:

$$Q_i \, \delta \, \phi_i = \delta E_i = M_t \, \delta \, \phi_i \left[U_i' \, (L) - U_i' \, (0) \right]$$

$$\therefore \; Q_i = M_t \left[U_i' \, (L) - U_i' \, (0) \right]$$

$$U_i' = \frac{i \pi}{L} \cos \frac{i \pi X}{L}$$

$$U_i' \, (L) = \frac{i \pi}{L} \cos i \pi$$

$$U_i' \, (0) = \frac{i \pi}{L}$$

$$\therefore \; Q_i = M_t \frac{i \pi}{L} (\cos i \pi - 1)$$

$$\therefore \quad Q_1 = -\frac{2\pi}{L} M_t$$

$$Q_2 = 0$$

$$Q_3 = -\frac{6\pi}{L} M_t$$

etc.

The thermal moment is derived in the following manner. For any temperature profile across the mast, the thermal stress is given by:

$$s = \epsilon E = C_T E (T - T_{ref})$$

Where T_{ref} is that temperature which occurs at a location where the first moments of stress on either side of this location are balanced. This location is the equivalent neutral axis. A temperature profile is shown in figure W-2.

The bending moment becomes:

$$M_t = 2 \int_o^{h_n} s_t \cdot W \cdot (h_n - h) \cdot dh$$

$$= 2 \int_o^{h_n} W \cdot C_T \cdot E \cdot (h_n - h) \cdot \left[T(h_n) - T(h) \right] dh$$

The neutral axis is defined by:

$$\int_o^{h_n} W \cdot C_T \cdot E \cdot (h_n - h) \cdot \left[T(h_n) - T(h) \right] dh =$$

$$\int_{h_n}^{h_o} W \cdot C_T \cdot E \cdot (h - h_n) \cdot \left[T(h) - T(h_n) \right] dh$$

For a uniform temperature gradient the thermal moment reduces to:

$$M_t = 2 \int_o^{h_o/2} W \cdot C_T \cdot E \cdot \left[\frac{h_o}{2} - h \right] \left[(T_o + \frac{\Delta T}{2}) - (T_o + \frac{\Delta T}{h_o} h) \right] dh$$

$$= 2 \cdot W \cdot C_T \cdot E \int_o^{h_o/2} \left[\frac{h_o}{2} - h \right] \left[\frac{\Delta T}{2 h_o} \right] \left[h_o - 2h \right] dh$$
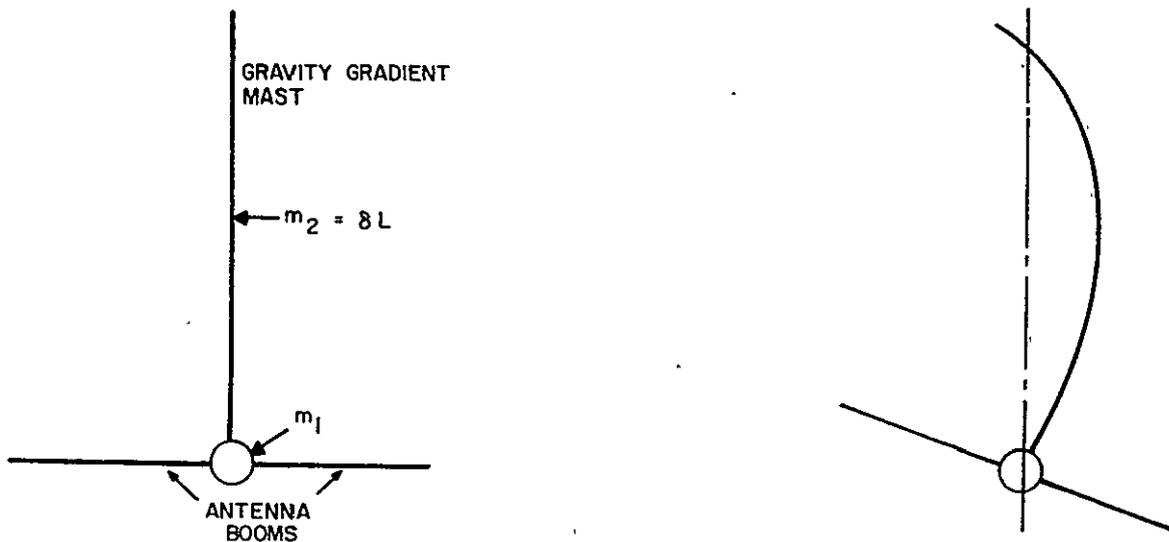
W-4

Figure W-1. Bending of Gravity Gradient Mast in Inertial Space
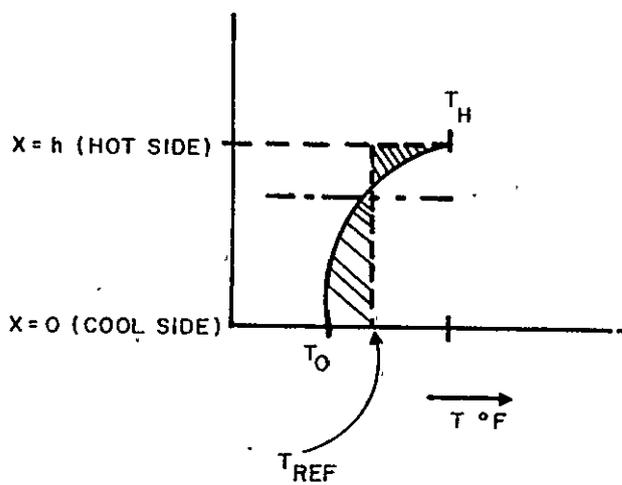

Figure W-2. Temperature Profile for Mast

$$= 2 \cdot W \cdot C_T \cdot E \cdot \frac{\Delta T}{2 h_o} \int_0^{h_o/2} \left[\frac{h_o^2}{2} - 2 h_o h + 2h^2 \right] dh$$

$$= W \cdot C_T \cdot \frac{\Delta T \ E}{h_o} \left[\frac{h_o^3}{4} - \frac{h_o^3}{4} - \frac{h_o^3}{12} \right]$$

$$= \frac{1}{12} W \cdot C_T \cdot \Delta T \ h_o^2 \ E = \frac{C_T \ \Delta T \ EI}{h_o}$$

For non-uniform gradients, as in dynamic responses, numerical methods are generally best used to determine the thermal moment due to the nature of the function which describes the temperature wave.

The thermal moment will assume a characteristic form in time which can be approximated by the following:

$$M_t \ (t) = M_t \ (\infty) \left[1 - e^{-t/\tau} \right] .$$

Applying this moment to the mast:

$$\ddot{\phi}_i + p_i^2 \ \phi_i = \frac{2 \pi}{\rho A L^2} \left[(\cos i - \pi 1) \right] \left[M_t \ (t) \right] ,$$

or

$$\ddot{\phi}_i + p_i^2 \ \phi_i = \frac{2 \pi}{\rho A L^2} \left[M_t \ (t) \right]_i$$

whence:

$$\phi_i = \frac{2 \pi}{\rho A L^2} \left\{ \frac{\left[M_t \ (\infty) \right]_i}{p_i^2 + \frac{1}{\tau^2}} \left[- \frac{\sin p_i t}{p_i \tau} - \frac{\cos p_i t}{p_i^2 \tau^2} \right] + \frac{\left[M_t \ (\infty) \right]_i}{p_i^2} \cdot \left[1 - \frac{p_i^2}{p_i^2 + \frac{1}{\tau^2}} \ e^{-t/\tau} \right] \right\}$$

The parameter of interest is the angle of the satellite with respect to the earth radial. This is

$$\theta_s = y' \ (0) = \sum_{i=1}^{\infty} \phi_i \ U_i' \ (0)$$

where:

$$U_i'(0) = \frac{i\pi}{L} \cos \left. \frac{i\pi X}{L} \right|_{X=0} = \frac{i\pi}{L}$$

The angular displacement of the ith mode of the mast at the satellite base, and therefore the satellite, is

$$\theta_{s_i} = \frac{i\pi}{L} \phi_i$$

$$\left| \theta_s \right|_i = \frac{2\pi^2}{\rho A L^3} \left[i^2 (\cos i\pi - 1) \right] M_t(\infty) \left\{ \frac{1}{p_i^2 + \frac{1}{\tau^2}} \left[-\frac{\sin p_i t}{p_i \tau} - \frac{\cos p_i t}{p_i^2 \tau^2} \right] + \right.$$

$$\left. \frac{1}{p_i^2} \left[1 - \frac{p_i^2}{p_i^2 + \frac{1}{\tau^2}} e^{-t/\tau} \right] \right\}$$

where:

$$M_t(\infty) = C_T \Delta T\, EI/h$$

and

$$p_i^2 = \frac{EI\,\pi^4}{\rho A L^4} i^4 .$$

The mast deflection, and therefore the satellite rotation, reduces to:

$$\left| \theta_s \right|_i = \left[\frac{4}{\pi^2} \frac{C_T \Delta T L}{i^2 h} \right] \left\{ \left[\frac{i}{1 + \frac{1}{p_i^2 \tau^2}} \right] \left[-\frac{\sin p_i t}{p_i \tau} - \frac{\cos p_i t}{p_i^2 \tau^2} + \left(1 + \frac{1}{p_i^2 \tau^2}\right) e^{-t/\tau} \right] \right\}$$

The rate is:

$$\left| \dot{\theta}_s \right|_i = \frac{1}{\tau} \left[\frac{4}{\pi^2} \frac{C_T \Delta T L}{i^2 h} \right] \left\{ \left[\frac{1}{1 + \frac{1}{p_i^2 \tau^2}} \right] \left[-\cos p_i t + \frac{\sin p_i t}{p_i \tau} + e^{-t/\tau} \right] \right\}$$

For
$$p_i \tau \gg 1$$

$$\left| \dot{\theta}_s \right|_i \approx \frac{2}{\tau} \left[\frac{4}{\pi^2} \frac{C_T \Delta T L}{i^2 h} \right]$$

For
$$p_i \tau \ll 1$$

$$\left| \dot{\theta}_s \right|_i \approx p_i \left[\frac{4}{\pi^2} \cdot \frac{C_T \Delta T L}{i^2 h} \right]$$

For this design,

$$p_i = .1039 \text{ sec}^{-1} \qquad \qquad \Delta T = 0.1°F$$
$$\tau = 24 \text{ sec.} \qquad \qquad C_T = 10^{-5}/°F$$
$$L = 2.4 \times 10^3 \text{ in} \qquad \qquad h = 0.5 \text{ in.}$$

$$p_i \tau = 0.333$$

$$\theta_s\Big|_i = (1.9 \times 10^{-3})\left[-.300 \sin p_i t - .900 \cos p_i t + 1 - .10 e^{-t/\tau} \right] \text{ radians}$$

and

$$\dot{\theta}_{s_i} = 0.0800 \times 10^{-3}\left[-0.10 \cos p_i t + 0.30 \sin p_i t + 0.10 e^{-t/\tau} \right] \text{ radians/sec.}$$

The time constant associated with thermal bending is primarily determined by the rate of change of solar flux as the satellite passes through the earth's penumbra. The penumbra is given by the apparent diameter of the sun when viewed from the earth's orbit.

$$\epsilon = \frac{\text{diameter of sun}}{\text{distance to sun}}$$

$$= \frac{751,680 \text{ nmi}}{80,700,000 \text{ nmi}}$$

$$= .0094 \text{ radians}$$

For an orbital rate of 2.48×10^{-4} rad/sec, the time required to pass from full shadow to full sunlight is 38 seconds. This can be represented by a simple exponential function with a time constant of 24 seconds.

The temperature drop across the mast is calculated by assuming that half of the absorbed heat is conducted to the cooler side, since the temperature drop is small. The heat absorbed is:

$$q = \alpha S \sin \theta A$$

where:

α = solar radiation absorptivity = .025

S = solar flux = 440 Btu/hr. ft^2

θ = angle between mast and solar flux = 21.5°

A = absorbing area of mast = 1/2" x length (L)

$\therefore q = .168$ W Btu/hr.

The heat conducted to the cool side is:

$$1/2 \, q = .084 \text{ W Btu/hr} = \frac{k A_c \Delta T}{L_c}$$

where:

k = thermal conductivity of Be Cu mast = 100 Btu/hr ft. F°

A_c = conduction area = 2 t L

t = mast wall thickness = .002"

L_c = conduction path length $\approx$ h = diameter of mast

Solving ΔT:

$\Delta T = 0.10°F$

W. 1. 2 Comparison of Mast Coordinates and Inertial Coordinates

With little error, the mast coordinates can be measured from a line connecting the end points of $\sin \frac{\pi x}{L}$ instead of the true inertial coordinates as the following shows.

Conservation of momentum for the mast fundamental yields:

$$\int y x \, dm = 0 = A\rho \int yx \, dx$$

$$= A\rho \int_0^L (y_0 \sin \frac{\pi x}{L} - \alpha x) x \, dx$$

$$= A\rho \left[y_0 \int_0^L x \sin \frac{\pi x}{L} \, dx - \int_0^L x^2 \, dx \right]$$

$$= A\rho \left[y_0 (\frac{L}{\pi})^2 \pi - \alpha \frac{L^3}{3} \right]$$

$$\therefore \alpha = \frac{3}{\pi} \frac{y_0}{L}$$

Now referring to figure W-3,

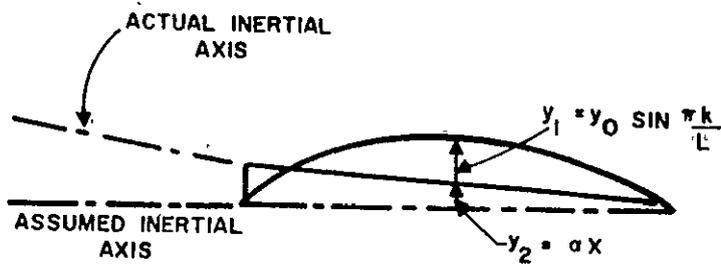$$\alpha_{max} = \frac{dy}{dx} \bigg|_{x=0} = \frac{\pi}{L} y_0$$

$$\therefore \alpha/\alpha_{max} = \frac{3}{\pi} \frac{y_0}{L} \cdot \pi \frac{L}{y_0} = 3/\pi^2$$

and

$$\alpha_1 \bigg|_{\substack{\text{inertially} \\ \text{corrected}}} = \alpha_{max} - \alpha = \frac{\pi y_0}{L} (1 - \frac{3}{\pi 2})$$

$$= .7 \alpha_{max}$$

For higher modes, the error is smaller. The second mode has

$$A\rho \int_0^L yx \, dx = A\rho \int_0^L y_0 (\sin \frac{2\pi x}{L}) x \, dx - A\rho \int_0^L \alpha x^2 \, dx$$

$$= y_0 (\frac{L}{2})^2 \left[-2\pi \right] - \frac{\alpha L^3}{3}$$

ACTUAL INERTIAL
AXIS

$y_1 = y_0 \sin \dfrac{\pi k}{L}$

ASSUMED INERTIAL
AXIS

$y_2 = \alpha X$

MAST COORDINATES AND INERTIAL COORDINATES
FIRST MODE (a)

ASSUMED INERTIAL AXIS

ACTUAL INERTIAL AXIS
SECOND MODE (b)

ACTUAL INERTIAL
AXIS

ASSUMED INERTIAL AXIS

α_{MAX}
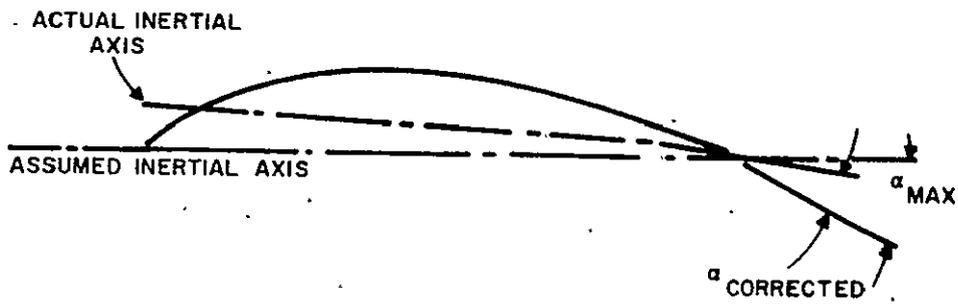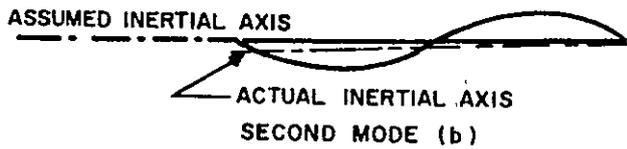
$\alpha_{CORRECTED}$

Figure W-3. Mast Coordinates

$$\alpha \text{ max} = y_0 \frac{2 \pi}{L}$$

$$\alpha_2|_{\substack{\text{inertially} \\ \text{corrected}}} = \alpha_{\text{max}} (1 + .075)$$

$$= 1.075 \, \alpha_{\text{max}}.$$

. Comparing actual curvature due to thermal bending moments with assumed flexure, the bending moment is found to be:

$$M_t = 2 \int_0^{h/2} y \cdot s(y) \cdot W(y) \cdot dy$$

$$= 2 \int_0^{h/2} E \, C_T \Big[(T_y - T_o) \, y \Big] \, W(y)$$

also

$$I = 2 \int_0^{h/2} y^2 \cdot W(y) \cdot dy$$

Assuming a uniform temperature gradient,

$$(T_y - T_o) = \frac{\Delta T/2}{h/2} \, y = \frac{\Delta T}{h} \, y$$

$$M_t = 2 \, EC_T \int_0^{h/2} \frac{\Delta T}{h} \, y^2 \cdot W(y) \cdot dy$$

$$= \frac{2 \, C_T \Delta T E}{h} \int_0^{h/2} y^2 \cdot W(y) \cdot dy$$

$$\frac{M_t}{I} = \frac{C_T \Delta T \, E}{h}$$

A beam deflects according to the following, for a moment applied to it, where θ is the slope at each end:

$$y'' = \frac{M}{EI} = \frac{1}{R} = \frac{2 \theta}{L}$$

$$\therefore \theta = \frac{ML}{EI} = 0.50 \, \frac{C_T \Delta TL}{h}$$

For the sinusoidal flexure,

$$\theta = \frac{4}{\pi^2} \, \frac{C_T \Delta T \, L}{h} = .405 \, \frac{C_T \Delta TL}{h}$$

$$\frac{\theta_{\text{sinusoidal}}}{\theta_{\text{actual}}} = \frac{.405}{.50} = 0.8$$

Combining this with the inertial correction for the fundamental:

$$\frac{\theta_{\text{theoretical}}}{\theta_{\text{actual}}} = \frac{\theta_{\text{sinusoidal}}}{\theta_{\text{actual}}} \cdot \frac{\alpha_{\text{max}}}{\alpha_{\text{inertially corrected}}}$$

$$= (0.8)/(0.7) = 1.1$$

$\therefore \ \theta_{\text{actual}} \approx .9 \ \theta_{\text{theoretical}}$

W.1.3 Analysis of Satellite 22A

    a. Known data (APL Report   TO: 514)

        Mast (Be Cu):

        $k = 100$ Btu/hr- FT^2- R°

        $\alpha = .4$

        $t = .002$ inches

        $h = .55$ inches

        $L = 100$ ft $= 1200$ inches

        $\rho = .3$ lb/in^3

    b. Performance

        (a) Static offset $= 10°$

        (b) Freq. of fundamental $= .055$ cps

        (c) Time Constant $= 20$ to 60 seconds

        (d) Peak ampl. of oscillation $= 1.2$ to 1.5 degrees

    c. Calculations

$$(1) \quad p_1^{\ 2} = \frac{EI\pi^4}{\rho AL^4}$$

$$p_1 = .273 \ \text{sec}^{-1}$$

$$f_1 = .0435 \ \text{cps}$$

$$(2) \quad y_1' = \frac{4}{\pi^2} \frac{C_T \Delta T L}{h} \left\{ \frac{1}{1 + \frac{1}{p_1^{\ 2}\tau^2}} \right\} \left\{ \frac{-\sin p_1 t}{p_1 \tau} - \right.$$

$$\left. \left\{ \frac{\cos p_1 t}{p_1^{\ 2}\tau^2} + 1 - e^{-t/\tau} + \frac{1}{p_1^{\ 2}\tau^2} \right\} \right.$$

where

$$p_1 \tau = 6.55$$

and

$$\Delta T = \frac{\alpha q A \ell}{2k A_c} = \frac{q h^2}{4k t} = 12.9^\circ F$$

$$\frac{4}{\pi^2} \frac{C_T \Delta TL}{h} = \frac{4}{\pi^2} \frac{(10^{-5})(12.9)(1200)}{(0.55)} = 0.11 \text{ radian}$$

The sinusoidal peak is

$$y'_{1 \text{ peak}} = (0.11)\left(\frac{1}{pi}\right) = .0168 \text{ rad}$$

$$= 1.0^\circ$$

The offset is

$$y'_{\text{offset}} = 0.11$$

$$= 6.4^\circ$$

    (3) Time Constant

$$\tau \approx .6(\theta_{\text{penumbra}})(\tau_{\text{orbit}}) = (6)(.0094)\left(\frac{6000 \text{ sec}}{2\pi}\right)$$

$$= 5.4 \text{ sec}$$

ITEM	PREDICTED	ACTUAL
1. Static offset (degrees)	6.4	10
2. Sinusoidal peak (degrees)	1.0	1.2 to 1.5
3. Freq. of oscillation (CPS)	.044	.055
4. Time Constant (sec)	5.4	20 to 60

W.2 MOTION OF THE ANTENNA BOOMS DUE TO THERMAL BENDING:

The kinetic energy (T) and potential energy (V) of the booms are

$$T = \frac{\rho A}{2} \int_0^L (\dot{y})^2 \, dx$$

$$V = \frac{EI}{2} \int_0^L (y'')^2 \, dx$$

Assuming the booms' curvature follows a half cosine function:

$$y = \sum \phi_i \, U_i(x)$$

where

$$U_i = 1 - \cos \frac{i \pi x}{2L}$$

whence

$$T = \frac{\rho A}{2} \int_0^L \left[\sum_{i=1}^{\infty} \phi_i \, u_i(x) \right]^2 dx$$

$$V = \frac{EI}{2} \int_0^L \left[\sum_{i=1}^{\infty} \phi_i \, u_i''(x) \right]^2 dx$$

Rayleigh[1] shows that

$$\int_0^L U_n U_m \, dx = 0 \text{ for normal modes.}$$

$$T = \sum_{i=1} \frac{\rho A}{2} \dot{\phi}_i^2 \int_0^L \left[U_i(x) \right]^2 dx$$

$$V = \sum_{i=1} \frac{EI}{2} \phi_i^2 \int_0^L \left[U_i'(x) \right]^2 dx$$

Let

$$F_1(i) = \frac{1}{L} \int_0^L \left[U_i(x) \right]^2 dx = \left[3/2 - \frac{4}{i\pi} \sin \frac{i\pi}{2} \right]$$

Let

$$F_2(i) = L^3 \int_0^L \left[U_i''(x) \right]^2 dx = \frac{\pi^4}{16} i^4 \left(\frac{1}{2} + \frac{\sin \frac{i\pi}{2}}{2\,i\pi} \right)$$

Performing the appropriate operations on the Lagrangian in a manner identical to the preeding section, the equations of motion are derived:

$$\rho AL\, F_1(i)\, \ddot{\phi}_i + \frac{ET}{L^3} F_2(i) \phi_i = Q_i$$

The generalized bending force Q_i associated with the ith mode of the boom is derived rom a consideration of the energy required to bend the boom:

$$\Delta E = M_t (\Delta \theta) = \int_0^L M_t \left(\frac{d\theta}{dx} \right) dx$$

[1] Rayleigh, J.W.S. - Theory of Sound Volumn I, MacMillan Co., 1945

$$= \sum_{i=1} M_t \int_0^L \phi_i \frac{dU_i'(x)}{dx} dx$$

$$= \sum_{i=1} M_t \phi_i \left[U_i'(L) - U_i'(0) \right]$$

For

$$U(x) = 1 - \cos\frac{i\pi}{2L},$$

$$U'(x) = \frac{i\pi}{2L} \sin\frac{i\pi}{2L}$$

For the ith mode,

$$|\Delta E|_i = M_t \phi_i \frac{i\pi}{2L} \sin\frac{i\pi}{2}$$

An incremental change in the energy results in

$$\delta E_i = Q_i \delta\phi_i = M_t \delta\phi_i \frac{i}{2L} \sin\frac{i\pi}{2}$$

The generalized force Q_i associated with the thermal bending of the boom is therefore

$$Q_i = M_t \frac{i\pi}{2L} \sin\frac{i\pi}{2}$$

$$0 = Q_2 = Q_4 = Q_6, \text{ etc.}$$

Allowing

$$\frac{i\pi}{2} \sin\frac{i\pi}{2} = F_3(i),$$

and since

$$M_t = (C_T \Delta_T EI / h)(1 - e^{-t/\tau})$$

The complete equation of motion is

$$\ddot{\phi}_i + \frac{EI}{\rho_{AL}4} \frac{F_2(i)}{F_1(i)} \phi_i = \frac{C_T \Delta_T EI}{\rho_{AL}3 h} \frac{F_3(i)}{F_1(i)} (1 - e^{-t/\tau})$$

The solution is

$$\phi_i = \frac{C_T \Delta_T EI}{\rho_{AL}2 h} \frac{F_3(i)}{F_1(i)} \frac{1}{p_i^2} \left\{ \left(\frac{1}{1 + \frac{1}{p_i^2 \tau^2}}\right) \left(\frac{-\sin p_i t}{p_i \tau} - \frac{\cos p_i t}{p_i^2 \tau^2}\right) + \right.$$

$$\left. \left(1 - \frac{1}{1 + \frac{1}{p_i^2 \tau^2}} e^{-t/\tau}\right) \right\}$$

where

$$p_i^2 = \frac{EI}{\rho A L^4} \frac{F_2(i)}{F_1(i)} \quad *$$

If the end slope of the boom is solved for the fundamental,

$$\frac{dy_1}{dx} = .618 \frac{C_T \Delta T\, L}{h} .$$

All modes, neglecting the modifying dynamic portion of the expression, yield

$$\frac{dy}{dx} = .733 \frac{C_T \Delta T L}{h} .$$

The actual slope is

$$\frac{dy}{dx} = 1.0 \frac{C_T \Delta T L}{h} .$$

Therefore the cosine function indicates a slope which is about 27 percent lower than the actual deflection.

The rate of change of the end slope for the ith mode is:

$$\dot{\phi}_i\, U_i'(L) = \left[\frac{C_T \Delta T L}{h}^2 \frac{F_3(i)}{F_2(i)} \frac{1}{1+\frac{1}{p_i^2 \tau^2}} \left[\frac{\cos p_i t}{\tau} + \frac{\sin p_i t}{p_i^2} + \frac{1}{\tau} e^{-t/\tau} \right] \left[\frac{i\pi}{2L} \sin \frac{i\pi}{2} \right] \right.$$

$$= \left[\frac{4}{\pi^2} \frac{C_T \Delta T L}{h \tau} \right] \left[\frac{1}{1+\frac{1}{p_i^2 \tau^2}} \right] \left[\frac{\sin^2 \frac{i\pi}{2}}{i^2 \left(\frac{1}{2} + \frac{\sin i\pi/2}{2i\pi} \right)} \right] \left[e^{-t/\tau} - \cos p_i t + \frac{1}{p_i \tau} \sin p_i t \right]$$

For $P_1 \tau = .91$ and $\Delta T = .25°F$

$$\dot{y}_1 = \left[\frac{4}{\pi^2} \frac{(10^{-5}/°)(.25°)(600\ in)}{(0.5\ in)(24\ sec)} \right] \left[\frac{1}{2.2} \right] \left[\frac{1}{.66} \right] \left[1.2 \right] = .042 \text{ milliradians/sec}$$

with

y' = 0.9 milliradians

W.3 MOTION OF THE ANTENNA BOOMS DUE TO SATELLITE MOTION:

In this case it is the motion of the reference axis from which strain deflections are measured that induces further boom motions in inertial space. If Y(x) is the displacement of the boom in inertial space, for small displacements,

$$Y(x) \approx y(x) + \theta x$$

---

*p_1^2 must be modified to account for end mass according to part 4 of this appendix.

where

   θ = angular rotation of reference axis

   y = deflection of boom from reference axis

   x = distance from origin to point on boom

then

$$\dot{Y} = \dot{y} + \dot{\theta} x$$

and

$$\dot{Y}^2 = \dot{y}^2 + \dot{\theta}^2 x^2 + 2\dot{y}\dot{\theta}x$$

In a manner similar to the preceding sections, the kinetic (T) and potential energies (V) are evaluated

$$T = \rho \frac{A}{2} \int_0^L (\dot{Y})^2\, dx = \rho \frac{A}{2} \int_0^L \dot{y}^2\, dx + \rho A \int_0^L \dot{\theta}\dot{y}x\, dx + \frac{\rho A}{2} \dot{\theta}^2 \int_0^L x^2 dx$$

Now

$$\int_0^L \dot{y}^2 dx = \sum_{i=1}^{\infty} \dot{\phi}_i^2 \int_0^L \left[U_i(x)\right]^2 dx = \sum_{i=1}^{\infty} \dot{\phi}_i^2 L\, F_1(i)$$

$$\int_0^L \dot{y}x\, dx = \sum_{i=1}^{\infty} \dot{\phi}_i \frac{L^2}{2}\left[1 - \frac{8}{(i\pi)^2}\cos\frac{i\pi}{2} - \frac{4}{i\pi}\sin\frac{i\pi}{2} + \frac{8}{(i\pi)^2}\right] = \sum_{i=1}^{\infty} \dot{\phi}_i \frac{L^2}{2} F_4(i)$$

$$\int_0^L x^2\, dx = \frac{L^3}{3}$$

Also

$$V = \frac{EI}{2} \int_0^L (y'')^2\, dx = \frac{EI}{2} \sum_{i=1}^{\infty} \phi_i^2 \frac{\pi^4}{16L^3} i^4 \left(\frac{1}{2} + \frac{\sin\frac{i\pi}{2}}{2\,i\pi}\right) = \frac{EI}{2} \sum_{i=1}^{\infty} \frac{F_2(i)}{L^2} \phi_i^2$$

Performing the necessary operations on the Lagrangian (L), where L = T - V,

$$\frac{\partial}{\partial t} \frac{\partial L}{\partial \dot{\phi}} = \frac{\rho A}{2} \sum_{i=1}^{\infty} \left[2\ddot{\phi}_i\, L\, F_1(i) + \ddot{\theta}L^2\, F_4(i)\right] \quad \text{and} \quad -\frac{\partial L}{\partial \phi} = \frac{EI}{L^3} F_2(i)\,\phi i$$

The equation of motion for the ith mode is therefore

$$\left(\frac{\rho A}{2}\right)(2LF_1(i)\ddot{\phi}_i + L^2 F_4(i)\ddot{\theta}) + \frac{EI}{L^3} F_2(i)\phi_i = 0$$

Rearranging,

$$\ddot{\phi}_i + \frac{EI}{\rho AL^4}\frac{F_2(i)}{F_1(i)}\phi_i = -\frac{L}{2}\frac{F_4(i)}{F_1(i)}\ddot{\theta}$$

where $\ddot{\theta}$ is synonomous with the acceleration of the satellite orientation due to the bending of the mast, as derived in section W.1 of this appendix. Note that the left side of the equation is identical with that of section W.2, thermal bending, as one would expect. Differentiating θ with respect to time twice yields the acceleration. Care must be exercised at this point to avoid confusing boom and mast parameters, since it is the latter which primarily determine the magnitude of the satellite rotation and the former which determine the response. Accordingly, the mast frequencies are designated by ω_k and the boom frequencies by p_i. The mast length is L' and the boom length is L. The magnitude of the acceleration corresponding to the kth mode of the mast is

$$
\ddot{\theta} = \frac{1}{\tau^2}\left[\frac{2\pi^2}{\rho A L'^3}\ \frac{M_t(\infty)}{\omega_k^2}\right]\left[k^2(\cos k\pi)\right]\left[\frac{1}{1+\frac{1}{\omega_k^2\tau^2}}\right]\left[\cos\omega_k t + \omega_k\tau\sin\omega_k t - e^{-t/\tau}\right]
$$

$$
= G(k)\left[\cos\omega_k t + \omega_k\tau\sin\omega_k t - e^{-t/\tau}\right]
$$

The solution for ϕ_i is:

$$
\phi_i = \frac{F_4(i)\ G_1(k)\ L}{2F_1(i)\ p_i^2}\left\{\frac{i}{1-\frac{\omega_k^2}{p_i^2}}\left[(\cos\omega_k t - \cos p_i t) + \omega_k\tau(\sin\omega_k t - \frac{\omega k}{p_i}\sin p_i t)\right]\right.
$$

$$
\left. + \frac{1}{1+\frac{1}{p_i^2\tau^2}}\left[\cos p_i t - \frac{1}{p_i\tau}\sin p_i t - e^{-t/\tau}\right]\right\}
$$

where it is assumed $\omega_k \neq p_i$. If $\omega_k = p_i$, then a large boom deflection is indicated. This will be limited by the effects of damping and finite system energy which were not included in this derivation. These effects are considered in the following sections of this appendix. Finally the deflection of the boom and its end slope are

$$
y = \sum_{i=1}^{\infty}\phi_i\left(1 - \cos\frac{i\pi}{2}\right)
$$

$$
y' = \frac{\pi}{2L}\sum_{i=1}^{\infty}i\phi_i\sin\frac{i\pi}{2}
$$

Note that if $\omega_k\tau$ is smaller than 1.0, corresponding to a quickly developed thermal moment, then the satellite angular acceleration for the fundamental mast mode is:

$$
\ddot{\theta}_1 = \left[\frac{4}{\pi^2}\ \frac{C_T\Delta T L'}{h}\ \omega_1^2\right]\left[e^{-t/\tau} - \cos\omega_1 t\right]
$$

which quickly diminishes to

$$
\theta_1 = -\left(\frac{4}{\pi^2}\ \frac{C_T\Delta T L'}{h}\ \omega_1^2\right)\cos\omega_1 t.
$$

W-18

For the disturbance frequency ω_k sufficiently lower than the resonant frequency of the boom p_i, the time independent part of the displacement becomes,

$$y_1 = \left(\frac{4}{\pi^2} \frac{C_T \Delta TL'}{h} \frac{\omega_1^2}{p_1^2}\right) \frac{L}{2} \frac{F_4(1)}{F_1(1)} = \frac{2}{\pi^2} \frac{C_T \Delta TL'}{h} \frac{\rho AL^5 F_4(1)}{EI F_2(1)} \omega_1^2$$

$$= \frac{2}{\pi^2} \frac{.53}{.66} \frac{16}{\pi^4} \left(\frac{C_T \Delta TL'}{h}\right) \rho AL^5 \omega_1^2 / EI = .0264 \left(\frac{C_T \Delta TL'}{h}\right) \rho AL^5 \omega_1^2 / EI$$

The equivalent static load applied to a cantilever beam yields

$$y = .0167 \left(\frac{C_T \Delta TL'}{h}\right) \rho AL^5 \omega_1^2 / EI$$

Therefore, the cosine flexure equation yields a deflection for the fundamental which is about 60 percent larger than the actual deflection for a cantilever beam of the same geometry and with the equivalent static load.

In evaluating the natural frequencies of the boom, Rayleigh notes that certain derived values of i must be used instead of the integral values 1, 2, 3, etc. corresponding to these modes. The natural frequencies are

$$p_n = a_n \sqrt{\frac{EI}{\rho AL^4}}$$

where

$$a_n \approx \left[\frac{1}{2}(2n-1)\pi\right]^2.$$

This value a_n corresponds to the previously derived quantity

$$\left[\frac{F_2(i)}{F_3(i)}\right]^{1/2} = \left[\frac{\frac{i^4 \pi^4}{16}\left(1/2 + \frac{\sin\frac{i\pi}{2}}{2i\pi}\right)}{3/2 - \frac{4}{i\pi}\sin\frac{i\pi}{2}}\right]^{1/2} = \frac{\pi^2}{4}i^2\left[\frac{\left(1/2 + \frac{\sin\frac{i\pi}{2}}{2i\pi}\right)}{3/2 - \frac{4}{i\pi}\sin\frac{i\pi}{2}}\right]^{1/2}$$

The proper values of i for the first, second, etc., modes can be derived by setting the above quantity equal to

$$\left[\frac{1}{2}(2n-1)\pi\right]^2,$$

where

n = 1, 2, etc.

or

$i \approx 1.31(2n-1)$ for n>1.

A more exact calculation yields the following:

n	i	a_n
1	0.92	3.5
2	3.97	22.4
3	7.13	61.7

W.4 CALCULATION OF NATURAL FREQUENCIES:

For booms and mast

$$E = 18 \times 10^6 \text{ PS1}$$

$$I/A \approx D^2/8 = .031 \text{ in}^2$$

For mast

$$g\ \rho = .3\ \text{lb/in}^3$$

and

$$L' = 200 \text{ ft} = 2.4 \times 10^3 \text{ inches}$$

For booms, cabling effectively triples the density of the material,

$$g\ \rho = .9\ \text{lb/in}^3$$

and

$$L = 50 \text{ ft} = 600 \text{ inches}$$

Mast:

$$\left[\frac{EI}{\rho A L^4}\right]^{1/2} = \left[\frac{18 \times 10^6 \text{ PS1} \times 0.031 \text{ in}^2 \times 386 \text{ in/sec}^2}{.3 \text{ lb/in}^3 \times 3.3\ 10^{13} \text{ in}^4}\right]^{1/2} = \left[2.18 \times 10^{-5} \text{ sec}^{-2}\right]^{1/2}$$

$$= 4.65 \times 10^{-3} \text{ sec}^{-1}$$

$$\omega_1 = \frac{2}{\pi} \times 4.65 \times 10^{-3} = 4.60 \times 10^{-2} \text{ sec}^{-1} = .0460 \text{ sec}^{-1}$$

$$\omega_3 = 9\pi^2 \times 4.65 \times 10^{-3} = 4.15 \times 10^{-1} \text{ sec}^{-1} = .415 \text{ sec}^{-1}$$

$$\omega_5 = 25\pi^2 \times 4.65 \times 10^{-3} = 1.15 \text{ sec}^{-1} = 1.15 \text{ sec}^{-1}$$

Boom:

$$\left[\frac{EI}{\rho^* A L^4}\right]^{1/2} = \left[\frac{18 \times 10^6 \text{ PS1} \times .031 \text{ in}^2 \times 386 \text{ in/sec}^2}{1.94 \text{ lb/in}^3 \times .13 \times 10^{12} \text{ in}^4}\right]^{1/2} = 2.92 \times 10^{-2} \text{ sec}^{-1}$$

$$p_1 = 3.5 \times 2.92 \times 10^{-2} = .102 \text{ sec}^{-1}$$

$$p_2 = 22.4 \times 2.92 \times 10^{-2} = .655 \text{ sec}^{-1}$$

$$p_3 = 61.7 \times 2.92 \times 10^{-2} = 1.80 \text{ sec}^{-1}$$

The boom frequencies are adjusted to account for the mass of the electronics mounted at the end. If the kinetic energy term is restated,

$$T = \frac{\rho A}{2} \int_0^L (\dot{y})^2 \, dx + \frac{1}{2} m \left[\dot{y}(L)\right]^2 = \frac{\rho A}{2} \sum \phi_i^2 \int_0^L \left[U_i(x)\right]^2 dx + \frac{m}{2} \sum \phi_i^2 \left[U_i(L)\right]^2$$

$$= \sum_i^\infty \phi_i^2 \left[\frac{\rho A L}{4} F_1(i) + \frac{m}{2} (1 - \cos\frac{i\pi}{2})^2\right]$$

ρ^* is adjusted to account for weight of cabling within boom $\Delta W = 3.0$ lbs.

The booms' resonant frequencies are thereby adjusted according to

$$p_i'^2 = p_i^2 \cfrac{1}{1 + \cfrac{m}{\rho AL}\left(\cfrac{1 - \cos\frac{i\pi}{2}}{F_1(i)}\right)^2}$$

where

$$F_1(i) = 3/2 - \frac{4}{i\pi}\sin\frac{i\pi}{2}$$

For

gm = 5.0 lbs

and

gρAL = 3.5 lbs,

the frequencies are

$$(k = 1) \quad p_1 = (.102)\cfrac{1}{\sqrt{1 + \cfrac{1.43}{.23}}} = -.038 \text{ sec}^{-1}$$

$$p_2 = (.655)\cfrac{1}{\sqrt{1 + 0}} = 0.655 \text{ sec}^{-1}$$

$$p_3 = (1.80)\cfrac{1}{\sqrt{1 + \cfrac{1.43}{1.7}}} = 1.33 \text{ sec}^{-1}$$

Similarly, since the satellite structure and the center of mass of the total system are displaced, the natural frequencies of the mast are likewise adjusted. The kinetic energy term is:

$$T = \sum_{i=1}^{\infty} \frac{\rho A}{2}\int_0^L \phi_i^2 \left[U_i(x)\right]^2 + \sum_{i=1}^{\infty} \frac{m}{2}\phi_i^2 \left[U_i(L')\right]^2 = \sum\phi_i^2\left[\frac{\rho AL}{4} + \frac{m}{2}\right]\left[\sin\frac{i\pi L'}{L}\right]^2$$

where

L'/L = 10'/200' = .05

$$T = \sum \phi_i^2 \frac{\rho AL}{4}\left[1 + \frac{2m}{\rho AL}\sin^2 i\pi(.05)\right]$$

Each value of ω_k^2 is accordingly adjusted by the factor

$$\frac{1}{1 + 400\sin^2(.05i\pi)}$$

$$\omega_1 = (.0460)\frac{1}{\sqrt{11}} = .0139 \text{ sec}^{-1}$$

$$\omega_3 = (.415)\frac{1}{\sqrt{81}} = .0460 \text{ sec}^{-1}$$

$$\omega_5 = (1.15)\frac{1}{\sqrt{201}} = .081 \text{ sec}^{-1}$$

RESPONSE OF BOOMS TO SATELLITE MOTIONS INDUCED BY THERMAL
BENDING OF GRAVITY GRADIENT MAST

A Deflection   Boom

		Mode 1		2		3	
	Freq, Sec^{-1}	.038		.655		1.33	
Mast Mode	Freq. Sec^{-1}	Deflection 10^{-3} Radians					
		y/L	y'	y/L	y'	y/L	y'
1	0.0139	0.536	.773	.005	0	*	.006
2	--	--	--	--	--	--	--
3	0.0460	.111	.160	*	0	*	*
4	--	--	--	--	--	--	--
5	0.081	.016	.024	*	0	*	*

*Less than 0.001

B   Rate   Boom

Mast Mode	Mode 1	2	3
	$\frac{d}{dt}(y')$ 10^{-3} Radians/Sec.		
1	.022	0	*
2	--	--	--
3	.012	0	*
4	--	--	--
5	.001	0	*

*Less than .001

W.5 DAMPING OF BOOM MOTION AND MAST MOTION BY MATERIAL HYSTERESIS.

The energy lost in mechanical hysteresis as a material is strained is related to the maximum stored energy[1] by

$$\Delta W \ (LOST) = \gamma W_{max}$$

For a complete cycle,

$$\Delta W = 2 \ \gamma W_{max}$$

The energy stored in either a boom or mast has the form:

$$W_{max} = \sum_{i=1}^{\infty} \phi_i^2 \ \frac{EI}{2} \ \int_0^L \left[U_i'' \ (X) \right]^2 dx$$

The energy lost can be expressed in terms of an equivalent damping factor and the rate of change of displacement:

$$\Delta W = FORCE \ x \ DISPLACEMENT$$

$$= \oint \sum_{i=1}^{\infty} (\beta_i \ \dot{\phi}_i) x \ (\dot{\phi}_i \ dt)$$

$$= \sum_{i=1}^{\infty} \beta_i \ \dot{\phi}_i^2 \ \oint \ sin^2 \omega t \ dt$$

$$= \sum_{i=1}^{\infty} \beta_i \ \dot{\phi}_i^2 \ \omega\pi$$

Where it is assumed the motion is sinusoidal,

$$\dot{\phi} = \omega \phi$$

$$Also \ \Delta W \ /cycle = 2 \gamma \ \sum_{i=1}^{\infty} \phi_i^2 \ \frac{EI}{2} \ \int_0^L (\frac{i \pi}{L})^4 \ sin^2 \ \frac{i \pi x}{L} \ dx$$

for the mast, where $U_i \ (x) = sin \ \frac{i \pi x}{L}$

$$\Delta W/cycle = 2 \ \gamma \sum_{i=1}^{\infty} \phi_i^2 \ \frac{EI}{2} \ (\frac{i \pi}{L})^4 \ \frac{L}{2}$$

$$= \gamma \ \frac{EI \ \pi^4}{2L^3} \ \sum_{i=1}^{\infty} \ \phi_i^2 \ i^4$$

$$\therefore \ \beta_i = \gamma \ \frac{EI \ \pi^3}{2L^3} \ \frac{i^4}{\omega}$$

[1]Newton, R.R., Damping of a Gravitationally Stabilized Satellite, APL Report TG-487. April 1963

For an equation of motion for the mast

$$\frac{1}{2} \rho AL \cdot \ddot{\phi}_i + \beta_i \dot{\phi}_i + \frac{EI\pi^4}{2L^3} i^4 \phi_i = Q_i.$$

The response when expressed in operator form has a characteristic quadratic:

$$\left(\frac{s^2}{\omega_n^2} + \frac{2\zeta}{\omega_n} s + 1\right) \phi$$

where

$$\frac{2\zeta}{\omega_n} = \frac{2\beta_i L^3}{EI\pi^4 i^4}$$

and

$$\omega_n^2 = \frac{EI\pi^4}{\rho AL^4 i^4}$$

For the ith mode, the equivalent damping factor ζ_i is given by

$$\zeta_i \doteq \beta_i \frac{\omega_n L^3}{EI\pi^4 i^4} \qquad \gamma \frac{EI\pi^3}{2L^3} \frac{i^4}{\omega} \frac{\omega_n}{EI\pi^4 i^4} L^3$$

$$= \frac{\gamma}{2\pi}$$

For free vibrations, the characteristic time constant for the decay is

$$\tau = \frac{1}{\zeta\omega_n} = \frac{2\pi}{\gamma\omega_n} \cong \frac{2\pi}{\gamma\omega_k}$$

Values of γ for most metals are about 0.1 or lower. The APL satellite 22A achieved $\gamma = 0.5$ on the mechanical spring in the motion damping system. The time constant for the first three odd harmonic of the mast and boom are given in table W-2.

For a mast disturbance of 1.9 milliradian, the time required for the displacement to reduce to .01 milliradians is 78.5 minutes with $\gamma = .5$. This defines the minimum period over which calibration would be required. Combined boom and mast velocities reduce from .10 milliradians/sec to .01 millirad/sec in 30 minutes.

W.6 CROSS COUPLING EFFECTS BETWEEN MAST AND BOOMS

When the phenomenon of resonance occurs between the mast and the booms, boom displacements can become large compared to the original mast displacement. The boom displacement can no longer be treated as a perturbation to the general satellite - mast motion. That the displacement is finite is shown in the following derivation. For simplicity, the motion is assumed to occur in a plane defined by the mast and two of the four booms.

TABLE W-2. CHARACTERISTIC TIME CONSTANT

MODE	BOOM			MAST		
	Freq Sec^{-1}	τ (Sec) $\gamma=.1$	τ (Sec) $\gamma=.5$	Sec^{-1}	τ (Sec) $\gamma=.1$	τ (Sec) $\gamma=.5$
1	.038	1640	1328	.0139	4480	896
3	.655	95	19	.0460	1360	272
5	1.33	47	9	.081	770	154

The general method is to assume that the mast and boom have similar geometry resulting in identical natural frequencies, then write the Lagrangian for the "n" components of the system and construct an "n" x "n" matrix for determining the eigenvectors and eigenvalues of the motion[1].

The potential energy of the booms and mast due to bending is:

$$V = \frac{K_2}{2} \left(\theta_1 - \theta_2 \right)^2 + \frac{K_3}{2} \left(\theta_1 - \theta_3 \right)^2 + \frac{K_4}{2} \left(\theta_1 - \theta_4 \right)^2$$

where K_2, K_3, K_4 are the spring constants if the booms and mast are assumed to be simple oscillators with only one mode of motion for each by itself.

The kinetic energy of the booms and mast plus the satellite structure (I_1) is

$$T = \frac{1}{2} I_1 \dot{\theta}_1^2 + \frac{1}{2} I_2 \dot{\theta}_2^2 + \frac{1}{2} I_3 \dot{\theta}_3^2 + \frac{1}{2} I_4 \dot{\theta}_4^2 .$$

Written in matrix form:

$$\underline{V} - \omega^2 \underline{T} = \begin{vmatrix} K_1 - \omega^2 I, & -K_2 & -K_3 & -K_4 \\ -K_2 & K_2 - \omega^2 I_2 & 0 & 0 \\ -K_3 & 0 & K_3 - \omega^2 I_3 & 0 \\ -K_4 & 0 & 0 & K_4 - \omega^2 I_4 \end{vmatrix} = 0$$

where $K_1 \equiv K_2 + K_3 + K_4$

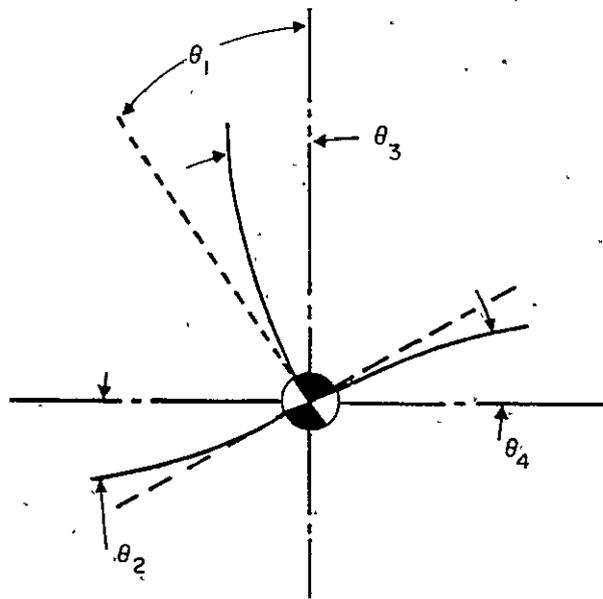[1] Goldstein - Classical Mechanics, Addison-Wesley Publishing Co., 1959

Figure W-4. Mast and Boom Coordinates for Cross Coupling Analysis

Solution of the determinent yields the eigenvalues ω_k. It is assumed that

$$\frac{K_2}{I_2} = \frac{K_3}{I_3} = \frac{K_4}{I_4} \quad ,$$

esulting in resonance:

$$\omega_1^2 = 0$$

$$\omega_2^2 = \omega_4^2 = \frac{K_2}{I_2}$$

$$\omega_3^2 = \frac{K_1}{I_1} \left(1 + \frac{1}{3} \frac{I_1}{I_2} \right)$$

Solution of the simultaneous equations yields the eigen vectors "a_k":

$$(K_1 - \omega_k^2 I_1) a_{11} - K_2 a_{21} - K_3 a_{31} - K_4 a_{41} = 0.$$

$$- K_2 a_{11} + (K_2 - \omega_k^2 I_2) a_{21} = 0.$$

$$- K_3 a_{11} + (K_3 - \omega_k^2 I_3) a_{31} = 0$$

$$- K_4 a_{11} + (K_4 - \omega_k^2 I_4) a_{41} = 0$$

For the case $\omega_1 = 0$, this implies pure rotation of the satellite as a rigid body. The motion of the satellite in toto is discussed in another section. This motion will be slower and not as critical as tne individual component motions.

Since the roots are triply degenerate $\left(\dfrac{K_2}{I_2} = \dfrac{K_3}{I_3} = \dfrac{K_4}{I_4} \right)$, the solution of the eigenvectors involves a straight forward solution of three and a construction of the fourth within the contraints of orthogonality requirements.

$$\underline{\omega_1 = 0} \quad \circ \atop \circ$$

$$a_{11} = a_{21} = a_{31} = a_{41} = \frac{1}{\sqrt{3 I_2 + I_1}}$$

$$\underline{\omega_2^{\,2} = \frac{K_2}{I_2}} \quad \circ\!\!\circ$$

$$a_{12} = a_{32} = 0$$

$$a_{22} = a_{42} = \frac{1}{\sqrt{2\,I_2}}$$

$$\underline{\omega_3^{\,2} = \frac{K_1}{I_1}\left(1 + \frac{1}{3}\frac{I_1}{I_2}\right) \quad \circ\!\!\circ}$$

$$a_{13} = -\frac{I_2}{I_1} \quad a_{23} = -\frac{I_3}{I_1} \quad a_{33} = -a_{43}\frac{I_4}{I_1} = \frac{1}{2\sqrt{I_1}}$$

Allowing $a_4 = a_{14} + a_{24} + a_{34} + a_{44}$ and

setting $a_4 \cdot a_2 = 0$

$\qquad a_4 \cdot a_1 = 0$

$\qquad a_4 \cdot a_3 = 0,$

all components of a_4 are solved and presented in the following table.

EIGENVALUE		EIGENVECTORS			
k	ω_k^2	a_{1k}	a_{2k}	a_{3k}	a_{4k}
1	0	$\dfrac{1}{\sqrt{3I_2 + I_1}}$	$\dfrac{1}{\sqrt{3I_2 + I_1}}$	$\dfrac{1}{\sqrt{3I_2 + I_1}}$	$\dfrac{1}{\sqrt{3I_2 + I_1}}$
2	$\dfrac{K_2}{I_2}$	0	$\dfrac{1}{\sqrt{2\,I_2}}$	0	$\dfrac{-1}{\sqrt{2\,I_2}}$
3	$\dfrac{3K_2}{I_2}\left(1 + \dfrac{1}{3}\dfrac{I_1}{I_2}\right)$	$\dfrac{1}{2\sqrt{I_1}}$	$\dfrac{-I_1/I_2}{2\sqrt{I_1}}$	$\dfrac{-I_1/I_2}{2\sqrt{I_1}}$	$\dfrac{-I_1/I_2}{2\sqrt{I_1}}$
4	$\dfrac{K_2}{I_2}$	0	$\sqrt{\dfrac{1}{6I_2}}$	$\sqrt{\dfrac{-2}{6I_2}}$	$\sqrt{\dfrac{1}{6I_2}}$
		(Satellite)	(Boom)	(Mast)	(Boom)

The normal modes are illustrated in figure W-5.

IST MODE

$\omega_1 = 0$
(PURE ROTATION)

2ND MODE

$\omega_2 = \sqrt{\dfrac{K_2}{I_2}}$

3RD MODE

$\omega_3 = \sqrt{\dfrac{3K_2}{I_1}\left(1 + \dfrac{I_1}{3I_2}\right)} >> \omega_2$

4TH MODE

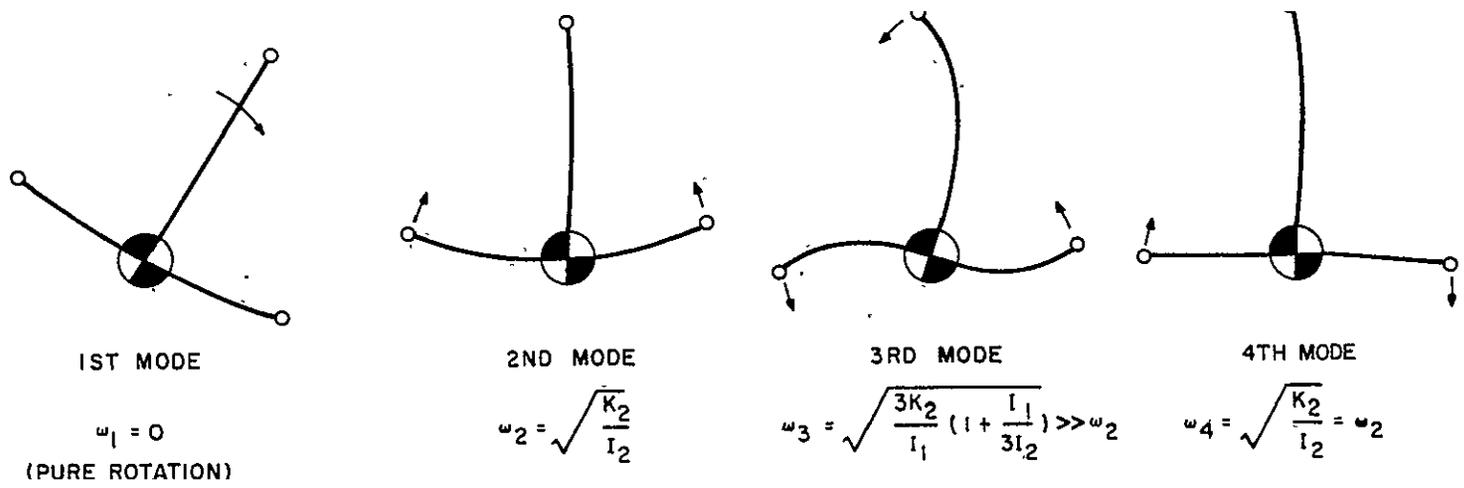$\omega_4 = \sqrt{\dfrac{K_2}{I_2}} = \omega_2$

Figure W-5. Normal Modes of Satellite, Mast and Boom Motions

The total motion of each of the four components is given by

$$\eta_i = \sum_k C_k \, a_{ik} \, e^{-j\omega_k t}.$$

where

η_i = displacement of ith component (boom, etc)

C_k = constant for k^{th} eigenvalue

a_{ik} = k^{th} component of ith eigenvector

ω_k = k^{th} eigenvalue

The constant C_k is determined from initial conditions:

Real part of $C_k = \sum_{ij} T_{ij} \, \eta_i \, (0) \, a_{jk}$

Imaginary part of $C_k = \dfrac{-1}{\omega_k} \sum_{ij} T_{ij} \, \dot{\eta}_i \, (0) \, a_{jk}$.

Where T_{ij} = appropriate inertia term

$(T_{11} = I_1, \ T_{22} = I_2$ etc).

Assuming that

$\dot{\eta}_i \, (0) = 0 \qquad\qquad i = 1, 2, 3, 4$

$\eta_i \, (0) = 0 \qquad\qquad i = 1, 2, 4$

$\eta_3 (0) = \theta$, which corresponds to a step or rapid displacement of the mast, the response of the boom is calculated.

$I_m C_k = 0$

$R_e C_k = \text{?}\ \theta \, a_{3k}$

$\therefore R_e C_1 = I_3 \theta \dfrac{1}{\sqrt{3I_2 + I_1}} = \dfrac{I_2 \theta}{\sqrt{3I_2 + I_1}}$.

$R_e C_2 = I_3 \theta \cdot (0) = 0$

$R_e C_3 = I_3 \theta \dfrac{-I_1/I_2}{2\sqrt{I_1}} = \sqrt{I_1} \dfrac{\theta}{2}$

$R_e C_4 = I_3 \theta \dfrac{-2}{\sqrt{6 I_2}} = -2 \theta \sqrt{\dfrac{I_2}{6}}$

The boom deflection η_2 is given by

$$\eta_2 = \sum_k C_k \, a_{2k} \, e^{-j\,\omega_k\,t}$$

$$= \wedge \cdot \sqrt{\frac{I_1 \theta}{2}} \quad \frac{-I_1/I_2}{2\sqrt{I_1}} \, e^{-j\,\omega_3\,t} \qquad\qquad (-2\theta)\sqrt{\frac{I_2}{6}} \, (\frac{1}{\sqrt{6I_2}}) \, e^{-j\,\omega_4\,t}$$

$$= \theta \left[\frac{1}{4} \frac{I_1}{I_2} \, e^{-j\,\omega_3\,t} - \frac{1}{3} \, e^{-j\,\omega_4\,t} \right]$$

The other boom is simply:

$$\eta_4 = \theta \left[-\frac{1}{4} \frac{I_1}{I_2} \, e^{-j\,\omega_3\,t} - \frac{1}{3} \, e^{-j\,\omega_4\,t} \right]$$

Since $I_1 \ll I_2$, the deflection is essentially

$$\eta_2 \approx \eta_4 = -\frac{\theta}{3} \, e^{-j\,\omega_4\,t}$$

Therefore it can be seen that for a finite step displacement θ of the mast, the boom executes a displacement in inertial space of $\theta/3$, in the opposite sense.

Note that the satellite structure rotates

$$\eta_1 = 0 + (-\sqrt{I_1} \, \frac{\theta}{2}) \, \frac{1}{2\sqrt{I_1}} \, e^{-j\,\omega_3\,t} + 0$$

$$= -\frac{\theta}{4} \cdot e^{-j\,\omega_3\,t}$$

Therefore, the displacement of the boom with respect to its equilibrium position varies in time from $\theta/3 - \theta/4 = .13\theta$ to $\theta/3 + \theta/4 = .58\theta$. This is in good agreement with the calculated response of paragraph W.3 of this appendix which shows the subresonant boom fundamental displaced by 0.28 of the disturbance. The conclusion of this analysis is that in a resonant condition and for a rapid displacement of the mast, the maximum dynamic displacement of the booms is not greater than that for the mast.

APPENDIX X
SAMPLE CALCULATIONS OF ATTITUDE DETERMINATION AND VEHICLE POSITION FIX

X. 1 GIVEN DATA

X. 1. 1 Reference Station Locations

Sta No.	Lat.	Long.
1	10°N	60°W
2	40°N	30°W
3	0°N	0°
4	0°N	75°W

X. 1. 2 Satellite Position

Altitude: 6000 nmi

Projection on earth surface: Lat. = 30°N, Long. = 30°W

X. 1. 3 Earth Configuration

A spherical earth is assumed for this illustrative example with radius = 3443 nmi

X. 2 MEASURED DATA

X. 2. 1 Interferometer Readings on Reference Stations

Interferometer No.	Ref Sta No.	Designation	Value
1	1	C_{11}	31. 666400
1	2	C_{12}	206. 97113
1	3	C_{13}	314. 55529
1	4	C_{14}	195. 21342
2	1	C_{21}	-274. 07753
2	2	C_{22}	-148. 83161
2	3	C_{23}	-81. 83879
2	4	C_{24}	-307. 09617

X. 2. 2 Satellite Readings on User Vehicle

Interferometer No. 1 $C_{1v} = 223. 69004$

Interferometer No. 2 $C_{2v} = -212. 09230$

Radar Range   6290. 669 nmi

X. 2. 3 Time Consideration

All measurements assumed to be simultaneous.

X. 3 PROBLEM

To find unknown latitude and longitude of user vehicle.

X. 3. 1 Outline of Method of Solution

    a. Satellite and reference station geographical coordinates are reduced to cartesian coordinates.

    b. Direction cosines of the range vectors from satellite to reference station are calculated.

    c. The direction cosines from (b) are entered as coefficients in a 4 x 4 linear system of equations. The interferometer measurements on reference stations enter as the right hand side of this system. The solution of the system yields interferometer orientation, scale factor, and delay. These values are calculated for each of the interferometers.

    d. Scale factor and delay from (c) are applied to the angular measurements on user vehicle.

    e. Corrected measurements from (d) are entered into two equations, the coefficients of the equations are the interferometer direction cosines solved for in (c). The solution of the equations gives 2 sets of direction cosines for the satellite to vehicle range vector.

    f. One set of direction cosines from (e) is eliminated. The range vector (satellite to vehicle) is obtained.

    g. The range vector is added to the satellite position vector. The result is converted into latitude and longitude designations.

X. 3. 2 Calculation of X, Y, Z Coordinates

    a. Reference station no. 1:

$$X_1 = R \cos \phi \cos \lambda$$
$$= 3443 \cos 10° \cos (-60°)$$
$$= 1695.3465$$

$\phi = $ latitude

$\lambda = $ longitude

$$Y_1 = R \cos \phi \sin \lambda$$
$$= 3443 \cos 10° \sin (-60°)$$
$$= -2936.4263$$

$$Z_1 = R \sin \phi$$
$$= 3443 \sin 10°$$
$$= 597.8707$$

    b. Similarly for reference stations no. 2, 3 and 4:

$$X_2 = 3443 \cos 40° \cos (-30°) = 2284.1342$$
$$Y_2 = 3443 \cos 40° \sin (-30°) = -1318.7455$$
$$Z_2 = 3443 \sin 40° = 2213.1177$$
$$X_3 = 3443 \cos 60° \cos 0° = 1721.5000$$
$$Y_3 = 3443 \cos 60° \sin 0° = 0$$
$$Z_3 = 3443 \sin 60° = 2981.7255$$

$X_4 = 3443 \cos 40° \cos (-75°) = 682.6329$

$Y_4 = 3443 \cos 40° \sin (-75°) = -2547.6207$

$Z_4 = 3443 \sin 40° = 2213.1177$

    c. Satellite:

$X_s = 9443 \cos 30° \cos (-30°) = 7082.2500$

$Y_s = 9443 \cos 30° \sin (-30°) = -4088.9389$

$Z_s = 9443 \sin 30° = 4721.5000$

X.3.3 Direction Cosines of Range Vectors

    a. Satellite to reference station no. 1:

$X_1 - X_s = 1695.3465 - 7082.2500 = -5386.9035$

$Y_1 - Y_s = -2936.4263 - (-4088.9389) = 1152.5126$

$Z_1 - Z_s = 597.8707 - 4721.5000 = -4123.6293$

Range:

$$R_{s_1} = \sqrt{(X_1 - X_s)^2 + (Y_1 - Y_s)^2 + (Z_1 - Z_s)^2} = 6881.2305$$

Direction cosines:

$$r_{1x} = \frac{X_1 - X_s}{R_{s_1}} = -0.78284015$$

$$r_{1y} = \frac{Y_1 - Y_s}{R_{s_1}} = 0.16748641$$

$$r_{1z} = \frac{Z_1 - Z_s}{R_{s_1}} = -0.59925755$$

In a similar manner the range and direction cosines for reference stations no. 2, 3 and 4 are calculated.

    b. Satellite to reference station no. 2:

Range:

$$R_{s_2} = 6081.7652$$

Direction cosines:

$r_{2x} = -0.78893473$

$r_{2y} = 0.455491672$

$r_{2z} = -0.41244313$

    c. Satellite to reference station no. 3:

Range:

$$R_{s_3} = 6963.0365$$

Direction cosines:

$r_{3x} = -0.76988682$

$r_{3y} = 0.58723502$

$r_{3z} = -0.24985859$

    d. Satellite to reference station no. 4:

Range:

$R_{s_4} = 7044.3412$

Direction cosines:

$r_{4x} = -0.90847631$

$r_{4y} = 0.21880232$

$r_{4z} = -0.35608473$

X.3.4 <u>Linear Equations for Interferometer Orientation and Constants</u>

    a. Interferometer no. 1:

        (1) System solution

$$r_{1x}(A_1 V_{1x}) + r_{1y}(A_1 V_{1y}) + r_{1z}(A_1 V_{1z}) - (A_1 D_1) = C_{11}$$

$$r_{2x}(A_1 V_{1x}) + r_{2y}(A_1 V_{1y}) + r_{2z}(A_1 V_{1z}) - (A_1 D_1) = C_{12}$$

$$r_{3x}(A_1 V_{1x}) + r_{3y}(A_1 V_{1y}) + r_{3z}(A_1 V_{1z}) - (A_1 D_1) = C_{13}$$

$$r_{4x}(A_1 V_{1x}) + r_{4y}(A_1 V_{1y}) + r_{4z}(A_1 V_{1z}) - (A_1 D_1) = C_{14}$$

With numerical values entered:

$$-.78284015 (A_1 V_{1x}) + .16748641 (A_1 V_{1y}) - .59925755 (A_1 V_{1z})$$
$$- (A_1 D_1) = 31.666400$$

$$-.78893473 (A_1 V_{1x}) + .45549167 (A_1 V_{1y}) - .41244313 (A_1 V_{1z})$$
$$- (A_1 D_1) = 206.97113$$

$$-.76988682 (A_1 V_{1x}) + .58723502 (A_1 V_{1y}) - .24985859 (A_1 V_{1z})$$
$$- (A_1 D_1) = 314.55529$$

$$-.90847631 (A_1 V_{1x}) + .21880232 (A_1 V_{1y}) - .35608473 (A_1 V_{1z})$$
$$- (A_1 D_1) = 195.21342$$

Solution of this 4 x 4 system gives the following values:

$$A_1 D_1 = 0.62796357$$

$$A_1 V_{1z} = 444.06309$$

$$A_1 V_{1y} = 313.99998$$

$$A_1 V_{1x} = -314.03019$$

Where V_{1x}, V_{1y}, V_{1z} are the direction cosines of the interferometer arm.

(2) Scale factor determination:

$$A_1^2 = (A_1 V_{1x})^2 + (A_1 V_{1y})^2 + (A_1 V_{1z})^2$$

$$= (-314.03019)^2 + (313.99998)^2 + (444.06309)^2$$

$$A_1 = \sqrt{394,402.9733} = 628.01511$$

(3) Delay determination:

$$D_1 = \frac{(A_1 D_1)}{A_1} = \frac{0.62796357}{628.01511} = 0.00099992$$

(4) Determination of the cosines of the vector that is aligned with interferometer no. 1:

$$V_{1x} = \frac{(A_1 V_{1x})}{A_1} = \frac{-314.03019}{628.01511} = -0.50003605$$

$$V_{1y} = \frac{(A_1 V_{1y})}{A_1} = \frac{313.99998}{628.01511} = 0.49998794$$

$$V_{1z} = \frac{(A_1 V_{1z})}{A_1} = \frac{444.06309}{628.01511} = 0.70708982$$

b. Interferometer no. 2:

(1) System Solution:

$$r_{1x} (A_2 V_{2x}) + r_{1y} (A_2 V_{2y}) + r_{1z} (A_2 V_{2z}) - (A_2 D_2) = C_{21}$$

$$r_{2x} (A_2 V_{2x}) + r_{2y} (A_2 V_{2y}) + r_{2z} (A_2 V_{2z}) - (A_2 D_2) = C_{22}$$

$$r_{3x} (A_2 V_{2x}) + r_{3y} (A_2 V_{2y}) + r_{3z} (A_2 V_{2z}) - (A_2 D_2) = C_{23}$$

$$r_{4x} (A_2 V_{2x}) + r_{4y} (A_2 V_{2y}) + r_{4z} (A_2 V_{2z}) - (A_2 D_2) = C_{24}$$

The solution of this system yields the values:

$$A_2 D_2 = 0.69113131$$

$$A_2 V_{2z} = 0.00001241$$

$$A_2 V_{2y} = 444.27517$$

$$A_2 V_{2x} = 444.23102$$

From these solutions, in the same manner used for interferometer no. 1, the following values are obtained:

(a) Sale factor:

$$A_2 = 628.26875$$

(b) Delay:

$$D_2 = 0.00110006$$

(c) Vector cosines:

$$V_{2x} = 0.70707165$$

$$V_{2y} = 0.70714191$$

$$V_{2z} = -0.00000002$$

At this point, the direction cosines describing orientations, scale factors, and delays have been calculated for both interferometers.

X.3.5 User Vehicle Position Fix Calculation

The cosines of the angles between the line of sight from the satellite interferometer axes to the vehicle are computed by applying the scale factors and delays to the actual measurements.

$$C_1 = \frac{C_{1v}}{A_1} + D_1 = \frac{223.69004}{628.01511} + .00099992 = 0.35718568$$

$$C_2 = \frac{C_{2v}}{A_2} + D_2 = \frac{-212.09230}{628.26875} + 0.00110006 = -0.33648207$$

The set of equations for the direction cosines (r_x, r_y, r_z) of the satellite to vehicle range vector are:

$$V_{1x} r_x + V_{1y} r_y + V_{1z} r_z = \cos \theta_1 = C_1$$

$$V_{2x} r_x + V_{2y} r_y + V_{2z} r_z = \cos \theta_2 = C_2$$

$$r_x^2 + r_y^2 + r_z^2 = 1$$

Solving this 3 x 3 system for r_z, the following quadratic equation in r_z is obtained:

$$1.9999040 \, r_z^2 - 1.0102020 \, r_z - 0.63162830 = 0$$

Solving this equation by the quadratic formula yields:

$$r_{z_1} = 0.86869345$$

$$r_{z_2} = -0.36356819$$

Solution of the 3 x 3 system of equations for r_x and r_y and applying the values of r_{z_1} and r_{z_2} to the system solutions, yields the following values:

$$r_{x_1} = 0.01914792$$

$$r_{y_1} = 0.49497985$$

$$r_{x_2} = -0.85219414$$

$$r_{y_2} = 0.37627559$$

The dot product test of two vectors is applied to determine which set of direction cosines is applicable to the problem solution. A vector from the center of the earth to the satellite and one from the satellite to the vehicle are shown in figure X-1.
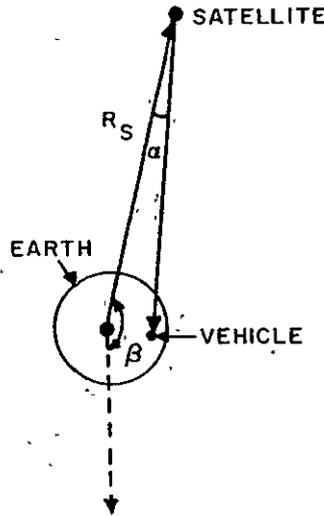

Figure X-1. Vector Orientation

The angle α in figure X-1 must always be $< 90°$ by nature of the vector geometry. Forming the dot product, places the two vectors involved in a tail-to-tail orientation. Under this condition, the angle β in figure X-1 is formed and is always $> 90°$. With this requirement, the product $\overline{R_s} \cdot \overline{r_s} < 0$ is the desired solution.

$$\overline{R_s} \cdot \overline{r_1} = R_{x_s} r_{x_1} + R_{y_s} r_{y_1} + R_{z_s} r_{z_1}$$

$$= (7082.2500)(.01914792) + (-4088.9389)(-.49497985) + (4721.5000)(.86869345)$$

By inspection, $\overline{R_s} \cdot \overline{r_1} > 0$. This is not the required result.

$$\overline{R_s} \cdot \overline{r_2} = R_{x_s} r_{x_2} + R_{y_s} r_{y_2} + R_{z_s} r_{z_2}$$

$$= (7082.2500)(-.85219414) + (-4088.9389)(.37627559) + (4721.5000)(-.36356819)$$

By inspection, $\overline{R_s} \cdot \overline{r_2} < 0$. This result meets the prescribed requirement. The r_2 values of the direction cosines are the values required for problem solution.

Using the calculated $\overline{r_2}$ direction cosines in conjunction with the radar range measurement, the components of the satellite to vehicle range vector are obtained.

$R_x = R \cdot rx = 6290.6647 \, (-.85219414) = -5360.8676$

$R_y = R \cdot ry = 6290.6647 \, (.37627559) = 2367.0236$

$R_z = R \cdot rz = 6290.6647 \, (-.36356819) = -2287.0856$

Adding this range vector to the satellite radius vector, the user vehicle position vector is obtained.

$X_v = R_{s_x} + R_x = 7082.2500 - 5360.8676 = 1721.3813$

$Y_v = R_{s_y} + R_y = -4088.9389 + 2367.0236 = -1721.9153$

$Z_v = R_{s_z} + R_z = 4721.5000 - 2287.0856 = 2434.4144$

$R_v = \sqrt{X_v^2 + Y_v^2 + Z_v^2} = 3443.0393$

Conversion, from rectangular to geographic polar coordinates is as follows:

Latitude $\phi = \sin^{-1} (Z_v/R_v) = \sin^{-1} (0.70705392) = 45°\ 0'.256$ N

Longitude $\lambda = \tan^{-1} (Y_r/X_v) = \tan^{-1} (-1.0003102) = 45°\ 0'.533$ W

BOOSTER WEIGHT CAPABILITY

This appendix describes the assumptions, derivations and relationships used in determining the payload weight that the various boosters or launch vehicles can orbit at different altitudes.

As previously described, there are three weight losses considered between a 100 nmi circular orbit, and the circular orbit at the desired altitude and inclination angle. These weight losses will vary with different boosters, altitudes and inclination angles. The expression for this variation will now be discussed.

Y.1 INCLINATION ANGLE WEIGHT LOSS

The objective of this section is to determine the loss of weight (ΔW_i) that a particular booster can orbit by changing the inclination angle from λ (the latitude of the launching station) to some greater value, i. For a given booster, let:

E = Energy capability of the booster

ΔKE_λ = Change of kinetic energy applied during launch to a 100 nmi altitude at an inclination angle, λ.

ΔKE_i = Change of kinetic energy applied during launch at an inclination angle, i.

ΔPE_λ = Change of potential energy applied during launch at an inclination angle, λ.

ΔPE_i = Change of potential energy applied during launch at an inclination angle, i.

Therefore

$$E = \Delta KE_\lambda + \Delta PE_\lambda$$

and

$$E = \Delta KE_i + \Delta PE_i.$$

or

$$\Delta KE_\lambda + \Delta PE_\lambda = \Delta KE_i + \Delta PE_i$$

but for the same orbital altitude

$$\Delta PE_\lambda = \Delta PE_i$$

Therefore

$$\Delta KE_\lambda = \Delta KE_i$$

but

$$\Delta KE_\lambda = \frac{1}{2} m_\lambda \ (\Delta V \lambda)^2$$

and

$$\Delta KE_i = \frac{1}{2} m_i (\Delta V_i)^2$$

so

$$\frac{1}{2} m_\lambda (\Delta V_\lambda)^2 = \frac{1}{2} m_i (\Delta V_i)^2$$

$$m_i = m_\lambda \frac{(\Delta V_\lambda)^2}{(\Delta V_i)^2}$$

or

$$W_i = W_\lambda \frac{(\Delta V_\lambda)^2}{(\Delta V_i)^2}$$

where

m_λ = mass of payload capable of being launched at an inclination angle, λ.

m_i = mass of payload capable of being launched at an inclination angle, i.

W_λ = weight of payload capable of being launched at an inclination angle, λ.

W_i = weight of payload capable of being launched at an inclination angle, i.

ΔV_λ = velocity increment which is added to the payload during launch to an inclination angle i.

ΔV_i = velocity increment which is added to the payload during launch to an inclination angle i.

Figure Y-1 describes the orbital plane at 100 nmi, and illustrates the various velocity vectors involved. The velocity increments of interest can be determined from the orbital plane geometry. These increments are:

$$\Delta V_\lambda = V_{100} - V_e$$

and

$$\Delta V_i = \sqrt{\left[V_{100} \cos(i - \lambda) - V_e\right]^2 + \left[V_{100} \sin(i - \lambda)\right]^2}$$

$$(\Delta V_i)^2 = V_{100}^2 \cos^2(i - \lambda) + V_e^2 - 2 V_{100} V_e \cos(i - \lambda) + V_{100}^2 \sin^2(i - \lambda)$$

$$= V_{100}^2 + V_e^2 - 2 V_{100} V_e \cos(i - \lambda).$$

Therefore

$$W_i = W_\lambda \frac{(V_{100} - V_e)^2}{V_{100}^2 + V_e^2 - 2 V_{100} V_e \cos(i - \lambda)}$$
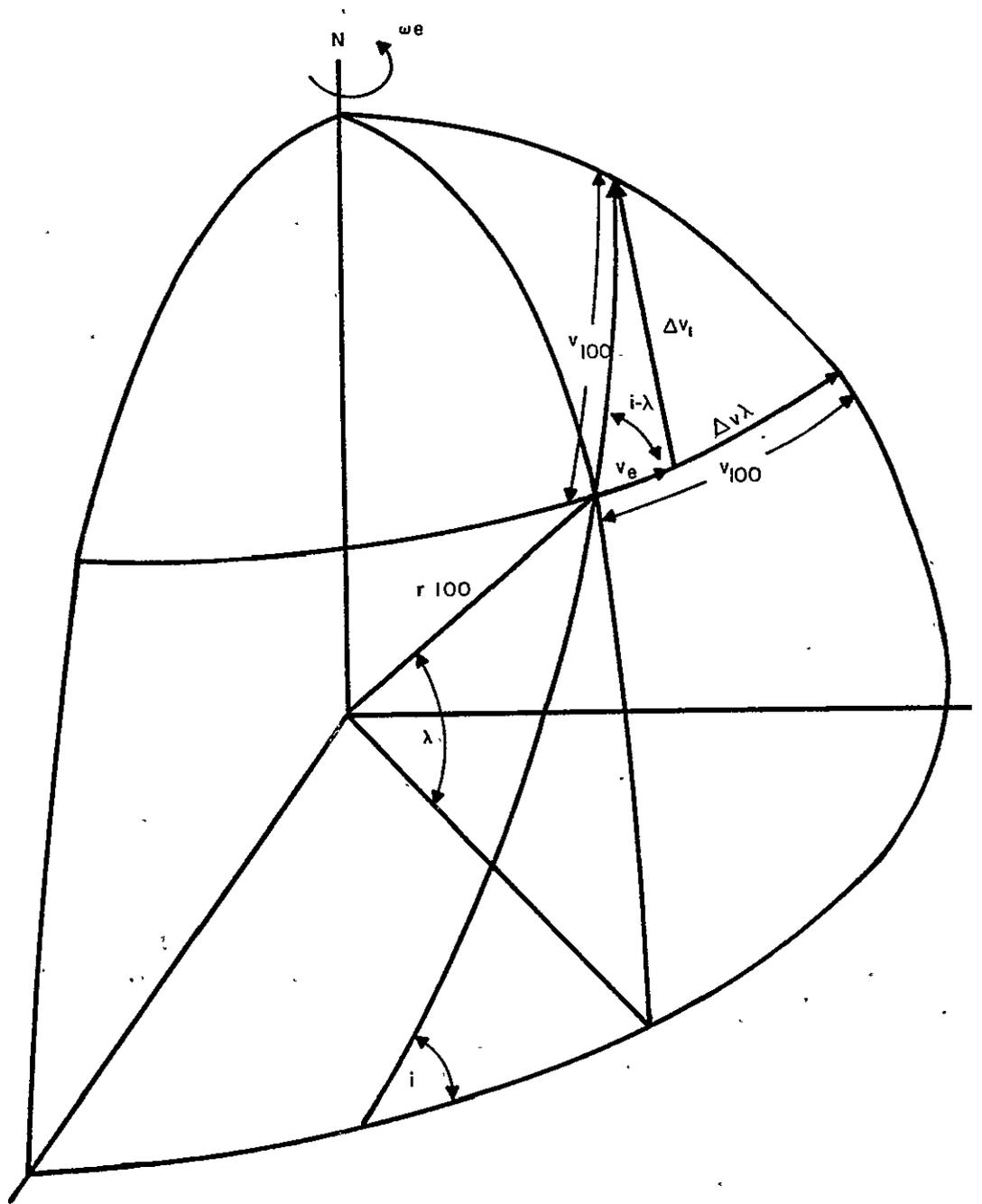
Figure Y-1. Orbital Plane at 100 Nautical Miles

but

$$\Delta W_i = W_\lambda - W_i$$

so

$$\Delta W_i = W_\lambda \left[1 - \frac{(V_{100} - V_e)^2}{V_{100}^2 + V_e^2 - 2 V_{100} V_e \cos(i - \lambda)} \right]$$

where

ΔW_i = inclination angle weight loss

The remaining terms in the above equations are:

$$V_e = r_e \, \omega_e \cos \lambda$$

$$V_{100} = \sqrt{\frac{g_o r_e^2}{r_{100}}}$$

ω_e = earth angular velocity

r_e = radius of earth

r_{100} = radius at 100 nmi altitude

g_o = gravitational acceleration at earth's surface

i = orbital plane inclination angle

λ = launching station latitude

V_e = tangential velocity at earth's surface

V_{100} = tangential velocity at 100 nmi altitude.

Y.2 PERIGEE WEIGHT LOSS

The next weight loss to be determined is that due to the injection of the payload at 100 nmi into an elliptical transfer orbit. The perigee is at 100 nmi and the apogee is at the desired orbital altitude.

It is assumed that the last stage of the booster injects the payload into the elliptical orbit by adding a velocity increment ΔV_p to the payload velocity at 100 nmi altitude. The necessary velocity increment is defined to be the difference between the 100 nmi circular velocity and the necessary perigee velocity.

Where

V_p = perigee velocity of ellipse.

V_{100} = circular velocity at 100 nmi

but*

$$V_{100} = \sqrt{\mu / r_p}$$

μ = Gravitational Constant (1.4×10^{16} ft^3/sec^2)

r_a = radius of apogee

r_p = radius of perigee

$$V_p = \sqrt{\frac{2 \mu r_a}{r_p (r_a + r_p)}}$$

---

*Jensen, Townsend, Kork and Kraft; "Design Guide to Orbital Flight" 1962

so

$$\Delta V_p = \sqrt{\frac{2\mu\, r_a}{r_p\, (r_a + r_p)}} - \sqrt{\mu/r_p}$$

$$\Delta V_p = \sqrt{\frac{\mu}{r_p}} \left(\sqrt{\frac{2\, r_a}{r_a + r_p}} - 1 \right)$$

For a given stage on a particular booster, the loss of payload carrying capability can be determined from the following expression:

$$e^{\Delta V_p / g_0 I_{sp}} = \frac{W_i}{W_i - W_p} \quad .$$

Where

      W_i = weight of payload at inclination angle i before injection

      W_p = stage propellent weight

      g_0 = gravitational acceleration at the earth's surface

      I_{sp} = propellent specific impulse

But the weight of the payload before injection is the sum of propellent weight, stage structure weight, and elliptical payload weight, i. e.

$$W_1 = W_e + W_s + W_p$$

Therefore

$$e^{\Delta V_p / g_0 I_{sp}} = \frac{W_e + W_s + W_p}{W_e + W_s}$$

where

      W_e = weight of payload injected into the elliptical orbit

      W_s = structure weight of the last stage

but

$$\delta_s = \frac{W_p}{W_s} \cdot$$

so

$$e^{\Delta V_p / g_0 I_{sp}} = \frac{W_e + (1 + 1/\delta_s)\, W_p}{W_e + (1/\delta_s)\, W_p}$$

where

      δ_s = stage mass ratio = $\dfrac{\text{propellent weight}}{\text{stage structure weight}}$ $\cdot$

Solving the above expression for W_p:

$$W_p = W_e \left[\frac{e^{\Delta V_p/g_o I_{sp}} - 1}{1 + 1/\delta_s - \frac{1}{\delta_s} e^{\Delta V_p/g_o I_{sp}}} \right]$$

For the stage mass ratios and ellipses considered in this model, the value of the denominator of the preceeding relationship remains very close to unity. Therefore, for simplification:

$$W_p \cong W_e \left(e^{\Delta V_p/g_o I_{sp}} - 1 \right)$$

As previously described:

$$W_i = W_e + W_s + W_p$$

or

$$W_i = W_e + W_p \left(1 + 1/\delta_s \right)$$

Combining the above equations for W_i and W_p

$$W_i = W_e + W_e \left(e^{\Delta V_p/g_o I_{sp}} - 1 \right) \left(1 + 1/\delta_s \right)$$

and solving for W_e

$$W_e = W_i \left[\frac{\delta_s / 1 + \delta_s}{e^{\Delta V_p/g_o I_{sp}} - 1/1 + \delta_s} \right]$$

but

$$\Delta W_p = W_i - W_e$$

or

$$\Delta W_p = W_i \left[1 - \frac{\delta_s / 1 + \delta_s}{e^{\Delta V_p/g_o I_{sp}} - 1/1 + \delta_s} \right]$$

where

ΔW_p = weight loss due to injection at perigee.

Y-3 APOGEE WEIGHT LOSS

The final weight loss to be determined is that loss due to the injection of the payload at the apogee of the elliptical transfer orbit into the desired circular orbit.

It is assumed that regardless of the booster used, an additional stage or rocket motor is included with the satellite for circular orbit injection at the apogee of the eliptical transfer orbit. The motor accomplishes this function by adding a velocity increment, ΔV_a. This

increment, the difference in the velocity at apogee of the ellipse and the velocity of the desired circular orbit at altitude h, is:

$$\Delta V_a = V_h - V_a$$

where

V_h = circular velocity at altitude h

V_a = apogee velocity of ellipse

but*

$$V_h = \sqrt{\mu/a}$$

$$V_a = \sqrt{\frac{2\mu \, r_p}{r_a (r_a + r_p)}}$$

so

$$\Delta V_a = \sqrt{\mu/a} \left(1 - \sqrt{\frac{2r_p}{r_a + r_p}}\right)$$

Further loss analysis is identical to the analysis used for determining the weight loss at perigee. Using the expression

$$e^{\Delta V_a/g_o I_{sp}} = \frac{W_e}{W_e - W_p}$$

where

W_e = weight of payload in the elliptical orbit

W_p = stage or motor propellent weight

It can be found that

$$W_p \cong W_f (e^{\Delta V_a/g_o I_{sp}} - 1)$$

where

W_f = final weight of the satellite payload injected at apogee

$W_e = W_f + W_s + W_p$

W_s = weight of the stage structure or rocket motor.

By combining these last two expressions and solving for W_f

$$W_f = W_e \left[\frac{\delta_s/1 + \delta_s}{e^{\Delta V_a/g_o I_{sp}} - 1/1 + \delta_s} \right]$$

but

$$\Delta W_a = W_e - W_f$$

___

*Ibid.

or

$$\Delta W_a = W_e \left[1 - \frac{\delta_s/1 + \delta_s}{e^{\Delta V_a/g_o I_{sp}} - 1/1 + \delta_s} \right]$$

where

ΔW_a = weight loss due to injection at apogee.

Y.4 SUMMARY

The three derived weight losses and the factors involved in calculating these losses are summarized in this section. The subscript j indicates the value of that quantity is dependent upon the booster used. The subscript m indicates the value of that quantity is dependent upon the type of rocket motor used for injection at apogee. The subscript h indicates the value is' dependent upon the altitude chosen for orbit. For a particular altitude, booster, and final stage motor, the total weight loss of that booster's capability can be determined as follows:

$$\Delta W_i = W_\lambda (1 - A)$$

$$\Delta W_p = W_i (1 - B)$$

$$\Delta W_a = W_e (1 - C)$$

where

$$A = \frac{(V_{100} - V_e)^2}{V_{100}^2 + V_e^2 - 2 V_{100} V_e \cos (i - \lambda)}$$

$$B = \frac{\delta_{s(j)}/1 + \delta_{s(j)}}{e^{\Delta V_p(h)/g_o I_{sp}(j)} - 1/1 + \delta_{s(j)}}$$

$$C = \frac{\delta_{s(m)} / 1 + \delta_{s(m)}}{e^{\Delta V_a(h)/g_o I_{sp}(m)} - 1/1 + \delta_{s(m)}}$$

The total weight loss, ΔW_t, has been defined as

$$\Delta W_t = \Delta W_i + \Delta W_p + \Delta W_a$$

or

$$\Delta W_t = W_\lambda (1-A) + W_i (1-B) + W_e (1-C)$$

From section Y.1

$$W_i = A W_\lambda$$

and from section Y.2

$$W_e = B \, W_i$$

or

$$W_e = ABW_\lambda$$

Substituting these values in the equation for ΔW_t yields

$$\Delta W_t = W_\lambda \, (1 - A) + W_\lambda \, (A) \, (1 - B) + W_\lambda \, (AB) \, (1 - C)$$

which reduces to

$$\Delta W_t = W_\lambda \, (1 - ABC)$$

The weight that can be put into orbit at altitude h by a given booster $W \, (j, h)$ is defined as the weight the booster can orbit at 100 nmi, $W_{\lambda \, (j)}$, less the weight lost in going to altitude h, $\Delta W_{t \, (j, h)}$, i.e.,

$$W_{(j, h)} = W_{\lambda \, (j)} - W_{t(j, h)}$$

or

$$W_{(j, h)} = W_{\lambda \, (j)} - W_{\lambda \, (j)} \, (1 - ABC)_{(h)}$$

Therefore

$$W_{(j, h)} = W_{\lambda \, (j)} \, (ABC)_{(h)}$$

where

$W_{(j, h)}$ = booster weight capability at altitude, h.

APPENDIX Z
DATA SYSTEM ANALYSIS AND PARAMETER CALCULATIONS

Z.1 INTRODUCTION

Of the five RF links in the Navigation Satellite System, three links carry a combination of radar and data on a time shared basis, one link exclusively carries radar and one link exclusively carries data. Since the power and bandwidth requirements are greater for the radar portion, the three combination links are sized for the radar requirements and are extensively analyzed in Appendix A along with the exclusive radar link. The link from satellite to vehicle, that exclusively carries data, is the subject of this analysis and is referred to as channel 2 in other sections of this report.

Since only data is carried by this channel, ionospheric refraction does not limit its frequency of operation to above 800 MC as required for the other four channels in the system. Since the satellite and vehicle antennas are wide beam, their gain is essentially independent of frequency and, the satellite power requirements increase as the square of the frequency. To minimize the power, the lowest possible frequency is desirable. However below about 100 MC, extraterrestial galactic noise rises to a level that causes the power requirements to again begin rising. Thus, the optimum frequency for minimum satellite power is approximately 100 MC. A frequency of 110 MC was chosen for this analysis.

Under present-day state-of-the-art, a peak power of approximately twenty watts within the satellite is feasible. This analysis starts with this constraint and determines the transmission reliability in terms of the detected message errors that are subject to correction by re-transmission. During the early stages of the program, when the system is lightly loaded, some of the system capacity may be utilized for error correction through redundant transmission. As the system is enlarged and more of its capacity is utilized, less system capacity can be applied to error correction. However, increases in satellite power capability shall be concurrent with the system growth and the requirement for message redundancy is decreased.

The error analysis presented in this appendix is based on the least desirable situation. This is when the satellite is near the vehicle horizon. Under this condition, it is shown that approximately one vehicle report in one hundred shall be in error and require re-transmission. When the satellite is overhead, the number of errors will be greatly reduced and will result in a negligible number of repeated messages. The actual number of repeated transmissions that are required will be the integral of the error probability

over the hemisphere above the vehicle. Since the least desirable case of one repeat in one hundred messages is within the capability of the system, it was deemed unnecessary to compute the actual system redundancy to show system feasibility.

Z.2 DATA SYSTEM BANDWIDTH REQUIREMENTS

Z.2.1 <u>Introduction</u>

In order to evolve a conceptual system model for purposes of evaluating the feasibility of power requirements, equipment weights and costs, etc., it is necessary to determine specific values for a number of highly complex system parameters. One of the more significant of these is the data channel bandwidth. This parameter is a function of a number of inter-related system variables as well as sub-system and equipment design choices. These can be enumerated as follows:

    a. System Variables

        (1) Data Rate

            -- Fix rate

            -- Total quantity of data

        (2) Doppler

            -- Satellite Altitude

            -- Operating Frequencies

            -- Vehicle Velocity

    b. Sub-system Design Choices

        -- Modulation Techniques

        -- Detection Techniques

        -- Error Rate Requirements

    c. Equipment Design Choices

        -- Component stabilities

        -- AFC/APC considerations

        -- Pulse characteristics

        -- Specific circuit choices

        -- Deviation ratio

A rigorous analysis of all of these factors is beyond the scope of this report since the results would only be of academic interest. The extensive effort would be justified only after the variables affecting data rate and doppler are more clearly defined. However, in this appendix assumptions shall be made covering these parameters and the significant factors in the choice of a system bandwidth shall be discussed. Finally, a value for use in evaluating a conceptual system shall be determined.

Z.2.2 <u>System Variables</u>

The data rate is dependent on the capacity of the system in terms of fix rate and total amount of data to be handled. The fix rate is a factor determined by the total number of

Z-2

users and the fix rate each user requires.. For purposes of determining the system band-width, it is assumed that a 2500 bit per second rate will handle the initial requirements of the system and provide fixes for up to nine vehicles per second. The total data per fix contains the basic fix data which consists of time, latitude, longitude and a limited amount of general and weather information.

The doppler shift due to satellite and vehicle velocities is discussed in Appendix P. Assuming a 6000 nautical mile satellite height, the curve in Appendix P shows the maximum doppler to be approximately (9.2×10^{-6}) (F_s) CPS. This is approximately ± 1 KC for the 110 MC link and ± 10 KC for the "L" band link.

The effect of this doppler shift on the bandwidth of the channel is dependent on the type of detection circuit. If a phase tracking loop were employed, no additional IF bandwidth shall be required to accommodate the doppler. However, since the cost and complexity of the vehicle equipment must be kept to a minimum, use of such techniques is not desirable. Therefore, the doppler shall be accommodated on the 110 MC link to the vehicle. Assuming use of AFC or APC on the satellite or frequency control in the ground station, the 10 KC doppler on the "L" band ground to satellite link can be neglected.

. Z. 2. 3 Sub-System Variables

The choice of the type of modulation to be employed in a system usually involves a highly complex analysis of trade-offs of various sophisticated techniques. However, in the case of the navigation satellite; certain factors make this decision relatively uncomplicated. First, the basic operational concepts dictate a pulsed system since the radio channels shall time share the data transmission with the radar pulses. Second, the constraint of minimum vehicle cost precludes any complex, and therefore expensive, techniques. This narrows the choice to conventional AM or FM (FSK) systems that employ simple modulator and detector/ discriminator circuits. The system chosen for evaluation can be defined as a PCM/FM system with the qualification that discreet messages; rather than binary coded characters that represent quantized samples of analog signals; are transmitted.

The error rate in the system is dependent on the signal-to-noise ratio in the decision circuit. This ratio is a function of a great many variables in both equipment and systems design. For purposes of determining bandwidth, it is necessary to determine the effect of band limiting on error rate. The problem in a PCM/FM system is to narrow the receiver IF and video bandwidth as much as possible to reduce the threshold and minimize the signal to noise ratio in the decision circuit. However, a limit exists where the errors increase rapidly due to the inability of the filter to pass the signal energy. McRae[1] shows that it is only necessary to have a post detection bandwidth equal to one half the bit rate.

---

[1] Consideration of RF Parameters for PCM Telemetry Systems, D. D. McRae, IRE Trans. in Space Elec. & Telemetry, June, 1959.

Thus, for the system under consideration, the ideal video filter would be 1250 CPS. McRae further points out that it is unnecessary for the receiver to pass frequency components higher than the 1250 CPS. The channel bandwidth required shall also include the separation between the "mark" and "space" frequencies. This separation is a function of the deviation ratio that is chosen. The rigorous solution to the choice of deviation ratio is beyond the scope of this report since it involves many specific design considerations. However, an approximation can be arrived at by considering that the minimum bandwidth is desirable to maintain minimum threshold. Since the maximum error rate will occur when the satellite is on the horizon (maximum path loss and fading), it is desirable to maintain a low threshold by sacrificing the FM improvement when the satellite is overhead and the signal levels are high with minimum fading. Thus, a deviation ratio in the order of unity is desirable.

From McRae, the ratio of channel bandwidth to bit rate for a deviation ratio of unity is approximately 2, if all components above 10% of the unmodulated carrier are to be passed. Thus, a channel bandwidth of 5 KC is a good approximation of the system requirements.

Z. 2. 4 Equipment Design Choices

Many of the equipment design choices have already been discussed as variables affecting sub-system parameters. The major design choice remaining is the component stabilities. Again, minimum cost of vehicle equipment dictates a system limitation. A stability of 1 part in 10^5 is considered economical on the vehicle. At the 110 MC frequency, the additional bandwidth allowance must then be approximately ±1. 1 KC.

Allowing an additional ±0. 5 KC to cover the AFC capabilities of the satellite, the total allowance would be ±1. 6 KC maximum or ±1. 2 KC RMS.

Z. 2. 5 Total Bandwidth

Allowing for the least desirable case, the total receiver IF bandwidth would be the sum of the doppler, information bandwidth and component instabilities. This bandwidth is 10. 2 KC. For purposes of this study, 10 KC shall be used for system evaluation.

Z. 3 EVALUATION OF PARAMETERS

Z. 3. 1 Free Space Attenuation

The free space attenuation between the satellite and vehicle is

$$L_{fs} = 37. 8 + 20 \log D + 20 \log f$$

where

L_{fs} = free space loss in db

D = straight line distance between satellite and vehicle in nautical miles

f = frequency in megacycles

$$L_{fs} = 37.8 + 20 \log 8496 + 20 \log 110$$
$$= 37.8 + 78.6 + 40.8$$
$$= 157.2 \text{ db}$$

Z.3.2 <u>Antenna Gains</u>

The satellite antenna gain, determined by the required coverage, is

$$G_s = 9.7 \text{ db}$$

The vehicle antenna gain is

$$G_v = 2 \text{ db}$$

The sky temperature contains contributions from the sun, oxygen and water vapor, and extra terrestial galactic noise. At 110 MC, the sun, and oxygen and water vapor components are negligible but, the galactic noise is significant. The temperature varies from about 300°K, at the galactic pole, to about 3000° K, at the center. The sum of incremental components, over the entire sky, has an average value of approximately 1450°K. Then:

$$T_a = 0.3 (290) + 0.7 (1450)$$
$$= 87 + 1010$$
$$= 1097°K$$

The effective noise temperature is calculated by the equation

$$T_e = T_a + 290 (F-1)$$

where

F is the receiver noise figure

On the vehicle, the noise figure is 5.5 db (3.54) and

$$T_e = 1097 + 290 (3.54-1)$$
$$= 1097 + 738$$
$$= 1835°K$$

Z.3.3 <u>Losses</u>

The losses in the satellite to vehicle path are

L	=	3 db	+	0.8 db	+	1.2 db
		(polarization)		(atmospheric)		(component)
	+	6 db	+	2 db	=	13 db
		(fading margin)		(safety factor)		

Z. 3. 4 Effective Noise Temperature

The vehicle antenna has an approximately uniform antenna pattern for its temperature characteristics. The side and back lobes, which constitute about three tenths of the entire pattern, sense the earth's temperature of 290°K. The hemispherical portion of the pattern virtually senses the entire sky. Thus, the vehicle antenna temperature can be found by:

$$T_a = .3 \,(290) + .7 \,(T_s)$$

where

T_s = average sky temperature.

Z. 3. 5 Receiver Noise Power

The receiver noise power is

$$N = K \, T_e \, B$$

$$N = (1.38 \times 10^{-23}) \,(1.835 \times 10^3) \,(10 \times 10^3)$$

$$= 25.32 \times 10^{-17} \text{ watts}$$

$$= -156 \text{ dbW } (-126 \text{ dbm})$$

Z. 3. 6 Calculation of Signal-to-Noise Ratio and Energy Contrast

Z. 3. 6. 1. Signal-to-Noise (S/N)

The signal received by the vehicle receiver in the absence of fading is

$$S = P_s + G_s + G_v = L_{fs} - L$$

(all values in db or dbm)

$$S = +43 + 9.7 + 2.0 - 157.2 - 7$$

$$= -109.5 \text{ dbm}$$

$$S/N = -109.5 - (-126)$$

$$S/N = 16.5 \text{ db}$$

Z. 3. 6. 2 Energy Contrast

Digital Systems require discrete elementary signals as information carriers. Such signals shall be separated in time and frequency. Each signal will occupy a bandwidth (W_L) in the low-pass-band for a duration of time (T).

The theoretical limit of bandwidth occupancy (W_T) of the elementary signal is

$$W_L = \frac{1}{2T}$$

This can only be achieved with $\frac{\sin x}{x}$ signals. Because the $\frac{\sin x}{x}$ signal is not limited to a time interval (T) (the distance between two zero crossings of the waveform), a more practical value of (W_L) is

$$W_L = \frac{2}{T}$$

The total signal energy (E_o) contained in the detected signal is

$$E_o = W_L T S$$

where S is the signal strength of the elementary signal. Dividing both sides by the received noise level to determine energy contrast, the result is

$$E_o/N = W_L T S/N = 2 S/N$$

For

$$S/N = 44.6 \ (16.5 \ db)$$

the energy contrast is

$$E_o/N = 2 S/N = 89.2 \ (19.5 \ db)$$

In the error analysis, the median value of energy contrast is required. Since the free space loss can be considered a mean or rms value and the fading is assumed to be Rayleigh distributed, the energy contrast of 19.5 db shall be corrected to median value of 1.6 db below the mean value. Therefore, the median energy contrast on the data link is

$$19.5 - 1.6 = 17.9 \ db.$$

Z.4 ERROR ANALYSIS UNDER CONDITIONS OF RAYLEIGH FADING

Z.4.1 Introduction

The results of a theoretical analysis of the message transmission reliability of the navigation satellite data transmission system is presented in this paragraph. Consideration is given to the feasibility of using either error-detecting or error-correcting coding to enhance the message transmission reliability.

The received signal power is assumed to be Rayleigh distributed in agreement with a curve plotted from an actual channel test between a satellite and a ground station. Curves of message transmission reliability are plotted vs. median received energy contrast. Conclusions and recommendations are made on the basis of a 17.9 db median energy contrast at the receiver. This value was given as a specified system design parameter.

The major conclusion of this presentation is that while the overall long-term average bit error rate in the data transmission channel is not good, most of these errors will be concentrated within a few messages that occur during fades. Thus, a reasonable message error rate is feasible at a 17.9 db median received energy contrast. In addition, most of these erroneous messages could be detected by a relatively simple error-detecting coding system. On the other hand, if it is desired to correct the erroneous messages rather than to request a retransmission, only the most complex and costly of error-correction-coding systems would be applicable.

There are many complex problems associated with a Navigation Satellite System, including the determination of accurate fixes of satellite numbers and orbits, equations for position calculations, etc. Once these are all determined one problem, perhaps the most important, remains. This problem is whether a data transmission complex can be set up between the satellites and possibly thousands of users so that the required number of position fixes can be accurately and quickly provided without overloading the system. A complete answer to the problem involves the consideration of message error-rate in the channel, expected channel transmission conditions, expected number of users, and the parameters of the transmitter and receiver system between the satellite and the user.

While it is desirable to have a negligible message error rate, it might be feasible to tolerate a few percent of erroneous messages if they can be detected and requests made for retransmission.

The purpose of this presentation was to make a theoretical observation of the expected message error rates under the specified system parameters. Based upon these calculations, recommendations were to be made on the feasibility of error-detecting or error-correcting coding to enhance the message transmission reliability to the user.

Z. 4. 2 Description of Message Transmission System and Format

    a. Communication System Parameters:

        (1) The received power is considered to be Rayleigh distributed.

        (2) The bit rate of transmission is 2.50 KC. The pulse width is 400μ sec.

        (3) FSK modulation is used in message transmission.

        (4) Detection is non-coherent, non-orthogonal frequency discrimination.

        (5) The median energy contrast at the receiver is 17.9 db.

    b. Message Format:

        (1) All messages begin with a sync code consisting of six bits (all marks). The timing circuits in the receiver are activated upon verification of the sync code. If the sync code is in error, the receiver shall disregard all transmission until a subsequent sync code is detected and verified.

        (2) Every sync code shall be followed by a four bit function code. The receiver shall decode the reference code and interpret it as one of the following:

            (a) Reference station fix command

            (b) Vehicle fix command

            (c) Vehicle report follows (airborne)

            (d) Special user vehicle report follows

            (e) Emergency report follows

            (f) Vehicle report follows (seaborne)

            (g) Other type report

(3) Every function code will be followed by either an eight bit reference station address, or a 24 bit vehicle address, depending on which function code is sent. The address will constitute the end of message transmission for a vehicle or reference station fix command. If the function code calls for a report, the report will immediately follow the vehicle address.

(4) The vehicle report consists of 153 bits of information including eight bits for error detection.

(5) There is built-in system error detection.

(a) If an addressee does not correctly decode a sync and/or function command that was intended to be a fix command, the addressee shall not respond to the range pulse. Its failure to respond shall be noted at the ground station.

(b) When an addressee responds to the range pulse following a fix command, it generates and transmits its address. The ground station shall determine if the proper addressee has responded to the range pulse by comparing the address transmitted by the addressee to the address originally transmitted by the ground station.

(c) When a vehicle has received a fix command, it shall start a clock that is preset to run a time (T). If the vehicle does not receive its report within time (T), the vehicle shall initiate a request for another fix report.

Z. 4. 3 Assumptions Made in Mathematical Model of Message Transmission System Analysis

A simplified mathematical model of the transmission system was assumed and approximate calculations, rather than extremely accurate calculations, were made because of time limitation. However, it is felt that the results still provide a good overall picture of the expected transmission channel behavior, as well as a bases for evaluating the feasibility of protective coding as applied to the data transmission.

Z. 4. 3. 1 Definition of Terms

This section contains some of the basic definitions used in the mathematical model.

a. Energy contrast - $\frac{E}{N_o}$ (Signal energy divided by noise power per cycle per second.) Usually taken to be the median E/N_o at the receiver.

b. Erroneous message - any message received with one or more bits in error.

c. Undetected error - any error which results in an invalid report being displayed by any vehicle.

d. Short Message - A message 50 bits in length, used in some places as a mathematical model of a vehicle fix command which is composed of somewhat fewer bits (including address, sync bits, etc.).

e. Long Message - a 187 bit message used as a mathematical model of the vehicle report message. The 187 bits include a 34 bit preamble consisting of addressing bits, synchronization bits, etc. A long message shall be said to have an undetected error

if the preamble is received correctly, but the data has one or more errors. The short message, by definition of its format, will always give an indication of an error (i. e., a synchronization bit is not received, or the wrong address is received, or a wrong command, etc.).

Z. 4. 3. 2 Assumptions

    a. Channel - The channel was assumed to be such that the received signal power was Rayleigh faded. This assumption was based on a graph made from data taken on an actual satellite-to-ground test where both the satellite and ground antennas were semi-directional.

    b. Detection – The detection was assumed to be based upon noncoherent, non-orthogonal FSK signals. A supplied curve gave probability of bit error in Gaussian noise as a function of E/N_o at the receiver. A Rayleigh distribution was superimposed upon this curve to supply the channel analysis in this document.

    c. Message format - Message transmission reliability was calculated for 50 bit and 200 bit messages. These calculations are good for messages of approximately the same sizes. Also, if a reliability figure is good for a longer word size, it shall always be good for a smaller word size.

Z. 4. 4 <u>Message Transmission Reliability Analysis</u>

Z. 4. 4. 1 Short Message

    Figure Z-1 is a plot of the probability of receiving a short word in error as a function of median received energy contrast. The probability of error was calculated for various bit error rates and the results were then averaged over a Rayleight distribution for each mean E/N_o. At the specified system E/N_o of 17. 9 db, it is noted that 6 out of 1000 short messages would be received in error.

Z. 4. 4. 2 Long Message

    Figure Z-2 presents essentially the same calculations for the 187 bit word at the specified system median E/N_o and the result is that 15 out of 1000 long messages shall be received in error.

    Figure Z-3 presents a plot of the probability of not detecting an error in a long message vs. median E/N_o for zero check bits and one parity check bit. More advanced error detecting systems are discussed in the following paragraph.

    Figure Z-3 is calculated on the basis of the 34 bit preamble (synch + function code + address) being correct in a 187 bit word with one or more of the remaining 153 bits being in error. This was calculated for various bit error rates and then the results averaged over a Rayleigh distribution. These results were halved for the one check – bit case since a single parity check shall detect all odd errors.
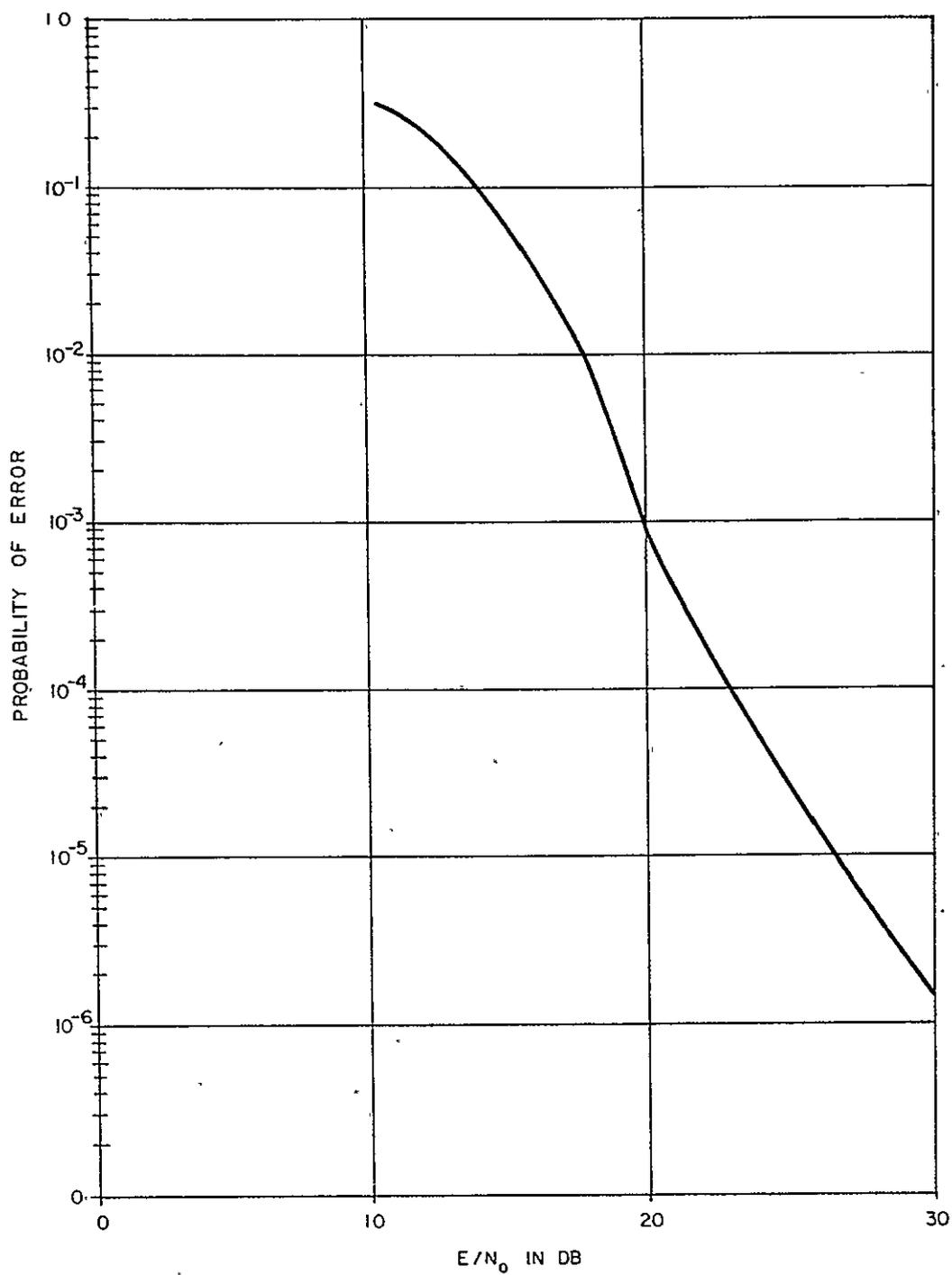
Figure Z-1. Probability of any Error (Detected or Undetected) in a
Vehicle Fix Command vs Median Energy Contrast
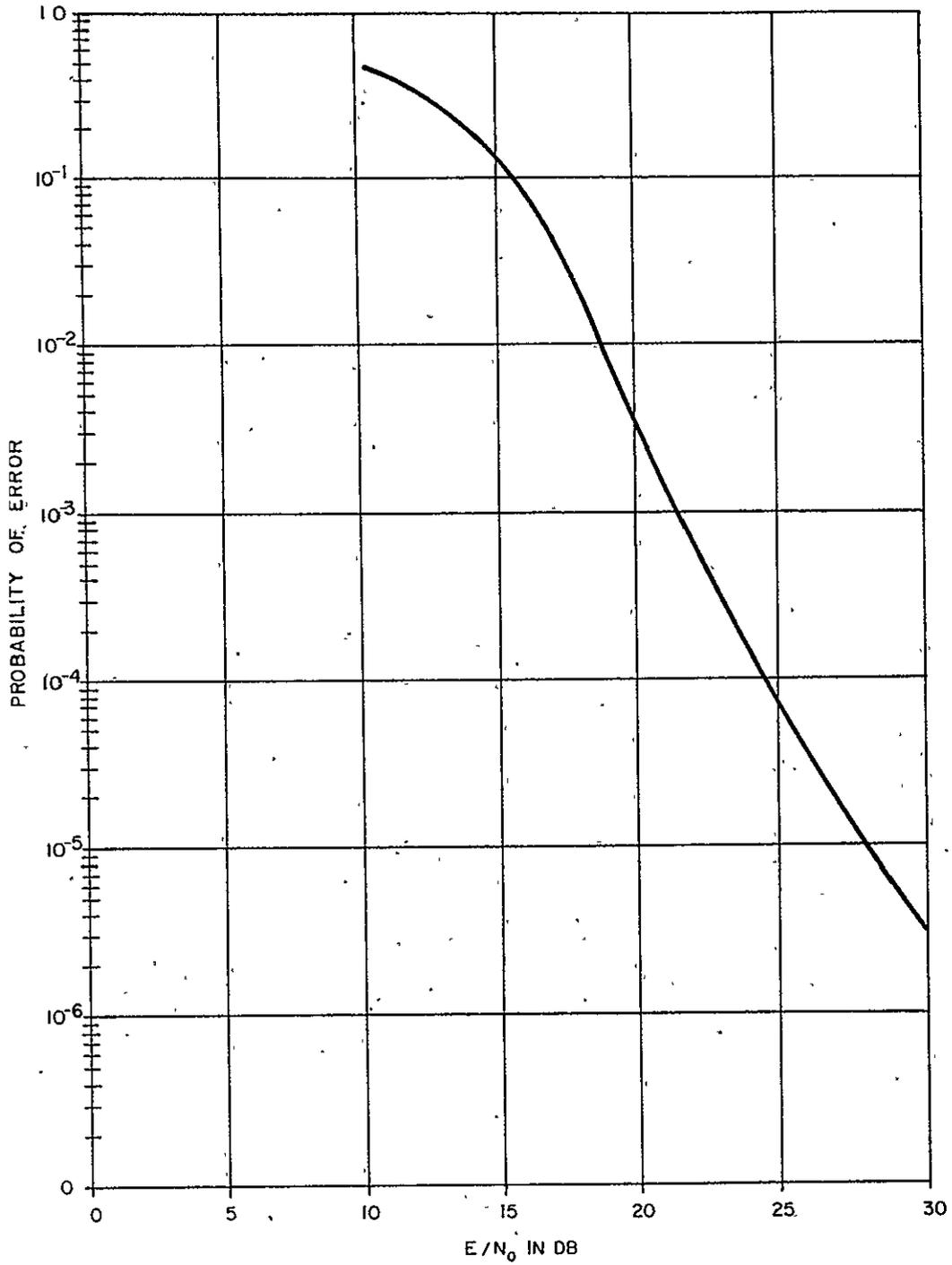
Figure Z-2. Probability of any Error (Detected or Undected) in a
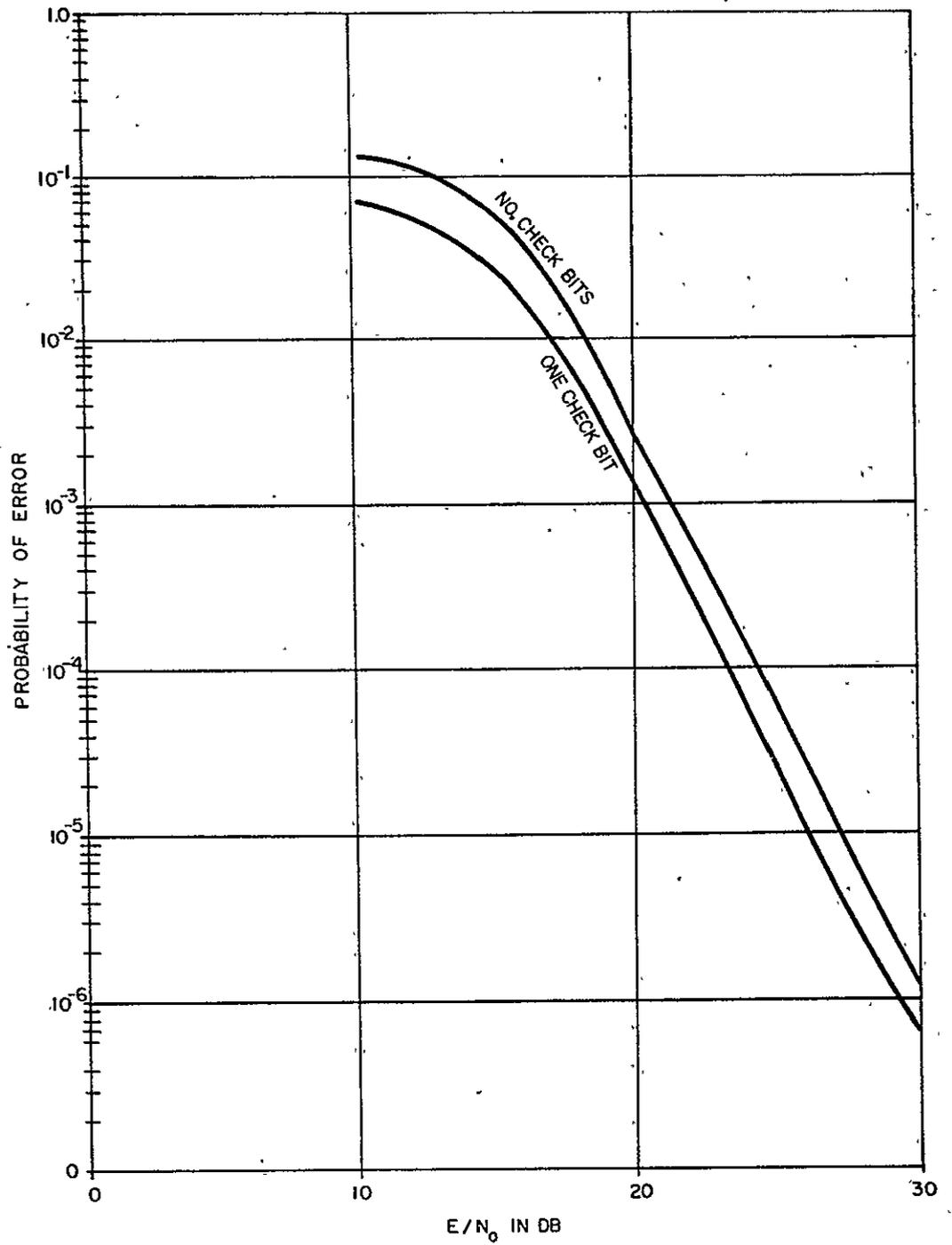Vehicle Report as a Function of Median $\frac{E}{N_o}$

Figure Z-3. Probability of an Undetected Error in a Vehicle Report with Zero and One Check Bit vs Median $\frac{E}{N_o}$

Note that at the specified system median receiver energy contrast of 17.9 E/N_o, 10 out of 1000 long messages shall get through with an undetected error if no check bit is used, while 5 out of 1000 will have undetected errors if one parity check bit is used.

Figure Z-4 is a plot of the difference between figures Z-2 and Z-3 and gives the probability of a detected error in a long message as a function of E/N_o for zero and one check bit.

Note that in all curves, the slope is steep and a difference of a few db in the median received energy contrast can make a signficant difference in the data transmission reliability. Thus, for all cases where the satellite is above the vehicles horizon, significantly better results can be expected.

Z.4.5 <u>Application of Protective Coding to Improve the Reliability of Message Transmission</u>

Z.4.5.1 General Considerations

There is an increasing need by communication systems for high speed and extremely reliable digital communication and data transmission complexes. Often, the desired transmission reliability is difficult to achieve within moderate equipment cost and complexity. In satellite systems, size becomes an even more important consideration than cost. In many cases it is becoming increasingly evident that ever tremendous increases in antenna size, transmitter power, etc. do not result in the desired reliability. This has brought about an increased interest in error control techniques (error-detecting and/or error-correcting coding) which, in many cases, can achieve the same improvement in transmission reliability at less cost.

Z.4.5.2 Error Correction Coding and Its Possible Application to the Satellite Data Transmission System

Past studies have shown that easily implementable error-correction techniques do not materially improve transmission reliability in a Rayleight fading channel. Only the more complex and expensive coders can be effective. Therefore, this document shall not study this application any further since the cost of error-correction equipment would be prohibitive.

The addition of a small amount of redundancy to a message, according to one of the many possible coding techniques, permits the detection of expected error patterns at the receiver. Cyclic forms of Bose-Chaudhuri codes can be used to detect a number of random errors or a larger number of errors in a burst. Other forms of codes, such as the Reed-Solomon codes, combat multiple bursts of errors. Although these error detection systems are efficient, they are only practicable where the erroneous message can be eliminated, or a request can be made for retransmission of the message.

The implementation of error-detecting coding is relatively simple. This method requires a linear sequential circuit of length equal to the number of check bits with codes at the
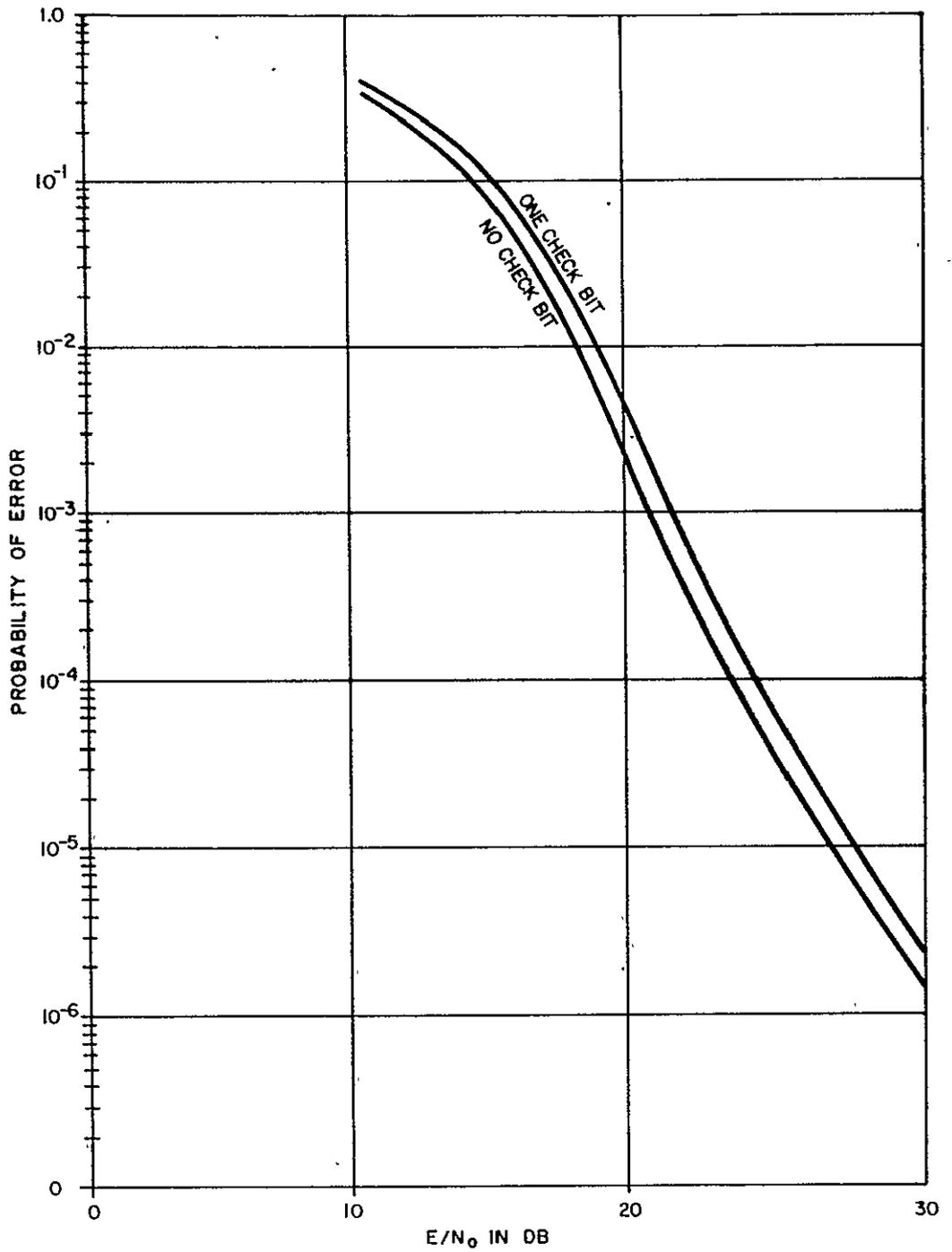
Figure Z-4. Probability of a Detected Error in a Vehicle Report with Zero and One Check Bit vs Median $\frac{E}{N_o}$

transmitter and receiver. A linear sequential circuit is a shift register with several feedback connections to exclusion OR gates.

For the particular long message, it is seen that the addition of one check bit would detect half of the erroneous messages. The analysis of the detecting properties of two or more check bits is extremely complicated and cannot be examined within the context of this document. It can be said, however, that the addition to the long message of from 10 to 20 check bits would permit the detection of possible 99% or more of erroneous messages.

Z.4.6 Conclusions and Recommedations

Z.4.6.1 Conclusions

As a result of this analysis of the message transmission reliability it is concluded that

a. The message transmission reliability is reasonable but not excellent at the specified 17.9 db median received energy contrast.

b. The message reliability is quite sensitive to changes of a few db in energy contrasts since the curves have a steep slope.

c. Error detection coding can possible provide a feasible means of signficantly reducing the probability of an undetected erroneous message.

d. Error-correcting coding is not feasible in the situation studied.

Z.4.6.2 Recommendations

a. Since the message transmission reliability is so sensitive to small changes in median energy contrast at the receiver, careful design of the system should be made to insure that it will be above the 17.9 db level in the actual expected environment.

b. Further study of the cost and error detecting capabilities of various longer error-detecting coding systems should be made to provide a means for making the data channel extremely reliable.

Z.4.6.3 Sample Calculation

As an example, the probability of an undetected error in a 187 bit word with a 34 bit address shall now be calculated for a median E/N_o of 15 db and zero check bits. For a fixed bit error rate (R), the probability of an undetected error is $P = \left\{ 1 - (1-R)^{153} \right\}$ $(1-R)^{34}$ in which $(1-R)^{34}$ is the probability of a correct preamble and $\left\{ 1 - (1-R)^{153} \right\}$ is the probability of one or more errors in the remaining 153 bits.

Error rates of 10^{-1}, 10^{-2}, 10^{-3}, 10^{-4}, 10^{-5}, 10^{-6}, 10^{-7}, 10^{-8} were chosen, and P was calculated for each. The results are:

R	10^{-1}	10^{-2}	10^{-3}	10^{-4}	10^{-5}	10^{-6}	10^{-7}	10^{-8}
P	.0275	.500	.101	1.19×10^{-2}	1.19×10^{-3}	1.19×10^{-4}	1.19×10^{-5}	1.19×10^{-6}

Using the relationship $P = 1/2\, e^{-E/2N_o}$, the energy contrasts were calculated for bit error rates halfway between the ones chosen above.

R	$.5 \times 10^{-1}$	5×10^{-2}	5×10^{-3}	5×10^{-4}	5×10^{-5}	5×10^{-6}	5×10^{-7}
E/N_o	6.5	9.8	11.5	12.8	13.7	14.8	15.2

The fraction of the time when E/N_o lies in each region can then be read from Rayleigh distribution graph paper for a median $E/N_o = 15$ db. The results are:

	Fraction of the Time
$\infty < E/N_o < 6.5$	.0075
$6.5 < E/N_o < 9.8$	.0925
$9.8 < E/N_o < 11.5$	.110
$11.5 < E/N_o < 12.8$	.110
$12.8 < E/N_o < 13.7$	.070
$13.7 < E/N_o < 14.8$	.090
$14.8 < E/N_o < 15.2$	.040
$15.2 < E/N_o < \infty$	.48

Multiplying the fraction of time by the appropriate error probability and summing, results in the average error probability, which in this case is 0.059.

For higher median E/N_o, the lower E/N_o's are not on the Rayleigh graph paper. In this case, the distribution shall be approximated by a straight line in this region, and the "fraction of the time" calculated by integating this curve.

Note that in the above calculations all $E/N_o > 15.2$ db are assumed to produce a bit error rate of 10^{-8}. This is not true. If $E/N_o > 15.62$, the bit error rate is closer to 10^{-9}, etc. However, in this particular calculation the 10^{-8} bit error rate has negligible contribution to the total probability of an undetected error. For higher median E/N_o, the smaller bit error rates contribute significantly to the error probability and error rates less than 10^{-8} might have to be considered.

APPENDIX AA

FORTRAN PROGRAM

This appendix contains the FORTRAN programs which compute the weights of the various satellite subsystems and the costs of the Navigation Satellite System according to the analysis presented in paragraph 7.4.1, entitled Optimization Studies.

The results presented in paragraph 7.4.1.2 were calculated by execution of these routines on the IBM 7094 digital computer.

```
       DIMENSION ALT(12),NGS(12),CGS(12),OMLAM(5),PUL(3),CBOO(5),
      XRELB(5),ACTCST(5),WW(5),WWE(5),WWH(5)
       DIMENSION ZBUSD(5)
       IRPUN=0
       NALT=12
       READ INPUT TAPE 5,1000,(ALT(I),I=1,NALT)
       READ INPUT TAPE 5,1001,(NGS(I),I=1,NALT)
       READ INPUT TAPE 5,1000,(CGS(I),I=1,NALT)
1001 FORMAT(12I3)
1000 FORMAT(6E11.4)
       OMLAM(1)=810.
       OMLAM(2)=920.
       OMLAM(3)=1500.
       OMLAM(4)=5000.
       OMLAM(5)=8500.
       PUL(1)=260.
       PUL(2)=350.
       PUL(3)=270.
       CBOO(1)=2.1E+06
       CBOO(2)=2.6E+06
       CBOO(3)=3.0E+06
       CBOO(4)=6.3E+06
       CBOO(5)=7.8E+06
       RELB(1)=0.95
       RELB(2)=0.75
       RELB(3)=0.75
       RELB(4)=0.6
       RELB(5)=0.5
       GMU=6.26E+04
       GG=5.3E-03
       RRP=3538.
       GLAMB=28.4*0.0174532925
       GGII=45.0*0.0174532925
       VV1=4.2064
       VVE=0.22
       DO 80 I=1,5
       ACTCST(I)=CBOO(I)/RELB(I)
80   CONTINUE
       TOMP=(VV1-VVE)**2/(VV1**2+VVE**2-2.0*VV1*VVE*COSF(GGII-GLAMB))
       DO 50 I=1,5
       WW(I)=OMLAM(I)*TOMP
50   CONTINUE
200  READ INPUT TAPE 5,1009,OH
1009 FORMAT(F10.3)
       IF(OH) 211,211,210
211  CALL EXIT
210  I=1
       IF(OH-ALT(1))10,10,20
20   DO 30 I=2,NALT
       IF(OH-ALT(I))40,10,30
```

```
30      CONTINUE
        I=NALT
        GO TO 10
40      I=I-1
10    - MNGS=NGS(I)
        RCGS=CGS(I)
        PHI=ACOSF(3424.9/(3438.+OH))-0.08727
        TEMP=3.1415927/ACOSF(COSF(PHI)/0.70711)
      , NSAT=TEMP+0.9999
        NSAT=NSAT*2
        CSTPS=1.5E+06
        TMSAT=NSAT
      · TOTCOS=TMSAT*CSTPS
        RRA=3438.+OH
        DELUP=SQRTF(GMU/RRP)*(-1.0+SQRTF(2.0*RRA/(RRA+RRP)))
        FAC1=0.7/(EXPF(DELUP/(GG*PUL(1)))-0.3)
        FAC2=0.7/(EXPF(DELUP/(GG*PUL(2)))-0.3)
        FAC4=0.5/(EXPF(DELUP/(GG*PUL(1)))-0.5)
        DELUA=SQRTF(GMU/RRA)*(1.0-SQRTF(2.0*RRP/(RRA+RRP)))
        FAC3=0.9/(EXPF(DELUA/(GG*PUL(3)))-0.1)
        DO 60 I=1,3
        WWE(I)=WW(I)*FAC1
60      CONTINUE
        WWE(4)=WW(4)*FAC4
        WWE(5)=WW(5)*FAC2
        DO 70 I=1,5
        WWH(I)=WWE(I)*FAC3
70      CONTINUE
888     CALL WEIGHT(OH,WTSAT,IRPUN)
        IF(IRPUN-2) 887,200,200
887     DO 90 I=1,5
        IF(WTSAT-WWH(I))100,100,90
90      CONTINUE
        GO TO 888
100     BOOST=TMSAT*ACTCST(I)
        NN=I
        COST1=BOOST+TOTCOS/RELB(NN)
        COST3=COST1+RCGS
        MSAT=NSAT/2
        SMSAT=MSAT
       ·GMSAT=SMSAT
        SATCOS=0.0
        WTPPL=SMSAT*WTSAT
        DO 169 I=1,5
169     ZBUSD(I)=0.0
175     IF(WTPPL-WWH(5))170,170,171
170   · DO 172 I=1,5
        IF(WTPPL-WWH(I)) 173,173,172
172     CONTINUE
173     ZBUSD(I)=ZBUSD(I)+1.0
        SATCOS=SATCOS+GMSAT*CSTPS/RELB(I)
       `GO TO 180
171`    ZMICH=0.0
181     ZMICH=ZMICH+1.0
        ZMACH=ZMICH*WTSAT
        IF(ZMACH-WWH(5)) 181,182,183
183     ZMICH=ZMICH-1.0
        ZMACH=ZMICH*WTSAT
182     ZBUSD(5)=ZBUSD(5)+1.0
        SATCOS=SATCOS+ZMICH*CSTPS/RELB(5)
        GMSAT=GMSAT-ZMICH
        WTPPL=WTPPL-ZMACH
        IF(WTPPL) 180,180,175
180     TPBOCT=0.0
        DO 190 I=1,5
        ZBUSD(I)=2.0*ZBUSD(I)
        TPBOCT=TPBOCT+ZBUSD(I)*ACTCST(I)
```

```
190   CONTINUE
      COST2=2.0*SATCOS+TPBOCT
      COST4=COST2+RCGS
999   A=A
      GO TO 888
      END(1,0,0,0,0,1,1,0,0,0,0,0,0,0,0)
```

SUBROUTINE WEIGHT(H,WS,IRPIN)   12/14/63

```
      SUBROUTINE WEIGHT(H,WS,IRPIN)
      DIMENSION G(2),A(2),FR(7),B(5),TNB(2),TN(5),F(7)
      DIMENSION R(2),C(2),PH(2),ALP(7),PNR(7),PNA(6),PN(7),PP(7),
     XS(5),PAO(5),PA(5)
      DIMENSION OG(2),OA(2),OF(7)
      DIMENSION TABLE(10,11),ICAS(11,85)
      IF(IRPIN) 6969,6969,6970
 6969 OG(1)=5.0
      OG(2)=5.0
      RE=3438.0
      PI=3.14159
      OSD=10.0
      OX1=29000.0
      OGV=1.5
      X2=1.6188E+05
      OA(1)=13.0
      OA(2)=13.0
      FR(1)=9.9E+08
      FR(2)=1.1E+08
      FR(3)=1.0E+08
      FR(4)=9.7E+08
      FR(5)=2.7E+09
      FR(6)=9.9E+08
      FR(7)=9.6E+08
      READ INPUT TAPE 5,1000,((TABLE(I,J),I=1,10),J=1,11)
 1000 FORMAT(5E10.3)
      READ INPUT TAPE 5,1001,((ICAS(I,J),I=1,11),J=1,30)
 1001 FORMAT(11I2)
      OGG=44.0
      X3=4.0E-21
      BR=1.6E+05
      OF(1)=6.4
      OF(2)=4.72
      OF(3)=4.72
      OF(4)=-7.6
      OF(5)=-7.6
      OF(6)=6.0
      OF(7)=6.0
      PPG=15.0
      PPT=3.6E+03
      SIGR=5.0E-02
      TPRW=3.2E-04
      BA=143.0
      SIGP=2.0E-01
      PE=1.0E-04
      GP4=50.0
      B(3)=0.0
      B(5)=0.0
      B(2)=5.0E+04
      TN(1)=1.66E-03
      TN(2)=1.028E-02
      TN(3)=1.156E-02
      TN(4)=1.856E-02
      TN(5)=2.556E-02
      TNB(1)=1.66E-03
      TNB(2)=1.92E-03
      TTV=1.0
      TTB=1.0
      BCN=4.0
      CUNV=PI/180.0
      G(1)=OG(1)*CUNV
      G(2)=OG(2)*CUNV
      SD=OSD*CUNV
      X1=OX1*CUNV**2
      GV=EXPF(0.2303*OGV)
      A(1)=EXPF(0.2303*OA(1))
      A(2)=EXPF(0.2303*OA(2))
      GG=EXPF(0.2303*OGG)
      DO 333 I=1,7
```

AA-4

```
333   F(I)=EXPF(0.2303*OF(I))
      ICO=1
6968 A=A
6970 IRPIN=1
      IF(ICO-1)6971,6971,6972
6972 IF(ICO-30 ) 6973,6973,6974
6974 IRPIN=2
      ICO=1
      RETURN
6973 J=ICO-1
      DO 6976 I=1,11
      IF(ICAS(I,J))6976,6976,6977
6977  I=I
      K=ICAS(I,J)
      GO TO(1,9,11,12,2,3,4,5,6,7,8),
1     L=1
      GO TO 13
9     L=4
      GO TO 13
11    L=6
      GO TO 13
12    L=7
13    FR(L)=TABLE(K,I)
      GO TO 6976
2     OGG=TABLE(K,I)
      GG=EXPF(0.2303*OGG)
      GO TO 6976
3     PPG=TABLE(K,I)
      GO TO 6976
4     PPT=TABLE(K,I)
      GO TO 6976
5     SIGR=TABLE(K,I)
      GO TO 6976
6     SIGP=TABLE(K,I)
      GO TO 6976
7     B(5)=TABLE(K,I)
      GO TO 6976
8     TTV=TABLE(K,I)
6976 CONTINUE
6971 ICO=ICO+1
      DO 10 I=1,2
      Z = RE*COSF(G(I))/(RE+H)
      B = Z*COSF(G(I))+SINF(G(I))*SQRTF(1.0-Z**2)
      R(I) = SQRTF(RE**2+(RE+H)**2-2.0*RE*(RE+H)*B)
      C(I) = ACOSF(B)
      PH(I) = 2.0*(PI*0.5-C(I)-G(I))+SD
10    CONTINUE
20    TEMP = X1*GV*(X2/R(1))**2/((4.0*PI)**2*A(1)*PH(1))
      DO 30 I = 1,3
      ALP(I) = TEMP*(1.0E+10/FR(I))**2
30    CONTINUE
      GO TO 80
82    IF(PP(I)-400.) 83,83,84
84    PA(I) = 3.0*PAO(I)
      GO TO 80
83    PA(I) = 3.5*PAO(I)
80    CONTINUE
      TPA = 5.0
      DO 89 I = 1,5
89    TPA=TPA+PA(I)
      WRT = 2.4*PAO(1)
      WCT = 23.0
      DO 90 I = 2,5
```

```
90      WCT = WCT+0.3*PAO(I)
        WSP = 0.5*TPA+10.0
        WR = WE+WAA+WRT
        WSTA = 10.0+50.348*((RE+H)/(RE+6000.))
        WET = WCT+WR+WSTA+WSP+10.0
        WSTU = 0.25*WET
        WS = 1.25*WET
        OH=H
        PH(1)=PH(1)/CUNV
        PH(2)=PH(2)/CUNV
        SR=4.343*LOGF(SR)
        SA=4.343*LOGF(SA)
        DL=6080.*DL
        DM=6080.*DM
        DS=6080.*DS
        S(2)=4.343*LOGF(S(2))
        S(3)=4.343*LOGF(S(3))
        S(5)=4.343*LOGF(S(5))
900     WRITE OUTPUT TAPE 6,9000
9000    FORMAT(1H1,10X)
        WAIT=WS
100     A=A
        RETURN
        END(1,0,0,0,0,1,1,0,0,0,0,0,0,0,0)
        ALP(6) = TEMP*(1.0E+10/FR(6))**2
35      TEMP = X1*GG*(X2/R(2))**2/((4.0*PI)**2*A(2)*PH(2))
        ALP(4) = TEMP*(1.0E+10/FR(4))**2
        ALP(5) = TEMP*(1.0E+10/FR(5))**2
        ALP(7) = TEMP*(1.0E+10/FR(7))**2
40      TEMP = BR*0.4
        PNR(1) = F(1)*TEMP
        PNR(4) = F(4)*TEMP
        PNR(6) = F(6)*TEMP
        PNR(7) = F(7)*TEMP
45      TEMP = BA*0.4
        PNA(4) = F(4)*TEMP
        PNA(6) = F(6)*TEMP
        PN(2) = F(2)*B(2)*0.4
        PN(3) = F(3)*B(3)*0.4
        PN(5) = F(5)*B(5)*0.4
        PN(7) = F(7)*B(2)*0.4
        SR = 0.75*(X2/BR)**2/(PI**2*SIGR**2*BR*TPRW)
        PP(1) = SR*PNR(1)*(PPG*PPT*ALP(6)*ALP(7)+PPT*ALP(6)*PNR(7)+PPG*
     X  ALP(7)*PNR(6)+PNR(6)*PNR(7))
        PP(1) = PP(1)/(PPG*PPT*ALP(6)*ALP(7)-SR*PPT*ALP(6)*PNR(7)-SR*PPG*
     X  ALP(7)*PNR(6)-SR*PNR(6)*PNR(7))
        PP(1)=PP(1)/ALP(1)
        TEMP = PP(1)*PPT*ALP(1)*ALP(6)*PNR(6)/((PP(1)*ALP(1)+PNR(1))*(PPG*
     X  ALP(7)+PNR(7)))
        TIMP = PPT*ALP(6)*PNR(1)/(PP(1)*ALP(1)+PNR(1))
        PP(6) = GP4*(PPT*ALP(6)*PNR(4)+PNR(4)*PNR(6))/(ALP(4)*(TEMP+
     X  TIMP+PNR(6)))
        PP(7) = GP4*(PPT*ALP(6)*PNA(4)+PNA(4)*PNA(6))/(ALP(4)*PNA(6))
        IF(PP(6)-PP(7)) 55,55,60
55      PP(4) = PP(7)
        GO TO 56
60      PP(4) = PP(6)
56      SA = PPT*ALP(6)/PNA(6)
        DL = X2*R(1)/(2.0*PI*SIGP*FR(6)*SQRTF(SA))
61      TUMP = X2/(2.0*FR(6)*SINF(0.5*PH(1)))
        IF(DL-TUMP) 62,62,63
62      DS = 0.0
        DM = 0.0
        GO TO 69
63      DS1 = TUMP
        TAMP = 2.0*X2/FR(6)
        IF(DS1-TAMP) 64,64,65
```

```
SUBROUTINE WEIGHT(H,WS,IRPIN)

65     DS = DS1
       GO TO 66
64     DS = TAMP
66     CC = X2/(2.0*PI*DS*FR(6)*SQRTF(SA
       TOMP = X2/(2.0*FR(6)*SINF(0.5*CC)
       IF(DL-TOMP) 67,67,68
67     DM = 0.0
       GO TO 69
68     DM = TOMP
69     S(2)=ABSF(LOGF(2.0*PE))
       S(3) = S(2)
       S(5) = S(2)
       PP(3) = PN(3)*S(3)/ALP(3)
       PP(5) = PN(5)*S(5)/ALP(5)
       PP(2) = (S(2)*PPG*ALP(7)*PN(2)+S(2)*PN(2)*PN(7))/(PPG*ALP(2)
      1ALP(7)-S(2)*ALP(2)*PN(7))
       PAO(3) = PP(3)
       PAO(5) = PP(5)
       DO 71 I = 1,2
71     PAO(I) = PP(I)*(TNB(I)/TTB+TN(I)/TTV)
       IF(DS) 72,73,72
73     PAO(4) = PP(4)*(BCN*TN(3)/TTB+TN(3)/TTV)
       WAA = 3648.0*DL+4.0
       WE = 20.0
       GO TO 74
72     IF(DM) 75,76,75
76     PAO(4) = PP(4)*(BCN*TN(4)/TTB+TN(4)/TTV)
       WAA = 3648.0*DL+8.0
       WE = 30.0
       GO TO 74
75     PAO(4) = PP(4)*(BCN*TN(5)/TTB+TN(5)/TTV)
       WAA = 3648.0*DL+12.0
       WE = 40.0
74     PA(1) = 3.0*PAO(1)+10.0
       DO 80 I = 2,5
       IF(PP(I)-50.0) 81,82,82
81     PA(I) = 4.0*PAO(I)
```